

Organic Substances and Sediments in Water

Volume 2

Processes and Analytical

Robert A. Baker

Editor

Ji - Rice
8-91

Organic Substances and Sediments in Water

Volume 2

Processes and Analytical

Robert A. Baker
Editor



LEWIS PUBLISHERS

Library of Congress Cataloging-in-Publication Data

Organic substances and sediments in water / Robert A. Baker,
Editor.

p. cm.

Papers from two symposia held at the American Chemical
Society Meeting in Boston, Apr. 22-27, 1990.

Includes bibliographical references and index.

Contents: v. 1. Humics and soils — v. 2. Processes and analytical — v. 3. Biological.

1. Organic water pollutants—Congresses. 2. Sediments, Suspended—Congresses. 3. Water chemistry—Congresses. 4. Biochemistry—Congresses. I. Baker, Robert Andrew, 1925— . II. American Chemical Society. Meeting (1990 : Boston, Mass.)

TD427.070753 1991

628.1'68--dc20 91-7855

ISBN 0-87371-342-7 (v. 1)

ISBN 0-87371-528-4 (v. 2)

**COPYRIGHT © 1991 by LEWIS PUBLISHERS, INC.
ALL RIGHTS RESERVED**

Neither this book nor any part may be reproduced or transmitted in any form or by any means, electronic or mechanical, including photocopying, microfilming, and recording, or by any information storage and retrieval system, without permission in writing from the publisher.

**LEWIS PUBLISHERS, INC.
121 South Main Street, Chelsea, Michigan 48118**

PRINTED IN THE UNITED STATES OF AMERICA

*To
Peggy Baker
for her continued understanding and encouragement*



Robert A. Baker is affiliated with the National Research Program, Water Resources Division of the U.S. Geological Survey. He holds a BChE from North Carolina State University, MChE and MS from Villanova University, and a D.Sc. from the Graduate School of Public Health, University of Pittsburgh. Dr. Baker's professional career has involved research, consultation, and management related to environmental science and engineering problems. He is active in professional societies and has authored over 70 books, patents, and papers.

Preface

Water resources managers, regulators, and researchers require definitive information that describes the highly correlated, interdisciplinary factors that influence fate and transport of water contaminants. Not unexpectedly, evolving questions stay ahead of advances in scientific and engineering developments. One of the most important and significant aspects currently being intensely investigated is the role of particulates and sediments in contaminant behavior. This three-volume compilation documents the proceedings of a symposium dedicated to the subject of organic substances and sediments in water. Stress was placed on the organic substances because so many of the anthropogenic contaminants which pose potential problems at all trophic levels are organic in nature.

The symposium program from which the proceedings derive included critical reviews which describe the state-of-the-science, and often identify major needs. This should be especially valuable to the reader, regardless of individual interest. As in any symposium proceedings, topics are treated with varying depth. However, coverage over the interdisciplinary subject is reasonably complete.

The first volume delves into the roles of humic substances and soils-sediments in the sorption and mobility of contaminants. Both regimes are introduced by comprehensive review papers, and both reviews are followed by papers that treat specific topics in depth.

The second volume combines papers that summarize various processes involved in contaminant fate and transport as well as analytical developments. The processes section has been divided into aquatic particle-organic chemical interaction (characterization and contaminant geochemistry); fate and transport; and interfacial and organic-inorganic processes. The processes and analytical sections present theoretical as well as case study developments.

The third volume is devoted to biological processes. It begins with a state-of-the-science summary which incorporates references to the other papers deriving from the symposium. The papers are divided under subheadings: integrating chemistry and toxicology of sediment-water interactions; uptake and accumulation (bioavailability and bioaccumulation); biodegradation (aerobic dechlorinations and co-metabolism).

This compilation extends over the broad interdisciplinary subject of organic substances and sediments in water. It should prove valuable to experienced scientists as well as those making initial inquiries.

Acknowledgments

An American Chemical Society symposium on the subject "Contaminants and Sediments" was held in Honolulu, April 1-6, 1979. A two-volume publication of the same title was published by Ann Arbor Science in 1980. These publications have frequently been cited in the literature. Several years ago colleagues suggested that the writer consider organization of another symposium to foster technology transfer and to update the proceedings of the previous state-of-the-science summary. This led to the symposium "Organic Substances and Sediments in Water" held at the American Chemical Society Meeting in Boston, April 22-27, 1990. The symposium emphasized organic substances and the complex processes effecting their fate and transport, particularly as these occur at the interface of suspended and fixed surfaces. Interdisciplinary contributions were solicited and development of topical sessions shared with recognized experts. These were: V. D. Adams, Tennessee Technical University; D. Armstrong, University of Wisconsin; S.A. Boyd, Michigan State University; C.T. Chiou, U.S. Geological Survey; B. Dempsey, Pennsylvania State University; B.J. Eadie, Great Lakes Environmental Research Laboratories; S.J. Eisenreich, University of Minnesota; P.F. Landrum, Great Lakes Environmental Research Laboratory; J. Leenheer, U.S. Geological Survey; R.L. Malcolm, U.S. Geological Survey; J.F. McCarthy, Oak Ridge National Laboratory; A.V. Palumbo, Oak Ridge National Laboratory; and A. Stone, Johns Hopkins University. Their dedication and cooperation was of the finest from onset through final manuscript peer review.

In addition to North American participants, scientists and engineers from other continents contributed. Five invited European scientists were: Jacques Buffle, University of Geneva, Switzerland; Hans Borén, Linköping University, Sweden; Egil Gjessing, Norwegian Institute for Water Research, Oslo, Norway; Jussi Kukkonen, University of Joensuu, Finland; and Paolo Sequi, Istituto D. Chimica Agraria, Bologna, Italy. Their perceptions and comments were as valuable as their technical contributions. A grant from the U.S. Environmental Protection Agency provided travel support for the invited speakers. Louis Swaby, Office of Exploratory Research, Washington, DC, and Wayne Garrison, Environmental Research Laboratory, Athens, Georgia provided program development assistance and liaison.

Chemical sciences are often an integral aspect of scientific and engineering processes perceived as nonchemical in nature. To improve knowledge of such situations and to facilitate communication among interdisciplinary contributions, the American Chemical Society, through its Committee on Science, has established a Pedagogical Symposium program. These tutorial symposia typically offer overview and research presentations by acknowledged experts in related fields. A competitive proposal to conduct a pedagogical symposium on

the same subject as the research symposium was awarded by the Committee on Science. The tutorial was held on April 24, 1990. The lecturers were: E.J. Bouwer, Johns Hopkins University; D.M.D. Toro, Manhattan College; J.W. Farrington, University of Massachusetts; I. Knight, University of Maryland; J.R. Pratt, Pennsylvania State University; R.E. Speece, Vanderbilt University; and J.A. Symons, University of Houston. Their presentations dramatically demonstrated the interdependence of various scientific and engineering processes as well as the benefits of interdisciplinary technology transfer. Drs. Pratt, Speece, and Knight contributed papers to these proceedings.

Financial support for the pedagogical symposium was from the Committee on Science and from the Environmental Chemistry Division of the American Chemical Society. The research symposium and the pedagogical symposium were held under the auspices of the Environmental Chemistry Division. Encouragement and support of the officers and members of these organizational units is gratefully acknowledged.

The endeavor would have been of no avail without the contribution of the scientists and engineers whose manuscripts are contained in these proceedings. The editor appreciates their willingness to share knowledge.

Contents

PART I AQUATIC PARTICLE-ORGANIC CHEMICAL INTERACTION: CHARACTERIZATION AND CONTAMINANT GEOCHEMISTRY

1. Preliminary Evaluation of the Potential of Gas Purging for Investigating the Air-Water Transfer of PCBs, *Michael W. Murray and Anders W. Andren* 3
2. Trace Element Cycling in Southern Lake Michigan: Role of Water Column Particle Components, *Martin M. Shafer and David E. Armstrong* 15
3. Sorption of Alkylbenzenes to Mineral Oxides, *Judith A. Perlinger and Steven J. Eisenreich* 49
4. Field-Measured Associations Between Polychlorinated Biphenyls and Suspended Solids in Natural Waters: An Evaluation of the Partitioning Paradigm, *Joel E. Baker, Steven J. Eisenreich, and Deborah L. Swackhamer* 79
5. The Role of Phytoplankton in the Partitioning of Hydrophobic Organic Contaminants in Water, *Deborah L. Swackhamer and Robert S. Skoglund* 91
6. Quantification and Characterization of Pore-Water Organic Colloids, *Yu-Ping Chin, Ann P. McNichol, and Philip M. Gschwend* 107
7. Adsorption of Surfactants, *Bruce J. Brownawell, Hua Chen, Wanja Zhang, and John C. Westall* 127
8. Partitioning and Sorption Kinetics of a PCB in Aqueous Suspensions of Model Particles: Solids Concentration Effect, *Patricia L. Van Hoof and Anders W. Andren* 149

PART II FATE AND TRANSPORT

9. Polycyclic Aromatic Hydrocarbons in Sediments and Pore Waters of the Lower Great Lakes: Reconstruction of a Regional Benzo(a)pyrene Source Function, *Brian J. Eadie, John A. Robbins, Warren R. Faust, and Peter F. Landrum*..... 171
10. Historical Deposition and Biogeochemical Fate of Polycyclic Aromatic Hydrocarbons in Sediments Near a Major Submarine Wastewater Outfall in Southern California, *Robert P. Eganhouse and Richard W. Gossett* 191
11. The Distribution of PCBs in Surface Sediments of Narragansett Bay, Rhode Island, *James S. Latimer, Lawrence A. LeBlanc, John T. Ellis, and James G. Quinn* 221
12. Carbon Cycling in Coastal Sediments: 2. An Investigation of the Sources of ΣCO_2 to Pore Water Using Carbon Isotopes, *Ann P. McNichol, Ellen R.M. Druffel, and Cindy Lee*..... 249
13. Diffusive Rate Limitations in the Sorption of Organic Chemicals, *William P. Ball and Paul V. Roberts* 273
14. Investigation of the Distribution of Natural Organic Compounds in the Sediments of Estuaries with Indication of Their Likely Sources, *Brian J. Harland, Malcolm J. Hetheridge, and Simon J. Molloy* 311
15. Environmental Response to Hazardous Chemicals, *R.E. Speece, N. Nirmalakhandan, and Diane J.W. Blum*..... 323

PART III INTERFACIAL AND ORGANIC-INORGANIC PROCESSES

16. Reduction of Hexachloroethane and Carbon Tetrachloride at Surfaces of Biotite, Vermiculite, Pyrite, and Marcasite, *Michelle Kriegman-King and Martin Reinhard* 349
17. The Effect of pH and Anions on the Solubility and Sorption Behavior of Acridine, *Robert A. Matzner, Douglas R. Hunter, and Roger C. Bales*..... 365
18. Surfactant-Enhanced Solubility of Hydrophobic Organic Compounds in Water and in Soil/Water Systems, *David A. Edwards, Zhongbao Liu, and Richard G. Luthy*..... 383

PART IV ANALYTICAL

19.	Determination of Anthropogenic Organic Compounds Associated with Fixed or Suspended Solids/Sediments: An Overview, <i>Martha J.M. Wells and V. Dean Adams</i>	409
20.	Determination of Polyvinyl Alcohol in Sewage, <i>C. Ellen Gonter, Lorraine C. Guyette, and Thomas G. Stevens</i>	481
21.	Use of ^{14}C Label to Study Fine Particulate Organic Matter Dynamics in Flowing Water, <i>J. Denis Newbold, Colbert E. Cushing, and G. Wayne Minshall</i>	493
22.	Synchronous Fluorescence Spectra of Dissolved Organic Matter, <i>Stephen E. Cabaniss</i>	503
	List of Authors.....	521
	Index	525

PART I

AQUATIC PARTICLE-ORGANIC CHEMICAL INTERACTION: CHARACTERIZATION AND CONTAMINANT GEOCHEMISTRY

CHAPTER 1

Preliminary Evaluation of the Potential of Gas Purging for Investigating the Air-Water Transfer of PCBs

Michael W. Murray and Anders W. Andren

INTRODUCTION

The processes affecting the air-water transfer of trace organic compounds such as polychlorinated biphenyls (PCBs) have become better understood in recent years with the aid of data generated by high-resolution gas chromatography analysis. PCB concentration data recently published for the water column of the Great Lakes,¹⁻⁶ the water of and air over Lake Superior,⁷ an estuarine system,⁸ the North Sea,⁹ and for the atmosphere¹⁰⁻¹² are useful in expanding the database of PCBs in the environment, and consequently in improving the predictive capability of recent modeling efforts.¹³⁻¹⁵

However, as noted by most authors, attempts to understand the partitioning of PCBs in water bodies are limited by the sampling technique generally employed, in which water is first filtered and then passed through an adsorbent; colloidal material and macromolecules with associated PCBs might either remain on the adsorbent or pass through the entire apparatus, as found for polycyclic aromatic hydrocarbons (PAHs) by Landrum and Giesy.¹⁶ Since only the truly free fraction of PCBs in lake waters is directly involved in diffusive or turbulent transfer both to the atmosphere and into organisms, it is desirable to have an alternative technique of determining this fraction in natural waters.

Gas purging is being investigated as a technique to determine the unbound fraction, or the fugacity, of PCBs in natural waters. While aeration has been used for decades in ore processing, packed column reactors, and other applications,¹⁷ it only recently appeared in the environmental literature as a technique (also called *dynamic headspace analysis*) for determining Henry's law constants (HLCs), first proposed by Mackay et al.¹⁸ and later used by others in investigations of HLCs and organic contaminant binding by particles.¹⁹⁻²⁴ Yin and Hassett recently reported on the use of the technique for investigating mirex fugacity in the Oswego River and Lake Ontario.²⁵

The technique for determining HLC involves bubble generation in an aqueous solution; if bubbles remain in the solution for a sufficient period of time, solute transfer to the bubble will occur until equilibrium is attained. This process is assumed to be described by a two-layer model of gas transfer.²⁶ Henry's law constant (or the ratio of gas- and liquid-phase concentrations at equilibrium) can be obtained by measuring the change in the gas concentration leaving the headspace via a trap,²³ the aqueous concentration change,¹⁸ or both concentrations at any one time.²²

For field determinations or investigation of partition coefficients, purge-gas flow rate and volume are adjusted such that the equilibrium between dissolved, colloidal, and particulate phases is not disturbed.²² In this manner, aqueous phase fugacity can be determined, and if the HLC is known, the free aqueous concentration can be calculated.

As noted by Fendinger and Glotfelty,²⁷ potential problems with the technique are lack of attainment of equilibrium and solute adsorption at the bubble-water interface (and associated transport to the upper region of the solution, reviewed in Lemlich, and later discussed by Valsaraj).^{28,29} These two problems were addressed in this study by purging at different flow rates (and thus using bubbles of different sizes and residence times), and by determining the solution concentration at depth and at the water surface following purging.

Additional concerns for field application are potential adsorption onto bubbles of contaminant-containing surface active organic material, and particle injection into the headspace following bubble bursting. Reviews on air-water hydrodynamics and exchange of particulate matter have summarized findings that even small bubbles can inject particles into the atmosphere on bursting.³⁰⁻³² The bubble-bursting phenomenon, and the consequent potential limitations of gas purging for fugacity investigations in the field, are under investigation. This chapter summarizes preliminary results of Henry's law constant determinations and field fugacity estimates for PCBs using the gas-purging technique.

EXPERIMENTAL

Henry's law constant determinations were made using an apparatus similar to that of Yin and Hassett.²² The vessel utilized was a 20-L glass carboy. Compressed air was introduced via two 0.125-in. stainless-steel (304) purge tubes terminating in fritted-glass gas-dispersion tubes (Ace Glass Co., Vineland, NJ), with nominal 4- to 8- μm pore sizes. Room-temperature experiments were conducted using six 0.5-mm holes in the ends of the purge tubes, before the dispersion tubes were added to the system.

The carboy is capped with a machined piece of Teflon, which is held tightly against the mouth by a metal collar, with a Viton O-ring forming the seal. The outflow of the headspace passes through a 0.25-in. Swagelok Teflon union to a

glass tube (4 mm i.d. by 10.5 cm length) packed with Florisil 30/60 mesh resin, with 3-mm plugs of silanized glass wool in each end. Traps are heated to 500°C for 6–8 hr, allowed to cool, and capped with brass end-caps prior to use.

During purging, high-purity (99.999%) compressed air passes through a flow controller, a Florisil trap, and the purge tubes, exits the dispersion tubes as bubbles that rise from the bottom of the solution, and exits the headspace via the adsorbent trap. The outflow then passes through a variable-area flow meter (Cole-Parmer Co., Chicago, IL), which is monitored during purging.

Henry's law constants were determined for 10 PCB congeners at room temperature (approximately 17 and 19°C) and at 25°C. For each determination, 0.7 mL of a 10-congener PCB solution in acetone was spiked into 19.7 L of Milli-Q water and allowed to equilibrate for at least 16 hr. The equilibration period was extended to 5 days for the 25°C experiment.

Before and after purging, two 100-mL subsamples of the water were taken and extracted with dichloromethane (3×20 mL). In order to investigate the possibility of net solute transport to the top of the solution during purging, subsamples were taken 1–2 cm below the surface and 1–2 cm above the vessel bottom immediately following purging in one experiment (at 5°C).

The water was purged at about 470 mL/min for the room-temperature experiments and at three different flow rates for the 25°C experiment. The traps were changed at regular intervals, with the purge time varying according to flow rate and expected mass purged. The traps were extracted with 60:40 acetone–hexane in a continuous-flow apparatus (similar to that described by Leuenberger and Pankow³³) for 2 hr, and all extracts were concentrated in hexane, transferred to *iso*-octane, and made to 1.0 mL, with congeners #30 and #204 added as internal standards. Analysis was performed on a Hewlett-Packard (HP) 5840 gas chromatograph with electron capture detector (GC-ECD) for the room-temperature experiments, and an HP 5890 GC-ECD for the 25°C experiment.

Field sampling was carried out at Little Lake Butte des Morts, Wisconsin. Duplicate 20-L surface water samples were pumped through Teflon lines into glass carboys, and the water was purged onsite; the temperature was measured before and after purging. The traps, including field blanks, were returned to the lab, kept refrigerated, spiked with congeners #14 and #166, and extracted as above.

Water samples were also taken for processing by a standard filtration/solid adsorption method³⁴ for comparison purposes. Samples of 17-L water were pressure-filtered (with nitrogen) from a stainless-steel container through a 293-mm ashed (450°C) glass-fiber filter (Type GC50, Micro Filtration Systems, Dublin, CA) and passed through a resin cartridge containing precleaned XAD-2 resin at flow rates of approximately 170 mL (4.5 bed volumes) per min. Resin samples were extracted with 60:40 acetone–hexane, reextracted with additional hexane in a separatory funnel, and concentrated to approximately 1.0 mL in hexane.

Field extracts were cleaned up on 60/100 mesh Florisil following the method

of Norstrom et al.,³⁵ reduced in hexane and transferred to *iso*-octane, spiked with congeners #30 and #204 as internal standards, made to 1.0 mL, and analyzed on an HP 5890 GC. The purge trap extracts were concentrated by nitrogen blowdown to 50 μ L and analyzed similarly. Response factors were obtained using congener mole fraction data from Mullin.³⁶

RESULTS AND DISCUSSION

Experimental Studies

Results of a HLC determination experiment for four congeners are shown in Figure 1.1, in which the cumulative amount of PCB purged is plotted vs time. It is apparent that the data remain on the linear portion of depletion curves for purge times up to 2.5 hr. The slight deviation from nonlinearity for congeners #128 and #153 (actually upward) is mostly due to an anomalously high value for the final run. These relatively straight curves are consistent with observations that the cumulative amounts purged are only a small fraction of the mass initially added to the vessel, and that the aqueous concentrations before and after purging are not significantly different ($p = .05$). Thus, each of the points on the plots represents an independent HLC determination for each congener, and HLCs can be calculated directly as the ratio of gas-phase and aqueous

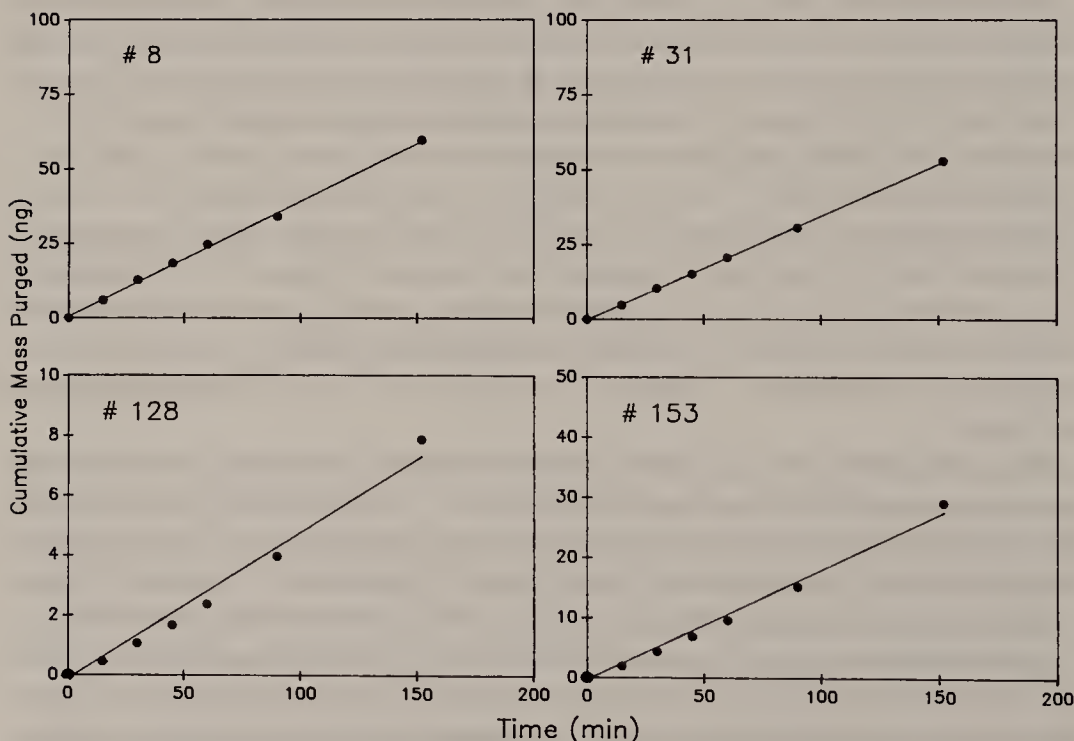


Figure 1.1. Plots of cumulative PCB mass purged vs. time for four PCB congeners in Henry's law constant experiment. Data are for six runs at 19°C.

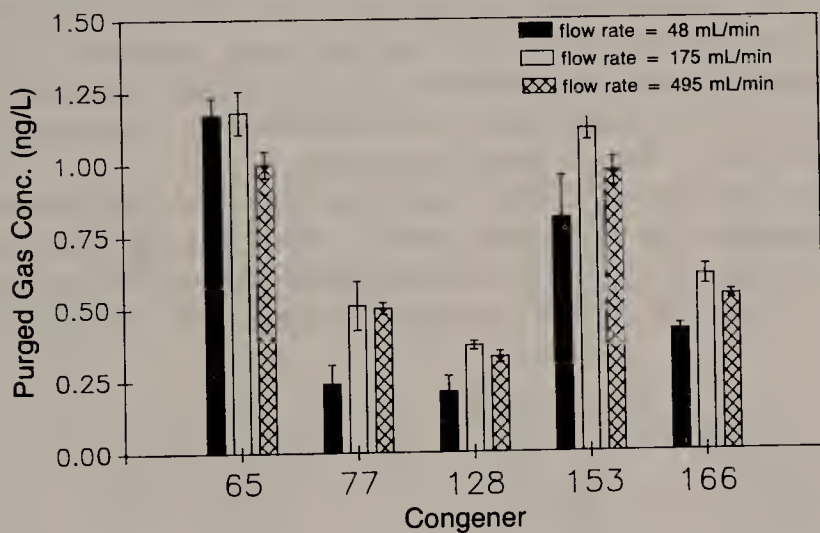
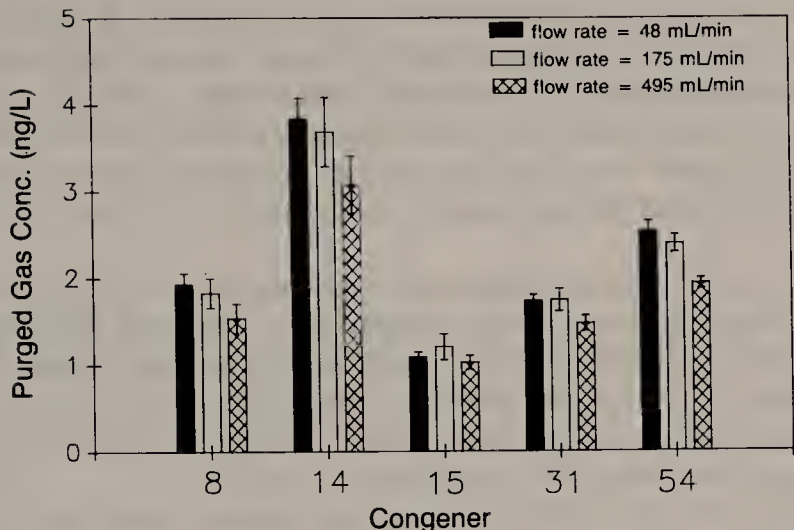


Figure 1.2. Effect of purge air flow rate on air-phase PCB concentrations for two sets of five congeners (25°C). Bars show mean and one standard deviation of three, four, and four runs at flow rates of 48, 175, and 495 mL/min, respectively.

concentrations. Similar curves were obtained for the congeners in the 25°C experiment.

Purged-gas congener concentrations for the 25°C experiment, in which purging was done at three flow rates, are shown in Figure 1.2. For the congeners shown in Figure 1.2a, generally higher concentrations at lower flow rates indicate slightly more efficient transfer to the bubbles, as would be expected. With the exception of the concentrations for congener #54 at the highest flow rate, there are no significant differences ($p = .05$) in concentration between flow rates for the these congeners.

Figure 1.2b shows anomalously low concentrations at the low flow rate for

congeners #77, #128, #153, and #166. It is not apparent why the concentrations for these congeners generally have higher standard errors, and in the case of congeners #128 and #166, are significantly different ($p = .05$) in concentration from those at 175 mL/min. For most congeners studied, however, the results indicate PCB transfer into the rising bubbles is independent of flow rate for the 10-fold range studied, and equilibrium appears to be attained for all 10 congeners.

Figure 1.3 shows aqueous congener concentrations at the surface and bottom of the vessel following 27 hr of purging in a separate experiment. The figure indicates no significant differences ($p = .05$) between surface and depth concentrations for nine of the congeners, and only a slight difference (4 percent) for congener #15. It appears that net transport of PCBs to the top of the solution during the course of purging is not significant.

The HLCs obtained in this study are, in general, consistent with other experimental^{23,37} and predicted³⁸ data, as shown in Table 1.1. Congeners with greater *ortho*-chlorine substitution (e.g., #54) have higher HLCs, and congeners with less *ortho*-chlorine substitution (e.g., #77) have lower HLCs. Although experiments 1 and 2 were conducted using perforated purge tubes, and experiment 3 using glass dispersion tubes (generating more numerous and smaller bubbles), the results indicate the expected trend, with slightly higher HLC values at 25°C than at room temperature.

Agreement with the HLC values of Dunnivant et al.²³ (obtained using a similar technique) and of Murphy et al.³⁷ (obtained using static headspace analysis) is better for the less chlorinated congeners than for congeners #128 and #153. Agreement with the calculated values of Burkhard³⁸ (calculated

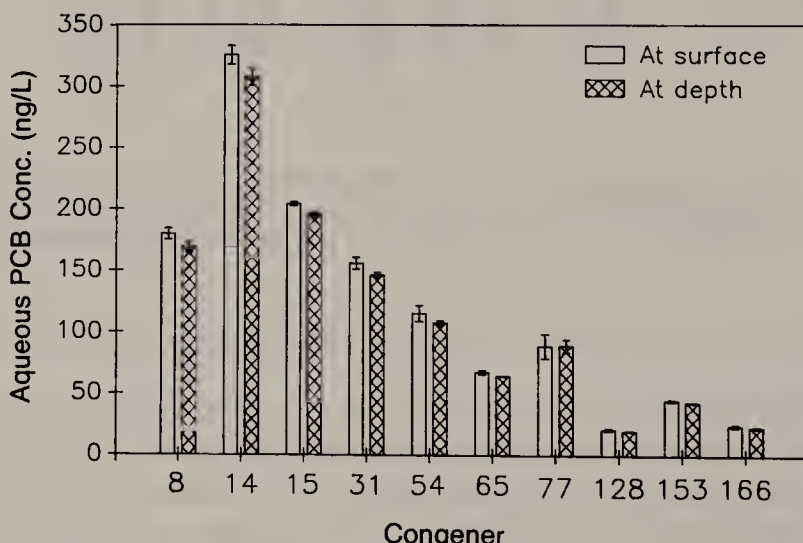


Figure 1.3. Effect of 27 hr of purging on aqueous PCB concentrations at the surface and at depth in the vessel. Bars show mean and one standard deviation of duplicate determinations 1–2 cm below top surface of water and 1–2 cm above water bottom.

Table 1.1. Experimental and Predicted Henry's Law Constants for 10 PCB Congeners

IUPAC #	Congener Name	H (x 10 ⁴ atm m ³ /mol)					
		This Study		Dunnivant et al. ²³		Murphy et al. ³⁷	
		19°C	17°C	25°C	25°C	20°C	25°
8	2,4'-DCB	2.01 (0.32) 1.47 (0.16)		2.59 (0.18)		2.80	2.46
14	3,5-DCB	2.20 (0.38) 1.63 (0.17)		2.83 (0.18)			1.65
15	4,4'-DCB	1.09 (0.18) 0.84 (0.10)		1.21 (0.07)			1.09
31	2,4',5-TCB	1.76 (0.24) 1.34 (0.08)		2.50 (0.10)		2.64	2.51
54	2,2',6,6'-TeCB	3.24 (0.49) 2.65 (0.26)		4.66 (0.27)		5.50	18.60
65	2,3,5,6-TeCB	2.25 (0.32) 1.97 (0.18)		3.46 (0.18)			2.69
77	3,3',4,4'-TeCB	0.35 (0.07) 0.33 (0.06)		0.43 (0.12)		0.94	0.43
128	2,2',3,3',4,4'-HCB	0.72 (0.15) 0.68 (0.15)		1.40 (0.37)		0.30	0.68
153	2,2',4,4',5,5'-HCB	1.59 (0.32) 1.30 (0.21)		2.78 (0.49)		1.32	0.99
166	2,3,4,4',5,6-HCB	1.18 (0.29) 1.06 (0.18)		2.33 (0.12)			2.22

Table 1.2. Estimated and Measured Aqueous Concentrations of Five PCB Congeners in Little Lake Butte des Morts (WI) on 11/30/89

Congener IUPAC #	Aqueous Conc. (pg/L)		Est./Meas.
	Estimated ^a	Measured	
4,10	99	73	1.4
6	181	65	2.8
17	243	233	1.0
18	198	178	1.1
53	33	40	0.8

^aCalculated from measured fugacities and Henry's law constants at 0°C from Burkhard.³⁸

from predicted values for solubility and vapor pressure based on thermodynamic and molecular surface area data) is good for most congeners, with similar patterns of change with chlorination in each data set. Current efforts in this laboratory using Aroclor mixtures are expected to yield HLC data for at least 50 PCB congeners.

Field Study

Field data on PCB aqueous fugacities obtained using gas purging are preliminary and reveal difficulties in analyzing levels near the detection limit. PCB concentrations in the surface water of Little Lake Butte des Morts, Wisconsin (obtained using the standard method) and expected concentrations (calculated based on aqueous fugacities and assuming equilibrium conditions prevailed) are compared in Table 1.2. HLC for 0°C were obtained from Burkhard.³⁸ The ratio of estimated to measured concentrations indicates overestimates by the gas purging method for at least three of the five congeners. Possible explanations for these results include

1. overestimate of the gas purging fraction due to aerosol generation and entrapment and/or uncertainties in working near the detection limit
2. underestimates of the operationally defined dissolved fraction due to breakthrough of colloidal matter past the resin during sampling
3. uncertainties in HLC at 0°C, and thus uncertainties in the predicted aqueous concentrations

Current work in this laboratory is addressing the question of aerosol generation and its effect on fugacity quantification in the field. Landrum and Giesy and others have noted the possibility of breakthrough of neutral hydrophobic compounds past Amberlite resins in the presence of dissolved organic matter.¹⁶ For the samples presented in Table 1.2, over 90% of the dissolved organic carbon passed through the resin column, and colloidal-bound PCBs may not have been retained. Apparently the traditional sampling technique gave a reasonable estimate of the truly dissolved component of PCBs for the surface water sample taken. HLC data obtained using aqueous Aroclor solutions maintained at different temperatures should yield more accurate estimates of aqueous PCB fugacities in the field.

Finally, sampling in more contaminated waters, or sampling with a flow-through technique (in which stripped water is continuously replenished in a floating apparatus), or both, is expected to yield more reliable aqueous fugacity measurements, and thus better determinations of the fugacity gradients for PCBs in natural waters.

CONCLUSION

As found by previous researchers, gas purging is an effective technique for determining Henry's law constants for trace organic compounds. HLCs obtained for 10 PCB congeners ranged from 0.4 to 4.7×10^{-4} atm m³/mol at 25°C and generally followed the trends of data from other experimental and predictive studies. Preliminary studies indicate little dependence of PCB transfer into the gas phase on flow rates over a 10-fold range, indicating equilibrium is maintained in the system. Additional data indicate no net transport of PCBs to the upper region of the solution during purging. Field data are preliminary and indicate the need for improved sensitivity of the gas-purging technique through sampling in highly contaminated waters or using a flow-through system in less-polluted natural waters.

REFERENCES

1. Baker, J. E., and S. J. Eisenreich. "PCBs and PAHs as Tracers of Particulate Dynamics in Large Lakes," *J. Great Lakes Res.* 15:84-103 (1989).
2. Mudroch, A., F. I. Onuska, and L. Kalas. "Distribution of Polychlorinated Biphenyls in Water, Sediment and Biota of Two Harbours," *Chemosphere* 18:2141-2154 (1989).
3. Oliver, B. G., and A. J. Niimi. "Trophodynamic Analysis of Polychlorinated Biphenyl Congeners and Other Chlorinated Hydrocarbons in the Lake Ontario Ecosystem," *Environ. Sci. Technol.* 22:388-397 (1988).
4. Swackhamer, D. L., and D. E. Armstrong. "Distribution and Characterization of PCBs in Lake Michigan Water," *J. Great Lakes Res.* 13:24-36 (1987).
5. Baker, J. E., P. D. Capel, and S. J. Eisenreich. "Influence of Colloids on Sediment-Water Partition Coefficients of Polychlorobiphenyl Congeners in Natural Waters," *Environ. Sci. Technol.* 20:1136-1143 (1986).
6. Capel, P. D., and S. J. Eisenreich. "PCBs in Lake Superior, 1978-1980," *J. Great Lakes Res.* 11:447-461 (1985).
7. Baker, J. E., and S. J. Eisenreich. "Concentrations and Fluxes of Polycyclic Aromatic Hydrocarbons and Polychlorinated Biphenyls Across the Air-Water Interface of Lake Superior," *Environ. Sci. Technol.* 24:342-352 (1990).
8. Duursma, E. K., J. Nieuwenhuize, and J. M. Van Liere. "Polychlorinated Biphenyl Equilibria in an Estuarine System," *Sci. Tot. Environ.* 79:141-155 (1989).
9. Duinker, J. C. "The Role of Small, Low Density Particles on the Partition of Selected PCB Congeners between Water and Suspended Matter (North Sea Area)," *Neth. J. Sea Res.* 20:229-238 (1986).

10. Manchester-Neesvig, J. M., and A. W. Andren. "Seasonal Variation in the Atmospheric Concentration of Polychlorinated Biphenyl Congeners," *Environ. Sci. Technol.* 23:1138-1148 (1989).
11. Duinker, J. C., and F. Bouchertall. "On the Distribution of Atmospheric Polychlorinated Biphenyl Congeners between Vapor Phase, Aerosols, and Rain," *Environ. Sci. Technol.* 23:57-62 (1989).
12. Hermanson, M. H., and R. A. Hites. "Long-Term Measurements of Atmospheric Polychlorinated Biphenyls in the Vicinity of Superfund Dumps," *Environ. Sci. Technol.* 23:1253-1258 (1989).
13. Mackay, D. "Modeling the Long-Term Behavior of an Organic Contaminant in a Large Lake: Application to PCBs in Lake Ontario," *J. Great Lakes Res.* 15:283-297 (1989).
14. Mackay, D., S. Peterson, and W. H. Schroeder. "Model Describing the Rates of Transfer Processes of Organic Chemicals between Atmosphere and Water," *Environ. Sci. Technol.* 20:810-816 (1986).
15. Andren, A. W. "Processes Determining the Flux of PCBs Across Air/Water Interfaces," in *Physical Behavior of PCBs in the Great Lakes*, D. Mackay, S. Paterson, M. S. Simmons, and S. J. Eisenreich, Eds. (Ann Arbor, MI: Ann Arbor Science, 1983), p. 127.
16. Landrum, P. F., and J. P. Giesy. "Anomalous Breakthrough of Benzo(a)pyrene During Concentration with Amberlite XAD-4 Resin from Aqueous Solutions," in *Advances in Identification and Analysis of Organic Pollutants in Water*, Vol. 1, L. H. Keith, Ed. (Ann Arbor, MI: Ann Arbor Science, 1981), p. 345.
17. Fuerstenau, D. W., and T. W. Healy. "Principles of Mineral Flotation," in *Adsorptive Bubble Separation Techniques*, R. Lemlich, Ed. (New York: Academic Press, 1972), p. 91.
18. Mackay, D., W. Y. Shiu, and R. P. Sutherland. "Determination of Air-Water Henry's Law Constants for Hydrophobic Pollutants," *Environ. Sci. Technol.* 13:333-337 (1979).
19. Matter-Muller, C., W. Gujer, and W. Giger. "Transfer of Volatile Substances from Water to the Atmosphere," *Water Res.* 15:1271-1279 (1981).
20. Oliver, B. G. "Desorption of Chlorinated Hydrocarbons from Spiked and Anthropogenically Contaminated Sediments," *Chemosphere* 14:1087-1106 (1985).
21. Hassett, J. P., and E. Milicic. "Determination of Equilibrium and Rate Constants for Binding of a Polychlorinated Biphenyl Congener by Dissolved Humic Substances," *Environ. Sci. Technol.* 19:638-643 (1985).
22. Yin, C., and J. P. Hassett. "Gas-Partitioning Approach for Laboratory and Field Studies of Mirex Fugacity in Water," *Environ. Sci. Technol.* 20:1213-1217 (1986).
23. Dunnivant, F. M., J. T. Coates, and A. W. Elzerman. "Experimentally Determined Henry's Law Constants for 17 Polychlorobiphenyl Congeners," *Environ. Sci. Technol.* 22:448-453 (1988).
24. Servos, M. R., and D. C. G. Muir. "Effect of Suspended Sediment Concentration on the Sediment to Water Partition Coefficient for 1,3,6,8-Tetrachlorodibenzo-p-dioxin," *Environ. Sci. Technol.* 23:1302-1306 (1989).
25. Yin, C., and J. P. Hassett. "Fugacity and Phase Distribution of Mirex in Oswego River and Lake Ontario Waters," *Chemosphere* 19:1289-1296 (1989).
26. Liss, P. S., and P. G. Slater. "Flux of Gases Across the Air-Sea Interface," *Nature* 247:181-184 (1974).
27. Fendinger, N. J., and D. E. Glotfelty. "A Laboratory Method for the Experi-

- tal Determination of Air-Water Henry's Law Constants for Several Pesticides," *Environ. Sci. Technol.* 22:1289-1293 (1988).
- 28. Lemlich, R., Ed. *Adsorptive Bubble Separation Techniques*, (New York: Academic Press, 1972).
 - 29. Valsaraj, K. T. "Binding Constants for Non-Polar Hydrophobic Organics at the Air-Water Interface: Comparison of Experimental and Predicted Values," *Chemosphere* 17:2049-2053 (1988).
 - 30. Blanchard, D. C. "Bubble Scavenging and the Water-to-Air Transfer of Organic Material in the Sea," in *Applied Chemistry at Protein Interfaces*, Symposium—166th Meeting of the American Chemical Society, (Washington, DC: American Chemical Society, 1975), p. 360.
 - 31. Winchester, J. W., and R. A. Duce. "The Air-Water Interface: Particulate Matter Exchange Across the Air-Water Interface," in *Fate of Pollutants in the Air and Water Environments*, Part 1, I. H. Suffet, Ed. (New York: Wiley-Interscience, 1977), p. 27.
 - 32. Coantic, M. "Mass Transfer Across the Ocean-Air Interface: Small Scale Hydrodynamic and Aerodynamic Mechanisms," *Physicochemical Hydrodynamics* 1:249-279 (1980).
 - 33. Leuenberger, C., and J. F. Pankow. "Tenax GC Cartridges in Adsorption/Solvent Extraction of Aqueous Organic Compounds," *Anal. Chem.* 56:2518-2522 (1984).
 - 34. Erickson, M. D. *Analytical Chemistry of PCBs* (Stoneham, MA: Butterworth Publishers, 1986).
 - 35. Norstrom, R. J., M. Simon, D. C. G. Muir, and R. E. Schweinsburg. "Organochlorine Contaminants in Arctic Marine Food Chains: Identification, Geographical Distribution, and Temporal Trends in Polar Bears," *Environ. Sci. Technol.* 22:1063-1071 (1988).
 - 36. Mullin, M. D. "PCB Workshop," U.S. EPA Large Lakes Research Station Workshop, Grosse Ile, MI, June 1985.
 - 37. Murphy, T. J., M. D. Mullin, and J. A. Meyer. "Equilibration of Polychlorinated Biphenyls and Toxaphene with Air and Water," *Environ. Sci. Technol.* 21:155-162 (1987).
 - 38. Burkhard, L. P. "Physical-Chemical Properties of the Polychlorinated Biphenyls: Measurement, Estimation, and Application to Environmental Systems," PhD Thesis, University of Wisconsin, Madison, WI (1984).

CHAPTER 2

Trace Element Cycling in Southern Lake Michigan: Role of Water Column Particle Components

Martin M. Shafer and David E. Armstrong

INTRODUCTION

Interactions with particles play a major role in controlling the concentration and fate of chemical contaminants in aquatic environments. Studies of both oceanic^{1,2} and freshwater^{3,4} systems have demonstrated that the vertical flux of particulate matter is one of the most important natural removal mechanisms for both organic and inorganic contaminants. Comparison of input and/or output fluxes, with contaminant concentrations in the water column, indicates that removal mechanisms must be quite efficient (short residence time). However, significant variations are observed between classes of contaminants, and systems.⁵ Recent work on trace metals points to even shorter residence times than previously indicated, reflecting lowering of many estimates of metal concentrations as "clean" techniques are adopted.⁶

Although the importance of particle-mediated removal of trace elements is well recognized, key questions remain unanswered concerning particle-contaminant specific interactions. Information on the particle types and phases controlling trace element removal in large lakes is limited. Even less clear is how the complex thermal and mixing cycles of lakes interact with particle production and external loading events to regulate trace element concentrations and fluxes over an annual cycle. Answers to these questions are needed to assess the rates of removal and release of specific metals by natural particulate matter and the influence of changes in the types and amounts of particles contributing to the particle flux.

This chapter presents estimates of the impact of specific particle events on the annual sedimentation flux of several trace elements for a 160-m water column in southern Lake Michigan. The approach involved combining data on water column concentrations and fluxes of significant particle components with trace element levels characteristic of the phases or components. Particle-

Table 2.1. Total Mass Flux at 72-m Trap Level

Deployment Interval	Mass Flux ($\text{g m}^{-2} \text{ d}^{-1}$)
April 7 – April 22	4.77
April 22 – May 4	3.04
May 4 – May 17	4.61
May 17 – June 3	3.73
June 3 – June 16	2.12
June 16 – June 30	1.22
June 30 – July 19	0.75
July 19 – Aug. 11	0.34
Aug. 11 – Aug. 30	0.16
Aug. 30 – Sept. 22	0.41
Sept. 22 – Oct. 21	0.63
Oct. 21 – Nov. 17	0.23
Nov. 17 – Dec. 7	0.12
Dec. 7 – March 29 ^a	6.17

^aOverwintering traps

specific elemental residence times, inferred from trace metal concentration data obtained using clean techniques over the course of this investigation, are also presented. The magnitude of specific metal transport vectors are compared with the total metal flux measured by sediment trapping and the burial flux determined from dated sediment cores.

MATERIALS AND METHODS

The station investigated is located at (42° 40' N, 87° 00' W), approximately in the center of the southern basin of Lake Michigan, at a water column depth of 160 m. The location was selected as representative of midlake conditions in the southern basin.

Field Procedures

Sediment Traps

A sediment trap array, moored at this station, was retrieved and redeployed 15 times over the course of the study period (early April 1982 to late March 1983). Deployment intervals, which averaged 3 weeks, are shown in Table 2.1.

Paired traps (3 diameters apart) mounted on epoxy-coated stainless-steel frames were deployed at 8 depths on a 3/4 inch polyester braided line. Traps (upper surface) were located at 4.2, 7.3, 13.0, 20.5, 49.4, 87.7, 116.7, and 131.1 m above the bottom. The upper trap (28.9 m below the water surface) was located below the depth of the summer thermocline. All buoyancy was subsurface; fiberglass spheres at 25 m provided the main support, with additional spheres at 60 m and 120 m. The array was anchored to the bottom with 225- to 450-kg concrete blocks. An acoustic release (Helle Engineering) located between the bottom trap and concrete anchor was used to uncouple the array from the bottom; when triggered, the array would rise to the surface at a rate

of $\sim 10 \text{ m min.}^{-1}$. A 70-kg weight kept tension on the line during ascent and retrieval. Swivels were located in the line at several points to release current-induced horizontal tension.

The cylindrical traps employed were similar in design to those described by Wahlgren and Nelson.⁷ The standard trap utilized had an aspect ratio of 4.0 (16 cm diameter), and an open area of 162 cm² with a baffle, 198 cm² without a baffle. At water velocities of 2.0 and 10.0 cm sec⁻¹ at 4°C, the trap produced Reynolds numbers of 2,070 and 10,400, respectively. The main body of the trap is made of plexiglass; the funnel, of conventional polyethylene; the baffle, of polystyrene; and the collector bottle, of clear polymethylpentene. All trap surfaces were washed in detergent, acid-leached, and thoroughly rinsed before use. Various modifications of the basic trap design were tested against the standard design. Traps with similar diameters, but with aspect ratios of 7.3 and 3.0, were used, as were traps without baffles.

One trap of each pair was poisoned with sodium azide. A vial packed with reagent-grade NaN₃ was placed in the collection bottle before redeployment; when deployed, the poison would slowly be released into the bottle through small holes in the vial.

Trapped particles, including those retained on the trap funnel, were kept at 4°C in the dark for transport to the laboratory for processing. The upper trap water was occasionally sampled, filtered, and chemically analyzed to compare with corresponding lake water samples.

Standing Crop

Standing-crop particulate matter was sampled using two techniques: niskin casts followed by filtration onto Nuclepore filters, and pumping-in-line sieving continuous-flow centrifugation, which enabled the collection of gram quantities of suspended particles.

A 10-L Teflon-coated General Oceanics Go-Flo sampler was used to obtain samples for filtration from 16 points in the water column on each cruise. Two casts from each depth were pooled. A 1-L subsample for total suspended particulate mass measurements was pressure-filtered (30 psi N₂) in an all-Teflon column/filter holder (Savilex) through tared 0.4-μm Nuclepore filters. Filtration was stopped when flow rate dropped below $\sim 10 \text{ mL min.}^{-1}$. Filters were rinsed with 2.0 mL of Milli-Q water, and excess water forced through the filter holder, after which filters were placed in acid-leached plastic petri dishes and immediately frozen. Filtrations were carried out on-board ship within a Class-100 laminar-flow bench. Control filters (one for every three field samples) were processed in a similar manner.

The pumping-in-line sieving continuous-flow centrifugation system consisted of a deck-mounted pumping system coupled to a plastic serial sieving unit, which in turn was coupled to two high-capacity continuous-flow tubular bowl centrifuges (Sharples Model AS-12V). Tubing (1-in. o.d. polyethylene) with a polyethylene-screened, weighted intake structure is let out to the desired

depth, and lake water pumped under vacuum to a deck-mounted platform by peristaltic pumps. The water is then passed through a series of four sieves (508-, 212-, 114-, and 63- μm openings), still under vacuum, before passing through the pump heads and into a tank, which serves as a buffer between the pumping-sieving unit and the centrifuges. From the tank (detention time: ~5 min), a peristaltic pump fed the lake water (now devoid of particles > 63 μm) into two large tubular bowl centrifuges at a rate of 3–5 L min⁻¹ per centrifuge. The centrifuges operated at 15,000 RPM, generating a maximum g force of 13,200 g. All surfaces of the centrifuge that came into contact with lake water were lined with Kynar (polyvinylidene fluoride) to reduce the possibility of contamination. An acid-leached mylar sheet was placed inside the circumference of the centrifuge bowl to enable rapid recovery of trapped particles.

Particles retained on the sieves were processed on-board ship by gently removing particles from the sieves with a stream of filtered lake water into 250-mL LPE bottles. The bottles were subsequently subsampled for optical microscopy, and the remaining solution gently filtered onto tared 5.0- μm Nuclepore filters, rinsed, and immediately frozen. Particles and lake water (4 L), retained in the centrifuge bowl after the self-sealing device isolated the bowl, were recovered and kept at 4°C for transport to the laboratory. Time delay from the collection to laboratory processing varied from 24 to 36 hr. At typical lake water particle concentrations of 1 mg L⁻¹ over 0.5 g of suspended particles could be collected in 1 hr.

Time limitation on station limited the number of depths sampled per cruise to six or seven. The depths chosen were selected to be representative of distinct layers of the water column and also to correspond to depths at which sediment traps were deployed.

Laboratory Procedures

Size Fractionation

Particles collected in the centrifuge (< 63 μm) were further size-fractionated in the laboratory by passage of the suspension through 8-in. diameter plastic sieves with mesh opening of 19 μm and 8.2 μm . The sieves were constructed of polyester mesh (PECAP) sealed to the bottom of 8-in. plexiglass cylinders. Particle loading was kept low (< 15 mg per sieve) to avoid clogging, and filtered centrifuge water was used when needed to aid in the processing. Particles retained on the sieves were washed by centrifugation in Milli-Q water. Subsamples were taken and fixed for optical microscopy, and the remaining suspension transferred to tared plastic vials and frozen. Particles that passed the 8.2- μm sieves—which in most samples was > 40% of the total sample mass—were collected on a variety of tared filter substrates, the type of filter dependent upon the final analytical protocol. For total mass determinations, 1.0-and 0.4- μm Nuclepore filters were employed. Loading on one of the 1.0- μm filters was kept low to estimate the fraction of mass between 0.4–1.0 and

1.0–8.2 μm . Appropriate filter blanks and controls were maintained with each set of samples and batch weighings. These were frozen along with samples. Frozen samples and controls were dried by lyophilization and reweighed on a Perkin-Elmer AD-2 microbalance (filters) or Mettler H51AR analytical balance (vials). After drying, samples were stored at $\sim 10^\circ\text{C}$ in desiccators.

Trap particles were size-fractionated in the laboratory in a manner similar to that described for the standing-crop particles. Four additional meshes, corresponding to those used in the pumping system sieve unit, were used to give complete correspondence with standing-crop size fractions.

In summary, for each trap or standing-crop sampling point, eight particle size fractions were created with nominal cutoffs of 508, 212, 114, 63, 19, 8.2, 1.0, and 0.4 μm . The 600 standing-crop and 1000 trap mass fractions were chemically analyzed for major and trace elemental composition, and particle types identified and enumerated by optical microscopy.

Chemical Analyses

Subsamples (< 20 mg) of standing-crop and trap particulate matter were solubilized by acid digestion in sealed all-Teflon bombs (Bombco, Inc.) in a procedure modified from Eggiman and Betzer.⁸ Use of this type of bomb with Ultrex (Baker) grade acids provides an essentially contaminant-free total digestion with no loss of volatile species. A two-step digestion proved adequate: 2 mL concentrated Ultrex HCl plus 1 mL concentrated Ultrex HNO₃ heated for 2 hr at 95°C in a water bath, followed by addition of 0.1 mL concentrated Ultrex HF and additional heating for 4 hr. Digestates were transferred to acid-leached LPE bottles and diluted to 30.00 mL. National Bureau of Standards river sediment (SRM 1645) and urban particulate matter (SRM 1648), as well as mixed-element liquid spikes, were used to check bomb performance.

Major element analyses of total digestates were performed by inductively coupled plasma emission spectrometry (ICP) (ARL Model 34000), except for Si, which was analyzed colorimetrically.⁹ Trace element analyses of particle digests were performed by graphite furnace atomic absorption (GFAA), as detailed below, except for zinc, where ICP data were used.

Biogenic silicon (BSI) was determined, with minor modifications, by the method of DeMaster.¹⁰ As adapted, the technique involved time course leaching of ≤ 20 -mg samples of particulate matter in 30 mL of 1.0% Na₂CO₃ in a water bath at 85°C. Oak Ridge-type LPE centrifuge tubes were used as reaction vessels. Subsamples were withdrawn at 2, 3.5, and 5 hr, filtered, and Si determined. Solution of nonbiogenic silicon is indicated by increasing Si concentrations with time beyond 2 hr. An equation for $\mu\text{g Si/mg/hr}$ is fit through the three points and used to correct for nonbiogenic silicon contribution. A select set of 15 samples of Lake Michigan suspended particulate matter fractions, each composed entirely of diatoms, was chosen to verify complete solution of BSI in 2 hr. Time course leaching showed, in all cases, slopes not significantly different from zero. Bomb digestions (HF) of splits of these same

samples gave Si values, within experimental error, identical with the carbonate leaching results, therefore documenting complete solution in 2 hr. Silica in leachates was quantified either colorimetrically (Technicon autoanalyzer procedure) or by nitrous oxide flame atomic absorption. Precision of replicate leachings was better than 2.1% at the 20 mg/L level.

Filtrable calcium was measured by a high-precision atomic absorption technique; and filtrable silicon, colorimetrically.⁹ A high-temperature, catalytic combustion technique (Perkin Elmer 240C) was used for particulate organic carbon determinations. Particulate inorganic (carbonate) carbon was measured on the same instrument by CO₂ evolution after treatment of the particles with phosphoric acid.

Total and Filtrable Trace Element Techniques

Samples for trace metal analysis were obtained with a Teflon-coated General Oceanics 10-L Go-Flo sampler on a stainless-steel hydrowire. Before use, the sampler was washed successively with detergent, 10% nitric acid, and Milli-Q water. Immediately upon retrieval, two samples (1 and 0.5 L) were drained from the sampler through a short length of Teflon tubing into linear polyethylene bottles. These samples were processed on-board ship within a Class-100 laminar-flow enclosure.

"Filtrable" metal samples were obtained by pressure filtration (30 psi N₂) of the 1-L subsamples, in an all-Teflon column-filter holder (Savilex), through 0.4-μm Nuclepore filters (47 mm). The Nuclepore filters were tared and pre-leached with 1 N Ultrex nitric acid. "Total" (500-mL subsample) and "filtrable" samples were acidified to pH 1.5 with concentrated Ultrex HNO₃. Metal samples were kept at 4°C for several days before storage at -10°C. Before analysis, the samples were thawed, respike with Ultrex HNO₃, and allowed to equilibrate at 4°C for 2 days. Control samples, which included lake water filtrates and Milli-Q water spiked with a mixed trace metal solution, and Milli-Q bottle blanks were prepared in the field to help put limits on loss and contamination resulting from handling and storage.

Trace metals were quantified by automated graphite furnace atomic absorption techniques (Perkin Elmer Model 400 furnace, 603 spectrometer, and As-40 autosampler). No preconcentration or matrix modification steps were employed. All sample manipulations were performed within a Class-100 laminar-flow bench, which in turn is located—as is the spectrometer—in laboratories with a 0.22 μm filtered air supply. Metal quantification was via standard addition techniques for approximately 50% of the samples. The remainder of the samples were quantified by matrix-matched standard curves, which did not introduce significant error since recoveries were very consistent.

Bottles used for sample storage were linear polyethylene, cleaned by the following sequential procedure: soak in 20% HCl (3 days, room temperature); soak in 20% HNO₃ (3 days, room temperature); rinse 3 times with Milli-Q water; store in 0.5% Ultrex HNO₃ until use; rinse 4 times with Milli-Q water.

Table 2.2. Diatom Major Element Composition

Element	Concentration (mg g ⁻¹)
Calcium	10.1
Potassium	6.74
Aluminum	4.58
Magnesium	2.56

Component Model

Major particle phases are described by application of a component model. The model calculates the weight percentages of major components comprising the total particulate matter pool. The three major components discussed in this chapter are excerpted from a more-detailed, eight-component model, described by Shafer.¹¹ The component model is based on chemical analyses of particle mass fractions, aided in part by optical microscopic techniques.

Major Element Contribution of Plankton

It was necessary in the model first to account for major element contributions of plankton before assigning amounts of these elements to other components. While literature values could have been applied, they would not have been specific to this system; therefore, we felt it best if these contributions were evaluated from data generated in this investigation. Since diatoms dominate plankton populations over much of the year (see model results), we decided to use these algae to evaluate major element contributions. Microscopy and elemental trends were used to select 53 standing-crop mass fractions as representative of pure diatoms. The major element concentrations of these fractions were tabulated, averaged (Table 2.2) and compared with biogenic silica content. Total aluminum, calcium, magnesium, and potassium concentrations in particulate matter were then corrected for the plankton contribution via measured biogenic silica content and the ratios mentioned above.

Biogenic Silica

Measured biogenic silicon mass was converted to biogenic silica by a factor of 2.139 (i.e., SiO₂/Si) and extended to include major elements (Ca, Mg, K, and Al) associated with the diatoms (see above) by including a factor of $1.024 \times 2.139 = 2.190$.

Organic Matter

Organic matter was estimated from organic carbon measurements via a multiplicative factor of 2.08. This factor was derived from the actual data set by selecting mass fractions as outlined above for diatoms, limiting the set to 24 epilimnetic samples only. Biogenic silica and other major element contributions were accounted for, and the remaining mass assumed to be organic matter. The ratio of this mass with measured organic carbon values was used

Table 2.3. Composition of Shale

Constituent	Weight %	mmole g ⁻¹
Si	26.52	9.442
Al	8.11	3.006
Ca	2.60	0.649
K	2.59	0.662
Mg	1.52	0.625
Na	0.56	0.244
CO ₂	3.63	0.826
C	0.90	0.750
Fe	4.18	0.748

to obtain the conversion factor. Only in a few fractions, particularly those dominated by zooplankton, did a factor of 2.08 apparently result in overestimates of organic matter. Analytical precision of the carbon measurements averaged 4.5%.¹²

Shale Model

Input from a shale model was required to evaluate the remaining components. Shale was chosen as the model rock because of the general sedimentological history and environment of the Lake Michigan region and due to a remarkable similarity in chemical composition of both bottom sediments and allochthonous water column particulate matter to average shale. The elemental composition of shales was culled from several sources¹³⁻¹⁶ and averaged to arrive at an average shale composition (Table 2.3). Variation among cited sources was typically small. Either aluminum or nonbiogenic silicon (crystalline Si = total Si - biogenic Si) could have been used as the key tracer (denominator) element. Precision of the aluminum data set exceeded that of the nonbiogenic silicon data; therefore, aluminum was chosen. The model assumes that aluminum is delivered to the lake solely in the form of shale-derived aluminosilicates. In the simplest application of the aluminum-shale model, the measured aluminum concentrations of lake particulates are multiplied by the ratio:

$$\frac{\text{shale total mass (carbonate free)}}{\text{aluminum mass}} = 11.35$$

to give mass of particles of terrigenous shale origin. The basic shale model has been extended to evaluate the contribution of eight major minerals to the allochthonous particulates (for details, see Shafer¹¹).

Calcite

Calcite is estimated from algal-corrected calcium data and model estimates of calcium contribution from noncalcite components. Correction for the algal calcium contribution was discussed above. The eight-component model is used

to estimate the calcium contribution from the only other significant calcium-containing phases, dolomite and anorthite.

Component Settling Rates

Component-specific settling rates were calculated from the ratios of sediment-trap-derived fluxes with the geometric mean of the standing-crop concentrations observed at the beginning and end of the deployment interval. This calculation was performed at each of the eight trap positions. The frequency of sampling was such that the movement of particle fronts through the water column could be followed. Settling rates of major particle species were also derived from the movement of particle fronts.

RESULTS

Component Concentrations and Fluxes

Calcite

Standing-crop concentrations (mg m^{-3}) and sediment trap fluxes ($\text{mg m}^{-2} \text{ d}^{-1}$) of calcite are shown in Figures 2.1 and 2.2, respectively. The primary sources of calcite are allochthonous phases, “old” autochthonous particles, and newly formed autochthonous precipitates. Isothermal mixing maintains a relatively uniform concentration ($\sim 40\text{--}50 \text{ mg m}^{-3}$) throughout the March–June period. Apparent fluxes during this period are high and do not reflect net sedimentation. Allochthonous and autochthonous particles from the previous year’s precipitation event make up the calcite pool. About 70–75% of total standing-crop calcium is found in the $8.2\text{--}0.4 \mu\text{m}$ size fraction. Epilimnetic calcite concentrations drop rapidly upon thermal stratification to levels approaching 5 mg m^{-3} ; fluxes also drop precipitously to around $5\text{--}7 \text{ mg m}^{-2} \text{ d}^{-1}$ in the upper water column. Some resupply of calcium to the epilimnion via atmospheric deposition is noted during the late June to early August period.

Autochthonous (precipitated) calcite totally dominates the late-summer–fall water column. Epilimnetic concentrations increase nearly 20-fold, from less than 50 to over 800 mg m^{-3} ; fluxes show a comparable increase, to over $700 \text{ mg m}^{-2} \text{ d}^{-1}$. Calcite concentrations in standing-crop particles exceed 70%, while concentrations of over 80% are reached in trapped particles. Active precipitation ceases by mid-September, and calcite settles from the water column at a rate of $\sim 2 \text{ m d}^{-1}$. Over 95% of autochthonous calcite is found in the $8.2\text{--}0.4 \mu\text{m}$ size fraction. Water column particles remain enriched in calcite (30–40%) until at least late November, just before fall turnover. Resuspension is evident both in standing-crop and flux diagrams from mid-August until turnover. The annual primary flux of calcite to the sediment surface (resuspension corrected) amounts to $33.9 \pm 3.1 \text{ g m}^{-2}$ (Table 2.4, Table 2.6), of

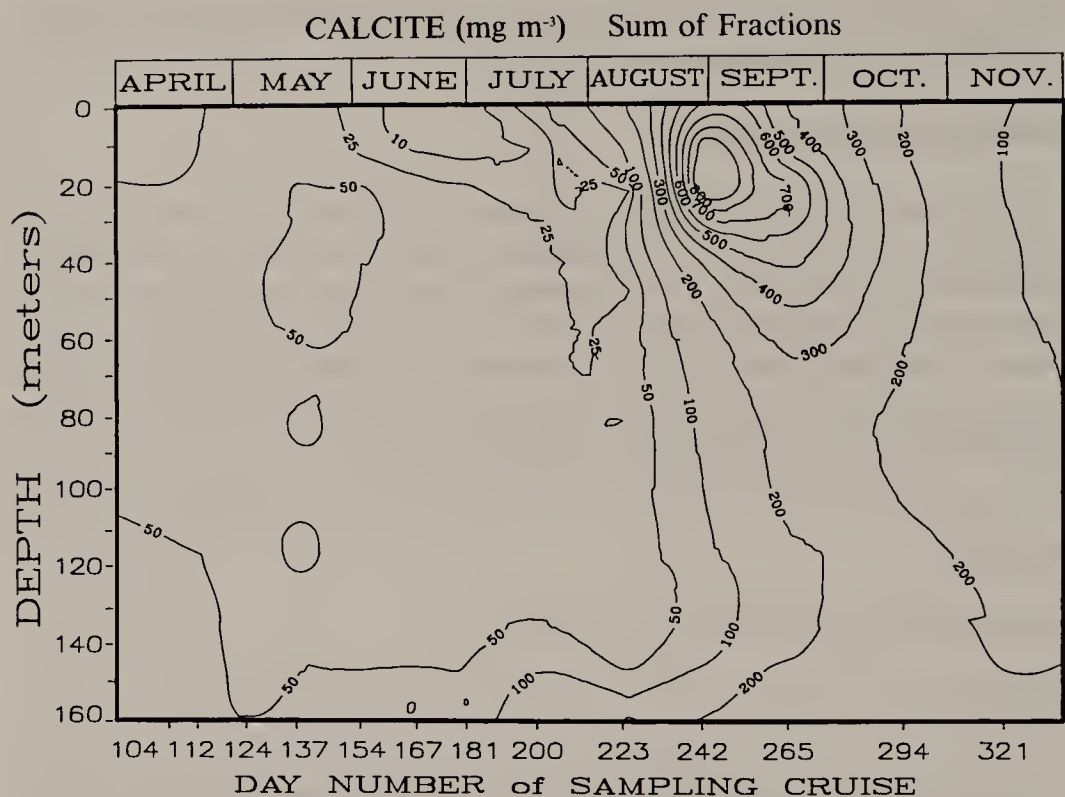


Figure 2.1. Calcite component plot, sum of size fractions: isopleth of standing-crop calcite concentration, mg m^{-3}

which 26.5 g m^{-2} represents freshly precipitated calcite. An examination of total calcite flux as a function of depth indicates that about 25% of total estimated production dissolves in the upper 100 m of the water column. Between 100 and 160 m, little change in calcite flux is noted.

Biogenic Silica

The dominant source of biogenic silica (BSI) to the water column is diatoms, with the primary input via the spring bloom (Figures 2.3 and 2.4). Smaller, but not insignificant, inputs also occur from overwintering species and resuspension of BSI produced in previous years. The spring bloom (dominated by *Melosira* species) raises water column BSI levels from less than 200 mg m^{-3} in early April to over 500 mg m^{-3} in mid-June. Water column mixing maintains nearly vertical profiles. Trap fluxes which would have otherwise declined (less mixing) over this period remain uniform due to this massive input of particles.

The bloom raises the biogenic silica content of standing-crop particles from less than 40% to over 60% in late June. Biogenic silica represents over 65% of the particle mass in mid-July trap collections. A secondary pulse of diatoms (predominantly *Fragilaria*) in late June to mid-July maintains high biogenic silica concentrations and fluxes until late August. Mid water column fluxes

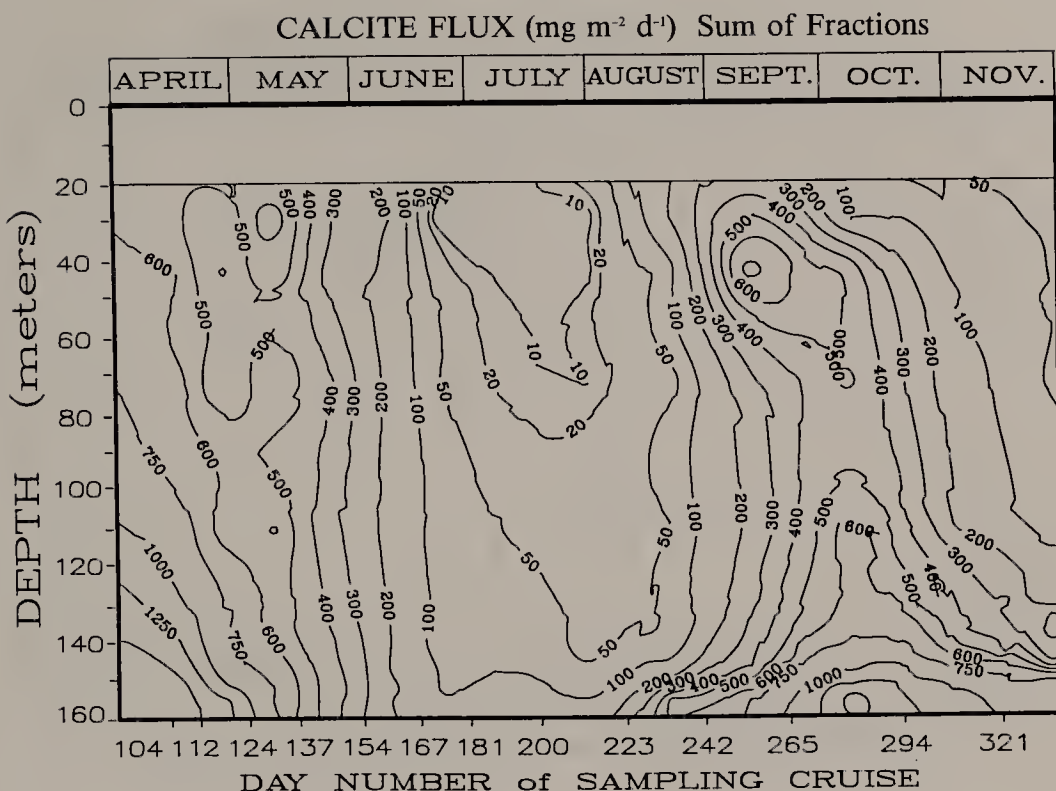


Figure 2.2. Calcite component plot, sum of size fractions: isopleth of calcite mass flux, $\text{mg m}^{-2} \text{ d}^{-1}$

over the stratified period range from 100 to over $700 \text{ mg m}^{-2} \text{ d}^{-1}$. Concentrations drop to 50–75 mg m^{-3} throughout the water column by mid-September, as does the biogenic silica content of particles, primarily as a result of dilution by calcite. Settling rates during the June–August period are typically in the range of 1.0 to 1.5 m d^{-1} . Total production estimates based on filtrable Si loss and

Table 2.4. Annual Flux of Model Components to the Sediment Surface

Component	Total Deposition (g m^{-2})
Diatoms	105.6 ± 7.4
Calcite (autochthonous)	30.4 ± 2.9
Σ Terrigenous	33.2 ± 5.8
Organic matter (not associated with 3 major components)	4.8 ± 0.5
Fecal pellets ^a	5 ± 2
Total Mass Flux	174.0 ± 16

Note: Corrections for mixed period net flux have been applied.

^aNot measured directly. Mass flux accounted for in other components.

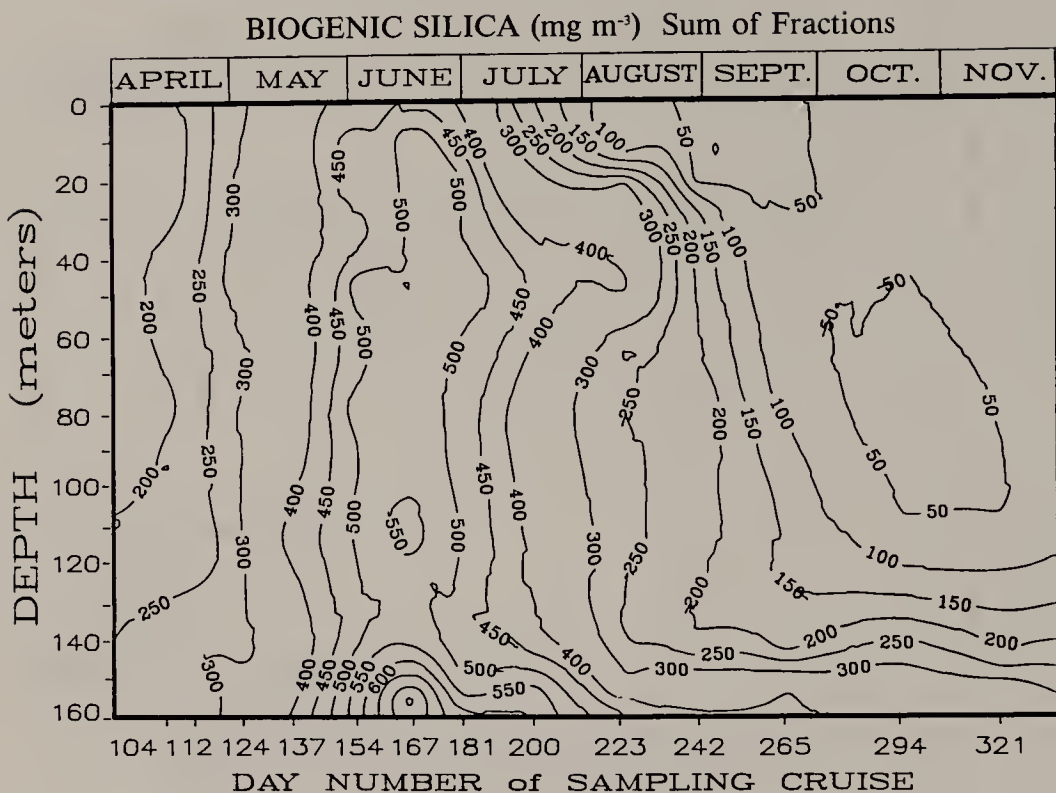


Figure 2.3. Biogenic silica component plot, sum of size fractions: isopleth of standing-crop BSI concentration, mg m^{-3}

biogenic silica particle profile development converge in the range of 85–90 g m^{-2} . Hypolimnetic (above 130 m) profiles of soluble silica over the stratified period show only small changes that could be attributed to water column silica dissolution (~2.5% of total production). Based on sediment trap work, Schelske et al. also found that little dissolution of silica occurs in the water column.¹⁷ Dissolution of biogenic silica occurs primarily in the nepheloid region, at or near the sediment surface.

The spring diatom bloom also nearly doubles the water column burden of organic matter. Diatom sedimentation also serves as the primary vector of organic matter delivery to the sediment surface. Using the carbon content of diatoms sedimenting into the nepheloid region, we estimate that 83% of annual organic matter deposition is associated with diatoms.

The annual primary flux of biogenic silica to the sediment surface (resuspension corrected) amounts to $84.5 \pm 5.8 \text{ g m}^{-2}$ (Table 2.6), more than double the next largest component. Schelske¹⁸ estimated a total annual biogenic silica flux of 85 g m^{-2} .

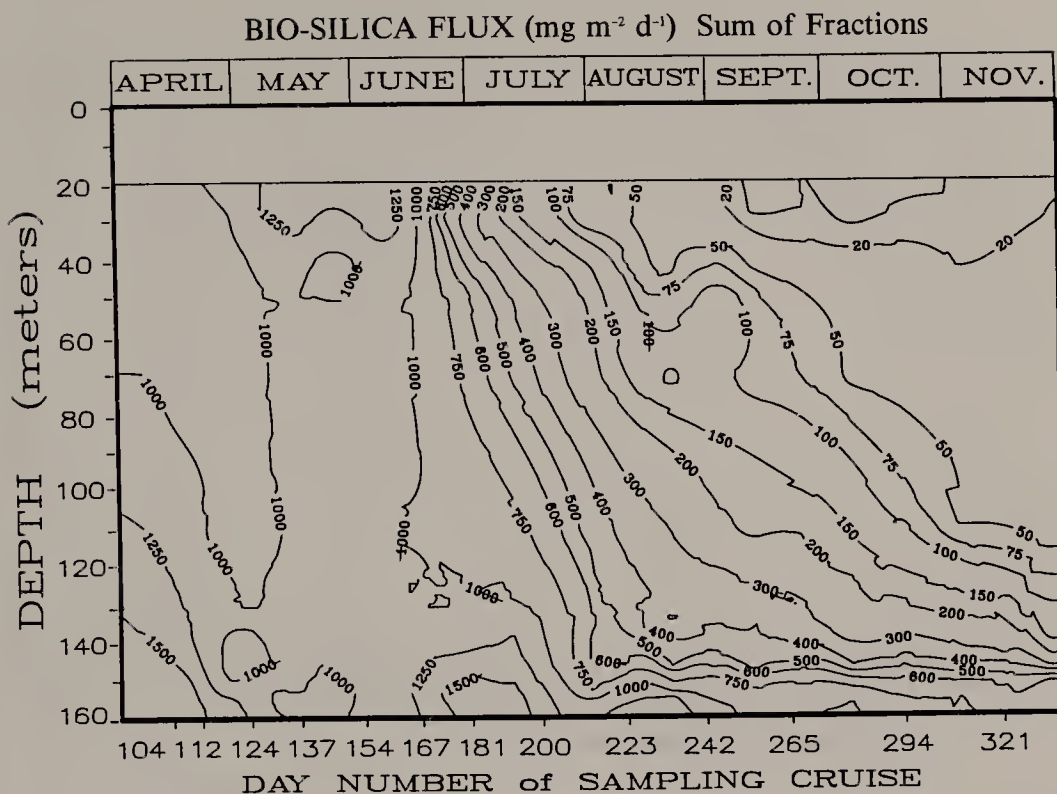


Figure 2.4. Biogenic silica component plot, sum of size fractions: isopleth of BSI mass flux, $\text{mg m}^{-2} \text{d}^{-1}$.

Allochthonous Components

The remaining components are allochthonous in origin, although a fraction of the dolomite may coprecipitate during calcite precipitation. Given their common origins, patterns of concentration and flux observed in the isopleths are very similar (Figures 2.5 and 2.6, Table 2.5). Dominant features include a relatively constant and uniform top-to-bottom standing-crop concentration distribution, resulting from spring isothermal mixing; a prominent and progressively developing nepheloid layer (resuspension), initiated at the time of mid-stratification; and very low upper water column concentrations from mid-

Table 2.5. Annual Flux of Model Allochthonous Components to the Sediment Surface

Component	Total Deposition (g m^{-2})
Clay	11.3 ± 1.7
Feldspar	4.09 ± 0.61
Quartz	7.57 ± 1.30
Iron oxide	1.70 ± 0.26
Calcite	3.53 ± 3.1
Dolomite	5.01 ± 0.66

Note: Corrections for mixed period net flux have been applied.

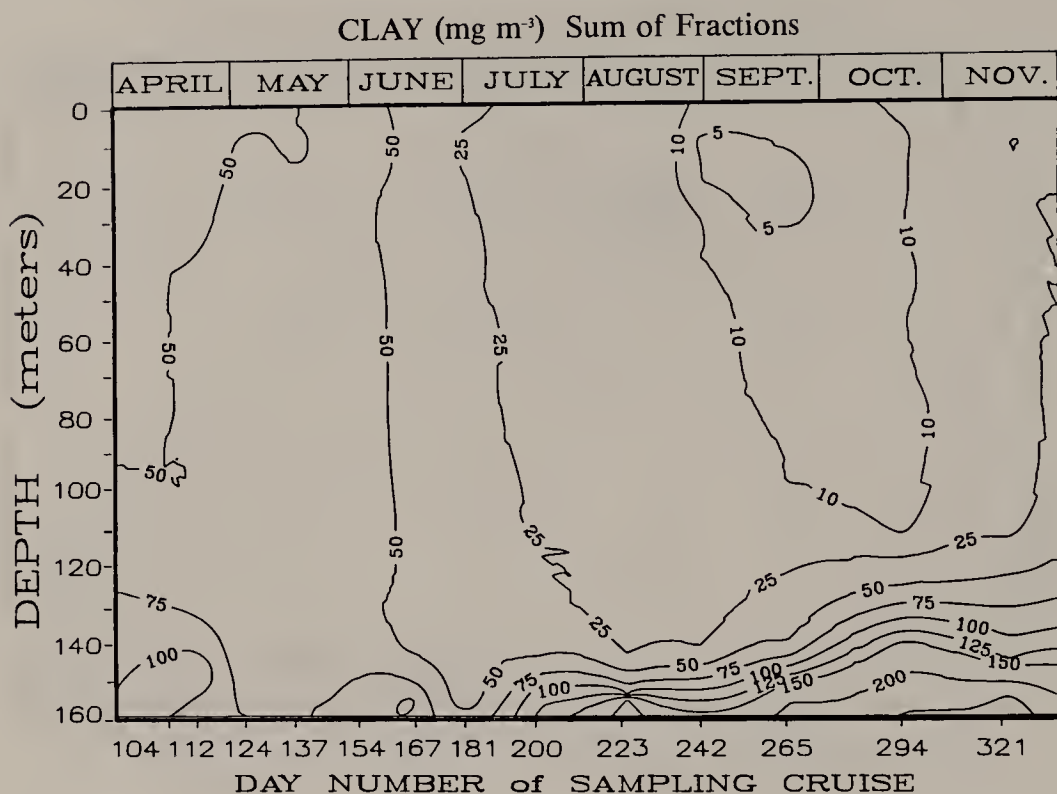


Figure 2.5. Clay component plot, sum of size fractions: isopleth of standing-crop clay concentration, mg m^{-3}

summer through early October. Resuspension, thermocline erosion, and fall storms introduce these components back into the upper water column beginning in mid-October.

Concentrations of clay and quartz in the upper water column drop to less than 5 mg m^{-3} , and those of feldspar and iron oxide to less than 2 mg m^{-3} , during August and September (Figure 2.5). Component fluxes drop in a corresponding fashion (Figure 2.6). Feldspar and clay settling rates were similar and generally higher than other components. Settling rates of all terrigenous components increased by almost a factor of two from August to October, reflecting scavenging by CaCO_3 .

Nepheloid-layer terrigenous component concentrations may be 20-fold greater than those in the upper water column (Figure 2.5). The differences in flux levels were even greater: increases of 50-to 150-fold were not uncommon (Figure 2.6). Significant resuspension of each of the components occurred up to 40 m off the bottom in late fall. The annual primary fluxes (resuspension corrected) of the allochthonous components to the sediment surface are given in Table 2.5. Assuming a bulk density of 1.05 g cm^{-3} and a dry weight fraction of 0.1 for the surface sediment floc, only 0.38 mm of sediment could supply the maximum observed water column burden of allochthonous phases, approximately half of average annual sedimentation at this location.

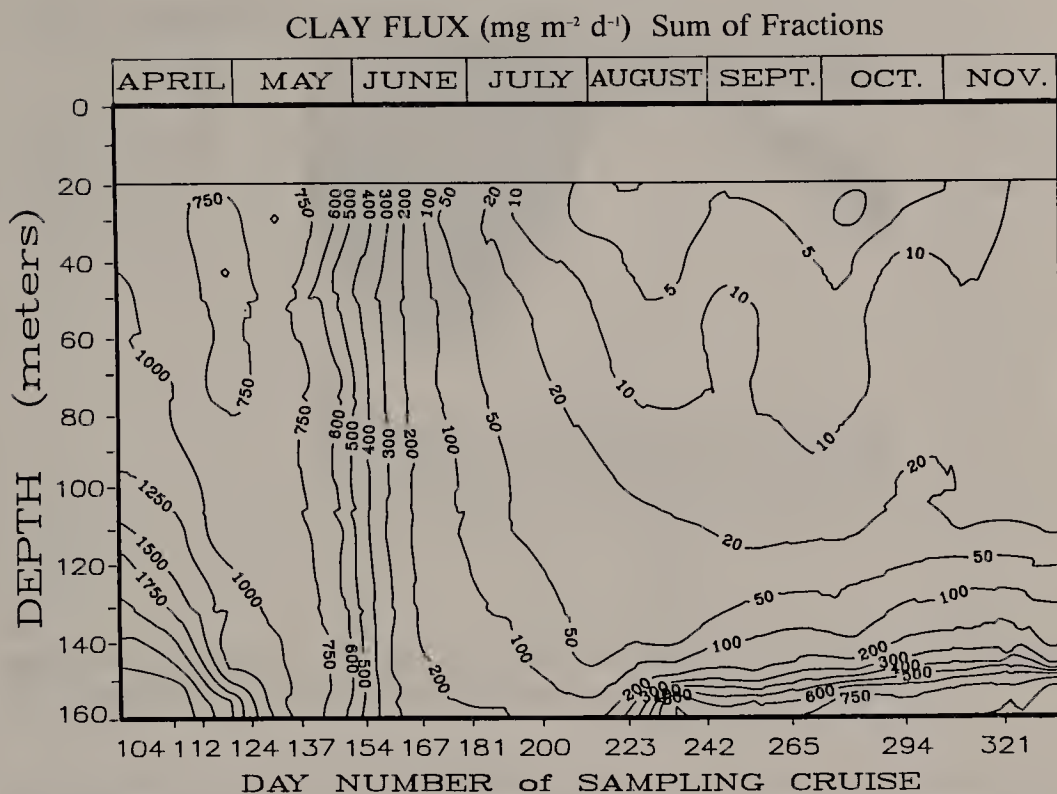


Figure 2.6. Clay component plot, sum of size fractions: isopleth of clay mass flux, $\text{mg m}^{-2} \text{ d}^{-1}$

Component Flux Summary

Component fluxes reaching the sediment surface as a function of time are summarized in Figure 2.7. Fluxes included an estimate for net sedimentation during the winter and early spring isothermal period, extending from mid-December through June 3. This period is characterized by high rates of water column mixing, which invalidates sediment trap use for net flux estimation. Levels of terrigenous components in the standing-crop were nearly constant over this period, suggesting a pseudo-steady state, i.e., little or no net flux. We have no independent way to estimate terrigenous component net flux during the isothermal season. However, comparison of integral filtrable silica loss with integral particulate biogenic silica gain on a cruise-by-cruise basis (2-week intervals) over the early April to June 3 period revealed a net loss of 2260 mg m^{-2} of Si, or 10.0% of estimated total production. Assuming that this percentage also applies to other components and using mean mixed-period standing-crop concentrations as an estimator of production, annual component fluxes can be corrected to include net loss during the mixed period. These estimates are shown in Table 2.6.

For the terrigenous components, mixed-period deposition accounts for

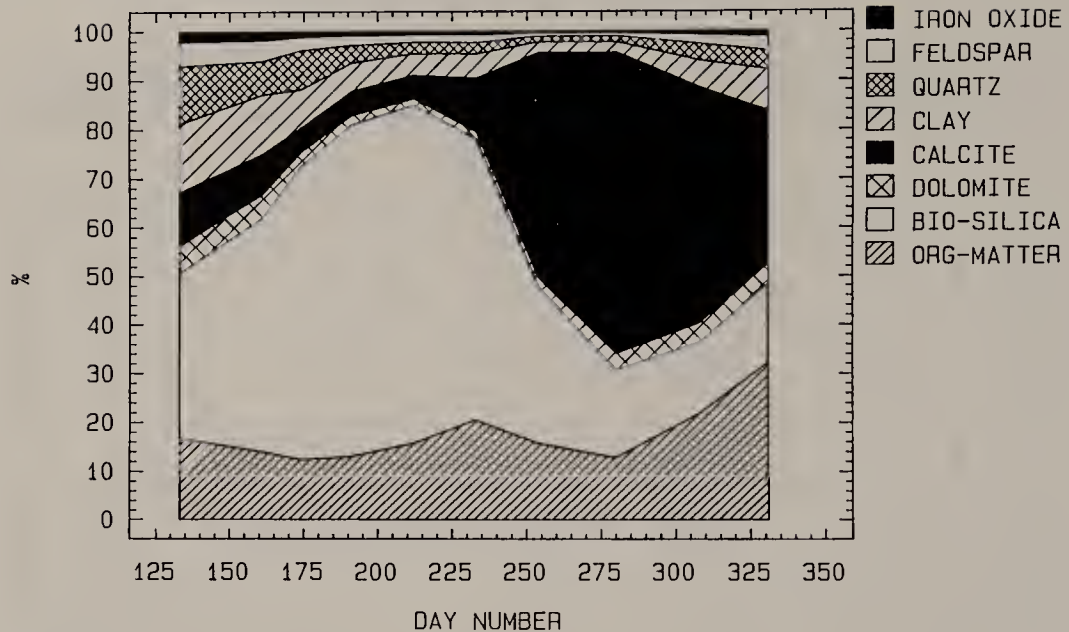


Figure 2.7. Sediment trap component summary, sum of size fractions: component breakdown of flux reaching sediment surface, percent of total mass flux.

8–11% of total annual flux. Lower percentages are seen for autochthonous components, whose major production and deposition occurs later in the year.

Total annual component fluxes are summarized in Table 2.4. Primary total mass flux amounts to $174.0 \text{ g m}^{-2} \text{ yr}^{-1}$, of which 26.5 g m^{-2} (15% of total) represents autochthonous calcite, and 105.6 g m^{-2} (61% of total) can be accounted for by diatoms (given a 20% mass contribution from organic matter). Total allochthonous flux amounts to 33.2 g m^{-2} (19% of total).

Table 2.6. Deposition During Mixed and Stratified Periods (Annual Flux)

	Mixed-Period Deposition (g m^{-2})	Stratified-Period Deposition (g m^{-2})	Total Deposition (g m^{-2})	Mixed Period (%)
Clay	0.93 ± 0.11	10.4 ± 1.7	11.3 ± 1.7	9.0
Feldspar	0.34 ± 0.037	3.75 ± 0.60	4.09 ± 0.61	9.0
Quartz	0.78 ± 0.093	6.79 ± 1.29	7.57 ± 1.30	11.0
Iron oxide	0.14 ± 0.015	1.56 ± 0.25	1.70 ± 0.26	9.0
Calcite	0.73 ± 0.058	33.2 ± 3.1	33.9 ± 3.1	2.2
Dolomite	0.37 ± 0.028	4.64 ± 0.65	5.01 ± 0.66	8.0
Organic matter	1.11 ± 0.079	24.8 ± 1.9	25.9 ± 1.9	4.5
Biogenic silica	2.26 ± 0.15	82.2 ± 5.8	84.5 ± 5.8	2.7

Note: Correction for mixed period net flux applied.

Table 2.7. Trace Element Concentrations ($\mu\text{g g}^{-1}$)

Metal	In Model Particulate Components		
	Diatoms	Calcite	Terrigenous
Cadmium	2.1 \pm 0.4	2.5 \pm 0.3	0.3
Chromium	41 \pm 7	95 \pm 13	95
Copper	54 \pm 6	39 \pm 4	51
Lead	63 \pm 11	32 \pm 6	20
Zinc	250 \pm 40	105 \pm 9	88

Metal	In Other Compartments		
	Recent Sediment ^a	Pre-Indust. Sediment ^b	Zooplankton ^c
Cadmium	1.1	0.5–0.7	2.8
Chromium	83	30–45	27
Copper	39	15–25	18
Lead	88	8–10	93
Zinc	198	40–50	142

^aCahill.¹⁹^bMudroch et al.³⁴^cThis study.

Trace Metal Content of Components

Trace metal concentrations in diatom and calcite components were estimated from particle mass fractions essentially clean with respect to either component (Table 2.7). Purity was verified by chemical analysis (component model) and optical microscopy. Ten representative particle fractions were chosen for each component, and trace element concentrations of the fractions averaged.

Trace element concentrations in the terrigenous component (Table 2.7) were estimated from data on trace element composition of shales, obtained from the same sources utilized for shale major element composition.^{13,14,16} Since trace element concentrations varied only slightly between sources, values were averaged. Data from elemental analyses of terrigenous-dominated fractions, supporting this approach, will be discussed later. Terrigenous metal fluxes calculated in this manner represent a resistant, probably nonlabile fraction. Direct or indirect surface uptake of metal from the water column by terrigenous components is not accounted for in the component model.

Component-Specific Metal Fluxes

Annual fluxes of the five trace elements associated with the major particle events occurring in the water column are shown in Table 2.8. The particle component fluxes employed were estimated from the component model and represent resuspension-corrected fluxes to the sediment surface, as discussed previously. For comparison, metal accumulation rates in bottom sediment are

Table 2.8. Component-Specific Annual Metal Fluxes (mg m^{-2})

Metal	Diatoms	Calcite	Terrigenous
Cadmium	0.22 (74)	0.066 (22)	0.010 (4)
Chromium	4.21 (43)	2.52 (25)	3.16 (32)
Copper	5.55 (67)	1.03 (12)	1.69 (21)
Lead	6.46 (81)	0.85 (11)	0.66 (8)
Zinc	25.7 (82)	2.78 (9)	2.92 (9)
Metal	Total Model Flux ^a	Recent Bottom Sediment Flux	Regeneration (%)
Cadmium	0.30	0.077	74
Chromium	9.9	5.8	41
Copper	8.3	2.7	67
Lead	8.0	6.2	23
Zinc	31.0	13.9	55

Note: Figures in parentheses are percents of total model flux.

^aTotal = Diatoms + Calcite + Terrigenous

also shown. Fluxes were calculated from average trace metal levels of recent bottom sediment¹⁹ and an average sedimentation rate of 70 g/m² year for southern basin sediments.²⁰

Diatoms are the dominant vector of trace metal supply to the surface sediment, transferring 82% of Zn, 81% of Pb, 74% of Cd, 67% of Cu, and 43% of Cr total annual flux. Calcite is a significant vector for Cd (22%) and Cr (25%), and terrigenous phases play a major role in Cr (32%) and Cu (21%) deposition. These values assume no selective loss of metal if partial dissolution of a carrier particle occurs in the water column.

In all cases, the combined influence of the component fluxes is more than sufficient to account for sediment-based metal fluxes. In fact, except for chromium, diatom deposition alone could account for the sediment metal flux. Calcite deposition could supply the sediment flux of cadmium, but not of the other metals. A large fraction of the sediment chromium and copper accumulation could be supplied by the terrigenous flux alone. Estimates of "long-term" recycling range from 23% for lead, to 74% for cadmium, with a mean of 52% for all metals. The recycled percentage for lead would be greater (61%) if the measured trap flux is used instead of model flux (see discussion). These values are higher than the 20% (average of four metals) reported by Sigg in Lake Constance.²¹ In comparison, 60% of total mass flux is regenerated, mostly from dissolution of diatoms and calcite, phases which account for most of the metal flux. Therefore, significant reassociation of metals with other phases must occur before burial.

Metal Residence/Removal Times for Various Depositional Processes

Data on filtrable trace element concentrations in southern Lake Michigan were also obtained. "Clean" sampling and analysis techniques were employed wherever possible. Mean (~180 data points per element) trace element concentrations observed at the 160-m station are summarized in Table 2.9. Based on

Table 2.9. Mean Filtrable Trace Element Concentrations Observed at the 160-m Station

Metal	$\mu\text{g/L}$	nM	$\text{mg m}^{-2\text{a}}$
Cadmium	0.019 \pm 0.006	0.17	2.99
Chromium	0.58 \pm 0.011	11.2	92.8
Copper	0.62 \pm 0.086	9.8	99.2
Lead	0.051 \pm 0.022	0.25	8.16
Zinc	0.57 \pm 0.17	8.7	91.2

^a160-m water column.

filtrable metal concentrations and the particulate metal fluxes (above), residence or removal times were calculated (Table 2.10). A comparison is made with residence times calculated from metal accumulation fluxes observed in bottom sediments.

Component-specific residence times of metals range from less than 1 to over 96 years, the range reflecting disparate biogeochemical properties of the elements and magnitude of mass fluxes of vectors. The trend among elements in residence time (component sum) agrees well with that seen in the bottom sediment, but the absolute magnitudes differ, reflecting regeneration at the sediment surface.

DISCUSSION

Component Fluxes

Chemical Phases

The chemical phases outlined in the eight-phase component model have all, except for FeOOH, been identified in the Lake Michigan basin. Other mineral phases have been documented but typically are found in minor quantities, and little additional interpretive value would be gained by attempting to add more mineral phases. All major elements, including Al, Ca, Mg, K, Na, Fe, C, and Si (in two chemical forms) were determined, although K and Na data were not directly utilized in the model. Particularly valuable was the differentiation of Si phases, which enabled the distinction of quartz from other mineral phases and, coupled with total Al data, provided a foundation for the shale model. Whenever possible, conversion factors were derived from the actual database.

Table 2.10. Water Column Residence Time, Various Depositional Processes (Years)

Metal	Diatoms	Calcite	Diatoms + Calcite		
			160-m Water Column	80-m Water Column	Bottom Sediment 80-m Water Column
Cadmium	14	45	11	5.3	20
Chromium	22	37	14	6.9	8.0
Copper	18	96	15	7.6	18
Lead	1.3	9.6	1.1	0.56	0.66
Zinc	3.6	33	3.2	1.6	3.3

Table 2.11. Model Analysis of Lake Michigan Particulates: Mass Accounting of Size Fractions

Size Fraction (μm)	Mean (mg g^{-1})	$\pm 1 \sigma$	n
Standing-Crop			
8.2 – 0.4	934.9	40.7	78
19 – 8.2	994.3	66.0	64
63 – 19	973.2	37.8	68
114 – 63	964.4	55.6	48
212 – 114	999.4	61.0	32
508 – 212	993.7	56.1	19
>508	971.0	60.5	11
Bulk	954.1	28.2	78
Sediment Traps			
8.2 – 0.4	1013.1	84.9	84
19 – 8.2	966.5	58.3	37
63 – 19	969.7	54.4	68
114 – 63	978.8	49.2	52
Bulk	1000.8	69.2	84
Sediment Core			
Bulk	961.1	19.9	15

An essentially independent analysis was performed for each component (except clay and feldspar, which are both tied to aluminum). Therefore, in lieu of direct confirmation of all phases with other techniques, the component mass sum is a good measure of model validity. The model is successful (Table 2.11), especially given the wide variation in composition between size fractions and the spatial and temporal variability of the particle system. Over 95% of the standing-crop mass and nearly 100% of sediment trap mass can be modeled.

The shale subset of the model analysis is partially validated by mass

Table 2.12. Model Analysis of Shale Mineralogy

Constituent	Concentration mg g^{-1}
Total feldspars	148.4
Anorthite	45.1
Albite	48.0
Microcline	55.3
Total clays	405.5
Chlorite	54.3
Illite	351.2
Total carbonates	61.9
Calcite	33.1
Dolomite	28.8
Quartz	267.4
Iron excess as FeOOH	58.1
Carbon as organic matter	18.0
Total Mass Accounting	959.3
	(96%)

accounting in Table 2.11. However, greater confirmation is obtained from a component reckoning of shale itself (Table 2.12). In total, 95.9% of shale mass is accounted for. Si, Al, Ca, K, and Mg are entirely reckoned—as is Fe if “excess Fe” is expressed as FeOOH; however, 25% of Na is not accounted for. The dominant phases and associated percentages (35% clay, 27% quartz, and 15% feldspars) are in good general agreement with information on mineralogy of Lake Michigan sediments.²²⁻²⁵

Elemental ratios and, in certain compartments, absolute elemental concentrations of Lake Michigan particulate matter agree remarkably well with published data on shale composition.^{15,26} The absolute concentrations of aluminum and nonbiogenic silicon (quartz and aluminosilicates) in bottom sediment core sections > 8 cm in depth are nearly identical to that of average shale. The nonbiogenic-silicon-to-aluminum ratio in suspended and trapped particulate matter is very similar (3.09 vs 3.14) to mean shale, which is also the case in bottom sediments. Absolute levels of potassium in buried sediment are also in good agreement with mean shale. Typical Lake Michigan sediments contain, in addition to shale components, significant but variable proportions of dolomite and calcite.¹⁹ These facts validate the general phase analysis and support the use of a shale framework for mineral composition of Lake Michigan particulate matter.

Comparison of Sediment Trap and Bottom Sediment Fluxes

Direct comparison of the trap-based fluxes with the component fluxes observed in the sediment core must be approached with caution. Assuming traps collect all particles with nearly 100% efficiency (a good assumption based on results of a trapping efficiency study¹¹), three major factors must be considered before a valid comparison can be made. First, a sedimentation rate for the core is required; second, the extent of bottom sediment focusing must be addressed; and finally, the degree of water column focusing must be estimated. Lead-210 dates on nearby cores, cited by Robbins and Edgington²⁰ and Armstrong and Swackhamer,²⁷ were used to estimate a mass sedimentation rate of 150 g m⁻² yr.⁻¹ A bottom sediment focusing factor of 2.17 was obtained from the ratio of the estimated core sedimentation rate with the basinwide average of 69 g m⁻² yr⁻¹ reported by Robbins and Edgington.²⁰ No data on horizontal distribution of particles and fluxes in the water column are available, so water column focusing is assumed to be negligible.

Comparisons of component flux estimates from traps with those calculated from the sediment core (Table 2.13) show sediment accumulation of terrigenous components is greater than the primary flux to the sediment surface. Allowing for errors in focusing correction and annual water column variability, it is apparent that at least 70% of calcite and 73% of organic matter are lost after deposition. For silica, the loss of 93% agrees well with reported retention values of 3–6%.^{18,28}

If the mass contribution of phases subject to relatively rapid dissolution

Table 2.13. Annual Flux of Model Components to Sediment Surface: Trap and Bottom Sediment Estimates ($\text{g m}^{-2} \text{ yr}^{-1}$)

	Trap	Bottom Sediment	Bottom Sediment/ Trap
Clay	11.3 \pm 1.7	17.4	1.54
Feldspar	4.09 \pm 0.61	6.32	1.54
Quartz	7.57 \pm 1.30	10.1	1.33
Iron oxide	1.70 \pm 0.26	2.64	1.68
Calcite	33.2 \pm 3.1	10.5	0.31
Dolomite	5.01 \pm 0.66	4.93	0.98
Organic matter	25.9 \pm 1.9	6.62	0.26
Biogenic silica	84.5 \pm 5.8	5.97	0.071

Note: Primary mass flux = $174.0 \text{ g m}^{-2} \text{ yr}^{-1}$

Diatoms = $105.6 \text{ g m}^{-2} \text{ yr}^{-1}$

Autochthonous calcite = $26.5 \text{ g m}^{-2} \text{ yr}^{-1}$

Terrigenous = $33.2 \text{ g m}^{-2} \text{ yr}^{-1}$

(i.e., carbonates and biogenic silica) are subtracted from the core, profiles of aluminum and nonbiogenic silicon become nearly constant with depth. Apparently, recent inputs of allochthonous phases to the lake have been relatively constant and, once buried, are stable for decades. The principal geochemical process controlling the bulk mineralogy of the core appears to be dissolution of autochthonous phases. Others have also noted that calcite and dolomite appear to be sensitive indicators of dissolution in Great Lakes sediments.²⁹

Metal Fluxes

Metal Concentrations in Particulate Matter Components

The trace metal contents of the vectors are those representative of natural "pure" phases. Particle fractions were selected to represent times and depths over which a given phase dominated in the water column. Although chemical and microscopic analysis were used to verify particle integrity, secondary chemical associations may also occur. Despite uncertainty about the exact nature of the metal-particle bonding mechanism, these phases are the major vectors of transport through the water column.

Variability in the metal content of "pure" components was relatively small, typically in the range of 10–15%, except for lead, where a higher degree of variability (20%) was found for the same particle group. The lead data may be explained by a greater level of water column scavenging (see below), in comparison with other metals.

Comparison of Component Model and Sediment Trap Fluxes

Model total metal flux estimates (Table 2.8) are compared with measured trap fluxes in Table 2.14. Trap fluxes of metals represent annual estimates calculated by summing all stratified deployment periods (resuspension corrected where necessary), and including a portion of mixed-period flux as described earlier.

Table 2.14. Comparison of Model Metal Flux Estimates with Measured Sediment Trap Metal Fluxes ($\text{mg m}^{-2} \text{ yr}^{-1}$)

Metal	Model ^a	Trap	Model/Trap
Cadmium	0.30	—	—
Chromium	9.9	9.4	1.05
Copper	8.3	7.1	1.16
Lead	8.0	16.2	0.49
Zinc	31	39	0.81

^aTotal flux = Diatoms + Calcite + Terrigenous

The agreement among estimates for chromium, copper, and zinc is good, validating the model approach, and indicating that all major vectors have been taken into account. The agreement also implies that little scavenging of these elements occurs during particle transit through the water column. A large (32%) terrigenous flux component (presumably less labile), coupled with the lithophilic, comparatively weak partitioning characteristics of dominant chromium species, may account for the close agreement (< 5% disparity) between chromium flux estimates. The model copper flux is slightly higher (16%) than the trap estimate, possibly reflecting a loss to the dissolved organic matter pool during particle diagenesis. The affinity of copper species for natural organic matter is well documented.^{30,31} A significant fraction (21%) of the copper flux is, like chromium, associated with terrigenous phases.

The annual zinc flux to the sediment surface, as measured in the sediment traps, is ~20% larger than the model estimate. The micronutrient zinc is accumulated by diatoms to levels 2.5 to 3 times greater than observed in calcite and terrigenous phases. This fact, coupled with the large diatom mass flux component, results in a delivery of a very large fraction (82%) of the total zinc primary flux by diatoms. Small errors in either diatom mass flux estimates or diatom-associated zinc levels could account for the small discrepancy between zinc flux estimates.

The twofold underestimate of lead flux cannot be explained by errors in component mass fluxes or particulate lead concentrations. Lead has the greatest particle affinity of the metals studied,³² and scavenging of dissolved lead by settling particles could account for a significant fraction of total lead flux at this deep station (160 m). Trap data during the stratified period showed increasing concentrations of lead in certain particle fractions as particles settled deeper in the lake, lending credence to the scavenging hypothesis. However, scavenging alone cannot account for the flux difference, since a nearly complete stripping of "dissolved" lead from the 160-m water column and a corresponding compensatory input source is required for the model flux to equal the trap-measured flux. Thus, model errors in concentrations of lead in terrigenous material or selective overtrapping of lead in sediment traps may contribute to the observed difference in flux estimates.

Diatoms are the major vector for metals because their mass flux exceeds other phases by 3-4 times and they accumulate metals to a greater extent than

Table 2.15. Comparison of Model Terrigenous Metal Flux with Preindustrial Metal Flux (mg m⁻² yr⁻¹)

Metal	Preindustrial	Model Terrigenous
Cadmium	0.03 – 0.05	0.010
Chromium	2.1 – 3.5	3.2
Copper	1.1 – 1.9	1.7
Lead	0.5 – 0.7	0.66
Zinc	2.7 – 3.5	2.9

Note: Preindustrial metal flux calculated from deep sediment core metal concentrations.

other components (except for enrichment of chromium in calcite and terrigenous phases). The selective impact of calcite on cadmium transport is consistent with similarities in calcium and cadmium ionic radii and potential for coprecipitation of CdCO_3 with CaCO_3 .³³

Comparison of Terrigenous Component and Preindustrial Sediment Fluxes

Model terrigenous metal fluxes are compared with metal fluxes calculated from preindustrial metal concentrations in deep sediment cores in Table 2.15. Historic (preindustrial) core metal concentrations were taken from Mudroch et al.,³⁴ and as discussed earlier, a focused-corrected sedimentation rate was used to obtain fluxes. A constant sedimentation rate for terrigenous material over the length of the core is assumed, a fact supported by the core component analysis. Agreement for all metals, except cadmium, is very good, indicating that terrigenous inputs could support historic metal accumulation in southern Lake Michigan, and that elevated metal concentrations in upper (recent) sediments result primarily from autochthonous removal mechanisms.

Fecal Pellet Transport of Metals

Fecal pellet production and sedimentation is a potentially significant vector for elemental and contaminant transport in both oceanic³⁵ and lake systems.³⁶ The importance of this flux component to metal transport in open-water Lake Michigan has not been directly quantified, but estimates can be made based on currently available data.

Using data on zooplankton standing stock obtained in this study, a mean annual areal concentration of 3540 mg m^{-2} is calculated. This value, based on particle samples obtained at 2- to 3-week intervals spanning April–December 1982, agrees well with other published estimates.^{37,38} Fecal material produced by cladocerans is loosely aggregated and unlikely to contribute to primary flux at the sediment surface.³⁹ In contrast, copepods pellets are securely enveloped in a peritrophic membrane.³⁹ Copepods represented ~60% of zooplankton biomass over the year. Applying a production-to-biomass ratio of 5:1,⁴⁰ an annual copepod production of 10.6 g m^{-2} is calculated. The fraction of production that reaches the sediment surface is uncertain. However, if all production

Table 2.16. Estimated Flux of Copepod Fecal Pellets to Sediment Surface

Metal	Concentration $\mu\text{g g}^{-1}$ in Pellet	Estimated Flux $\text{mg m}^{-2} \text{ yr}^{-1}$	% of Total Model Flux
Cadmium	2.8	0.014	4.7
Copper	27	0.14	1.7
Chromium	18	0.090	0.9
Lead	93	0.47	5.9
Zinc	142	0.71	2.3

Note: Pellet mass flux = $5 \text{ g m}^{-2} \text{ yr}^{-1}$

is packaged⁴⁰ and the average settling distance before breakup is 60 m,³⁶ an upper bound on pellet mass transport to sediment surface would be in the range of 2 to $4 \text{ g m}^{-2} \text{ yr}^{-1}$.

Ferrante and Parker measured a copepod pellet number flux of $0.9 \text{ cm}^{-2} \text{ day}^{-1}$ at a 100-m station in southern Lake Michigan.³⁶ Annualizing this flux, and using typical pellet dimensions of $40 \times 120 \mu\text{m}$ and density of 1.25 g cm^{-3} ,^{36,41} results in a pellet mass flux of $0.63 \text{ g m}^{-2} \text{ yr}^{-1}$, similar to previous estimates.

It was mentioned previously that ~80% of annual organic carbon flux was associated with diatoms, and only a small percentage (< 10%) of this is packaged in pellets. Assuming that one-half of the remaining (20%) organic carbon flux is delivered to the sediment surface in the form of fecal pellets in mid-summer to early fall, a fecal pellet organic matter flux of $4.5 \text{ g m}^{-2} \text{ yr}^{-1}$ is obtained. If organic matter comprises 50% of diatom-dominated fecal pellets, and 100% of late summer pellets, an annual pellet mass flux of 7.3 g m^{-2} results.

One additional estimate of zooplankton pellet production may be obtained using season-specific community clearance rates for epilimnetic offshore Lake Michigan.⁴² Applying Scavia and Fahnenstiel's carbon-based estimates, an annual carbon flux through zooplankton of between 25 and 30 g C m^{-2} is obtained.⁴² A copepod carbon clearance of 8.1 g m^{-2} is calculated, given a 60% copepod biomass contribution and production/biomass ratios of 5:1 and 20:1 for copepods and cladocerans, respectively.⁴⁰ The 8 g C m^{-2} equates to a pellet mass flux of 20 g m^{-2} using an average 40% carbon content. If 25% of this production were to survive transit, the primary fecal pellet mass flux is about $5 \text{ g m}^{-2} \text{ yr}^{-1}$.

The estimates of fecal pellet flux tend to converge around 5 g m^{-2} a mass flux comparable to some mineral components, but an order of magnitude smaller than major vectors.

Concentrations of the trace elements in whole zooplankters measured over the study period (Table 2.7) are coupled with pellet mass flux to obtain primary metal flux associated with fecal pellets (Table 2.16). For chromium, copper, and zinc, pellet flux is only 1–2% of total metal flux, whereas for cadmium and lead the corresponding value is about 5%. If phytoplankton metal concentrations are applied instead of those for zooplankton, estimates

for cadmium and lead would be reduced slightly, and chromium, copper and zinc percentages would rise to 2–4%. Thus, fecal pellet transport appears to be a minor vector for metal deposition to sediment in this system. However, the impact of pellet transport is greater during mid-to late summer, when pellet production peaks and other vectors are in decline or not yet operative.

Metal Fluxes and Residence Times

Published data on water-column-based metal fluxes for Lake Michigan are few. Parker et al. give estimates of the annual deposition of Zn and Cd in the southern basin of Lake Michigan of 90 mg m^{-2} and 1 mg m^{-2} respectively, about three times higher than estimated here.⁴³ Their estimates were based on short-term uptake experiments in the summer epilimnion and involve assumptions that may not hold true on an annual basis. Eadie et al. estimated, based on stratified-period epilimnetic trap fluxes, that the net annual lead flux to the southern basin sediments was $12 \pm 9 \text{ mg m}^{-2} \text{ yr}^{-1}$,⁴⁴ close to the model estimate of $8.0 \pm 1.5 \text{ mg m}^{-2} \text{ yr}^{-1}$ and measured trap flux of $16.2 \text{ g m}^{-2} \text{ yr}^{-1}$ reported in this study. Most other reports of metal flux were derived from bottom sediment data. Edgington and Robbins, using ^{210}Pb -dated sediment cores, estimated a stable lead flux of $15 \text{ mg m}^{-2} \text{ yr}^{-1}$ for southern Lake Michigan.⁴⁵ Tisue and Fingleton reported a zinc depositional flux, calculated from the ratio of sediment zinc concentrations with published bottom sediment lead values, of $18.3 \text{ mg m}^{-2} \text{ yr}^{-1}$.⁴⁶

The depositional fluxes measured here are compared with reported atmospheric loadings in Table 2.17.^{47,48} A relatively small portion of chromium and copper depositional flux is supported by atmospheric inputs, while the atmospheric input is more than sufficient to supply observed lead depositional flux. The atmospheric input represents ~60% of cadmium and zinc depositional flux, elements with very similar chemical properties. The same trends in significance of atmospheric deposition relative to total metal loadings and sedimentation flux have been noted by Coale and Flegal⁶ and Sigg.²¹

Metal Residence Times and Partitioning

Several recent papers have noted a strong correlation between residence times of metals in aquatic environments and measures of the partitioning characteristics of the metals. Two distinct strategies have been applied:

1. a partition coefficient approach ($K_d = C_p/C_w$), e.g., Morel and Hudson,⁴⁹ using published oceanic water column, sediment, and crustal metal data
2. a more mechanistic correlative approach, where a chemical property which influences partitioning behavior is employed, e.g., Whitfield and Turner, who correlated degree of hydrolysis with residence time⁵⁰

An integrated estimator of particle affinity available directly from our field data is the partition coefficient, K_d . Partition coefficients with respect to five particle phases are given in Table 2.18. These data are comparable in magni-

Table 2.17. Comparison of Annual Deposition of Metals to Sediment Surface (Model Estimates) with Whole Lake Averaged Atmospheric Loading (mg m^{-2})

	Atmospheric Loading		Particle Flux
	Eisenreich ⁴⁷	Schmidt and Andren ⁴⁸	This Study
Cadmium	0.19	—	0.30
Chromium	—	1.67	9.9
Copper	2.07	3.97	8.3
Lead	11.0	11.0	8.0
Zinc	19.1	—	31

tude to those given by Sigg for Lake Constance and Lake Zurich, one of the few reports of values for freshwaters.⁵ The K_d 's given by Sigg represent average bulk settling particles (sediment trapped), possibly accounting for the slightly lower values than obtained for Lake Michigan speciated standing-crop particles. Bulk trapped particles contain a seasonally variable fraction of particles with low sorption capacity (allochthonous minerals) and may be biased toward larger particles. Both factors would lower K_d 's in comparison with the Lake Michigan data presented here. Filtrable trace element concentrations are similar for Lake Michigan and Lake Constance.

Metal residence time in the water column should be inversely related to the tendency of the metal to associate with particulate phases. Mass sedimentation rate also affects total metal residence time and must be considered when comparing systems. Regression analysis shows a good relationship between relative residence time (i.e., τ_m/τ_w) and K_d (diatoms); K_d accounts for 96.4% of the variation in basin residence time (Figure 2.8). Diatoms were chosen because they are the principal autochthonous removal vector (see Table 2.4). The relationship is further improved by including autochthonous calcite via a multiple linear regression model (Figure 2.9); nearly 99% of the variation in residence time is modeled. Thus, the partition coefficient approach can be used for residence time prediction and frames the mechanistic interpretation of removal in terms of sorption to the two major autochthonous particle phases.

Lead, the metal with the greatest particle affinity, has the shortest southern basin residence time, only 0.3–0.6 years. Coale and Flegal, comparing atmospheric fluxes and surface water concentrations, reported an epilimnetic residence time of about 1 week for lead in Lake Ontario.⁶ The basin residence time reported here corresponds to an epilimnetic residence time of about 1 month.

Table 2.18. Trace Element Partition Coefficients (L Kg^{-1})

Metal	Diatoms	Calcite	Terrigenous	Recent Bottom Sediment	Zooplankton
Cadmium	1.1×10^5	1.3×10^5	1.6×10^4	5.8×10^4	1.5×10^5
Chromium	7.1×10^4	1.6×10^5	1.6×10^5	1.4×10^5	4.7×10^4
Copper	8.7×10^4	6.3×10^4	8.2×10^4	6.3×10^4	2.9×10^4
Lead	1.2×10^6	6.3×10^5	3.9×10^5	1.7×10^6	1.8×10^6
Zinc	4.4×10^5	1.8×10^5	1.5×10^5	3.5×10^5	2.5×10^5

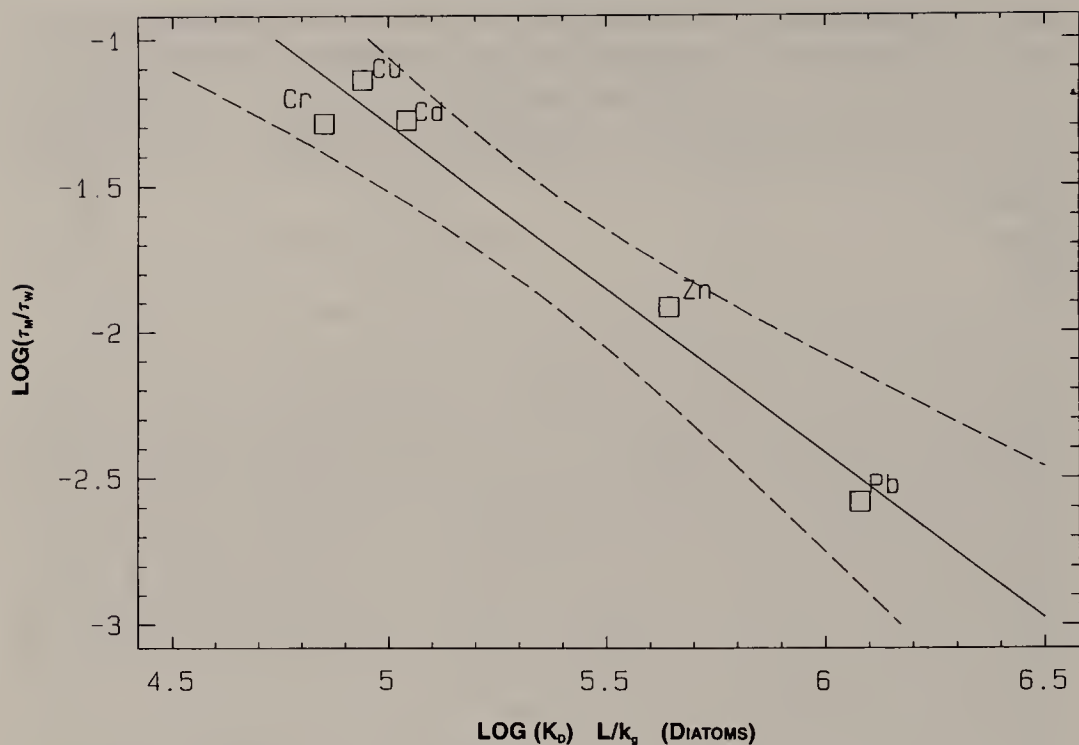


Figure 2.8. Regression of relative residence time of metals on partition coefficient with respect to diatoms.

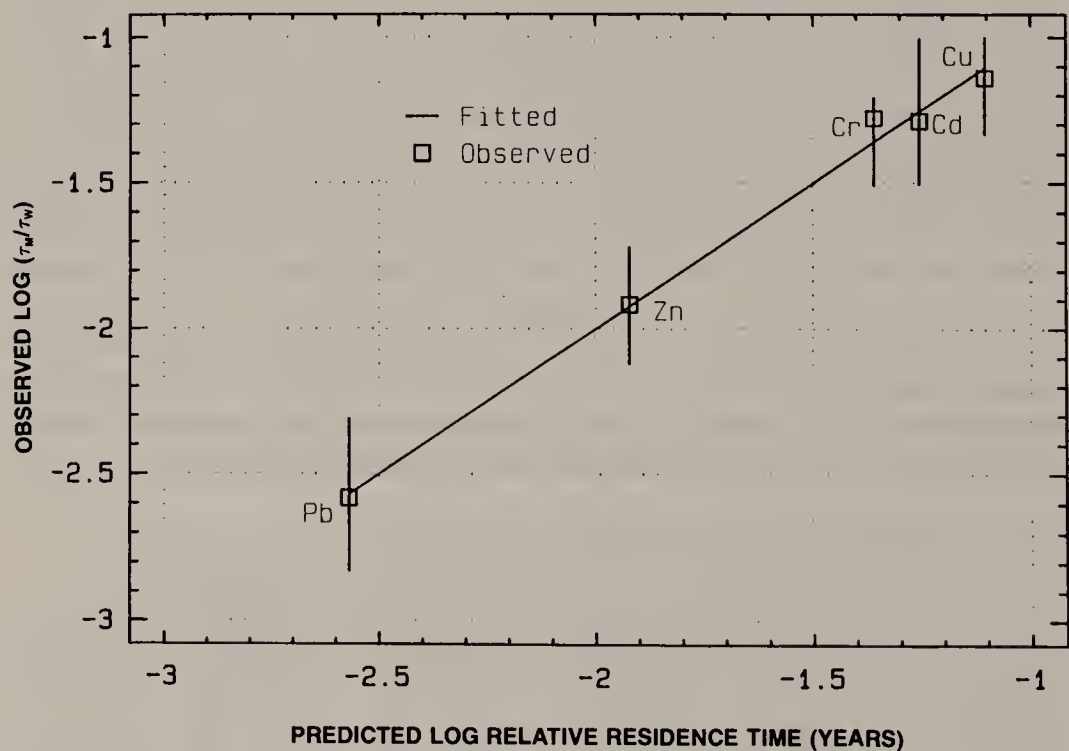


Figure 2.9. Plot of multiple regression model predictions of relative residence time of metals vs observed relative residence times.

The agreement is good, considering the widely disparate sampling, analytical, and computational strategies employed, and points clearly to very rapid particle scavenging of lead. The overall trend in residence time among metals reported by Coale and Flegal⁶ and Sigg⁵ is consistent with residence time and K_d trends reported here. Zinc, a biophilic element, also has a short residence time, on the order of 1.5 years. Copper has the longest residence time among the metals examined, averaging 7 years. Selective affinity of copper for colloidal and dissolved organic matter results in a comparatively long residence time.^{31,51} Adsorption of copper onto humic-coated particles decreases as pH increases from neutral to moderately alkaline values typical of Lake Michigan, whereas sorption increases for most other metals.⁴⁹ Tisue and Fingleton⁴⁶ used recent estimates of water column trace element concentrations and bottom-sediment-based sedimentation fluxes to calculate residence times of 15 and 2 years for cadmium and zinc, respectively. For comparison, we measured an average particle residence time at this station of approximately 0.3 years.

Our Lake Michigan partitioning data are unique in reflecting nearly pure major particle phases in the natural environment. Most data are based on either synthetic phases in laboratory studies or sediment trap values. Although constrained by operational size cutoffs and kinetics (both under investigation), these data advance our understanding of "real world" partitioning mechanisms and prediction of contaminant fate.

The observed K_d reflects an integration of many factors, including bonding characteristics and speciation of the metal, and biogeochemistry of particles and solution phases. Variation between metals (differing by up to a factor of 40), is greater than between particle types (up to a factor of 10), though in certain combinations the influences are comparable. The partition data confirm hypotheses (e.g., Morel and Hudson,⁴⁹ Whitfield and Turner,⁵⁰ and Sigg⁵) that algal/zooplankton cell surfaces have a higher affinity for metals (particularly Cu, Pb, and Zn) than other common aquatic particle surfaces. Affinity for metals, coupled with dominance of algal material (intact cells or coatings of algal-derived material on other particles) explains the dominant role, in Lake Michigan, of phytoplankton (especially diatoms, which generate a large vertical flux) in metal transport to the surface sediment.

Removal from the water column is primarily controlled by phytoplankton; however, phases controlling total metal concentration in the water column on time scales of years to decades are less certain. Redistribution of metals between phases must occur during vector particle dissolution/diagenesis at the sediment surface (93% of SiO_2 , 70% of CaCO_3 , and 73% of organic matter are lost at or near sediment surface). To support recent metal accumulation rates in bottom sediments, a significant fraction of the trace element flux delivered via autochthonous vectors must reassociate with other phases. The fraction left unassociated (regenerated) averaged—over all metals—52% (62% if terrigenous flux is considered nonlabile) and corresponds closely with total mass regeneration of 50 or 60%. The observed metal retention values correlate weakly with K_d . However, variation among metals in retention percentages is

smaller, particularly if the sediment-trap-based flux of Pb is used. The similarity in regeneration suggests either the formation of a new controlling phase or general similarity in particle reactivity in the sediment environment. The correlation between residence time and metal partition coefficient observed between water and recent bottom sediment is highly significant ($r^2 = .95$), indicating components of the sediment may exert a long-term influence over residence times.

ACKNOWLEDGMENTS

This work was funded by the University of Wisconsin Sea Grant College Program under grants from the Office of Sea Grant, National Oceanic and Atmospheric Administration, U.S. Department of Commerce, and from the State of Wisconsin (Federal Grants NA80AA-D-00086, Project R/MW-24, and NA84AA-D-0065, Project R/MW-37).

REFERENCES

1. Prahl, F. G., and R. Carpenter. "The Role of Zooplankton Fecal Pellets in the Sedimentation of Polycyclic Aromatic Hydrocarbons in Dabob Bay, Washington," *Geochim. Cosmochim. Acta* 43:1959-1972 (1979).
2. Jickells, T. D., W. G. Deuser, and A. H. Knap. "The Sedimentation Rates of Trace Elements in the Sargassum Sea Measured by Sediment Trap," *Deep-Sea Res.* 31:1169-1178 (1984).
3. Sigg, L., M. Sturm, and D. Kistler. "Vertical Transport of Heavy Metals by Settling Particles in Lake Zurich," *Limnol. Oceanogr.* 32:112-130 (1987).
4. Eadie, B. J., R. L. Chambers, W. S. Gardner, and G. L. Bell. "Sediment Trap Studies in Lake Michigan: Resuspension and Chemical Fluxes in the Southern Basin," *J. Great Lakes Res.* 10:307-321 (1984).
5. Sigg, L. "Surface Chemical Aspects of the Distribution and Fate of Metal Ions in Lakes," in *Aquatic Surface Chemistry: Chemical Processes at the Particle-Water Interface*, W. Stumm, Ed. (New York: John Wiley and Sons, 1987), pp. 319-349.
6. Coale, K. H., and A. R. Flegal. "Copper, Zinc, Cadmium, and Lead in Surface Waters of Lakes Erie and Ontario," *Sci. Total Environ.* 87/88:297-304 (1989).
7. Wahlgren, M. A., and D. M. Nelson. "Factors Affecting the Collection Efficiency of Sediment Traps in Lake Michigan," Argonne National Laboratory Report ANL-76-88 (1976), pp. 103-106.
8. Eggiman, D. W., and P. R. Betzer. "Decomposition and Analysis of Refractory Oceanic Suspended Material," *Anal. Chem.* 48:886-890 (1976).
9. Strickland, J. D. H., and T. R. Parsons. *A Practical Handbook of Seawater Analysis*, 2nd ed., Bull. Fish. Res. Bd. Can. No. 167 (1972).
10. DeMaster, D. J. "The Supply and Accumulation of Silica in the Marine Environment," *Geochim. Cosmochim. Acta* 45:1715-1732 (1981).
11. Shafer, M. M. "Biogeochemistry and Cycling of Water Column Particulates in Southern Lake Michigan," PhD Thesis, University of Wisconsin, Madison, WI (1988).

12. Fullerton, M. K. "Particulate Organic Carbon in Lake Michigan: Spacial, Temporal, and Size Distribution," Master's Thesis, University of Wisconsin, Madison, WI (1988).
13. Krauskopf, K. B. *Introduction to Geochemistry* (New York: McGraw-Hill, 1967).
14. Fairbridge, R. W., Ed. *The Encyclopedia of Geochemistry and Environmental Sciences*, Encyclopedia of Earth Sciences Series, Vol. IVa (New York: Van Nostrand Reinhold, 1972).
15. Holland, H. D. *The Chemistry of the Atmosphere and Oceans* (John Wiley and Sons, 1978).
16. Reeves, R. D., and R. R. Brooks. *Trace Element Analysis of Geological Materials* (John Wiley and Sons, 1979).
17. Schelske, C. L., B. J. Eadie, and G. L. Krausse. "Measured and Predicted Fluxes of Biogenic Silica in Lake Michigan," *Limnol. Oceanogr.* 29:99–110 (1984).
18. Schelske, C. L. "Biogeochemical Silica Mass Balances in Lake Michigan and Lake Superior," *Biogeochemistry* 1:197–218 (1985).
19. Cahill, R. A. "Geochemistry of Recent Lake Michigan Sediments," Illinois Inst. Nat. Resources, State Geol. Survey Circular 517 (1981).
20. Robbins, J. A., and D. N. Edgington. "Determination of Recent Sedimentation Rates in Lake Michigan Using Pb-210 and Cs-137," *Geochim. Cosmochim. Acta* 39:285–304 (1975).
21. Sigg, L. "Metal Transfer Mechanisms in Lakes; The Role of Settling Particles," in *Chemical Processes In Lakes*, W. Stumm, Ed. (New York: John Wiley and Sons, 1985), pp. 283–310.
22. Shimp, N. F., H. V. Leland, and W. A. White. "Distribution of Major, Minor, and Trace Constituents in Unconsolidated Sediments from Southern Lake Michigan," Ill. State Geol. Survey, Environ. Geol. Notes 32 (1970).
23. Tisue, G. T., and G. Merk. "Sedimentological and Mineralogical Characteristics of Recent Sediments at Selected Sites in the Southern Basin of Lake Michigan," Argonne National Laboratory, Annual Report (1977), pp. 93–98.
24. Lineback, J. A., C. I. Dell, and D. L. Gross. "Glacial and Postglacial Sediments in Lakes Superior and Michigan," *Geol. Soc. Am. Bull.* 90:781–791 (1979).
25. Goldberg, E. D., V. F. Hodge, J. J. Griffin, M. Koide, and D. N. Edgington. "Impact of Fossil Fuel Combustion on the Sediments of Lake Michigan," *Environ. Sci. Technol.* 15:466–471 (1981).
26. Hurlbut, C. S. *Dana's Manual of Mineralogy* (John Wiley and Sons, 1971).
27. Armstrong, D. E., and D. L. Swackhamer. "PCB Accumulation in Southern Lake Michigan Sediments: Evaluation from Core Analysis," in *Physical Behavior of PCBs in the Great Lakes*, D. Mackay, S. Paterson, S. J. Eisenreich, and M. S. Simmons, Eds. (Ann Arbor, MI: Ann Arbor Science, 1983), pp. 229–244.
28. Parker, J. I., H. L. Conway, and E. M. Yaguchi. "Dissolution of Diatom Frustules and Recycling of Amorphous Silicon in Lake Michigan," *J. Fish. Res. Board Can.* 34:545–551 (1977).
29. Rea, D. K., R. A. Bourbonniere, and P. A. Meyers. "Southern Lake Michigan Sediments: Changes in Accumulation Rate, Mineralogy, and Organic Content," *J. Great Lakes Res.* 6:321–330 (1980).
30. Sholkovitz, E. R., and D. Copland. "The Coagulation, Solubility and Adsorption Properties of Fe, Mn, Cu, Ni, Cd, Co and Humic Acids in a River Water," *Geochim. Cosmochim. Acta* 45:181–189 (1981).
31. Buffle, J. "Natural Organic Matter and Metal-Organic Interactions in Aquatic

- Systems," in *Metal Ions in Biological Systems*, H. Sigel, Ed. (New York: Marcel Dekker, 1984), pp. 154-221.
- 32. Hunter, K. A. "The Adsorptive Properties of Sinking Particles in the Deep Ocean," *Deep-Sea Res.* 30:669-675 (1983).
 - 33. Salomoms, W., and U. Förstner. *Metals in the Hydrocycle* (New York: Springer-Verlag, 1984).
 - 34. Mudroch, A., L. Sarazin, and T. Lomas. "Summary of Surface and Background Concentrations of Selected Elements in the Great Lakes Sediments," *J. Great Lakes Res.* 14:241-251 (1988).
 - 35. Pilskaln, C. H., and S. Honjo. "The Fecal Pellet Fraction of Biogeochemical Particle Fluxes to the Deep Sea," *Global Biogeochemical Cycles* 1:31-48 (1987).
 - 36. Ferrante, J. G., and J. I. Parker. "Transport of Diatom Frustules by Copepod Fecal Pellets to the Sediments of Lake Michigan," *Limnol. Oceanogr.* 22:92-98 (1977).
 - 37. Hawkins, B. E., and M. S. Evans. "Seasonal Cycles of Zooplankton Biomass in Southeastern Lake Michigan," *J. Great Lakes Res.* 5:256-263 (1979).
 - 38. Laird, G. A., D. Scavia, G. L. Fahnenstiel, L. A. Strong, J. M. Malczyk, G. A. Lang, and W. S. Gardner. "Southern Lake Michigan Nutrients, Temperature, Chlorophyll, Plankton, and Water Movement During 1983 and 1984," NOAA Technical Memorandum ERL GLERL-67 (1987).
 - 39. Turner, J. T., and J. G. Ferrante. "Zooplankton Fecal Pellets in Aquatic Ecosystems," *Bioscience* 29:670-676 (1979).
 - 40. Yan, N. D., G. L. Mackie, and D. Boomer. "Seasonal Patterns in Metal Levels of the Net Plankton of Three Canadian Shield Lakes," *Sci. Total Environ.* 87/88:439-461 (1989).
 - 41. Komar, P. D., A. P. Morse, L. F. Small, and S. W. Fowler. "An Analysis of Sinking Rates of Natural Copepod and Euphausiid Fecal Pellets," *Limnol. Oceanogr.* 26:172-180 (1981).
 - 42. Scavia, D., and G. L. Fahnenstiel. "Dynamics of Lake Michigan Phytoplankton: Mechanisms Controlling Epilimnetic Communities," *J. Great Lakes Res.* 13:103-120 (1987).
 - 43. Parker, J. I., K. A. Stanlaw, J. S. Marshall, and C. W. Kennedy. "Sorption and Sedimentation of Zn and Cd by Seston in Southern Lake Michigan," *J. Great Lakes Res.* 8:520-531 (1982).
 - 44. Eadie, B. J., R. L. Chambers, W. S. Gardner, and G. L. Bell. "Sediment Trap Studies in Lake Michigan: Resuspension and Chemical Fluxes in the Southern Basin," *J. Great Lakes Res.* 10:307-321 (1984).
 - 45. Edgington, D. N., and J. A. Robbins. "Records of Lead Deposition in Lake Michigan Sediments Since 1800," *Environ. Sci. Technol.* 10:266-274 (1976).
 - 46. Tisue, T., and D. Fingleton. "Atmospheric Inputs and the Dynamics of Trace Elements in Lake Michigan," in *Toxic Contaminants in the Great Lakes*, J. O. Nriagu and M. S. Simmons, Eds. (New York: John Wiley and Sons, 1984), pp. 81-103.
 - 47. Eisenreich, S. J. "Atmospheric Input of Trace Metals to Lake Michigan," *Water Air Soil Poll.* 13:287-301 (1980).
 - 48. Schmidt, J. A., and A. W. Andren. "Deposition of Airborne Metals into the Great Lakes: An Evaluation of Past and Present Estimates," in *Toxic Contaminants in the Great Lakes*, J. O. Nriagu and M. S. Simmons, Eds. (New York: John Wiley and Sons, 1984), pp. 81-103.

49. Morel, F. M., and R. J. Hudson. "The Geobiological Cycle of Trace Elements in Aquatic Systems: Redfield Revisited," in *Chemical Processes In Lakes*, W. Stumm, Ed. (New York: John Wiley and Sons, 1985), pp. 251-281.
50. Whitfield, M., and D. R. Turner. "The Role of Particles in Regulating the Composition of Seawater," in *Aquatic Surface Chemistry: Chemical Processes at the Particle-Water Interface*, W. Stumm, Ed. (New York: John Wiley and Sons, 1987), pp. 457-493.
51. Wallace, G. T. "The Association of Copper, Mercury and Lead with Surface-Active Organic Matter in Coastal Seawater," *Marine Chem.* 11:379-394 (1982).

CHAPTER 3

Sorption of Alkylbenzenes to Mineral Oxides

Judith A. Perlinger and Steven J. Eisenreich

INTRODUCTION

Nonpolar, hydrophobic organic chemicals (HOCs) have become common groundwater contaminants. Because these compounds are used extensively in society, groundwater contamination has become a widespread problem.^{1,2} Most of these contaminants have relatively high aqueous solubilities and low hydrophobicities, and thus sorb to aquifer solids to a limited degree.

An understanding of the sorption process of HOCs is critical to understanding the transport of HOCs in groundwater for numerous reasons. First, natural processes other than sorption that speed the degradation of HOCs or decrease their aqueous concentration in surface environments (e.g., biodegradation, photolysis, volatilization) tend to occur at very slow rates—or not at all—in subsurface environments. Sorption to minerals is the major mechanism by which the transport of the HOC with the groundwater is retarded. Second, even though HOCs do not sorb to subsurface materials that are low in organic matter as strongly as to the relatively higher organic matter surface materials, interactions between these chemicals and mineral surfaces are important. Over long distances and periods of time, even a small retardation factor will alter the shape and size of a contaminant plume.³ Third, it is often economically infeasible or impossible to sample a contaminant plume extensively and frequently enough to monitor the plume over time. Therefore, models are employed to predict the contaminant transport. The accuracy of these models is dependent on an accurate description of the sorption process. Finally, an understanding of the sorption (desorption) process is necessary to accurately estimate the volume of water that must be pumped and treated to attain aquifer remediation.

For very low f_{oc} (fractional organic carbon content) sorbents, mineral surfaces provide sorption sites for HOCs. The f_{oc} of the subsurface decreases with depth^{4,5} and is typically less than 0.001 in unconsolidated aquifers. Karickhoff demonstrated that “mineral phase” sorption was most pronounced for those sorbents with a substantial clay-mineral:organic-carbon ratio.⁶

Sorption of HOCs to mineral surfaces has been the subject of few studies. A comprehensive theoretical (or empirical) model for sorption of HOCs to mineral surfaces does not exist. Before such a model can be developed, a fundamental understanding of the properties of the solute, solvent, and sorbent that influence the sorption process must be gained. Until recently, analytical methods were inadequate to measure the low extent of HOC sorption to mineral surfaces. In addition, researchers studying sorption to mineral surfaces frequently used sorbents that were not thoroughly characterized, or that consisted of a composite of minerals with varying characteristics, or both. This made the determination of the influence of particular characteristics of the sorbent on sorption of HOCs impossible.

The general objectives of this research were twofold:

1. to develop and evaluate the use of a headspace analysis method for studying sorption of HOCs to mineral surfaces
2. to study the mechanism of sorption of HOCs to well-characterized mineral oxides

The objectives of this chapter are, first, to review past studies on sorption of HOCs. Proposed mechanisms of sorption of HOCs to minerals and explanations for the particle concentration effect are reviewed. Second, the conventions for expressing activity of HOCs are examined. Third, the headspace analysis method used in this study and a series of experiments that verify the use of headspace analysis for studying sorption are summarized. Finally, the findings of a set of sorption experiments using headspace analysis, in which benzene was the solute and corundum was the sorbent, are discussed. The results of the benzene-corundum experiments suggest that by using headspace analysis, changes in the sorbed activity of the solute under varying experimental conditions can be observed.

SORPTION TO MINERAL SURFACES

Few studies of HOC sorption to mineral surfaces exist compared to sorption studies in which the solids contain organic matter. One explanation for the paucity of studies is that mineral sorption is viewed as unimportant in surface waters because organic matter dominates the sorption reactions.

The predominance of organic matter in controlling sorption of HOCs has been verified for a variety of compounds on many types of soils and sediments.⁶⁻¹² Dividing the measured sorption coefficient, K_d = sorbed concentration (mole/g solid)/aqueous concentration (mole/L), by the fractional organic carbon, f_{oc} (g C/g solid), of the solids produces a sorption coefficient, K_{oc} , which is less variable for a given compound when sorbed to various sediments and soils:

$$K_{oc} = K_d/f_{oc} \quad (3.1)$$

When organic matter is present in or on the solids in sufficient amounts, the sorption mechanism is thought to be one of partitioning of the HOC into the organic matter. This can be understood in thermodynamic terms by examining the terms in the sorption coefficient as described by Schwarzenbach et al.¹³ Similar descriptions have been given by Chiou et al.¹⁰ and Karickhoff.⁶ The sorption coefficient normalized to the natural organic matter of the solids is

$$\begin{aligned} K_{om} &= C_{om}/C_w \\ &= (\text{moles sorbed}/\text{mass om})/(\text{moles dissolved}/\text{volume water}) \end{aligned} \quad (3.2)$$

Because $C = x/V$, where C is concentration, x is mole fraction, and V is molar volume,

$$K_{om} = \frac{x_{om} (\# \text{ mole/tot # mole})/V_{om} (\text{kg/tot # mole})}{x_w (\# \text{ mole/tot # mole})/V_w (\text{L/tot # mole})} \quad (3.3)$$

where x_{om} and x_w refer to the mole fraction concentrations in the organic matter and water solutions, respectively, and V_{om} and V_w are the molar "volumes" of the two phases. The activity coefficients of the solute in each phase (τ) are related by Raoult's convention to the saturation mole fraction according to the free energy equation for the solute in equilibrium with the pure liquid phase of the solute. For a solute in the aqueous phase:

$$\Delta G = RT(\ln \tau_w + \ln x_w - \ln \tau_o - \ln x_o) = 0 \quad (3.4)$$

where RT are the universal gas constant and absolute temperature (K), respectively, and the subscripts w and o represent the water and pure liquid solute phases, respectively. By assuming that τ_o and x_o are equal to 1, Equation 3.4 simplifies to

$$\ln \tau_w = -\ln x_w \quad (3.5)$$

or

$$\tau_w = 1/x_w \quad (3.6)$$

A similar derivation for the solute in the organic matter leads to the expression:

$$\tau_{om} = 1/x_{om} \quad (3.7)$$

The activity coefficients for the solute in each phase (water and organic matter) at mole fractions less than saturation are assumed to be not significantly different from their saturation values (this assumption is discussed further below). Thus, the sorption coefficient expression can be rewritten as

$$K_{om} = \tau_w V_w / \tau_{om} V_{om} \quad (3.8)$$

For a series of organic compounds of increasing hydrophobicity sorbing to the same sorbent, τ_{om} would be expected to be similar, and variation in τ_w would cause the principal variation in K_{om} . Because $\tau_w V_w = 1/C_w^{sat}$, where C_w^{sat} is the solubility of the compound (moles/L), K_{om} would be expected to decrease with increasing C_w^{sat} . This relation has been observed by various investigators.^{8,10,14,15} The partitioning process of HOCs between water and organic matter is similar to partitioning of HOCs between water and organic solvents. Indeed, empirical equations have been developed to relate the sorption coefficient to the octanol-water partition coefficient of the form:

$$\log K_{om} = a \log K_{ow} + b \quad (3.9)$$

where K_{ow} is the octanol-water partition coefficient. Values for the coefficients a and b have been published for different classes of compounds.^{6,8,14-16} Similar correlations between the partition coefficient and solubility^{6,10} and total surface area of the HOC¹⁷ have been determined.

Mineral surfaces are presumed to be insignificant sorbents for HOCs because they are typically hydrophilic and preferentially bind water.⁹ The organic matter is believed to be a better sorbent because of its hydrophobic and polyelectrolyte character. Chiou and Shoup demonstrated this by measuring the sorption of *m*-dichlorobenzene and 1,2,4-trichlorobenzene to dehydrated wood-burn soil ($f_{oc} = 0.019$), and then increasing the relative humidity and measuring sorption again.¹⁸ On dry soils, the sorption isotherms were nonlinear and could be modeled using a BET sorption model for multilayer coverage. As relative humidity increased above 0.5, isotherms became linear and sorption capacities were reduced by as much as 100-fold. Call found similar results.¹⁹

Chiou and Shoup suggested that water suppressed the sorption of HOCs on mineral soils.¹⁸ The sorption that occurred in the presence of water at relative humidities > 0.5 was attributed to partitioning of the HOC to soil organic matter. To support their conclusions, the authors cited previous results of Jurinak and Volman, who found that uptake of ethyl dibromide (EDB) on various clays was a function of BET surface area.²⁰ Rhue et al. have found similar results.²¹ These studies demonstrate the ability of water to outcompete HOCs for mineral surfaces. Chiou summarized the most commonly held view of sorption of HOCs to natural sorbents:²²

The diverse sorption characteristics with dry and wet soils can thus be reconciled by the postulate that the soil behaves as a dual sorbent, in which the mineral matter functions as a conventional solid adsorbent and the organic matter as a partition medium. . . . In aqueous solution, adsorption of organic compounds by minerals is suppressed by water, and hence the soil uptake consists mainly of solute partitioning into soil organic matter. The strong vapor sorption by dry soil and subsequent suppression by moisture is attributed to mineral adsorption that

predominates over the simultaneous uptake by partitioning into soil organic matter.

In groundwater environments, however, natural organic matter can be quite sparse,⁴ and thus sorption to mineral surfaces can be important. Even small sorption coefficients will cause retardation of a contaminant plume in groundwater.³ Thus, in the past few years, sorption studies using HOCs and inorganic sorbents have become more common.

An f_{oc} equal to 0.001 has been suggested as the critical value needed for the partitioning process to dominate over sorption to mineral surfaces.^{15,23} More recent studies have confirmed this value.^{6,24-28} Below an f_{oc} of 0.001, measured sorption coefficients normalized to fractional organic carbon are higher than would be predicted by the partitioning models. Schwarzenbach and Westall¹⁵ measured K_{oc} values that were up to 2.5 orders of magnitude higher than would be predicted by their partitioning model. Curtis et al.^{26,29} and Piwoni and Banerjee²⁸ have found similar results.

It should be noted that Lee et al. conducted batch and column experiments with two aquifer solids having f_{oc} s of 0.00034 and 0.00025.³⁰ They used a two-site sorption model to describe the data: one type of site was allowed to reach equilibrium, and the other was kinetically hindered from attaining equilibrium. They attributed the kinetically hindered sorption step to diffusion into sorbent organic matter. Other investigators have suggested that the same process may be a dominant cause of the slow approach to equilibrium when higher f_{oc} sorbents are used.³¹⁻³⁴ Bouchard et al. did not observe nonequilibrium conditions for a column experiment in which the sorbent had an f_{oc} of 0.00033.³¹ However, there is some indication that slow diffusion into organic matter may occur at $f_{oc} < 0.001$.³⁰

The paucity of measurements of sorption to mineral surfaces has made it difficult to determine the mechanisms of the process, and appropriate models for sorption remain difficult to discern. In an early attempt, McCarty et al. expressed the sorption coefficient, K_p , in terms of sorption to the organic matter of the sorbent, K_{oc} , as well as sorption to the inorganic material of a solid, K_{io} :²³

$$K_p = f_{io} K_{io} + f_{oc} K_{oc} \quad (3.10)$$

where f_{io} and f_{oc} are the weight fractions of the inorganic and organic materials, respectively. Assuming $K_{oc} >> K_{io}$ and $f_{io} \approx 1$, the critical f_{oc} , below which sorption to inorganic material would become important, was obtained as

$$f_{oc}^* = K_{io}/K_{oc} \quad (3.11)$$

The authors measured K_{io} values by performing column sorption experiments with silica as sorbent, and benzene, chlorinated benzenes, naphthalene, and

tri- and tetra-chloroethylene as solutes. They derived an expression to approximate HOC sorption to silica surfaces as

$$K_s^s = (S K_{ow}^{0.16})/200 \quad (3.12)$$

where K_s^s (mL/g) is the equilibrium sorption coefficient relating the surface and solution concentrations and S is specific surface area (m^2/g). The authors viewed the sorption process as a minimization of the HOC surface exposed to water (hydrophobic effect) by sorbing to the mineral surface. Thus, the more hydrophobic the HOC, the greater the sorption constant. In addition, the greater the specific surface area of the sorbent available for sorption, the greater the sorption constant.

By combining the two expressions above, the authors derived an expression for f_{oc}^* in terms of solute and sorbent properties:

$$f_{oc}^* = S/(200 K_{ow}^{0.84}) \quad (3.13)$$

This expression implies that the f_{oc} needed to maintain a partitioning process must increase as the mineral surface area increases. For sorption experiments using low f_{oc} solids, specific surface area has been found to influence the magnitude of the sorption coefficient.^{5,6,35} Sorbent specific surface area also has been observed to influence the sorption coefficient when dehydrated sorbents are used, as previously discussed. Notably, Piwoni and Banerjee found no relationship between the sorption coefficient and specific surface area.²⁸ However, specific surface areas were measured for only four of the sorbents used in their sorption experiments, and three of the four specific surface areas were within a factor of four of one another. Equation 3.13 also implies that for partitioning into organic matter to dominate over sorption to the mineral surface, a higher f_{oc} is necessary for less hydrophobic compounds relative to more hydrophobic compounds. In agreement with Equation 3.12, sorption studies using mineral sorbents have reported positive correlations between sorption coefficients and solute hydrophobicity for sorption experiments using low f_{oc} sorbents.^{15,26,28,29} Although the model of McCarty et al.²³ has not been applied to data outside their study, it does provide an expression for the influence of specific surface area and solute hydrophobicity on the sorption coefficient for low f_{oc} sorbents which has also been observed by other investigators.

Another mechanism of sorption of HOCs to mineral surfaces that may occur in addition to surface adsorption was presented by Schwarzenbach et al.¹³ They pictured the mineral surface as being surrounded by water molecules that are capable of interacting with the mineral surfaces by van der Waals forces, dipole-dipole forces, and hydrogen bonding. These highly attractive forces cause the water molecules near the surface (the vicinal water) to orient themselves so as to maximize their binding to the surface, resulting in structural organization that extends many layers into solution. Thus, the HOC

molecules are viewed as partitioning into the ordered layer of water adjacent to the mineral surface in addition to adsorbing onto the surface. The main energetic advantage for a HOC to partition into the vicinal water volume vs the bulk water is that once the cavity in the vicinal water is created for the HOC, little energy is required to restructure the vicinal water around the organic molecule; it is already structured due to its interaction with the mineral surface. The authors generated a predictive correlation between the sorption coefficient to kaolinite and silica, K_{\min} , and the infinite dilution activity coefficients of the sorbates, τ_w , from reported sorption coefficients of various HOCs to kaolinite and silica:

$$\log K_{\min} (\text{L/m}^2) = 1.4 \log \tau_w - 11 \quad (3.14)$$

In this case, K_{\min} was normalized to the surface area of the sorbent (m^2) rather than the mass of sorbent (g). This accounts for the vicinal water volume if the thickness of the vicinal water layer is assumed to be constant for different solids. Because $\log K_{\min}$ increased linearly with $\log \tau_w$, the tendency to escape solution was a determinant of the magnitude of the sorption coefficient. Equation 3.14 supports either a surface adsorption or a vicinal water partitioning mechanism.

The models of McCarty et al.²³ and Schwarzenbach et al.¹³ are similar in that both empirically relate the sorption coefficient to sorbent specific surface area and solute hydrophobicity. The primary difference between the two models is that the former is based on a mechanism of adsorption to the mineral phase, while the latter is based on a mechanism of dissolution into vicinal water in addition to surface adsorption. Characteristics of the mineral sorption process can be examined to attempt to distinguish which mechanism may be operative.

The kinetics of HOC sorption to minerals indicate that sorption is not rate limited for mineral surfaces, but is rate limited for sorbents containing organic matter; thus, HOCs do not diffuse into the mineral matrix.^{32,33,36,37} However, this does not indicate whether surface adsorption or dissolution into vicinal water occurs.

Thermodynamically, the overall sorption reaction is weakly exothermic as determined by enthalpy measurements.^{38,39} However, after accounting for solution enthalpies, the enthalpy values of sorption are neutral or weakly endothermic. This indicates that no strong HOC-surface interactions are involved, and that differences in adsorption from one chemical to another are due primarily to variations in their aqueous activity coefficients.¹³ This supports the empirical models that predict sorption is a function of solute hydrophobicity, not mineral properties.

If dissolution into vicinal water is the sorption mechanism, then changes in bulk water parameters such as pH and ionic strength might be expected to influence the sorption process. If the vicinal layer thickness is assumed to be independent of mineral type,¹³ mineral type would be important only if surface

adsorption is the mechanism. Very few studies have been carried out in which specific surface area has been kept constant while mineral type, pH, or ionic strength is varied. Horzempa and DiToro examined the effects of pH and ionic strength on sorption of HCBP to montmorillonite ($f_{oc} < 0.001$).⁴⁰ They observed a decrease of approximately twofold in the sorption coefficient as pH was increased from 4 to 11. Although they did not observe an influence of ionic strength in the range 10^{-4} to 10^{-2} M for NaCl electrolyte, they did observe a twofold increase in the sorption coefficient as ionic strength increased from 10^{-4} to 10^{-2} M when CaCl₂ was used as electrolyte. They suggested the increase could have been due to flocculation of small (colloidal) clay particles that would be efficiently removed from solution by centrifugation, and thus cause an increase in the measured sorbed concentration. The need to physically separate liquid and solid phases to measure the sorption coefficient thus obscured the analysis.

Stauffer and MacIntyre similarly observed a decrease in sorption of HOCs to low f_{oc} sorbents under basic conditions (high pH) and low ionic strengths.²⁴ However, they also observed a decrease in the sorption coefficient depending on sorbent type in the order surface soil ($f_{oc} = 0.014$) > > FeO(OH) > aquifer material > aluminum oxide. This change in sorption coefficient may have been a result of variations in f_{oc} (not measured for all solids) or variations in mineral type. As discussed previously, water molecules have been found to outcompete HOCs for the mineral surface. Also, linear isotherms have been observed in batch sorption experiments for sorbents having $f_{oc} < 0.001$.^{15,26,30,37,41} Linear isotherms for low f_{oc} solids suggests dissolution or partitioning of the HOCs into vicinal water. Thus, although there are indications that dissolution into vicinal water could be an important sorption mechanism of HOCs to mineral surfaces, conclusive evidence is lacking.

PARTICLE CONCENTRATION EFFECT ON SORPTION COEFFICIENTS

Numerous investigators have observed a decrease in the sorption coefficient of HOCs to natural solids with increasing particle concentration. These observations have been reported for both laboratory batch experiments^{40,42-47} and field measurements.⁴⁸⁻⁵⁰ A decrease in the binding coefficient of HOCs to very small particles (colloids) has also been indicated for studies in which DOC was used as the indicator of colloid concentration.⁵¹⁻⁵⁴ Four principal causes— incomplete phase separation, kinetics, particle interaction, and particle aggregation—for the effect of particle concentration on the sorption coefficient have been suggested and will be reviewed here.

The incomplete phase separation of colloidal-sized material ($\sim 0.001\text{--}1 \mu\text{m}$) in natural samples may be the cause of the observed effect.^{43,55,56} Once a HOC is equilibrated between a natural sorbent and water, the sorbent and solvent phase are physically separated by either centrifugation or filtration. Because colloids are smaller than the pore size of most filters, they pass through the

filter or remain suspended following centrifugation. Because colloids bind HOCs during equilibration, the colloid-bound HOC contributes to the measured aqueous concentration, causing it to be artificially high.

Gschwend and Wu measured indicators of colloids (dissolved organic carbon, light absorbance, and total dissolved solids) and found that the indicators increased with increasing particle concentration.⁵⁵ They suggested from these measurements that the colloidal organic material was in dynamic equilibrium with the particulate organic matter. Washing the sorbents prior to the sorption experiment greatly reduced the solids effect. A three-phase equilibrium model was developed by Gschwend and Wu to explain the results. Assuming reversible partitioning between water, particulate organic carbon, and colloidal organic carbon, the sorption coefficient can be described as

$$K_p = f_{oc}^p K_{oc}^p / (1 + f_{oc}^c K_{oc}^c) \quad (3.15)$$

where f_{oc}^c and f_{oc}^p are the fractional organic carbon in the colloidal and particulate phases, respectively, and K_{oc}^c and K_{oc}^p are the respective partition coefficients normalized for organic carbon content. The ratio of the true sorption coefficient to the observed distribution coefficient is given as

$$K_p/K_d = 1 + f_{oc}^c K_{oc}^c \quad (3.16)$$

Sorption experiments should give true sorption coefficients when K_{oc}^c is small or when sorbent organic matter is removed from the supernatant (i.e., when f_{oc}^c is small).

The incomplete separation of colloids cannot explain observations of the particle concentration effect for cases in which the phases were not physically separated to measure the sorption coefficient.^{47,57} Thus, other mechanisms must be invoked to explain the data. Moreover, as discussed below, the influence of sorption kinetics cannot be distinguished from the influence of colloids in short-term (24–48 hr) sorption experiments using sorbents with significant organic matter content.

Nonattainment of sorption equilibrium may be the cause of the particle concentration effect on the sorption coefficient.^{6,58,59} Recent studies have pointed out that the kinetics of sorption are much slower than previously thought, even when low f_{oc} sorbents are used.^{6,26,34,58–61} Early studies observed a rapid increase in sorbed concentration, followed by a leveling off of the sorbed concentration. Analytical techniques were not sensitive enough to detect small changes in concentration at later times. Thus, many sorption experiments were not taken to equilibrium. Karickhoff proposed a two-component sorption capacity: one component sorbs HOCs rapidly and attains sorption equilibrium, and the second component sorbs HOCs at a much slower rate.⁶² The second component is likely to be reversibly sorbed, but requires much longer equilibration times (weeks) than the first component (minutes to hours).

There is increasing evidence that suggests that the slower sorption step may

in many cases be due to diffusion of the HOC into particulate organic matter.³² Brusseau and Rao compiled literature data on column experiments that exhibited nonequilibrium sorption.³³ Compiled sorption coefficients spanned seven orders of magnitude, and the rate constants spanned six orders of magnitude. Paradoxically, an inverse relationship between the sorption coefficient and rate constant was observed. After elimination of other possible mechanisms (physical nonequilibrium, chemical nonequilibrium, intraminerall diffusion) for the observed nonequilibrium, they postulated that intra-organic-matter diffusion explained the relationship.

Other recent column sorption studies have suggested the same phenomenon.^{30,31,34} Szecsody and Bales studied the kinetics of sorption of substituted benzenes to surface-modified silica particles.³⁷ Batch and column studies were carried out with aliphatic-coated (C_1 , C_8 , and C_{18}) particles and with particles coated with aliphatic chains terminating in a phenyl group. Batch experiments required up to 100 hr to reach equilibrium. Diffusion through immobile fluid explained some, but not all, of the slow sorption in column experiments. In addition, diffusion through the organic phase did not completely explain the results because of small diffusional path lengths. Slow binding and release at strong sorption sites on the phenyl polymer-modified silica was thought to cause the tailing in column experiments. However, chemical nonequilibrium has not been observed for HOCs as a rate-controlling step when natural sorbents are used. Diffusion into particulate organic matter is thought to be a very important rate-limiting step for natural sorbents.

Because the sorption coefficient is proportional to organic matter, and if the rate-limiting step is diffusion into organic matter, then the approach to equilibrium would be slowed by addition of particulate organic matter (i.e., by increasing suspended solids containing organic matter), thus causing an apparent particle concentration effect due to nonattainment of equilibrium. A kinetic study of sorption of 4-monochlorobiphenyl to monodisperse polystyrene spheres ($f_{oc} = 0.92$) demonstrated a diminishing particle concentration effect with time on the scale of months.⁶³ Increased particle concentration appeared to slow the approach to equilibrium for both adsorption and desorption processes. Attainment of equilibrium deserves much more attention in future sorption studies.

A third possible explanation of the influence of particle concentration on HOC sorption is particle-induced desorption of the reversibly sorbed fraction of the HOC.^{40,44,64,65} In an attempt to demonstrate particle-induced desorption, DiToro et al. centrifuged a preequilibrated solute/sediment suspension and removed some of the supernatant.⁶⁴ The authors assumed that the colloid concentration remained unchanged while the solids concentration increased. Because the particle concentration effect on the sorption coefficient was observed, the authors proposed that an increased frequency of particle collisions at higher particle concentrations was responsible. Although the observed particle concentration effect may be attributable to incomplete separation of colloids from the aqueous phase,⁵⁶ DiToro proposed that a particle-induced

desorption reaction caused the particle concentration effect.⁶⁶ Based on DiToro and Horzempa's model, for which sorption components are characterized as either easily desorbed (reversible) or resistant to desorption,⁶⁰ the particle interaction model predicts that at low particle concentrations, the partition coefficient for the reversible component approaches the classical partition coefficient. At high particle concentrations, however, the reversible partition coefficient approaches the ratio v_x/m , where v_x is the ratio of the kinetic rate constants for adsorption and particle-induced desorption ($v_x = k_{ads}/k_{p-d}$), and m is the particle concentration.

The main shortcoming of DiToro's model is that it lacks a mechanistic explanation for the particle-induced desorption reaction. Mackay and Powers developed a particle interaction model that supports DiToro's model but uses a mass transfer approach rather than a chemical reaction approach.⁶⁵ When a particle collides with another particle, partial desorption of the loosely associated HOC occurs. Sorption with time resembles a saw-toothed pattern, with asymptotic sorption followed by rapid desorption. It is questionable whether the energy of particle collision is adequate to cause desorption.⁶³ Furthermore, the experiments used to demonstrate this model are not free of the confounding effects of colloids.

Aggregation of particles as particle concentration increases also has been noted as a possible cause for the decrease in the sorption coefficient. Aggregation would cause a decrease in surface area for sorption and an increase in diffusional path length.^{56,67} A decrease in surface area could cause a decrease in the sorption coefficient, and an increase in diffusional path length could result in nonattainment of sorption equilibrium during short-term sorption experiments. Brusseau and Rao reviewed models that describe physical nonequilibrium caused by intraaggregate diffusion in column studies.³² Analytical techniques for monitoring aggregation during batch HOC sorption experiments have only recently been applied.⁶³ Particle aggregation warrants further attention in future studies on sorption.

ACTIVITY IN THE AQUEOUS AND SORBED PHASES

Raoult's and Henry's Conventions

Raoult's and Henry's conventions are used to determine the aqueous activity coefficient (τ) of HOCs. The differences and the relation between them will be discussed here. The fugacity in the liquid phase according to Raoult's convention and Henry's convention are equal:⁶⁸

$$f_L = x\tau f_R^\circ = x\tau^* K_{H,x} \quad (3.17)$$

Raoult's Convention	Henry's Convention
$\tau \rightarrow 1$ as $x \rightarrow 1$	$\tau^* \rightarrow 1$ as $x \rightarrow \infty$

where f_L = liquid-phase fugacity
 x = mole fraction of solute in the liquid
 f_R° = pure component reference fugacity
 τ = Raoult's convention activity coefficient
 τ^* = Henry's convention activity coefficient
 $K_{H,x}$ = Henry's law constant, mole fraction basis

The liquid fugacity has units of pressure. The relation between τ and τ^* is graphically demonstrated in Figure 3.1. Under Raoult's convention, the activity coefficient at aqueous saturation, τ_w , is $1/x_w$, where x_w is mole fraction solubility. Thus, different compounds having a range of x_w would have τ_w as shown. The relationship between τ and x in the range of mole fractions between infinite dilution and saturation ($x_w^\infty > x > x_w$) has been measured in only a few cases, but τ has been empirically related to x as

$$\log \tau = K(1 - x)^2 \quad (3.18)$$

and is shown for a compound i in Figure 3.1, where τ_{wi} approaches τ_{wi}^∞ asymptotically.⁶⁹ K was set equal to $\log \tau_{wi} = -\log x_{wi}$. In addition, the activity coefficient according to Henry's convention, τ_i^* , is proportional to τ_i by a factor of $f_{Ri}^\circ/K_{H,xi}$. Notice that the aspect ratios above and below zero on the y-axis are different.

The activity coefficients of the two conventions provide different information about the solute. Applying Equation 3.17 at mole fractions greater than infinite dilution and at infinite dilution, the following relation can be derived:

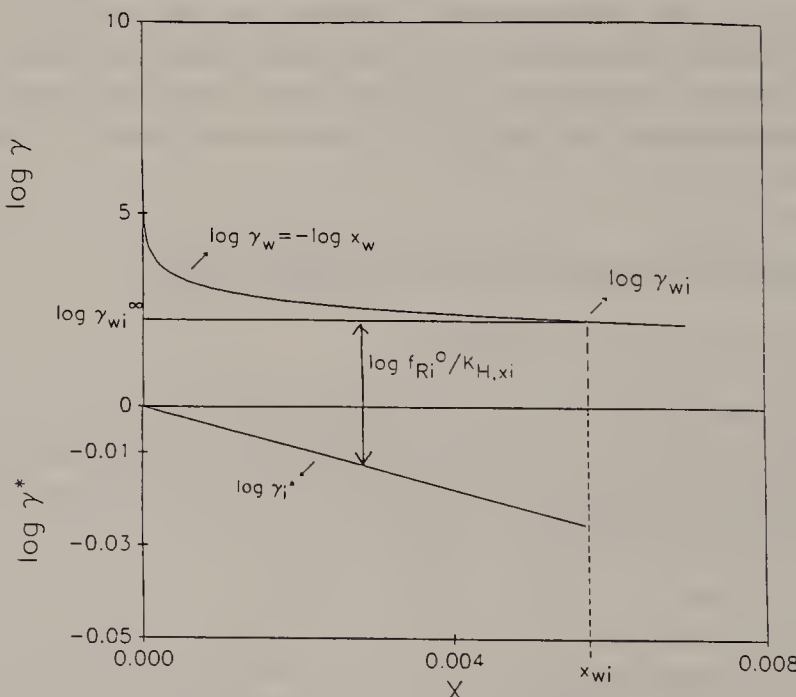


Figure 3.1. Relationship between Henry's and Raoult's law conventions.

$$\begin{aligned} & (x\gamma(x \geq x_w^\infty) f_R^\circ) / (x\gamma(x = x_w^\infty) f_K^\circ) \\ &= (x\gamma^*(x \geq x_w^\infty) K_{H,x}) / (x\gamma^*(x = x_w^\infty) K_{H,x}) \end{aligned} \quad (3.19)$$

However, because $\tau^* = 1$ at $x = x_w^\infty$, the relation simplifies to:

$$\gamma(x \geq x_w^\infty) / \gamma(x = x_w^\infty) = \gamma^*(x \geq x_w^\infty) \quad (3.20)$$

In this manner, the Henry's convention activity coefficient, τ^* , describes the deviation of the solute from ideality. Without the infinite dilution activity coefficient, $\tau(x = x_w^\infty)$, no information can be gained about how ideally a solute behaves in a given solution using Raoult's convention.

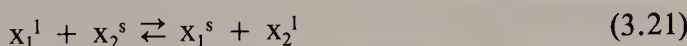
The Raoult's convention activity coefficient, τ , expresses the relative hydrophobicity of compounds having different solubilities. As τ increases, the hydrophobicity of the compound increases. Therefore the Raoult's convention activity coefficient is useful in thermodynamic discussions.⁷⁰

In this study, the Henry's law convention was used to describe the liquid-phase fugacity because it was desirable to observe whether the behavior of the solute deviated from ideality at mole fractions of 10^{-8} to 10^{-6} . From Figure 3.1, the deviation from ideal behavior is expected to be small (< 2%) for the alkylbenzene series used in this study because their mole fraction solubilities are relatively low (1.7×10^{-6} to 4.1×10^{-4}). No measurable deviation from ideal behavior was observed.⁴¹ Munz and Roberts also observed no deviation from ideal behavior for HOCs having mole fraction solubilities ranging from 6.1×10^{-7} to 1.2×10^{-3} .⁶⁸ For nondissociated substituted 2-nitrophenols which have (subcooled) liquid solubilities of 2.1×10^{-6} to 6.1×10^{-4} , Schwarzenbach et al. measured ideal behavior up to saturation concentrations.⁷¹ For nitrophenols where intramolecular hydrogen bonding was disturbed or not possible, however, Schwarzenbach et al. observed significant deviations from ideal behavior.⁷¹ These studies provide evidence that relatively insoluble HOCs behave ideally in aqueous solution.

Activity in Sorption Studies

Most sorption studies carried out with HOCs and natural solids in water apply sorption models developed by physical chemists. The use of these models involves assumptions about the solvent-solute-solid system under study. Although several models have been applied to data from HOC sorption experiments (e.g., Freundlich, Toth, BET^{72,73}), the Langmuir sorption model provides a commonly used example.

For the case of dilute solutions, the Langmuir equation for sorptive equilibrium is written as



corresponding to an exchange reaction between solute (x_1^l) and solvent (x_2^s) on the solid surface, where the number of solvent molecules sorbed per solute molecule is assumed to be one and the superscripts denote the surface (s) and

liquid (l) phases.⁷² The Langmuir model assumes that once all of the solvent has been displaced from the sorbent by the solute, no further adsorption occurs. A constant monolayer concentration is reached as solute aqueous concentration is increased.

The model also assumes that the energy of adsorption is constant and that there is no migration of the solute on the sorbent surface. The corresponding equilibrium coefficient is given as

$$K_x = a_1^s a_2^l / a_1^l a_2^s \quad (3.22)$$

where a is activity. Because $a = \tau x$, where τ is the activity coefficient and x is mole fraction, the complete expression is

$$K_x = \tau_1^s x_1^s \tau_2^l x_2^l / \tau_1^l x_1^l \tau_2^s x_2^s \quad (3.23)$$

In applying the Langmuir model to experimental data a number of assumptions are made to simplify the expression for the sorption coefficient. First, in dilute solution, x_2^l is assumed equal to one. Second, the equilibrium expression (Equation 3.21) is usually further simplified by assuming that the solvent forms a distinct liquid phase adjacent to the solid surface such that the mole fraction of sorbed solvent, x_2^s , is equal to one. The equilibrium expression is rewritten as the following:⁷⁴

$$x_1^l \rightleftharpoons x_1^s \quad (3.24)$$

In addition, the solvent is assumed to have the same activity in the liquid and sorbed phases, and the solute is assumed to behave ideally in both the sorbed and liquid phases. The sorption coefficient according to the above expression is thus $K_x = x_1^s / x_1^l$, or because the concentration of solute in the sorbed and aqueous phases, c_1^s and c_1^l , is usually measured rather than the mole fraction,

$$K = c_1^s / c_1^l = x_1^s v_m Q / x_1^l \quad (3.25)$$

where v_m is the molar volume of the solvent and Q is the total number of sites/g. This is the expression used to compute the sorption coefficient for HOCs sorbing to natural sorbents from water.

Two principal assumptions underlie this simplification of the expression for the sorption coefficient. The first is that the solvent has the same activity in the bulk liquid and sorbed phases. For the system of interest, that is, water as solvent and mineral oxide as sorbent, this assumption may not be valid.^{36,72,74} Strong hydrogen bonding between adsorbed water and the mineral surface may change the structure of the adsorbed water and alter its activity. The second assumption, that the solute behaves ideally in both sorbed and liquid phases, also may not be valid for the present system. The charge of the mineral surface may cause a "salting out" effect near the mineral surface.

Most analytical techniques for measuring sorption are not capable of measuring τ_1^1 , τ_1^s , τ_2^1 , or τ_2^s . In one exception, activity coefficients for the solute (ethanol) and solvent (water) in the sorbed and liquid phases were determined for adsorption to silicalite particles.³⁶ Significant deviations from ideality were found for all of the activity coefficients in the ethanol concentration range studied (0.1 to 1 mole fraction). Although the solute aqueous mole fraction range of this study (10^{-8} to 10^{-6}) is significantly lower than that employed by Farhadpour and Bono for ethanol,³⁶ it is still possible that the solute or solvent behaves nonideally in the liquid or sorbed phases.

METHOD AND MATERIALS

A headspace analysis method was used to study the sorption process primarily to avoid analytical artifacts that have plagued previous sorption studies. Typical analytical methods employed by environmental chemists to study sorption have been demonstrated to have inherent analytical artifacts that complicate interpretation of the results. In particular, batch experiments require the physical separation of the liquid and solid phases to determine the amount of HOC in each. However, colloidal-size particles that are broken off of larger particles during sorption experiments bind the HOC molecules. These particles are not completely separated from the liquid phase by conventional phase separation techniques (filtration, centrifugation). Headspace analysis allows determination of the concentrations of HOC in the aqueous and solid phases without the necessity for physical separation of phases. Thus, artifacts generated by incomplete phase separation are avoided with headspace analysis. In addition, headspace analysis can be used to study the aqueous activity of HOCs.

The use of headspace analysis to study sorption of volatile, hydrophobic organic compounds from solution to sorbents is not novel.⁵⁷ Numerous investigators have used the equilibrium partitioning in closed systems (EPICS) technique of Lincoff and Gossett to study partitioning of HOCs to solids and micelles.^{30,75-81} The EPICS method employs two closed containers: one containing water and air only, and one containing water, air, and sorbent. When the same amount of solute is added to each container, the difference in the gas-phase concentration in the two containers is proportional to the amount of solute sorbed. In this way, the sorption coefficient is determined.

The method employed in this study is different from the EPICS method in that only one container is used to measure the sorbed concentration. The amount sorbed is computed from the difference between the total mass added and that calculated to be present in the water and headspace based on application of Henry's law to the measured headspace concentration.^{41,82} This method assumes that the solute behaves ideally in the gaseous and aqueous phases and that no reactions other than volatilization and sorption occur for the study compounds in the concentration ranges employed. The assumption of ideal

gas behavior has been discussed further by Mackay and Shiu.⁷⁰ The assumptions of ideal behavior in the aqueous phase was verified as discussed above, and the absence of other reactions was verified and will be discussed below.

The headspace analyzer used in this study was designed after a prototype instrument built by Hussam and Carr.⁸³ In contrast to previously reported headspace analysis methods that have been used in the environmental field, it is semiautomated and provides rapid sample analysis and precision of $\leq 2\%$ for replicate samples. A description of the headspace analyzer can be found in Perlinger⁴¹ and Perlinger et al.⁸²

The compounds selected for this study were a homologous series of alkylbenzenes including benzene, toluene, ethylbenzene, propylbenzene, and butylbenzene. The physical-chemical properties of these compounds are similar to those of many common, low-molecular-weight pollutants (Table 3.1).^{70,84-86} These compounds are used in a variety of applications and are common groundwater contaminants. They are manufactured primarily by petroleum refining and coal and coal tar processing. Uses include the manufacture of plastics and resins, aviation and automobile fuel, paints and coatings, and solvents. The major source of alkylbenzenes in the environment is through the use of gasoline.⁸⁷ The high solubility and Henry's law constants of the alkylbenzenes were required for this study because of the relatively high detection limits of the detection method employed (flame ionization). The alkylbenzenes exhibit a range of physical-chemical properties, and thus the influence of these properties on the sorption process can be studied.

The sorbent chosen for the sorption experiments discussed here was corundum (α -Al₂O₃). In contrast to some of the previous studies of HOCs to natural mineral sorbents, the sorbent used in this study consisted of one mineral, rather than a mixture of minerals. It was thoroughly characterized so that the influence of characteristics of the sorbent on sorption could be studied. It had fixed crystalline structure—in contrast to amorphous solids, the molecular structure of which can vary with time. In contrast to clay minerals, it has few exchangeable cation sites, does not have variable molecular composition, and does not have interlamellar layers that are known to sorb HOCs to varying degrees. Thus, this sorbent has reproducible properties that can be quantified to assess their influence on HOC sorption.

The aluminum oxide was obtained from Alcan Chemicals (Cleveland, OH). It was combusted for approximately 24 hr at 500°C to oxidize any organic matter to CO_{2(g)}. The aluminum oxide was characterized by X-ray diffraction to have the crystalline structure of α -Al₂O₃ (corundum) and is virtually free of organic carbon ($f_{oc} = 0.000012$). The mean diameter of the corundum is $6.0 \pm 0.5 \mu\text{m}$. The specific surface area of the corundum is $0.55 \text{ m}^2/\text{g}$, which is within a factor of two of the value computed by assuming that the particles are nonporous spheres with a diameter of $6.0 \mu\text{m}$. The particles are characterized by a high surface charge, with a pH_{zpc} equal to 9.0 ± 0.1 . Further details of the methods used to characterize the corundum and the results can be found elsewhere.⁴¹

Table 3.1. Physical and Chemical Properties of Alkylbenzenes

	Saturated Vapor Pressure (atm)	Solubility (25°C, mg/L) ^a	$K_H, 25^\circ\text{C}$ (10^{-3} atm m ³ /mol) ^a	$\log(K_{\text{ow}})$	Surface Tension, 20°C (dyne/cm) ^b	Density, 20°C (g/cm ³) ^c	Molar Volume, 20°C (cm ³ /mol) ^c	Total Surface Area (Å ²) ^d
Benzene	78.11	0.125	1780	5.4 ± 0.25	2.13	28.88	0.879	88.9
Toluene	92.11	0.0375	515	6.6 ± 0.35	2.65	28.52	0.867	106.2
Ethylbenzene	106.17	0.0125	152	7.9 ± 0.7	3.13	29.29	0.867	122.5
Propylbenzene	120.19	0.0044	55	6.9 ± 3	3.69	28.98	0.862	139.4
Butylbenzene	134.21	0.00132	12.6	13.0 ± 2.5	4.28	29.23	0.860	156.1

^aFrom Mackay and Shiu.⁷⁰^bFrom Jasper.⁸⁴^cFrom Timmermans.⁸⁵^dFrom Pearlman.⁸⁶

The headspace analysis approach permitted the study of sorption to mineral particles while eliminating analytical artifacts typical of batch sorption experiments. Phase separation was not required to determine the amount of HOC sorbed using headspace analysis. If sorption to mineral colloids occurred, only the truly dissolved HOC available for air-water exchange was measured. The system was virtually organic carbon free. Therefore, intra-organic-matter diffusion was expected to be absent, and sorptive equilibrium rapidly reached (minutes to hours). Size distributions for particles greater than 2 μm in diameter were measured before and after the sorption experiment to monitor for particle aggregation over the course of the sorption experiment. This provided an indicator of changes in the aggregation state of the particles, which could be correlated with changes in the sorption coefficient. Thus, this analysis technique allowed the various explanations of the particle concentration effect to be examined.

RESULTS AND DISCUSSION

Verification of Method

The method for determination of the concentrations of solute in the gaseous, aqueous, and sorbed phases was verified before performance of sorption experiments. Correct use of the method is dependent upon the absence of losses from the cell by leakage, the absence of processes other than air-water exchange and sorption to the mineral surface, and the establishment of equilibrium between the three phases.

The cell was tested for leakage by adding an equimolar alkylbenzene mixture to water in the cell, allowing the alkylbenzenes to equilibrate between the air and the water at 20°C, and measuring the gaseous concentration of the alkylbenzenes over time. After an initial rapid decrease in gaseous concentration during solute dissolution of the alkylbenzenes, the measured gaseous concentrations varied by 1.1% or less over 5 days. The variation was random, with no systematic decrease in the gaseous concentration over time, indicating that no measurable leakage from the cell occurred.

Titration of a mixture of alkylbenzenes into water in the cell to give mole fractions in the range of 10^{-8} to 10^{-6} and measurement of the equilibrium gaseous concentration of the alkylbenzenes resulted in a linear increase in gaseous concentration with aqueous concentration.^{41,82} Linear regressions through the data points for each alkylbenzene exhibited zero-intercepts. The Henry's law constants (slopes of air/water regression lines) are given in Table 3.2, together with the data of Ashworth et al. for comparison.⁸⁸ The gaseous concentration increased linearly with aqueous concentration, indicating that the alkylbenzenes participated in no reactions other than volatilization in this concentration range. Reactions such as sorption to the glass above or below the air-water interface and sorption to the air-water interface do not occur in

Table 3.2. Measured Henry's Law Constants ($\times 10^3$ atm m³/mole)

	Perlinger ^{41a}	Ashworth et al. ⁸⁸
Benzene	4.54 \pm 2.21%	4.52 \pm 4.82%
Toluene	4.92 \pm 2.46%	5.55 \pm 2.61%
Ethylbenzene	5.75 \pm 2.72%	8.01 \pm 3.46%
Propylbenzene	8.37 \pm 1.60%	8.81 \pm 1.24%
Butylbenzene	11.0 \pm 2.84%	— ^b

^a20°C, values from this study based on 36 replicates.^bNot measured.

this concentration range. The aqueous activity coefficients for the alkylbenzenes do not differ from one as aqueous concentration increases.

It is important to verify that sorption equilibrium is reached when gas from the cell is sampled. In air-water and air-water-solid systems, equilibrium was judged to have been reached when the measured air concentration changed by less than 2% over time. The coefficient of variance of replicate samples from the cell or the gas bulb standard was $\leq 2\%$. The approach to equilibrium in an air-water-solid system was studied by adding an alkylbenzene mixture to a cell containing water and 1.0 g/L of aluminum oxide at 20°C and sampling the headspace of the cell over time (Figure 3.2). The area counts were initially high during dissolution of the alkylbenzenes and gradually leveled off. Samples taken over 200 hr showed that the area counts became constant after approxi-

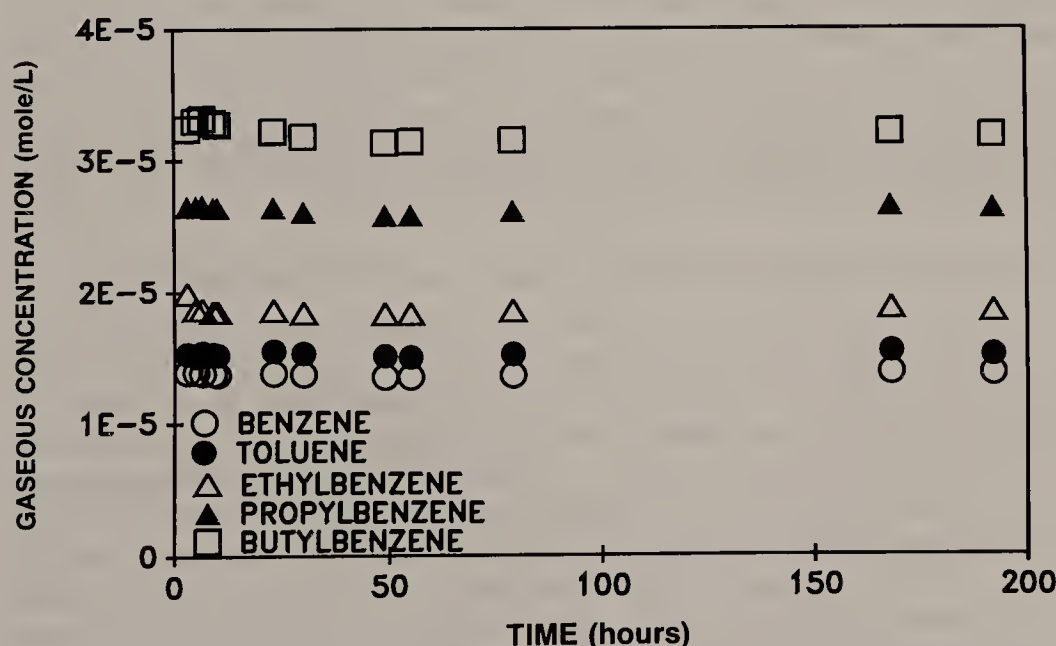


Figure 3.2. Time required for equilibrium between sorbed, aqueous, and gaseous alkylbenzenes. An equimolar mixture (198 mL) was added to the 4270 mL cell containing 4.0 L water and a corundum concentration of 1.0 g/L at 20°C. The measured area counts of all of the alkylbenzenes in gas samples taken over time became constant after approximately 350 min.

Table 3.3. Freundlich Model Parameters for Sorption Isotherms

Freundlich Model: $C_s = K \cdot C_w^n$ ($n = 1$)				
Solids conc: (g/L)	1.0	2.75	6.0	10
K (mL/g)	47 ± 3.5	19 ± 1.2	12 ± 0.6	5 ± 0.3
y-intercept ($\times 10^7$)	-0.3 ± 17	-1.1 ± 3.3	1.0 ± 2.7	-0.07 ± 3
r^2	.885	.930	.950	.882
n	25	22	24	26

mately 350 min of equilibration. No slow sorption step appears to occur for this system. In routine sorption experiments, an equilibrium time of at least 6.5 hr was used when working with alkylbenzene mixtures in air-water-solid systems.

Benzene-Corundum Sorption Experiments

To investigate the sorption process at low surface coverages, four sorption experiments were carried out with corundum at particle concentrations of 1.0, 2.75, 6.0, and 10.0 g/L using benzene alone as the solute (pH, 7.0; ionic strength, 0.01 M; temperature, 20°C). A sorption isotherm was generated at each particle concentration. Linear regression through the data points of each isotherm yielded y-intercepts that were not significantly different from zero (Table 3.3). The slopes of the regression of each isotherm (equivalent to the sorption constant using the Freundlich model, $n = 1$) decreased with increasing particle concentration (Table 3.3 and Figure 3.3).

Comparison of Measured Sorption Coefficients with Literature Values

In general, the sorption coefficients for benzene reported in Table 3.3 are higher than sorption coefficients from the literature (Table 3.4).^{15,25,26,28,30,37,89} All sorption experiments from the literature summarized in Table 3.4 are for HOC sorption to solids having $f_{oc} < 0.001$. The particle concentrations at which the sorption coefficients were determined were much higher (56 to 5000 g/L) than the particle concentrations of the experiments here (1 to 10 g/L). The particle concentration effect that causes the decrease of approximately one order of magnitude in the sorption coefficients (Table 3.3) may be the cause of the difference between sorption coefficients measured here and those in the literature. An equation correlating the measured values of log K with the log of the particle concentration (Figure 3.3) for the benzene-corundum sorption experiments was computed to allow extrapolation to the particle concentration range of the sorption experiments reported in the literature:

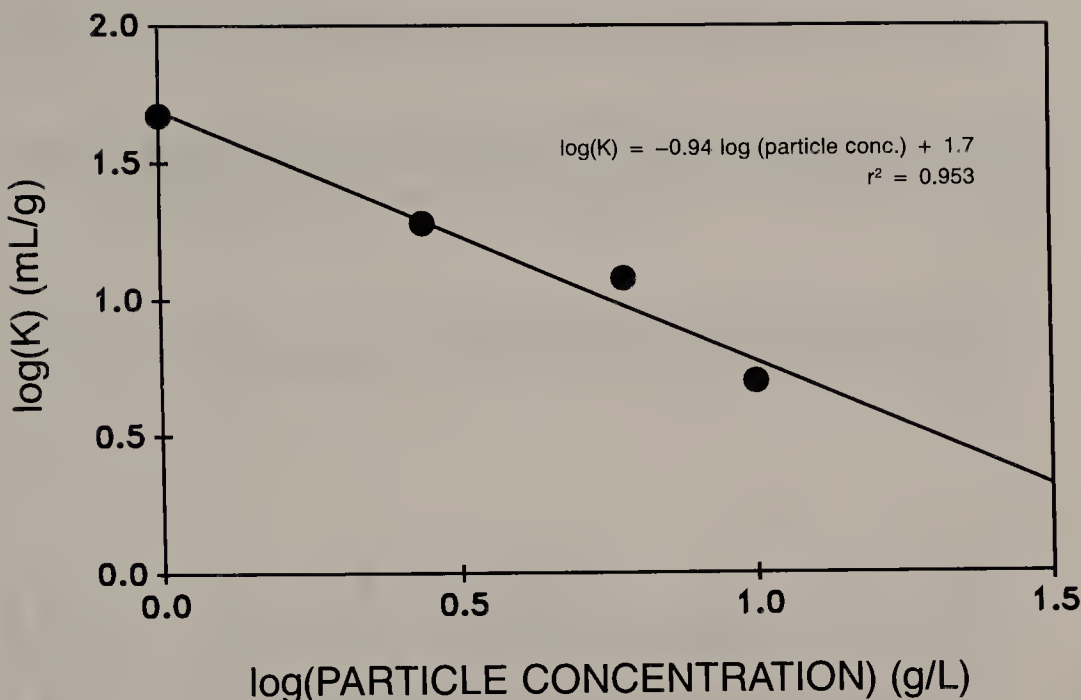


Figure 3.3. Log(K) versus log(particle concentration) for sorption of benzene to corundum (pH, 7.0; ionic strength, 0.01 M; temperature, 20°C). The sorption coefficients decrease with increasing particle concentration.

$$\log K = -0.94 \log(\text{particle conc.}) + 1.7 \quad (3.26)$$

$$n = 4; r^2 = .953$$

where the units of particle concentration are g/L. At particle concentrations of 56 and 5000 g/L, the sorption coefficients computed by the above relationship would be 1.1 mL/g and 0.017 mL/g, respectively. These values are close to the values reported in Table 3.4.

Cause of the Particle Concentration Effect at Low Surface Coverages

The observed decrease in the sorption coefficient with increasing particle concentration is surprising in that a number of the possible causes that have been suggested for the decrease cannot be invoked for these experiments. Because physical separation of the solid phase from the aqueous phase was not necessary for the determination of the sorbed and aqueous concentrations, incomplete separation of colloid-associated HOC from the aqueous phase cannot be the explanation. If HOC is sorbed to colloidal-sized mineral particles, it is measured in the same way as HOC associated with larger particles.

The only way that the presence of colloids could affect the sorption coefficient in these experiments would be if the mass ratio of colloidal-size particles to larger particles changed as a function of particle concentration. To decrease the sorption coefficient with increasing particle concentration, the ratio would

Table 3.4. Literature Values of Sorption Coefficients Measured at Low Values of *foc*

<i>K</i> (mL/g)	<i>SS</i> (g/L)	<i>Solid</i>	<i>foc</i> %	<i>SSA</i> (m ² /g)	<i>Compound</i>	<i>log(Kow)</i>	<i>Aq. Conc.</i> Range (μg/L)	<i>Ref.</i>
0.78	200	Tinker aquifer	0.0096	9.2	naphthalene	3.36	1–2000	89
0.47	200	Carswell aquifer	0.027	9.5	naphthalene	3.36	1–2000	89
0.57	200	Barksdale aquifer	0.105	7.5	naphthalene	3.36	1–2000	89
0.61	200	Traverse City aquifer	0.011	0.2	naphthalene	3.36	1–2000	89
0.28	200	Borden aquifer	0.016	0.3	naphthalene	3.36	1–2000	89
0.27	200	Lula aquifer	0.02	11.8	naphthalene	3.36	1–2000	89
0.44	200	Tinker aquifer	0.0096	9.2	<i>m</i> -naphthalene	2.29	1–2000	89
0.45	200	Carswell aquifer	0.027	9.5	<i>m</i> -naphthalene	2.29	1–2000	89
0.96	200	Barksdale aquifer	0.105	7.5	<i>m</i> -naphthalene	2.29	1–2000	89
0.71	200	Traverse City aquifer	0.011	0.2	<i>m</i> -naphthalene	2.29	1–2000	89
0.65	200	Borden aquifer	0.016	0.3	<i>m</i> -naphthalene	2.29	1–2000	89
0.51	200	Lula aquifer	0.02	11.8	<i>m</i> -naphthalene	2.29	1–2000	89
0.1	200	Tinker aquifer	0.0096	9.2	<i>o</i> -dichlorobenzene	3.38	1–2000	89
0.18	200	Carswell aquifer	0.027	9.5	<i>o</i> -dichlorobenzene	3.38	1–2000	89
0.3	200	Barksdale aquifer	0.105	7.5	<i>o</i> -dichlorobenzene	3.38	1–2000	89
0.36	200	Traverse City aquifer	0.011	0.2	<i>o</i> -dichlorobenzene	3.38	1–2000	89
0.3	200	Borden aquifer	0.016	0.3	<i>o</i> -dichlorobenzene	3.38	1–2000	89
0.14	200	Lula aquifer	0.02	11.8	<i>o</i> -dichlorobenzene	3.38	1–2000	89
0.038	200–500	subsurface core	0.031	0.8	benzene	2.1	10–300	28
0.088	200–500	subsurface core	0.031	0.8	trichloroethylene	2.3	10–300	28
0.35	200–500	subsurface core	0.031	0.8	tetrachloroethylene	2.9	10–300	28
0.34	200–500	subsurface core	0.031	0.8	dichlorobenzene	3.4	10–300	28
0.026	200–500	subsurface core	0.021	11	benzene	2.1	10–300	28
0.032	200–500	subsurface core	0.021	11	trichloroethylene	2.3	10–300	28
0.19	200–500	subsurface core	0.021	11	tetrachloroethylene	2.9	10–300	28
0.082	200–500	subsurface core	0.021	11	dichlorobenzene	3.4	10–300	28
0.035	200–500	subsurface core	0.028	30	benzene	2.1	10–300	28
0.076	200–500	subsurface core	0.028	30	trichloroethylene	2.3	10–300	28
0.18	200–500	subsurface core	0.028	30	tetrachloroethylene	2.9	10–300	28
0.23	200–500	subsurface core	0.028	30	dichlorobenzene	3.4	10–300	28
0.47	2000	homogenized subsurface S1	0.015	1.04	perchloroethylene	2.6	30	25
0.41	2000	subsurface core	0.014	1.06	perchloroethylene	2.6	30	25
0.56	2000	subsurface core	0.014	1.04	perchloroethylene	2.6	30	25

Table 3.4. continued

K (mL/g)	SS (g/L)	Solid	foc %	SSA (m²/g)	Compound	log(Kow)	Aq. Conc. Range (μg/L)	Ref.
0.54	2000	subsurface core	0.014	1.02	perchloroethylene	2.6	30	25
0.466	2000	subsurface core	0.016	0.95	perchloroethylene	2.6	30	25
0.165	2000	bulk Borden sand	0.02	0.8	carbon tetrachloride	2.7	31	26
0.173	2000	bulk Borden sand	0.02	0.8	bromoform	2.3	32	26
0.46	2000	bulk Borden sand	0.02	0.8	perchloroethylene	2.6	30	26
0.76	2000	bulk Borden sand	0.02	0.8	1,2-dichlorobenzene	3.4	332	26
0.814	2000	bulk Borden sand	0.02	0.8	hexachloroethane	3.6	20	26
4.8	118	silica	NA	200	p-nitrotoluene	1010	37	
2.7	56	silica	NA	NA	1,4-dichlorobenzene	3.38	810	37
3.9	56	silica	NA	NA	1,4-dichlorobenzene	3.38	6000	37
26	56	silica	NA	250	pentachlorobenzene	30	30	37
0.1	5000	Borden aquifer	0.025	0.3	trichloroethylene	2.42	2000–4500	30
0.23	5000	Borden aquifer	0.025	0.3	p-xylene	3.15	4000–1400	30
0.17	5000	Lula aquifer	0.034	7.7	trichloroethylene	2.42	100–800	30
0.17	5000	Lula aquifer	0.034	7.7	p-xylene	3.15	1000–8000	30
0.48	5000	Lula aquifer	0.034	7.7	chlorobenzene	2.71		15
0.6	166–417	Kaolin	≤ 0.06	12	1,4-dichlorobenzene	3.38		15
1.1	166–417	Kaolin	≤ 0.06	12	1,2,4-trichlorobenzene	4.05		15
2.4	166–417	Kaolin	≤ 0.06	12	1,2,4,5-tetrachlorobenzene	4.72		15
4.9	166–417	Kaolin	≤ 0.06	12	chlorobenzene	2.71		15
0.6	166–417	Alumina	≤ 0.01	120	1,4-dichlorobenzene	3.38		15
0.9	166–417	Alumina	≤ 0.01	120	1,2,4-trichlorobenzene	4.05		15
1.5	166–417	Alumina	≤ 0.01	120	1,2,4,5-tetrachlorobenzene	4.72		15
2.2	166–417	Alumina	≤ 0.01	120	chlorobenzene	2.71		15
4.2	166–417	Silica	≤ 0.01	500	1,4-dichlorobenzene	3.38		15
6	166–417	Silica	≤ 0.01	500	1,2,4-trichlorobenzene	4.05		15
7.6	166–417	Silica	≤ 0.01	500	1,2,4,5-tetrachlorobenzene	4.72		15
12.1	166–417	Silica	≤ 0.01	500				

have had to decrease, thus decreasing the surface area available for sorption. Such an aggregation of particles was not apparent from particle size distributions of particles $> 2 \mu\text{m}$ in diameter measured by coulter counter before and after the sorption experiments.⁴¹ Even though these particle size distributions do not give information about particles $< 2 \mu\text{m}$ in diameter, it seems likely that aggregation should be apparent for particles $> 2 \mu\text{m}$ if it were occurring. It is concluded that neither the presence of colloids nor particle aggregation can explain the decrease in the sorption coefficient.

Lack of attainment of sorption equilibrium cannot explain the particle concentration effect. Slow sorption kinetics would not be expected for this system because the corundum was shown to be nonporous, and therefore intraminal diffusion is negligible. The corundum has a low natural organic carbon content ($f_{\text{oc}} = 0.000012$), and thus intra-organic-matter diffusion is probably negligible. As previously discussed, particle size distributions taken before and after the sorption experiments do not change. Thus, particle aggregation does not occur, and therefore intraaggregate diffusion cannot be invoked to explain the particle concentration effect.

Of the explanations that have been put forth for the particle concentration effect, only the particle interaction explanation of DiToro,⁶⁶ expanded upon by Mackay and Powers,⁶⁵ can be invoked to explain these data. An interesting feature of the experiments of this work is that at equilibrium, all of the sorbed alkylbenzenes would be expected to be at the mineral surface (rather than in particle aggregates, pores, or natural organic matter). Other investigators have indicated that it is the surface-associated HOC that is influenced by the particle concentration effect. According to Mackay and Powers,⁶⁵ it is the "loosely sorbed" HOC which is capable of being desorbed by particle collisions. Similarly, the particle interaction model of DiToro⁶⁶ is based on DiToro and Horzempa's reversible-resistant model,⁹⁰ for which sorption components are characterized as a fraction easily desorbed versus a fraction resistant to desorption. Only the reversible component is affected by the particle concentration effect according to DiToro's particle interaction model.

The data of van Hoof support this view: the particle concentration effect observed in batch sorption experiments of 4-monochlorobiphenyl to well-characterized polystyrene particles was greatest initially and decreased with exposure time (i.e., the sorption coefficient of batch experiments carried out at different particle concentrations approached the same value over time).⁶³ If it is assumed that the initial mechanism by which monochlorobiphenyl binds to the surface is surface adsorption followed by diffusion of the PCB molecule into the bulk solid, then there may be a particle concentration effect exerted on surface adsorption.⁶³ The results of the experiments carried out in this study support this view.

We suggest that the particles, and perhaps the HOC molecules, alter the structure of water at the particle surface, changing the activity coefficients of sorbed water (vicinal water), sorbed solute, and/or bulk water. Changes in these activity coefficients would cause changes in the sorption coefficient. As

discussed earlier, the activity coefficient τ_1^1 for dissolved benzene was determined to be one in the mole fraction range of this study in the absence of particles.⁴¹ However, τ_1^s , τ_2^1 , and τ_2^s are assumed to be one. If, in reality, they vary in response to changes in experimental conditions (i.e., changing particle concentration), the measured sorption coefficient, $K = c_s/c_w$, would also change. These results suggest that the nonideal behavior of the solvent and/or solute caused changes in the sorption coefficient as particle concentration was increased. Further research is needed to understand the mechanism by which increasing particle concentration causes the observed decrease in the sorption coefficient when ideal behavior is assumed.

SUMMARY

Two mechanisms have been suggested for the sorption of HOCs to mineral oxides. Too few data exist, however, to confirm which mechanism is operative under various conditions. Headspace analysis is useful for studying sorption of HOCs to minerals because incomplete phase separation is avoided. The headspace analysis method used in this study was verified to give accurate and precise results because reactions other than volatilization and sorption to the suspended particles do not occur for the alkylbenzenes in the concentration range employed in the sorption studies. The particle concentration effect observed in the results of the benzene-corundum sorption experiments does not appear to be caused by incomplete phase separation, nonattainment of sorption equilibrium, or particle aggregation. Rather, these results suggest that when activity coefficients are assumed to be one, the measured sorption coefficient changes in response to changes in the activity coefficients of the solute and/or solvent.

REFERENCES

1. Pye, V. I., and R. Patrick. "Groundwater Contamination in the United States," *Science* 222:1:713-721 (1983).
2. Westrick, J. J., J. W. Mello, and R. F. Thomas. "The Groundwater Supply Survey," *Journal AWWA* 76:52-59 (1984).
3. Roberts, P. V., M. N. Goltz, and D. M. Mackay. "A Natural Gradient Experiment on Solute Transport in a Sand Aquifer: 3. Retardation Estimates and Mass Balances for Organic Solutes," *Water Resour. Res.* 22:2047-2058 (1986).
4. Thurman, M. *Organic Geochemistry of Natural Water*, (Dordrecht: Nijhoff/Junk Publ., 1985).
5. Banerjee, P., M. D. Piwoni, and K. Ebeid. "Sorption of Organic Contaminants to a Low Carbon Subsurface Core," *Chemosphere* 14:1057-1067 (1985).
6. Karickhoff, S. W. "Organic Pollutant Sorption in Aquatic Systems," *J. Hydraulic Eng.* 110:707-735 (1984).
7. Steen, W. C., D. F. Paris, and G. L. Baughman. "Partitioning of Selected Polychlorinated Biphenyls to Natural Sediments," *Water Res.* 12:655-756 (1978).

8. Karickhoff, S. W., D. S. Brown, and T. A. Scott. "Sorption of Hydrophobic Pollutants on Natural Sediments," *Water Res.* 13:241-248 (1979).
9. Chiou, C. T., L. J. Peters, and V. H. Freed. "A Physical Concept of Soil-Water Equilibria for Nonionic Organic Compounds," *Science* 206:831-832 (1979).
10. Chiou, C. T., P. E. Porter, and D. W. Schmedding. "Partition Equilibria of Non-ionic Organic Compounds between Soil Organic Matter and Water," *Environ. Sci. Technol.* 17:227-297 (1983).
11. Brown, D. S., and E. W. Flagg. "Empirical Prediction of Organic Pollutant Sorption in Neutral Sediments," *J. Environ. Qual.* 10:382-386 (1981).
12. Means, J. C., and R. Wijayaratne. "Role of Natural Colloids in the Transport of Hydrophobic Pollutants," *Science* 215:968-970 (1982).
13. Schwarzenbach, R. P., P. M. Gschwend, and D. M. Imboden. *Environmental Organic Chemistry: Emphasis on Aquatic Systems* (New York: Wiley-Interscience, in press).
14. Means, J. C., S. G. Wood, J. J. Hassett, and W. L. Banwart. "Sorption of Polynuclear Aromatic Hydrocarbons by Sediments and Soils," *Environ. Sci. Technol.* 14:1524-1528 (1980).
15. Schwarzenbach, R. P., and J. Westall. "Transport of Nonpolar Organic Compounds from Surface Water to Groundwater. Laboratory Sorption Studies," *Environ. Sci. Technol.* 15:1360-1367 (1981).
16. Dzombak, D. A., and R. B. Luthy. "Estimating Adsorption of Polycyclic Aromatic Hydrocarbons on Soils," *Soil Science* 137:292-308 (1984).
17. Rao, P. S. C., A. G. Hornsby, D. P. Kilcrease, and P. Nkedi-Kizza. "Sorption and Transport of Hydrophobic Organic Chemicals in Aqueous and Mixed Solvent Systems: Model Development and Preliminary Evaluation," *J. Environ. Qual.* 14:376-383 (1985).
18. Chiou, C. T., and T. D. Shoup. "Soil Sorption of Organic Vapors and Effects of Humidity on Sorptive Mechanism and Capacity," *Environ. Sci. Technol.* 19:1196-1200 (1985).
19. Call, F. "The Mechanism of Sorption of Ethylene Dibromide on Moist Soils," *J. Sci. Food Agric.* 8:630-639 (1957).
20. Jurinak, J. J., and D. H. Volman. "Application of Brunauer, Emmett, and Teller Equation to Ethylene Dibromide Adsorption by Soils," *Soil Sci.* 83:487-496 (1957).
21. Rhue, R. D., P. S. C. Rao, and R. E. Smith. "Vapor-Phase Adsorption of Alkylbenzenes and Water on Soils and Clays," *Chemosphere* 17:727-741 (1988).
22. Chiou, C. T. "Theoretical Considerations of the Partition Uptake of Nonionic Organic Compounds by Soil Organic Matter," in *Reactions and Movement of Organic Chemicals in Soils*, B. L. Sawhney and K. Brown, Eds. (Madison, WI: Soil Science Society of America, 1989), pp. 1-29.
23. McCarty, P. L., M. Reinhard, and B. E. Rittmann. "Trace Organics in Groundwater," *Environ. Sci. Technol.* 15:40-49 (1981).
24. Stauffer, T. B., and W. G. MacIntyre. "Sorption of Low-Polarity Organic Compounds on Oxide Minerals and Aquifer Material," *Environ. Tox. Chem.* 5:949-955 (1986).
25. Mackay, D. M., W. P. Ball, and M. G. Durant. "Variability of Aquifer Sorption Properties in a Field Experiment on Groundwater Transport of Organic Solutes: Methods and Preliminary Results," *J. Contam. Hydrol.* 1:119-132 (1986).
26. Curtis, G. P., P. V. Roberts, and M. Reinhard. "A Natural Gradient Experiment

- on Solute Transport in a Sand Aquifer: 4. Sorption of Organic Solutes and Its Influence on Mobility," *Water Resour. Res.* 22:2059–2067 (1986).
27. Mehran, M., R. L. Olsen, and B. M. Rector. "Distribution Coefficient of Trichloroethylene in Soil-Water Systems," *Ground Water* 25:275–282 (1987).
28. Piwoni, M. D., and P. Banerjee. "Sorption of Volatile Organic Solvents from Aqueous Solution onto Subsurface Solids," *J. Contam. Hydrol.* 4:163–179 (1989).
29. Curtis, G. P., M. Reinhard, and P. V. Roberts. "Sorption of Hydrophobic Organic Compounds by Sediments," in *Geochemical Processes at Mineral Surfaces*, J. A. Davis and K. F. Hayes, Eds., ACS Symposium Series 323 (Washington, DC: American Chemical Society, 1986), pp. 191–216.
30. Lee, L. S., P. S. C. Rao, M. L. Brusseau, and R. A. Ogwada. "Nonequilibrium Sorption of Organic Contaminants during Flow through Columns of Aquifer Materials," *Environ. Toxicol. Chem.* 7:779–793 (1988).
31. Bouchard, D. C., A. L. Wood, M. L. Campbell, P. Nkedi-Kizza, and P. S. C. Rao. "Sorption Nonequilibrium during Solute Transport," *J. Contam. Hydrol.* 2:209–223 (1988).
32. Brusseau, M. L., and P. S. C. Rao. "Sorption Nonideality during Organic Contaminant Transport in Porous Media," *CRC Critical Reviews in Environ. Contr.* 19:33–109 (1989).
33. Brusseau, M. L., and P. S. C. Rao. "The Influence of Sorbate-Organic Matter Interactions on Sorption Nonequilibrium," *Chemosphere* 18:1691–1706 (1989).
34. Nkedi-Kizza, P., M. L. Brusseau, P. S. C. Rao, and A. G. Hornsby. "Nonequilibrium Sorption during Displacement of Hydrophobic Organic Chemicals and Ca-45 through Soil Columns with Aqueous and Mixed Solvents," *Environ. Sci. Technol.* 23:814–820 (1989).
35. Karickhoff, S. W., and D. S. Brown. "Paraquat Sorption as a Function of Particle Size in Natural Sediments," *J. Environ. Qual.* 7:246–252 (1978).
36. Farhadpour, F. A., and A. Bono. "Adsorption from Solution of Nonelectrolytes by Microporous Crystalline Solids: Ethanol-Water/Silicalite System," *J. Colloid Interface Sci.* 124:209–227 (1988).
37. Szecsody, J. E., and R. C. Bales. "Sorption Kinetics of Low-Molecular Weight Hydrophobic Organic Compounds on Surface-Modified Silica," *J. Contam. Hydrol.* 4:181–203 (1989).
38. Mills, A. C., and J. W. Biggar. "Adsorption of 1,2,3,4,5,6-Hexachlorocyclohexane from Solution: The Differential Heat of Adsorption Applied to Adsorption from Dilute Solutions on Organic and Inorganic Surfaces," *J. Colloid Interface Sci.* 29:720–731 (1969).
39. Boucher, F. R., and G. F. Lee. "Adsorption of Lindane and Dieldrin on Unconsolidated Aquifer Sands," *Environ. Sci. Technol.* 6:538 (1972).
40. Horzempa, L. M., and D. M. DiToro. "PCB Partitioning in Sediment-Water Systems: The Effect of Sediment Concentration," *J. Environ. Qual.* 12:373–380 (1983).
41. Perlinger, J. A. "Use of Headspace Analysis to Study Sorption of a Homologous Series of Alkylbenzenes to Mineral Oxides," MS Thesis, University of Minnesota, Minneapolis, MN (1990).
42. O'Connor, D. J., and J. P. Connolly. "The Effect of Concentration of Adsorbing Solids on the Partition Coefficient," *Water Res.* 14:1517–1523 (1980).
43. Voice, T. C., C. P. Rice, and W. J. Weber, Jr. "Effect of Solids Concentration on

- the Sorptive Partitioning of Hydrophobic Pollutants in Aquatic Systems," *Environ. Sci. Technol.* 17:513-518 (1983).
44. DiToro, D. M., J. S. Jeris, and D. Ciarcia. "Diffusion and Partitioning of Hexachlorobiphenyl in Sediments," *Environ. Sci. Technol.* 19:1169-1175 (1985).
 45. Oliver, B. G. "Desorption of Chlorinated Hydrocarbons from Spiked and Anthropogenically Contaminated Sediments," *Chemosphere* 14:1087-1106 (1985).
 46. Staples, C. A., and S. J. Geiselmann. "Influence of Sorbent Concentration on Sorption of Kepone to Solids," *Environ. Toxicol. Chem.* 7:139-142 (1988).
 47. Servos, M. R., and D. C. G. Muir. "Effect of Suspended Sediment Concentration on the Sediment to Water Partition Coefficient for 1,3,6,8-Tetrachlorodibenzo-p-dioxin," *Environ. Sci. Technol.* 23:1302-1305 (1989).
 48. Capel, P. D., and S. J. Eisenreich. "PCB's in Lake Superior, 1978-1980," *J. Great Lakes Res.* 11:447-461 (1985).
 49. Baker, J. E., P. D. Capel, and S. J. Eisenreich. "Influence of Colloids on Sediment-Water Partition Coefficients of Polychlorinated Biphenyl Congeners in Natural Waters," *Environ. Sci. Technol.* 20:1136-1143 (1986).
 50. Duinker, J. C. "The Role of Small, Low Density Particles on the Partition of Selected PCB Congeners between Water and Suspended Matter (North Sea Area)," *Netherlands J. Sea Res.* 20:229-238 (1986).
 51. Carter, C. W., and I. H. Suffet. "Binding of DDT to Dissolved Humic Materials," *Environ. Sci. Technol.* 16:735-780 (1982).
 52. Landrum, P. F., S. R. Nihart, B. J. Eadie, and W. S. Gardner. "Reverse-Phase Separation Method for Determining Pollutant Binding to Aldrich Humic Acid and Dissolved Organic Carbon of Natural Waters," *Environ. Sci. Technol.* 18:187-192 (1984).
 53. Hassett, J. P., and E. Milicic. "Determination of Equilibrium and Rate Constants for Binding of a Polychlorinated Biphenyl Congener by Dissolved Humic Substances," *Environ. Sci. Technol.* 19:638-643 (1985).
 54. McCarthy, J. F., and B. D. Jimenez. "Interactions between Polycyclic Aromatic Hydrocarbons and Dissolved Humic Material: Binding and Dissociation," *Environ. Sci. Technol.* 19:1072-1076 (1985).
 55. Gschwend, P. M., and S. Wu. "On the Constancy of Sediment-Water Partition Coefficients of Hydrophobic Organic Pollutants," *Environ. Sci. Technol.* 19:90-96 (1985).
 56. Morel, F. M. M., and P. M. Gschwend. "The Role of Colloids in the Partitioning of Solutes in Natural Waters," in *Aquatic Surface Chemistry*, W. Stumm, Ed. (New York: John Wiley and Sons, 1987), pp. 405-422.
 57. Capel, P. D. "Distributions and Diagenesis of Chlorinated Hydrocarbons in Sediments," PhD Thesis, University of Minnesota, Minneapolis, MN (1986).
 58. Karickhoff, S. W., and K. R. Morris. "Sorption Dynamics of Hydrophobic Pollutants in Sediment Suspensions," *Environ. Toxicol. Chem.* 4:469-479 (1985).
 59. Coates, J. T., and A. W. Elzerman. "Desorption Kinetics for Selected PCB Congeners from River Sediments," *J. Contam. Hydrol.* 1:191-210 (1986).
 60. DiToro, D. M., and L. M. Horzempa. "Reversible and Resistant Components of PCB Adsorption-Desorption Isotherms," *Environ. Sci. Technol.* 16:594-602 (1982).
 61. Wu, S., and P. M. Gschwend. "Sorption Kinetics of Hydrophobic Organic Compounds to Natural Sediments and Soils," *Environ. Sci. Technol.* 20:717-725 (1986).

62. Karickhoff, S. W. "Sorption Kinetics of Hydrophobic Pollutants in Natural Sediments," in *Contaminants and Sediments*, Vol. 2, R. A. Baker, S. Paterson, S. J. Eisenreich, and M. Simmons, Eds. (Ann Arbor, MI: Ann Arbor Science, 1980), pp. 193-205.
63. Van Hoof, P. L. "Partitioning and Sorption Kinetics of a Polychlorinated Biphenyl in Aqueous Suspensions of Model Particles: A Solids Concentration Effect," PhD Thesis, University of Wisconsin, Madison, WI (1989).
64. DiToro, D. M., J. D. Mahony, P. R. Kirchgraber, A. L. O'Bryne, L. R. Pasquale, and D. C. Piccirilli. "Effects of Nonreversibility, Particle Concentration, and Ionic Strength on Heavy-Metal Sorption," *Environ. Sci. Technol.* 20:55-61 (1986).
65. Mackay, D., and B. Powers. "Sorption of Hydrophobic Chemicals from Water: A Hypothesis for the Mechanism of the Particle Concentration Effect," *Chemosphere* 16:745-757 (1987).
66. DiToro, D. M. "A Particle Interaction Model of Reversible Organic Chemical Sorption," *Chemosphere* 14:1503-1538 (1985).
67. Honeyman, B. D., and P. H. Santschi. "Metals in Aquatic Systems," *Environ. Sci. Technol.* 22:862-871 (1988).
68. Munz, C., and P. V. Roberts. "Effects of Solute Concentration and Cosolvents on the Aqueous Activity Coefficient of Halogenated Hydrocarbons," *Environ. Sci. Technol.* 20:830-836 (1986).
69. Mackay, D., and S. Paterson. "Calculating Fugacity," *Environ. Sci. Technol.* 15:1006-1014 (1981).
70. Mackay, D., and W. Y. Shiu. "A Critical Review of Henry's Law Constants for Chemicals of Environmental Interest," *J. Phys. Chem. Ref. Data* 10:1175-1199 (1981).
71. Schwarzenbach, R. P., R. Stierli, B. R. Folsom, and J. Zeyer. "Compound Properties Relevant for Assessing the Environmental Partitioning of Nitrophenols," *Environ. Sci. Technol.* 22:83-92 (1988).
72. Parfitt, G. D., and C. H. Rochester. "Adsorption of Small Molecules," in *Adsorption from Solution at the Solid/Liquid Interface*, G. D. Parfitt and C. H. Rochester, Eds. (New York: Academic Press, 1983), pp. 3-47.
73. Kinniburgh, D. G. "General Purpose Adsorption Isotherms," *Environ. Sci. Technol.* 20:895-904 (1986).
74. Karger, B. L., L. R. Snyder, and C. Horvath. *An Introduction to Separation Science* (New York: John Wiley and Sons, 1973).
75. Hayase, K., and W. Hayano. "The Distribution of Higher Alcohols in Aqueous Micellar Solutions," *Bull. Chem. Soc. Jap.* 50:83-85 (1977).
76. Spink, C. H., and S. Colgan. "Thermodynamics of Alcohol Binding to Deoxycholate Micelles and the Hydrophobic Effect," *J. Phys. Chem.* 87:888-894 (1983).
77. Garbarini, D. R., and L. W. Lion. "Evaluation of Sorptive Partitioning of Non-ionic Pollutants in Closed Systems by Headspace Analysis," *Environ. Sci. Technol.* 19:1122-1128 (1985).
78. Garbarini, D. R., and L. W. Lion. "Influence of the Nature of Soil Organics on the Sorption of Toluene and Trichloroethylene," *Environ. Sci. Technol.* 20:1263-1269 (1986).
79. Valsaraj, K. "On the Physico-Chemical Aspects of Partitioning of Non-Polar Hydrophobic Organics at the Air-Water Interface," *Chemosphere* 17:875-887 (1988).
80. Valsaraj, K. T., and L. J. Thibodeaux. "Relationships between Micelle-Water and

- Octanol-Water Partition Constants for Hydrophobic Organics of Environmental Interest," *Water Res.* 23:183-189 (1989).
81. Lincoff, A. H., and J. M. Gossett. "The Determination of Henry's Constant for Volatile Organics by Equilibrium Partitioning in Closed Systems," in *Gas Transfer at Water Surfaces*, W. Brutsaert and G. H. Jirka, Eds. (Dordrecht: Reidel Publ., 1984), pp. 17-25.
 82. Perlinger, J. A., S. J. Eisenreich, P. D. Capel, P. W. Carr, and J. H. Park. "Adsorption of a Homologous Series of Alkylbenzenes to Mineral Oxides at Low Organic Carbon Content Using Headspace Analysis," *Water Sci. Technol.* 22:7-14 (1990).
 83. Hussam, A., and P. W. Carr. "A Study of a Rapid and Precise Methodology for the Measurement of Vapor Liquid Equilibria by Headspace Gas Chromatography," *Anal. Chem.* 57:793-801 (1985).
 84. Jasper, J. J. "The Surface Tensions of Pure Liquid Compounds," *J. Phys. Chem. Ref. Data* 1:841 (1972).
 85. Timmermans, J. *Physico-Chemical Constants of Pure Organic Compounds*, Vol. 2 (New York: Elsevier, 1965).
 86. Pearlman, R. S. "Molecular Surface Areas and Volumes and Their Use in Structure/Activity Relationships," in *Physical and Chemical Properties of Drugs*, S. H. Yalkowsky, A. A. Sikula, and S. C. Valvani, Eds. (New York: Marcel Dekker, 1980).
 87. Verschueren, K. *Handbook of Environmental Data on Organic Chemicals*, 2nd ed. (New York: Van Nostrand Reinhold, 1983).
 88. Ashworth, R. A., G. B. Howe, M. E. Mullins, and T. N. Rogers. "Air-Water Partitioning Coefficients of Organics in Dilute Aqueous Systems," *J. Haz. Mat.* 18:25-36 (1988).
 89. Stauffer, T. B., W. G. MacIntyre, and D. C. Wickman. "Sorption of Nonpolar Organic Chemicals on Low-Carbon-Content Aquifer Materials," *Environ. Toxicol. Chem.* 8:845-852 (1989).
 90. DiToro, D. M., and L. M. Horzempa. "Reversible and Resistant Component Model of Hexachlorobiphenyl Adsorption-Desorption Resuspension and Dilution," in *Physical Behavior of PCB's in the Great Lakes*, D. Mackay, S. Peterson, S. J. Eisenreich, and M. Simmons, Eds. (Ann Arbor, MI: Ann Arbor Science, 1983), pp. 89-113.

CHAPTER 4

Field-Measured Associations between Polychlorinated Biphenyls and Suspended Solids in Natural Waters: An Evaluation of the Partitioning Paradigm

Joel E. Baker, Steven J. Eisenreich, and Deborah L. Swackhamer

K_d is a much studied parameter, particularly for adsorption in the laboratory, and enjoys a voluminous literature heritage beyond the point of realistic application in the natural environment.

L. J. Thibodeaux¹

BACKGROUND

The aquatic behaviors of many organic chemicals depend strongly upon their high affinities for suspended and settling solids in the water column. These associations control the speciation, reactivity, and bioavailability of slightly soluble hydrophobic organic contaminants (HOCs), including polycyclic aromatic hydrocarbons (PAHs) and polychlorinated biphenyls (PCBs). Due to the critical importance of HOC-solid associations in surface waters, considerable efforts have been dedicated both to understand the underlying mechanisms and to develop predictive models of contaminant sorption to natural solids.² In a vast majority of these studies, sorption of individual chemicals or simple mixtures to sediments or soils has been measured in laboratory experiments. Thermodynamic-based partitioning models resulting from such studies have been incorporated into surface water quality models. Surprisingly, there have been very few reported measurements of HOC partitioning in the field under ambient conditions. In an earlier paper,³ we described the field-measured partitioning of PCB congeners in Lake Superior. We expand that analysis in this chapter by evaluating reported PCB distributions in a number of freshwater and marine environments. These data suggest that several assumptions of HOC partitioning models are violated in surface waters and that partitioning models inadequately predict HOC speciation within the water column.

Our current understanding of HOC-solid associations is largely based upon

the experimental work of Karickhoff and coworkers^{4,5} and subsequent theoretical development by Chiou et al.⁶ The magnitude of HOC-particle associations directly vary with contaminant hydrophobicity, as parameterized by the octanol-water partition coefficient (K_{ow}) or aqueous solubility. As was found earlier for sorption of pesticides to soils, Karickhoff et al. determined that the extent of HOC-solids associations also depends directly upon the organic matter content of the solids.⁴ These findings were interpreted by Chiou et al.⁶ as evidence that HOC-solid associations result from partitioning of contaminants into the relatively nonpolar organic matter portion of natural solids. Chiou et al. employed the Flory-Huggins model of solubilization within polymeric matrices to develop a mechanistic description of contaminant partitioning, using measured relationships among HOC partition coefficients, K_{ow} , and the solid organic matter content.⁶ The resulting semiempirical equations, which have been widely used to estimate contaminant partitioning, take the form:

$$\log K_{oc} = A (\log K_{ow}) + B \quad (4.1)$$

where the organic carbon-normalized partition coefficient K_{oc} is the ratio of particulate organic carbon bound and dissolved contaminant concentrations, and A and B are regression coefficients. This partitioning paradigm implicitly assumes that HOCs have equal affinities for all particulate organic matter, that mass transfer rates are relatively rapid and, therefore, partitioning is at equilibrium, and that the dissolved phase and particulate-bound HOCs can be unambiguously separated.

In our earlier study, we reported the failure of the above semiempirical equations to describe the observed particle associations of PCB congeners in Lake Superior.³ This failure was attributed to the relative importance of contaminant-binding colloidal matter in this oligotrophic lake. As described by Gschwend and Wu,⁷ colloids that complex contaminants and are not separated by filtration decrease the *apparent* contaminant K_d :

$$K_d = (P/M)/[(D + N)/V] \quad (4.2)$$

where P = mass of PCB sorbed to filterable solids
 N = mass of PCB sorbed to colloids
 D = mass of PCB dissolved in solution
 M = the mass of filterable particles
 V = volume of water

Note the distinction between K_p , the true thermodynamic partition coefficient, and K_d , the measured distribution coefficient. Assuming that the complexation of PCBs by colloidal matter can be described as an equilibrium partitioning process analogous to their sorption to sediment organic matter, rearrangement of Equation 4.2 yields

$$K_d = K_p [1 + K_c (M_c/V)]^{-1} \quad (4.3)$$

where K_p and K_c are the partition coefficients to filterable and nonfilterable particles, respectively, and M_c is the mass of colloids. Further, Baker et al.³ argued that the colloid concentration (M_c/V) is likely proportional to the filterable solids concentration (M/V) and that K_c is proportional to K_p , yielding

$$K_d = K_p[1 + CK_p(M/V)]^{-1} \quad (4.4)$$

where the proportionalities above are combined into the constant C. This three-phase model predicts the following:

1. At low values of K_p (i.e., more soluble species), K_d approaches K_p , and the "colloid artifact" is negligible.
2. The observed distribution coefficient becomes *independent* of K_p and approaches a value of $1/[C(M/V)]$ for highly hydrophobic compounds (i.e., the *apparent* partitioning of all highly hydrophobic compounds will be the same).
3. The observed distribution appears to vary inversely with the suspended solids concentration due to the proportional contribution of colloidal-bound HOC to the concentration.

In the following section, several PCB partitioning data sets resulting from field measurements are used to evaluate the partitioning paradigm described above and to further investigate the potential importance of colloids in the aquatic geochemistry of HOCs.

DESCRIPTION OF PCB PARTITIONING DATA SETS

The distribution of PCB congeners in natural waters has been investigated in several studies by separating the particle-bound and dissolved congeners using either high-volume filtration or centrifugation. Dissolved-phase PCBs are isolated either by passage through an adsorptive resin (e.g., Amberlite XAD-2) or by liquid-liquid extraction. PCB distribution coefficients are calculated as the ratio of the particle-bound and dissolved-phase concentrations in units of ng/kg and ng/L, respectively. To test the applicability of the partitioning paradigm, reported PCB distribution coefficients were regressed against the congener K_{ow} values,⁸ as summarized in Table 4.1.

PCB distribution coefficients measured in Lake Superior surface waters in 1980,⁹ 1983,³ and 1986¹⁰ are plotted against their K_{ow} 's in Figure 4.1. The 1980 and 1983 data were used to calibrate the three-phase partitioning model in our earlier paper.³ The log K_d values of all PCB congeners in Lake Superior averaged 5.67, 4.91, and 4.85 during these three years, respectively. As was noted previously,³ K_d values of individual congeners vary more than one order of magnitude, far exceeding the estimated analytical uncertainty. In addition, K_{ow} is a poor predictor of these observed K_d values, explaining at most 30% of the variation in K_d in 1986. Rather than the systematic two- to threefold variation

Table 4.1. Apparent Distribution Coefficients of PCB Congeners

	Log K _d		Log K _d = A(Log K _{ow}) + B			r ²
	Mean ± SD	N	A	B		
Lake Superior						
1980	5.67 ± 0.66	364	0.01 ± 0.06	5.6 ± 0.6		0.00
1983	4.91 ± 0.49	797	0.37 ± 0.03	2.7 ± 0.5		0.16
1986	4.85 ± 0.49	122	0.34 ± 0.05	2.7 ± 0.4		0.30
Lake Michigan						
1980	5.76 ± 0.45	221	0.11 ± 0.06	5.0 ± 0.5		0.02
1986	5.53 ± 0.33	126	0.17 ± 0.04	4.4 ± 0.3		0.11
Green Bay, Lake Michigan						
1980	5.44 ± 0.45	56	0.23 ± 0.09	4.0 ± 0.4		0.10
1987 ^a	5.29 ± 0.35	71	0.16 ± 0.05	4.3 ± 0.3		0.15
1987 ^b	5.68 ± 0.55	71	0.00 ± 0.08	5.7 ± 0.6		0.00
Lake St. Clair and Detroit River						
All OCs	6.32 ± 0.43	24	0.33 ± 0.05	4.4 ± 0.3		0.62
PCBs	6.49 ± 0.33	11	0.35 ± 0.10	4.2 ± 0.2		0.57
North Sea						
1981	5.60 ± 0.49	29	0.36 ± 0.12	3.3 ± 0.5		0.24

^aHigh volume filtration.^bContinuous-flow centrifugation.

in log K_d among PCB congeners predicted by the semiempirical partitioning equations, the highly variable observed values are largely invariant with K_{ow}.

Results of PCB partitioning studies conducted in Lake Michigan, including Green Bay, are similar to those obtained in the Lake Superior studies. In 1980, Swackhamer and Armstrong found that PCB log K_d values in Lake Michigan averaged 5.76 and were poorly correlated with K_{ow} (Figure 4.2).¹¹ Similarly, Lefkowitz measured an average log K_d of 5.53 during three cruises in 1985 (Figure 4.2).¹² Samples collected in Green Bay, Lake Michigan, in 1980 and 1988 yield comparable PCB distribution coefficients,^{11,13} which are again poorly correlated with K_{ow} (Figure 4.3). In 1987, matched samples collected in Green Bay using coincident high-volume filtration and continuous-flow centrifugation resulted in comparable partition coefficients, suggesting that these two methods isolate the same particle size classes from surface waters.

The distribution coefficients reported by Lau et al. in the St. Clair and Detroit Rivers were determined by continuous-flow centrifugation followed by extraction of dissolved contaminants from the centrifugate with dichloromethane.¹⁴ In addition to PCB congeners, this data set includes chlorinated benzenes and other more soluble organochlorines. As shown in Figure 4.4 and Table 4.1, Lau et al. observed a relatively good correlation between K_d and K_{ow}, perhaps due either to the inclusion of a wider range of compounds or to the avoidance of artifacts in their sampling procedure.¹⁴

Two samples collected in the North Sea exhibit PCB partitioning behavior remarkably similar to that observed in the Great Lakes (Figure 4.5),¹⁵ suggesting little systematic difference between HOC-particle associations in marine

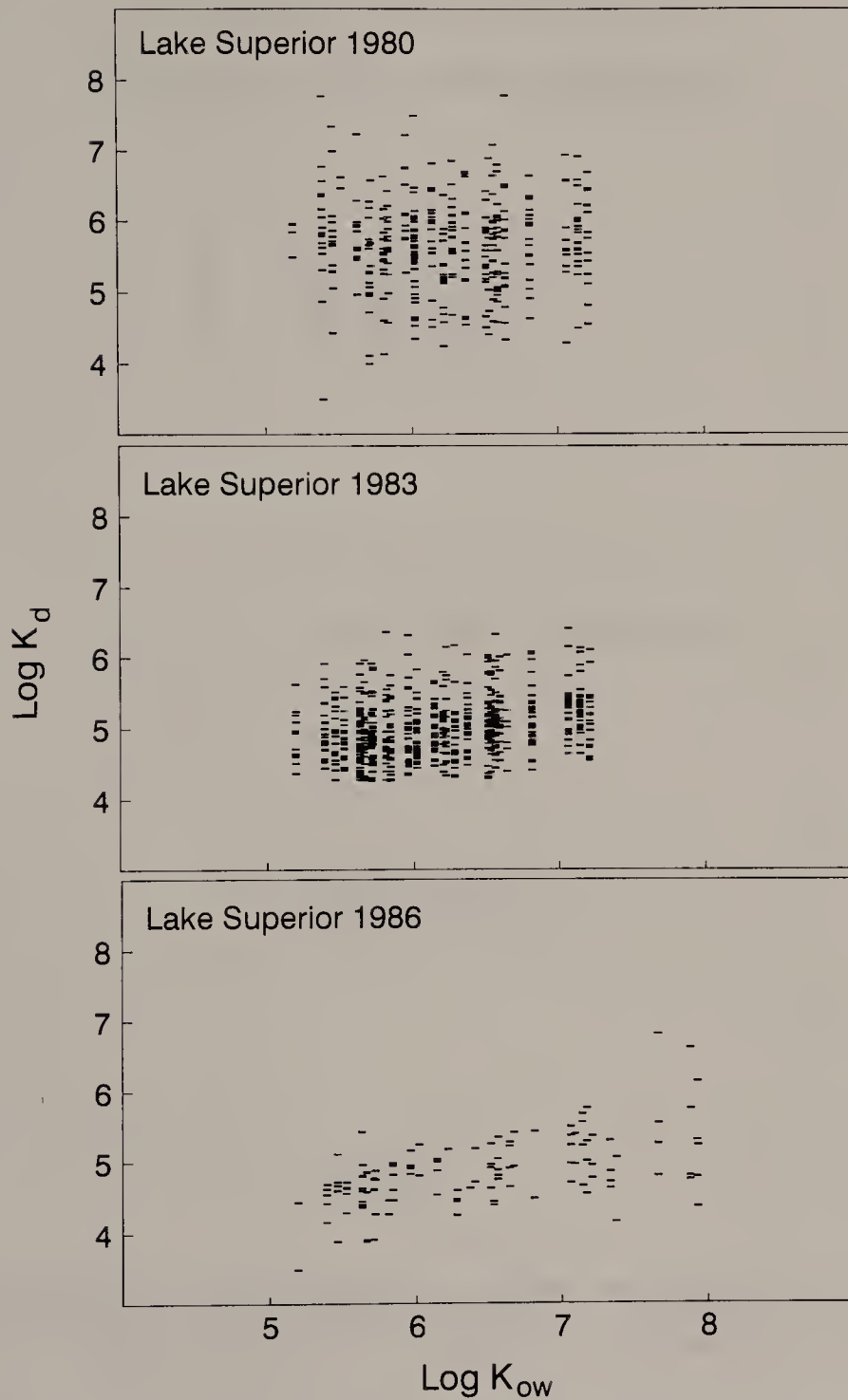


Figure 4.1. PCB congener distribution coefficients versus octanol-water partition coefficients, Lake Superior. From Baker et al.,³ Capel and Eisenreich,⁹ and Baker and Eisenreich.¹⁰

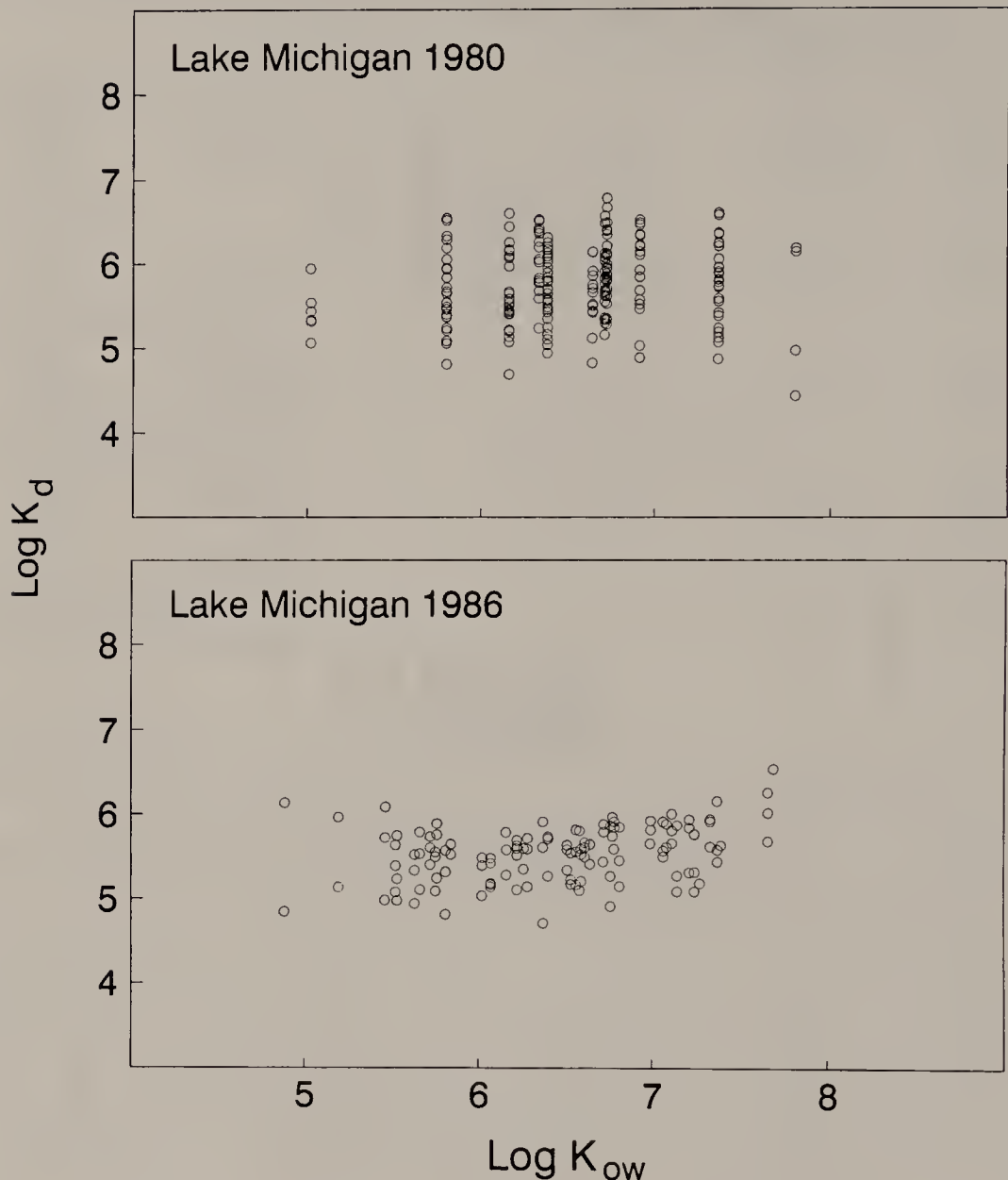


Figure 4.2. PCB congener distribution coefficients versus octanol-water partition coefficients, Lake Michigan. From Swackhamer and Armstrong¹¹ and Lefkowitz.¹²

and freshwaters. Finally, the PCB distribution coefficients measured in two small lakes in Wisconsin (shown in Figure 4.6) also show only a slight dependence of K_d and K_{ow}.¹⁶

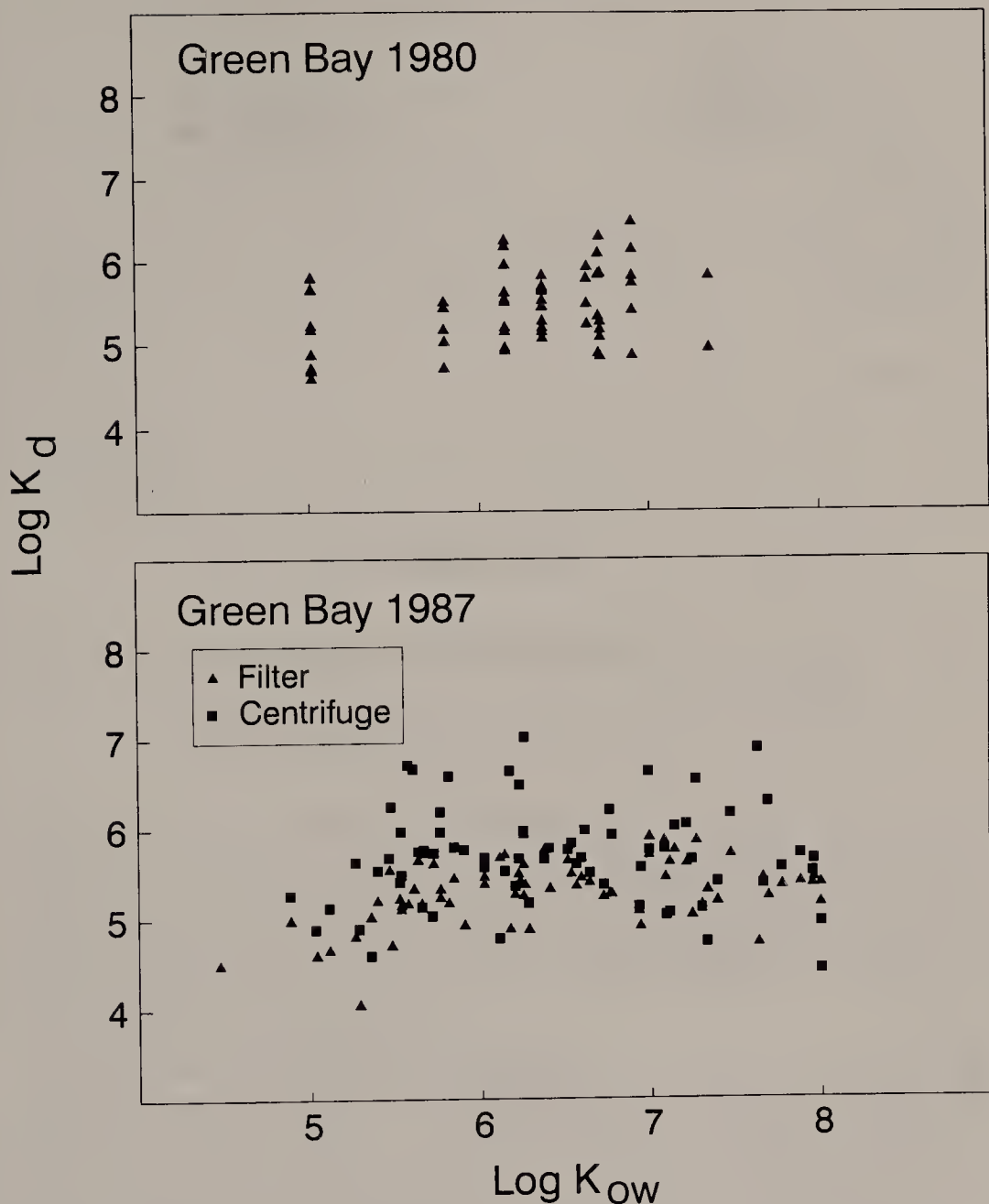


Figure 4.3. PCB congener distribution coefficients versus octanol-water partition coefficients, Green Bay, Lake Michigan. From Swackhamer and Armstrong¹¹ and Swackhamer.¹³

DISCUSSION

The data presented above show a remarkably consistent PCB distribution in surface waters, with relatively little dependence on the collection methodologies or the properties of the compounds (e.g., K_{ow}). Limited data available

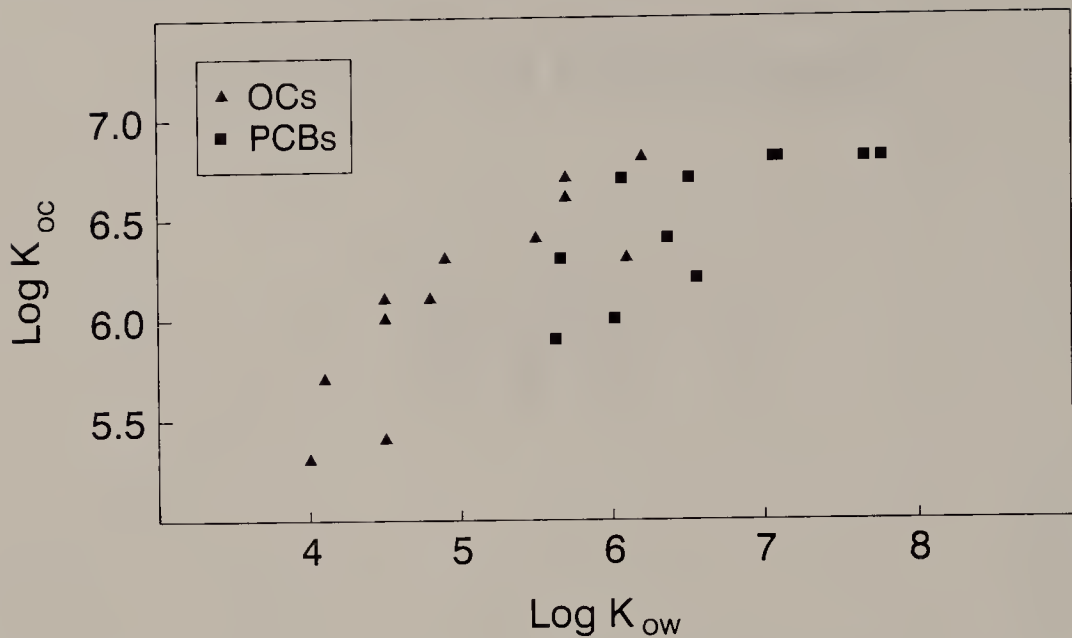


Figure 4.4. PCB and other organochlorine distribution coefficients versus octanol-water partition coefficients measured in the Detroit and St. Clair Rivers. From Lau et al.¹⁴

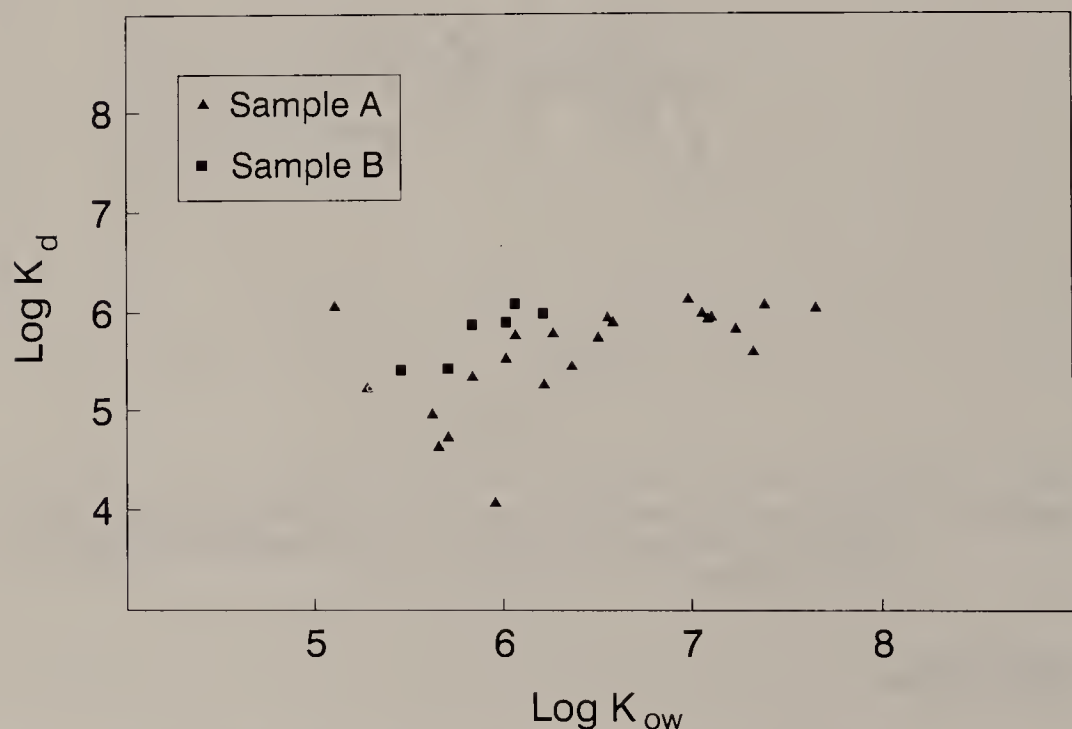


Figure 4.5. PCB congener distribution coefficients versus octanol-water partition coefficients in two samples collected in the North Sea. From Duinker.¹⁵

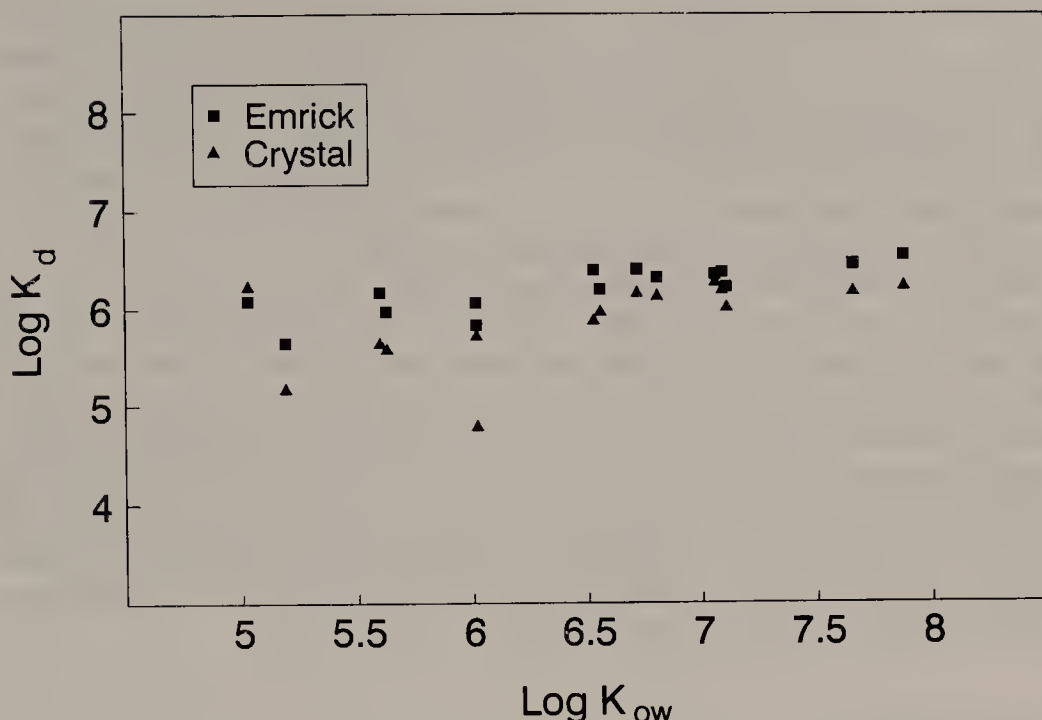


Figure 4.6. PCB congener distribution coefficients versus octanol-water partition coefficients, Crystal and Emrick Lakes, Wisconsin.¹⁶

also suggest poor correlations between PCB K_d values and the organic carbon content of surface water solids.^{3,11} The weak relationship between PCB partitioning and particulate organic matter may be due to the substantial spatial and temporal variability in organic matter composition and to the relative slow rates of sorption into the organic matter matrix. In short, the observed PCB distributions, while highly variable, are poorly explained by our current understanding of HOC-solid associations.

The presence of PCB-complexing colloids may explain the observed PCB partitioning data if colloids are abundant relative to filterable particles. This sampling artifact results in an overestimation of dissolved-phase PCB concentrations, with the error increasing for more hydrophobic congeners. If colloid and filterable particle concentration are proportional, this sampling artifact results in K_d values which appear to vary inversely with the concentration of filterable solids. Models that incorporate a "solids concentration effect" to mimic this observed behavior may greatly overestimate the actual dissolved-phase PCB concentrations, which may lead to erroneous estimates of HOC water column residence times and organismal exposure levels.

Recently, Swackhamer et al. have suggested an alternative explanation for the relative consistency in observed PCB distribution coefficients in surface waters.¹⁷ They demonstrate that the rate of uptake of PCB congeners by phytoplankton is slow relative to algal growth rates, and that therefore partitioning is not at equilibrium. They show that the more soluble PCB congeners

approach equilibrium more rapidly than do the highly chlorinated congeners ($\log K_{ow} > 7$). The lack of dependence of K_d on K_{ow} observed in surface water may result from particulate concentrations of the more hydrophobic congeners that are lower than their final, equilibrium values. If slow uptake kinetics are controlling PCB distributions in surface waters, then the measured dissolved phase concentrations of more hydrophobic HOCs are accurate and greater than predicted by equilibrium partitioning.

It is likely that both the colloid artifact and slow uptake kinetics are driving the observed partitioning behavior of PCBs in surface waters. While we cannot infer the relative importance of these two processes from the field-measured distribution coefficients, it is clear from the data compiled in this chapter that our current understanding of HOC-particle associations is insufficient to accurately model HOC distributions in natural waters. Improved methods for measuring dissolved HOC concentrations in natural waters and further characterization of the rates of HOC uptake and release by natural particles are necessary to further understand the distributions—and therefore aquatic behaviors—of these particle-reactive contaminants.

REFERENCES

1. Thibodeaux, L. J. "Theoretical Models for Evaluation of Volatile Emissions to Air During Dredged Material Disposal with Application to New Bedford Harbor, Massachusetts," U.S. Army Corps of Engineers Final Report, Contract No. DACW39-87-M-2487 (1989).
2. Baker, R. A. *Contaminants and Sediments* (Ann Arbor, MI: Ann Arbor Science, 1980).
3. Baker, J. E., P. D. Capel, and S. J. Eisenreich. "Influence of Colloids on the Sediment-Water Partition Coefficients of Polychlorobiphenyl Congeners in Natural Waters," *Environ. Sci. Technol.* 20:1136–1143 (1986).
4. Karickhoff, S. W., D. S. Brown, and T. A. Scott. "Sorption of Hydrophobic Pollutants on Natural Sediments," *Water Res.* 13:241–248 (1979).
5. Karickhoff, S. W. "Pollutant Sorption in Aquatic Systems," *J. Hydr. Div. ASCE* 110:707–735 (1984).
6. Chiou, C. T., L. J. Peters, and V. H. Freed. "A Physical Concept of Soil-Water Equilibria for Nonionic Organic Compounds," *Science* 206:831–832 (1979).
7. Gschwend, P. M., and S. C. Wu. "On the Constancy of Sediment-Water Partition Coefficients of Hydrophobic Organic Pollutants," *Environ. Sci. Technol.* 19:90–96 (1985).
8. Franz, T. P. "PCBs in Rural Minnesota Precipitation," MS Thesis, University of Minnesota, Minneapolis, MN (1990).
9. Capel, P. D., and S. J. Eisenreich. "PCBs in Lake Superior, 1978–1980," *J. Great Lakes Res.* 11:447–461 (1985).
10. Baker, J. E., and S. J. Eisenreich. "PCBs and PAHs as Tracers of Particle Dynamics," *J. Great Lakes Res.* 15:84–103 (1989).
11. Swackhamer, D. L., and D. E. Armstrong. "Distribution and Characterization of PCBs in Lake Michigan Water," *J. Great Lakes Res.* 13:24–36 (1987).

12. Lefkowitz, L. F. "The Particle-Mediated Fractionation of PCBs in Lake Michigan," MS Thesis, University of Wisconsin, Madison, WI (1987).
13. Swackhamer, D. L., and S. J. Eisenreich. "Intercomparison of Methodologies for Measuring PCBs in Particulate and Dissolved Phases in Green Bay Water," U.S. EPA Final Report, Grant R-005968-01, U.S. EPA Great Lakes National Program Office, Chicago, IL, 1989.
14. Lau, Y. L., B. G. Oliver, and B. G. Krishnappan. "Transport of Some Chlorinated Contaminants by the Water, Suspended Sediments, and Bed Sediments in the St. Clair and Detroit Rivers," *Environ. Tox. Chem.* 8:293-301 (1989).
15. Duinker, J. "The Determination of Polychlorinated Biphenyls in Open Ocean Waters," IOC Technical Series 26, UNESCO (1984).
16. Swackhamer, D. L. "The Role of Water-Particle Partitioning and Sedimentation in Controlling the Fate and Transport of PCBs in Lakes," PhD Dissertation, University of Wisconsin, Madison, WI (1985).
17. Skoglund, R. S., and D. L. Swackhamer, "Bioaccumulation of PCB Congeners by Algae," presented at the 31st Conference on Great Lakes Research, McMaster University, Hamilton, Ontario, 17-20 May 1988.

CHAPTER 5

The Role of Phytoplankton in the Partitioning of Hydrophobic Organic Contaminants in Water

Deborah L. Swackhamer and Robert S. Skoglund

INTRODUCTION

The fate and transport of hydrophobic organic compounds (HOCs) in aquatic systems are largely controlled by their association with particles. By definition, their hydrophobic nature drives them to partition from water to particulate matter in the water column. The source, transport, and fate pathways of the particulate matter thus controls the fate of the HOCs.

This particulate matter is a heterogeneous mixture—both biotic and abiotic in nature—that is derived from multiple sources and results in a diverse and dynamic particle size distribution. HOCs do not associate with all particles in a similar manner, preferring to sorb to particles high in organic carbon or lipid.¹ A large part of the particulate matter in the water column can be derived from primary production, consisting of both live and detrital phytoplankton. This material can range from 3 to 30% lipid by weight, and thus has a high affinity for HOCs. It can be consumed by higher trophic levels, can settle out and become incorporated into bottom sediments, or can be mineralized by heterotrophs in the recycling of nutrients. Thus, phytoplankton plays a crucial role in the fate of HOCs because it is the primary entrance of particulate-associated HOCs into the food chain, and because it can be a major removal mechanism of HOCs from the water column via sedimentation.

Hydrophobic organic compounds generally include those contaminants that have low solubilities (< 10 µg/L) and high octanol-water partition coefficients ($\log K_{ow} > 4$). Many of these compounds have chemical structures that are resistant to degradation, and thus they tend to accumulate in tissue lipids and bioaccumulate in food webs. Examples of HOCs are the polychlorinated biphenyls (PCBs); chlorinated pesticides, such as DDT and its metabolites, dieldrin, chlordane, toxaphene, and heptachlor and its epoxide; and industrial contaminants, such as hexachlorobenzene, polychlorinated dibenzo-*p*-dioxins (PCDDs), and polychlorinated dibenzofurans (PCDFs).

This chapter will provide an assessment of the role of phytoplankton in the overall fate of HOCs in water by integrating what is known about the association of HOCs and phytoplankton with current work being done in our laboratory. A discussion of the factors that control uptake, the mechanism of uptake, and the kinetics of uptake will be included.

METHODS

We have conducted experiments to determine the relative importance of sorbent and sorbate properties in controlling the bioaccumulation of HOCs by phytoplankton. Our experimental design also included time course studies to establish the kinetics of uptake. Under controlled laboratory conditions, single phytoplankton species in batch cultures were exposed to a mixture of 40 PCB congeners. This suite of compounds was chosen to represent HOCs in general and spanned a wide range of physical-chemical properties. Initial phytoplankton mass was 10 mg/L. A spike of PCB was added by acetone carrier, resulting in a total concentration of 7 ng/mL. Cultures were maintained at a specified temperature with a lighting regime of 16 hours light and 8 hours dark. Aliquots were taken at specified time intervals and separated into algal and media phases by centrifugation. Determinations of lipid, mass, and PCB concentrations were made on each aliquot.

PCBs were batch-extracted from the media with hexane and isolated by Soxhlet extraction of the biomass with 1:1 hexane-acetone. Surrogate standards were added prior to extraction to monitor extraction efficiencies in all samples and included congeners #14, #65, and #166 (3,5-di-, 2,3,5,6-tetra-, and 2,3,4,4',5,6-hexachlorobiphenyl, respectively). All extracts were cleaned by alumina and silica gel column chromatography. Columns contained 2–3 g anhydrous sodium sulfate over 7 g of 10% deactivated neutral alumina (80–200 mesh, activated at 450°C for 4 hr) over 1 g 6% deactivated silica gel (100–200 mesh, activated at 300°C for 4 hr) and were eluted with 3 × 15 mL hexane. Cleaned extracts were reduced in volume, received internal standards, and analyzed by capillary column gas chromatography (GC) with electron capture detection. The internal standards were congeners #30 (2,4,6-trichlorobiphenyl) and #204 (2,2',3,4,4',5,6,6'-octachlorobiphenyl). A Hewlett-Packard 5890 GC with 30 m × 0.25 mm capillary column, ^{63}Ni electron capture detector, autoinjector, and Waters-Millipore Maxima data system was used with the following conditions:

- injection port: 225°C
- carrier gas: H₂, 2 mL/min
- oven: programmed from 100 to 280°C at 1°/min
- makeup gas: 95%/5% argon in methane, 20 mL/min
- detector: 350°C

All quantitation was done by the internal standard method.

Field samples were collected by pumping water through sequential filters of differing pore size to isolate discrete size fractions of particulate matter, and isolating dissolved PCBs on XAD-2 resin. Complete details of sampling and analysis of samples from two remote Wisconsin lakes are detailed elsewhere.² Samples from Green Bay, Lake Michigan, were size-fractioned into > 102 µm (predominantly zooplankton), 10–102 µm (predominantly phytoplankton), and 0.7–10 µm (detritus, nannoplankton). Collections were made at two sites in April 1989, July 1989, and February 1990. Samples were extracted in the same manner as the laboratory samples and cleaned using a column containing fully activated alumina and anhydrous sodium sulfate, eluted with 3 × 15 mL of 2% dichloromethane in hexane. Extracts were analyzed on a 60-m DB-5 capillary column for all environmentally significant congeners after the method of Mullin,³ using the same chromatographic conditions as the laboratory samples.

FACTORS CONTROLLING PARTITIONING OF HOCs TO PHYTOPLANKTON

The equilibrium concentration of an HOC in phytoplankton can be described by the bioaccumulation factor (BAF), defined as the ratio of the HOC concentration in the phytoplankton (C_a , ng/kg, dry weight) and the HOC concentration dissolved in the surrounding water ($C_{w,d}$, ng/L), expressed in equivalent units (L/kg):

$$\text{BAF} = C_a/C_{w,d}$$

The BAF is often normalized to the fraction lipid in the phytoplankton, analogous to the organic carbon-normalized water-particle partition coefficient, K_{oc} .¹

Many researchers have reported BAFs for a variety of HOCs taken up by different species of phytoplankton. A compilation of earlier reviews^{4,5} and more recently published values is provided in Table 5.1. All BAFs are reported in terms of wet weight, using a dry weight conversion factor of 5.5 where needed.⁶ All of these data were laboratory generated, using axenic cultures in most cases. Equilibration times ranged from 1 hour to 3 days. Differences in these reported BAFs can be seen for different compounds and for different species, as well as among species for the same compound. These variations can be attributed to differences in compound properties, differences in surface and lipid properties of the phytoplankton, differences in experimental protocols among laboratories (e.g., equilibration times, analytical methodologies), and kinetic considerations.

The physical-chemical properties of the compounds that may affect uptake

Table 5.1. BAF (Wet Weight) for a Variety of HOCs and Phytoplankton Species

Chemical	Phytoplankton Species	BAF	Reference
DDT	<i>Selenastrum capricornutum</i>	12,000	13
DDT	<i>Syracosphaera carterae</i>	25,000	36
DDT	<i>Amphidirium carteria</i>	80,000	36
DDT	<i>Thalassiosira fluviatilis</i>	25,000	36
DDT	<i>Ankistrodesmus</i>	61,600	19
Aldrin	<i>Anabaena cylindrica</i>	1,300	37
Aldrin	<i>Chlorella</i>	12,600	16
Aldrin	<i>Chlorella</i>	12,300	12
Dieldrin	<i>Anabaena cylindrica</i>	200	37
Dieldrin	<i>Scenedesmus</i>	233 ^a	28
Dieldrin	<i>Benthic algae</i>	1000–300,000	38
Dieldrin	<i>Ankistrodesmus</i>	32,000	19
Toxaphene	<i>Chlorella pyrenoidosa</i>	11,000	39
Phenanthrene	<i>Selenastrum</i>	4,362 ^a	11
Pyrene	<i>Selenastrum</i>	6,601 ^a	11
Mirex	<i>Dunaliella tertiolectra</i>	4,100	40
PCBs	<i>Chlorella</i>	16,000	41
PCBs	Centric marine diatoms	65,500–255,000 ^a	24
PCBs-1254	Nat. assemblage— <i>Skeletomema</i>	20,000	23
PCBs-1254	Nat. assemblages in field	40,000	23
PCBs-1254	<i>Dunaliella</i>	30,000	42
Biphenyl	<i>Chlorella</i>	540	16
2-PCB	<i>Chlorella</i>	2,700	16
2-PCB	<i>Chlorella fusca</i>	4,980	21
3-PCB	<i>Chlorella</i>	8,960	16
4-PCB	<i>Selenastrum</i>	3,300 ^a	32
4-PCB	<i>Chlorella</i>	4,776	22
5-PCB	<i>Chlorella</i>	11,500	16
5-PCB	<i>Selenastrum</i>	1,800 ^a	32
5-PCB	<i>Chlorella</i>	9,530	21
6-PCB	<i>Scenedesmus quadricauda</i>	82	29
6-PCB	<i>Selenastrum capricornutum</i>	12,000	13
6-PCB	<i>Selenastrum</i>	10,000–1,000,000	32
6-PCB	<i>Fragilaria crotonensis</i>	18,000–55,000	9
6-PCB	<i>Ankistrodesmus folcatus</i>	110,000–220,000	9
6-PCB	<i>Microcystis sp.</i>	10,000–1,000,000	9
6-PCB	<i>Microcystis sp.</i>	10,000–1,000,000	31
6-PCB	<i>Microcystis sp.</i>	18	29
6-PCB	<i>Cyclotella</i>	450	29
6-PCB	<i>Chlorella</i>	10,000	22
8-PCB	<i>Chlorella</i>	10,700	22
10-PCB	<i>Chlorella</i>	8,670	22

^aAssume dry weight/5.5 = wet weight (see Hansen⁶).

by phytoplankton include the octanol-water partition coefficient (K_{ow}), aqueous solubility (S), molecular weight, steric configuration, molar volume, and parachor (molar volume corrected for surface tension). The phytoplankton properties that may be important include lipid fraction, lipid class distribution, surface area, surface type, growth, and excretion rate. The relative importance of these factors is dependent on the mechanism of the HOC uptake by phytoplankton. The possible mechanisms and the associated factors that would be most important are listed in Table 5.2.

Table 5.2. Possible Mechanisms for HOC Bioaccumulation by Phytoplankton and Factors Associated with Those Mechanisms

	Factors	
	Compound Properties	Phytoplankton Properties
Thermodynamic lipid-water partitioning	K_{ow} S	lipid fraction lipid composition
Surface sorption	S	surface area surface type
Active metabolic uptake	assimilation efficiency exudate binding constant	uptake rate excretion rate
Multistep mechanism	K_{ow} S steric effects	lipid fraction surface area surface type

Mechanism of Uptake

The most commonly held theory is that the partitioning of HOCs between the lipids of the organism and the dissolved aqueous phase is a thermodynamic process that is driven by the concentration or fugacity gradient between the phases.⁷ Thus, at equilibrium it follows that for lipophilic compounds the BAF should be directly proportional to the K_{ow} of the compound and indirectly proportional to the aqueous solubility.^{7,8} Differences among species in BAFs for a given compound should be eliminated by normalization of the BAF to fraction lipid. However, Lederman and Rhee report that differences in BAFs for three genera of phytoplankton were not eliminated by lipid normalization in laboratory experiments.⁹ These results may be due to compositional differences in lipids, or to differences in the rates of uptake among genera, since the experiments were not taken to equilibrium.

Several researchers have reported a correlation between the log of the lipid-normalized BAF and $\log K_{ow}$.¹⁰⁻¹³ Fugacity theory suggests that BAF and K_{ow} are directly correlated, and that the slope of the regression of the log transformed values should be one.⁷ Mailhot reported that hydrocarbon BAFs correlated most strongly with the HPLC capacity factor and K_{ow} than with other physical-chemical properties such as parachor, molar volume, connectivity index, or solubility.¹³ These and other relationships are described in Table 5.3. This supports the thermodynamic lipid-partitioning mechanism. Note that in all cases the slope of the line is less than the hypothetical value of one,⁷ suggesting a lack of equilibrium. Field-measured phytoplankton BAFs from two small Wisconsin lakes and from several sites in the Great Lakes failed to show a relationship between BAF and K_{ow} for PCBs (see below).² Our laboratory has tested this hypothesis using 40 PCB congeners with a range of $\log K_{ow}$'s from 4 to 9 in axenic cultures of *Scenedesmus* sp. For congeners with $\log K_{ow}$ less than 7, we obtained a strong relationship between BAF and K_{ow} (Table 5.3 and Figure 5.1) at or near equilibrium

Table 5.3. Relationships between Phytoplankton BAFs and Physical-Chemical Properties

Equation	n	r ²	Species	Reference
$\log \text{BAF} = 0.36 \log K_{\text{ow}} + 2.1$	7	0.81	<i>Selenastrum capricornutum</i>	13
$\log \text{BAF} = 0.68 \log K_{\text{ow}} + 0.16$	41	0.81	<i>Chlorella</i>	12
$\log \text{BAF} = 0.7 \log K_{\text{ow}} - 0.26$	8	0.93	<i>Scenedesmus</i>	10
$\log \text{BAF} = 0.46 \log K_{\text{ow}} + 2.36$	8	0.83	<i>Selenastrum</i>	11
$\log \text{BAF} = 0.78 \log K_{\text{ow}} + 3.4$	40	0.84	<i>Scenedesmus</i>	this study
$\log \text{BAF} = -0.46 \log S + 4.55$	34	0.77	<i>Chlorella</i>	16
$\log \text{BAF} = 0.86 \log k' + 2.9^a$	28	0.89	<i>Selenastrum</i>	13

^ak' = HPLC capacity factor.

(see below). An explanation for the apparent differences between field and laboratory data will be offered below.

The type of lipids in the organism may also affect the BAF. Different classes of lipids may have different binding constants, which would increase or decrease the BAF as a function of lipid composition. No work has been done on phytoplankton at this time to elucidate this question. Recent work on binding of benzo(a)pyrene to different lipid classes in benthic invertebrates did not indicate any difference in binding coefficients.¹⁴

Uptake of HOCs by phytoplankton may be simple surface sorption, which would be affected by the hydrophobicity of the compound (1/S) and by the area and type of cell surface available for sorption. The log BAF has been

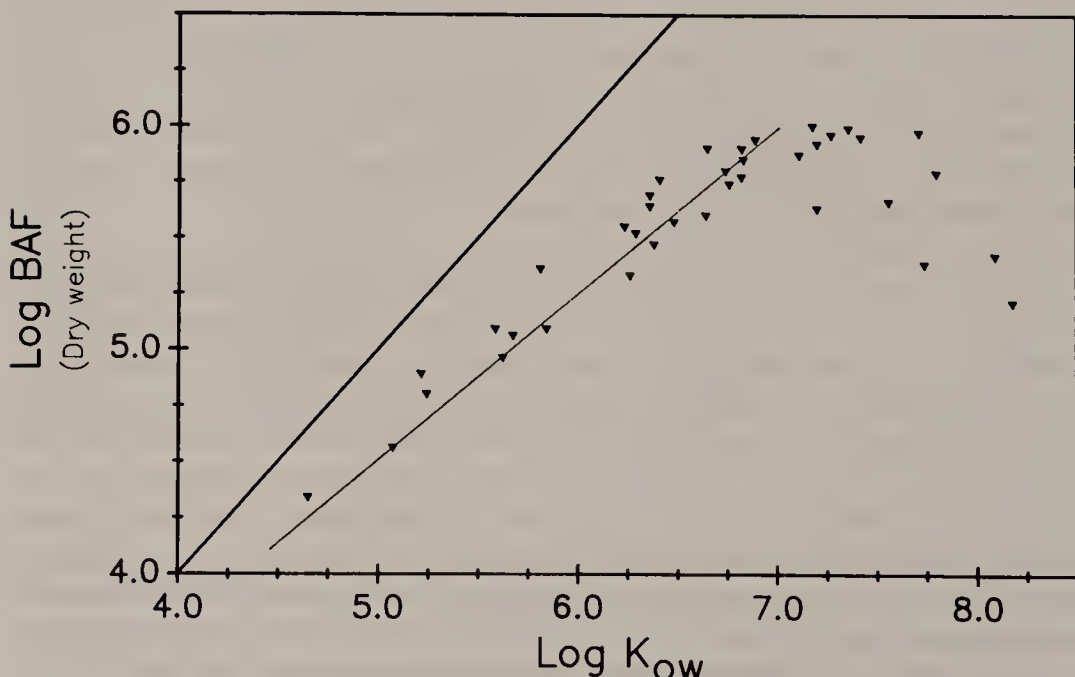


Figure 5.1. Relationship of log BAF vs log K_{ow} (from Hawker and Connell⁴³) under low-growth conditions (0.03 day^{-1}) after 20 days exposure to 40 PCB congeners. For congeners with $\log K_{\text{ow}} < 7$, $r^2 = 0.84$ and slope = 0.78. Reference line has a slope of 1.0.

reported to be inversely related to aqueous solubility.^{4,15,16} An inverse relationship between BAF and cell size (i.e., direct relationship between BAF and surface area) has been reported by Rice and Sikka¹⁷ and Hiraizumi et al.,¹⁸ although the interpretation of the 1973 data was questioned by Neudorf and Khan.¹⁹ Lederman and Rhee found that the uptake of a hexachlorobiphenyl by the filamentous diatom *Fragilaria* increased significantly when the filamentous chains were broken up by sonication, increasing the surface area available for sorption.⁹ The authors were careful to point out, however, that this difference may have been due to alterations of the cells by the sonication treatment.

Surface sorption would be affected by characteristics of the surface. Hansen studied the uptake of lindane by two species of *Chlorella* having different surface types.⁶ *C. pyrenoidosa* had a gelatinous surface, while *Chlorella* sp. did not. The uptake of lindane by *C. pyrenoidosa* was significantly enhanced in uptake experiments over 3 days. This supports the mechanism of surface sorption, with increased uptake by the more organic-rich surface offered by *C. pyrenoidosa*. Lederman and Rhee conducted a series of well-conceived experiments on the absorption and desorption of ¹⁴C-2,2',4,4',5,5'-hexachlorobiphenyl by the diatom *Fragilaria*.⁹ The study design included experiments with live cells, heat-killed cells, acid-killed cells stripped of mucilage, and frustules only. Although their experiments did not reach equilibrium in some cases, differences in uptake over time were observed. The uptake for mucilage-stripped cells was approximately two times less than for the other treatments. Frustules alone showed approximately 30% less uptake in the first 60 min, with no further significant uptake after that. These experiments indicate that surface type is important, especially in the initial period of uptake, but that it is not the only factor controlling uptake. Field measurements of PCB concentrations in phytoplankton from two Wisconsin lakes suggested that the BAFs were lower when the community was dominated by diatoms than by nondiatoms.²

The question of whether there is active metabolic uptake of HOCs by phytoplankton has been approached by conducting uptake experiments with live and dead cells, both heat-killed and chemically treated; all of the investigators concluded that uptake was a passive process. Several studies found no difference in uptake of HOCs by live vs dead cells.^{17,20,21} In several other cases dead cells had greater BAFs than live cells.^{9,17,22,23} Rice and Sikka found that five of six test species showed no difference in DDT bioaccumulation with live and dead cells, but that dead *Amphidinium* took up 2 to 2.5 times greater DDT than live cells.¹⁷ The increase in uptake by dead cells may be due to greater loss by excretion by live cells,²³ or by cellular alterations by the treatments used to kill the cells.⁹

A two-step mechanism involving an initial surface sorption followed by a transfer to the lipid complex in the cell has been suggested.^{21,24} Experiments by Harding and Phillips indicated that PCBs reached sensitive sites within the cell that disrupted the cellular photosynthetic apparatus within hours of

exposure.²⁴ Wang et al. washed exposed cells with solvent and found that the extraction of a PCB congener decreased from 96% initially to 74% after 48 hr and concluded that the PCB had been transferred into, and stabilized by, the cell matrix.²¹ The experiments by Lederman and Rhee discussed above, which compared uptake by diatoms vs frustules only, are consistent with this proposed mechanism.⁹ Experiments in our laboratory support this mechanism.²⁵ Uptake of PCB congeners was initially rapid (hours), plateaued for up to 24 hr, followed by a much slower increase in PCB over time (days to weeks). A more detailed discussion of the kinetics of uptake is included below.

Transport across, or incorporation into, cell membranes may be affected by molecular size and shape.²⁶ Our laboratory has conducted experiments designed to determine the effect of molecular configuration on the uptake of PCB congeners. The BAFs were measured for a series of tetrachlorinated biphenyls having from zero to four chlorines in the *ortho* position. Chlorines not in the *ortho* position were in the *meta* position. An increase in the number of *ortho* chlorines causes an increase in the nonplanarity of the molecule. There was a strong inverse relationship between the log BAF and the number of *ortho* chlorines, as shown in Figure 5.2. The differences are not explained by the log K_{ow} 's of the compounds, which differ by less than an order of magnitude. These results are consistent with other reports in the literature that indicate that bioaccumulation is strongly influenced by the planarity of the molecule (e.g., preferential 2,3,7,8-tetrachlorinated dioxin uptake by carp²⁷).

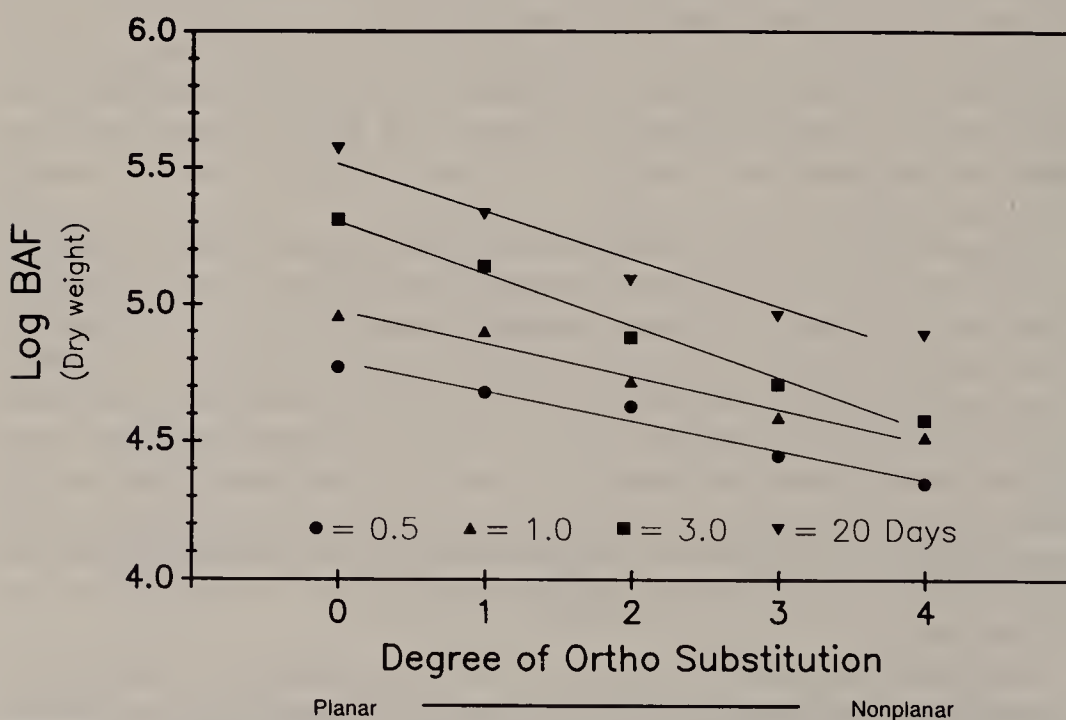


Figure 5.2. Relationship of log BAF vs number of *ortho* chlorines for five tetrachlorinated biphenyls at four time points, under low-growth conditions.

"Bulkier" molecules may have more resistance to transfer across structured membranes, so that bioaccumulation is controlled by more than lipid content only.

KINETIC CONSIDERATIONS

Most earlier reports have concluded that equilibrium between HOCs and phytoplankton was achieved within hours.^{4,6,12,17,20,28,29} There are no published uptake experiments lasting more than 3 days. However, Neudorf and Khan¹⁹ and Wang et al.²¹ noted that their BAFs were still increasing slowly with time at the end of their experiments (3 and 28 hr, respectively), indicating a lack of equilibrium.

Experiments were carried out in this laboratory for up to 20 days under conditions where algal growth was minimized by temperature (0.03 day^{-1}) and under normal growth conditions (0.13 day^{-1}). Under low-growth conditions, the BAFs for congeners with $\log K_{ow} < 7$ were related to $\log K_{ow}$ (Figure 5.1). However, the BAF values increased continually over the time frame of the experiment, with most congeners not reaching equilibrium even after 20 days of exposure. The rate of uptake was rapid initially, with 40–90% of the uptake occurring in the first 24 hr. Uptake then appeared to level off, then gradually began to show a small, but steady, increase that continued throughout the experiment. This is highly consistent with the two-step mechanism for bioaccumulation in phytoplankton. It is our belief that previous investigators misinterpreted the decrease in the initial uptake rate of their experiments as equilibrium, and terminated the exposures before observing the slow but continued uptake. Our observed BAFs at 24 hr are similar to those reported in the literature, but the BAFs after 30 days exposure are considerably greater. We conclude that the overall uptake kinetics are considerably slower than previously believed. For congeners with $\log K_{ow} > 7$, there was no direct relationship between BAF and K_{ow} . Since their BAFs continually increased over the course of the experiment, it is possible that they might eventually reach their K_{ow} -defined equilibrium value. It is also possible that their size, shape, or both caused a significant resistance to transfer into the cell matrix.

Different results were obtained when cultures were maintained under typical growth conditions. For most congeners, the log BAFs were independent of the $\log K_{ow}$'s (Figure 5.3). BAFs were lower for normal-growth conditions than for low-growth conditions. These experiments indicate that growth is a major factor controlling the uptake of HOCs by phytoplankton, and may be more important than K_{ow} under nonequilibrium conditions. For growth conditions typical of the Great Lakes ($0.06\text{--}0.60\text{ day}^{-1}$),³⁰ it is likely that equilibrium would not be reached.

The effect of growth may be a decrease in uptake of HOCs due to a contin-

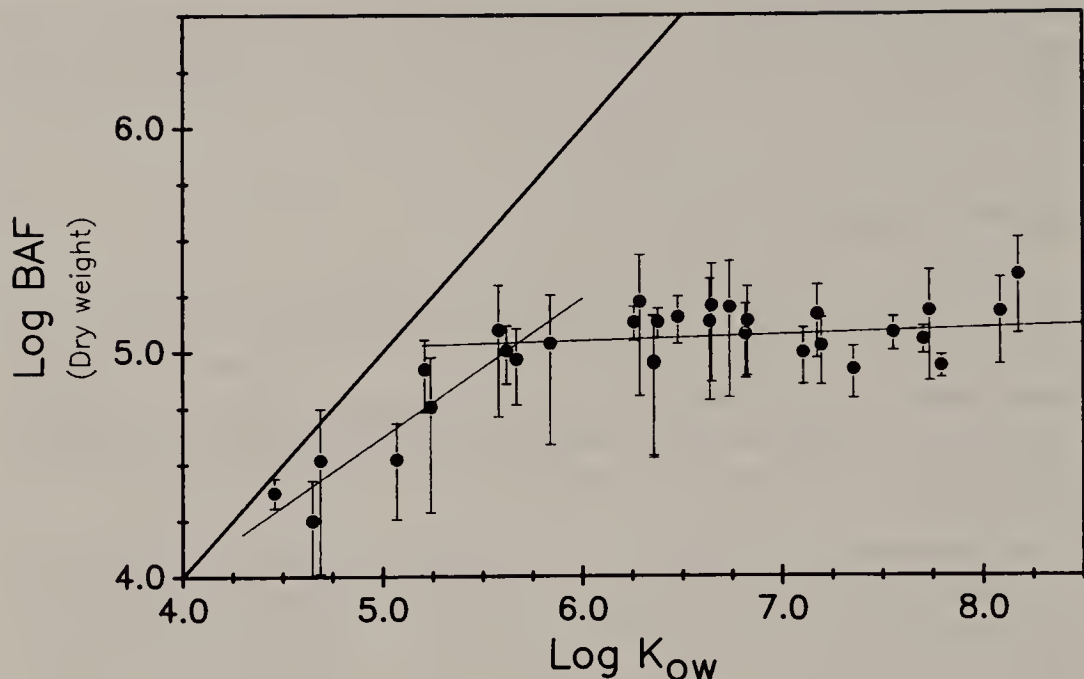


Figure 5.3. Relationship of log BAF vs log K_{ow} under normal-growth conditions (0.13 day^{-1}) for 40 PCB congeners. Data are averages of all time points between 8 and 30 days throughout the exposure period; error bars are 1 standard deviation. For congeners with $\log K_{ow} > 5$, slope is not statistically different from zero.

ual dilution of the biomass, or an increase in the elimination of HOCs, related to an increase in excretion of extracellular products resulting from increased cellular metabolism. This elimination pathway may be enhanced as a function of HOC exposure.³¹ It has been reported that excretion of glycolates by *Selenastrum* was increased concurrently with an increase in photosynthesis, with no net change in growth at certain concentrations of DDT.³² However, the importance of this elimination depends on the magnitude of the association constants of the HOC and phytoplankton exudates, which are currently unknown.

Desorption of HOCs from phytoplankton has not been studied as much as uptake. Despite differences in experimental design, phytoplankton species, and experimental compounds under consideration, all reports agree that there is a hysteresis effect, with the desorption kinetics being significantly slower than the sorption kinetics.^{9,20,24,29}

The importance of kinetics in algal uptake of HOCs that is indicated in our laboratory experiments is also borne out in field observations. Figure 5.4 shows measured BAFs for different size fractions of particulate matter in the water column of Emrick Lake, Wisconsin, as a function of K_{ow} for selected PCB congeners. These data were obtained during summer when growth would be expected to be high. The 10-to 50- μm size fraction, consisting of phytoplankton biomass as confirmed by microscopic analysis, shows a

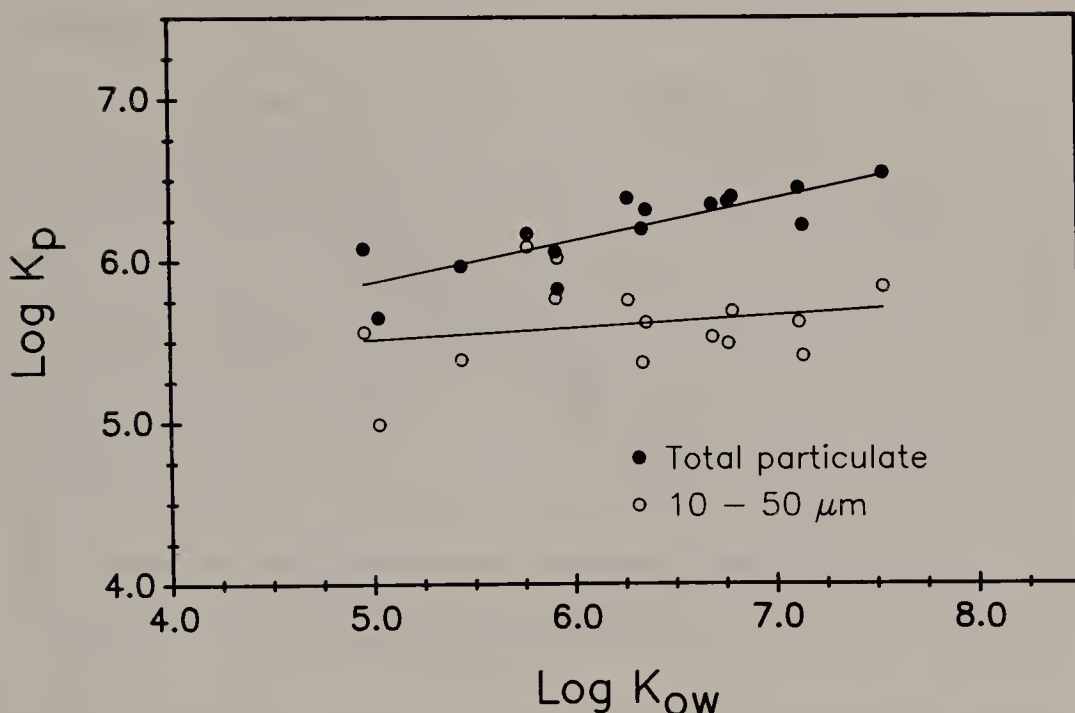


Figure 5.4. Relationship of $\log K_p$ vs $\log K_{ow}$ for total water column particulate matter (slope = 0.26, $r^2 = 0.66$) and the phytoplankton size fraction (10–50 μm , slope = 0.08, $r^2 = 0.04$) in Emrick Lake, WI.

weak BAF- K_{ow} relationship. The other size fractions, consisting of zooplankton and detritus, show a strong BAF- K_{ow} relationship. These data are interpreted as indicating that PCBs have not reached equilibrium with phytoplankton from these lakes during this time period.

Similar field samples have been collected from Green Bay, Lake Michigan, during spring, summer, and winter months of 1989–1990. The results for spring and summer were very similar, and different from the winter results. The relationship of the BAFs to K_{ow} are shown in Figure 5.5. The results from the spring and summer sampling are similar to the earlier results from the Wisconsin lakes and show a poor relationship of BAF to K_{ow} . These data look remarkably similar to the laboratory experimental data under normal-growth conditions, where phytoplankton growth prevented equilibrium from being reached. In contrast, the winter data show a very strong relationship of BAF to K_{ow} , which is similar to the laboratory results under low-growth conditions. This is consistent with the minimal-growth conditions expected in Green Bay during ice cover, where both light and temperature would be limiting. This research is leading us to develop a dynamic model for predicting phytoplankton bioaccumulation of HOCs as a function of phytoplankton growth rate and K_{ow} .

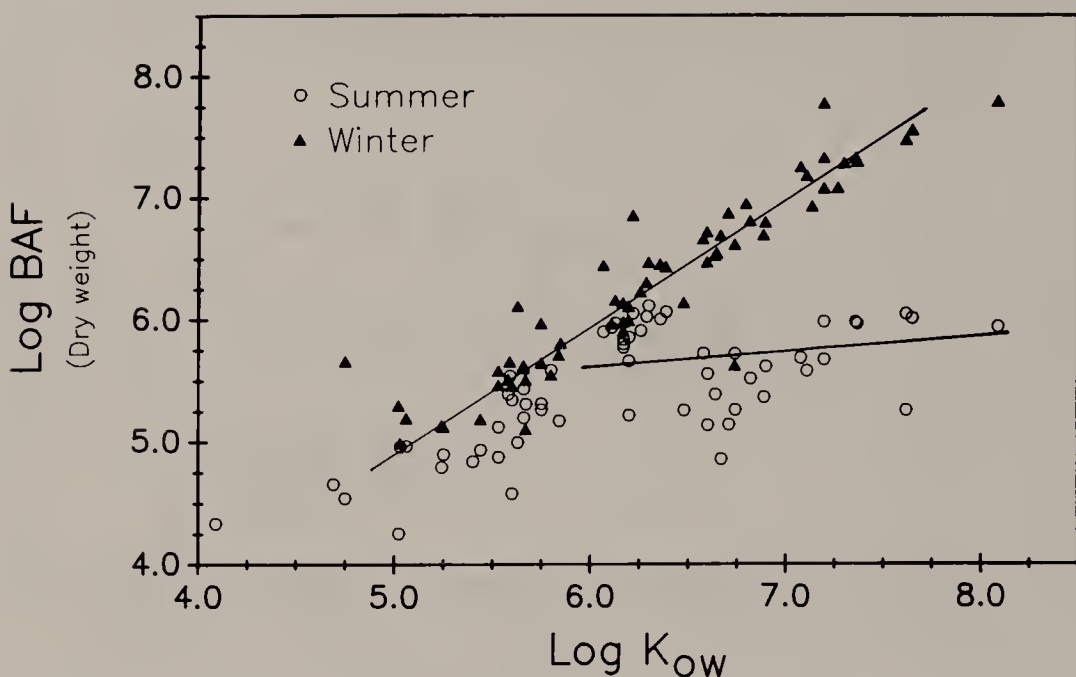


Figure 5.5. Relationship of log BAF vs log K_{OW} for winter (slope = 0.93, r^2 = 0.86) and summer (slope = 0.40, r^2 = 0.46) field collections of phytoplankton size fraction (10–102 μm) in Green Bay, Lake Michigan.

FATE OF HOCs BY PHYTOPLANKTON

The algal composition is a determining factor in HOC fate. In the Great Lakes, the biomass is thought to be dominated by nannoplankton (< 20 μm).^{33,34} Their high rates of production and high levels of excretion may limit HOC concentrations during productive periods. On the other hand, their large surface-area:volume ratio may promote uptake. The role of nannoplankton in HOC fate is largely unexplored and requires future attention.

HOCs associated with nannoplankton may be more available to the food chain because zooplankton grazing generally favors the smaller forms of phytoplankton.³⁵ They also have slower settling velocities than larger phytoplankton, leading to longer residence times in the water column. The rates of phytoplankton production relative to zooplankton grazing can also determine the importance of food-chain transfer compared to sedimentation. High grazing rates in areas of low primary production, such as open waters, may favor HOC transfer to the food chain; in areas of high productivity with moderate grazing pressure, transfer to sediments may dominate HOC fate over food-chain uptake. More information is needed on temporal phytoplankton compositions and size distributions, production and grazing rates, and settling velocities, to form a complete context to evaluate HOC fate in the field.

SUMMARY

Phytoplankton play a critical role in controlling the fate of HOCs in the water column because they are high in lipids and because they serve as the base of the food chain and as vectors for transport to the bottom sediments. The relative importance of these pathways in a given system is dependent on species composition and characteristics of the food chain. Previous studies that demonstrate a relationship of BAF to K_{ow} and to phytoplankton surface properties, as well as the data presented here, support the hypothesis that the mechanism of HOC uptake is a rapid surface sorption followed by a slower transfer into lipids in the cell matrix. Our work on the kinetics of uptake indicates that equilibrium is reached slowly and that the rate of uptake is of a similar magnitude as phytoplankton growth under normal field conditions. Thus, a critical factor that controls the bioaccumulation of HOCs is the growth rate of the phytoplankton itself. It is unlikely that HOCs reach equilibrium in phytoplankton during normal growth periods, therefore indicating that models used to predict HOC concentrations in phytoplankton must use a dynamic approach.

ACKNOWLEDGMENTS

This research has been funded, in part, by the Minnesota Sea Grant College Program supported by the NOAA Office of Sea Grant, Department of Commerce, under grant no. NO86AA-D-SG112; by grant no. RO-05028, from the U.S. Environmental Protection Agency, Great Lakes National Program Office, Chicago, IL; and by BRSG 507 RR 055448, awarded by the Biomedical Research Support Grant Program, Division of Research Resources, National Institute of Health. We thank Karen Brademeyer for preparation of the manuscript.

REFERENCES

1. Karickhoff, S. W., D. S. Brown, and T. A. Scott. "Sorption of Hydrophobic Pollutants on Natural Sediments," *Water Res.* 13:241-248 (1979).
2. Swackhamer, D. L. "The Role of Water Particle Partitioning and Sedimentation in Controlling the Fate and Transport of PCBs in Lakes," PhD Thesis, University of Wisconsin, Madison, WI (1985).
3. Mullin, M. Workshop on Analysis of PCB Congeners, Grosse Ile, MI (1985).
4. Baughman, G. L., and D. F. Paris. "Microbial Bioconcentration of Organic Pollutants from Aquatic Systems—A Critical Review," *CRC Crit. Rev. Microbiol.* 1:205-228 (1981).
5. Butler, G. L. "Algae and Pesticides," *Residue Rev.* 66:19-61 (1977).
6. Hansen, P.-D. "Experiments on the Accumulation of Lindane (τ -BHC) by the Primary Producers *Chlorella* spec. and *Chlorella pyrenoidosa*," *Arch. Environ. Contam. Toxicol.* 8:721-731 (1979).

7. Mackay, D. "Correlation of Bioconcentration Factors," *Environ. Sci. Technol.* 13:1218-1223 (1982).
8. Chiou, C. T. "Partition Coefficients of Organic Compounds in Lipid-Water Systems and Correlations with Fish Bioconcentration Factors," *Environ. Sci. Technol.* 19:57-62 (1985).
9. Lederman, T. C., and G.-Y. Rhee. "Bioconcentration of Hexachlorobiphenyl in Great Lake Planktonic Algae," *Can. J. Fish. Aquat. Sci.* 39:380-387 (1982).
10. Ellgehausen, H., J. A. Guth, and H. O. Esser. "Factors Determining the Bioaccumulation Potential of Pesticides in the Individual Compartments of Aquatic Food Chains," *Ecotoxicol. Environ. Saf.* 4:134-157 (1980).
11. Casserly, D. M., E. M. Davis, T. D. Downs, and R. K. Guthrie. "Sorption of Organics by *Selenastrum capricornutum*," *Water Res.* 17:1591-1594 (1983).
12. Geyer, H., G. Politzki, and D. Freitag. "Prediction of Ecotoxicological Behaviour of Chemicals: Relationship between *n*-Octanol/Water Partition Coefficient and Bioaccumulation of Organic Chemicals by Alga *Chlorella*," *Chemosphere* 13:269-284 (1984).
13. Mailhot, H. "Prediction of Algal Bioaccumulation and Uptake Rate of Nine Organic Compounds by Ten Physicochemical Properties," *Environ. Sci. Technol.* 21:1009-1013 (1987).
14. Gardner, W. S., P. F. Landrum, and J. F. Cavaletto. "Lipid Partitioning and Deposition of Benzo[a]pyrene and Hexachlorobiphenyl in Lake Michigan *Pontoporeia hoyi* and *Mysis relicta*," *Environ. Toxicol. Chem.* 9:1269-1278 (1990).
15. Korte, F., D. Freitag, H. Geyer, W. Klein, A. G. Kraus, and E. Lahaniatis. "Ecotoxicology Profile Analysis. A Concept for Establishing Ecotoxicologic Priority Lists for Chemicals," *Chemosphere* 7:79-102 (1978).
16. Geyer, H., R. Viswanathan, D. Freitag, and F. Korte. "Relationship between Water Solubility of Organic Chemicals and Their Bioaccumulation by the Alga *Chlorella*," *Chemosphere* 10:1307-1313 (1981).
17. Rice, C. P., and H. C. Sikka. "Uptake and Metabolism of DDT by Six Species of Marine Algae," *J. Agr. Food Chem.* 21:148-152 (1973).
18. Hiraizumi, Y., M. Takahashi, and H. Nishimura. "Adsorption of Polychlorinated Biphenyl onto Sea Bed Sediment, Marine Plankton, and Other Adsorbing Agents," *Environ. Sci. Technol.* 13:580-584 (1979).
19. Neudorf, S., and M. A. Q. Khan. "Pick-Up and Metabolism of DDT, Dieldrin and Photodieldrin by a Fresh Water Alga (*Ankistrodesmus amalloides*) and a Microcrustacean (*Daphnia pulex*)," *Bull. Environ. Contam. Toxicol.* 13:443-450 (1975).
20. Sodergren, A. "Uptake and Accumulation of ¹⁴C-DDT by *Chlorella* sp. (Chlorophyceae)," *Oikos* 19:126-131 (1968).
21. Wang, K., B. Rott, and F. Korte. "Uptake and Bioaccumulation of Three PCBs by *Chlorella fusca*," *Chemosphere* 11:525-530 (1982).
22. Urey, J. C., J. C. Kricher, and J. M. Boylan. "Bioconcentration of Four Pure PCB Isomers by *Chlorella pyrenoidosa*," *Bull. Environ. Contam. Toxicol.* 16:81-85 (1976).
23. Biggs, D. C., C. D. Powers, R. G. Rowland, H. B. O'Connors, Jr., and C. F. Wurster. "Uptake of Polychlorinated Biphenyls by Natural Phytoplankton Assemblages: Field and Laboratory Determinations of ¹⁴C-PCB Particle-Water Index of Sorption," *Environ. Poll.* 22:101-110 (1980).
24. Harding, L. W., Jr., and J. H. Phillips, Jr. "Polychlorinated Biphenyls: Transfer

- from Microparticulates to Marine Phytoplankton and the Effects on Photosynthesis," *Science* 202:1189-1191 (1978).
25. Swackhamer, D. L., and R. S. Skoglund. Submitted for publication.
 26. Shaw, G. R., and D. W. Connell. "Physicochemical Properties Controlling Polychlorinated Biphenyl (PCB) Concentrations in Aquatic Organisms," *Environ. Sci. Technol.* 18:18-23 (1984).
 27. Keuhl, D. W., P. M. Cook, A. R. Batterman, D. B. Lothenbach, B. C. Butterworth, and D. L. Johnson. "Bioavailability of 2,3,7,8-Tetrachlorodibenzo-p-dioxin from Municipal Incinerator Flyash to Freshwater Fish," *Chemosphere* 14:427-437 (1985).
 28. Reinert, R. E. "Accumulation of Dieldrin in an Alga (*Scenedesmus obliquus*), *Daphnia magna*, and the Guppy (*Poecilia reticulata*)," *J. Fish. Res. Bd. Can.* 29:1413-1418 (1972).
 29. Autenrieth, R. L. "Sorption and Desorption Partition Characterization of Selected Organochlorine Compounds with Phytoplankton," PhD Thesis, Clarkson University, Potsdam, NY (1986).
 30. Fahnstiel, G. L., and D. Scavia. "Dynamics of Lake Michigan Phytoplankton: Primary Production and Growth," *Can. J. Fish. Aquat. Sci.* 44:499-508 (1987).
 31. Gotham, I. J., and G.-Y. Rhee. "Effect of a Hexachlorobiphenyl and Pentachlorophenol on Growth and Photosynthesis of Phytoplankton," *J. Great Lakes Res.* 8:328-335 (1982).
 32. Rhee, G.-Y. "Persistent Toxic Substances and Phytoplankton in the Great Lakes," in *Toxic Contaminants and Ecosystem Health: A Great Lakes Focus*, M.S. Evans, Ed. (New York: John Wiley and Sons, 1988), pp. 513-526.
 33. Munawar, M., I. F. Munawar, L. R. Chip, and G. Dupuis. "Relative Importance of Nannoplankton in Lake Superior Biomass and Community Metabolism," *J. Great Lakes Res.* 4:462-480 (1978).
 34. Fahnstiel, G. L., L. Sicko-Goad, D. Scavia, and E. F. Stoermer. "Importance of Picoplankton in Lake Superior," *Can. J. Fish. Aquat. Sci.* 43:235-240 (1986).
 35. Porter, K. C. "Selective Grazing and Differential Digestion of Algae by Zooplankton," *Nature* 244:179-180 (1973).
 36. Cox, J. L. "Low Ambient Level Uptake of ¹⁴C-DDT by Three Species of Marine Phytoplankton," *Bull. Environ. Contam. Toxicol.* 5:218 (1970).
 37. Schauberger, C. W., and R. B. Wildman. "Accumulation of Aldrin and Dieldrin by Blue-Green Algae and Related Effects on Photosynthetic Pigments," *Bull. Environ. Contam. Toxicol.* 17:534 (1977).
 38. Rose, F. L., and C. D. McIntire. "Accumulation of Dieldrin by Benthic Algae in Laboratory Streams," *Hydrobiologia* 35:481 (1970).
 39. Paris, D. F., D. L. Lewis, and J. T. Barnett. "Bioconcentration of Toxaphene by Microorganisms," *Bull. Environ. Contam. Toxicol.* 17:564 (1977).
 40. Hollister, R. A., G. E. Walsh, and J. Forester. "Mirex and Marine Unicellular Algae: Accumulation, Population Growth, and Oxygen Evolution," *Bull. Environ. Contam. Toxicol.* 10:753 (1975).
 41. Sodergren, A. "Accumulation and Distribution of Chlorinated Hydrocarbons in Cultures of *Chlorella pyrenoidosa* (Chlorophyceae)," *Oikos* 22:215-220 (1971).
 42. Scura, E. D., and G. H. Theilacker. "Transfer of the Chlorinated Hydrocarbon PCB in a Laboratory Marine Food Chain," *Mar. Biol.* 40:317-325 (1977).
 43. Hawker, D. W., and D. W. Connell. "Octanol-Water Partition Coefficients of Polychlorinated Biphenyl Congeners," *Environ. Sci. Technol.* 22:382-397 (1988).

CHAPTER 6

Quantification and Characterization of Pore-Water Organic Colloids

Yu-Ping Chin, Ann P. McNichol, and Philip M. Gschwend

INTRODUCTION

Many marine and freshwater sediment beds are heavily polluted by hydrophobic organic contaminants (HOCs). In some coastal marine waters, such as Boston and New Bedford Harbors (Massachusetts), elevated levels of polycyclic aromatic hydrocarbons (PAH) and polychlorinated biphenyls (PCBs), respectively, have been found in sediments.^{1,2} Efforts currently under way to reduce or eliminate the point source discharges of these substances into receiving waters include the upgrading of municipal and industrial treatment facilities and the relocation of outfalls to offshore sites. Unfortunately, the organic pollutants currently in the sediments may continue to be harmful to aquatic organisms at all trophic levels for decades to come, even after major steps have been taken to limit further chemical inputs.

Hydrophobic organic pollutants are particle reactive and transported to the sediment bed from the water column by association with sinking detrital matter. In an undisturbed environment, the main mode of pollutant transport back to the water column is by molecular diffusion, hindered by the tortuosity of the sediment bed and processes such as sorption. Such transport is slow, and one would anticipate yearly fluxes of contaminants back into the water column to be small. Actual benthic deposits, however, are constantly being reworked by burrowing animals, such as shellfish, bottom-feeding fish, and worms. This biological activity can facilitate the movement of particle-bound substances from lower depths to the sediment-water interface, where the target compound can desorb back into the water column.³⁻⁵ Worm burrows can also "irrigate" sediments by flushing pore fluids, enhancing fluxes of HOCs back into the overlying water.⁶⁻⁸ Quantification of these irrigation and mixing processes is essential for understanding fluxes of organic contaminants from sediment beds to overlying waters. Particle-reactive radionuclides, such as ²¹⁰Pb and ²³⁴Th, can be utilized to elucidate sediment mixing rates,^{9,10} while more

soluble radioactive substances, such as ^3H or ^{222}Rn , are used to study irrigation processes.^{7,11}

Sediment-bed-to-overlying-water releases of organic contaminants are further complicated by the presence of organic colloids in the pore fluids. These colloids include macromolecules that are comprised of both humic and labile components. Recent evidence has shown that HOCs can be bound by organic colloids, and thereby affect their ability to sorb onto sediments.¹²⁻¹⁷ While macromolecules have lower diffusivities than HOCs, these colloids can enhance the total amount of hydrophobic substances in the pore waters, as observed by Brownawell and Farrington, who found that PCBs in Buzzards Bay sedimentary pore-waters were primarily associated with the colloidal phase.¹⁸

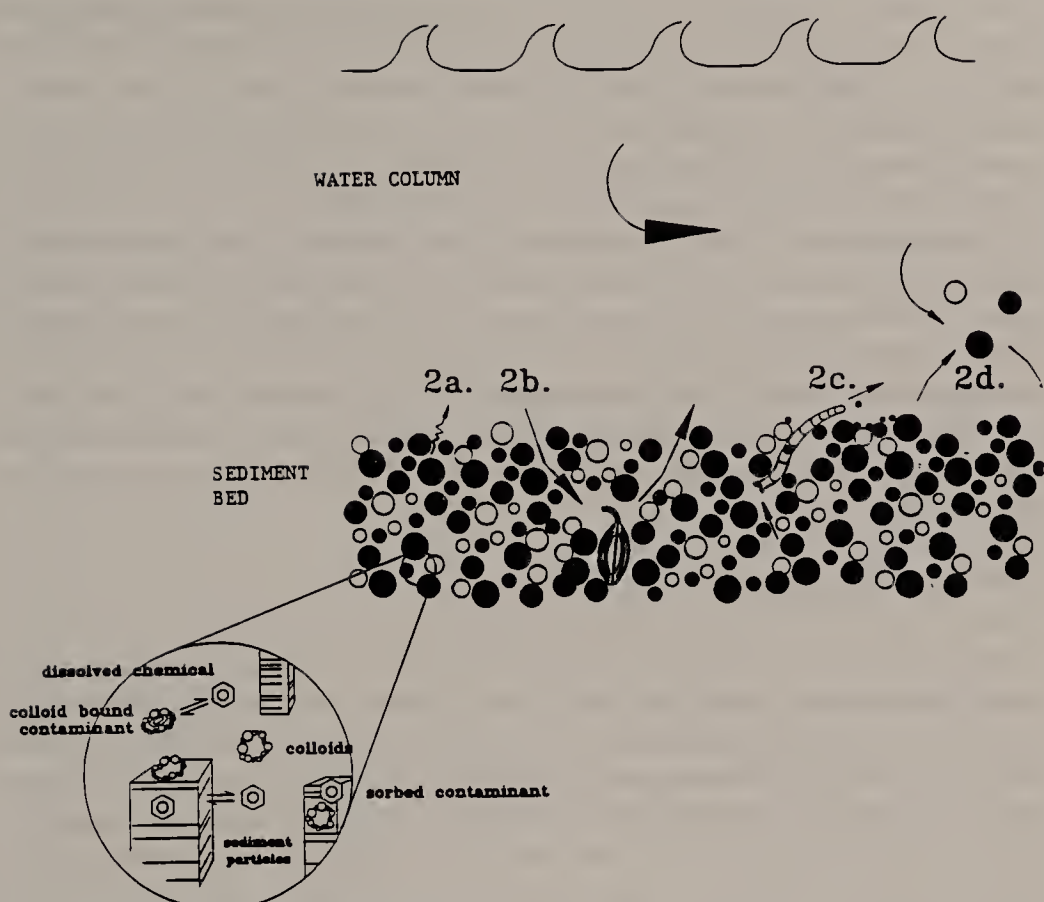
The propensity for a particular compound to be bound by a colloid is dependent upon the aqueous solubility of the compound and the size and polarity of the colloid.^{15-17,19} Therefore, it is likely that the presence of certain HOCs in pore water may be greatly enhanced by the presence of interstitial-fluid colloidal matter, while other contaminants are less affected (Figure 6.1). This phenomenon, coupled with bioirrigation processes, can significantly increase releases of organic pollutants from sediment beds over fluxes arising solely by molecular diffusion of the target compounds.

As part of our efforts to understand the enhanced release of hydrophobic organic contaminants from sediment beds, we have studied the size, quantity, and organic pollutant binding properties of "real world" colloids from both marine and lacustrine environments. Total organic carbon analysis (TOC), ultrafiltration (UF), and high-pressure size-exclusion chromatography (HPSEC) were chosen to determine the pore-fluid colloid concentrations and molecular-weight distributions. Free liquid diffusivities of the colloids were subsequently estimated based upon the colloids' measured sizes. Other aspects of this work included measuring equilibrium partition coefficients using two PAH probes, pyrene and phenanthrene, in an effort to understand the sorbent properties of pore-fluid colloids. Finally, the bioirrigation rates from two sites in Boston Harbor using ^{222}Rn were determined. Using this information, we made preliminary estimates of sediment-bed-to-overlying-water organic contaminant fluxes in the presence or absence of pore-water colloids.

MATERIALS AND METHODS

Sample Collection and Preparation

Sediment cores were taken from three sites in Boston Harbor: at Deer Island Flats (DIF), near Spectacle Island (SI), and in the Inner Harbor outside Fort Point Channel (FPC). A lacustrine sample was collected at Upper Mystic Lake (UML) in Arlington, MA. Sediments were collected using a gravity or box corer and sectioned shortly after sampling. The sediment sections were placed



1. Solid-Water Exchange, including colloids in suspension

Figure 6.1. Various processes contributing to the transport of toxic chemicals within and out of sediment beds: (1) microscopic-scale sorptive exchanges between water, colloids, and larger particles, coupled with macroscopic-scale processes controlling phase contact; (2a) diffusion and groundwater exfiltration, (2b) pore-water irrigation by infauna, (2c) bed turnover by infauna, (2d) resuspension.

in 5 M HNO₃-rinsed polycarbonate bottles and centrifuged at 600 g for 1 hr. The supernatants were drawn off and passed through two type A/E glass-fiber filters (Gelman Science, Ann Arbor, MI). The pH for the marine samples was determined to be 8.1; the lacustrine pore fluid had a pH of 6.5. Samples were then stored in the dark at 4°C until analysis.

A commercial humate (Aldrich Chemicals, Milwaukee, WI) and Suwanee River fulvate (International Humic Substances Society, Denver, CO) were used to enable comparisons of our protocol to the procedures reported in the literature for assaying the size of colloids. The fulvate was used without any pre-treatment, but the humate was extensively cleaned before use by dissolution in 0.01 M NaOH solution, followed by centrifugation and separation of the supernatant from the solids. Subsequent acidification of the supernatant precipitated the humic acids, which were separated by centrifugation and redis-

solved in base. This procedure was repeated several times before diluting the humic acid solution with a phosphate buffer to working concentrations. Final pH values for the fulvic and humic acid samples were 7.7 and 7.2, respectively. NaCl was added to some samples to assess ionic strength matrix effects on some of the analytical techniques.

Organic carbon analyses for all samples were conducted on an Ionics 555 TOC analyzer (Ionics, Inc., Watertown, MA). This instrument uses conditions similar to the method recommended by Sigimura and Suzuki.²⁰ Combustion of organic matter occurs in a quartz reactor tube packed with platinum and heated to 900°C. The technique proved to be precise ($\pm 5\%$), and was able to assay both marine and freshwater samples by direct aqueous injection. Analysis of organic colloids by ultraviolet/visible spectrophotometry was conducted on a Beckman DU-7 scanning spectrophotometer (Beckman Instruments, Fullerton, CA).

Molecular Size Analysis

High-pressure size-exclusion chromatography was performed using a Waters 501 solvent pump coupled with a Waters 484 variable wavelength detector, and a Rheodyne rotary injector valve equipped with either a 20- or 200- μ L sample loop (Waters Assoc., Milford, MA). A Waters 300SW modified silica column was employed for this study, which has a general molecular weight cutoff of 1000 to 2000 based upon the configuration of random coiled macromolecules. The column packing was selected based upon its low residual hydrophobicity and minimal ion exchange capacity.

Mobile phases were comprised of Milli-Q water (Millipore, Bedford, MA) and phosphate buffers (pH = 6.9). Sodium chloride was added to vary the ionic strength from 0.004 M to 0.6 M (approximately that of seawater). A large polystyrene sulfonate (molecular weight = 104K) random coil polymer was used to determine the void volume, while acetone was used to measure the permeation volume. The column was calibrated to both random coil macromolecules comprised of polystyrene sulfonates (18K, 8K, 4.6K, 1.8K) and proteins (bovine serum albumin, 67K; carbonic anhydrase, 29K; aprotinin, 6.5K). Sodium benzoate was also used to elucidate stationary-phase charge-exclusion effects.

Ultrafiltration experiments were done using Centricon microconcentrators (Amicon, Danvers, MA) equipped with 30K, 10K, and 3K membranes. Each device was extensively rinsed and cleaned in Norganic water (Millipore, Bedford, MA). Blanks, using distilled water analyzed for organic carbon after ultrafiltration, showed no appreciable leaching of organic matter from the membrane or housing materials. Sample (2 mL) was added to the top reservoir of each concentrator and capped to minimize evaporative losses. Each apparatus was centrifuged at 1000 g until the volume of liquid from the upper compartment passed through the membrane into the lower reservoir. The ultrafiltrate was assayed by both TOC and UV/visible spectrophotometry.

PAH-Colloid Binding Studies

Fluorescence quenching^{15,16,21} was applied to study the binding of two PAH probes, phenanthrene and pyrene, to pore-water organic colloids taken from the Fort Point Channel site. Fluorescence measurements were obtained using a Perkin-Elmer LS-5 spectrofluorometer. Optimum excitation/emission wavelength pairs were determined to be 230 nm/390 nm for pyrene and 230 nm/373 nm for phenanthrene. Interfering fluorescence from the organic colloids was observed to be minimal at these wavelengths. Saline solutions ($I = 0.6$ M NaCl) were spiked with 10 μ L of the probe dissolved in an acetonitrile carrier. Saline solutions containing no PAH were used as controls to quantify the amount of interfering fluorescence from the colloids. Both the blank and sample were transferred to quartz cuvettes, and initial fluorescence emissions were recorded. Following this, 100 μ L of raw pore water was added to each cuvette and allowed to equilibrate. Previous investigators observed short equilibration times (less than 1 min).^{15,16,21} We allowed our samples to sit for about 4 minutes before making another reading. This process was repeated four or five times depending upon the amount of pore fluid available. In between fluorometric readings, the cuvettes were transferred to the UV/visible spectrophotometer for absorbance measurements to account for inner-filter effects.^{15,16} The corrected fluorescence data, along with measured colloid concentrations (expressed as organic carbon), were used to determine the equilibrium binding constant, K_{oc} .

Radon Analysis

^{222}Rn was assayed to quantify the intensity of bioirrigation at the Deer Island Flats and Spectacle Island sites (this procedure is described in detail elsewhere²²). Briefly, sediments from each section were transferred to glass bottles containing seawater and sealed with silicone sealant. The samples were slurried, and the ^{222}Rn was stripped into gas scintillation counting cells. ^{222}Rn activity was corrected for the decay that occurred subsequent to sampling. Ingrown radon activity was measured several weeks later to determine the supported ^{222}Rn activities.

RESULTS AND DISCUSSION

Detection of Colloids by TOC and UV Analysis

The quantification of colloids has been conducted by ultraviolet spectrophotometry and total organic carbon analysis.^{23,24} Such observations show a linear relationship between TOC and absorbance. A number of separation techniques, such as HPSEC, rely on TOC-absorbance correlations for quantifying colloid fractions. This approach, however, assumes that the extinction coeffi-

Table 6.1. Downcore Extinction Coefficients of Raw and Ultrafiltered (< 10K) Pore Waters Extracted from Deer Island Flats Sediments

Depth Interval (cm)	Raw Pore Water		Ultrafiltered Pore Water	
	E (L/mole-oc cm)	OC (mg/L)	E (L/mole-oc cm)	OC (mg/L)
3	140	27	140	12
5	67	45	82	22
8	120	30	96	23
12	120	37	90	29
16	100	44	110	24
21	100	49	110	25
Average	108 ± 25		105 ± 20	
Aldrich humate	1000	42	900	8.0
Sewanee fulvate	530	5.5	nd	nd

Note: nd = not determined.

cient of the mixture of colloids is constant for a specific wavelength both before and after any operation that might alter the original mixtures.

We measured extinction coefficients (ϵ) at 280 nm for raw and ultrafiltered pore-water colloids extracted from different sections of the Deer Island Flats core (Table 6.1). These coefficients appeared to vary only slightly with depth, with an average value of 108 ± 25 L/mole-oc cm, a number in good agreement with observations made by Stuermer, who reported a value of 149 L/mole-oc cm for a coastal marine fulvic acid.²⁵ Aldrich humate and Suwanee fulvate ϵ values, however, were a factor of 10 and 5 higher, respectively (Table 6.1), suggesting that our colloids are comprised of humic materials with fewer conjugated bonds, or may be composed of terrestrial humic matter diluted by other macromolecules (e.g., polysaccharides) that do not absorb at 280 nm.

Removal of macromolecular organic carbon by ultrafiltration (amounting to 40–50% of the total initial organic carbon) does not consistently change the extinction coefficients of the mixtures (Table 6.1). This suggests that the molar absorptivity for these marine pore-water colloids was similar to that of the smaller organic components. Thus, detection of our colloid fractions by UV and conversion to an organic carbon concentration basis using $\epsilon \approx 100$ L/mole-oc cm appears justified.

Coiling and Uncoiling of Organic Colloids

High-pressure size-exclusion chromatograms of colloidal material from the Deer Island pore fluids show very different patterns when this analytical system uses mobile phases with different ionic strengths (Figure 6.2). This was representative for all the marine pore-water samples tested. When the concentration of the mobile-phase electrolyte (sodium chloride) approaches that of seawater, all the multipeak chromatograms, observed using lower ionic strength eluents, merged into one peak (Figure 6.2c). One interpretation has been that results, such as shown in Figure 6.2a, are indicative of a mixture of very large, small, and intermediate colloid classes. Upon increasing the

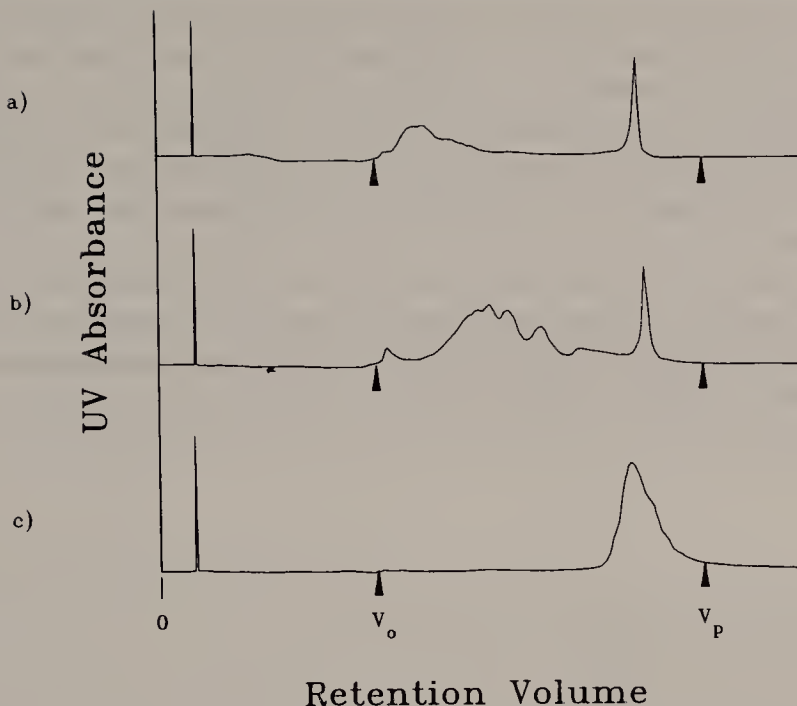


Figure 6.2. Separation of pore-water colloids from the Deer Island Flat site (10–14 cm) by HPSEC with aqueous mobile phases of different strengths: (a) $I = 4 \times 10^{-4}$, (b) $I = 0.012$, (c) $I = 0.6$.

mobile-phase ionic strength, they coalesce into one peak because of the overwhelming influence of adsorption (onto the stationary phase).²⁶ However, if such adsorption occurs, we would expect to see retention of colloids beyond the permeation volume of the column (V_p). The colloids studied here always eluted well before the permeation retention volume. This implies that other processes are responsible for variable elution behavior.

One plausible mechanism that could be controlling the separation of macromolecules by HPSEC is the dynamic *in situ* coiling and uncoiling of the colloids as they are being eluted. A number of investigators proposed a random coil configuration for humic substances which is able to contract and expand as a function of ionic strength and pH.^{27,28} A sample containing concentrated dissolved salts, entering the column being run with a low ionic strength mobile phase, might have a certain population of its colloids at the front of the mixing zone of the analyte and mobile phase where the electrolyte concentration is lower. This would cause these macromolecules to expand and increase their hydrodynamic radii, preventing the target species from diffusing into the smaller pores of the stationary phase. Thus, the population of macromolecules uncoiled at the front of the analyte input would proceed quickly through the size-exclusion column. Similar molecules in the rear of the injectate would move ahead into the electrolyte-rich zone, recoil, and then elute with that population of colloids. Humic macromolecules associated with the center zone of the salt plug would remain coiled and be able to diffuse into the smaller

pores. These types of multimodal polyelectrolytic effects have been documented for the separation of well-characterized substances such as polyacrylonitrile sulfonate and nylon 66 by polar solvents.²⁹ The addition of electrolytes to the mobile phase, to match that of the sample matrix, suppresses the propensity of the organic colloid to change its conformation during analysis and allows consistent size exclusion to occur throughout the analyte-column interaction.

In order to test further the *in situ* coiling/uncoiling mechanism hypothesis, HPSEC analysis of Aldrich humic acid in 0.6 M NaCl solution was performed using a low ionic strength mobile phase (0.03 M). The chromatograms resulted in a bimodal distribution (Figure 6.3)—similar behavior was seen for pore-

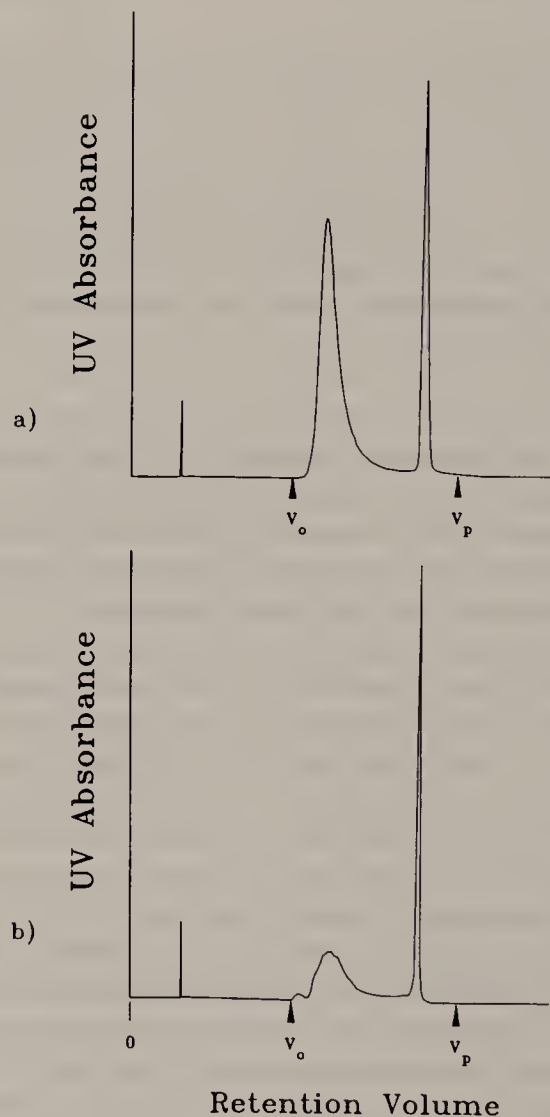


Figure 6.3. Separation of Aldrich humic acid in a 0.6 M NaCl solution by HPSEC (mobile phase I = 0.03): (a) whole sample, (b) reinjected second peak from previous sample.

water colloids. The last peak of this HPSEC run was collected and reinjected onto the column under identical conditions at a higher detector sensitivity. Accurate separation by size in the initial analysis should have reproduced one peak with the same retention time; however the rechromatographed sample resembled the original whole colloid chromatogram (Figure 6.3b), suggesting that the last peak contained a representative mixture of the original macromolecules in coiled configuration. When rechromatographed this produced the original bimodal distribution by allowing some of the contracted colloids to expand. Thus, artifact peaks may be produced in SEC analyses of colloidal mixtures if sample matrix and mobile-phase ionic strengths are not carefully matched. Consequently, we believe the results obtained (as indicated for Figure 6.2c) most accurately reflect the true colloidal size distribution for these pore-water materials.

Charge Repulsion Effects in SEC

Charge repulsion between colloids and the stationary phase is another mechanism which may affect the separation of colloids by HPSEC. Several researchers attributed a decreased retention of the analyte with the diminishing mobile-phase ionic strength as evidence for the expansion of the macromolecules;^{30,31} however, we believe that it is difficult to distinguish between size- and charge-exclusion effects in such cases. The composition of size-exclusion chromatography stationary phases (with the possible exception of some of the newer resin-based materials) consists of polar substances bonded to silica; since some of the silica surface may be uncovered, negative surface groups are present at mobile phase pH's above silica's pH_{zpc} (2–4). Polyelectrolytes, such as humic substances, may be prevented from diffusing into the stationary-phase pores due to these charged sites on the silica support. Addition of an indifferent electrolyte to the mobile phase shrinks the thickness of the surface double layer to sizes that are small relative to pore openings, thereby allowing diffusion of charged solutes into the narrow channels of the packing material. A mobile-phase buffer composition that exceeds a critical ionic strength (CIS), where the double layer is compressed to a thickness sufficient to enable analyte entry to the pores, is necessary before we can isolate effects due to coiling and uncoiling of the polymer.

In order to test this hypothesis, we observed the retention behaviors as a function of pH for sodium benzoate and Suwanee fulvate. Matching the ionic strength and pH of the mobile phase to that of the fulvate sample matrix resulted in the elution of one peak. The CIS, under these circumstances, is identified as the ionic strength at which the retention behavior of benzoate approaches that of an uncharged probe, acetone. The elution volume for benzoate approached a constant value between an ionic strength of 0.03 and 0.1 M (Figure 6.4). This suggests that at an ionic strength of 0.03 or higher, the effect of charge exclusion on benzoate is suppressed for this packing material. The fulvate retention ratio also becomes constant near this mobile-phase ionic

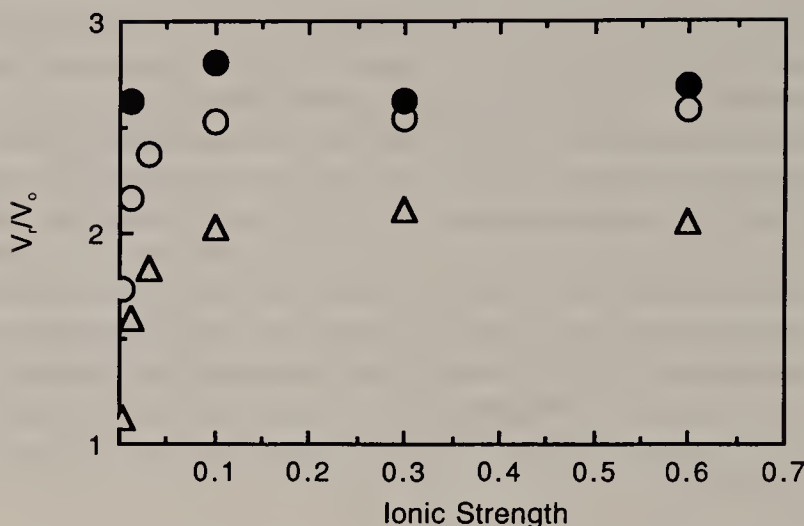


Figure 6.4. Normalized retention volume (V_r/V_o) for acetone (filled circles), benzoate (open circles), and Suwanee fulvic acid (triangles) as a function of mobile-phase ionic strength.

strength; thus, it is impossible to discern between charge exclusion and coiling/uncoiling effects below this critical ionic strength. Consequently, charge exclusion appears to be an important process and may cause inaccurate assessment of analyte molecular weights if mobile-phase ionic strengths are too low.

Elucidation of Colloid Molecular Weight by HPSEC

HPSEC analyses of our colloids, in light of charge exclusion and in situ macromolecular configurational changes discussed above, were done using high ionic strength mobile phases. Sodium chloride (0.6 M) was added to our freshwater samples before analysis, and the colloids were assumed to have attained a coiled configuration. Random coil and protein molecular weight standards were eluted under similar conditions. The relationship between V_r/V_o for the random coil polystyrene sulfonate samples, eluted with a high ionic strength mobile phase ($I = 0.6$), and their respective log molecular weights (MW) was

$$\log MW = 6.99 - 1.73(V_r/V_o) \quad (6.1)$$

$$n = 5; r = 0.99$$

The compact globular protein standards yielded a different regression equation:

$$\log MW = 7.17 - 1.51(V_r/V_o) \quad (6.2)$$

$$n = 3; r = 0.99$$

Table 6.2. Estimated Organic Colloid Molecular Weights and Liquid Diffusivities Based upon Random Coiled and Globular Configurations

Sample	Random Coil		Globular Protein	
	MW	D _l (cm ² /sec)	MW	D _l (cm ² /sec)
Deer Island Flats	2000	5.9 × 10 ⁻⁶	9100	1.4 × 10 ⁻⁶
Upper Mystic Lake	2100	5.9 × 10 ⁻⁶	9300	1.3 × 10 ⁻⁶
Aldrich Humate	4300	4.8 × 10 ⁻⁶	17000	1.2 × 10 ⁻⁶
Sewanee Fulvate	2500	5.5 × 10 ⁻⁶	11000	1.3 × 10 ⁻⁶

Presumably, the variation in these correlations reflects the differences in hydrodynamic size between random coil and globular macromolecules of the same molecular weight. While humic molecules cannot coil as tightly as globular proteins, we suspect that the presence of branching (as opposed to being linear) prohibits them from extending to maximal lengths in low ionic strength water for their particular molecular weights. Thus, humic substances probably lie between the stretched and globular extremes, and the molecular weight distributions for our organic colloid samples were therefore estimated using both Equations 6.1 and 6.2 (Table 6.2).

The molecular weight of Suwanee fulvate, based upon a random coil configuration, is in reasonable agreement with the value of 1910 reported by Beckett et al.³² Conversely, our Aldrich humate value is a factor of three smaller than the molecular weight (14,500) measured by flow field flow fractionation.³² During our Aldrich humate cleanup procedure, we removed a large number of particles by centrifugation. The inclusion of these particles in an untreated sample would result in a higher observed molecular weight irrespective of the technique used. Thus, our reported value represents the size of Aldrich humates purged of these interfering constituents.

The magnitudes of liquid macromolecular diffusivities are governed by the size and shape of the macromolecules. Such diffusivities can be estimated using the following expression:³²

$$D_l = aM_n^{-b} \quad (6.3)$$

where D_l is polymer liquid diffusivity, and a and b are empirical constants. For polystyrene sulfonates, a was determined to be 1.42×10^{-4} and b = 0.422. Using the data of Wahlund and Giddings,³³ we deduced a different set of constants for globular shapes where a = 5.76×10^{-5} and b = 0.411.

Based on these expressions, and our measured molecular weights of DIF and UML pore-water colloids, we estimated the diffusion coefficients of these macromolecules using Equation 6.3 (Table 6.2). Note that the results for Upper Mystic Lake pore-water colloids were obtained using HPSEC analysis with the mobile-and sample-phase ionic strength adjusted to 0.6 M so as to avoid charge-exclusion effects. One would suspect that in the lake, these colloids exist in a more extended configuration and would therefore have lower diffusivities than indicated in Table 6.2.

There is only a small difference in estimated diffusivities between the colloids from various sources (< 25%). Differences in diffusivities based upon the two macromolecular configurations, however, vary by a factor of four. As for molecular weight, we suspect that the pore-water colloids probably exhibit diffusivities between these limits.

Vertical Distributions of Organic Colloids in Sedimentary Pore Waters

Total and macromolecular organic carbon (that fraction retained by an ultrafilter with 3000 globular protein molecular weight cutoff) core profiles from four sites indicated that colloid concentrations were enriched in the deeper layers for all the samples and depleted near the sediment-water interface (Figure 6.5). Bioirrigation and biotransformation could explain this depletion of macromolecular organic matter. This suggests that part of the colloids, in the upper layer of sediment beds, are being released back into the water column. We also observed that the organic colloids were not a constant fraction of the total organic carbon in the pore water, although both macromolecular and total organic carbon profiles appeared similar.

Binding of PAH by Pore-Water Organic Colloids

Quenching of pyrene and phenanthrene fluorescence was observed for pore-water organic colloids extracted from Fort Point Channel sediments (Figures 6.6 and 6.7). Organic carbon concentrations represent the macromolecular fraction (> 3000 globular protein MWCO) as measured by ultrafiltration. Quenching of pyrene by the ultrafiltrate was determined to be insignificant (Figure 6.6). The linear relationship between colloid concentration and inverse fluorescence of the probe suggests that quenching processes in this system can be described by the Stern-Volmer equation.^{15,16} The slopes of the lines yield K_{oc} values of 1.01×10^5 mL/g for pyrene and 6.89×10^4 mL/g for phenanthrene. The measured pyrene binding coefficient is fairly consistent with values reported by other authors for Aldrich humic acid,^{15,16} while the experimentally determined K_{oc} for phenanthrene is slightly higher. In both cases our marine colloidal matter appears to bind the HOCs rather extensively. It is plausible that the presence of electrolytes in high concentrations causes the configuration of the colloids to be optimal for binding hydrophobic substances. A number of investigators reported an increase in K_{oc} by as much as a factor of 2.5 when the ionic strength was varied from 10^{-4} to 0.5 M.^{12,15} The K_{oc} values we report here are within such a factor of values found in the literature.

Estimated PAH Fluxes from Boston Harbor Sediments

^{222}Rn profiles from the DIF and SI cores indicate bioflushing of the upper sediment layers (Figure 6.8). In the absence of any fluxes, the observed and

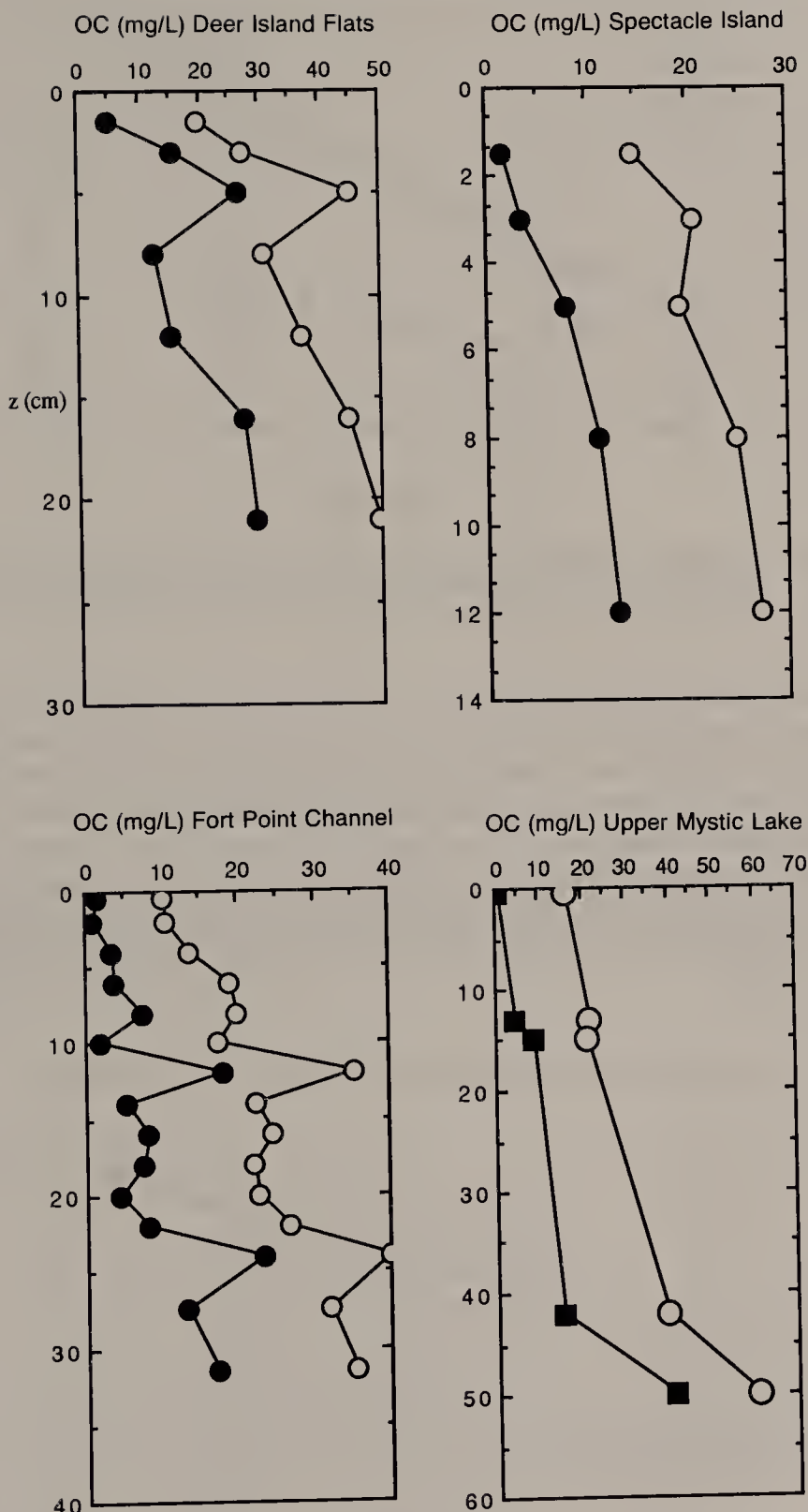


Figure 6.5. Total (*open symbols*) and macromolecular (*filled symbols*) pore-water organic carbon from Boston Harbor sites and Upper Mystic Lake.

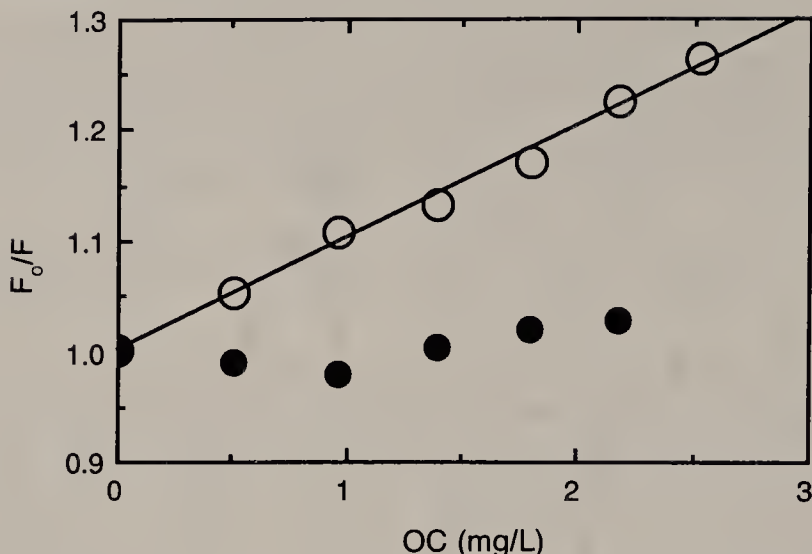


Figure 6.6. Binding of pyrene by Fort Point Channel pore-water colloids (*open circles*). Ultrafiltered pore water (*filled circles*) exhibits little propensity to bind pyrene. F_0/F is the ratio of unquenched to quenched fluorescence intensity.

supported profiles should be identical. There was a marked depletion of ^{222}Rn in the upper few centimeters far in excess of expectations from diffusion alone. The SI core shows ^{222}Rn depletion all the way to the bottom of the interval sampled. Obviously intense flushing was occurring to greater depths at that site. These observations support the idea that the depletion of organic macromolecules near the sediment-water interface at these sites is at least partially due to bioirrigation. We also noted that the irrigation of pore waters by benthic organisms is a significant process in areas (e.g., DIF) where sediments appear anoxic.

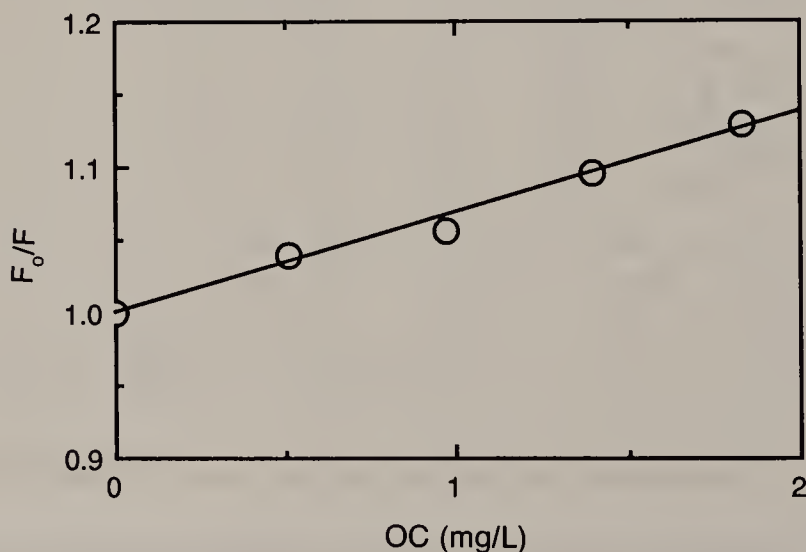


Figure 6.7. Binding of phenanthrene by Fort Point Channel pore-water colloids.

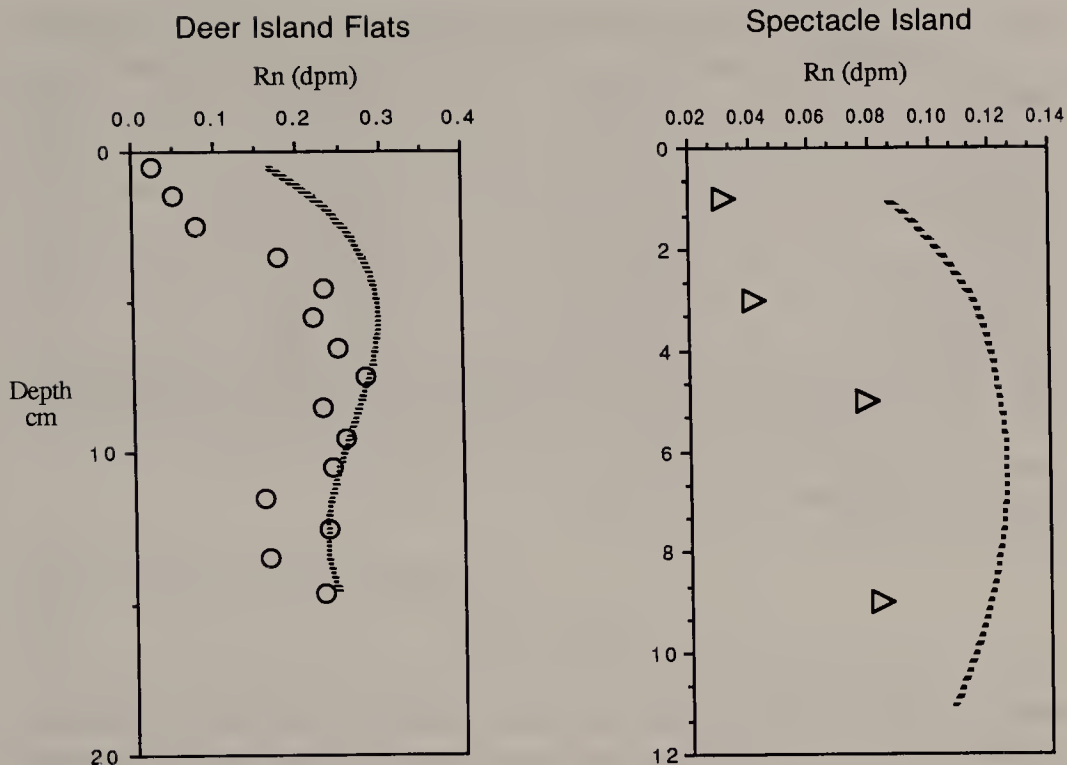


Figure 6.8. Supported (dashed lines) and observed (open symbols) ^{222}Rn profiles from Deer Island Flats and Spectacle Island.

The ^{222}Rn data can be used to quantify bioirrigation. The total flux term, J_t , is comprised of diffusion and irrigation components and can be approximated using the following equation:

$$J_t = -\phi D_{\text{eff}} \frac{\Delta C_{\text{pw}}}{\Delta Z} - \phi D_{\text{oc}} \frac{\Delta C_{\text{oc}}}{\Delta Z} - \phi Z [\alpha_s (C_{\text{pw}} - C_{\text{ol}}) + \alpha_{\text{oc}} (C_{\text{oc}} - C_{\text{ol}})] \quad (6.4)$$

where ϕ = sediment porosity

D_{eff} = substance's sediment diffusivity

D_{oc} = colloid's sediment diffusivity

α_s = solute nonlocal exchange term¹¹

α_{oc} = colloid nonlocal exchange term¹¹

Z = depth of the irrigation zone

C_{oc} = colloid concentration

C_{pw} = average concentration of the substance in the pore fluid

C_{ol} = average concentration of the substance in the overlying water

Sediment diffusivity for a compound can be estimated from its free liquid diffusivity (D_f):

Table 6.3. Estimates of Benzo(a)pyrene and Pyrene Releases from Boston Harbor Sediments

Parameter	BaP	Pyrene	Colloid
$D_{\text{eff}}(\text{cm}^2/\text{day})$	0.2	0.2	0.1
$\alpha(\text{day}^{-1})$	0.3	0.3	0.1
$C_{\text{sediment}}(\mu\text{g/g}_{\text{oc}})$	6.0	10.0	—
$C_{\text{pw}}(\mu\text{g/cc})$	1.2×10^{-6}	1.2×10^{-4}	5.0
$C_{\text{oil}}(\mu\text{g/cc})$	0	0	0.5
$K_{\text{oc, colloid}}(\text{cc/g})$	2.1×10^6 ^a	1.0×10^5 ^b	—
$K_{\text{oc, sediment}}(\text{cc/g})$	5.0×10^6 ^c	8.0×10^4	—
$J_{\text{woc}}(\mu\text{g/cm}^2/\text{yr})$	1.8×10^{-4}	1.9×10^{-2}	—
$J_t(\mu\text{g/cm}^2/\text{yr})$	7.7×10^{-4}	2.1×10^{-2}	—

Notes: Average porosity of the sediments was determined to be 0.6. J_{woc} denotes estimated fluxes in the absence of colloids, and J_t is the total flux with colloids.

^aSee Landrum et al.³⁶

^bMeasured using fluorescence quenching.

^cSee Reinbold et al.³⁸

$$D_{\text{eff}} = \frac{D_l}{\theta^2} \quad (6.5)$$

where θ is the tortuosity of the sediment.³⁴ Since it is difficult to determine tortuosity based upon the geometry of the sediments, it can be estimated indirectly if the sediment's porosity is known:

$$\theta^2 = \phi(\phi^{-n}) \quad (6.6)$$

where the coefficient n was empirically determined to be 2 for a variety of coastal marine sediments.³⁴

To establish the magnitude of nonlocal exchange parameters, this model can be used on ^{222}Rn data, adjusting the solute's α as necessary. For the Deer Island site, α_{Rn} was determined to be 0.6/day. Assuming that irrigational transport across burrow walls is by molecular diffusion, and that the mechanisms of ^{222}Rn transport and of other substances across burrow walls are similar, the nonlocal exchange term for other substances can be estimated from α_{Rn} using the following relationship:

$$\alpha = \frac{D_l}{D_{\text{Rn}}} \alpha_{\text{Rn}} \quad (6.7)$$

where D_{Rn} is the liquid diffusion coefficient of radon.

Estimated releases of benzo(a)pyrene (BAP) and pyrene from Boston Harbor sediments at Deer Island Flats were calculated using Equation 6.4 (Table 6.3). The porosity is an average value measured for these sediments, while the diffusion coefficients for pyrene and BAP were estimated using the Wilke-Chang equation.³⁵ The equilibrium binding constants, as well as the sediment organic carbon normalized partition coefficients for both solutes, were measured or taken from the literature.³⁶⁻³⁸ We were able to extract all the other requisite model parameters from measured values and the ^{222}Rn data.

Estimated total fluxes (diffusion and bioirrigation) for these two compounds with and without the influences of colloids are reported in the last two rows of Table 6.3. Because of the uncertainties involved in estimating the colloid and PAH nonlocal exchange parameters (both components being much larger than radon), the reported fluxes are maximum predictions. Sediment bed releases in the absence of colloids are relatively small for the highly particle-reactive benzo(a)pyrene as compared to the more water-soluble pyrene. The presence of organic colloids increases the flux of BAP by approximately a factor of four, but is less significant for pyrene. Thus, it appears that the mobility of highly particle-reactive HOCs may be substantially enhanced by colloids.

SUMMARY AND CONCLUSIONS

Sediment-bed-to-overlying-water releases of recalcitrant organic contaminants may be facilitated by the presence of organic colloids and bioirrigation processes. We have observed the presence of macromolecular organic matter in marine and freshwater pore waters. These colloids appear to undergo alterations in their configuration in response to ionic strength changes. Molecular weights measured by high-pressure size-exclusion chromatography suggest that our colloids were between 2000 daltons (based upon the shape of random coil macromolecules) and 10,000 daltons (based upon globular protein configurations). These colloids bind hydrophobic organic compounds very extensively (as determined by fluorescence quenching), and when coupled with bioirrigation processes, are able to enhance sediment-bed-to-water fluxes of particle reactive pollutants.

ACKNOWLEDGMENTS

We gratefully acknowledge the generous assistance of John MacFarlane, Deb Backhus, Paul Sherblom, John Farrington, Gordon Wallace, Hovey Clifford, and Sue McGroddy for their invaluable assistance during sampling and data analysis. This work was conducted with support by the National Science Foundation, grant no. 8714110-CES, Dr. Edward H. Bryan, program director; by a grant provided to the Massachusetts Institute of Technology by the National Sea Grant College Program Office, a part of the National Oceanic and Atmospheric Administration; by a grant from the National Institute of Environmental Health Sciences (grant no. 2P30E502109-11); and by the Massachusetts Water Resources Authority.

REFERENCES

1. Shiaris, M. P., and D. Jambard-Sweet. "Polycyclic Aromatic Hydrocarbons in Surficial Sediments of Boston Harbor, MA (USA)," *Mar. Poll. Bull.* 17:469-472 (1986).
2. Farrington, J. N., A. C. Davis, B. J. Brownawell, B. W. Tripp, C. V. Clifford, and J. B. Livramento. "The Biogeochemistry of PCBs in the Acushnet River Estuary, MA," in *Organic Marine Geochemistry*, ACS Symposium Series 305 (Washington, DC: American Chemical Society, 1986), pp. 174-197.
3. Benninger, L. K., R. C. Aller, J. K. Cochran, and K. K. Turekian. "Effect of Biological Sediment Mixing on the ^{210}Pb Chronology and Trace Metals Distribution in a Long Island Sound Sediment Core," *Earth Planet. Sci. Lett.* 43:241-259 (1979).
4. Fischer, J. B., W. J. Lick, P. L. McCall, and J. A. Robbins. "Vertical Mixing of Lake Sediments by Tubificid Oligochaetes," *J. Geophys. Res.* 85:3997-4006 (1980).
5. Karickhoff, S. N., and K. R. Morris. "Impact of Tubificid Oligochaetes on Pollutant Transport in Bottom Sediments," *Environ. Sci. Technol.* 19:51-56 (1985).
6. Aller, R. C. "Quantifying Solute Distributions in the Bioturbated Zone of Marine Sediments by Defining an Average Microenvironment," *Geochim. Cosmochim. Acta* 44:1955-1965 (1980).
7. Emerson, S., P. Jahnke, and D. Heggie. "Sediment-Water Exchange in Shallow Water Estuaries," *J. Mar. Res.* 42:709 (1984).
8. McNichol, A. P. "A Study of Remineralization of Organic Carbon in Nearshore Sediments Using Carbon Isotopes," Woods Hole Oceanographic Institution, Woods Hole, MA (1986).
9. Robbins, J. A., and D. N. Edington. "Determination of Recent Sedimentation Rates in Lake Michigan Using ^{210}Pb and ^{137}Cs ," *Geochim. Cosmochim. Acta* 39:285 (1975).
10. Aller, R. C., and J. K. Cochran. " $^{234}\text{Th}/^{236}\text{U}$ Disequilibrium in Nearshore Sediments: Particle Reworking and Diagenetic Timescales," *Earth Planet. Sci. Lett.* 29:37 (1976).
11. Martin, W. R., and F. L. Sayles. "Seasonal Cycles of Particles and Solute Transport Processes in Nearshore Sediments: $^{222}\text{Rn}/^{226}\text{Ra}$ and $^{234}\text{Th}/^{238}\text{U}$ Disequilibrium at a Site in Buzzards Bay, MA," *Geochim. Cosmochim. Acta* 51:927 (1987).
12. Carter, C. W., and I. H. Suffet. "Binding of DDT to Dissolved Humic Material," *Environ. Sci. Technol.* 16:735 (1982).
13. Landrum, P. F., S. R. Nihart, B. J. Eadie, and W. S. Gardner. "Reverse Phase Separation Method for Determining Pollutant Binding to Aldrich Humic Acid and Dissolved Organic Carbon of Natural Waters," *Environ. Sci. Technol.* 19:187 (1984).
14. Gschwend, P. M., and S. Wu. "On the Constancy of Sediment-Water Partition Coefficients of Hydrophobic Organic Pollutants," *Environ. Sci. Technol.* 19:90 (1985).
15. Gauthier, T. D., E. C. Shane, W. F. Guerin, W. R. Seitz, and C. L. Grant. "Fluorescence Quenching Method for Determining Equilibrium Constants for Polycyclic Aromatic Hydrocarbon Binding to Dissolved Humic Materials," *Environ. Sci. Technol.* 20:1162 (1986).
16. Gauthier, T. D., W. R. Seitz, and C. L. Grant. "Effects of Structural and Composi-

- tional Variations of Dissolved Humic Materials on Pyrene K_{oc} Values," *Environ. Sci. Technol.* 21:243 (1987).
- 17. Chin, Y. P., and W. J. Weber, Jr. "Estimating the Effects of Dispersed Organic Polymers on the Sorption of Contaminants by Natural Solids: 1. A Predictive Thermodynamic Humic Substance-Organic Solute Interaction Model," *Environ. Sci. Technol.* 23:978 (1989).
 - 18. Brownawell, B. J., and J. N. Farrington. "Biogeochemistry of PCBs in Interstitial Waters of Coastal Marine Sediment," *Geochim. Cosmochim. Acta* 50:157 (1986).
 - 19. Chiou, C. T., D. E. Kile, T. I. Brinton, R. L. Malcolm, J. A. Leenheer, and P. MacCarthy. "A Comparison of Water Solubility Enhancement of Organic Solutes by Aquatic Humic Materials and Commercial Humic Acids," *Environ. Sci. Technol.* 21:1231 (1987).
 - 20. Sigimura, Y., and Y. Suzuki. "A High Temperature Catalytic Oxidation Method for the Determination of Non-Volatile Dissolved Organic Carbon in Seawater by Direct Injection of a Liquid Sample," *Mar. Chem.* 24:105 (1988).
 - 21. Backhus, D. A., and P. M. Gschwend. "Fluorescent Polycyclic Aromatic Hydrocarbons as Probes for Studying the Impact of Colloids on Pollutant Transport in Groundwater," *Environ. Sci. Technol.* 24:1214 (1990).
 - 22. Mathieu, G. " $^{222}\text{Rn}/^{226}\text{Ra}$ Technique of Analysis," in *Annual Report to ERDA, Transport and Transfer Rates in the Waters of the Continental Shelf* (1977), Appendix 1.
 - 23. Randtke, S. J., and C. P. Jepsen. "Effects of Salts on Activated Carbon Adsorption of Fulvic Acids," *Journal AWWA* 74:84 (1982).
 - 24. Weber, W. J., Jr., M. Pirbazari, J. B. Long, and D. A. Barton. "Potential Mechanisms for Removal of Humic Acids from Water by Activated Carbon," in *Activated Carbon Adsorption of Organics from the Aqueous Phase* (Ann Arbor, MI: Ann Arbor Science, 1980), p. 317.
 - 25. Stuermer, D. H. "The Characterization of Humic Substances in Sea Water," PhD Thesis, Woods Hole Oceanographic Institution, Woods Hole, MA (1975).
 - 26. Hine, P. T., and D. B. Bursill. "Gel Permeation Chromatography of Humic Acid: Problems Associated with Sephadex Gel," *Water Res.* 18:1461 (1984).
 - 27. Ghosh, K., and M. Schnitzer. "Macromolecular Structures of Humic Substances," *Soil Sci.* 129:266 (1980).
 - 28. Cornel, P. K., R. S. Summers, and P. V. Roberts. "Diffusion of Humic Acid in Dilute Aqueous Solution," *J. Colloid. Interface Sci.* 110:149 (1986).
 - 29. Yau, W. W., J. J. Kirkland, and D. D. Bly. *Modern Size Exclusion Chromatography: Practice of Gel Permeation and Gel Filtration Chromatography* (New York: John Wiley and Sons, 1979).
 - 30. DeHaan, H., R. I. Jones, and K. Salonen. "Does Ionic Strength Affect the Configuration of Aquatic Humic Substance, as Indicated by Gel Filtration?" *Freshwater Biol.* 17:453 (1987).
 - 31. Ceccanti, B., M. Calcina, M. Bonmati-Pont, C. Ciardi, and R. Tarsitano. "Molecular Size Distribution of Soil Humic Substances with Ionic Strength," *Sci. Total Environ.* 81/82:471 (1989).
 - 32. Beckett, R., Z. Jue, and J. C. Giddings. "Determination of Molecular Weight Distributions of Fulvic and Humic Acids Using Flow Field Flow Fractionation," *Environ. Sci. Technol.* 21:289 (1987).
 - 33. Wahlund, K.-G., and J. C. Giddings. "Properties of an Asymmetrical Flow Field

- Flow Fractionation Channel Having One Permeable Wall," *Anal. Chem.* 59:1332 (1987).
- 34. Ullman, W. J., and R. C. Aller. "Diffusion Coefficients in Nearshore Sediments," *Limnol. Oceanog.* 27:552 (1982).
 - 35. Wilke, C. R., and P. Chang. "Correlation of Diffusion Coefficients in Dilute Solutions, *J. Al. Ch. E.* 1:264 (1956).
 - 36. Landrum, P. F., M. D. Reinhold, S. R. Nihart, and B. J. Eadie. "Predicting the Bioavailability of *P. hoyi* in the Presence of Humic and Fulvic Materials, and Natural Dissolved Organic Matter," *Environ. Toxicol. Chem.* 4:459 (1985).
 - 37. Karickhoff, S. N., D. S. Brown, and T. A. Scott. "Sorption of Hydrophobic Pollutants on Natural Sediments," *Water Res.* 13:241 (1979).
 - 38. Reinbold, K. A., J. J. Hassett, J. C. Means, and W. L. Banwart. "Adsorption of Energy Related Organic Pollutants: A Literature Review," U.S. EPA Report-600/3-79-086 (1979).

CHAPTER 7

Adsorption of Surfactants

Bruce J. Brownawell, Hua Chen, Wanjia Zhang, and John C. Westall

INTRODUCTION

Surfactants are used in increasingly large quantities in a number of consumer and industrial products.¹ Total 1988 U.S. production of surfactants was 7.3 billion pounds. Anionic (62% of total U.S. surfactant production), neutral (27%), and cationic (10%) surfactants are all important classes of organic chemicals; production of nonionic and cationic surfactants is growing faster than that of anionic surfactants.¹ Adsorption of surfactants to surfaces of suspended particles affects their removal in waste treatment plants,^{2,3} bioavailability and toxicity,^{2,4,5} rates of biodegradation,⁵ and distribution and fate in receiving waters, particularly those with high suspended solids concentrations. There are also several indirect effects that surfactants, through adsorption on surfaces, can have on the distribution and fate of other pollutants that tend to adsorb.⁶⁻⁸

Despite the fundamental importance of adsorption processes, there have been relatively few systematic studies of surfactant adsorption on environmental sorbents.⁸⁻¹⁰ The adsorption of ionic and nonionic surfactants to other materials, such as minerals and textiles, has been studied much more thoroughly,¹¹⁻¹³ although the majority of studies have been conducted at high concentrations (greater than 10 μM) in order to achieve high surface coverages. In general, the sorption of surfactants onto natural materials has been studied much less than the sorption of nonpolar compounds. For nonpolar organic compounds,¹⁴⁻¹⁶ the results of numerous laboratory and field studies have led to the development of mechanistic and predictive models for distributions. Such models have not been developed for amphiphilic organic compounds in natural waters. We do not know the relative importance of hydrophobic, electrostatic, and specific chemical interactions that control adsorption, nor do we have sufficient empirical information that would allow predictions of surfactant adsorption under various environmental conditions. This information is particularly lacking at low (submicromolar), environmentally significant concentrations of surfactants.

We summarize here results from a number of batch adsorption studies that were conducted to characterize surfactant adsorption.¹⁷⁻²⁰ We examine the effects of surfactant structure, solution composition ($[H^+]$, $[Na^+]$, and $[Ca^{2+}]$), and sorbent properties on the distributions of cationic, neutral, and anionic surfactants. The results presented here have been chosen to illustrate the relative importance of these variables on the extent of adsorption and shed some light on the mechanisms involved.

METHODS

Materials

The ^{14}C -labeled cationic, anionic, and neutral surfactants used in this study are shown in Table 7.1. The only cationic surfactant used was N-[1- ^{14}C]-dodecylpyridinium (DP). The anionic surfactants were uniformly ring-labeled homologues of 4-alkylbenzenesulfonates containing 10, 12, and 14 carbons in the alkyl chain, referred to as C-10, C-12, and C-14 LAS. The neutral surfactants were homologues of monoalkyl ethers of poly(ethylene glycol), also known as alcohol ethoxylates, referred to as AEs. The hydrophobic chain of each of the AEs contained 13 carbons (1- ^{14}C) and the hydrophilic chain contained 3, 6, or 9 oxyethylene (-CH₂CH₂O-) units; these compounds are referred to as AE₃, AE₆, and AE₉. Thus, the AE homologues differed in hydrophilic chain length, while the LAS homologues differed in hydrophobic chain length. The DP is a permanently charged cation. The LAS compounds are moderately strong acids that are anionic at all environmentally relevant pH values, and the AEs are neutral. The ^{14}C -labeled compounds were used to enable the determination of surfactant distribution at environmentally relevant submicromolar concentrations.

The labeled DP was synthesized by Pathfinder Laboratories, Inc. (St. Louis, MO); LAS compounds were obtained through the Soap and Detergent Association from Proctor and Gamble; and AE compounds were obtained through the Soap and Detergent Association from Shell Research. The specific activities of DP, C-10, C-12, C-14 LAS, AE₃, AE₆, and AE₉ were 10.6, 1.46, 13.4, 12.9, 6.9, 21.3, and 6.6 Ci/mol, respectively. The purity of the DP and LAS compounds was greater than 99% as determined by HPLC; the purity of the AE compounds was 95–98% as determined by TLC and HPLC. Thus, the purity of the compounds used in this study is very high compared to the mixtures of homologues that are generally used in commercial formulations. Primary standards were prepared in methanol, and spiking standards in 95% ethanol; they were stored at ~0°C.

The sorbents were five sediments and soils from the “EPA collection” (EPA-1, -12, -13, -16, and -25), which were provided by John J. Hassett of the University of Illinois. The properties of the sorbents are listed in Table 7.2. The sorbents exhibit a wide range of characteristics that can influence surfac-

Table 7.1. Surfactants Used in This Study

	A. Alkylpyridinium	B. LAS	C. AE		
ID ^a	Name	n ^b	M ^c	Elemental Composition	CAS Registry Number
A. Alkylpyridinium					
DP	dodecylpyridinium	10	248	C ₁₇ H ₃₀ N	15416-74-7
B. LAS	"linear alkylbenzenene sulfonate"				
C-10 LAS	4-(1-methylnonyl)benzenesulfonate	7	297	C ₁₆ H ₂₅ O ₃ S	
C-12 LAS	4-(1-methylundecyl)benzenesulfonate	9	325	C ₁₈ H ₂₉ O ₃ S	18767-50-5
C-14 LAS	4-(1-methyltridecyl)benzenesulfonate	11	353	C ₂₀ H ₃₃ O ₃ S	
C. AE	"alcohol ethoxylate"				
AE ₃	monotridecyl ether of tri(ethylene glycol)	3	332	C ₁₉ H ₄₀ O ₄	4403-12-7
AE ₆	monotridecyl ether of hexa(ethylene glycol)	6	464	C ₂₅ H ₅₂ O ₇	930-09-6
AE ₉	monotridecyl ether of nona(ethylene glycol)	9	596	C ₃₁ H ₆₄ O ₁₀	7300-80-3

^aAbbreviation used in this study.^bValue of n in structure above.^cMolar mass, g/mol.

Table 7.2. Properties of Sorbents

Sediment	Organic Carbon (%)	Sand (%)	Silt (%)	Clay (%)	CEC (mmol/g)	pH ^a (1:1)	pH ^b (1:20)	Surface Area ^c (m ² /g)
EPA-16	1.20	0.5	60.5	39.0	0.110	6.50	6.76	18
EPA-13	3.04	20.3	27.1	52.6	0.119	6.90	7.08	13
EPA-12	2.33	0	64.6	35.4	0.135	7.63	7.52	12
EPA-25	0.76	41.9	37.6	20.5	0.089	7.65	7.57	8
EPA-1	0.22	93.9	0	6.1	0.011	7.30	—	0.8

Source: Hassett et al.²¹

^aSolution was 0.01 M NaCl, 1 g sediment to 1 mL solution.

^bSolution was 0.01 M NaN₃, 1 g sediment to 20 mL solution.

^cDetermined courtesy of Jeff Fahey, Teledyne Wah-Chang, Albany, Oregon.

tant adsorption, including fraction organic carbon (f_{oc}), surface area, particle size distribution and mineralogy, and cation exchange capacity (CEC).²¹

Determination of Distribution Ratios in Batch Experiments

The adsorption of surfactants on suspended sediments and soils was studied by equilibrating solutions in batch at 25°C. The methods that were used to determine the distribution of surfactants between adsorbed and aqueous phases were essentially the same for each class of compound and are summarized below; the procedures are described in detail elsewhere.¹⁷⁻²⁰

The equipment used for equilibrations and phase separations in the adsorption experiments included a New Brunswick Model G-24 thermostatted shaker and a Beckman Model J2-21 thermostatted centrifuge. The radioactivity of the surfactants was determined with a Beckman Model LS 7800 scintillation counter. Labeled compounds adsorbed to sediment or soil were converted to CO₂ by combustion with a Harvey Model 300 Oxidizer. The solution pH was determined with an Orion Model 8102 combination glass electrode. Concentrations of major ions were determined by inductively coupled plasma emission spectrometry.

Before sorbents were equilibrated with solutions of surfactants, they were washed eight times to reduce the amounts of suspended particles that are not removed from the water phase by centrifugation. Association of organic compounds with nonseparable or colloidal materials can affect the observed distributions in batch experiments.²² Washing of the sorbents also decreased the amounts of major ions which desorbed or dissolved during the equilibration step,¹⁹ and decreased the concentrations of dissolved organic carbon and UV absorbance in the supernatant solution.

The sorbents were washed by adding 0.05–1.0 g of air-dried sorbent to 35-mL Corex centrifuge tubes, adding 20 mL of distilled and deionized (Milli-Q) water, shaking for 1 hr at 500 rpm and 25°C on the shaker, and centrifuging for 10 min at 11,000 g and 25°C. The supernatant was removed by aspiration with a pipet, and the procedure repeated seven more times. After the last wash the contents of the tube were freeze-dried and reweighed. Generally, 2% or less

of the sediment mass was removed by the washing procedure. In selected experiments, we determined that there were no discernible effects of the freeze-drying procedure.¹⁹

The freeze-dried sorbents were then resuspended by adding 20 mL of electrolyte solution to the centrifuge tube. The ratio of mass of solids to volume of liquid, $C_s(w)$, for all of these experiments was in the range 0.015–0.050 g/mL. In studies in which effects of $C_s(w)$ were examined,^{18–20} only slight effects of $C_s(w)$ on adsorption were observed, and they could be attributed either to isotherm nonlinearity or to variations in $[Ca^{2+}]$ which was released from the solids during equilibration. Unless otherwise specified, the electrolyte solution was 0.01 M NaN_3 . The equilibrations were conducted in the presence of azide to inhibit microbial degradation of labeled compounds, which was evident in several LAS and AE experiments that were run with NaCl or deionized water.^{18,19} The type of anion, whether chloride or azide, did not have a significant effect on adsorption of LAS or DP.^{17,19}

The resuspended sorbents were shaken for 1 hr, the suspensions were centrifuged, and surfactants were added as 10–200 μ L spikes in 95% ethanol. The purpose of this procedure was to minimize the contact between sorbents and localized high concentrations of surfactants. Isotherms were developed by adding different amounts of surfactant to different tubes having the same solids-to-liquid ratio. The tubes were sealed with PTFE-lined caps, and the contents shaken at 500 rpm for 4–12 hr. Adsorption kinetic experiments showed that the approach to equilibrium was virtually complete for DP and LAS in 4 hr;^{17,19} adsorption kinetics for the AE homologues were slower, and suspensions were equilibrated on the shaker for 12 hr.¹⁸ After shaking, the suspensions were centrifuged for 1 hr at 11,000 g to separate particles from the aqueous phase.

After centrifugation the concentrations of labeled surfactants were determined in three fractions: the water, the sorbent, and the tube walls. From these data were calculated the recovery of the label added to the tube and the concentration distribution ratio, D_c :

$$D_c = C_i(s)/C_i(w) \quad (L/kg) \quad (7.1)$$

where $C_i(s)$ (mol/kg) and $C_i(w)$ (mol/L) are the total concentrations of surfactant in the sorbent and water phases, respectively.

Activities of the labeled compound associated with each phase were determined by similar methods. Aliquots of the aqueous phase, 0.2–1.0 mL, were obtained with glass pipets and added to vials containing Beckman HP/b scintillation fluid. The amount of surfactant adsorbed to sediment or soil was determined by removing the excess supernatant solution, freeze-drying the sorbent in the tube, transferring replicate subsamples of the dried sorbent (weighing 10–200 mg) to quartz combustion boats, oxidizing the subsamples at 900°C in oxygen, and trapping the resulting $^{14}CO_2$ in a mixture of 5 mL Packard Carbo-sorb and 5 mL of Permafluor V scintillation fluid. The walls

of the centrifuge tubes were brushed clean and extracted with 20 mL of 95% ethanol, which was sampled in a similar manner as the aqueous-phase samples. The activity of each sample was determined by liquid scintillation counting and calibrating with spikes added to each phase. The precision of the aqueous- and sorbent-phase determinations was estimated to be better than 2 and 5% relative standard deviation, respectively. The overall recoveries for each experiment were excellent, averaging 97% for all experiments. The amount of surfactant found on the container walls did not exceed 10% of the total amount adsorbed. The fraction on the walls increased as the D_c increased; the walls were more important for cationic than anionic surfactants and at lower sorbent-to-solution ratios.

For the study of the effect of pH on surfactant adsorption, the pH was adjusted through additions of HCl or NaOH. The solution pH was determined before and after equilibration with surfactant. The effect of $[Na^+]$ on surfactant adsorption was investigated by addition of NaCl (DP and the AE homologues) or NaN_3 (C-12 LAS). The effect of $[Ca^{2+}]$ on surfactant adsorption was investigated with solutions containing variable concentrations of $CaCl_2$ and 0.01 M NaN_3 . Concentrations of Ca, Na, and other major elements in solution that were released from the sediments and soils during equilibration were determined in selected experiments.¹⁹

RESULTS AND DISCUSSION

Adsorption of amphiphilic compounds to natural surfaces can involve a combination of hydrophobic, electrostatic, and specific chemical interactions with the surface. We examine here the effects of (1) surfactant charge and structure, (2) sorbent properties, and (3) selected solution properties on the adsorption of surfactants to surfaces of suspended particles.

Because of possible solute-solute or sorbate-sorbate interactions among surfactant molecules, the concentration range of the study is important. At low surface concentrations of surfactant, surface-sorbate interactions control adsorption. As the surfactant accumulates at the surface, sorbate-sorbate interactions can become important. At high surface coverages of surfactant, favorable hydrophobic cooperative effects and unfavorable electrostatic effects may be significant. Cooperative hydrophobic effects are thought to account for hemimicelle formation of surfactants on a number of surfaces.^{11,12,23} For the studies presented here, there should be little influence of solute-solute or sorbate-sorbate interactions because of the low solution and surface concentrations of surfactants.

Adsorption Isotherms of Different Surfactants

The adsorption isotherms for each of the seven surfactants on EPA-12 sorbent are shown in Figure 7.1. This figure illustrates clearly the nonlinearity

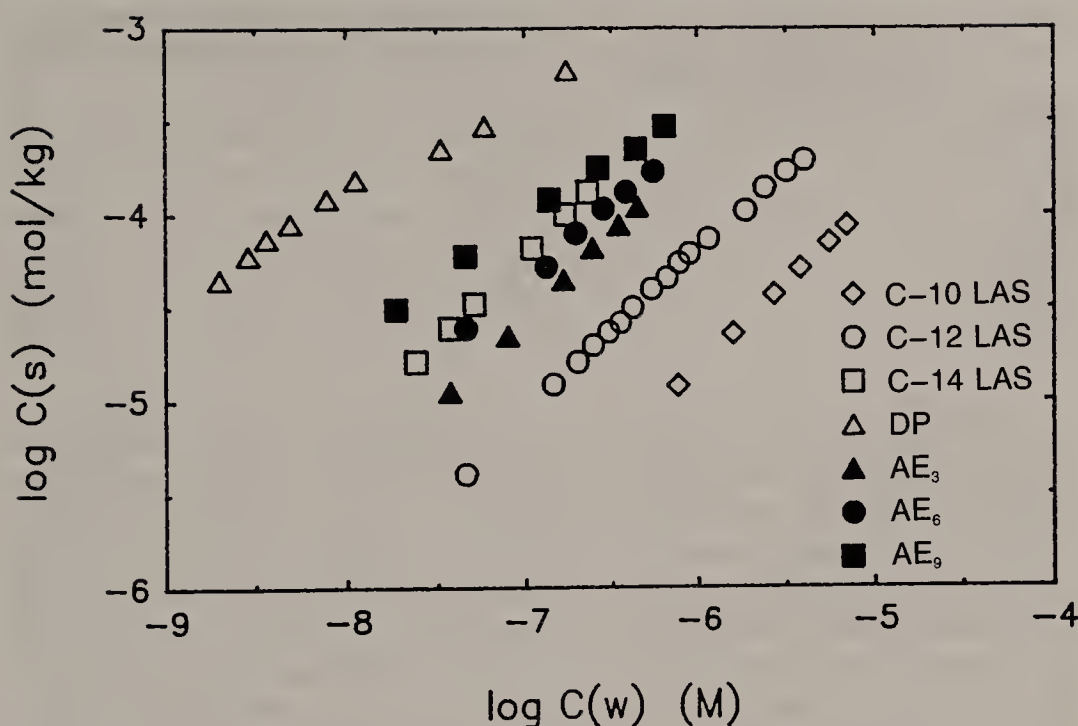


Figure 7.1. Comparison of adsorption of different classes of surfactants. Adsorption isotherms of seven surfactants on EPA-12 sorbent in 0.01 M NaN_3 ; $C_s(w) = 0.025 \text{ g/mL}$ for AEs and DP, 0.015 g/mL for C-12 LAS, and 0.050 g/mL for C-10 and C-14 LAS. Freundlich isotherm parameters in Table 7.3.

of all the isotherms and the differences in adsorption energy among the three classes of surfactants and the LAS and AE homologues, as discussed below.

Nonlinearity

The isotherms determined for EPA-12, and all other combinations of surfactants and sorbents examined in the low concentration range, were reasonably well described by the Freundlich equation:

$$\log C_i(s) = \log K + n \log C_i(w) \quad (7.2)$$

where K and n are empirical constants. The values of K and n for the isotherms in Figure 7.1 are given in Table 7.3. A value of $n = 1$ corresponds to a linear isotherm. Despite the low concentrations of surfactants, isotherms were distinctly nonlinear ($n < 1$) for all compounds, as shown in the table. At these low concentrations of surfactants, the estimated fractional surface coverages are well below those of a uniform monolayer. The estimated fractional surface coverages are in the range of 0.01 to 2.8%, based on surface concentrations in the range of 2.5 to 560 nmol/g, area occupied by a sorbed molecule of 1 nm^2 , and specific surface area of the sorbent (EPA-12) of $12 \text{ m}^2/\text{g}$.

In the absence of cooperative sorbate-sorbate interactions, isotherm nonlinearity can be due to (1) variable electrostatic interactions as the concentration

Table 7.3. Values of Parameters in Freundlich Equation for Adsorption Isotherms on Sorbent EPA-12. From Figure 7.1 and Equation 7.2; log K reported for C(w) in mol/L and C(s) in mol/kg

Surfactant	log K	n
DP	0.43	0.54
AE ₃	1.90	0.92
AE ₆	1.22	0.79
AE ₉	0.35	0.63
C10-LAS	0.58	0.90
C12-LAS	0.98	0.86
C14-LAS	2.27	0.93

of the ionic LAS or DP sorbate increases; (2) presence of an assemblage of heterogeneous adsorption sites and saturation of the more energetically favored sites; and (3) unrecognized artifacts (e.g., changes in solution concentrations of major ions caused by adsorption of the target compound). After having considered electrostatic energy and the other factors listed above, we have interpreted most of the isotherm nonlinearity of the AEs and DP over this concentration range to be caused by filling of heterogeneous adsorption sites. In the case of the AEs, these are sites that interact specifically with the oxyethylene units, and for DP, they are cation exchange sites.^{17,18} In the case of the three LAS homologues, the isotherms of which are the most linear ($n = 0.83\text{--}0.93$), there may be some contribution of electrostatic repulsion of adsorbed LAS to D_c at the highest concentrations.¹⁹ Hand and Williams reported linear three-point isotherms for LAS on sediments over a similar concentration range.¹⁰

Adsorption Energy

For compounds that sorb with a linear isotherm, a comparison of sorption energies follows directly from a comparison of values of log K. However, such a comparison is not strictly justifiable for the values of log K in Table 7.3 since the isotherms are nonlinear. Nonetheless, a reasonable estimate of comparative adsorption energies can be made by comparing D_c at constant $C_i(s)$ or $C_i(w)$, whichever is thought to be the major source of nonlinearity. In this study, we attribute most of the nonlinearity to surface heterogeneity; thus, comparison at constant $C_i(s)$ is indicated. Irrespective of this issue, a simple qualitative comparison of the isotherms in Figure 7.1 reveals that energy of adsorption increases from anionic to neutral to cationic surfactants of approximately the same size. This observation is one indication of the importance of electrostatic interactions of surfactants with negatively charged natural particle surfaces.

For the three LAS homologues, adsorption increases as expected,²⁴ with increasing alkyl chain length due to hydrophobic interactions: at very low concentrations, $d \log D_c / d \log n_{\text{CH}_2^-} \approx 0.40$ (Figure 7.1). This value is close to the value of 0.45 determined by Hand and Williams for LAS adsorption.¹⁰

For the three AE homologues, an increase in the number of oxyethylene

(-CH₂CH₂O-) units leads to an increase in adsorption and an increase in the nonlinearity of the isotherm (Figure 7.1). Presumably the ether oxygen atoms and the terminal hydroxy group contribute to the specific adsorption of the AEs. The isotherm of AE₃, which is the most hydrocarbon-like of the neutral surfactants, is the most linear, consistent with a relatively nonspecific sorption behavior. The stronger adsorption of the AEs with increasing number of oxyethylene units is evident despite a concomitant increase in aqueous solubilities. The critical micelle concentrations (CMC) of AEs increase with increasing number of oxyethylene units. For example, the CMC of A₁₂E₂, A₁₂E₄, A₁₂E₆, and A₁₂E₈ at 25°C are 33, 64, 82, and 100 μM, respectively.¹³

The increase in log D_c with number of oxyethylene units, at constant C_{i(s)}, is not linear: at C_{i(s)} = 100 nmol/g, d log D_c/d n_(-CH₂CH₂O-) = 0.045 and 0.15 for the difference between AE₃ and AE₆, and AE₆ and AE₉, respectively. These values of d log D_c/d n_(-CH₂CH₂O-) depend on C_{i(s)} as well. There are few reports of the effect of the number of oxyethylene units on adsorption in the low concentration region of the isotherm. In a study of AE adsorption on carbon black, the value of d log D_c/d n_(-CH₂CH₂O-), calculated for infinite dilution, was 0.11.²⁵ Apparently the longer hydrophilic chains allow multiple interactions to occur between the surfactant molecule and the surface, resulting in the increase of d log D_c/d n_(-CH₂CH₂O-) with length of the hydrophilic chain. With our data, we cannot yet determine the nature of these interactions.

Adsorption of Surfactants on Different Sorbents

The adsorption isotherms of DP, C-12 LAS, and AE₆ on the different sorbents are presented in Figures 7.2–7.4. For each compound, the extent of adsorption varied from sorbent to sorbent; of interest is the effect of sorbent properties, particularly f_{oc} and CEC, on extent of adsorption. Adsorption isotherms were described well by Equation 7.2 for all surfactant-sorbent combinations; the parameters of the Freundlich equation are found in Table 7.4 for the data in Figures 7.2–7.4.

Dodecylpyridinium

The slopes of the Freundlich isotherms (Figure 7.2 and Table 7.4) for DP were similar for all five sorbents; the low values of n (0.56–0.62) correspond to a large degree of isotherm nonlinearity. The adsorption of DP on the five sorbents increases in the order: EPA-1 < EPA-12 < EPA-25 ≈ EPA-16 < EPA-13 and follows the relative increase of the cation exchange capacity (CEC) of the sorbent, with the notable exception of EPA-12 soil, which exhibited lower adsorption despite having the largest CEC. There are no other properties that we have measured (Table 7.2), such as surface area or f_{oc}, that suggest why the behavior of EPA-12 is somewhat anomalous. Qualitative clay mineral analysis by X-ray diffraction indicates that swelling clays (smectites) are present in high amounts in EPA-16 and EPA-25 sorbents, but in lower

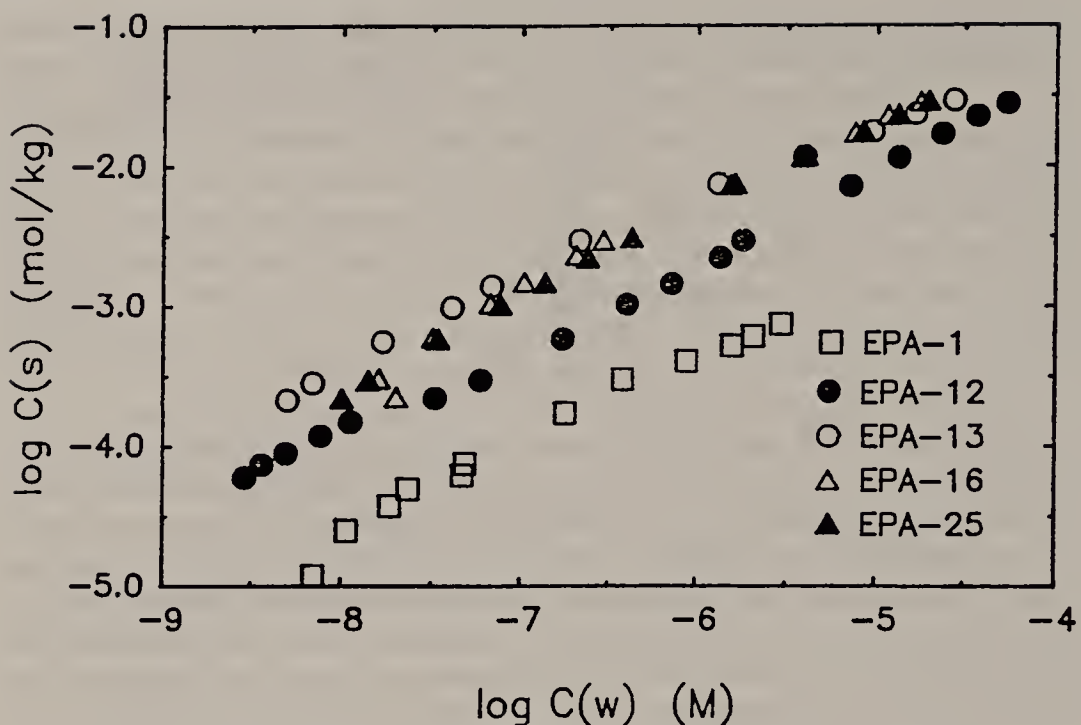


Figure 7.2. Adsorption isotherms for DP on five sorbents in 0.01 M NaN_3 ; $C_s(w) = 0.025$ g/mL for each sorbent. Freundlich isotherm parameters in Table 7.4.

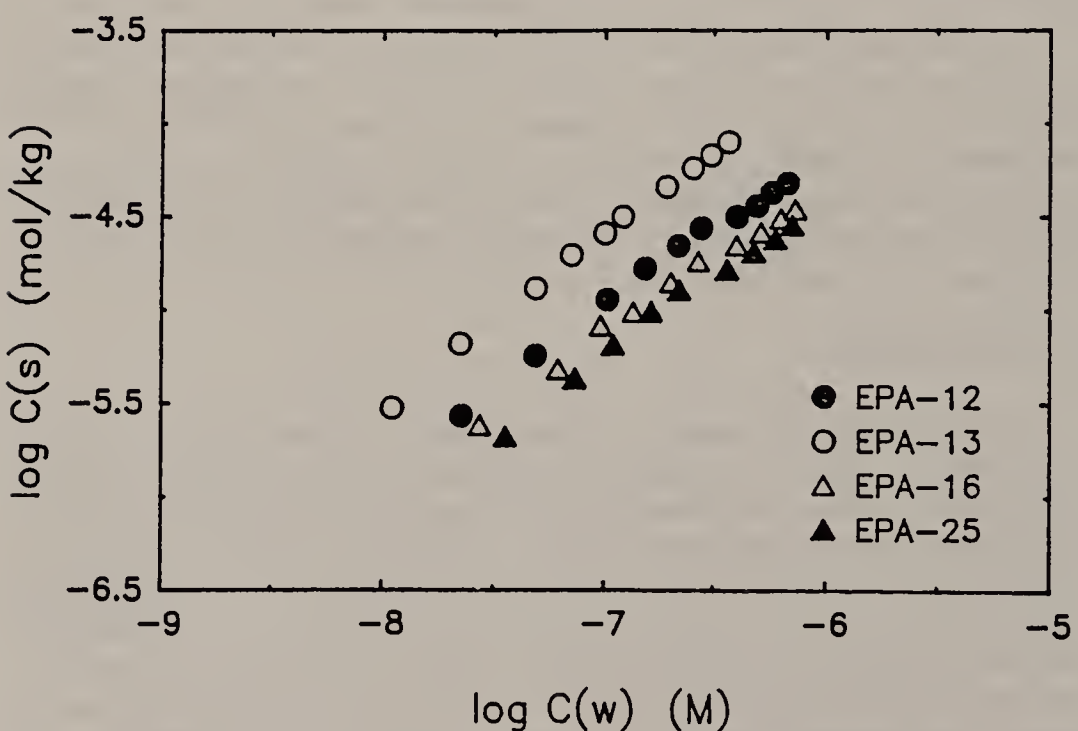


Figure 7.3. Adsorption isotherms for C-12 LAS on four sorbents in 0.01 M NaN_3 ; $C_s(w) = 0.025$ g/mL for each sorbent. Freundlich isotherm parameters in Table 7.4.

Table 7.4. Values of Parameters in Freundlich Equation for Adsorption of DP, C12-LAS, and AE₆ on Different Sorbents. From Figures 7.2–7.4 and Equation 7.2; log K Reported for C(w) in mol/L and C(s) in mol/kg. (Values of log K and n were Calculated from Data in Figures; Values Reported Here for DP, C-12 LAS, and AE₆ on EPA-12 Differ Slightly from Values in Table 7.3 Due to Different Subsets of Data in Figure 7.1 and Figure 7.2–7.4.)

Surfactant	Sorbent	log K	n
DP	EPA-1	0.42	0.63
DP	EPA-12	1.03	0.62
DP	EPA-13	1.08	0.56
DP	EPA-16	1.59	0.65
DP	EPA-25	1.49	0.63
C12-LAS	EPA-12	0.85	0.83
C12-LAS	EPA-13	1.84	0.92
C12-LAS	EPA-16	0.46	0.80
C12-LAS	EPA-25	0.68	0.85
AE ₆	EPA-12	1.79	0.88
AE ₆	EPA-13	1.77	0.74
AE ₆	EPA-16	1.78	0.78
AE ₆	EPA-25	1.60	0.75

amounts in EPA-12. Cationic and nonionic surfactants are known to intercalate in smectites, while anionic surfactants do not.^{26–28}

The adsorption capacity (the amount adsorbed at plateau adsorption) of DP was found to correspond closely to the cation exchange capacity of the sorbent in a study with aquifer materials, clay minerals, and with EPA-12 soil.¹⁷ Studies on the adsorption of methylacridinium and paraquat with soils and sediment have also determined that both adsorption capacity and intensity can be estimated from the CEC of the sorbent.^{29,30} Given these observations and the effects of pH and salt concentration (which are presented below), it appears that cation exchange is a dominant mechanism for adsorption of organic cations.¹⁷ The isotherm nonlinearity cannot be accounted for by variable electrostatic interactions nor by the filling of a single type of cation exchange site. The application of a multisite model in which cation exchange and adsorption of ion pairs are important reactions has been reported elsewhere.¹⁷

Linear Alkylbenzenesulfonate

The isotherms of C-12 LAS shown in Figure 7.3 and Table 7.4 were all determined with C_s(w) = 0.025 g/mL. There was very weak adsorption of LAS on EPA-1, and the data are not included in Figure 7.2. In all cases, the isotherms were slightly nonlinear and the slopes of the Freundlich isotherms were very similar; the nonlinearity actually increases with concentration. The intensity of adsorption of C-12 LAS increased with increasing fraction organic carbon, f_{oc}, of the sorbent, suggesting relatively nonspecific sorption of this compound. The values of D_c increase in the order: EPA-1 < EPA-25 ≈ EPA-16 < EPA-12 < EPA-13, which is the same order of the fraction organic carbon of the sorbents. There is a roughly proportional increase in adsorption

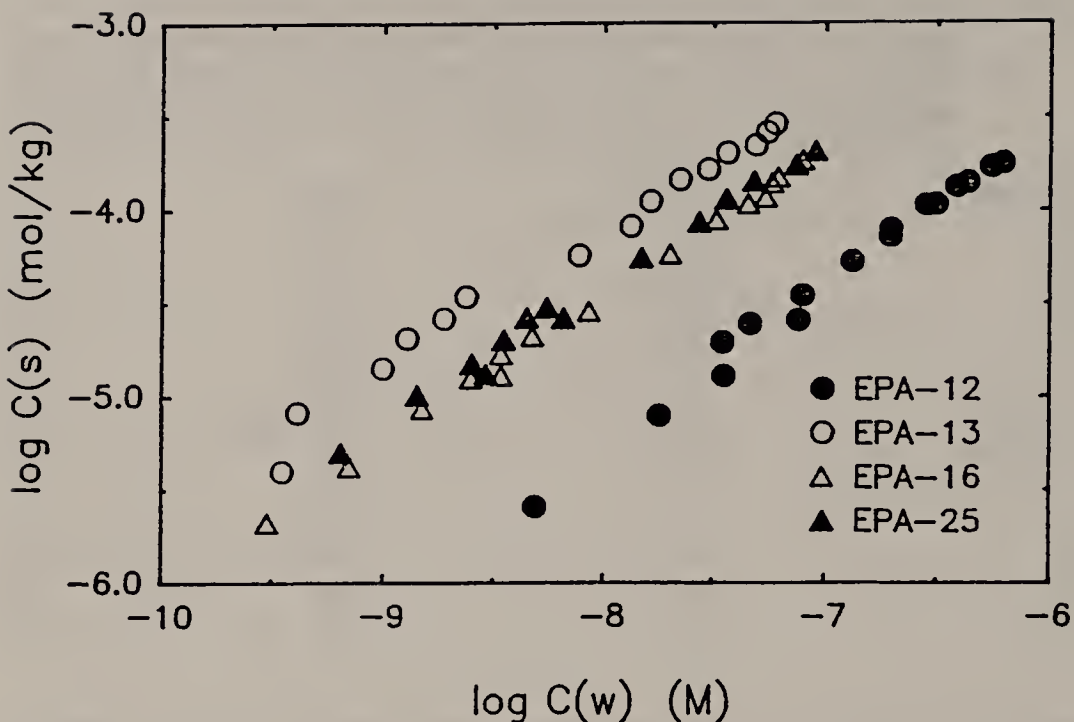


Figure 7.4. Adsorption isotherms for AE₆ on four sorbents in 0.01 M NaN₃; C_{s(w)} = 0.025–0.029 g/mL for each sorbent. Freundlich isotherm parameters in Table 7.4.

intensity with f_{oc}, as is observed with nonpolar organic compounds.^{14,31} Values of K_{oc} were derived by fitting the sorption data to a linear sorption model and dividing the resulting K by f_{oc} of the sorbent.¹⁹ Estimates of K_{oc} ranged between 4400 L/kg_{oc} for EPA-12 and 8600 L/kg_{oc} for EPA-13; the average value was 6400 L/kg_{oc} for the five sorbents. No relationships between sorption and the other properties of sorbents were apparent. Other authors have observed a correlation between the sorption of alkylbenzenesulfonates and f_{oc} of soils and sediments.^{9,10} In a comparable study,¹⁰ the values of K_{oc} for C-12 LAS were 7000–9000 L/kg_{oc} for two sediments, but much higher than this range for two additional sediments. Other studies with soils have shown a correlation between adsorption of alkylbenzenesulfonate (and other ions such as sulfate and phosphate) and the sesquioxide (extractable Al and Fe) content.^{32,33} We have no information on the sesquioxide content of our sorbents. The nonlinearity of the LAS isotherms, while slight, may be due to specific interactions and saturation of energetic sesquioxide surface sites. The extent of nonlinearity at higher concentration cannot be explained completely by variable electrostatic energy, although such interactions could be contributing.¹⁹

Alcohol Ethoxylates

The effect of sediment properties on adsorption of AE₆ (Figure 7.4) is similar to that for DP, except that the adsorption onto EPA-12 soil is even

more reduced relative to that of the other sorbents. Our results are consistent with those of Podoll et al., who found that adsorption of polyethylene glycols to sediment was related to the fraction of swelling clays (montmorillonite + vermiculite) of the sorbent, but not to organic carbon content.³⁴ Certainly the properties of the sorbent that affect AE are complicated and deserve further attention.

Effect of Solution Properties on Adsorption

The effects of solution concentrations of H^+ , Na^+ , and Ca^{2+} on adsorption of each of the classes of surfactant are shown in Figures 7.5–7.7. The data are from the low concentration range of the isotherm and are all for the common sorbent EPA-12. Experiments were conducted with a constant amount of surfactant in the system and varying pH or concentration of Na^+ or Ca^{2+} .

The observed effect of solution property on D_c can be complicated by non-linearity of the isotherm and the total surfactant concentration (i.e., concentrations above and below those at which solute-solute or sorbate-sorbate interactions become significant).¹⁷ However, in these studies, neither of these problems significantly affects our interpretation of the results; the sorbate concentration was low and did not vary by more than a factor of two.

Dodecylpyridinium

In contrast to the anionic surfactants, solution pH had negligible effect on the adsorption of cationic DP (Figure 7.5a)—an observation not inconsistent with electrically neutral cation exchange reactions. The same result was obtained in another study for Lula aquifer material.¹⁷

The effects of $[Na^+]$ (Figure 7.6) and especially $[Ca^{2+}]$ (Figure 7.7) on adsorption were large: $d \log D_c/d \log [M]$ ranged from approximately -0.3 to -0.6 for a range of sorbent materials including EPA-12, for which the data are shown.¹⁷ The effect of metal concentration on adsorption of amphiphilic organic cations has been explained by electrically neutral cation exchange and ion-pair reactions.¹⁷

Linear Alkylbenzenesulfonates

The adsorption of each of the LAS homologues increased with increasing $[H^+]$ (Figure 7.5b), $[Na^+]$ (Figure 7.6), and $[Ca^{2+}]$ (Figure 7.7). The measured effect of pH for all three LAS homologues was $d \log D_c/d \log [H^+] \approx 0.17$. The effect of pH may be due to the influence of H^+ as a surface potential determining ion or to specific pH-dependent surface complexation or ligand exchange reactions (e.g., ligand exchange with $-OH$ of $=FeOH$ or $=AlOH$ groups). Competitive adsorption by SO_4^{2-} and HPO_4^{2-} on LAS has been observed^{32,33} and supports the importance of specific surface interactions.

An increase in Na^+ concentration results in a relatively large increase in LAS

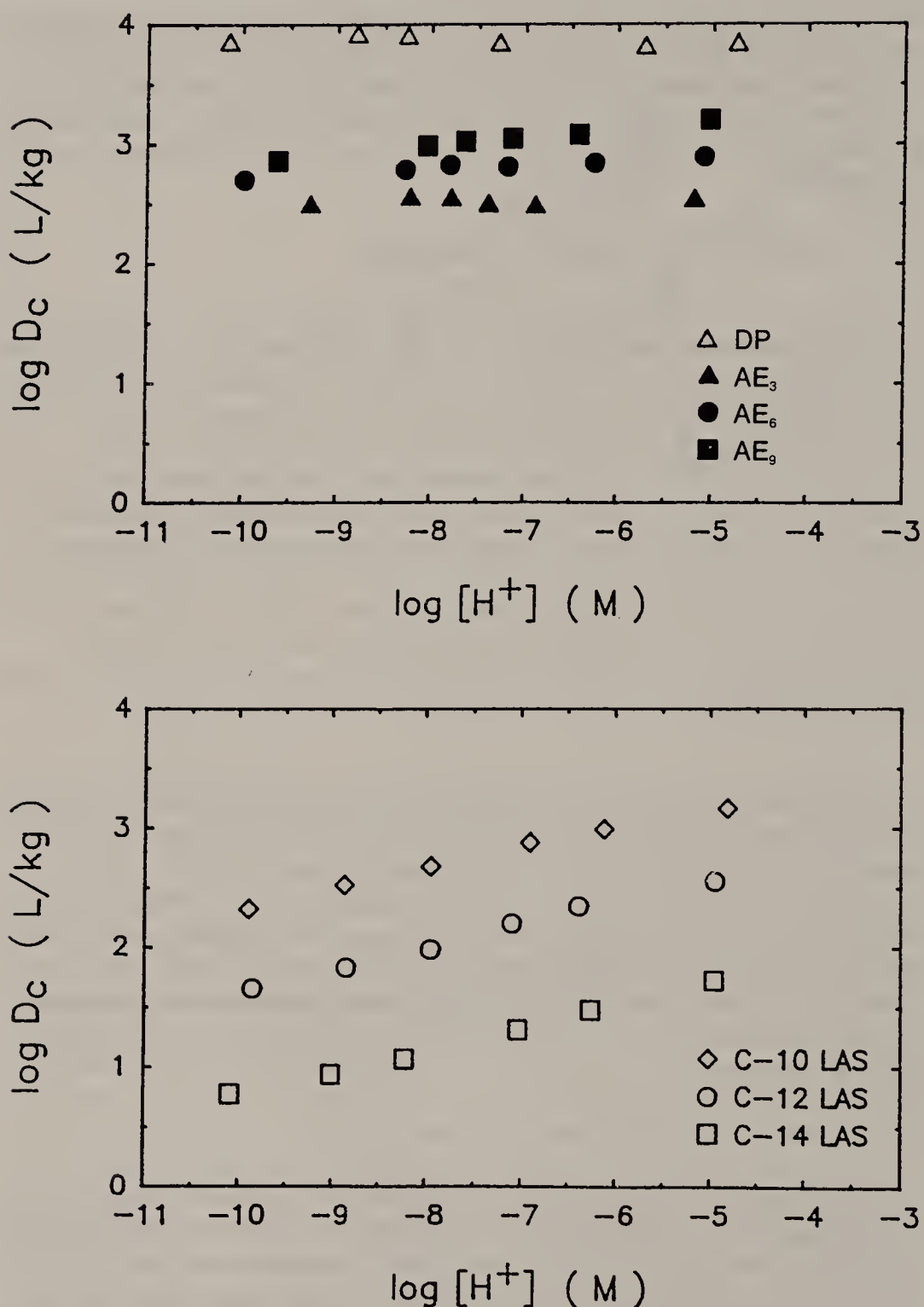


Figure 7.5. Effect of pH on adsorption (a) of cationic and nonionic surfactants by EPA-12 sorbent in 0.01 M NaN_3 ; $C_s(w) = 0.025$ g/mL; (b) of LAS homologues by EPA-12 sorbent in 0.01 M NaN_3 ; $C_s(w) = 0.05$ g/mL.

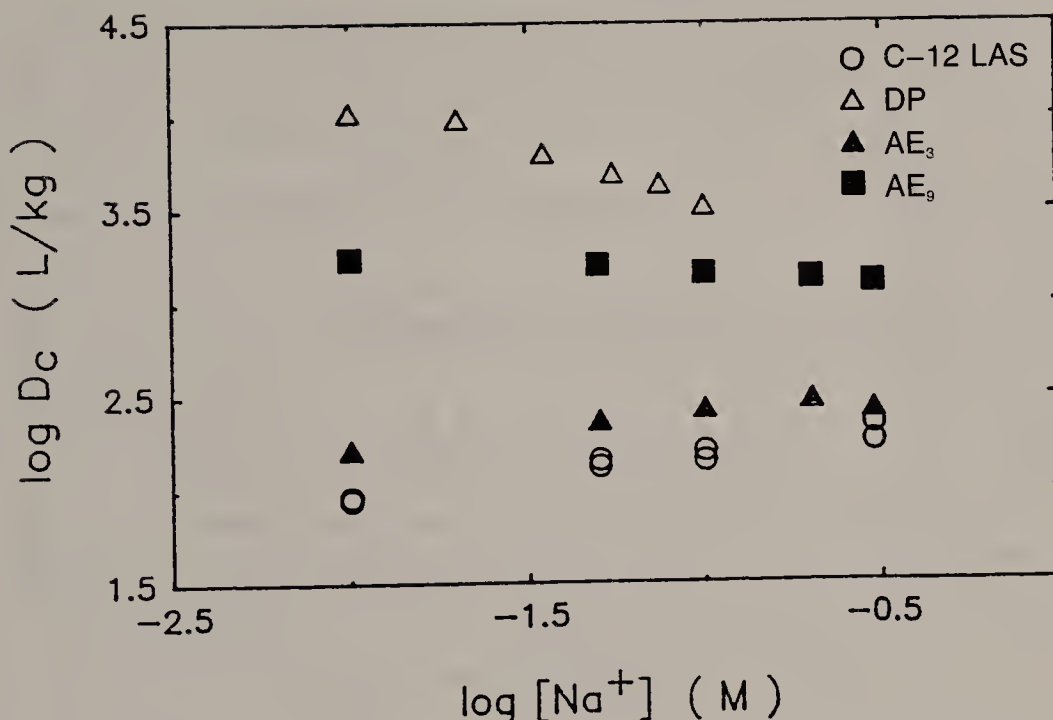


Figure 7.6. Effect of $[Na^+]$ on adsorption of surfactants by EPA-12 sorbent in 0.01 M NaN_3 . $[Na^+]$ was varied by addition of NaCl (DP) or NaN_3 (LAS and AE); $C_s(w) = 0.005$, 0.025, and 0.050 g/mL for DP, AEs, and LAS, respectively. Data for C-12 LAS represent replicate determinations.

adsorption: $d \log D_c/d \log [Na^+] \approx 0.23$ (Figure 7.6). The magnitude of this effect is consistent with the attenuation of the electrostatic repulsion between LAS and the surface by the presence of nonspecifically adsorbed Na^+ in the diffuse part of the electric double layer.

The effect of low concentrations of Ca^{2+} (0.1–1.0 mM) in the presence of higher concentrations of Na^+ (10 mM) were appreciable ($d \log D_c/d \log [Ca^{2+}] \approx 0.23$) (Figure 7.7) and comparable to the effects of Na^+ itself. The effect of calcium on LAS adsorption cannot be explained simply by the attenuation of electrostatic repulsion by nonspecifically adsorbed Ca^{2+} in the diffuse part of the electric double layer; such electrostatic repulsion would be masked by the relatively high concentrations of Na^+ . A specific surface complex of LAS with surface adsorbed Ca^{2+} is suggested by these results. The effect of Ca^{2+} is consistent with the observed increase in LAS adsorption in naturally hard waters compared to that in 0.01 M KCl.¹⁰

Alcohol Ethoxylates

For the nonionic surfactants, there were minor, yet significant, effects over the range of properties measured. There was no discernible effect of pH (Fig-

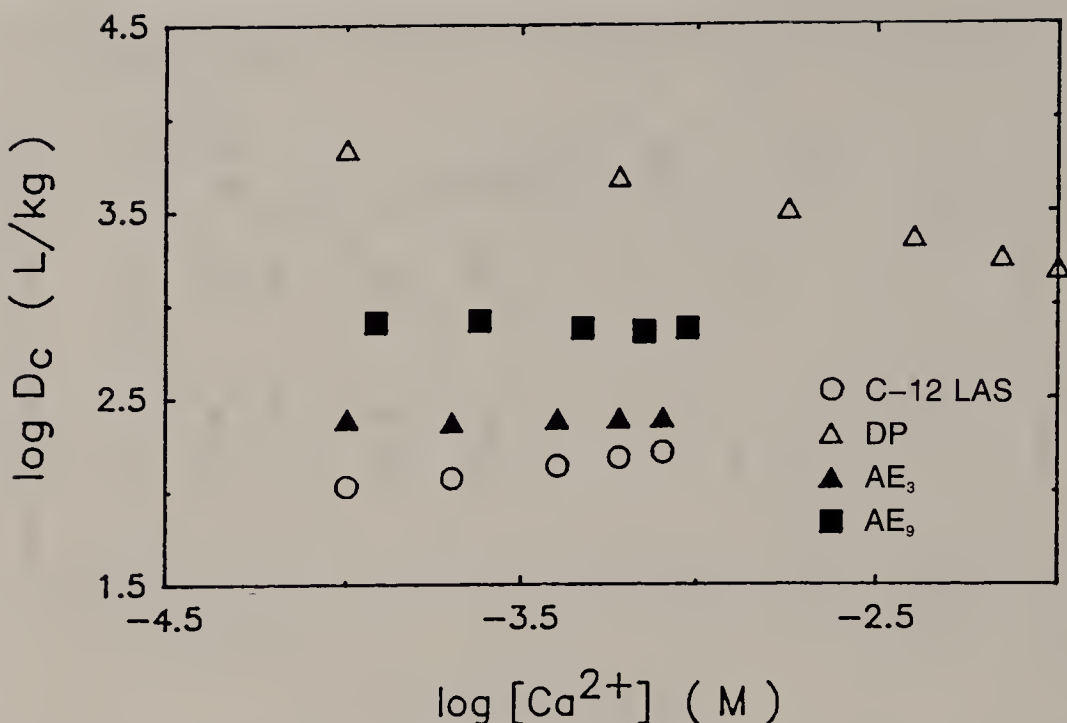


Figure 7.7. Effect of $[Ca^{2+}]$ on adsorption of surfactants by EPA-12 sorbent in the presence of 0.01 M NaN_3 ; $C_s(w) = 0.005$ g/mL for DP and 0.010 g/mL for LAS and AEs.

ure 7.5a) on the adsorption of AE_3 . For homologues with a greater number of oxyethylene units, there was a greater effect of pH ($d \log D_c/d \log [H^+] \cong 0.07$ for AE_9). Larger effects of pH have been observed for alkylphenol "ethoxyate" (APE) adsorption on surfaces with pH-dependent surface charge, such as those of quartz, silica, and carboxycellulose.³⁵⁻³⁹ The interactions have been attributed to the ether oxygen behaving as a weak H-bond acceptor or to chemisorption of the terminal hydroxyl group.³⁵⁻³⁹

Sodium ion concentration has a small but measurable effect on adsorption of AE_3 and AE_9 (Figure 7.6); however, the direction of the effect was reversed for the two homologues. In the case of AE_3 , adsorption increased approximately twofold when $[Na^+]$ was increased from 10 to 300 mM. The magnitude of the increase in D_c is consistent with salting out of this more hydrocarbon-like homologue. However, the functional relation between $\log D_c$ and $[Na^+]$ does not correspond very well to that predicted by the Setchenow equation,⁴⁰ which describes the effect of electrolyte concentration on the solubility of hydrophobic solutes.

The D_c of AE_9 decreased with increasing NaN_3 , from 1850 to 1280 L/kg. This decrease in adsorption must be due to a decreased interaction of the oligo(ethylene glycol) chain with the surface, although the mechanism of this effect is unknown. Savintseva and coworkers have reported that APE adsorption on silica is reduced by addition of NaCl; the effect was even greater for sodium phosphate.^{38,39}

Calcium has virtually no effect on adsorption in the presence of 10 mM NaN_3 (Figure 7.7). This result suggests that the energy of the Ca^{2+} interaction is not high relative to that of the Na^+ interaction, and the effect of Ca^{2+} is masked by the high concentration of Na^+ .

SUMMARY OF SURFACTANT ADSORPTION

Many properties of surfactant, solution, and sorbent were observed to affect adsorption. The effects of sorbent and solution properties that control adsorption are quite different for different classes of surfactants, as are the important mechanisms.

DP adsorption was affected strongly by the concentrations of co-ions such as Na^+ and Ca^{2+} , but was independent of solution pH. These results, and those reported for other large hydrophobic organic cations, indicate the importance of cation exchange reactions. Organic cations exhibit very nonlinear adsorption isotherms with natural soil and sediment sorbents. We interpret this behavior to be the result of the heterogeneity of the surface. The adsorption intensity and capacity of organic cations both generally follow the CEC of the sorbent, although this was not the case for the EPA-12 soil, where the adsorption energy was lower.

LAS adsorption was affected by hydrophobic, electrostatic, and specific chemical interactions, although it is extremely difficult to separate specific and electrostatic effects. The importance of nonspecific hydrophobic interactions is evident from the regular effect of alkyl chain length, the correspondence of the adsorption intensity with the organic carbon content of the sorbent, and the small amount of isotherm nonlinearity as compared to the other surfactant classes studied. While it is difficult to separate the magnitudes of hydrophobic and electrostatic/specific chemical contributions to the total adsorption energy, the contributions appear to be additive; that is, solution properties (e.g., pH, $[\text{Na}^+]$, $[\text{Ca}^{2+}]$) that influence electrostatic or specific chemical interactions have the same regular effect for the different alkyl homologues.

The concentrations of Ca^{2+} , Na^+ , and H^+ all have significant effects on adsorption of LAS. The effect of a decade increase in these properties acts to increase $\log D_c$ by 0.23, 0.23, and 0.17 units, respectively. The effect of sodium is probably due to an attenuation of long-range electrostatic interactions. The effect of calcium is more specific and is likely due to complexation with LAS that occurs on the surface or in solution. The influence of pH on adsorption is also important. It is not known whether its effect is due to the dependence of surface potential (electrostatic energy) or specific ligand exchange reactions on pH. The nonlinearity of the isotherms exhibited at low concentration and the correlation of adsorption with sesquioxide content of soils reported in the literature^{32,33} indicate that some specific chemical interactions can be important.

AE adsorption depended primarily on the nature of the sorbent and on the number of oxyethylene units; the solution properties examined had relatively

little effect. The oxyethylene units were specifically adsorbed. The adsorption energy and the degree of nonlinearity both increased with increasing number of oxyethylene units. The nonlinearity is interpreted as an indication of specific interactions of the oxyethylene group with a limited number of surface functional groups. Adsorption was not well correlated with any measured property of the sorbents. The possible influence of swelling clays has been recognized previously and should be examined in greater detail.³⁴

The results of our work indicate that the adsorption of surfactants on natural materials can be important in environments with high solids concentrations. Adsorption was greatest for the cationic surfactant; the D_c for DP (at 10 nM in solution) was greater than 10⁴ L/kg for all of the sorbents, with the exception of the sandy EPA-1 sorbent. Association with suspended particles can be expected to affect the speciation of cationic surfactants that are the size of DP or greater in all but the most oligotrophic surface waters or surface waters of high salinity. Given the range of distribution ratios determined in this study, nonionic AEs and anionic LAS homologues will be significantly adsorbed only in highly eutrophic surface waters, and in waste treatment facilities in which wastewaters have large amounts of suspended solids. The extent of adsorption in a given environment will depend on the hydrophobicity and structural properties of the surfactant. Finally, adsorption onto particle surfaces will affect the fate and transport of all surfactants that accumulate in porous media environments, such as soils, aquifer environments, and surface sediments.

Predictive Models

In this study we have examined the sensitivity of surfactant adsorption to various parameters, and we have proposed some mechanisms to explain some of the observations. Studies of this sort are a first step toward the goal of understanding the processes well enough to develop predictive models for surfactant adsorption to environmental surfaces. Toward this goal we offer the following two observations.

This synthesis of surfactant adsorption studies has shown that, under similar conditions, different classes of surfactants behave quite differently. Thus, it is better to try to understand the behavior of surfactants one class at a time, rather than to attempt *a priori* to solve the problem for surfactants in general.

These studies with environmental sorbents have illustrated parameters to which adsorption is sensitive. Since the sorbent materials with which we worked were so heterogeneous, it is very difficult to reach definitive conclusions about mechanisms. The next step is to use carefully selected homogeneous sorbents (e.g., oxides, clays, carbonates, organic polymers) in experiments at low surface coverage, to examine the working hypotheses for adsorption mechanisms that we have proposed and to develop more quantitative models. Then the results from studies of the two types of sorbents must be thoughtfully integrated.

CONCLUSIONS

Conclusions concerning the adsorption of surfactants by suspended particles that can be derived from these and other studies include the following:

1. Adsorption of cationic surfactants onto negatively charged surfaces of soils and sediments is favored over nonionic and anionic compounds of similar size.
2. Alkyl homologue effects on the adsorption energy are regular and reasonably well predicted.
3. Isotherms are nonlinear, even at very low, environmentally relevant concentrations; this fact complicates the comparison of adsorption energies.
4. Results presented here suggest that the slopes of the Freundlich equations are similar for the same surfactants on different sorbents. This observation may facilitate the application of empirical or mechanistically based adsorption models.
5. Solution pH has a significant effect on adsorption of anionic surfactants, but not for cationic or nonionic classes.
6. Na^+ and Ca^{2+} concentrations are important determinants of LAS adsorption.
7. The adsorption of AEs increases with the number of oxyethylene units.
8. Adsorption of amphiphilic organic cations such as DP is largely controlled by cation exchange reactions.

ACKNOWLEDGMENTS

This research was funded partially by the Soap and Detergent Association. Other funding was provided by the U.S. Environmental Protection Agency through assistance agreement CR-814501 to Oregon State University. This work has not been subjected to EPA review, and therefore it does not reflect the views of the EPA and no official endorsement should be inferred. The U.S. EPA grant was administered through the R. S. Kerr Environmental Research Laboratory in Ada, OK.

REFERENCES

1. Greek, B. F., and P. L. Layman. "Detergent Industry Ponders Products for New Decade," *Chem. Eng. News* 68(5):37-60 (1990).
2. McEvoy, J., and W. Giger. "Determination of Linear Alkylbenzenesulfonates in Sewage Sludge by High-Resolution Gas Chromatography/Mass Spectrometry," *Environmental Science and Technology* 20:376-383 (1986).
3. Ahel, M., T. Conrad, and W. Giger. "Persistent Organic Chemicals in Sewage Effluents. 3. Determinations of Nonylphenoxy Carboxylic Acids by High Resolution Gas Chromatography/Mass Spectrometry and High-Performance Liquid Chromatography," *Environ. Sci. Technol.* 21:697-703 (1987).
4. Lewis, M. A., and D. Suprenant. "Comparative Acute Toxicities of Surfactants to Aquatic Invertebrates," *Ecotoxicol. Environ. Safety* 7:313-322 (1983).

5. Boethling, R. S. "Environmental Fate and Toxicity in Wastewater Treatment of Quaternary Ammonium Surfactants," *Water Res.* 18:1061-1076 (1984).
6. Beveridge, A., and W. F. Pickering. "The Influence of Surfactants on the Adsorption of Heavy Metal Ions by Clays," *Water Res.* 17:215-225 (1983).
7. Mortland, M. M., S. Shaobai, and S. A. Boyd. "Clay-Organic Complexes as Adsorbents for Phenol and Chlorophenols," *Clays Clay Miner.* 34:581-585 (1986).
8. Bouchard, D. C., R. M. Powell, and D. A. Clark. "Organic Cation Effects on the Sorption of Metals and Neutral Organic Compounds on Aquifer Material," *J. Environ. Sci. Health A23:585-601* (1988).
9. Urano, K., M. Saito, and C. Murato. "Adsorption of Surfactants on Sediments," *Chemosphere* 13:293-297 (1984).
10. Hand, V. C., and G. K. Williams. "Structure-Activity Relationships for Sorption of Linear Alkylbenzenesulfonates," *Environ. Sci. Technol.* 21:370-373 (1987).
11. Hough, D. B., and H. M. Rendall. "Adsorption of Ionic Surfactants," in *Adsorption from Solution at the Solid/Liquid Interface*, G. D. Parfitt and C. H. Rochester, Eds. (New York: Academic Press, 1983), pp. 247-319.
12. Clunie, J. S., and B. T. Ingram. "Adsorption of Nonionic Surfactants," in *Adsorption from Solution at The Solid-Liquid Interface*, G. D. Parfitt and C. H. Rochester, Eds. (New York: Academic Press, 1983), pp. 105-152.
13. Rosen, M. J. *Surfactants and Interfacial Phenomena* (New York: John Wiley and Sons, 1978).
14. Karickhoff, S. W., D. S. Brown, and T. A. Scott. "Sorption of Hydrophobic Pollutants on Natural Sediments," *Water Res.* 13:241-248 (1979).
15. Chiou, C. T., L. J. Peters, and V. H. Freed. "A Physical Concept of Soil-Water Equilibria for Nonionic Compounds," *Science* 206:831-832 (1979).
16. Chiou, C. T., P. E. Porter, and D. W. Schmedding. "Partition Equilibria of Non-ionic Organic Compounds between Soil Organic Matter and Water," *Environ. Sci. Technol.* 17:227-231 (1983).
17. Brownawell, B. J., H. Chen, J. M. Collier, and J. C. Westall. "Adsorption of Organic Cations to Natural Materials," *Environ. Sci. Technol.* 24:1234-1240 (1990).
18. Westall, J. C., B. J. Brownawell, H. Chen, and W. Zhang. "Adsorption of Non-ionic Surfactants on Natural Materials," *Environ. Sci. Technol.* (in preparation).
19. Westall, J. C., B. J. Brownawell, H. Chen, and W. Zhang. "Adsorption of Linear Alkylbenzenesulfonates on Sediment Materials: A Study of Mechanisms," *Environ. Sci. Technol.* (in preparation).
20. Westall, J. C., B. J. Brownawell, and H. Chen. "Adsorption of Cationic Surfactants on Natural Materials," *Environ. Sci. Technol.* (in preparation).
21. Hassett, J. J., J. C. Means, W. L. Banwart, and S. G. Wood. "Sorption Properties of Sediments and Energy-Related Pollutants," U.S. Environmental Protection Agency, Report EPA-600/3-80-041, NTIS, Springfield, VA (1980).
22. Gschwend, P. M., and S.-C. Wu. "On the Constancy of Sediment-Water Partition Coefficients of Hydrophobic Organic Pollutants," *Environ. Sci. Technol.* 19:90-96 (1985).
23. Fuerstenau, D. W. "Streaming Potential Studies on Quartz in Solutions of Ammonium Acetates in Relation to the Formation of Hemi-Micelles at the Quartz-Solution Interface," *J. Phys. Chem.* 60:981-985 (1956).

24. Tanford, C. *The Hydrophobic Effect* (New York: Wiley-Interscience, 1980), pp. 1-20.
25. Klimenko, N. A. "Calculation of Isotherms for Adsorption of Nonionic Surfactants from Aqueous Solutions on a Carbon Sorbent below the Critical Micelle Concentration," *Kolloidn. Zh.* 41:1105-1109 (1978).
26. Greenland, D. J., and J. P. Quirk. "Adsorption of 1-n-Alkyl Pyridinium Bromides by Montmorillonite," in *Proceedings of the Ninth National Conference on Clays and Clay Minerals*, A. Swineford, Ed. (New York: Pergamon Press, 1962), pp. 484-499.
27. Law, J. P., and G. W. Kunze. "Reaction of Surfactants with Montmorillonite: Adsorption Mechanisms," *Soil Sci. Soc. Amer. Proc.* 30:321-327 (1966).
28. Theng, B. K. G. *The Chemistry of Clay-Organic Reactions* (New York: John Wiley and Sons, 1974), pp. 136-238.
29. Karickhoff, S. W., and D. S. Brown. "Paraquat Sorption as a Function of Particle Size in Natural Sediments," *J. Environ. Qual.* 7:246-252 (1978).
30. Brown, D. S., and G. J. Combs. "A Modified Langmuir Equation for Predicting Sorption of Methylacridinium Ion in Soils and Sediments," *J. Environ. Qual.* 14:195-199 (1985).
31. Schwarzenbach, R. P., and J. C. Westall. "Transport of Nonpolar Organic Compounds from Surface to Groundwater. Laboratory Sorption Studies," *Environ. Sci. Technol.* 15:1360-1367 (1981).
32. Krishna Murti, G. S. R., V. V. Volk, and M. L. Jackson. "Soil Adsorption of Linear Alkylate Sulfonate," *Soil Sci. Soc. Amer. Proc.* 30:685-688 (1966).
33. Inoue, K., K. Kaneko, and M. Yoshida. "Adsorption of Dodecylbenzenesulfonates by Soil Colloids and Influence of Soil Colloids on Their Degradation," *Soil Sci. Plant Nutr.* 24:91-102 (1978).
34. Podoll, R. T., K. C. Irwin, and S. Bredlinger. "Adsorption of Water-Soluble Oligomers on Sediments," *Environ. Sci. Technol.* 21:562-568 (1987).
35. Doren, A., D. Vargas, and J. Goldfarb. "Nonionic Surfactants as Flotation Collectors," *J. Inst. Min. Metall. Trans. (C)* C34-38 (1975).
36. van den Boomgaard, T., T. F. Tadros, and J. J. Lyklema. "Adsorption of Nonionic Surfactants on Latices and Silica in Combination with Stability Studies," *J. Coll. Int. Sci.* 116:8-16 (1987).
37. Krings, P., M. J. Schwuger, and C. H. Krauch. "Wasch-und Reinigungsmittel mit unlöslichen Ionen austauschern," *Naturwiss.* 61:75-77 (1974).
38. Savintseva, S. A., Z. A. Grankina, I. M. Romashenko, and A. F. Koretskii. "Infrared Spectroscopic Investigation of the Mechanism of the Adsorption of Nonionic Surfactants on Aerosil," *Kolloidn. Zh.* 42:592-594 (1980).
39. Savintseva, S. A., I. M. Sekisova, V. A. Kolasanova, and A. F. Koretskii. "Effect of Modification of Nonionic Surfactants on Their Adsorptivity," *Kolloidn. Zh.* 47:901-906 (1985).
40. McDevit, W. F., and F. A. Long. "The Activity Coefficient of Benzene in Aqueous Salt Solutions," *J. Amer. Chem. Soc.* 24:1773-1778 (1952).

CHAPTER 8

Partitioning and Sorption Kinetics of a PCB in Aqueous Suspensions of Model Particles: Solids Concentration Effect

Patricia L. Van Hoof and Anders W. Andren

INTRODUCTION

A particle concentration effect on the sorption of a variety of hydrophobic solutes (organic and inorganic) in aqueous suspensions of natural particles has been noted by several investigators.¹⁻³ This decrease in the amount adsorbed with increasing particle concentration is most pronounced for compounds characterized by large partitioning ($K_p > 10^3$ mL/g) and is not predicted by thermodynamic first principles.² If partitioning is a function of particle concentrations, then there are many practical ramifications concerning the measurement and modeling of hydrophobic organic compounds (HOCs). For example, laboratory measurements of HOC partitioning made at large particle concentrations (10^2 – 10^4 mg/L) cannot be linearly extrapolated to the low particle concentrations typical of suspended particulate matter (10^{-1} – 10^1 mg/L). Also, in environmental models, different partition coefficient values, K_p —the equilibrium ratio of solute concentration in the solid phase (g/g) to that in the aqueous phase (g/mL)—would be required for suspended versus bottom sediments, even for different times of the year if resuspension and storm inputs are significant. It is therefore essential that the mechanism(s) for this particle concentration dependency be understood and incorporated into environmental fate models.

Several theories and models have been proposed to explain this sorption phenomenon. One explanation involves a third phase consisting of colloidal matter (macromolecules and microparticles, 0.001–1 μm in linear dimensions) which cannot be separated from the aqueous phase by filtration or centrifugation. Thus, the “dissolved” phase contains truly dissolved and sorbed components, resulting in a reduced K_p .⁴⁻⁶ The concentration of these colloids increases with particle concentration and the organic matter content of the sediment or soil, and consequently lowers solute partitioning.⁵

Another explanation for the particle concentration effect on K_p suggests that particle interactions induce desorption of the labile fraction of sorbed HOCs as a result of the increased frequency of particle collision with increased particle concentration.^{3,7,8}

A third factor that has been suggested to account for this phenomenon is increased coagulation or aggregation of particles at higher concentrations.⁹⁻¹¹ An increase in the aggregated state of the system would result not only in less surface area, but also in an increase in the diffusive path length. In addition, recent evidence has shown that sorption equilibrium does not occur as quickly as once thought.¹⁰⁻¹² A period of fast uptake (minutes to hours) is followed by a much slower sorption process (days to months). The determination of complete equilibrium between the two phases requires sufficient analytical accuracy and precision to detect small changes in aqueous solute concentrations. Consequently, the nonattainment of adsorption equilibrium within the short incubation periods used in the past (24-48 hr) may have resulted in lower K_p 's at higher particle concentrations.

Undoubtedly, no single explanation will suffice for all possible compound/particle systems. There is little doubt that a colloidal effect exists; field and laboratory studies have provided extensive evidence. However, it remains to be shown whether other mechanisms may not also be contributing to a partitioning dependency on particle concentration.

In order to further elucidate the mechanism(s) responsible for the particle concentration dependency of HOC partitioning, the sorption behavior of a model HOC (4-monochlorobiphenyl, abbreviated 4-MCB) in a simplified model particle suspension is investigated. The model system consists only of clean monodisperse polystyrene microspheres and water, thereby eliminating any confounding effects due to the presence of colloidal or aggregated phases. The influence of parameters such as solute concentration, particle size, and stirring rate on sorption uptake rates and partitioning are examined. A radial diffusion model based on Fick's law of diffusion is applied to the kinetic uptake data to demonstrate how well it predicts the intraparticle diffusion process of this system.

EXPERIMENTAL METHOD

Details of the experimental methods are given elsewhere.¹³ Briefly, a radiolabeled chlorinated biphenyl congener (4-MCB) was obtained from Sigma Chemical Company (St. Louis, MO). An aqueous solution of the compound was obtained by plating the congener out of iso-octane onto the walls of a glass bottle. After the solvent evaporated, Milli-Q water (Millipore, Bedford, MA) was added, and the solution continuously stirred for a week prior to its use in any experiment.

Monodisperse polystyrene microspheres (MPM) with diameters of $5.87 \pm 0.11 \mu\text{m}$ and $0.53 \pm 0.005 \mu\text{m}$, and low surface charge densities ($5 \mu\text{eq-SO}_4^-/\text{g}$)

for the 5.87- μm MPM) were obtained from Polysciences, Inc. (Warrington, PA). A carboxylate-modified MPM, $3.07 \pm 0.09 \mu\text{m}$ in diameter and exhibiting a more hydrophilic surface ($67 \mu\text{eq COO}^-/\text{g}$), was purchased from Interfacial Dynamics Corporation (Portland, OR). To ensure that these surfactant-free particle suspensions were free of monomer, low-molecular-weight oligomer, benzaldehyde, and other impurities, a diafiltration process was used to clean the particles.¹⁴ Diafiltration has been shown to be just as effective in removing impurities from MPM suspensions as dialysis and ion exchange, but more expedient.¹⁵ Surface charge densities were characterized by conductometric titration.¹⁶

Adsorption Equilibration

Microspheres were added to $14 \mu\text{g}$ 4-MCB/L aqueous solutions, 1% of the compound's saturation solubility. A 10% saturation solution was also tested with $0.53\text{-}\mu\text{m}$ MPM suspensions. Particle concentrations of 1, 10, 100, and 1000 mg/L were placed in 1- to 2-L screw-cap bottles and equilibrated in a temperature controlled water bath ($25 \pm 2^\circ\text{C}$). The pH of these samples was 5.6. The suspensions were stirred on a submersible stir plate with a Teflon-coated stir bar at a rate of 170 rpm. A slower stir rate of 60 rpm was also applied to 10-mg/L samples to test the effect of the hydrodynamic regime on hydrophobic partitioning.

Duplicate subsamples for aqueous phase, solid phase, total 4-MCB, and particle concentration were taken after approximately 5, 50, 80, 125, and 240 days of equilibration for the $3.07\text{-}\mu\text{m}$ and $5.87\text{-}\mu\text{m}$ particles. The $0.53\text{-}\mu\text{m}$ particles were subsampled at 5, 35, and 100 days.

Partition Measurements

The approach to sorption equilibrium was determined by measuring the distribution coefficient, K_d , over time. K_d is defined as the ratio of solute concentration in the particulate phase (C_p , g/g) to that in the aqueous phase (C_w , g/mL).

The particulate and aqueous phases were separated by filtration. The effectiveness of the filter used in separating the phases is crucial for accurate partitioning measurements. Four filters were tested for 4-MCB sorption and $0.53\text{-}\mu\text{m}$ particle retention. Sorption of 4-MCB was evaluated by measuring the recovery of a filtered aqueous sample. Retention of $0.53\text{-}\mu\text{m}$ particles was evaluated by examining the amount of light scattered as a laser passed through the filtrate. Glass-fiber filters (Gelman) were found to be adequate for filtering $3.07\text{-}\mu\text{m}$ and $5.87\text{-}\mu\text{m}$ particles, but not $0.53\text{-}\mu\text{m}$ particles. Recently developed anodized alumina filters (Anotec Separations, New York) were found to be adequate on both counts and allowed for fast filtration. Consequently, glass-fiber filters were used for the larger particles, and alumina filters for the $0.53\text{-}\mu\text{m}$ particles.

The following procedures were chosen based on the recommendations of Dunnivant for solvent extraction of sediments.¹⁷ Aqueous-phase 4-MCB was extracted from 45 mL of filtrate with iso-octane, 4 mL followed by 1 mL. Extraction efficiencies were >95%. Sorbed 4-MCB was extracted from MPM (0.5–50 mg collected on filters) using 2 mL acetone and 10 mL hexane. The extraction vials were then placed next to a sonic probe (475-watt SON-1M-1 Ultrasonic Processor) at 50% relative output and sonicated for 25 min. Extraction solvent (5 mL) was added to liquid scintillation cocktail and counted. Total 4-MCB was measured to verify a mass balance. A 20 mL volume of total sample, 100 mL of acetone, and 15 mL of iso-octane were placed in a 250-mL dissolved oxygen bottle and sonicated for 25 min. The sample was then back-extracted by placing it in a 1-L volumetric flask along with 750 mL of Milli-Q water and shaken vigorously for 3 min. After phase separation, the iso-octane was subsampled and counted.

Since the particle concentration parameter is as important in calculating the K_d as the 4-MCB concentrations, MPM concentrations were also carefully measured as a function of time. Polycarbonate Nuclepore filters (0.1- μm pore size) were found to be adequate for filtering all particle sizes.

RESULTS AND DISCUSSION

Approach to Sorption Equilibrium

The kinetic approach to sorption equilibrium of 4-MCB in aqueous suspensions of polystyrene microspheres of three particle sizes ($d = 0.53, 3.07,$ and $5.87 \mu\text{m}$) is illustrated by an increase in the distribution coefficient, K_d , with time (Figures 8.1 and 8.2). An initial period of fast uptake is followed by considerably slower rates of sorption for all three particle sizes. In addition, the time required to reach equilibrium increased with increasing solids concentration. While the approach to equilibrium for the higher solids samples is slower, it appears that K_p values similar to those of the 10-mg/L samples will eventually be attained. In fact, the 100-mg/L K_d values for the 0.53- μm MPM (data sets 1 and 2) are not significantly different from the 10-mg/L values after 96 to 110 days of equilibration ($p < .05$). The 1000-mg/L K_d values are still significantly different at this point, but appear to be approaching the lower solids K_p value.

One possible explanation for slower sorption kinetics with increasing particle concentration is an associated increase in aggregation. However, these suspensions remained stable throughout the experiment, exhibiting very little aggregation. This was verified either by light microscopy (3.07 and 5.87- μm MPM) or light-scattering (0.53- μm MPM) techniques.

The rate of stirring in the incubation bottles was varied to test the effect of the hydrodynamic regime on partitioning. If transport in the aqueous phase is limiting, increasing the shear force of the system will increase the rate of

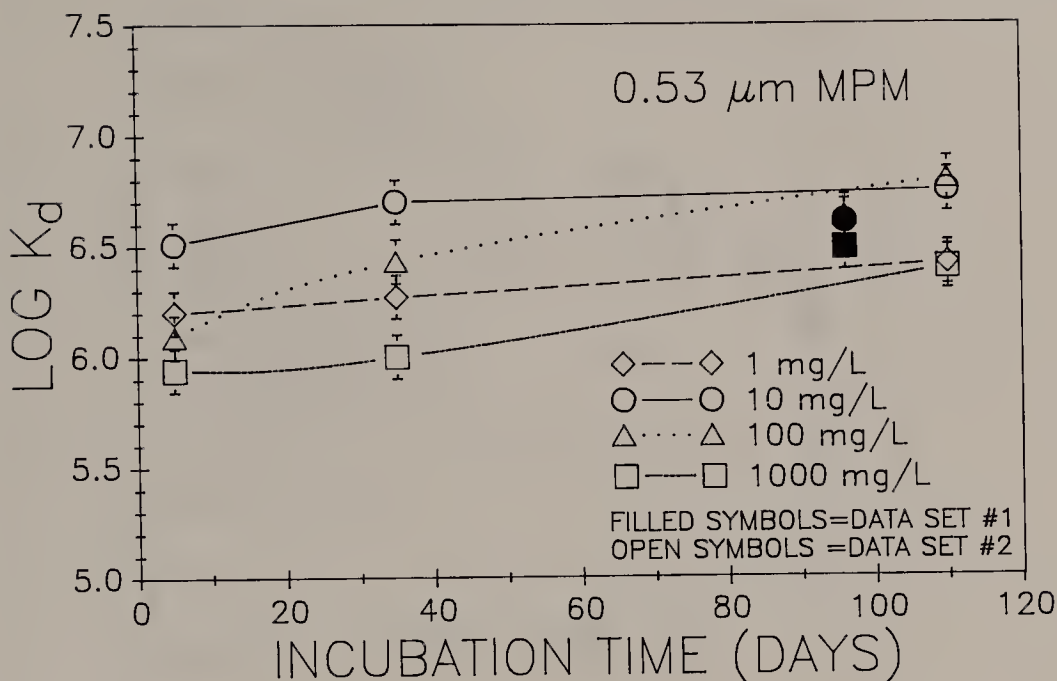


Figure 8.1. Time course of $\log K_d$ for $0.53\text{-}\mu\text{m}$ MPM suspensions of varying particle concentrations. Error bars represent two standard deviations.

sorption. The 3.07- and $5.87\text{-}\mu\text{m}$ MPM 10-mg/L samples were stirred at 60 rpm (slow) and 170 rpm (fast); all other samples were stirred at 170 rpm. No significant difference in uptake was observed between the fast and slow regimes, indicating that transport through the aqueous phase is not limiting (Figure 8.2). This is supported by a ten-order-of-magnitude decrease in the effective diffusivity of 4-MCB in polystyrene microspheres ($10^{-17} - 10^{-16}\text{ cm}^2/\text{s}$, see Radial Diffusion Model), relative to that in water ($6.51 \times 10^{-6}\text{ cm}^2/\text{s}$).¹⁸

As expected, particle size is an important parameter in determining the time required to reach sorption equilibrium. Smaller particles exhibit a faster approach to equilibrium than larger particles due to shorter diffusional paths. For the 10-mg/L solids samples, equilibrium appears to be reached after 35 days for the $0.53\text{-}\mu\text{m}$ MPM, 123 days for the $3.07\text{-}\mu\text{m}$ MPM, and 247 days for the $5.87\text{-}\mu\text{m}$ MPM. For the higher solids samples, longer equilibration times are required.

In addition, initial uptake is limited by particle surface area. This is best demonstrated by comparing the rate of uptake, represented by an increase in $\log K_d$ with time, to a ratio of surface areas (projected surface area of 4-MCB added less the equilibrium aqueous concentration:surface area of the particles, Figure 8.3). The ratio of surface areas (SA) represents a sorption driving force normalized to the surface area of the sorbent. For a particular particle size, the rate of uptake is positively correlated to the SA ratio. For the 3.07- and $5.87\text{-}\mu\text{m}$ MPMs, however, this only holds for ratios less than 0.75. At ratios greater than 0.75, the rate of uptake decreases with increasing SA ratio. This decline is

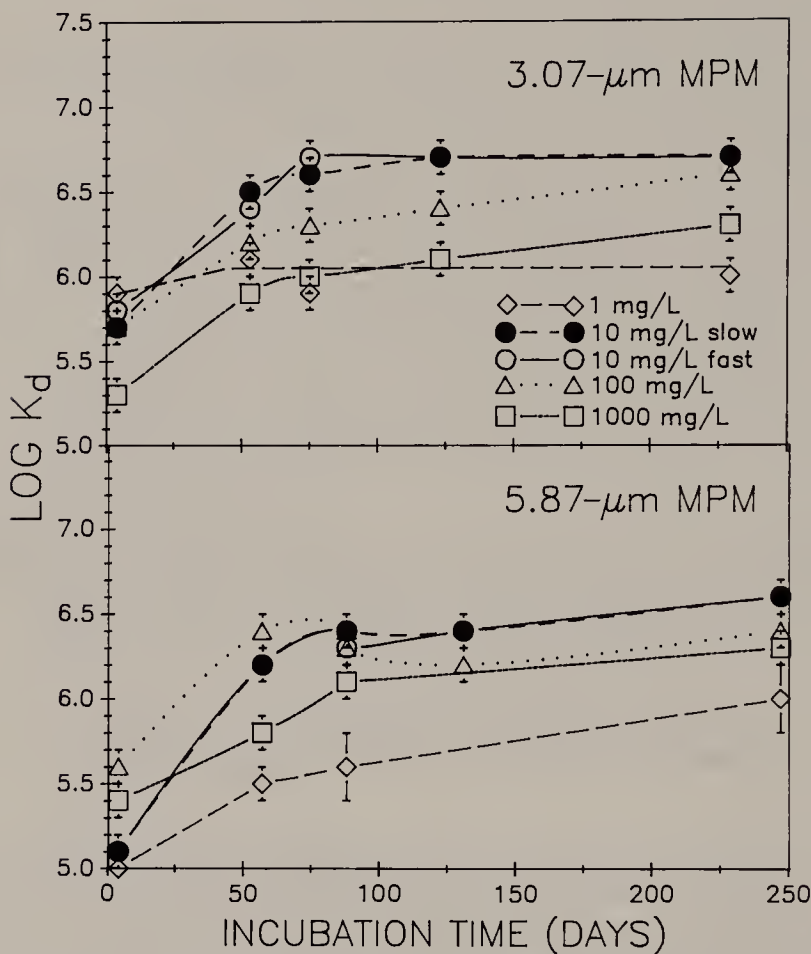


Figure 8.2. Time course of $\log K_d$ for 3.07-and 5.87- μm MPM suspensions of varying particle concentrations. Slow and fast stir rates are 60 and 170 rpm, respectively.

probably the result of particle surface saturation. Since diffusion of 4-MCB in polystyrene is extremely slow (see below), it is the limiting step. Therefore, 4-MCB partitioning in these suspensions is limited by intraparticle diffusion. The reason for the decline of solute uptake with decreasing SA ratios (or increasing particle concentration) during both early (Figure 8.3a) and later (Figure 8.3b) time intervals is not immediately apparent.

In contrast, the extent of partitioning appears to be independent of particle size. The K_p values of the 10-mg/L samples are 4×10^6 mL/g and 5×10^6 mL/g for the 5.87- μm and 3.07- μm MPMs, respectively. The 0.53- μm MPM K_p values are 4×10^6 mL/g (data set 1) and 5×10^6 mL/g (data set 2). If surface adsorption is significant, then K_p values should increase with decreasing particle size. Although there is a slight increase in partitioning between the 5.87- and 3.07- μm MPMs, the particle with the largest specific surface area (0.53- μm MPM) has K_p values which are not significantly different from those of the larger particles. These results support the conceptual model of HOCs partitioning into an organic phase, in addition to surface associations.¹⁹

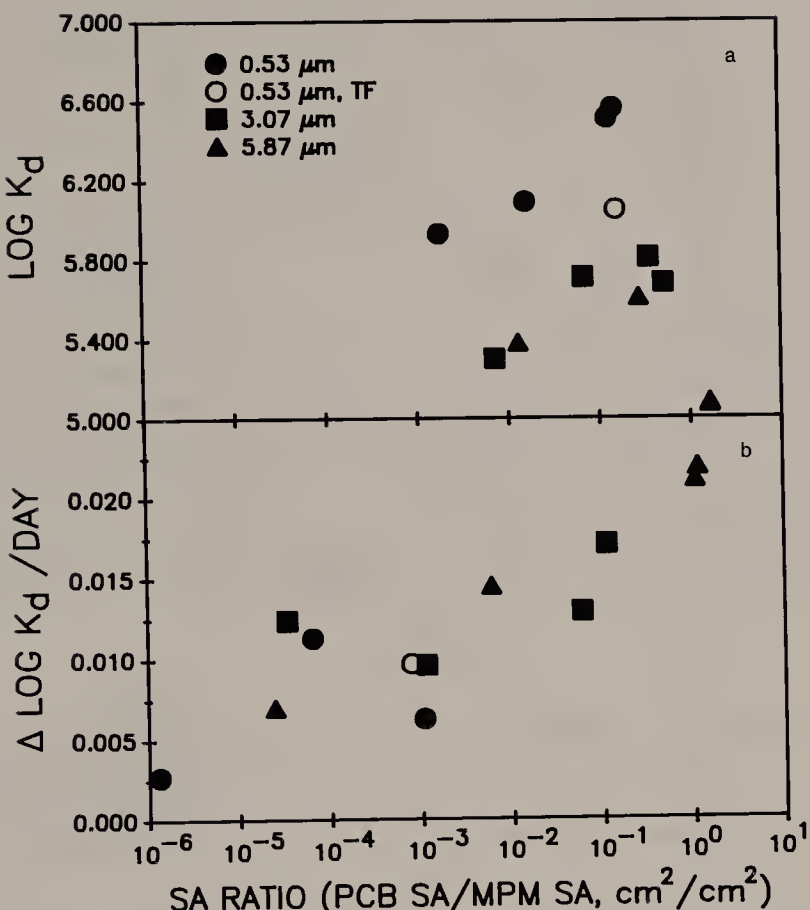


Figure 8.3. Relationship between the increase in $\log K_d$ and the surface area ratio of PCB:MPM between (a) 0–5 days and (b) 5–35 days for 0.53- μm MPM, and 5–53 days for 3.07- and 5.87- μm MPMs.

Adsorption Isotherms

The four-order-of-magnitude range in particle concentration results in a similar range for C_w and C_p values, which can be plotted as an adsorption isotherm (Figure 8.4). It should be noted that not all of the data are at equilibrium. The approach to sorption equilibrium for each of the particle concentrations of the 0.53- μm and 5.87- μm MPMs is traced by a dashed line. For the 0.53- μm MPM, a linear region with a slope of one, and a K_p of 5×10^6 mL/g, is evident for suspensions with C_p values less than 2 mg/g. Although the K_d of the highest solids sample (1000 mg/L) is slightly less than this K_p after 110 days, it appears to be approaching the value (Figure 8.4, far left data set). For the 5.87- μm MPM, a linear region is also evident, but the slope appears greater than one. Consequently, the data could be represented by a Freundlich isotherm with $n > 1$. However, it is more likely that the nonunity slope is an artifact of the higher solids suspensions and larger particle size requiring more time to reach equilibrium, even after 247 days of equilibration.

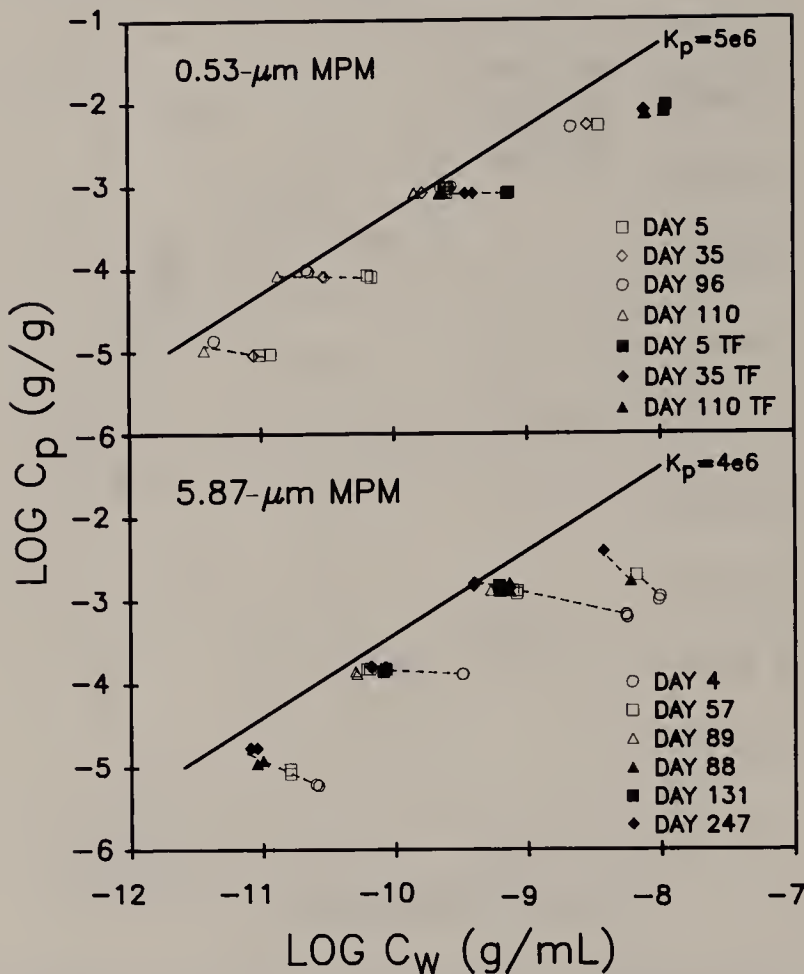


Figure 8.4. Relationship of $\log C_p$ to $\log C_w$ as a function of time for the 0.53- and 5.87- μm MPMs. $\log C_w$ varied with particle concentration—1 mg/L (fourth data set from left) to 1000 mg/L (far left data set)—and 4-MCB concentration ($TF = 10$ -fold 4-MCB concentration). Dashed lines follow approach to equilibrium.

Absent from this discussion so far has been the lowest solids suspension, 1 mg/L. These suspensions generally have lower K_d values than their higher solids counterparts. After 230 days of equilibration, the K_d values of the 1-mg/L 5.87- μm and 3.07- μm MPM suspensions average $1.3 \pm 0.4 \times 10^6 \text{ mL/g}$ (Figure 8.2). The K_d value of the 0.53- μm MPM 1-mg/L sample is twice as high, $2.3 \times 10^6 \text{ mL/g}$, after 110 days (Figure 8.1). When the adsorption isotherm of each particle size is examined, it is apparent that the 1-mg/L samples are not in the linear region (Figure 8.4). Whether the K_d 's of these suspensions have reached equilibrium early on, or are approaching higher values at extremely slow rates, is difficult to ascertain.

In addition to varying the solids concentration, the concentration of 4-MCB was varied by an order of magnitude for the 10- and 100-mg/L 0.53- μm MPM samples. While the sorptive uptake of the 100-mg/L 0.53- μm MPM sample equilibrated with 140- $\mu\text{g}/\text{L}$ 4-MCB is greater than the 14- $\mu\text{g}/\text{L}$ 4-MCB sample,

the K_d time courses of the two systems are not significantly different (Figures 8.3a and 8.5). The partitioning kinetics of the 10-mg/L 0.53- μm MPM samples also appear to be independent of the 4-MCB concentration; however, the extent of partitioning is significantly less at the higher 4-MCB concentration. In addition, this sample exhibits a greater reduction in partitioning than the 1-mg/L sample exposed to 14- $\mu\text{g}/\text{L}$ 4-MCB, despite having the same 4-MCB:MPM mass ratio. Thus, the extent of partitioning is both dependent on (>2 mg 4-MCB/g MPM) and independent of (<2 mg 4-MCB/g MPM) the mass ratio of solute to sorbent. The approach to sorption equilibrium can also be a function of the solute-to-sorbent mass ratio; however, the kinetics appear to be influenced mainly by particle concentration, and less by solute concentration, except initially when the surface becomes saturated.

One possible explanation for the reduced partitioning at higher 4-MCB:MPM mass ratios is the presence of heterogenous "sites" within the polystyrene microsphere. Dual modes of sorption have been suggested as an explanation for the behavior of gases sorbed at high pressures in glassy polymers:

1. sorption into preexisting voids or micropores which act in a manner equivalent to that of specific sites
2. sorbate dissolution into the polymer with more-or-less random distribution.^{20,21}

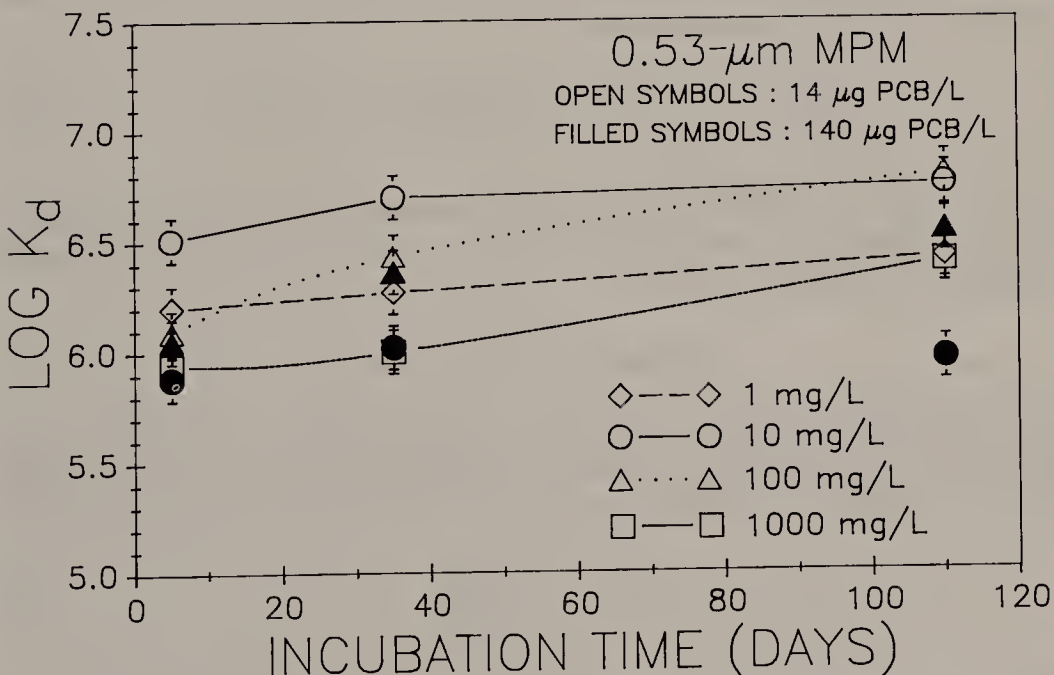


Figure 8.5. Time course of $\log K_d$ for 0.53- μm MPM suspensions as a function of particle and 4-MCB concentration.

Although polymer-sorbate interactions are relatively strong, they are not specific as in the case of site-sorbate interactions.²¹

Radial Diffusion Model

The uptake of a solute by a sorbent can be analyzed by an intraparticle diffusion model, assuming that external mass transfer to the particle is not rate limiting. The radial diffusion model has been used successfully to model adsorption rates of solutes into activated carbon,²² ion exchange resins,²³ heterogenous catalysts,²⁴ sediment and soil particles,²⁵ and soil columns.²⁶ The applicability of this model is restricted to systems where rigid boundary conditions can be assumed. Consequently, the size and shape of the solid phase must be well defined. Since the particles of the 4-MCB-MPM system are spherical and monodisperse, Crank's analytical solution to the intraparticle diffusion equation²⁷ can be used, rather than a numerical solution which is required for polydisperse systems (e.g., Wu and Gschwend's model²⁸). Other assumptions of the model include:

1. particles are internally porous and homogenous
2. bulk solution concentration is uniform, but not necessarily constant
3. K_p and the effective intraparticle diffusion coefficient, D_{eff} , are spatially invariant
4. sorption is controlled by linear, reversible isotherms
5. local equilibrium holds.

Under these conditions the fractional approach to equilibrium of a well-stirred solution of limited volume is given by

$$\frac{M_t}{M_{eq}} = 1 - \sum_{n=1}^{\infty} \frac{6\alpha(\alpha + 1)\exp(-D_{eff} q_{n2} t/R^2)}{9 + 9\alpha + q_{n2} \alpha^2}, \quad (8.1)$$

where $\alpha = 3V/(4\pi R^3 K_p)$. M_{eq} is the sorbed concentration (g/g) at equilibrium, R is the radius of the particle, V is the aqueous volume, and q_n is given by the nonzero roots of the equation

$$\tan(q_n) = 3q_n/(3 + \alpha q_{n2}). \quad (8.2)$$

Equation 8.2 is solved for q_n using the secant method. Since M_{eq} was not measured for those samples which did not reach equilibrium, it was calculated using K_p (from 10-mg/L data), solids concentration (p), and the equations

$$C_{w(eq)} = \frac{C_{w(o)}}{1 + pK_p}, \quad (8.3)$$

and

$$M_{eq} = K_p C_{w(eq)}. \quad (8.4)$$

Table 8.1. Uptake of 4-MCB by Polystyrene Microspheres

Incubation Period (Days)	Log K_d (mL/g)			M/M _{eq}		
	TSS (mg/L)			10	TSS (mg/L)	M/M _{eq}
	10	100	1000			
0.53-μm MPM						
5	6.51	6.09	5.93	0.95	0.95	0.97
35	6.70	6.43	6.01	0.96	0.97	0.98
110	6.75	6.80	6.44	1.00	1.00	1.00
3.07-μm MPM						
4	5.81	5.71	5.30	0.88	0.97	1.00
53	6.45	6.18	5.91	0.98	0.98	1.00
75	6.71	6.34	6.08	0.99	0.97	1.00
123	6.72	6.45	6.08	1.00	1.00	1.00
229	6.71	6.59	6.30	1.00	1.00	1.00
5.87-μm MPM						
4	5.08	5.61	5.38	0.57	0.98	1.00
57	6.20	6.40	5.76	0.97	1.00	1.00
89	6.38	6.45	6.08	0.98	1.00	1.00
131	6.38	6.23	—	0.99	1.00	—
247	6.61	6.40	6.29	1.00	1.00	1.00

The model is generally fit to M_t/M_{eq} versus time curves with D_{eff} as the only fitting parameter. However, because the early portion of the uptake curve was not measured, and the M_t/M_{eq} ratio changes only slightly, optimization of D_{eff} from this type of plot is less accurate. By day 4, all of the solids concentrations of the 0.53- μm MPM had sorbed 95% of their M_{eq} . For the larger particles, the 10-mg/L samples sorbed as much as 57% (5.87- μm MPM) and 88% (3.07- μm) of their M_{eq} , while the 100- and 1000-mg/L samples sorbed 95–100% by day 4 (Table 8.1). It would appear, then, that these suspensions reach equilibrium very quickly, with the higher solids samples approaching M_{eq} faster than the lower solids samples. Regardless, conclusions drawn from the K_d -time relationships indicate that the opposite is true: sorption equilibrium is reached very slowly, and lower solids samples equilibrate faster than higher solids samples (Figures 8.1 and 8.2, and Table 8.1).

Clearly, the former type of presentation illustrates only what is going on in the solid phase, while the K_d reflects the approach to equilibrium of both phases. For systems with high partitioning, due to the hydrophobicity of the solute and/or the large organic fraction of the sorbent, the amount of solute associated with the solid phase is much greater than that of the aqueous phase. Thus, while the solid-phase concentration appears to level off, small transfers from the aqueous phase still occur, resulting in observable increases in K_d .

Simulated uptake curves with a range of D_{eff} values are shown in Figure 8.6 along with the K_d data sets of each particle size. It is obvious that a single D_{eff} cannot be applied to all the solids concentrations, or very often even within a solids concentration for all times. Because the computer simulation did not

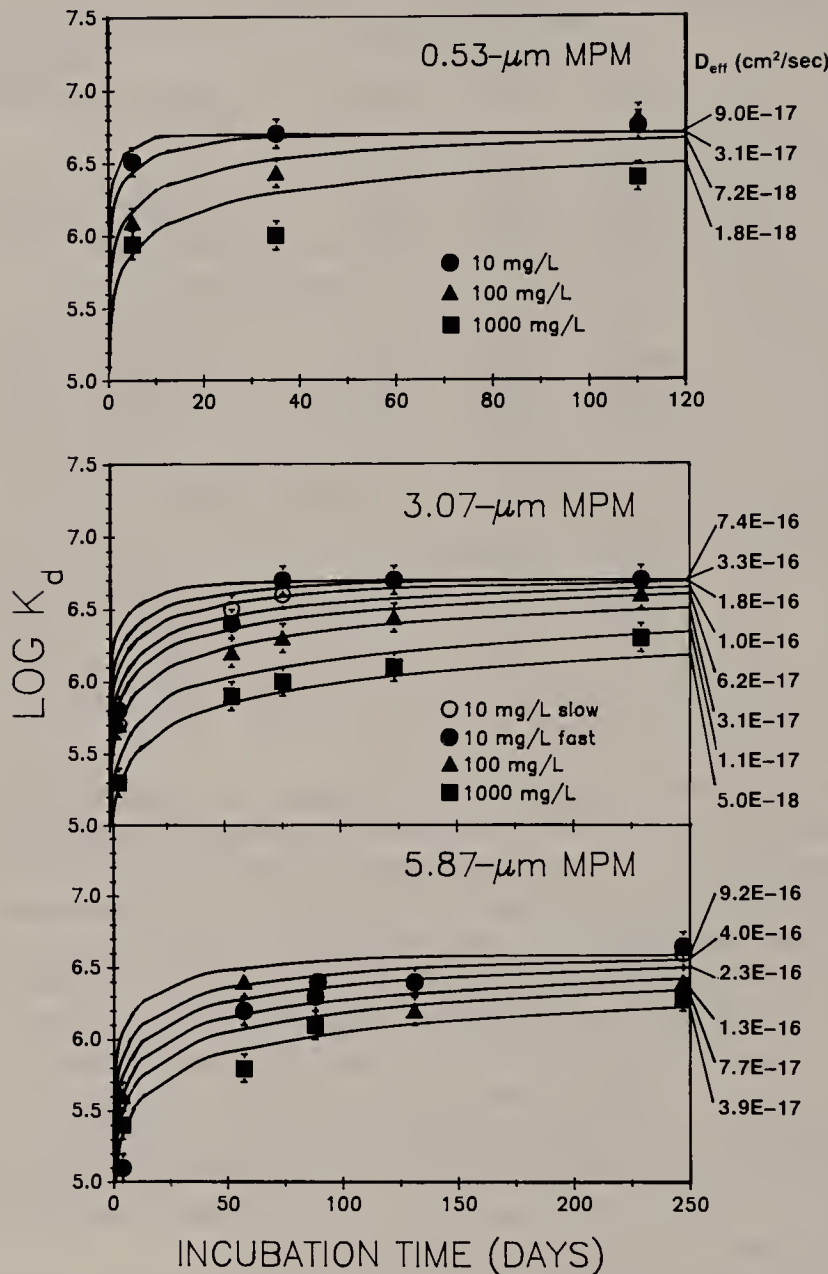


Figure 8.6. Radial diffusion model curves for varying D_{eff} values compared with experimental results for 0.53-, 3.07-, and 5.87- μm MPM suspensions at particle concentrations of 10, 100, and 1000 mg/L.

allow for a statistical best fit, visual best-fit ranges of D_{eff} are listed in Table 8.2. These D_{eff} result from fitting the center portion of the curve. The D_{eff} values, ranging from 1.5×10^{-18} cm^2/s to 9×10^{-16} cm^2/s , generally appear to decrease with increasing solids concentration and decreasing particle size. Thus, an increase in particle number or associated surface area is adversely affecting the rate of sorptive uptake of 4-MCB.

Table 8.2. Radial Diffusion Model D_{eff} Estimates ($10^{17} \text{ cm}^2/\text{sec}$)

Particle Size (μm)	Particle Concentration (mg/L)		
	10	100	1000
0.53	3–9	0.15–0.7	
3.07	(< 70 days)	6–10	2–6
	(> 70 days)	18–70	0.5–1.1
5.87		10–20	4–8

The radial diffusion model tends to overestimate early (day 4) K_d values and underestimate the later K_d values. The initial overestimation occurs for those samples whose SA ratios indicated an initial saturation of the surface (i.e., 10- and 100-mg/L 5.87- μm MPM, and 10-mg/L 3.07- μm MPM suspensions). The model's initial partitioning boundary condition does not account for the mass transfer limitation that occurs when PCB:MPM SA ratios are greater than 0.75. Additionally, the apparent increase of D_{eff} at later times and the increase of the coefficient with decreasing solids concentration are unaccounted for by simple Fickian diffusion. One possible explanation for these phenomena is a concentration dependency of D_{eff} . However, when the concentration of 4-MCB is increased 10-fold the rate of uptake is unaffected (Figure 8.5). This suggests that a solute concentration dependency of the intraparticle D_{eff} is not important at these low levels.

An estimate of the concentration effect on D_{eff} for the 4-MCB-MPM system can be made using a relationship established for the benzene vapor-polystyrene system:²⁹

$$D = D_{(0)} \exp(\alpha v_p) \quad (8.5)$$

where v_p is the volume fraction of sorbed penetrant, and $D_{(0)}$ is the diffusivity at zero volume fraction. For benzene, α is equal to 52. The parameter α does not vary considerably with solute, ranging from 35 to 58 for a variety of halogenated and nonhalogenated hydrocarbons in polystyrene at 25°C.²⁹ Using the particulate 4-MCB concentrations for the 10-mg/L (~1000 μg 4-MCB/g MPM) and 1000-mg/L (~10 μg 4-MCB/g MPM) 0.53- μm suspensions at equilibrium, the D_{eff} would be expected to increase by only 5% as solids concentrations decreased. Initially, however, the sorbed 4-MCB is associated with a small fraction of the particulate volume; consequently, the solute concentrations are much higher. At these solute concentrations, the D_{eff} of the low solids suspensions would be expected to increase significantly according to Equation 8.5, but the high solids D_{eff} value would not be affected. It is therefore possible that the concentration dependency of the intraparticle diffusivity could account for the 0.5-to 2-orders-of-magnitude increase in D_{eff} associated with the 2-orders-of-magnitude decrease in solids concentration. Further experimental and modeling studies are required to support this hypothesis, and to explain the contradictory result shown in Figure 8.5.

Solute Diffusion in Polymers

Solute diffusion through a polymer matrix is determined by properties of the polymer, which in turn can be functions of temperature, solute concentration, and time (for a review, see Rogers²¹). For a polymer which is soft or rubbery (i.e., above its glass transition temperature), polymer strand relaxation is rapid in response to changes in conditions (e.g., temperature, solute concentration). Solute diffusion behavior in this type of polymer can be adequately described by a concentration-dependent form of Fick's law. For a hard or glassy polymer (i.e., below its glass transition temperature), such as polystyrene, stress to polymer strands is slow to decay. Additional sorption results as a consequence of the increase in free volume of the polymer matrix with segment relaxation.²¹ Relaxation times decrease with increasing temperature or solute concentration. Thus, the overall sorption process reflects polymeric relaxation motions and their consequences that occur on a time scale comparable to, or greater than, the time scale of the concurrent diffusion process. This type of behavior results in a time-dependent D_{eff} .

Examples of non-Fickian diffusion in glassy polymers include organic vapors, such as methylene chloride and benzene, diffusing in polystyrene,^{29,30} cellulose nitrate,³¹ and cellulose acetate.^{32,33} Non-Fickian systems exhibit sorption curves that are sigmoid in shape. For the PCB-MPM system, the uptake curves do not appear sigmoid. However, early times (< 24 hr) have not been examined. While there is no conclusive evidence specifically for non-Fickian behavior in this system, it seems highly likely given the tendency of polystyrene, and the increase in anomalous behavior with increasing molecular size of the solute.

As mentioned previously, solute partitioning to glassy polymers is complicated by their heterogenous nature. Free segmental rotations of the polymer chains are restricted in the glassy state, resulting in microvoids in the polymer matrix.³⁴ These "holes" act to significantly retard solute diffusion by entrapment or binding at high energy sites. Support of the theory of dual modes of sorption in glassy polymers is found in its ability to account for anomalously high partitioning and negative sorption enthalpies³⁴ and in pulsed NMR evidence.³⁵ For a number of studies, the highly nonlinear isotherms can be decomposed into partitioning and Langmuir contributions. However, it has not yet been established whether two modes of diffusion are also operative.

Polymers as Models for Natural Organic Matter

The intended use of polystyrene microspheres was not that these particles act as specific surrogates for natural organic matter, but rather as particles of well-defined size, shape, and organic composition in a partitioning study of the solids concentration effect. However, it became clear that a thermodynamic answer may not be what is required to explain the solids effect, but rather a kinetic one. Although these particles are sufficient for thermodynamic

sorption studies, they may not be suitable for kinetic studies. The following are a few observations and recommendations concerning the use of polymers as models for natural organic matter in sorption studies.

Concerning thermodynamic partitioning, the $\log K_{oc}$ for the 4-MCB-MPM system is 6.7. This K_{oc} (mL/g) value is two orders of magnitude greater than its partitioning in the octanol-water system ($\log K_{oc} = 4.5$).³⁶ The 4-MCB-MPM K_{oc} value is three orders of magnitude greater than the predicted K_{oc} for natural organic matter using the relationship of Chiou et al. for PCBs ($\log K_{oc} = 3.51$).³⁷ Looking at the water-saturated solubility parameters of each solvent, δ (cal/cm³)^{0.5}, it is expected that polystyrene ($\delta = 9.3$)³⁸ have higher K_{oc} s than octanol ($\delta = 10.3$) or soil humus ($\delta = 13.0$)³⁷ for solutes with $\delta < 10$ (e.g., trichlorobiphenyl, naphthalene, phenanthrene).³⁸ However, the K_{oc} of the MPMs is disproportionately higher. One possible cause for this partitioning relates to the concept of dual-mode sorption in glassy polymers. Applying the dual-mode sorption model of Vieth and Sladek²⁰ to the measured isotherms, a $\log K = 6.8$ for specific-site sorption (Langmuir isotherm contribution), and a $\log K = 5.1$ for dissolution into the polymer (linear partitioning contribution) were calculated. Thus, without the specific sites provided by micropores, the partitioning in these microspheres would be much lower. If this hypothesis is correct, an amorphous but nonglassy polymer (above its glass temperature at room temperature, and therefore no micropores) with an equivalent δ should have a $\log K_{oc}$ of about 5 for 4-MCB.

Although octanol is well suited for predicting equilibrium partitioning, it cannot be used as a surrogate for natural organic matter with regard to sorption kinetics due to structural differences between the phases and diffusive path lengths. Nonglassy amorphous polymers would be better surrogates for the polymeric component (called *humin* or *kerogen*) that is present in most sediments.³⁹ These polymers behave as simple hydrocarbon liquids whose thermodynamic properties are homogenous.⁴⁰ In addition, their transport properties are not time dependent. Therefore, a polymer such as polymethyl acrylate, which has a glass temperature below room temperature (8°C) and a $\delta = 10.4$, would be a good surrogate. However, intraparticle geometric parameters, such as macroporosity and tortuosity, that contribute to sorption kinetic rates in natural particles are generally absent from these systems.

SUMMARY AND CONCLUSIONS

A solids concentration effect on 4-MCB sorption was observed in aqueous suspensions of polystyrene microspheres. The microspheres were carefully cleaned so that any DOC or colloidal effect was effectively eliminated. This apparent inverse relationship of 4-MCB partitioning with particle concentration diminished with time, demonstrating that nonattainment of equilibrium results in the observed phenomenon. The 10-, 100-, and 1000-mg/L samples of the smallest particles (0.53-μm MPM) effectively reached the same K_p after 96

days. Consequently, the effect of particle concentration on solute partitioning requires a kinetic explanation rather than a thermodynamic one.

As in many natural particle suspensions, a period of initial fast uptake was followed by impeded intraparticle diffusion for the 4-MCB-MPM system. The fast uptake is characterized by a surface area dependency, implying that the surface concentration becomes saturated (SA ratio > 0.75) when the rate of intraparticle diffusion limits the uptake process. For SA ratios < 0.75 (nonsaturated), another surface area dependency is evident, with partitioning decreasing as the SA ratio decreases. This latter dependency occurs during the period of slow uptake as well.

The independence of K_p with particle size ($4\text{--}5 \times 10^6 \text{ mL/g}$) agrees with the conceptual model of dissolution of HOCs within the sediment/soil organic phase, in addition to adsorption to hydrophobic surfaces. Although equilibrium partitioning within the 4-MCB-MPM system is independent of particle size, the kinetics of adsorption is not. For the 10-mg/L sample to reach sorption equilibrium, it required approximately 35 days for the 0.53- μm MPM, 123 days for the 3.07- μm MPM, and 247 days for the 5.87- μm MPM. As expected, the smaller particles reached equilibrium faster due to the shorter diffusional path. However, the intraparticle diffusivity of 4-MCB within 0.53- μm particles, obtained as a fitting parameter for a radial diffusion model, is significantly lower than those for the 3.07-and 5.87- μm MPMs. In addition, the D_{eff} appears to decrease with increasing particle concentration. These results suggest that the number of particles, or amount of surface area, in a suspension affects the rate of intraparticle diffusion of 4-MCB.

A mechanistic explanation for the inverse relationship of particle concentration and sorption uptake rates is not immediately obvious. Impeded diffusion as a result of aggregation at higher solids concentrations can be discounted in this case, since these particles remained monodispersed. The nonlinearity of the adsorption isotherm provided evidence for heterogenous modes of sorption (specific sites, along with random dissolution) within these polystyrene microspheres. A result of this dual-mode sorption mechanism—observed in polystyrene, as well as other rigid polymers—is a concentration dependency of D_{eff} . Preliminary estimates indicate that the magnitude of the dependency is large enough to account for the 0.5-to 2-orders-of-magnitude increase in D_{eff} associated with the 2-orders-of-magnitude decrease in solids concentration.

The radial diffusion model applied in this study, Crank's analytical solution for intraparticle diffusion, overestimates early partitioning values for those samples whose SA ratio indicates saturation, and slightly underestimates later partitioning values, implying that D_{eff} increases with time. Therefore, 4-MCB diffusion through these particles cannot be described by simple Fickian diffusion. Non-Fickian behavior, such as time-dependent D_{eff} 's or surface concentrations, and heterogeneity of sorption modes, results in much more complex sorption partitioning and kinetics. Whether non-Fickian diffusion is responsible for the solids concentration effect on sorption uptake rates cannot be

determined without finer time resolution of the uptake process as a function of solute and solids concentrations.

More important, however, is to ascertain whether an inverse relationship of HOC sorption uptake rates with solids concentration occurs in natural particles and their organic components. Since it is very difficult to eliminate colloidal effects in these natural suspensions, a cleaner system made up of amorphous nonglassy polymer particles is recommended. These rubbery polymers have the advantage of behaving as simple hydrocarbon liquids with respect to their thermodynamic properties, and exhibit simple Fickian diffusion.

ACKNOWLEDGMENTS

The authors would like to thank David Armstrong, Marc Anderson, Pasupati Mukerjee, George Zografi, and Chad Jafvert for their insightful discussions. We gratefully acknowledge Stewart Rounds for providing a FORTRAN version of the radial diffusion model. This work was funded by the University of Wisconsin Sea Grant Institute under grants from the National Oceanic and Atmospheric Administration, U.S. Department of Commerce, and from the State of Wisconsin (Federal Grant No. NA84AA-D-00065, Project No. R/MW43).

REFERENCES

1. Lotse, E. G., D. A. Graetz, G. Chesters, G. F. Lee, and L. W. Newland. "Lindane Adsorption in Lake Sediments," *Environ. Sci. Technol.* 2:353-357 (1968).
2. O'Connor, D. J., and J. P. Connolly. "The Effect of Concentration of Adsorbing Solids on the Partition Coefficient," *Water Res.* 14:1517-1523 (1980).
3. DiToro, D. M., J. S. Jeris, and D. Ciarcia. "Diffusion and Partitioning of Hexachlorobiphenyl in Sediments," *Environ. Sci. Technol.* 12:1169-1176 (1985).
4. Voice, T. C., C. P. Rice, and W. J. Weber, Jr. "Effect of Solids Concentration on the Sorptive Partitioning of Hydrophobic Pollutants in Aquatic Systems," *Environ. Sci. Technol.* 17:513-518 (1983).
5. Gschwend, P. M., and S. C. Wu. "On the Constancy of Sediment-Water Partition Coefficients of Hydrophobic Organic Pollutants," *Environ. Sci. Technol.* 19:9-96 (1986).
6. Hassett, J. P., and E. Milicic. "Determination of Equilibrium and Rate Constants for Binding of a Polychlorinated Biphenyl Congener by Dissolved Humic Substances," *Environ. Sci. Technol.* 19:638-643 (1985).
7. DiToro, D. M., J. D. Mahony, P. R. Kirchgraber, A. L. O'Bryne, L. R. Pasquale, and D. C. Picirilli. "Effects of Nonreversibility, Particle Concentration, and Ionic Strength on Heavy Metal Sorption," *Environ. Sci. Technol.* 20:55-61 (1986).
8. Mackay, D., and B. Powers. "Sorption of Hydrophobic Chemicals from Water: A Hypothesis for the Mechanism of the Particle Concentration Effect," *Chemosphere* 16:745-757 (1987).
9. Anderson, M. A., M. I. Tejedor-Tejedor, and R. R. Stanforth. "Influence of

- Aggregation on the Uptake Kinetics of Phosphate by Goethite," *Environ. Sci. Technol.* 19:632-637 (1985).
10. Karickhoff, S. W., and K. R. Morris. "Sorption Dynamics of Hydrophobic Pollutants in Sediment Suspensions," *Environ. Toxic. Chem.* 4:469-479 (1985).
 11. Coates, J. T., and A. W. Elzerman. "Desorption Kinetics for Selected PCB Congeners from River Sediments," *J. Contaminant Hydrol.* 1:191-210 (1986).
 12. Karickhoff, S. W. "Organic Pollutant Sorption in Aquatic Systems," *J. Hydraul. Eng.* 110:707-735 (1984).
 13. Van Hoof, P. L. "Partitioning and Sorption Kinetics of a Polychlorinated Biphenyl in Aqueous Suspensions of Model Particles: A Solids Concentration Effect," PhD Dissertation, University of Wisconsin, Madison, WI (1989).
 14. Ahmed, S. M., M. S. El-Asser, G. H. Pauli, G. W. Poehlein, and J. W. Vanderhoff. "Cleaning Latexes for Surface Characterization by Serum Replacement," *J. Colloid Interf. Sci.* 73:388-405 (1980).
 15. Wilkinson, M. C., J. Hearn, P. Cope, and M. Chainey. "A Microfiltration Technique for Cleaning Polymer Latices," *Br. Polym. J.* 13:82-89 (1981).
 16. Labib, M. E., and A. A. Robertson. "The Conductometric Titration of Latices," *J. Colloid Interf. Sci.* 77:151-161 (1980).
 17. Dunnivant, F. M. "Determination of Polychlorinated Biphenyl Concentrations in Selected Sediments Using a Sonication Extraction Technique," Master's Thesis, Clemson University, Clemson, SC (1985).
 18. Lyman, W. J., W. F. Reehl, and D. H. Rosenblatt. *Handbook of Chemical Property Estimation Methods* (New York: McGraw-Hill, 1982).
 19. Chiou, C. T., L. J. Peters, and V. H. Freed. "A Physical Concept of Soil-Water Equilibria for Nonionic Organic Compounds," *Science* 206:831-832 (1979).
 20. Vieth, W. R., and K. J. Sladek. "A Model for Diffusion in a Glassy Polymer," *J. Colloid Sci.* 20:1014-1033 (1965).
 21. Rogers, C. E. "Permeation of Gases and Vapors in Polymers," in *Polymer Permeability*, J. Comyn, Ed. (New York: Elsevier Applied Science, 1985), pp. 11-73.
 22. Weber, W. J., Jr., and R. R. Rumer. "Intraparticle Transport of Sulfonated Alkylbenzenes in a Porous Solid: Diffusion with Non-Linear Adsorption," *Water Resour. Res.* 1:361-369 (1965).
 23. Helffrich, F. *Ion-Exchange* (New York: McGraw-Hill, 1962), pp. 259-262.
 24. Satterfield, C. W. *Mass Transfer in Heterogeneous Catalysis* (Cambridge, MA: MIT Press, 1970).
 25. Wu, S. C., and P. M. Gschwend. "Sorption Kinetics of Hydrophobic Organic Compounds to Natural Sediments and Soils," *Environ. Sci. Technol.* 20:717-725 (1986).
 26. Rao, P. S. C., J. M. Davidson, R. E. Jessup, and H. M. Selim. "Evaluation of Conceptual Models for Describing Nonequilibrium Adsorption-Desorption of Pesticides During Steady-Flow in Soils," *Soil Sci. Soc. Am. J.* 43:22-28 (1979).
 27. Crank, J. *The Mathematics of Diffusion*, 2nd ed. (Oxford: Clarendon Press, 1975), pp. 93-96.
 28. Wu, S. C., and P. M. Gschwend. "Numerical Modeling of Sorption Kinetics of Organic Compounds to Soil and Sediment Particles," *Water Resour. Res.* 24:1373-1383.
 29. Park, G. S. "The Diffusion of Some Organic Substances in Polystyrene," *Trans. Faraday Soc.* 47:1007-1013 (1951).

30. Long, F. A., and R. J. Kokes. "Diffusion of Benzene and Methylene Chloride Vapors into Polystyrene," *J. Am. Chem. Soc.* 75:2232-2237 (1953).
31. Dreschel, P., J. L. Hoard, and F. A. Long. "Diffusion of Acetone into Cellulose Nitrate Films and Study of the Accompanying Orientation," *J. Polymer Sci.* 10:241-252 (1953).
32. Mandelkern, L., and F. A. Long. "Rate of Sorption of Organic Vapors by Films of Cellulose Acetate," *J. Polymer Sci.* 6:457-469 (1951).
33. Park, G. S. "An Experimental Study of the Influence of Various Factors on the Time Dependent Nature of Diffusion in Polymers," *J. Polymer Sci.* 11:97-115 (1953).
34. Vieth, W. R., J. M. Howell, and J. H. Hsieh. "Dual Sorption Theory," *J. Membrane Sci.* 1:177-220 (1976).
35. Assink, R. A. "Investigation of the Dual Mode Sorption of Ammonia in Polystyrene by NMR," *J. Polymer Sci., Polymer Phys. Ed.* 13:1665-1673 (1975).
36. Woodburn, K. B., W. J. Doucette, and A. W. Andren. "Generator Column Determination of Octanol/Water Partition Coefficients for Selected Polychlorinated Biphenyls," *Environ. Sci. Technol.* 18:457-459 (1984).
37. Chiou, C. T., P. E. Porter, and D. W. Schmedding. "Partition Equilibria of Non-ionic Organic Compounds between Soil Organic Matter and Water," *Environ. Sci. Technol.* 17:227-231 (1983).
38. Barton, A. F. M. *Handbook of Solubility Parameters and Other Cohesion Parameters* (Boca Raton, FL: CRC Press, 1983).
39. Freeman, D. H., and L. S. Cheung. "A Gel Partition Model for Organic Desorption from a Pond Sediment," *Science* 214:790-792 (1981).
40. Michaels, A. S., and H. J. Bixler. "Solubility of Gases in Polyethylene," *J. Polymer Sci.* 50:393-412 (1961).

PART II

FATE AND TRANSPORT

CHAPTER 9

Polycyclic Aromatic Hydrocarbons in Sediments and Pore Waters of the Lower Great Lakes: Reconstruction of a Regional Benzo(a)pyrene Source Function

Brian J. Eadie, John A. Robbins, Warren R. Faust, and Peter F. Landrum

INTRODUCTION

In the Great Lakes, as in most aquatic systems, the rapid and efficient processes of sorption and settling scavenge hydrophobic organic contaminants (HOC) from the water column, with the result that the largest fraction of persistent trace contaminant inventories presently resides in sediments. However, studies of the long-term behavior of certain fallout radionuclides and stable contaminants in the Great Lakes have shown that higher levels persist in the lakes than would be expected if settling and burial were the sole transport process. Toxic materials return from sediments due primarily to resuspension.¹ Constituents initially transferred to sediments are homogenized via bioturbation, creating a mixed layer corresponding to a decade or more of accumulation. These are resuspended back into the water column during the isothermal period and are available for uptake by pelagic biota. A second, poorly quantified return pathway to pelagic biota is via the direct uptake of sediment-bound contaminants by benthos and food web transfer.

The processes of sorption, settling and resuspension, bioturbation, and burial together control the phase distribution, long-term behavior, and, to some degree, bioavailability of most trace contaminants in aquatic systems.¹ The degree of partitioning of a constituent between particulate and dissolved phases, generally presented as the ratio (K_d), is a function of the compound's intrinsic properties and the composition (e.g., particle size, fraction organic carbon) of the substrate. Once the HOC is associated with particulate matter, its water column residence time is relatively short (ca. months in the 100-m deep Great Lakes). Mean particle settling velocities of approximately 1 m/day have been estimated for the period of thermal stratification in several large lakes in the world,² and values during the isothermal period are greater. At a

depth of approximately 10–20 m above the bottom, particles enter the benthic nepheloid layer (BNL), a region of elevated particle concentration and mass flux. The BNL is a regular feature in all of the Great Lakes and appears to be composed primarily of resuspended sediments. The BNL is frequently recharged from a variety of sources in addition to the particles settling down from above. In shallow waters, surface and internal waves, and occasional strong currents, resuspend sediments, sorting the particles and transporting them horizontally as well as vertically. During the long period when the system is not thermally stratified, there appears to be local resuspension even in deeper regions, and the resuspended sediments are well mixed throughout the water column.^{3,4} With the onset of stratification, vertical turbulence is markedly reduced below the thermocline, and the bulk of resuspended materials resettle to the BNL and lake bottom. The long-term consequence of seasonal resuspension and redeposition is the eventual accumulation of particle-associated contaminants in least turbulent areas of the lakes. The resultant lateral inhomogeneity of sediment-associated trace constituents, called *focusing*, operates strongly in the Great Lakes system.

At the sediment surface, freshly deposited materials are mixed with older sediments as a result of the movement and feeding activities of organisms inhabiting the upper layers of sediment (1–10 cm thick). As a result of mixing, materials which would have been buried are reintroduced into the resuspensible pool. Several studies have shown that, in general, organisms occur in sufficient numbers throughout the Great Lakes to homogenize near-surface sediments, representing the input of years to decades.^{5,6} In the Great Lakes, the amphipod *Diporeia* sp. is the predominant benthic organism, constituting 65% of the macroinvertebrate population biomass.⁷ Note that *Diporeia* sp. is a new genus and was previously classified as *Pontoporeia hoyi*.⁸ *Diporeia* lives at the interface, although it does burrow down a few centimeters and mixes sediments in a dispersive manner. *Diporeia* can also swim up into the water column. Oligochaete worms are also major contributors to sediment mixing in the lakes. These animals characteristically burrow several centimeters down into the sediments and spend a significant amount of their time feeding in a head-down position while excreting from tails protruding through the sediment-water interface. This particle-selective conveyor-belt process has the effect of bringing buried materials back into the resuspensible pool and ultimately homogenizing near-surface deposits. This mixed layer zone has been shown to be directly related to the vertical distribution and numbers of organisms that can mix sediments at a given site.^{5,6} The reintroduction of homogenized materials from the sediment mixed layer into the water via resuspension allows constituents to move toward new sorption equilibria.

The polycyclic aromatic hydrocarbons (PAH) constitute a large class of compounds generally formed in the incomplete combustion of fossil fuels.⁹ At relatively low combustion temperatures, the multiringed PAH contain a large number of alkyl side chains. The abundance of these side chains decreases as combustion temperature increases, so that at temperatures above approxi-

mately 750°C, the unsubstituted parent ring structures predominate. Studies of several combustion sources and sediments have shown that several PAH are ubiquitous and relatively abundant. Among the most common and easily identified are phenanthrene, fluoranthene, pyrene, and benzo(a)pyrene (BAP). The structures of these PAH are given in Figure 9.1. In this chapter, we examine the distribution of these four PAH within the highly industrialized lower Great Lakes in well-characterized sediments going back to before 1800 in an attempt to (1) estimate the historical fluxes of PAH to these lakes and compare them to other lake systems and (2) use this information to reconstruct a historical source function for BAP for the lower Great Lakes.

METHODS

Sediment samples were collected aboard the Canadian RV *Limnos* with a 0.25-m² box corer at two sites in eastern Lake Ontario (described in detail in Eisenreich et al.¹⁰) and a high depositional site in eastern Lake Erie (42°31'00" N, 79°53'38" W). For the Lake Ontario samples, 3-in. diameter subcores were taken, extruded and sectioned at 1-cm intervals in the field, and stored frozen until extraction. Larger (5-in.) subcores were collected from the Lake Erie box core, and the extruded 2-cm sections were stored in refrigeration until centrifuged. Radionuclide analyses were performed on adjacent 3-in. subcores (from the same box core) sectioned at 0.5-to 1-cm intervals.

Pore waters were separated from the Lake Erie sediments by centrifugation; then 2-cm sections from two adjacent 5-in. subcores were combined. These large wet sediment samples (> 500 mL) were placed in precleaned 1-L high-density polyethylene bottles and spun at 2500 rpm for 20 min in an IEC Model K centrifuge. Small chunks of dry ice were placed inside the centrifuge to keep the temperature below ambient. Under these conditions, 290–375 mL of pore water was separated per 2-cm section. The water was decanted and immedi-

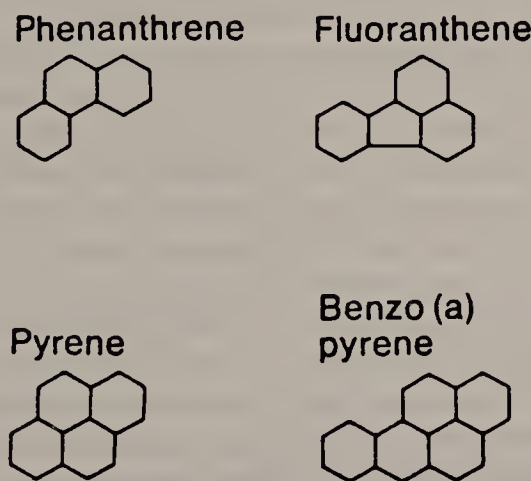


Figure 9.1. Ring structure of the four combustion PAH discussed in this chapter.

ately filtered through precombusted (4 hr at 400°C) Whatman GFF glass-fiber filters (nominal cutoff < 1 μM). Dissolved organic carbon (DOC) was analyzed from subsamples by the wet oxidation method. The remainder of the pore water was dosed with two radiolabeled PAH compounds as tracers for the analytical methodology and extracted three times with approximately 10% of the water volume using methylene chloride.

Sediments were Soxhlet extracted (wet) with 125 mL MeOH for approximately 4 hr. After cooling, 250 mL of CH_2Cl_2 was added and extraction continued overnight. The extracts were transferred to 500-mL separatory funnels and washed with 3 \times 50 mL of CH_2Cl_2 extracted distilled water. The solvent portion of the extracts was then reduced in volume by rotary evaporation (equipped with a cold finger trap to increase efficiency) to approximately 5 mL, transferred to a 50-mL round-bottom flask, and 15 mL of pentane was added. Rotary evaporation was continued until the sample was reduced in volume to approximately 2 mL; then this step was repeated. The extract, now in pentane, was evaporated to approximately 0.5 mL with a stream of clean nitrogen gas. This was introduced onto a column (12 \times 0.5 cm) that had been slurry packed with fully activated (8 hr at 200°C; stored at 120°C) silica gel. The upper 1 cm of the column was dry packed with precleaned sodium sulfate to trap any remaining water. The first elution, 12 mL of pentane, removed primarily the saturated hydrocarbons. The second elution, calibrated for each batch of silica gel, used 10–12 mL of 9–14% CH_2Cl_2 in pentane to elute the PAH. A 15-mL wash of CH_2Cl_2 recovered the remainder of the extract. These eluents were evaporated to 0.5 mL in a stream of dry nitrogen, and 50 μL was removed for counting of radiotracer. Extraction yields were based on the average of the recovery of spiked radiotracers. The radioactivity was measured on a Packard 460C liquid scintillation spectrometer. Sample quench was corrected using the external standards method after subtracting background.

Analysis was performed on a Hewlett Packard 5880 gas chromatograph equipped with an autoinjection system, programmed in a dual column mode. An injection was made into each 20-m capillary column (DB-1 and DB-5) at 100°C. The program was then automatically started (4°C/min to 280°C) with detection on a pair of HNU photoionization detectors (10.2 eV) optimized for PAH.¹¹ These detectors are 20–50 times more sensitive than FID for the aromatic compounds. Compound identification was based on retention times on both columns being within 0.5% of mixed external standards run on the same day. Samples were quantified by running a set of three standards, covering an order of magnitude in concentration (responses were within linear range), at the beginning of each programmed autosample run. If the response of the sample fell outside of the standard runs, the sample concentration was altered by dilution or evaporation and rerun. Solvent blanks were run between each sample/standard to ensure that there was no memory. For 12 sets of three concentrations of the PAH standards, the measured standard deviation was less than 10% of the mean values for each compound.

A problem common to analyses of trace contaminants in the environment is

our ability to collect a representative sample and the quality of data achievable with existing technologies. We have previously reported on the precision of our analyses for PAH in sediments;^{12,13} coefficients of variation for extractions of a homogenized, split sediment sample for the PAH were 34% (Phen), 21% (Fl), 20% (Py), and 19% (BAP). Analysis of two other samples similarly collected on two subsequent cruises did not substantially change the means or coefficients of variation. For this study, we regard the precisions cited above to be realistic.

RESULTS AND DISCUSSION

Sediment Geochronology

The Lakes Erie and Ontario cores selected for analysis were collected as part of a more comprehensive evaluation of tracers in lake sediments. Core geochronology is based on the analysis of fallout ^{137}Cs and natural ^{210}Pb . The geochronology of the two Lake Ontario cores is analyzed in detail elsewhere.^{10,14} The latter treatment includes a correction for the recent (past 80 years) increase in the concentration of organic carbon and CaCO_3 , both related to nutrient-enhanced productivity. Both cores appear to have an uninterrupted record of deposition over their length, and their recent accumulation rates differ by a factor of 1.8. The first of these cores, designated E-30, has a base sediment accumulation rate of $0.040 \text{ g/cm}^2 \text{ year}$ until approximately 1900, after which it increased to a maximum of about $0.055 \text{ g/cm}^2 \text{ year}$ due to the carbon dilution mentioned above. The second core, G-32, had a base sedimentation rate of $0.090 \text{ g/cm}^2 \text{ year}$, which began increasing at the same time to a maximum of about $0.115 \text{ g/cm}^2 \text{ year}$.

The down-core distribution of the ^{137}Cs and ^{210}Pb for the eastern Lake Erie core is presented in Figure 9.2. The ^{137}Cs peak corresponds with the maximum load in 1963. The ^{137}Cs data were least-squares fitted to a rapid steady-state mixing (RSSM) model,^{5,15} from which the thickness of the sediment mixed layer (3.35 g/cm^2) and sediment accumulation rate ($0.60 \text{ g/cm}^2 \text{ year}$) are optimized. The solid line in Figure 9.2a is the fit to the measured ^{137}Cs points. Using these same parameters, the model was fit to the ^{210}Pb constant source function, with excellent results (Figure 9.2b), increasing our confidence in the parameter values. Thus, the sediment accumulation rate in the core from eastern Lake Erie is 5–10 times that of the Lake Ontario cores.

Combustion PAH in Sediments

The PAH concentrations measured in these three Great Lakes cores (Figure 9.3) fall within the range of measurements in other locations, and as is expected, they are more representative of highly populated, industrialized sites. Laflamme and Hites, in their analysis of sediments from around the

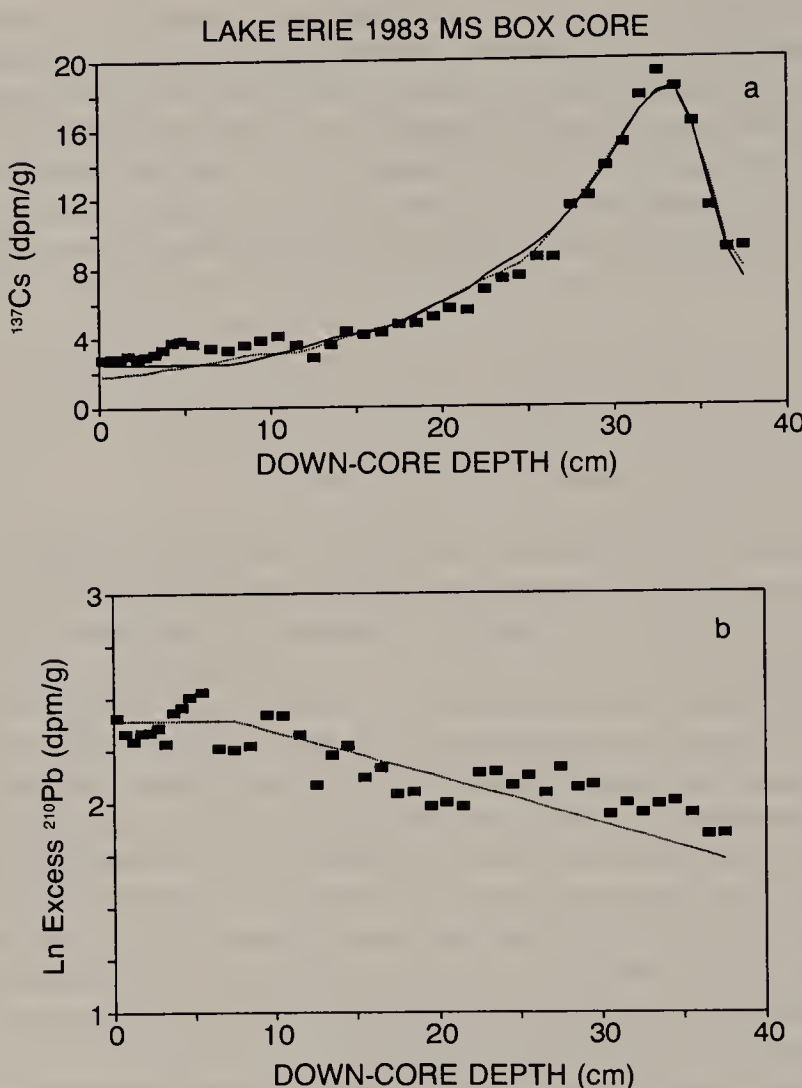


Figure 9.2. (a) The depth profile of ^{137}Cs measured in the Lake Erie 1983 MS box core. The two lines represent the results of the rapid steady-state mixing (RSSM) model (solid) and an external integration model (dashed); the differences are negligible. Results from the RSSM are the mixed layer depth (3.35 g/cm^2) and sediment accumulation rate ($0.60 \text{ g/cm}^2 \text{ year}$). (b) The depth profile of excess ^{210}Pb . The line represents the results of applying the RSSM with ^{137}Cs -derived parameters to the ^{210}Pb source function. The agreement with the Pb data increases our confidence in the RSSM parameters.

world, found a background concentration from remote environments to be a few tens of ng/g.¹⁶ This is similar to the values that we measured in the two Lake Ontario cores in sections from before approximately 1850. Similar background concentrations have also been reported, for the four combustion PAH discussed in this chapter, in remote lake sediments from the Adirondacks.¹⁷ The surface and subsurface maximum concentration are also within the range already described in the literature. The Charles River (Boston, MA) and New

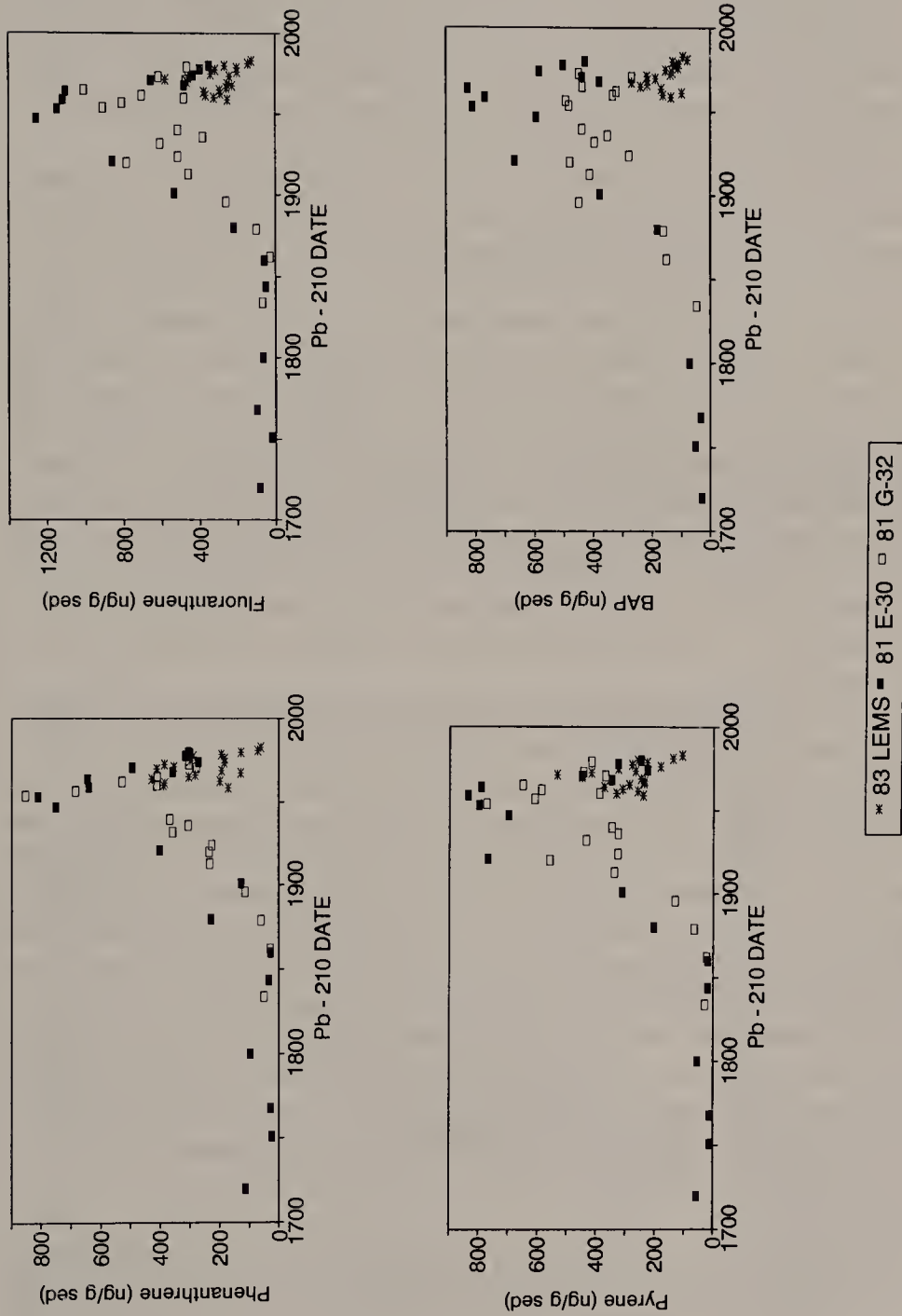


Figure 9.3. Depth profiles of the four combustion PAH in three sediment cores: Lake Erie 1983 MS data (asterisks), 1981 Lake Ontario G-32 core (open rectangles), and 1981 E-30 core (filled-in rectangles). All concentration data are plotted against ^{210}Pb estimates of the date. Peak values were recorded in the 1950s and were approximately two to three times as large as present concentrations.

York Bight, for example, have higher reported concentrations,¹⁶ as do some of the cores from the Greifensee.¹⁸ These sites are in highly industrialized areas and most likely receive localized inputs. More surprising is the high surface sediment concentration in remote Adirondack lakes,¹⁷ whose source of PAH is predominantly atmospheric (from combustion-related activities in the Great Lakes region). Furlong et al. also found very high concentrations and fluxes of combustion PAH in Adirondack lakes.¹⁹ If the source assumption is correct, then these findings imply a relatively long-range (hundreds of kilometers) transport of large amounts of the combustion PAH.

The PAH profiles that we measured in Lake Ontario exhibit a clear subsurface maximum (Figure 9.3). In many recently collected sediments, the maximum reported value for the combustion-related PAH is at the surface.^{17,18,20} Undoubtedly, the primary source of these compounds is incomplete combustion of fossil fuels. In the Great Lakes region, the major industrial energy source (coal) and home heating (coal and wood) were being replaced by cleaner-burning oil and natural gas by the late 1950s. These changes, plus emission controls subsequently imposed by environmental legislation, have resulted in an observable decrease in the concentration of BAP in regional air and in the delivery of PAH to Lake Ontario. Profiles of PAH with subsurface maxima have been reported for Puget Sound²¹ and some small lakes in the northeast United States.^{19,22} Concentration maxima in these systems occurred between 1940 and 1955, similar to those described in this chapter, and subsequent reductions have also been attributed to changes to cleaner fuels and emission controls.

Surface concentrations of PAH in the Lake Erie core (Figure 9.4) were low relative to other (near-shore) sediments reported for Lake Erie,^{13,23} but well within the range reported for the other open Great Lakes. Based on the radionuclide interpretation, the core covers the period of approximately 1959 (38–40 cm) to the collection date of 1983; thus, each 2-cm section represents less than 2 years of accumulation. Peak PAH concentrations (approximately two times the surface concentrations) were observed between 20 and 30 cm (approximately 1964–1970). In Figure 9.3 the sediment PAH are presented as concentration versus radionuclide model estimated date. This allows the two Lake Ontario cores to be superimposed and presented along with the Lake Erie core described above. It is clear from this figure that the Lake Erie core was too short to reach the peak concentrations of PAH. These values occurred in the mid-1950s (Table 9.1); the error in the time estimate is approximately ± 5 years. Since the Lake Erie core did not reach PAH background, it is not included in Table 9.1.

Concentrations of the four PAH show background levels of a few tens of ng/g, presumably produced by natural forest fires, until the middle of the 19th century. The subsequent increase in PAH concentration, presumably anthropogenic in origin, corresponds to the growth of population and industrial development in the region.²⁴ Surface sediment concentration of these PAH were higher in the Ontario cores than in the Erie core. This is mainly due to the

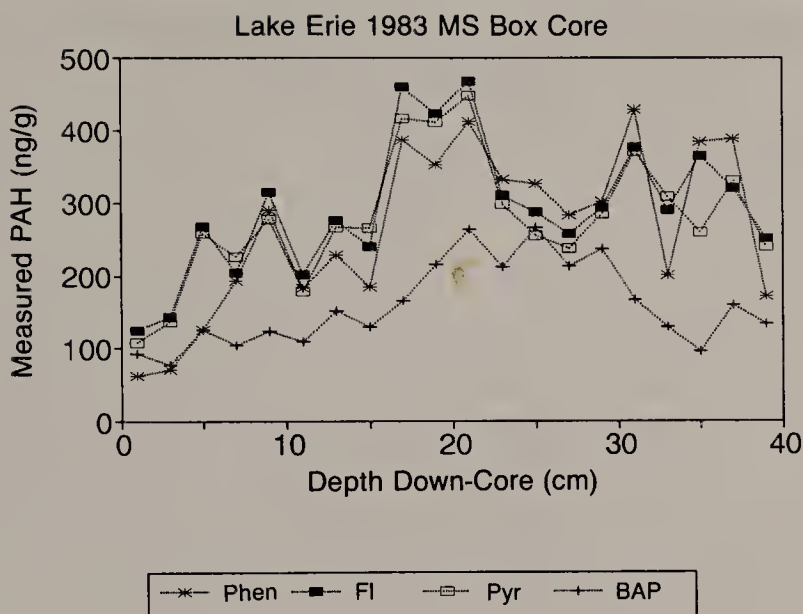


Figure 9.4. Combustion PAH measured in the 1983 Lake Erie MS box core. Each line represents the concentration of phenanthrene, fluoranthene, pyrene, or benzo(a)pyrene as identified in the legend. The core spans the period of approximately 1959 to the time of collection, 1983. The reduction near the surface is significant, a factor of 2–3 less than the peak.

Table 9.1. PAH Concentrations (ng/g sed) in Lake Ontario Sediments

Core 81E-30				
PAH	Max	Year	PAH	Max/1981
Phenanthrene	812	1953	307	2.6
Fluoranthene	1145	1953	349	3.7
Pyrene	839	1959	249	3.3
Benzo(a)pyrene	809	1959	425	1.9
Core 81G-32				
PAH	Max	Year	PAH	Max/1981
Phenanthrene	854	1954	301	2.8
Fluoranthene	909	1954	466	1.9
Pyrene	773	1954	418	1.8
Benzo(a)pyrene	494	1957	300	1.7

Accumulation ($\mu\text{g}/\text{cm}^2$) 1830–1981

		E-30	G-32	Ratio
Mass	(g/cm^2)	5.4	9.3	1.73
Focusing factor		1.17	1.74	1.49
Organic carbon	($\text{mg C}/\text{cm}^2$)	138.0	273.0	1.98
Phenanthrene	($\mu\text{g}/\text{cm}^2$)	1.9	2.7	1.42
Fluoranthene		3.5	4.6	1.31
Pyrene		2.5	3.3	1.32
Benzo(a)pyrene		2.5	3.3	1.32

Table 9.2. Lake Erie (83MS Box) Pore-Water Concentrations (ng/L) and Equilibrium Distribution Coefficients for Sediment PAH

Compound	Mean Pore-Water Conc.		Mean $K_d \pm SD$
	$\pm SD$		
Phenanthrene	198 \pm 92		1247 \pm 1141
Fluoranthene	26 \pm 16		11396 \pm 5147
Pyrene	28 \pm 18		13319 \pm 6437
BAP	17 \pm 14		9120 \pm 5950

higher mass accumulation rate in the Lake Erie sediment resulting in more dilution by inert materials. Considering the errors involved in these analyses, the peak concentrations of PAH at the two Ontario sites are approximately equal, except for BAP, which was generally higher in concentration at station E-30. Since these sites are in the same depositional basin of Lake Ontario and are only separated by about 30 km, it is difficult to understand this difference in BAP. For all four PAH, peak concentrations in the mid-1950s were approximately two to three times present values. The total accumulation of the four PAH, from background levels around 1860, was greater in core G-32. The ratio of PAH accumulation in the two cores was substantially lower than the ratio of mass or organic carbon accumulation and more closely approximated the accumulation of ^{137}Cs and ^{210}Pb from which the focusing factors are derived.

Pore Waters

Understanding the distribution of HOC within the sediment matrix is important for understanding the exposure of organisms to these contaminants. Organisms that live and feed in the surface sediments suffer elevated exposure to HOCs from both the inventory attached to particles in the sediments and that in the interstitial water.^{13,25-27} Models applied to measured PAH concentrations, assumed to be in equilibrium among Great Lakes sediments, pore waters, overlying waters, and benthos, implied that a large fraction of the combustion PAH in oligochaetes and the amphipod *Diporeia* resulted from exposure to pore water and sediments.^{13,25}

Pore-water samples were extracted from this core in an attempt to measure the PAH concentrations. Ambient measurements of trace organics in pore waters are rare since samples are relatively small, and low concentrations generally force analyses to near the detection limit. In this case, this was most apparent for BAP. Based on separate analyses of a large pore-water sample, split to approximately this size, we estimate our coefficient of variation to be 100% for these four PAH.

Overlying water concentration of BAP in Lake Erie is estimated as 0.3 ng/L, and average pore-water concentration (Table 9.2) is 17 ± 14 ng/L.^{23,28} In laboratory toxicokinetic studies, the pore-water contribution to bioaccumulation was modified by the presence of DOC, which reduced the bioavailability of HOC.^{29,30} The uptake of the unassociated fraction of PAH in pore waters by

Diporeia was similar to the uptake from overlying water. Estimates of the fraction bound to DOC in these sediments can be made from laboratory measurements of the mean equilibrium distribution coefficient of BAP to DOC (K_b) of 32,000 and the average DOC in this core (12.3 mg C/L).^{31,32} The result is that approximately 70% of the BAP in pore water is not associated with DOC and is thus potentially available to benthos. The balance of the two sediment source terms, ingested particles and respired interstitial water, remains in question, but the contribution of the interstitial water pathway is apparently large for compounds such as phenanthrene and pyrene and smaller, but still significant, for compounds such as 2,4,5,2',4',5'-hexachlorobiphenyl.³³

Pyrene concentrations in Lake Erie pore waters are shown in Figure 9.5 along with the sediment values for the same intervals. The structure in the pore-water concentration profile is not different from a constant concentration with this measurement error. Calculated mean equilibrium distribution coefficients (Table 9.2) are significantly (> 20 times) lower than values reported for ambient Great Lakes water samples,³² possibly a consequence of the mysterious particle concentration effect on K_d observed in laboratory studies.³⁴ These smaller distribution coefficients imply an elevated bioavailability of these compounds to benthic organisms.

PAH Inventories/PAH Fluxes

If we assume that there is little degradation of the combustion-based PAH within aquatic systems, we can compute and compare fluxes estimated from concentration profiles in radiometrically dated cores. In order to compare regional fluxes from these sediment calculations, we would need to correct for within-system sediment-focusing effects. Sediment focusing results in the lateral inhomogeneous distribution of sediment and constituent accumulation.^{6,10} Maximum sediment accumulation is usually, but not always, coincident with maximum lake depths. Focusing factors are calculated as the inventory of a constituent in a core to its total areal load to the system. Radionuclides are excellent for this purpose since the inputs of ^{137}Cs and ^{210}Pb are reasonably well known. The average values for Lake Ontario cores E-30 and G-32 are reported in Eisenreich et al.¹⁰ The sampling range for the Lake Erie box core does not cover a sufficient length of time to reach preindustrial background; thus, we cannot calculate an inventory of PAH. Lacking focusing factors, it is not possible to estimate whether the core-derived fluxes are representative of the entire lake system or region.

In their analysis of PAH in cores from nine lakes, summarized into four regions, Furlong et al. report the post-1890 inventory of the sum of the four combustion PAH that we examined for Lake Ontario plus chrysene, triphenylene, benzo(e)pyrene, and benzo(ghi)perylene.¹⁹ These combustion PAH are well correlated with each other, a property of a common source. In our experience, these four extra compounds generally account for approximately 30% of

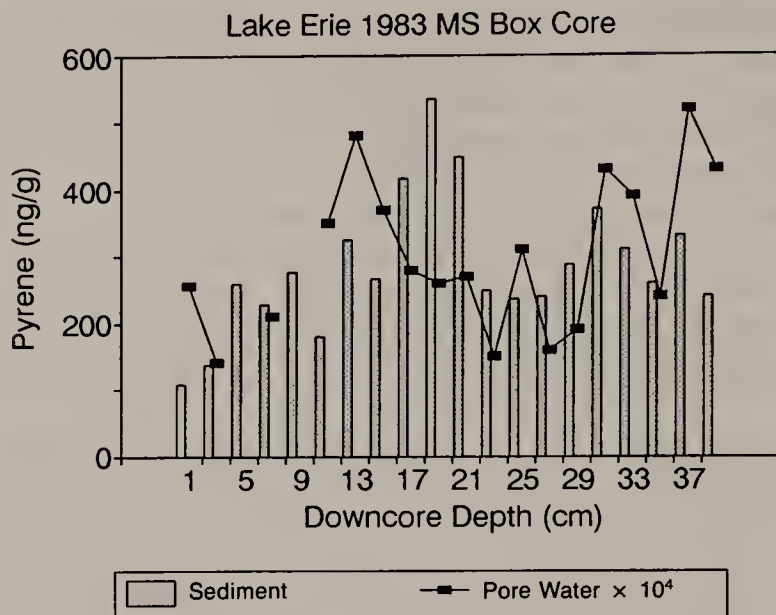


Figure 9.5. The depth profile of pyrene concentration in Lake Erie sediment (bars) and the pore-water concentration (filled-in rectangles) at each 2-cm increment. The pore-water values have been multiplied by 10,000 for scaling. Large errors in the analysis of these small pore-water samples render the structure meaningless, not different from a constant value of 28 ng/L.

the sum; we will use this approximation to reduce their calculated fluxes in order to compare the different cores. Tan and Heit report the postindustrial accumulation of the four PAH in the Adirondack sediments of Lakes Sagamore and Woods.¹⁷ We compare the postindustrial inventories with those that we measured for Lake Ontario in Table 9.3.

This comparison shows that the highly populated and industrialized Great Lakes has received more combustion PAH than has been measured in cores from areas with less local PAH production. As is evident from the inventories of the two Lake Ontario cores, the focusing correction is very important in estimating regional accumulations, and therefore the comparison among regions. Estimates of recent PAH fluxes are in the range reported by Gschwend and Hites, with Lake Ontario in the range of their high values.²²

Deriving a Lower Great Lakes BAP Source Function

In the following section, we use the measured down-core concentrations of BAP in the Lake Ontario sediments along with the radionuclide-determined mixing and accumulation values to reconstruct the load of BAP to the lakes. We then test this source function against the measured down-core concentration of BAP in Lake Erie and some published atmospheric measurements.

The sedimentary profiles of BAP for Lake Ontario E-30 and G-32 are redrawn in Figure 9.6a, after normalizing the concentrations in core G-32 by multiplying the measured concentration by the ratio of the inventories of BAP

Table 9.3. PAH Fluxes (ng/cm² year) and Postindustrial Inventories (ng/cm²)

Location	Recent Flux	Inventory	Focus-Corrected Inventory
Lake Ontario E-30	119	10450	8932
Phenanthrene	26	1930	
Fluoranthene	31	3500	
Pyrene	24	2509	
BAP	38	2511	
Lake Ontario G-32	156	13978	8033
Phenanthrene	28	2735	
Fluoranthene	50	4559	
Pyrene	41	3331	
BAP	37	3353	
Ontario average	96 ^a	12214	8483
Sagamore Lake		1150	
Woods Lake		1400	
Adirondacks	91	5040	
North of Great Lakes	12	546	
No. Florida Lakes	27	525	
No. New England Lakes	26	1190	

^aRecent flux average for Lake Ontario is focus corrected.

in the two cores (1.34). The smoothed line, a least-squares Gaussian fit to the data (after a background BAP concentration of 36 ng/g was subtracted), was then used as the uncorrected source function for a simulation of BAP in a coupled lakes model optimized for ¹³⁷Cs.^{35,36} Since measured distribution coefficients for BAP and ¹³⁷Cs are similar (500,000 mL/g), the transport parameters used for ¹³⁷Cs were not changed for this simulation. The inventory of sedimentary BAP calculated by the model was then divided into the focus-factor-corrected inventory of BAP (2100 ng/cm²) measured in cores G-32 and E-30. This ratio was then used to correct the Gaussian source function, resulting in our estimate of the total BAP source function for Lake Ontario (Figure 9.6b). The calculation shows a peak input of approximately 2 ng/cm² month in 1947, declining to an input of 1.45 ng/cm² month in 1981. The modeled cumulative inventory of BAP in Lake Ontario (Figure 9.6c) shows that over the period 1830–1981, approximately 2100 ng/cm² were stored in the sediments, the equivalent of 400 ng/cm² have flowed out of the lake through the St. Lawrence River, and a small amount, approximately 30 ng/cm², is in the water column. This converts to a total concentration of approximately 4 ng/L in the water.

We attempt to evaluate the validity of the Lake Ontario sediment-derived BAP source function by examining independent data from Lake Erie. There are two separate data sets that are available: (1) the BAP that we measured in the core from the eastern basin (Figure 9.4) and (2) BAP concentrations measured locally in the atmosphere by the EPA from 1966 through 1979.^{37,38} We convert the measured sediment concentrations in a similar manner to that used

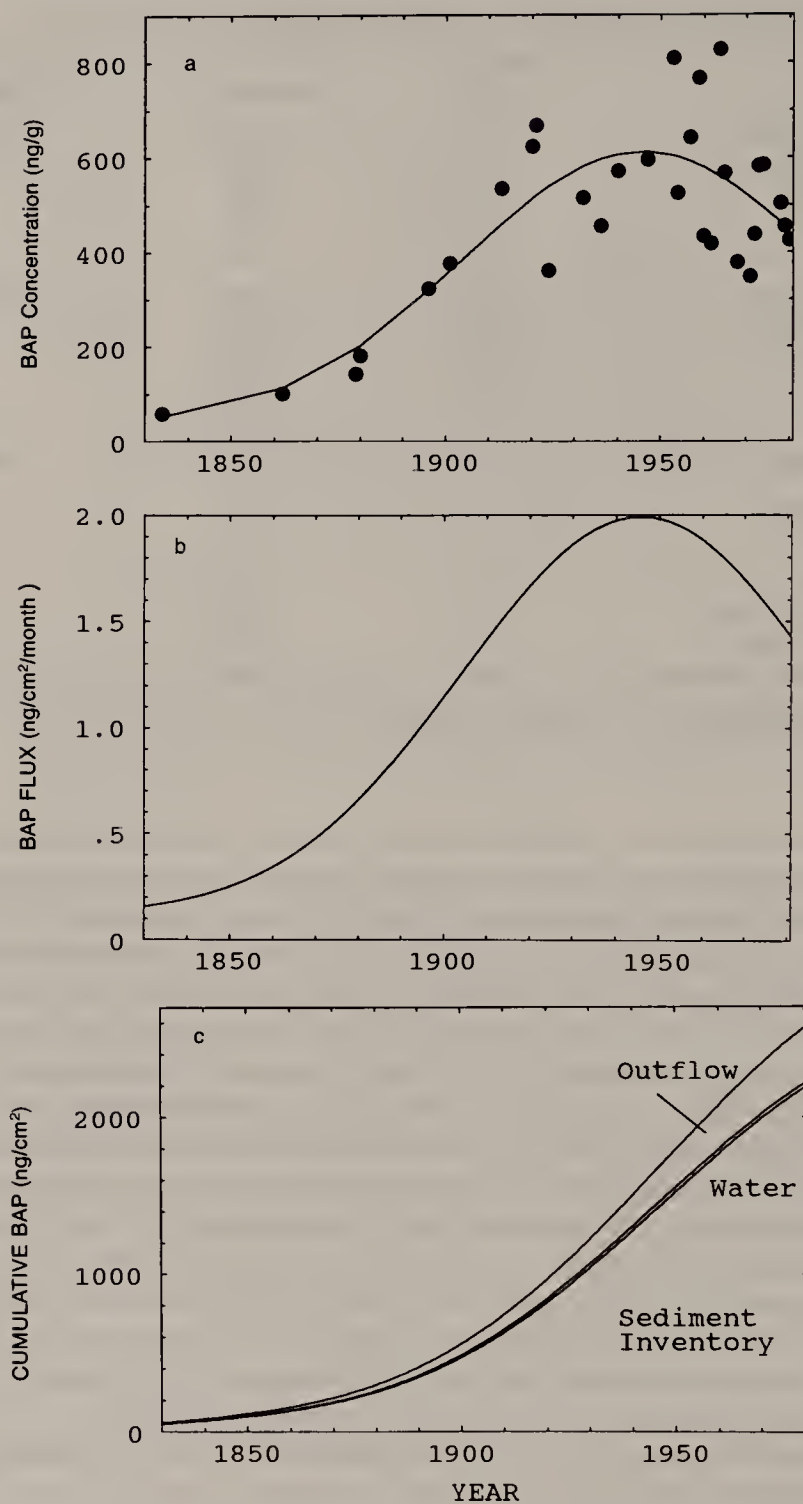


Figure 9.6. (a) The depth profile of BAP in the Lake Ontario cores (filled-in circles), with the G-32 concentrations multiplied by 1.34, the ratio of the BAP inventories from 1830 to 1981. The line is a least-squares fitted Gaussian used as input to the coupled lakes model. (b) The reconstructed BAP source function for the lower Great Lakes (see text for value). (c) The coupled lakes modeled cumulative distribution of BAP in Lake Ontario. The small region between the lines is the inventory in the water column.

for the Lake Ontario calculations. The mass accumulated in each 2-cm section of the Lake Erie core was multiplied by the BAP concentration to yield the uncorrected BAP flux. In order to compare this to the regional flux, it must be corrected for focusing. The ^{137}Cs focusing factor for this core is 6.3, meaning that 6.3 times as much ^{137}Cs is stored at this site than in the average lake sediment. Dividing the calculated BAP fluxes by this correction results in the flux values (*filled-in rectangles*) illustrated in Figure 9.7. The agreement with the solid line, which is the Lake Ontario sediment-derived source function, supports the idea of a generalized regional source for the lower lakes, without significant local sources to either lake.

A second independent confirmation for this source function from the atmospheric measurements at Toledo, Ohio (on the western shore of Lake Erie) is also illustrated in Figure 9.7. The measured concentrations were converted to fluxes using the Pelletier-Whipple-Wedlick (PWW) model,³⁹ which relates monthly deposition rates to atmospheric concentrations. The model has been calibrated with measured atmospheric concentrations and deposition of radionuclides in the Great Lakes region.³⁵

$$\text{deposition (ng/cm}^2/\text{month}) = 1.7 \times \text{atmos. conc. (ng/m}^3)$$

The atmospheric BAP concentration at Toledo declined from a maximum of 2 ng/m³ in 1967 to values around 1 by the early 1970s. Atmospheric BAP con-

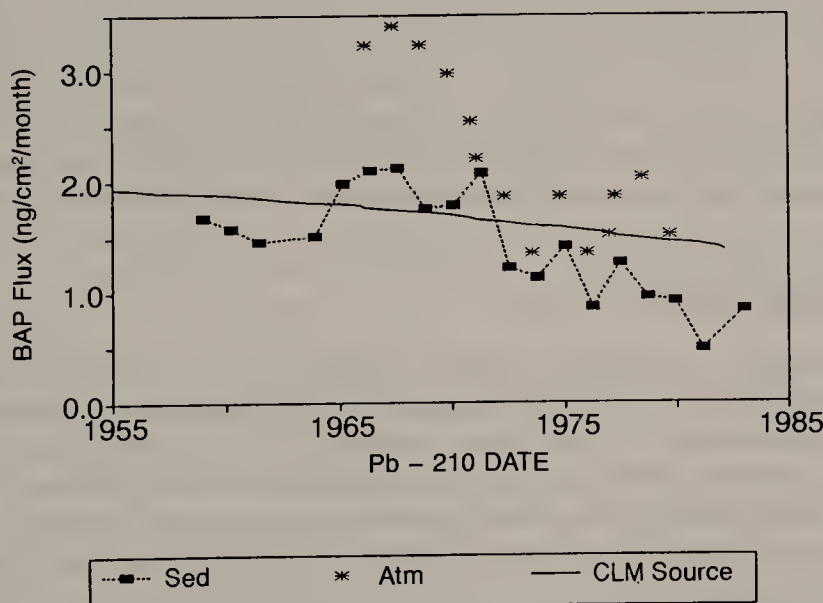


Figure 9.7. Validating the lower Great Lakes BAP source function: the portion of our calculated source function for the time period covered by the independent Lake Erie sediment and atmospheric data (solid line), the BAP fluxes calculated from the 1983 Lake Erie box core concentration measurements (filled-in rectangles), and the fluxes calculated from the measured atmospheric concentrations of BAP in Toledo, Ohio (asterisks).

centrations of approximately 1 ng/m³ are also reported by several investigators for the lower Great Lakes region for the 1970s.^{23,40-43} After 1972, the fluxes calculated from these data are in excellent agreement with the sediment-derived source function, supporting the magnitude of the source function and the underlying assumptions of rapid transfer from atmosphere to sediments with little decomposition.

These relatively successful independent tests of the source function give us confidence that our approach has been valid. Our estimate of the BAP source function for the lower Great Lakes, as illustrated in Figure 9.6b, is

$$\text{BAP (ng/cm}^2 \text{ month)} = \text{BAP}_b + \text{BAP}_{\max} \exp -(\text{t} - \text{t}_m)^2 / 2\sigma^2$$

where $\text{BAP}_b = 0.12$

$\text{BAP}_{\max} = 1.88$

$\text{t}_m = 1946$

$\sigma = 41.7$

Since there are many major cities and industrial complexes on Lakes Erie and western Ontario, and the prevailing wind is from the southwest, the source for the upper (and upwind) Great Lakes may be somewhat different—presumably smaller.

It is clear from the sedimentary profiles presented that the fluxes and resultant concentrations of combustion PAH are lower than peak values reached in the 1950s. However, this reduction of approximately 25% from the peak is much smaller than the three-to five-times reductions in chlorinated hydrocarbons (CHC) in these same cores¹⁰ and reductions of PCB in fish, which have dropped by more than a factor of five since the early 1970s.⁴⁴ The lakes have responded rapidly and efficiently to the regulatory controls applied to the CHC; less stringent controls have been applied to combustion emissions, and the fluxes may again begin to increase with increased fossil energy usage.

ACKNOWLEDGMENTS

We would like to thank Jim Barrett, Brian Lake, and Allan Frank, undergraduate students, and Nancy Morehead of the Great Lakes Environmental Research Laboratory (GLERL), who assisted in the preparation of samples for analysis. We also express our sincere appreciation to the Canada Centre for Inland Waters (CCIW) for providing time aboard their fine vessel, the RV *Limnos*, and for their cooperation in collection of sediments. Special thanks to Rick Bourbonniere of CCIW for his efforts. GLERL contribution #725.

REFERENCES

1. Eadie, B. J., and J. A. Robbins. "The Role of Particulate Matter in the Movement of Contaminants in the Great Lakes," in *Sources and Fates of Aquatic Pollutants*,

- R. A. Hites and S. J. Eisenreich, Eds., American Chemical Society Advances in Chemistry Series 216 (Washington, DC: American Chemical Society, 1987), pp. 319–364.
2. Eadie, B. J., H. A. Vanderploeg, J. A. Robbins, and G. L. Bell. "Significance of Sediment Resuspension and Particle Settling," in *Large Lakes: Ecological Structure and Function*, M. M. Tilzer and C. Serruya, Eds. (New York: Springer Verlag, 1990), pp. 196–209.
 3. Eadie, B. J., R. L. Chambers, W. S. Gardner, and G. L. Bell. "Sediment Trap Studies in Lake Michigan: Resuspension and Chemical Fluxes in the Southern Basin," *J. Great Lakes Res.* 10:307–321 (1984).
 4. Robbins, J. A., and B. J. Eadie. "Seasonal Cycling of Trace Elements, ^{137}Cs , ^7Be and $^{239+240}\text{Pu}$ in Lake Michigan," *J. Geophys. Res.* (submitted).
 5. Robbins, J. A., J. R. Krezski, and S. C. Mozley. "Radioactivity in Sediments of the Great Lakes: Postdepositional Redistribution by Deposit Feeding Organisms," *Earth Planet. Sci. Lett.* 36:325–333 (1977).
 6. Robbins, J. A. "Stratigraphic and Dynamic Effects of Sediment Reworking by Great Lakes Zoobenthos," in *Developments in Hydrobiology: 9. Sediment Freshwater Interaction*, P. G. Sly, Ed. (The Hague: Dr W. Junk Publ., 1982), pp. 611–622.
 7. Nalepa, T. F. "Estimates of Macroinvertebrate Biomass in Lake Michigan," *J. Great Lakes Res.* 15:437–443 (1989).
 8. Bousfield, E. L. "Revised Morphological Relationships within the Amphipod Genera *Pontoporeia* and *Gammaracanthus* and the "Glacial Relict" Significance of Their Past Glacial Distributions," *Can. J. Fish. Aquat. Sci.* 46:1714–1725 (1989).
 9. Neff, J. M. *Polycyclic Aromatic Hydrocarbons in the Aquatic Environment: Sources, Fates and Biological Effects* (London: Applied Sciences Publ., 1979).
 10. Eisenreich, S. J., P. D. Capel, J. A. Robbins, and R. Bourbonniere. "Accumulation and Diagenesis of Chlorinated Hydrocarbons in Lacustrine Sediments," *Environ. Sci. Technol.* 23:1116–1126 (1989).
 11. Driscoll, J. N. "Review of Photoionization Detection in Gas Chromatography: The First Decade," *J. Chromo. Sci.* 23:488–492 (1985).
 12. Eadie, B. J., W. R. Faust, P. F. Landrum, N. R. Morehead, W. S. Gardner, and T. Nalepa. "Bioconcentration of PAH by Some Benthic Organisms of the Great Lakes," in *Polynuclear Aromatic Hydrocarbons: Metabolism and Measurement*, M. W. Cooke and A. J. Dennis, Eds. (Columbus, OH: Battelle Press, 1982), pp. 437–449.
 13. Eadie, B. J., W. R. Faust, W. S. Gardner, and T. Nalepa. "Polycyclic Aromatic Hydrocarbons in Sediments and Associated Benthos in Lake Erie," *Chemosphere* 11:185–191 (1982).
 14. Schelske, C. L., J. A. Robbins, W. S. Gardner, D. J. Conley, and R. A. Bourbonniere. "Sediment Record of Biogeochemical Responses to Anthropogenic Perturbations of Nutrient Cycles in Lake Ontario," *Can. J. Fish. Aquat. Sci.* 45:1291–1303 (1988).
 15. Robbins, J. A., and D. N. Edgington. "Determination of Recent Sedimentation Rates in Lake Michigan Using Pb-210 and Cs-137," *Geochim. Cosmochim. Acta* 39:285–304 (1975).
 16. Laflamme, R. E., and R. A. Hites. "The Global Distribution of Polycyclic Aromatic Hydrocarbons in Recent Sediments," *Geochim. Cosmochim. Acta* 42:289–303 (1978).

17. Tan, Y. L., and M. Heit. "Biogenic and Abiogenic Polynuclear Aromatic Hydrocarbons in Sediments from Two Remote Adirondack Lakes," *Geochim. Cosmochim. Acta* 45:2267-2279 (1981).
18. Wakeham, S. G., C. Schaffner, and W. Giger. "Polycyclic Aromatic Hydrocarbons in Recent Lake Sediments: I. Compounds Having Anthropogenic Origins," *Geochim. Cosmochim. Acta* 44:403-413 (1980).
19. Furlong, E. T., L. R. Cessar, and R. A. Hites. "Accumulation of Polycyclic Aromatic Hydrocarbons in Acid Sensitive Lakes," *Geochim. Cosmochim. Acta* 51:2965-2975 (1987).
20. Hites, R. A., R. E. Laflamme, and J. W. Farrington. "Sedimentary Polycyclic Aromatic Hydrocarbons: The Historical Record," *Science* 198:829-831 (1977).
21. Bates, T. S., S. E. Hamilton, and J. D. Cline. "Vertical Transport and Sedimentation of Hydrocarbons in the Central Main Basin of Puget Sound, Washington," *Environ. Sci. Technol.* 18:300-305 (1984).
22. Gschwend, P. M., and R. A. Hites. "Fluxes of Polycyclic Aromatic Hydrocarbons to Marine and Lacustrine Sediments in the Northeastern United States," *Geochim. Cosmochim. Acta* 45:2359-2367 (1981).
23. Eadie, B. J. "Distribution of Polycyclic Aromatic Hydrocarbons in the Great Lakes," in *Toxic Contaminants in the Great Lakes*, J. O. Nriagu and M. S. Simmons, Eds., Advances in Environmental Science and Technology 14 (New York: John Wiley and Sons, 1984), pp. 195-211.
24. Statistical Abstracts of the United States (SAUS), U.S. Government Printing Office (1988).
25. Eadie, B. J., W. R. Faust, P. F. Landrum, and N. R. Morehead. "Factors Affecting Bioconcentration of PAH by the Dominant Benthic Organisms of the Great Lakes," in *Polynuclear Aromatic Hydrocarbons: Mechanisms, Methods and Metabolism*, M. W. Cooke and A. J. Dennis, Eds. (Columbus, OH: Battelle Press, 1985), pp. 363-377.
26. Landrum, P. F., B. J. Eadie, W. R. Faust, N. R. Morehead, and M. J. McCormick. "Role of Sediment in the Bioaccumulation of Benzo(a)pyrene by the Amphipod *Pontoporeia hoyi*," in *Polynuclear Aromatic Hydrocarbons: Mechanisms, Methods and Metabolism*, M. W. Cooke and A. J. Dennis, Eds. (Columbus, OH: Battelle Press, 1985), pp. 799-812.
27. Landrum, P. F., W. R. Faust, and B. J. Eadie. "Bioavailability and Toxicity of a Mixture of Sediment Associated Chlorinated Hydrocarbons to the Amphipod *Pontoporeia hoyi*," American Society for Testing and Materials, Spec. Tech. Pub. 1027 (1989), pp. 315-329.
28. Strachan, W. M. J., and S. J. Eisenreich. "Mass Balancing of Toxic Chemicals in the Great Lakes: The Role of Atmospheric Deposition," Workshop Report, International Joint Commission, Windsor, Ontario (1988).
29. Landrum, P. F., M. D. Reinhold, S. R. Nihart, and B. J. Eadie. "Predicting the Bioavailability of Organic Xenobiotics to *Pontoporeia hoyi* in the Presence of Humic and Fulvic Materials and Natural Dissolved Organic Matter," *Environ. Toxicol. Chem.* 4:459-467 (1985).
30. Landrum, P. F., S. R. Nihart, B. J. Eadie, and L. R. Herche. "Reduction of Bioavailability of Organic Contaminants to the Amphipod *Pontoporeia hoyi* by Dissolved Organic Matter of Sediment Interstitial Waters," *Environ. Toxicol. Chem.* 6:11-20 (1987).
31. Morehead, N. R., B. J. Eadie, B. Lake, P. F. Landrum, and D. Berner. "The

- Sorption of PAH onto Dissolved Organic Matter in Lake Michigan Waters," *Chemosphere* 15:403-412 (1986).
32. Eadie, B. J., N. R. Morehead, and P. F. Landrum. "Three Phase Partitioning of Hydrophobic Organic Compounds in Great Lakes Waters," *Chemosphere* 20:161-178 (1990).
 33. Landrum, P. F., and J. A. Robbins. "Bioavailability of Sediment Associated Contaminants to Benthic Organisms," in *Sediment Chemistry and Toxicity of In-Place Pollutants*, R. Baudo, J. P. Giesy, and H. Muntau, Eds. (Ann Arbor, MI: Lewis Publishers, 1990), pp. 237-263.
 34. DiToro, D. M. "A Particle Interaction Model of Reversible Organic Chemical Sorption," *Chemosphere* 14:1503-1538 (1985).
 35. Robbins, J. A. "Great Lakes Regional Fallout Source Functions," GLERL Technical Memo ERL-GLERL-56, Ann Arbor, MI (1985).
 36. Robbins, J. A. "The Coupled Lakes Model for Estimating the Long-Term Response of the Great Lakes to Time Dependent Loadings of Particle Associated Contaminants," GLERL Technical Memo ERL-GLERL-57, Ann Arbor, MI (1985).
 37. Faoro, R. B., and J. A. Manning. "Trends in Benzo(a)pyrene, 1966-77," *J. Air Poll. Control Assoc.* 31:62-64 (1981).
 38. Ackland, J. Personal communication: computer printout of the NASN BaP data 1975-1981, U.S. EPA, Research Triangle Park, NC (1982).
 39. Pelletier, C. A., G. H. Whipple, and H. L. Wedlick. "Use of Surface Air Concentration and Rainfall Measurements to Predict Deposition of Fallout Radionuclides," in *Radioactive Fallout from Nuclear Weapons Tests*, Proc. 2nd Conference, U.S. AEC Technical Information, Germantown, MD (1965), pp. 723-736.
 40. Andren, A. W., and J. W. Strand. "Atmospheric Deposition of Particulate Organic Carbon and PAH to Lake Michigan," in *Atmospheric Pollutants in Natural Waters*, S. J. Eisenreich, Ed. (Ann Arbor, MI: Ann Arbor Science, 1981), pp. 459-479.
 41. Katz, M., T. Sakuma, and A. Ho. "Chromatographic and Spectral Analysis of PAH - Quantitative Distributions in Air of Ontario Cities," *Environ. Sci. Technol.* 12:909-915 (1978).
 42. "Polycyclic Aromatic Hydrocarbons - A Background Report Including Available Ontario Data," ARB-TDA report 58-79, Ministry of Environment (MOE), Toronto, Ontario (1979).
 43. Strand, J. W., and A. W. Andren. "PAH in Aerosols over Lake Michigan, Fluxes to the Lake," in *Polynuclear Aromatic Hydrocarbons: Chemistry and Biological Effects*, A. Bjorseth and A. J. Dennis, Eds. (Columbus, OH: Battelle Press, 1980), pp. 127-137.
 44. DeVault, D. S., W. A. Wilford, R. J. Hesselberg, D. A. Nortrup, E. G. S. Rundberg, A. K. Alwan, and C. Bautista. "Contaminant Trends in Lake Trout from the Upper Great Lakes," *Arch. Environ. Contam. Toxicol.* 15:349-356 (1986).

CHAPTER 10

Historical Deposition and Biogeochemical Fate of Polycyclic Aromatic Hydrocarbons in Sediments Near a Major Submarine Wastewater Outfall in Southern California

Robert P. Eganhouse and Richard W. Gossett

INTRODUCTION

Over the last two decades a tremendous amount of research has been directed at understanding the environmental behavior and fate of polycyclic aromatic hydrocarbons (PAH), primarily because of their demonstrated carcinogenicity and global distribution.^{1,2} PAH have been found in many estuarine and coastal environments,³⁻¹⁰ and it has repeatedly been shown that the highest concentrations in and fluxes to sediments typically occur in areas adjacent to urban centers.¹¹⁻¹⁴ The possible sources of PAH near such urbanized sites include atmospheric deposition,¹⁵ surface runoff,^{16,17} municipal waste effluents,^{18,19} industrial effluents,²⁰⁻²² spills and leakage during transport and production of fossil fuels,²³ natural seepage,^{10,24,25} and erosion of exposed shales^{26,27} and coal seams.²⁸⁻³⁰ Whereas direct biosynthesis is generally believed to be insignificant, numerous PAH may be formed from biogenic precursors within relatively short periods of time (years to decades) during the early stages of diagenesis. Examples of the latter include retene, an alkylated phenanthrene derived from abietic acid;^{2,31} perylene, a pentacyclic PAH whose diagenetic precursor(s) and pathway(s) remain controversial (see references in Venkatesan³²); and numerous tetra-and pentacyclic PAH derived from triterpenoidal precursors.^{2,33-35}

One of the most consistent observations has been the similarity of PAH assemblages in many marine sediments from locations throughout the world.² The compositions indicate a dominantly pyrogenic (as opposed to uncombusted fossil fuel) origin and are presumed to reflect the widespread dispersal of combustion-derived PAH in the atmosphere.³⁶ Contributions of combustion PAH near urban centers are often augmented by inputs related to the use and disposal of fossil fuels. Offshore dispersal via currents is thought to be

restricted,^{37,38} and many of the (lower-molecular-weight) PAH derived from uncombusted fossil fuels are relatively labile compared to those found in association with combustion particles.^{8,39-41} This explains the dominance of combustion-derived PAH in offshore sediments and the mixed compositions sometimes found in heavily urbanized embayments and estuaries (e.g., Lake et al.⁷). Differences in the transport dynamics and susceptibility of individual PAH to biodegradation reflect variations in their physicochemical properties and phase associations, the latter of which may be established prior to introduction to the marine environment.^{11,42-45}

The vertical distribution of PAH in well-preserved, age-dated sediment cores typically shows increasing concentrations in the post-1900 period.^{11,12,44,46,47} This parallels the rapid onset of modern industrialization and increased use of fossil fuels in the northern hemisphere.⁴⁸ Because similar profiles have been reported for both lacustrine and marine environments from widely separated locales, the depositional records would appear to document historical anthropogenic inputs on a regional, if not global, scale. The major caveat to this statement is that regional variations in anthropogenic activities related to fossil fuel consumption may cause minor differences in the character (e.g., rate of change, occurrence of subsurface maxima) of the downcore patterns.⁴⁹

Published information on the composition and abundance of PAH in municipal wastewater effluents and the fate of these compounds in receiving waters is relatively limited.^{18,19,50} This makes it difficult to evaluate the importance of such discharges vis-à-vis other inputs of PAH to coastal and estuarine environments. This chapter extends previous studies^{19,51} aimed at describing the detailed organic chemical composition of municipal waste effluents in southern California. Here we present data on the composition and concentration of PAH in one of these effluents, that discharged by the Los Angeles County Sanitation District (LACSD). Because the LACSD receives a significant contribution of industrial (especially petrochemical) waste to its influent, the emissions of petroleum hydrocarbons from this plant exceed those of any major treatment facility in the region.⁵² Our primary interest in investigating the LACSD effluent was to establish the origin of the PAH and estimate their rates of discharge to nearby coastal waters. Comparison of effluent PAH compositions with those of sediments deposited near the outfall system affords an opportunity to investigate the short-term fate of these compounds. In this context, we have also examined sections of a sediment core collected from the Palos Verdes Shelf during the LACSD's coring program in 1981. Sediments from this core have previously been analyzed for elemental abundance, stable isotopic composition, molecular markers, and a variety of inorganic and chlorinated organic trace constituents.^{53,54} Because the core is so well characterized, we felt it would provide an opportunity to estimate the accumulation rate of PAH at this site and to draw some conclusions regarding the origin(s) and postdepositional fate of PAH in this waste-impacted environment.

STUDY AREA

Figure 10.1 shows the location of the LACSD outfall system and the sediment coring (station 3C1). In 1979 the LACSD discharged approximately 1.4×10^9 L/day of effluent, 100% of which received advanced primary treatment. The outflow of water, solids, oil and grease, and hydrocarbons from this facility accounted for 35, 41, 45, and 39%, respectively, of the combined emissions by the four major treatment plants in southern California at that time.⁵² Mass emission rates of total hydrocarbons, saturated hydrocarbons, and aromatic hydrocarbons were estimated at 8000, 4500, and 3500 metric tons/year. The final effluent is discharged from two outfalls, the termini of which are located below the thermocline at a water depth of 60 m.

Sediments deposited on the shelf adjoining the Palos Verdes peninsula have for some time been heavily contaminated with DDT and a complex assemblage of trace inorganic and organic substances (see references in Eganhouse and Kaplan⁵³). Because the prevailing subsurface currents generally transport water and effluent particles along isobaths in a northwesterly direction, concentration isopleths of these contaminants tend to be centered on the 60-m depth

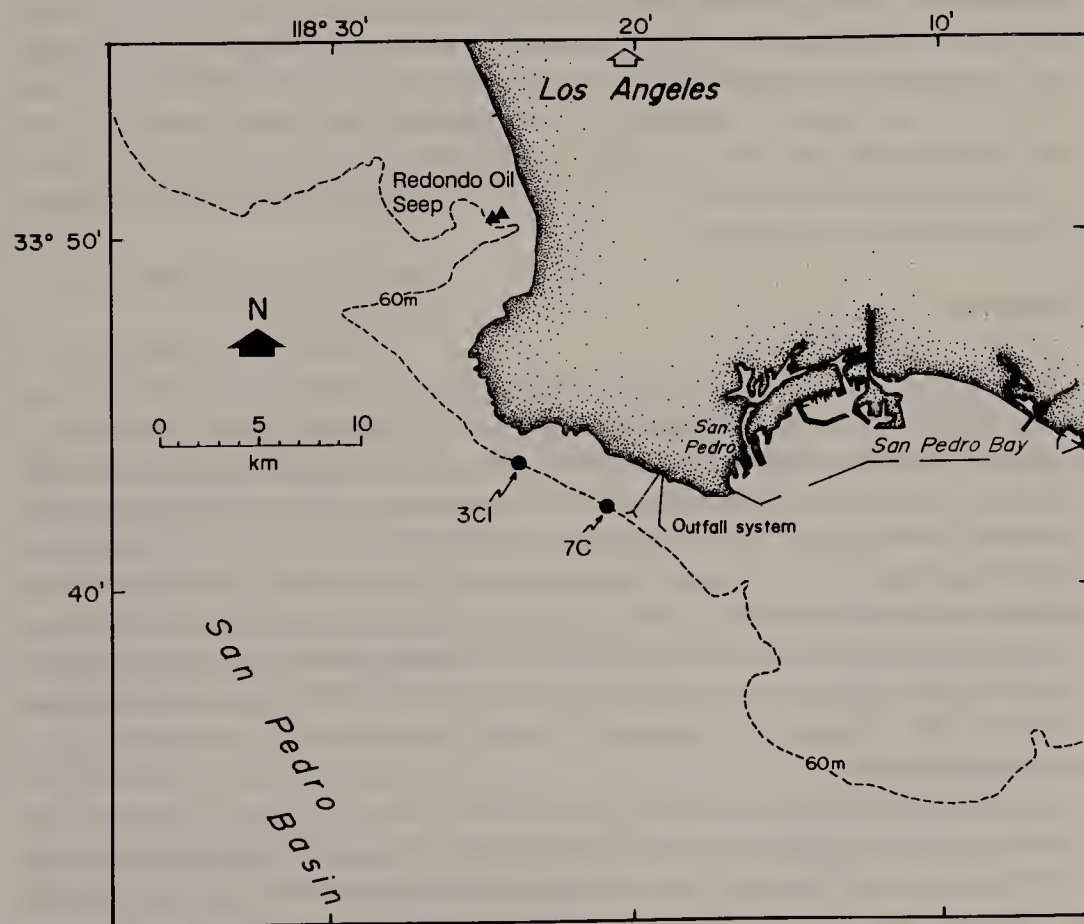


Figure 10.1. Location of the LACSD outfall system, sediment sampling stations (3C1 and 7C), and the Redondo oil seep.

contour and extend northward into Santa Monica Bay. The existence of the deep water outfall system since the early 1950s has resulted in the accumulation of more than 60 cm of organic-rich, effluent-derived material near the outfalls. We chose to investigate a site 6 km downcurrent from the outfalls because of the ability to collect material (by gravity coring) deposited before the onset of significant waste inputs.

EXPERIMENTAL

Sample Collection

Twelve monthly flow-proportioned 24-hr composites of final effluent were collected from the LACSD treatment plant (Carson, CA) during 1979. Details of the procedures used in these collections can be found elsewhere.⁵² Samples were returned to the laboratory and processed as described below. Results presented here pertain to unfiltered effluent samples extracted directly with chloroform.

Sediments were collected using a gravity corer during April 1981 as described by Eganhouse et al.⁵⁵ Although the design and method of deploying the coring device were intended to minimize disruption of the sediment surface and avoid unnecessary compaction, it is probable that some portion of the flocculent surface layer was lost. The sediments were extruded while frozen, cut into 2-cm intervals, trimmed of the outer 2 cm, and stored in a freezer until analyses could be performed.

Analyses

Details of the procedures used to isolate hydrocarbons from effluent and sediment samples can be found elsewhere.^{52,55} Briefly, the effluents were extracted with chloroform; the sediments were extracted with a CH₂Cl₂-MeOH solution. These extracts were treated for removal of water and elemental sulfur, after which they were analyzed gravimetrically for total extractable organic matter. Following esterification of fatty acids, an aliquot of the extract was applied to thin layers of silica gel for isolation of the total hydrocarbon fraction (THC). In some cases, total saturated hydrocarbon and total aromatic hydrocarbon (TAH) fractions were also separated by thin layer chromatography. Yields of these fractions were subsequently determined by microgravimetry.

Aromatic hydrocarbon subfractions suitable for instrumental analysis were obtained from the THC fraction using adsorption chromatography on activated silica gel as described in Anderson and Gossett.⁵⁶ Recovery surrogates (12.5 µg/L of naphthalene-d₈, acenaphthene-d₁₀, phenanthrene-d₁₀, chrysene-d₁₂, and perylene-d₁₂ in hexane) were added to the column along with the THC fraction, and the PAH were collected (f₂: hexane-benzene, 60:40) following

elution of a fraction corresponding to the saturated hydrocarbons (f_1 : hexane). Fraction 2 was concentrated under a stream of N_2 gas, amended with a measured volume of the internal standard solution (anthracene-d₁₀), and adjusted to a known volume by addition of hexane for subsequent instrumental analysis.

Measurement of individual PAH concentrations was accomplished using a Hewlett-Packard 5970 MSD. A 30 m \times 0.25 mm i.d. capillary column coated with DB-5 (0.25- μ m film thickness) was used with splitless injection at 50°C. The column was temperature programmed to 275°C at 4°C/min with an isothermal hold at the upper temperature. Mass spectra were acquired by scanning from 50–400 amu/sec at an ionizing voltage of 70 eV. Peak identifications were based on relative retention times of authentic standards coupled with positive confirmation of the mass spectra. Quantitation of individual PAH was performed by comparison of the integrated peak areas of selected ions for each PAH using the internal standard method. In the case of alkylated homologues of naphthalene and phenanthrene/anthracene, the summed areas of individual homologue peaks were used for quantitation following mass spectral verification. With the exception of naphthalene-d₈, recoveries generally exceeded 90%. Consequently, no correction of PAH concentrations has been made for recovery. Naphthalene recoveries averaged 73 and 43%, respectively, for effluent and sediment samples. Precision is estimated at $\pm 20\%^{56}$.

RESULTS AND DISCUSSION

PAH in Wastewater Effluent

Compositional Features

Table 10.1 provides data on the concentrations of 19 parent PAH and 6 alkylated homologue groups in the LACSD effluent. When summed, the PAH determined by gas chromatography-mass spectrometry comprise < 2% of the total hydrocarbons and $\leq 6\%$ of the total aromatic hydrocarbons measured gravimetrically (following thin layer chromatographic separation).⁵² High-resolution gas chromatography confirms that the TAH fraction consists largely of an unresolved complex mixture (UCM), with resolved PAH representing, at most, a minor component of the total.¹⁹ The vast majority (> 90%) of the resolved PAH contain two or three rings, and naphthalene + (C₁₋₃) alkylated homologues make up 50–75% of the total (Table 10.1). Hoffman et al. report finding similar results for sewage effluents from Rhode Island.¹⁷ The dominance of the PAH assemblage by di-and tricyclic species is consistent with the hypothesis that most of the hydrocarbons in these effluents are derived from petroleum,^{3,19} and not from the thermal alteration of organic matter. The LACSD treatment plant receives wastes from all but one of the petrochemical plants in the Los Angeles basin, and it is presumed that these inputs represent a

Table 10.1. Concentration of PAH in LACSD Final Effluent ($\mu\text{g/L}$) During 1979, 1987^b

Compound ^a	Jan	Feb	Mar	Apr	May	Jun	Jul	Aug	Sep	Oct	Dec	Mean	1987 ^b
Naph	7.0	3.7	1.7	16.3	7.4	1.7	17.8	13.0	8.1	6.9	2.0	7.8	3.92
$\Sigma\text{C}_1\text{-Naph}$	16.2	15.5	22.2	53.3	19.3	12.6	21.3	7.5	22.8	13.7	10.6	23.2	4.85
$\Sigma\text{C}_2\text{-Naph}$	30.1	26.6	46.7	81.5	25.3	29.4	24.9	75.8	45.3	21.2	16.3	38.5	
$\Sigma\text{C}_3\text{-Naph}$	45.9	38.2	90.0	134.4	46.4	54.4	40.4	121.0	87.8	37.3	30.6	66.0	
Biphenyl	1.8	1.2	4.6	5.7	2.8	2.5	5.9	6.6	2.9	2.9	4.4	3.7	
Aceny	c											0.3	
Acenaph													
Florene	1.4	0.7	2.6	3.3	1.2	1.8	5.4	3.6	2.7	4.2	1.1	2.5	
Phen	7.1	5.4	15.3	17.5	7.8	9.6	21.0	19.7	18.0	23.6	5.8	13.7	0.99
$\Sigma\text{C}_1\text{-Phen/A}$	13.7	11.4	22.3	37.4	12.4	19.3	15.8	36.6	37.8	20.4	9.8	21.5	
$\Sigma\text{C}_2\text{-Phen/A}$	11.3	8.4	48.8	34.9	10.7	16.3	10.9	35.4	55.8	16.6	8.4	23.4	
$\Sigma\text{C}_3\text{-Phen/A}$	3.6	1.9	6.1	15.6	5.2	7.6	4.3	17.3	36.8	6.9	2.6	9.8	
Anthracene												0.9	
Fluoran	0.4		0.8	1.4	1.0	0.7	0.5	2.3	0.9	1.2	1.0	2.2	
Pyrene	1.5	0.6	2.4	2.7	1.3	1.6	4.7	3.8	5.5	5.0	1.4	2.4	
B[a]Anthr					0.7	0.4	0.6	1.4	1.1	3.8	1.8	0.8	
Chrys/Tri	0.5		0.2	1.4	1.4	1.4	2.4	2.9	9.6	3.1	0.8	1.0	
B[b]Fluoran												2.1	
B[k]Fluoran												0.2	
B[e]Pyrene												0.02	
B[a]Pyrene												0.09	
Perylene												0.01	
9,10-DPA												<0.1	
DB[a,h]Anthr												<0.1	
B[ghi]Peryl												<0.1	
ΣPAH^d	138.7	112.5	261.6	403.6	139.4	157.1	180.5	382.5	346.8	167.7	91.4	216.5	—
%2,3-ring ^e	98.3	99.5	98.6	98.5	97.3	97.2	93.2	97.5	91.5	92.0	96.5	96.4	
%Naph + ^f	71.5	74.7	61.4	70.8	70.6	62.5	57.8	67.2	47.3	47.2	65.1	63.3	
$\Sigma\text{C}_1\text{-Phen/Phen}$	1.9	2.1	1.5	2.1	1.6	2.0	0.8	1.9	2.1	0.9	1.7	1.7	1.26
Fluoran/Pyrene	0.24	—	0.45	0.38	0.51	0.31	0.49	0.23	0.25	0.47	1.09	0.40	0.65

^aNaph = Naphthalene; Aceny = Acenaphthylene; Acenaph = Acenaphthene; Phen = Phenanthrene; Fluoran = Fluoranthene; B[a]Anthr = Benz[a]Anthracene; Chrys/Tri = Chrysene/Triphenylene; B[b]Fluoran = Benzo[b]Fluoran; B[k]Fluoran = Benzo[k]Fluoran; B[e]Pyrene = Benzo[e]Pyrene; B[a]Pyrene = Benzo[a]Pyrene; B[ghi]Perylene = Benzo[ghi]Perylene.

^bData for 1987 mean concentrations reported by Baird et al.⁵⁷

^cNot detected.

^d ΣPAH = summation of individual PAH excluding biphenyl.

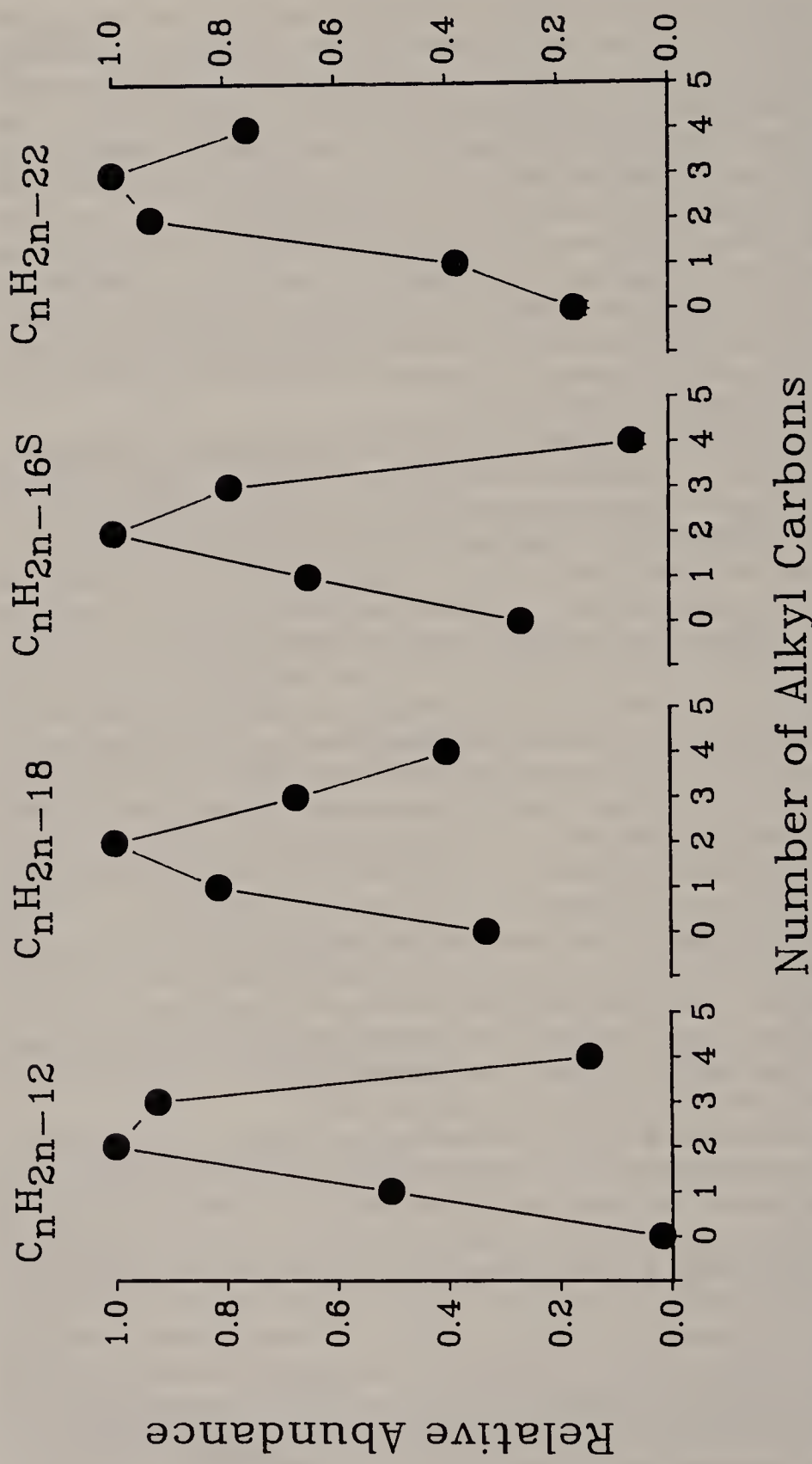
^e2,3-ring = Naphthalene, phenanthrene, anthracene + alkylated homologues.

^fNaph + = Naphthalene + alkylated homologues.

primary source of hydrocarbons and PAH to the plant. The major PAH having four or five rings are fluoranthene, pyrene (and alkylated homologues), and chrysene/triphenylene. Other compounds, including benzo[ghi]perylene, were observed variably and generally at low concentrations (< 1 µg/L), an exception being the benzopyrenes, which were found at concentrations exceeding 2 µg/L during the month of September. Notable for their absence, even in the September sample, are 9,10-diphenylanthracene and benzo[k]fluoranthene (see below). Analyses performed by the LACSD on effluent collected in 1987 indicate that some of these higher-molecular-weight PAH are consistently present in the effluent (e.g., benzo[a]pyrene, benzo[e]pyrene, benzofluoranthenes, and perylene).⁵⁷ However, the concentrations they determined were typically at or below the detection limit of the methodology used here (ca. 0.05 µg/L; see Table 10.1).

Figure 10.2 illustrates the alkyl homologue distributions (AHD) of the naphthalene (C_nH_{2n-12}), phenanthrene/anthracene (C_nH_{2n-18}), dibenzothiophene ($C_nH_{2n-16}S$), and fluoranthene/pyrene (C_nH_{2n-22}) series for the September effluent sample. The compositions depicted in this figure are representative of all of the samples with some minor exceptions discussed below. In all cases, the AHDs are dominated by the C_{2-3} homologues rather than the parent compounds. This agrees with findings of Barrick¹⁸ and further supports an uncombusted fossil fuel origin for the majority of these compounds.³⁶ The naphthalene series is either absent or in low abundance in combustion particles,^{58,59} whereas the phenanthrene/anthracene series represents an overlap between the two sources. In contrast, the fluoranthene/pyrene series is typically found in small quantities in crude oil, while it often represents the most abundant PAH in soot, atmospheric particles, and marine sediments.^{11,47,59,60} For this reason, Sportsøl et al. have suggested that the fluoranthene/pyrene series is a more definitive indicator of combustion vs fossil sources for the higher-molecular-weight PAH.⁵⁹ Based on the relatively low abundance of these tetracyclic compounds (F/P + C_{1-3} -homologues, ca. 2% total PAH) in the effluent and the prevalence of their higher alkylated homologues, contributions of combustion products to the higher-molecular-weight PAH pool in these effluent samples would appear to be small. Similar conclusions were reached by Baird et al., who examined the LACSD effluent in 1987.⁵⁷

Close examination of the ΣC_1 -phenanthrene:phenanthrene ratio, however, suggests that lower values are generally found for samples having higher relative abundances of the 4- and 5-ring PAH (Table 10.1). In the case of the July and October samples, the ratios are less than 1.0. These particular samples also exhibit fluoranthene + pyrene concentrations that exceed 2% of total PAH and are only slightly less abundant than the higher alkylated homologues (Table 10.1). Although the effect is minor, these trends indicate that some combustion-derived PAH are present in the effluent and constitute a variable component of the higher-molecular-weight species. Unlike treatment systems such as the METRO in Seattle,¹⁸ the LACSD plant is largely decoupled from inputs due to surface runoff. Consequently, pyrogenic PAH are unlikely to



Number of Alkyl Carbons

Figure 10.2. Distribution of naphthalene (C_nH_{2n-12}), phenanthrene/anthracene (C_nH_{2n-16S}), dibenzothiophene (C_nH_{2n-16S}), and fluoranthene/pyrene (C_nH_{2n-22}) alkyl homologue series for LACSD effluent sample taken September 13, 1979. Abundances are based on summation of integrated molecular ion current for each level of alkylation.

arise from contributions by surface runoff. This may also account for the lack of any discernable seasonal pattern in the PAH composition and/or concentrations. Products of high-temperature catalytic cracking or other industrial pyrolytic processes,^{61,62} on the other hand, might reasonably be expected to be entering the system. Other possible sources are the wastes generated by car washes, gasoline stations, and other vehicular service industries.⁶³

It is also interesting to note that the fluoranthene:pyrene ratio is, with one exception (sample taken December 1979), less than unity in all effluent samples (mean $\pm 1\sigma = 0.40 \pm 0.27$). In 1987, Baird et al. reported similar ratios for the LACSD effluent (mean $\pm 1\sigma = 0.65 \pm 0.49$).⁵⁷ The fluoranthene:pyrene ratio is almost universally near or greater than one in combustion particles, atmospheric aerosols, and sediments contaminated by pyrogenic sources.^{1,2,11,14,15,22,34,37,38,48} In contrast, crude oils and refined petroleum products typically show ratios less than 1.0.^{11,64} This again signals a dominantly petroleum origin for the high-molecular-weight PAH in the effluent. Comparable data for municipal wastewater effluents were reported by Grzybowski et al., who found fluoranthene and pyrene concentrations within ranges of 0.5–5.0 and 11.0–27.0 $\mu\text{g/L}$, respectively.⁵⁰

Estimation of Mass Emission Rates

Table 10.2 presents a summary of the mass emission rates of the individual and ΣPAH from the LACSD plant for the year 1979. These data were developed by applying the concentrations determined for each monthly sample to the flow for that date. The daily mass emissions were then multiplied by the number of days in each month, and the monthly estimates were summed to produce an annual figure. Also provided are estimates reported by Barrick for the Seattle METRO treatment plant during the period 1977–1979.¹⁸ With the exception of phenanthrene, these data represent particulate concentrations. The particulate-based data are comparable with those reported here (i.e., total concentrations) because the vast majority of the higher-molecular-weight PAH in municipal wastes and urban runoff are associated with filterable (0.45–1.2 μm) particulate matter.^{17,57}

If one computes the ratio of annual mass emissions of individual PAH for the LACSD and METRO effluents, it is apparent that the LACSD discharge rate greatly exceeds that of the METRO (LACSD/METRO: range, 8–50; mean, 33.4). Normalization of mass emissions to the population served reduces the difference to factors ranging from 1.0 to 6.4 (mean_{LACSD/METRO} = 4.3). By comparison, the average ratio (of daily per capita mass emissions) for total hydrocarbons is $5.9/3.12 = 1.89$.^{18,52} Thus, the LACSD effluent would appear to have been discharging significantly greater amounts of hydrocarbons and, especially, PAH to coastal waters of the southern California Bight during 1979 than the METRO plant was to Puget Sound. This probably reflects the large petrochemical input to the former. Recent work by Baird et al. has revealed significantly lower concentrations of PAH in the LACSD

Table 10.2. Mass Emission Rates (metric tons/year) of Individual PAH from the LACSD and Seattle METRO Wastewater Treatment Plants

Compound ^a	MER(mta)		Per capita MER (mg/cap day)	
	LACSD ^b	METRO ^c	LACSD	METRO
Naph	3.99		2.99	
ΣC_1 -Naph	11.9		8.94	
ΣC_2 -Naph	19.7		14.8	
ΣC_3 -Naph	33.8		25.4	
Biphenyl	1.91		1.44	
Aceny	0.13		0.10	
Acenaph	0.43		0.32	
Fluorene	1.30		0.98	
Phen	7.00	0.18	5.26	0.9
ΣC_1 -Phen/A	11.0	0.22	8.24	1.2
ΣC_2 -Phen/A	11.9	0.25	8.94	1.4
ΣC_3 -Phen/A	4.92		3.70	
Anthracene	0.45		0.34	
Fluoran	0.55	0.067	0.41	0.4
Pyrene	1.40		1.05	
B[a]Anthr	0.94	0.014	0.36	0.08
Chrys/Tri	0.48	0.028	0.78	0.2
B[b]Fluoran	0.11		0.08	
B[e]Pyrene	0.22	0.013	0.17	0.07
B[a]Pyrene	0.17		0.12	
Perylene	0.03		0.02	
DB[ah]Anthr	0.01		0.01	
B[ghi]Peryl	0.03		0.02	
ΣPAH^d	110.5		83.0	

^aCompound names given in Table 10.1.^bThis study. Effluent samples collected 1979.^cData from Barrick¹⁸ for effluent collected 1977–1979.^d ΣPAH = summation of individual PAH excluding biphenyl.

effluent (Table 10.1).⁵⁷ With the exception of naphthalene, individual PAH and associated alkylated homologue groups appear to have been present in lower concentrations in 1987 than they were in 1979 by more than an order of magnitude. This is probably due to a combination of industrial source control and improvements in treatment. Between 1979 and 1987, the fraction of effluent that received full secondary treatment at the LACSD changed from 0 to 54%. However, it is more likely that the reduction in PAH emissions during this period was achieved by aggressive source control measures, as evidenced by the nearly parallel decreasing trends in influent and effluent oil and grease mass inputs starting in the late 1970s.⁶⁵

PAH in Sediments

PAH Composition and Sources

Table 10.3 summarizes the PAH composition of surficial (0–2 cm) sediments collected from station 3C1 (see Figure 10.1) on the Palos Verdes Shelf. Data are also provided from two investigations in which surficial sediments were

Table 10.3. PAH Concentrations (ng/dry g) in Sediments of the Palos Verdes Shelf

Compound ^a	This study ^b (3C1; 1981)	Swartz et al. ⁶⁶ (7C; 1980)	Anderson and Gossett ⁵⁶ (7C; 1986)
Naph	— ^c	29	87
ΣC_1 -Naph	—	NR ^d	104
ΣC_2 -Naph	—	NR	415
ΣC_3 -Naph	—	NR	462
Biphenyl	—	NR	22
Aceny	—	160	57
Acenaph	—	NR	—
Fluorene	—	NR	16
Phen	—	290	197
ΣC_1 -Phen/A	—	NR	773
ΣC_2 -Phen/A	—	NR	1193
ΣC_3 -Phen/A	—	NR	701
Anthracene	—	623	52
Fluoran	17	294	157
Pyrene	127	838	401
B[a]Anthr	36	1330	166
Chrys/Tri	88	606	274
B[b]Fluoran	207	633	746
B[e]Pyrene	217	NR	317
B[a]Pyrene	212	NR	323
Perylene	105	NR	353
9,10-DPA		NR	4
DB[a,h]Anthr	38	NR	NR
B[ghi]Peryl	205	NR	217
Σ PAH	1252		7037

^aCompound names given in Table 10.1.^bData are for 0–2 cm section.^cBelow detection limit.^dNot reported.

analyzed for PAH at station 7C, in close proximity to the outfall termini (see Figure 10.1).^{56,66}

In the case of the 3C1 sediments, di-and tricyclic PAH were not detected in the 0–2 cm section, and Σ PAH concentrations were 1.25 $\mu\text{g}/\text{dry g}$. By comparison, significant amounts of di-and tricyclic PAH were found in sediments collected at station 7C, and the concentration of Σ PAH in these sediments is more than a factor of five greater (7.04 $\mu\text{g/g}$). These differences probably reflect variations in sediment accumulation rates of waste-derived particles at the two sites (see below and Kettenring⁶⁷). Deeper sections of the 3C1 core were found to contain small, but measurable, quantities of phenanthrene, anthracene, and their alkylated homologues. However, the lower-molecular-weight species (e.g., naphthalene, biphenyl, etc.) were generally below detection limits.

Gas chromatograms of the f_2 fractions of all core sections reveal an unresolved complex mixture similar to that reported by Venkatesan et al. for sediments from San Pedro Basin.¹⁰ The resolved PAH represent only a small fraction of the total aromatics isolated in the f_2 fraction. Examination of the AHDs for the fluoranthene/pyrene series in the 3C1 sediments (Figure 10.3)

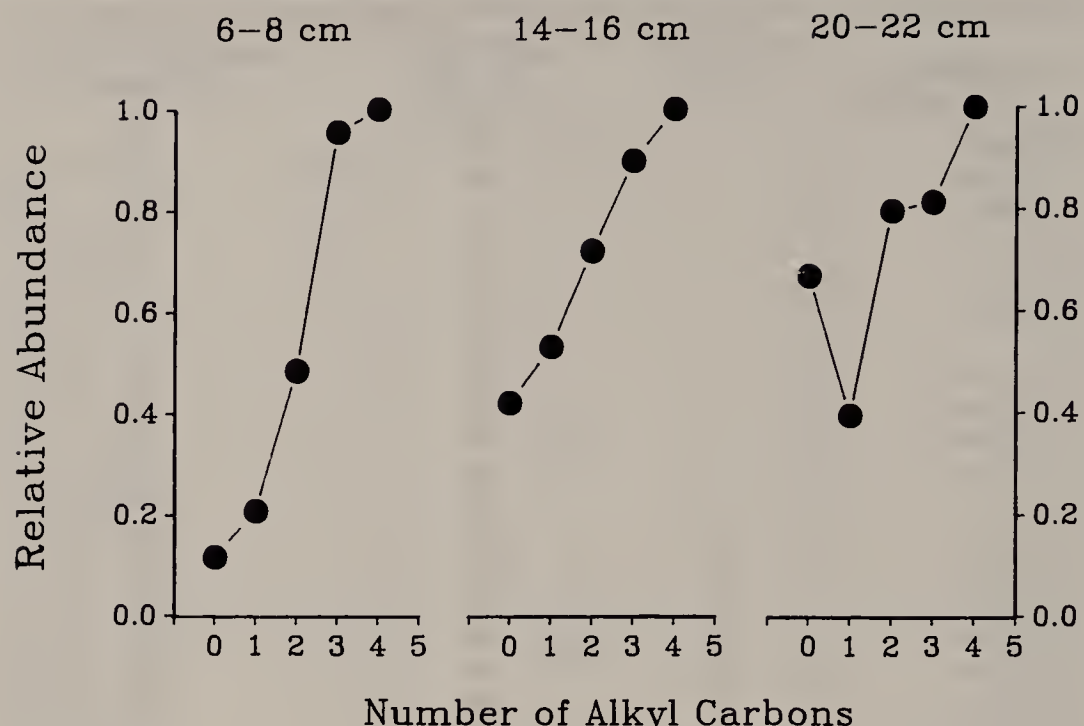


Figure 10.3. Distribution of fluoranthene/pyrene alkyl homologue series for sediment sections from core 3C1. Abundances are based on summation of integrated molecular ion current for each level of alkylation.

typically show increasing amounts of higher alkylated homologues up to at least the C₄-substituted species, indicating a petroleum origin. Similar trends have been reported by Venkatesan et al. for surface (0–5 mm) sediments from the San Pedro Basin floor.³⁸ Moreover, the F/P ratios in the 3C1 sediments range from 0.13 to 0.75 (mean $\pm 1\sigma = 0.42 \pm 0.22$) and are essentially indistinguishable from ratios reported in Table 10.1 for the LACSD effluent (mean $\pm 1\sigma = 0.40 \pm 0.27$). Because of the occurrence of submarine oil seepage in this region,^{68,69} however, the PAH in these sediments probably originate from a combination of petroleum residues discharged from the LACSD outfall system and natural oil seepage. Similarities between the distribution of higher-molecular-weight PAH found in the effluent and near-surface sediments at 3C1 (Figure 10.4) are suggestive of a linkage between the waste discharge and the sedimentary PAH.

Recent work by Eganhouse and Kaplan has shown that the vast majority (85–100%) of the hydrocarbons found in the upper 24 cm of this core are derived from municipal effluent.⁵³ These authors found correlations between the vertical distribution of specific molecular markers of the LACSD effluent (e.g., linear alkylbenzenes, DDT) and oil seepage (17 α (H),18 α (H),21 β (H)-28,30-bisnorhopane) and the historical discharge of wastes from the LACSD treatment plant. Some of these results are summarized in Figure 10.5, where vertical concentration profiles of Σ PAH, total hydrocarbons, and the

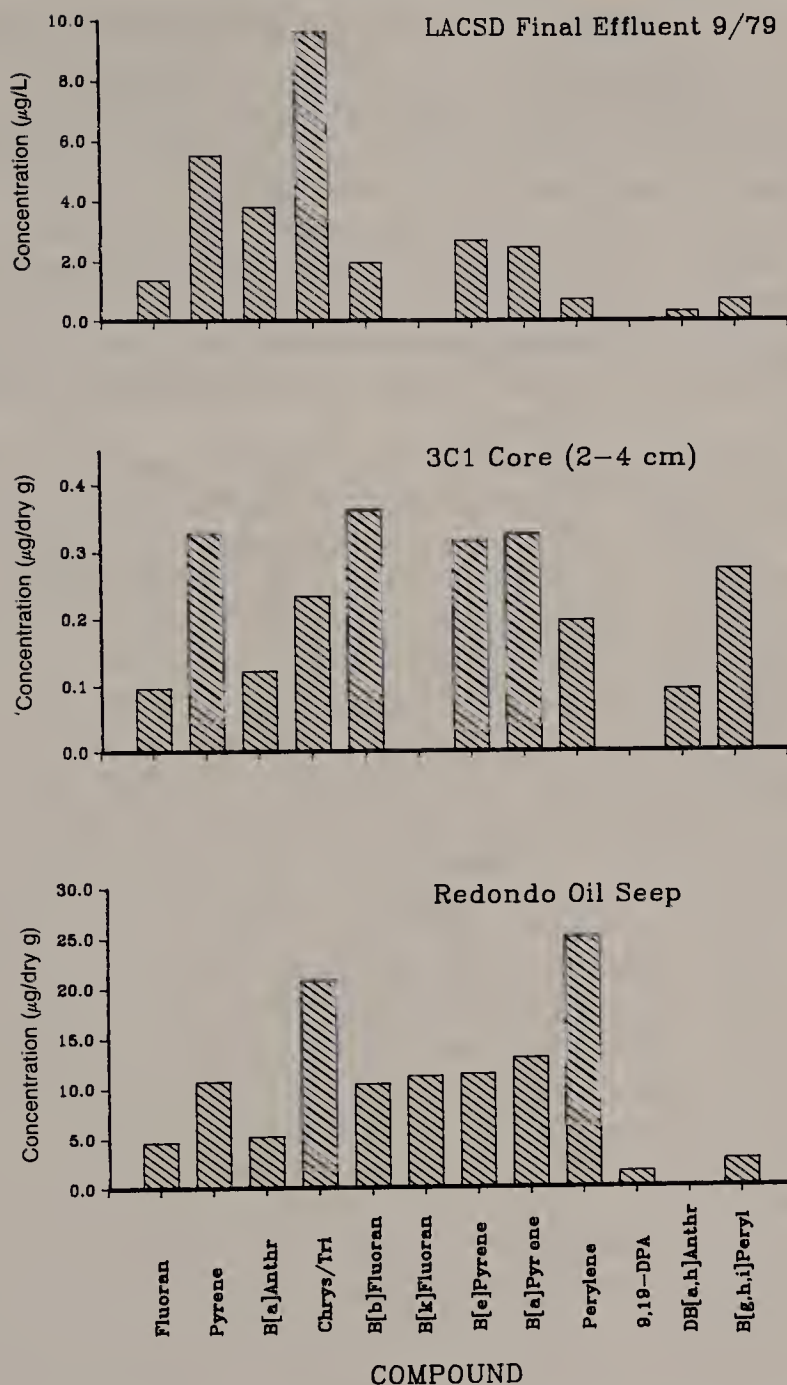


Figure 10.4. Composition of PAH in LACSD final effluent (September 1979), near-surface sediments (2–4 cm) from station 3C1, and a sample of the Redondo oil seep. For compound names see Table 10.1.

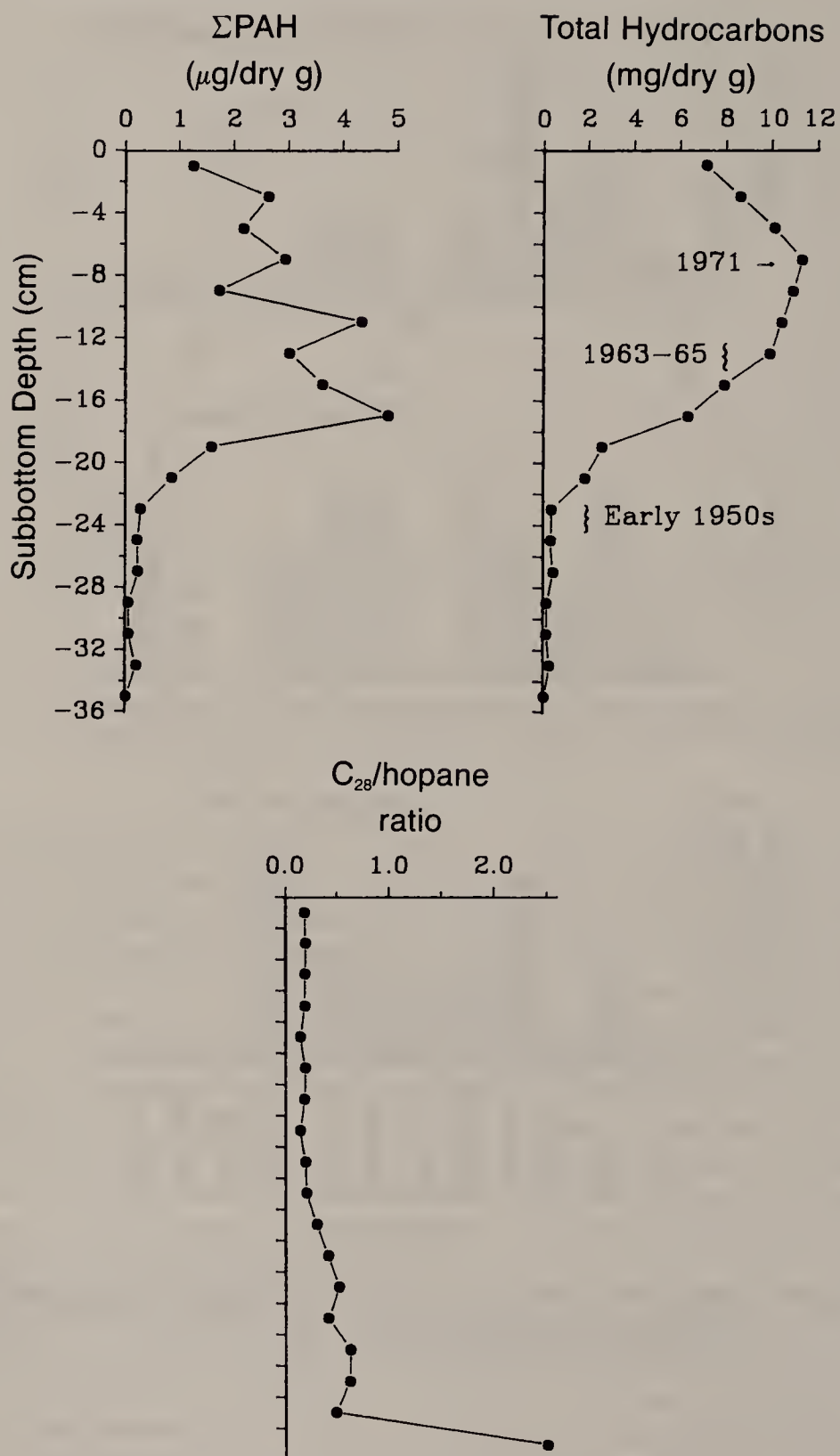


Figure 10.5. Vertical concentration profiles of total PAH and total hydrocarbons and the $17\alpha(\text{H}), 18\alpha(\text{H}), 21\beta(\text{H})$ -28,30-bisnorhopane:hopane ratio in the 3C1 core.

$17\alpha(H),18\alpha(H),21\beta(H)$ -28,30-bisnorhopane:hopane ratios are provided. The bisnorhopane (C_{28}^*) is a pentacyclic triterpane found abundantly in the Monterey shale and California oils (see references in Simoneit and Kaplan⁶⁸) but only in trace quantities in the LACSD effluent.^{19,53} Because of the restricted occurrence of this compound in other (non-California) oils and its pervasive distribution in sediments in this region, the bisnorhopane has been proposed as a unique molecular indicator of natural seepage in the southern California Bight.⁶⁸ Hopane, on the other hand, is an ubiquitous constituent of fossil organic matter and is used here as a normalizing factor to distinguish between the effluent (C_{28}^* :hopane ratio < 0.09) and seepage oil (C_{28}^* :hopane ratio > 1.0).⁵³

In this figure, the concentration of total hydrocarbons exhibits a distinct maximum at a subbottom depth of 6–8 cm, declines rapidly at greater depth, and reaches apparent background levels at ca. 24 cm. The subsurface maximum has been assigned a tentative date of ca. 1971 because this corresponds to the year of maximum solids emissions from the LACSD,⁶⁵ whereas the 22–24 cm horizon is believed to correspond to ca. 1950, a period when waste discharges to the shelf began to become important.^{55,65,70} Other effluent-derived contaminants show subsurface maxima at the same depth in these sediments,^{55,56} and Eganhouse and Kaplan have demonstrated strong correlations among concentrations of organic carbon, organic nitrogen, extractable organics, and THC.⁵³ Together, these results support the hypothesis that the sediment profiles record the history of waste emissions to the Palos Verdes Shelf. By comparison, the Σ PAH concentration appears to increase irregularly downcore to ca. the 16–18 cm section. Thereafter, concentrations decline with increasing depth until near-background levels are reached, again at ca. 24 cm. The elevated Σ PAH concentrations in the upper 24 cm of this core approximate the trends for total hydrocarbons and organic carbon, indicating that these related organic compound groups probably originate from the same source. However, a well-defined subsurface maximum is not apparent for the PAH, and the highest concentration is found at a greater subbottom depth than the THC maximum. Assuming these discrepancies cannot be ascribed to diagenetic effects, the patterns suggest that historical changes in the emissions of solids from the LACSD plant alone did not control the accumulation rates of PAH in these sediments. The trend for the C_{28}^* :hopane ratio (Figure 10.5) is essentially the reverse of that exhibited by the PAH and THC, with highest ratios (i.e., greatest seepage inputs) found within the 34–36 cm section. This is consistent with the hypothesis that the input of wastewater hydrocarbons (and, therefore, the PAH) has dominated contributions made by natural seepage over the time period represented by the upper 34 cm of this core.⁵³

Figure 10.4 shows PAH distributions for the LACSD effluent (September 1979), the 2–4 cm section of core 3C1, and a sample of the Redondo oil seep⁶⁹ (for sampling locations see Figure 10.1). Differences between the seep and effluent PAH distributions include

1. the absence of benzo[k]fluoranthene and 9,10-diphenylanthracene in the effluent (see Table 10.1)
2. the absence of dibenz[a,h]anthracene from the seep material
3. the greater relative abundance of perylene in the seep oil

Examination of the PAH distribution in the core sediments indicates that both benzo[k]fluoranthene and 9,10-diphenylanthracene were undetected, dibenz[a,h]anthracene is present in approximately the same amount (relative to benzo[ghi]perylene) as found in the effluent sample, and perylene is less abundant than the benzopyrenes, unlike the seep oil. These relations strongly suggest that the PAH in near-surface sediments at 3C1 are dominated by waste, not seepage, inputs. The same patterns are found throughout the core with one exception: the abundance of perylene relative to the benzopyrenes is somewhat variable.

Short-Term Biogeochemical Fate of Waste-Derived PAH

The behavior and fate of PAH in aquatic environments may depend upon the phases with which these compounds become associated during formation.^{42,43} For example, it has recently been suggested that PAH present in combustion particles may be occluded within the ash or soot matrix and thereby be prevented from release to surrounding waters.⁴² This is thought to account for the extreme uniformity of PAH composition in a sediment core collected in the Tamar Estuary.⁴⁴ Oil-derived PAH, on the other hand, are expected to be largely adsorbed to surfaces of particles or present as agglomerations, where they are more readily available for release and metabolism. Based on the earlier discussions, it is clear that the PAH associated with the LACSD effluent particles (including the 4-to 6-ring compounds) are largely petroleum derived. It is, therefore, likely that these PAH would be subject to exchange during and after sedimentation.

Comparison of data provided in Tables 10.1 and 10.3 indicates that virtually all of the 2-and 3-ring PAH which dominate effluent compositions are absent in surficial sediments at station 3C1. These compounds are sufficiently soluble in water so that a significant portion would be expected to be present in the dissolved phase of the effluent. This expectation is, in fact, met.⁵⁷ However, the absence of 2-and 3-ring PAH in the sediments indicates that the particle-bound fraction of these compounds is effectively removed prior to incorporation of waste particles into the sediments at station 3C1. The higher-molecular-weight PAH (four to six rings) have very low solubilities in water and strongly sorb to particulate matter.⁶² Not surprisingly, they are found entirely in the filterable particulate phase (i.e., < ~0.5 µm) of the effluent,⁵⁷ and they are the dominant PAH in the sediments.

One means of estimating the magnitude of PAH removal during sedimentation is by comparing the particulate organic carbon normalized concentrations of PAH in the effluent and in surficial sediments. Because of the difficulty of detecting all of the 4- to 6-ring PAH in many of the effluent samples, we have

Table 10.4. Organic Carbon Normalized PAH Concentrations ($\mu\text{g/g}$ OC) in LACSD Effluent (9/13/79) and Near-Surface Sediments (2–4 cm) from Core 3C1

Compound ^a	Effluent	Sediments	% PAH Lost ^b
Fluoran	13.8	1.55	88.8
Pyrene	54.8	5.25	90.4
B[a]Anthr	37.8	1.95	94.8
Chrys/Tri	95.7	3.74	96.1
B[b]Fluoran	19.6	5.79	71.4
B[e]Pyrene	26.9	5.06	81.2
B[a]Pyrene	24.5	5.22	78.7
Perylene	7.3	3.15	56.8
DB[a,h]Anthr	3.2	1.5	53.0
B[ghi]Peryl	7.3	4.37	40.2
Σ PAH	3459	42.0	98.8

^aCompound names given in Table 10.1.^b%PAH lost is calculated as $\{1 - [\text{Conc.}_{\text{sed}}/\text{Conc.}_{\text{effl}}]\} \times 100$.

selected the September 1979 sample (which exhibited the highest concentrations of high-molecular-weight PAH) for purposes of comparison. As noted earlier, these compounds are entirely associated with filterable particulate matter. Thus, it is reasonable to compute POC-normalized concentrations for the effluent sample. The organic carbon normalized concentrations for each compound (sediments) exhibited no discernible trend with depth, and given the time period over which the sediments in this core were presumably deposited, the variation was surprisingly low. One exception is that the concentrations of all compounds tended to maximize at a depth of 16–18 cm. As noted earlier, this may correspond to a period of intense PAH input to the LACSD plant.

When one compares the PAH concentrations in the 2–4 cm sediment section with those obtained for the September effluent sample (Table 10.4) and then computes the difference as a percentage, apparent "losses" of 40–96% are obtained for individual PAH. This computation assumes that the organic carbon is refractory, which is clearly not the case. Investigating the short-term decomposition of LACSD effluent particles in coastal waters, Myers found organic carbon concentration to decrease by approximately 25% within a period of approximately 1 week.⁷⁰ If such a correction is applied to the present data to account for loss of particulate organic carbon, one finds that the apparent losses range from 47 to 112%. Given the uncertainties associated with use of the September effluent sample and Myers' estimates for the decomposition of organic carbon, the corrected losses fall within an acceptable range. More importantly, however, the magnitude of the lost fraction appears to be inversely related to the log solubility of the compound (Figure 10.6). The data depicted in this figure suggest that PAH having solubilities lower than approximately 10^{-7} moles/L are lost during the earliest stages of sedimentation.

A similar exercise can be performed using the total hydrocarbon concentration as normalizing factor (Table 10.5 and Figure 10.6). In this case, one must assume that the character of the hydrocarbons discharged by the LACSD

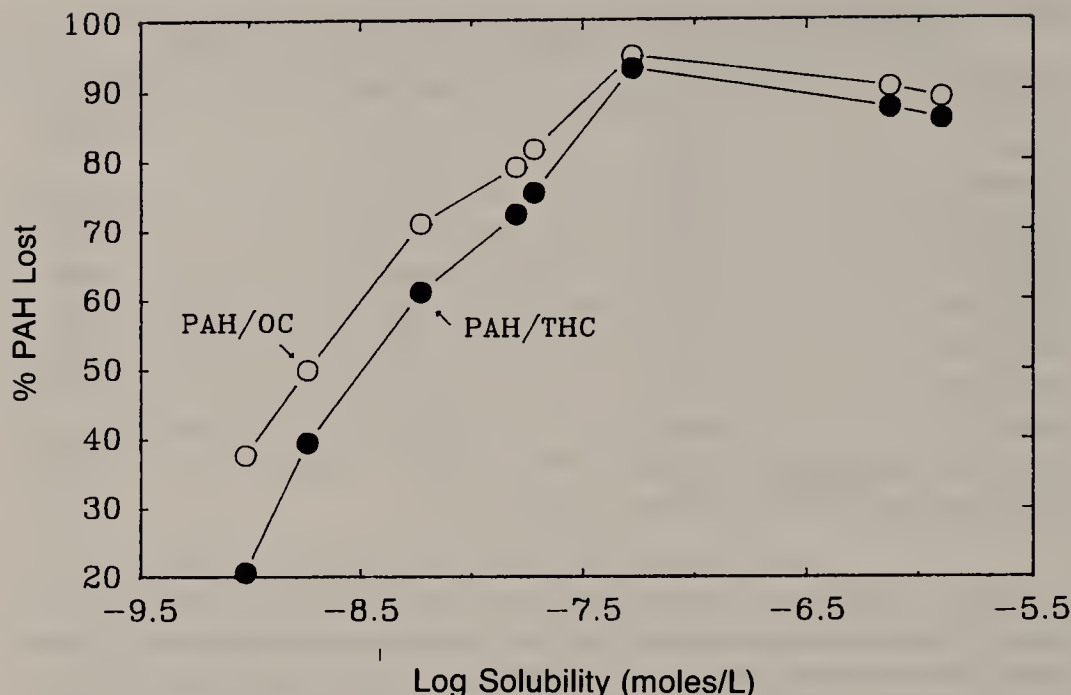


Figure 10.6. Percent PAH lost during early sedimentation vs log molar solubility of 4-, 5-, and 6-ring PAH in sediments of core 3C1.

through time has not changed significantly. Judging from the uniformity of the high-resolution gas chromatographic profiles of the total hydrocarbon fractions of effluent samples taken over a 12-month period¹⁹ and from sediments throughout the 3C1 core,⁵³ this assumption seems tenable. The estimated fraction of "lost" PAH ranges from 21 to 95%. Agreement between estimates based on OC-normalized and THC-normalized concentrations is quite good for the more soluble compounds. In the extreme case of benzo[ghi]perylene, differences in estimates of the lost fraction fall within a factor of 1.9.

Table 10.5. Total Hydrocarbon Normalized PAH Concentrations (mg/g THC) in LACSD Effluent (9/13/79) and Near-Surface Sediments (2–4 cm) from Core 3C1

Compound ^a	Effluent	Sediments	% PAH Lost ^b
Fluoran	76.5	11.3	85.3
Pyrene	303	38.1	87.4
B[a]Anthracene	209	14.2	93.2
Chrysanthrene	530	27.2	94.9
B[b]Fluoran	108	42.0	61.2
B[e]Pyrene	149	36.7	75.4
B[a]Pyrene	136	37.9	72.1
Perylene	40.3	22.9	43.2
DB[a,h]Anthracene	17.7	10.9	38.3
B[ghi]Perylene	40.4	31.7	21.5
Σ PAH	19300	304.6	98.4

^aCompound names given in Table 10.1.

^b% PAH lost is calculated as $\{1 - [\text{Conc.}_{\text{sed}}/\text{Conc.}_{\text{effl}}]\} \times 100$.

The discrepancy may indicate a greater relative lability of the hydrocarbons (compared with total organic carbon). Although the magnitude of the "lost fraction" of the high-molecular-weight PAH remains uncertain, it is systematically related to the solubility of the individual PAH. Examination of Figures 10.2 and 10.3 shows that the fluoranthene/pyrene AHDs of effluent and sediments are different. The effluent exhibits a maximum at the C₃-alkyl homologue, whereas the sediment AHD more typically shows a monotonic increase in abundance with degree of alkylation.³⁸ Because the log solubilities of PAH within a homology decrease linearly with increasing molar volume,⁷¹ this difference is another manifestation of solubility-controlled removal.

Several processes may be responsible for the compositional changes that take place between the time of discharge and the accumulation of effluent-derived PAH in bottom sediments. The most important of these are desorption and biological degradation. Photochemical oxidation is unlikely to be significant because the wastewater effluent is discharged below the thermocline, and except under unusual circumstances during nonstratified conditions, effluent particles do not enter the photic zone. Numerous studies of the desorption kinetics of hydrophobic organic compounds have demonstrated that sorbate release occurs in two phases: (1) a rapid desorption step in which 25–60% of the sorbate is released within minutes to hours and (2) slow desorption of the remainder over a time scale of days to months.^{72–75} Once discharged, the effluent experiences rapid dilution with seawater in the range of 100:1 to 300:1. Consequently, rapid desorption of the PAH from effluent particles during initial dilution could account for release of as much as 25–60% of the PAH. The fact that virtually all of the 2- and 3-ring PAH in the effluent are absent from sediments heavily impacted by the discharge indicates that if desorption were the only process involved during sedimentation of effluent particles, it must have taken place over time scales in excess of hours. This is consistent with estimates of the average time that effluent particles require to reach the bottom on this part of the shelf (days) and the likelihood that once deposited, most of the particles experience repeated resuspension and redeposition prior to incorporation into the permanent sediments. In effect, this would act to increase their residence time in the water column.

Karickhoff⁷² and Karickhoff and Morris⁷³ presented a sorption kinetics model consisting of "labile" and "nonlabile" compartments that simulated the results of laboratory desorption experiments. They showed that the slow desorption step could be characterized by a rate constant, k_d , that was inversely related to the equilibrium partition coefficient, K_p , of a given hydrophobic organic substance. Rate constants ranging from 0.49 hr⁻¹ (naphthalene) to 0.031 hr⁻¹ (pyrene) were reported. Similar results were obtained by Wu and Gschwend, who developed a radial diffusion model to simulate sorption-desorption kinetics.⁷⁴ In the latter case, experimental data could be fitted using a single effective diffusivity parameter, D_{eff} , which again was inversely related with K_p . The common conceptual feature of these two models is the requirement that desorption (and adsorption) rates are limited by diffusive processes

occurring within particle pores, the sorbent matrix, and/or intraaggregate pore spaces. Regardless which mechanism(s) or matrix is most important, the experimental data suggest that the more hydrophobic (i.e., less soluble) PAH should desorb more slowly from particles. Thus, desorption kinetics could explain the trend of increasing PAH loss with increasing solubility (Figure 10.6).

At the same time, numerous microcosm studies have demonstrated that the rate at which PAH are degraded by microorganisms in the water column and sediments increases with decreasing molecular size (i.e., increasing solubility).^{39,41,76,77} Within the water column, higher-molecular-weight PAH are particularly susceptible to photodegradation,^{76,78} whereas the lower-molecular-weight species (e.g., naphthalene, phenanthrene, anthracene) are removed primarily by evaporation and microbial degradation. Hinga et al. reported little biodegradation of benz[a]anthracene within the water column of a marine mesocosm.⁷⁹ Rather, metabolism was found to occur in surface (0–1 cm) sediments; degradation was apparently slowed in deeper anoxic layers. Herbes was unable to establish degradation of 4- and 5-ring PAH (i.e., benzo[a]pyrene and dibenz[a,h]anthracene) in incubated sediments taken downstream of a coal-coking plant, whereas 2- and 3-ring compounds showed measurable degradation in both water and sediment compartments.³⁹ Gardner et al. also noted that the rate of PAH removal in sediments decreases with increasing molecular weight and reduced oxygen availability.⁸⁰ This effect of redox conditions has been confirmed by others.⁸¹ Together these results suggest that the lower-molecular-weight species are probably rapidly removed during sedimentation by a combination of desorption and biodegradation. Transport times for effluent particles through the water column are expected to be on the order of days. Judging from the results of previous microcosm experiments (which were conducted on similar time scales), the residence time of effluent particles in the water column is probably insufficient to bring about the complete physical release of the high-molecular-weight PAH. Consequently, the partial losses of 4-, 5-, and 6-ring PAH largely occur after initial deposition during the period when the particles reside within the oxidizing layer of the surface sediments.

Postdepositional Alteration

The foregoing discussion points to differential rates of removal for the higher-molecular-weight PAH within the surface layers of the sediments on the Palos Verdes Shelf. If kinetically controlled removal (i.e., coupled desorption and metabolism) of 4-, 5-, and 6-ring PAH were to continue following incorporation and burial of effluent particles, one would expect to see systematic changes in PAH composition with increasing subbottom depth. This assumes, of course, that the quality of the source PAH has not changed significantly with time. Such systematic changes over time have been reported for lower-molecular-weight species (i.e., naphthalenes and phenanthrenes) introduced to

intertidal sediments during a fuel oil spill²³ and in microcosm studies.⁷⁷ However, Readman et al. observed uniform higher-molecular-weight PAH compositions throughout a 50-cm core from the Tamar Estuary.⁴⁴ In the latter case, the lack of compositional variation with depth was attributed to the occlusion of (predominantly) pyrogenic PAH in the source particles. Examination of downcore variations in PAH composition at station 3C1 should reveal whether kinetically controlled removal continues after burial.

Table 10.6 presents a Pearson correlation matrix for sediment concentrations of ten 4-, 5-, and 6-ring PAH in the 3C1 core. All correlations are significant ($p \leq 0.001$). High correlation coefficients are found for many pairs. However, the best coefficients were generally obtained when both PAH were present in higher concentrations, presumably the result of improved analytical precision. In general, these correlations suggest that kinetically controlled, compound-specific removal of these higher-molecular-weight PAH is not occurring during burial. This is nicely illustrated in Figure 10.7, which shows a scatterplot of pyrene vs benzo[ghi]perylene. As discussed earlier (Tables 10.4 and 10.5, Figure 10.6), these two compounds represent extremes with respect to apparent PAH removal rates during the earliest stages of sedimentation. Nevertheless, the relative abundances of these PAH are maintained throughout the core. Although no data are available on the variation of redox conditions with subbottom depth at 3C1, it is known that the presence of hydrogen sulfide in surface sediments has varied in response to wastewater solids emissions and advances by the echiuran *Listriolobus pelodes*.⁸² Because of the high depositional flux of labile organic matter at this site, it is presumed that the sediments are anoxic only a short distance below the sediment-water interface. Under these conditions, the resistance of all PAH to biodegradation would be enhanced.⁷⁹⁻⁸¹

In contrast to the findings of Readman et al. for sedimentary PAH in the Tamar Estuary,⁴⁴ the PAH in these sediments are derived primarily from uncombusted petroleum. Consequently, the compositional uniformity of the PAH cannot be attributed to occlusion within combustion particles. Exchange of the high-molecular-weight PAH between pore waters and the overlying water column (or deeper in the core) by molecular diffusion and/or transport in association with pore-water colloids is limited by the hydrophobicity of these compounds and the lack of significant pore-water advection at depth.⁸³ Thus, the virtual cessation of PAH degradation, presumably in response to the onset of reducing conditions within the sediment, is the most plausible explanation for the uniformity of PAH composition in these sediments.

Historical Accumulation Rates of PAH

Using tentative assignments for the ages of different depths of this core,⁵³ one can calculate average accumulation rates of total and individual PAH on the Palos Verdes Shelf. Table 10.7 presents estimates based on such calculations. Although approximate, these estimates show that the average accumula-

Table 10.6. Pearson Correlation Matrix for PAH Concentrations in Core Sediments

Variable ^a	Fluoran	Pyrene	B[a]Anthr	Chrys/Tri	B[b]Fluoran	B[e]Pyrene	B[a]Pyrene	Perylene	DB[a,h]Anthr
Fluoran	1.000	*	*	*	*	*	*	*	*
Pyrene	.921	1.000	*	*	*	*	*	*	*
B[a]Amthr	.936	.961	1.000	*	*	*	*	*	*
Chrys/Tri	.836	.909	.897	1.000	*	*	*	*	*
B[b]Fluoran	.894	.959	.909	.898	1.000	*	*	*	*
B[e]Pyrene	.904	.950	.901	.910	.979	1.000	*	*	*
B[a]Pyrene	.842	.924	.886	.905	.967	.982	1.000	*	*
Perylene	.800	.942	.855	.849	.972	.929	.933	1.000	*
DB[a,h]Anthr	.860	.751	(.731)	(.707)	.805	.865	.828	(.695)	1.000
B[ghi]Pery	.878	.944	.924	.863	.979	.940	.931	.952	(.730)

Note: p < .001 for all values except for those in parentheses, which were p = .001.

^aCompound names given in Table 10.1.

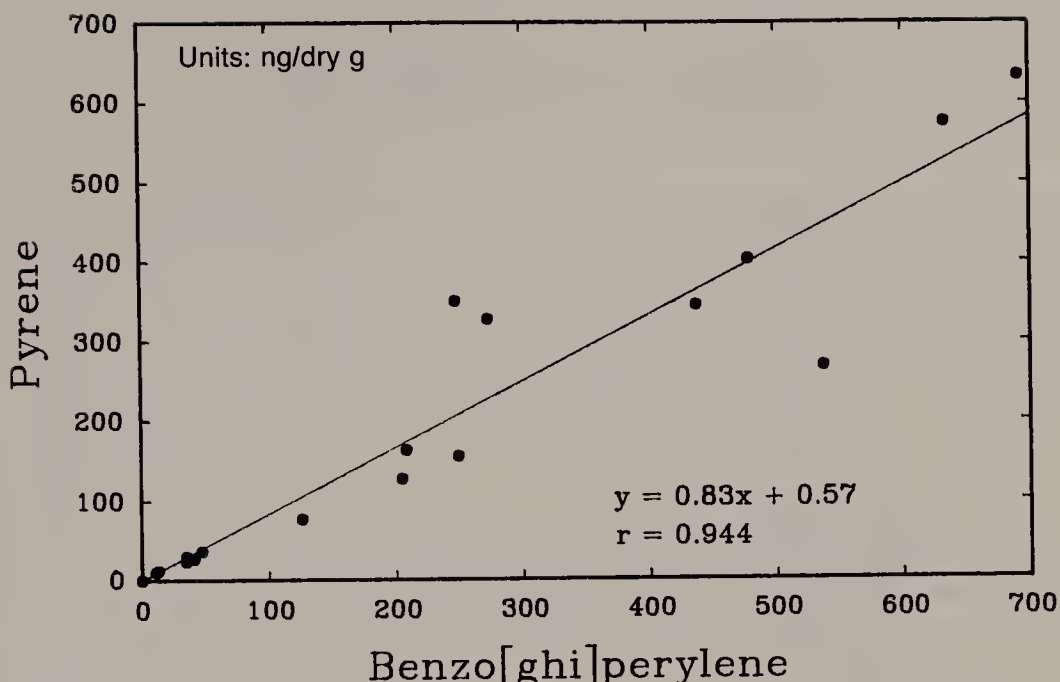


Figure 10.7. Scatter diagram of pyrene vs benzo[ghi]perylene concentration in sediments of core 3C1. Line and equation represent results of linear regression analysis.

tion rates of individual and total PAH after ca. 1950 are an order of magnitude greater than those for the pre-1950 period. Moreover, the average accumulation rates appear not to have changed significantly during the three decades subsequent to 1950. The rates determined for deep sections of the core (i.e., > 24 cm) are similar to those reported by Gschwend and Hites¹¹ for sediments near urban centers such as Boston Harbor and Buzzards Bay, MA, and by Barrick¹⁸ for a site within Central Puget Sound near the Seattle METRO wastewater outfall (Table 10.7). They are, however, at least an order of magnitude higher than those found at remote locations where sedimentary fluxes are dominated by atmospheric deposition.^{11,15} This suggests that even the deeper sections of the 3C1 core, predating 1950, may have been heavily influenced by local inputs of fossil PAH, with direct atmospheric deposition playing only a minor role.

CONCLUSIONS

The LACSD treats and discharges wastes originating from a multitude of domestic and industrial sources. To the extent that it receives an unusually large proportion of petrochemical wastes and little surface runoff, it may be considered an uncommon municipal treatment plant. These factors undoubtedly influence the composition and quantity of PAH in its effluent. We estimate that as of 1979 the LACSD discharged approximately 110 metric tons

Table 10.7. Average Accumulation Rates of PAH in Sediments at Station 3C1, 1981, and Other Sites

Depth Interval (cm)	Approximate Date Interval	Accumulation rate (ng/cm ² year)						Site
		Fluoran	Pyrene	B[a]Anthr	Chrys/Tri	B[e]Pyrene	B[a]Pyrene	
0-8	1971-81	77	273	89	172	285	274	2280 Palos V.
8-14	1962-71	65	335	76	134	316	304	2660 Palos V.
14-24	1950-62	117	283	80	124	333	276	2550 Palos V.
24-34	1937-50	18	28	8	12	25	23	228 Palos V.
Urban sites ^{a,b}	1900-present modern	37	39	19	23	14	17	- ^c Boston H. Puget Snd.
Remote sites(av.s.) ^a	present ca. 1950 ca. 1900	46	-	19	30	23	-	- Average for 5 lacustrine sites
Atmospheric deposition ^d	1980 1980	0.6 0.6	0.4 0.5	-	-	-	0.9 1.1	Sequim Quillayute

^aAfter Gschwend and Hites.¹¹^bAfter Barrick.¹⁸^cNot reported.^dAfter Prahl et al.¹⁵

PAH/year. Present indications suggest that the LACSD may have reduced emissions of PAH to the ocean by more than an order of magnitude during the period 1979–1987, mostly as a result of source control. This reinforces the effectiveness of source control measures (as opposed to treatment upgrades) in large centralized urban treatment systems.

The vast majority of the PAH in the LACSD effluent are of petroleum origin and consist of lower-molecular-weight species (2-and 3-ring PAH) and their alkylated homologues. Upon discharge to the ocean, these compounds are apparently rapidly removed such that little, if any, evidence of them are found in heavily contaminated surficial sediments 6 km downcurrent from the outfall system. The effluent particles are probably buried too rapidly for complete release/removal of the higher-molecular-weight PAH (4-, 5-, and 6-ring compounds). Nevertheless, a fraction of these compounds appears to be lost prior to incorporation into the permanent sediments. The extent of removal is directly related to (the logarithm of) their aqueous solubility. Thus, the 6-ring PAH tend to survive better than the 4-and 5-ring PAH. It is unclear whether these changes are brought about by simple physical release (desorption), microbial degradation processes or both. However, once incorporated into the sediments, the composition of the high-molecular-weight PAH does not change with time. Either they are metabolized at identical rates or not metabolized at all. Evidence from other microcosm studies suggests that under the reducing conditions that prevail below the sediment-water interface at this site, the latter hypothesis is more likely. Because the PAH in these sediments are of petroleum (rather than combustion) origin, physical occlusion (as proposed for pyrogenic PAH) should not be regarded as a unique prerequisite for preservation in the sedimentary column.

ACKNOWLEDGMENTS

The authors wish to thank K. Billingsley and M. Eganhouse for extraordinary moral support during the writing of this chapter. We also appreciate the donation of core material by the LACSD and the technical assistance of D. Blumfield. Financial support was provided, in part, by the Department of Energy, Contract No. EY-76-3-03-0034.

REFERENCES

1. Lunde, G., and A. Bjorseth. "Polycyclic Aromatic Hydrocarbons in Long-Range Transported Aerosols," *Nature* 268:518–519 (1977).
2. LaFlamme, R. E., and R. A. Hites. "The Global Distribution of Polycyclic Aromatic Hydrocarbons in Recent Sediments," *Geochim. Cosmochim. Acta* 42:289–303 (1978).
3. Boehm, P. D., and J. W. Farrington. "Aspects of the Polycyclic Aromatic Hydrocarbon Geochemistry of Recent Sediments in the Georges Bank Region," *Environ. Sci. Technol.* 18:840–845 (1984).

4. Colombo, J. C., E. Pelletier, C. Brochu, M. Khalil, and J. A. Catoggio. "Determination of Hydrocarbon Sources Using *N*-Alkane and Polyaromatic Hydrocarbon Distribution Indexes. Case Study: Rio de La Plata Estuary, Argentina," *Environ. Sci. Technol.* 23:888-894 (1989).
5. Johnson, A. C., P. F. Larsen, D. F. Gadbois, and A. W. Humason. "The Distribution of Polycyclic Aromatic Hydrocarbons in the Surficial Sediments of Penobscot Bay (Maine, USA) in Relation to Possible Sources and to Other Sites World Wide," *Mar. Environ. Res.* 15:1-16 (1985).
6. Knap, A. H., P. J. L. Williams, and E. Lysiak. "Petroleum Hydrocarbons in Sediments of Southampton Water Estuary," *Mar. Environ. Res.* 7:235-249 (1982).
7. Lake, J. L., C. Norwood, C. Dimock, and R. Bowen. "Origins of Polycyclic Aromatic Hydrocarbons in Estuarine Sediments," *Geochim. Cosmochim. Acta* 43:1847-1854 (1979).
8. Readman, J. W., R. F. C. Mantoura, M. M. Rhead, and L. Brown. "Aquatic Distribution and Heterotrophic Degradation of Polycyclic Aromatic Hydrocarbons (PAH) in the Tamar Estuary," *Est. Coastal Shelf Sci.* 14:369-389 (1982).
9. Thompson, S., and G. Eglinton. "Composition and Sources of Pollutant Hydrocarbons in the Severn Estuary," *Mar. Poll. Bull.* 9:133-136 (1978).
10. Venkatesan, M. I., S. Brenner, E. Ruth, J. Bonilla, and I. R. Kaplan. "Hydrocarbons in Age-Dated Sediment Cores from Two Basins in the Southern California Bight," *Geochim. Cosmochim. Acta* 44:789-802 (1980).
11. Gschwend, P. M., and R. A. Hites. "Fluxes of Polycyclic Aromatic Hydrocarbons to Marine and Lacustrine Sediments in the Northeastern United States," *Geochim. Cosmochim. Acta* 45:2359-2367 (1981).
12. Pruell, R. J., and J. G. Quinn. "Geochemistry of Organic Contaminants in Narragansett Bay Sediments," *Est. Coastal Shelf Sci.* 21:295-312 (1985).
13. Shiaris, M. P., and D. Jambard-Sweet. "Polycyclic Aromatic Hydrocarbons in Surficial Sediments of Boston Harbour, Massachusetts, USA," *Mar. Poll. Bull.* 17:469-472 (1986).
14. Windsor, J. G., Jr., and R. A. Hites. "Polycyclic Aromatic Hydrocarbons in Gulf of Maine Sediments and Nova Scotia Soils," *Geochim. Cosmochim. Acta* 43:27-33 (1979).
15. Prahl, F. G., E. Crecelius, and R. Carpenter. "Polycyclic Aromatic Hydrocarbons in Washington Coastal Sediments: An Evaluation of Atmospheric and Riverine Routes of Introduction," *Environ. Sci. Technol.* 18:687-693 (1984).
16. Eganhouse, R. P., B. R. T. Simoneit, and I. R. Kaplan. "Extractable Organic Matter in Urban Stormwater Runoff: 2. Molecular Characterization," *Environ. Sci. Technol.* 15:315-326 (1981).
17. Hoffman, E. J., G. L. Mills, J. S. Latimer, and J. G. Quinn. "Urban Runoff as a Source of Polycyclic Aromatic Hydrocarbons to Coastal Waters," *Environ. Sci. Technol.* 18:580-587 (1984).
18. Barrick, R. C. "Flux of Aliphatic and Polycyclic Aromatic Hydrocarbons to Central Puget Sound from Seattle (Westpoint) Primary Sewage Effluent," *Environ. Sci. Technol.* 16:682-692 (1982).
19. Eganhouse, R. P., and I. R. Kaplan. "Extractable Organic Matter in Municipal Wastewaters: 2. Hydrocarbons: Molecular Characterization," *Environ. Sci. Technol.* 16:541-551 (1982).
20. Bieri, R. H., C. Hein, R. J. Huggett, P. Shou, H. Slone, C. Smith, and C.-W. Su.

- "Polycyclic Aromatic Hydrocarbons in Surface Sediments from the Elizabeth River Subestuary," *Int. J. Environ. Anal. Chem.* 26:97-113 (1986).
21. Merrill, E. G., and T. L. Wade. "Carbonized Coal Products as a Source of Aromatic Hydrocarbons to Sediments from a Highly Industrialized Estuary," *Environ. Sci. Technol.* 19:597-603 (1985).
 22. Bjorseth, A., J. Knutzen, and J. Skei. "Determination of Polycyclic Aromatic Hydrocarbons in Sediments and Mussels from Saudafjord, W. Norway, by Glass Capillary Gas Chromatography," *Sci. Total Environ.* 13:71-86 (1979).
 23. Teal, J. M., K. Burns, and J. Farrington. "Analyses of Aromatic Hydrocarbons in Intertidal Sediments Resulting from Two Spills of No. 2 Fuel Oil in Buzzards Bay, Massachusetts," *J. Fish. Res. Bd. Can.* 35:510-520 (1978).
 24. Reed, W. E., and I. R. Kaplan. "The Chemistry of Marine Petroleum Seeps," *J. Geochem. Explor.* 7:255-293 (1977).
 25. Stuermer, D. H., R. B. Spies, P. H. Davis, D. J. Ng, C. J. Morris, and S. Neal. "The Hydrocarbons in the Isla Vista Marine Seep Environment," *Mar. Chem.* 11:413-426 (1982).
 26. Rowland, S. J., and J. R. Maxwell. "Reworked Triterpenoid and Steroid Hydrocarbons in a Recent Sediment," *Geochim. Cosmochim. Acta* 48:617-624 (1984).
 27. Eganhouse, R. P., and M. I. Venkatesan. "Chemical Oceanography and Geochemistry," in *Ecology of the Southern California Bight* (in preparation), Chapter 3.
 28. John, E. D., M. Cooke, and G. Nickless. "Polycyclic Aromatic Hydrocarbons in Sediments Taken from the Severn Estuary Drainage System," *Bull. Environ. Contam. Toxicol.* 22:653-659 (1979).
 29. Tripp, B. W., J. W. Farrington, and J. M. Teal. "Unburned Coal as a Source of Hydrocarbons in Surface Sediments," *Mar. Poll. Bull.* 12:122-126 (1981).
 30. White, C. M., and M. L. Lee. "Identification and Geochemical Significance of Some Aromatic Components of Coal," *Geochim. Cosmochim. Acta* 44:1825-1832 (1980).
 31. Simoneit, B. R. T. "Diterpenoid Compounds and Other Lipids in Deep-Sea Sediments and Their Geochemical Significance," *Geochim. Cosmochim. Acta* 41:463-476 (1977).
 32. Venkatesan, M. I. "Occurrence and Possible Sources of Perylene in Marine Sediments - A Review," *Mar. Chem.* 25:1-27 (1988).
 33. Chaffee, A. L., and R. B. Johns. "Polycyclic Aromatic Hydrocarbons in Australian Coal: I. Angularly Fused Pentacyclic Tri-and Tetraaromatic Components of Victorian Brown Coal," *Geochim. Cosmochim. Acta* 47:2141-2155 (1983).
 34. Tan, Y. L., and M. Heit. "Biogenic and Abiogenic Polynuclear Aromatic Hydrocarbons in Sediments from Two Remote Adirondack Lakes," *Geochim. Cosmochim. Acta* 45:2267-2279 (1981).
 35. Wakeham, S. G., C. Schaffner, and W. Giger. "Polycyclic Aromatic Hydrocarbons in Recent Lake Sediments: II. Compounds Derived from Biogenic Precursors during Early Diagenesis," *Geochim. Cosmochim. Acta* 44:415-429 (1980).
 36. Blumer, M., and W. W. Youngblood. "Polycyclic Aromatic Hydrocarbons in Soils and Recent Sediments," *Science* 188:53-55 (1975).
 37. Larsen, P. F., D. F. Gadbois, and A. C. Johnson. "Polycyclic Aromatic Hydrocarbons in Gulf of Maine Sediments: Distributions and Mode of Transport," *Mar. Environ. Res.* 18:231-244 (1986).
 38. Venkatesan, M. I., E. Ruth, S. Steinberg, and I. R. Kaplan. "Organic Geochemis-

- try of Sediments from the Continental Margin off Southern New England, U.S.A.: Part II. Lipids," *Mar. Chem.* 21:267-299 (1987).
39. Herbes, S. E. "Rates of Microbial Transformation of Polycyclic Aromatic Hydrocarbons in Water and Sediments in the Vicinity of a Coal-Coking Wastewater Discharge," *Appl. Environ. Microbiol.* 41:20-28 (1981).
40. Jones, D. M., S. J. Rowland, A. G. Douglas, and S. Howells. "An Examination of the Fate of Nigerian Crude Oil in Surface Sediments of the Humber Estuary by Gas Chromatography and Gas Chromatography-Mass Spectrometry," *Int. J. Environ. Anal. Chem.* 24:227-247 (1986).
41. Pruell, R. J., and J. G. Quinn. "Polycyclic Aromatic Hydrocarbons in Surface Sediments Held in Experimental Mesocosms," *Toxicol. Environ. Chem.* 10:183-200 (1985).
42. Prahl, F. G., and R. Carpenter. "Polycyclic Aromatic Hydrocarbon (PAH) Phase Associations in Washington Coastal Sediment," *Geochim. Cosmochim. Acta* 47:1013-1023 (1983).
43. Readman, J. W., R. F. C. Mantoura, and M. M. Rhead. "The Physico-Chemical Speciation of Polycyclic Aromatic Hydrocarbons (PAH) in Aquatic Systems," *Fres. Z. Anal. Chem.* 319:126-131 (1984).
44. Readman, J. W., R. F. C. Mantoura, and M. M. Rhead. "A Record of Polycyclic Aromatic Hydrocarbon (PAH) Pollution Obtained from Accreting Sediments of the Tamar Estuary, U.K.: Evidence for Non-Equilibrium Behaviour of PAH," *Sci. Total Environ.* 66:73-94 (1987).
45. Socha, S. B., and R. Carpenter. "Factors Affecting Pore Water Hydrocarbon Concentrations in Puget Sound Sediments," *Geochim. Cosmochim. Acta* 51:1273-1284 (1987).
46. Grimmer, G., and H. Böhnke. "Profile Analysis of Polycyclic Aromatic Hydrocarbons and Metal Content in Sediment Layers of a Lake," *Cancer Lett.* 1:75-84 (1975).
47. Wakeham, S. G., C. Schaffner, and W. Giger. "Polycyclic Aromatic Hydrocarbons in Recent Lake Sediments: I. Compounds Having Anthropogenic Origins," *Geochim. Cosmochim. Acta* 44:403-413 (1980).
48. Hites, R. A., R. E. Laflamme, and J. W. Farrington. "Sedimentary Polycyclic Aromatic Hydrocarbons: The Historical Record," *Science* 198:829-831 (1977).
49. Ohta, K., N. Hand, and E. Matsumoto. "Trends and Factors Governing Polycyclic Aromatic Hydrocarbon Levels in Tokyo Bay Sediments," *Geochim. Cosmochim. Acta* 47:1651-1654 (1983).
50. Grzybowski, J., A. Radecki, and G. Rewkowska. "Isolation, Identification, and Determination of Polycyclic Aromatic Hydrocarbons in Sewage," *Environ. Sci. Technol.* 17:44-47 (1983).
51. Eganhouse, R. P. "Organic Matter in Municipal Wastes and Storm Runoff: Characterization and Budget to the Coastal Wastes of Southern California," PhD Thesis, University of California, Los Angeles, CA (1982).
52. Eganhouse, R. P., and I. R. Kaplan. "Extractable Organic Matter in Municipal Wastewaters. 1. Petroleum Hydrocarbons: Temporal Variations and Mass Emission Rates to the Ocean," *Environ. Sci. Technol.* 16:180-186 (1982).
53. Eganhouse, R. P., and I. R. Kaplan. "Depositional History of Recent Sediments from San Pedro Shelf, California: Reconstruction Using Elemental Abundance, Isotopic Composition and Molecular Markers," *Mar. Chem.* 24:163-191 (1988).
54. Stull, J. K., R. B. Baird, and T. C. Heesen. "Marine Sediment Core Profiles of

- Trace Constituents Offshore of a Deep Wastewater Outfall," *J. Water Poll. Control Fed.* 58:985-991 (1986).
55. Eganhouse, R. P., D. L. Blumfield, and I. R. Kaplan. "Long-Chain Alkylbenzenes as Molecular Tracers of Domestic Wastes in the Marine Environment," *Environ. Sci. Technol.* 17:523-530 (1983).
56. Anderson, J. W., and R. W. Gossett. "Polynuclear Aromatic Hydrocarbon Contamination in Sediments from Coastal Waters of Southern California," report to California State Water Resources Control Board (1987).
57. Baird, R., L. Neisess, and J. P. Gute. "Characterization of Toxic Organic Constituents in POTW Discharges," LACSD report to California State Water Resources Control Board (1987).
58. Lee, M. L., G. P. Prado, J. B. Howard, and R. A. Hites. "Source Identification of Urban Airborne Polycyclic Aromatic Hydrocarbons by Gas Chromatographic Mass Spectrometry and High Resolution Mass Spectrometry," *Biomed. Mass Spectrom.* 4:182-186 (1977).
59. Sportsøl, S., N. Gjøs, R. G. Lichtenthaler, K. O. Gustavsen, K. Urdal, F. Oreld, and J. Skei. "Source Identification of Aromatic Hydrocarbons in Sediments Using GC/MS," *Environ. Sci. Technol.* 17:282-286 (1983).
60. Cautreels, W., and K. Van Cauwenbergh. "Determination of Organic Compounds in Airborne Particulate Matter by Gas Chromatography-Mass Spectrometry," *Atmos. Environ.* 10:447-457 (1976).
61. Harrison, R. M., R. Perry, and R. A. Wellings. "Polynuclear Aromatic Hydrocarbons in Raw, Potable and Waste Waters," *Water Res.* 9:331-346 (1975).
62. Neff, J. M. *Polycyclic Aromatic Hydrocarbons in the Aquatic Environment: Sources, Fates and Biological Effects* (London: Applied Science Publishers, 1979).
63. Nellor, M. LACSD Industrial Waste Section, personal communication.
64. Platt, H. M., and P. R. Mackie. "Analysis of Aliphatic and Aromatic Hydrocarbons in Antarctic Marine Sediment Layers," *Nature* 280:576-577 (1979).
65. Stull, J. K., and C. I. Haydock. "Wastewater Discharges and Environmental Responses: The Palos Verdes Case," in *Proceedings of the Symposium, Managing Inflows to California's Bays and Estuaries* (Sausalito, CA: The Bay Institute, 1986), pp. 44-49.
66. Swartz, R. C., D. W. Schults, G. R. Ditsworth, W. A. DeBen, and F. A. Cole. "Sediment Toxicity, Contamination, and Macrofaunal Communities near a Large Sewage Outfall," in *ASTM STP 865* (Philadelphia, PA: American Society for Testing and Materials, 1985), pp. 152-175.
67. Kettenring, K. N. "The Trace Metal Stratigraphy and Recent Sedimentary History of Anthropogenic Particulates on the San Pedro Shelf, California," PhD Thesis, University of California, Los Angeles, CA (1981).
68. Simoneit, B. R. T., and I. R. Kaplan. "Triterpenoids as Molecular Indicators of Paleoseepage in Recent Sediments of the Southern California Bight," *Mar. Environ. Res.* 3:113-128 (1980).
69. Hartman, B., and D. E. Hammond. "The Use of Carbon and Sulfur Isotopes as Correlation Parameters for the Source Identification of Beach Tar in the Southern California Borderland," *Geochim. Cosmochim. Acta* 45:309-319 (1981).
70. Myers, E. P. "The Concentration and Isotopic Composition of Carbon in Marine Sediments Affected by a Sewage Discharge," PhD Thesis, California Institute of Technology, Pasadena, CA (1974).

71. Eganhouse, R. P., and J. C. Calder. "The Solubility of Medium Molecular Weight Aromatic Hydrocarbons and the Effects of Hydrocarbon Co-Solutes and Salinity," *Geochim. Cosmochim. Acta* 40:555-561 (1976).
72. Karickhoff, S. W. "Sorption Kinetics of Hydrophobic Pollutants in Natural Sediments," in *Contaminants and Sediments*, Vol. 2, R. A. Baker, Ed. (Ann Arbor, MI: Ann Arbor Science, 1980), p. 193-205.
73. Karickhoff, S. W., and K. R. Morris. "Sorption Dynamics of Hydrophobic Pollutants in Sediment Suspensions," *Environ. Toxicol. Chem.* 4:469-479 (1985).
74. Wu, S.-C., and P. M. Gschwend. "Sorption Kinetics of Hydrophobic Organic Compounds to Natural Sediments and Soils," *Environ. Sci. Technol.* 20:717-725.
75. Brusseau, M. L., and P. S. C. Rao. "The Influence of Sorbate-Organic Matter Interactions on Sorption Nonequilibrium," *Chemosphere* 18:1691-1706 (1989).
76. Lee, R. F., W. S. Gardner, J. W. Anderson, J. W. Blaylock, and J. Barwell-Clarke. "Fate of Polycyclic Aromatic Hydrocarbons in Controlled Ecosystem Enclosures," *Environ. Sci. Technol.* 12:832-838 (1978).
77. Farrington, J. W., B. W. Tripp, J. M. Teal, G. Mille, K. Tjessem, A. C. Davis, J. B. Livramento, N. A. Hayward, and N. M. Frew. "Biogeochemistry of Aromatic Hydrocarbons in the Benthos of Microcosms," *Toxicol. Environ. Chem.* 5:331-346 (1982).
78. Hinga, K. R., M. E. Q. Pilson, G. Almquist, and R. F. Lee. "The Degradation of 7,12-Dimethylbenz[a]anthracene in an Enclosed Marine Ecosystem," *Mar. Environ. Res.* 18:79-91 (1986).
79. Hinga, K. R., M. E. Q. Pilson, R. F. Lee, J. W. Farrington, K. Tjessem, and A. C. Davis. "Biogeochemistry of Benzanthracene in an Enclosed Marine Ecosystem," *Environ. Sci. Technol.* 14:1136-1143 (1980).
80. Gardner, W. S., R. F. Lee, K. R. Tenore, and L. W. Smith. "Degradation of Selected Polycyclic Aromatic Hydrocarbons in Coastal Sediments: Importance of Microbes and Polychaete Worms," *Water Air Soil Poll.* 11:339-347 (1979).
81. Hambrick, G. A., III, R. D. DeLaune, and W. H. Patrick, Jr. "Effect of Estuarine Sediment pH and Oxidation-Reduction Potential on Microbial Hydrocarbon Degradation," *Appl. Environ. Microbiol.* 40:365-369 (1980).
82. Stull, J. K., C. I. Haydock, and D. E. Montagne. "Effects of *Listriolobus pelodes* (Echiura) on Coastal Shelf Benthic Communities and Sediments Modified by a Major California Wastewater Discharge," *Est. Coastal Shelf Sci.* 22:1-17 (1986).
83. Brownawell, B. J., and J. W. Farrington. "Biogeochemistry of PCBs in Interstitial Waters of a Coastal Marine Sediment," *Geochim. Cosmochim. Acta* 50:157-169.

CHAPTER 11

The Distribution of PCBs in Surface Sediments of Narragansett Bay, Rhode Island

James S. Latimer, Lawrence A. LeBlanc, John T. Ellis, and James G. Quinn

INTRODUCTION

Particle-Associated Pollutant Transport Processes

Sediments are an important sink for many pollutants in the marine environment. Present-day sediments are derived from the erosion of materials in the watersheds and washed through the rivers and estuaries. In addition to the natural weathering of continental rock, the activities of humans have added to the loads contained in rivers. The suspended solids that are transported in the rivers are not, in many cases, simply mineral particles, but are particles that have been coated with the breakdown products of natural organics, commonly known as humic materials.¹ This organic coating is very effective at adsorbing or partitioning anthropogenic contaminants such as polychlorinated biphenyls (PCBs) and other thermodynamically stable hydrophobic organic compounds (HOCs).² The concentrations of these contaminants on the particles are dependent upon the nature of the particle itself (for example, the organic carbon content [humic material coating], size, and mineral type) and the chemical nature of the sorbed compound (for example, its octanol-water partition coefficient). In Narragansett Bay, PCBs have been observed, primarily, in the particulate fraction of water samples, although they have been found in the soluble phase of some tributary samples.³

Primary productivity and the consequent secondary productivity (i.e., both living and dead material) add to the suspended matter derived from sediment erosion and from the activities of humans. With the sun as the source of energy, phytoplankton, using the dissolved inorganic carbon and dissolved nutrients in the water, periodically build up large concentrations of organic particulates. Subsequently, zooplankton populations increase, thus forming the first layer of the food web. The rapid increase in biomass may alter the balance of a hydrophobic substance among the dissolved, colloidal, and particulate phases. The process of bioconcentration involves the taking of sub-

stances out of solution by direct partitioning into the fatty portions of the organism.⁴ That which is not retained is excreted—sometimes in a degraded state—back into the particulate pool, in the form of fecal pellets. Fluid excretions would be subject to adsorption and partitioning processes that eventually lead to particulate forms. Alternately, colloidal materials in the water, including humic substances, serve to keep hydrophobic contaminants from sorbing to larger particles, causing them to remain in a semidissolved state.

A fraction of the total amount of suspended solids and associated organic contaminants will settle to the sediment-water interface, depending on the size, shape, and chemical properties of the particles. The interface layer is a dynamic area, in which resuspension takes place. This boundary layer may be divided into a region of very turbid water just above the actual sediment bed and a region encompassing the upper portion of the bed itself. The first section has been termed the *benthic nepheloid layer* (BNL); the second, the active sediment layer.⁵ Under the active sediment layer, which may be from 1 to 10 cm in depth, are the permanently buried sediments. The BNL is formed in areas where the energy of the system, expressed as surface turbulence in the case of shallow systems, or as internal waves or currents in the deeper systems, is high enough to lift particles of varying diameters into the water column. Once resuspended, they may be transported to areas of less energy. The cause and the results of turbulence are generally characteristic of the system itself—for example, the season of the year, the prevailing wind-induced circulation, the velocity of currents, the geometry of the basin, and even the size, density, and chemical characteristics of the suspended solids and the water column chemistry itself. Thus, there will be locations where the resuspended sediments tend to accumulate; these areas will include topographic depressions and mixing zones between fresh-and saltwater. In areas where the Coriolis force steers currents into wide, more quiescent locations, the suspended load will also be deposited. The result of this action is sediment focusing, which can be observed with seismic reflection instrumentation. Reflection profiles indicate lenses of fine-grained sediment in some areas, while other areas are completely barren.

The heterogeneity of the benthic environment, with respect to depth, extent, and location of sediment lenses, complicates the estimation of pollutant mass reservoirs associated with the sediments. The accumulation patterns of recent fine-grained sediments (i.e., those with large surface areas and high levels of organic matter) have been found to be the controlling factor in the distribution of PCBs in the Hudson-Raritan estuary system.⁶ The areas that trap fine-grained sediments and the associated contaminants serve to focus and magnify them from considerably larger regions. In the Hudson-Raritan region, sheltered environments such as harbors, dredged channels, and certain bays may have sediment deposition rates that are orders of magnitude greater (1–70 cm/year) than the rates in adjacent, more open locales (1–3 mm/year).⁶ These more quiescent environments contain and trap the bulk of the particulate PCB contamination, although dissolved and colloidally bound constituents may

leave the estuary. If sediments were homogeneously distributed throughout an area, geochemists would only need to estimate the contaminant concentration and multiply by the area and depth of the sediments to gain an understanding of the magnitude of the pollutant reservoir. However, in most cases, detailed seismic profiling with resolutions on the order of a few meters is necessary, along with adequate pollutant concentration data, to accurately quantify the extent of anthropogenic contamination.

In contrast to sediment focusing, which can be thought of as an advective force transporting sediments horizontally, bioturbation, which can also be occurring in the active sediment zone, can be thought of as a vertical force, causing deeper deposits to be transported to the surface, making them available for resuspension.^{5,7} Organisms such as benthic worms and certain bivalve mollusks, by their dietary activities, serve to bring up sediments from below, either through their gut (conveyer-belt type) or by their movements. This causes the deeper sediments to be mixed with the surficial deposits and vice versa. This activity will tend to homogenize the sediments.

Another process operating in the sediments is partitioning. Since the sediments contain pore waters which usually have extremely high concentrations of dissolved organic matter, the partitioning of a contaminant among the dissolved, colloidal, and particulate phases may be altered in such a way as to cause HOCs to act as dissolved constituents. For example, very high concentrations of dissolved PCBs have been observed in the pore waters of sediments.^{8,9} Changes in the partitioning of contaminants may begin to occur in the BNL because of the phenomenon associated with the very high suspended solids concentrations, which have been shown to cause shifts in the partitioning of sorbed species.¹⁰ Although the mechanism for this "solids effect" has not been definitively determined, these changes may be due to the interactions of the various phases in the water column and on the solids.

General Information and Geographic Area of Interest

PCBs are particularly susceptible to the processes outlined above since they are hydrophobic, resistant to degradation, and ubiquitous in the aquatic environment. These compounds, marketed by the Monsanto Chemical Company under the trade name Aroclor, were produced from 1930 to 1977. Their primary use was in the electrical industry, particularly in transformers and capacitors.^{11,12} Much of the original electrical equipment is still in use today, since only the manufacture, and not the use, of PCBs was banned by the EPA in 1979. The production and sales records of PCBs are not as important as the uses they had in the marketplace with respect to their impact on the near-shore marine environment. While U.S. PCB production ended in 1976, it has been estimated that, as of January 1988, 690 million kg (31% of total produced) of PCBs are still in use, in millions of pieces of electrical equipment throughout the country, and that it will be 20 or 30 years before all PCBs still in use are disposed of or destroyed.¹³ On a worldwide basis, it has been estimated that

65% of the PCBs produced are still in use in electrical equipment and other products and are in landfills and dumps.¹⁴ The U.S. mobile environmental reservoir (MER)—that which is available for environmental redistribution on land—has been estimated to be 10% of the total amount produced since 1930, or approximately 53 million kg.^{15,16} On a worldwide basis, the MER (terrestrial and coastal: river + lake + sediment + biota) has been estimated to be 12% of the total PCB production, or approximately 140 million kg.¹⁴ Thus, even though the production has ceased, the amount affecting the ecosystems is still substantial.

Narragansett Bay sediments have been well studied for a variety of contaminants, including petroleum hydrocarbons,¹⁷⁻¹⁹ and polycyclic aromatic hydrocarbons.¹⁹ There is some information on PCBs in the bay, but these studies were limited in scope and dated.^{17,20-22} The purpose of the present study is to examine, in greater detail, the distribution of PCBs in surface sediments in order to assess the degree of contamination and to evaluate recent inputs to the bay.

METHODS

Sampling

The spatial distribution of PCBs was assessed by their determination in 26 surface sediment sites (top 0.5 cm, collected in 1985 and 1986) from throughout Narragansett Bay.²³ The sediments were diver collected along a transect from the upper Providence River to the mouth of the bay, including both an eastern and western branch, in order to give the widest spatial network for the evaluation of PCBs to date (Figure 11.1). Ancillary data on total organic carbon (TOC) content as well as other parameters were determined in order to better characterize geochemical interactions and aid in the evaluation of the data (Quinn, unpublished data).²³ Once collected, the surface sediment samples were placed in solvent-cleaned jars and frozen at -20°C until analysis.

Extraction

An aliquot each of thawed sediment was removed for water content determination, TOC analysis, and organic component analysis. Usually, a sample of sediment (equivalent to 1–10 g dry weight) was placed into a round-bottom flask for the organic determinations. Many different types of organics were determined in the sediments, including total organic carbon (loss on ignition, 450°C),²³ petroleum hydrocarbons, polycyclic aromatic hydrocarbons (Quinn, unpublished data), phthalates,²³ coprostanol,²³ and substituted benzotriazoles.^{3,23} The specific analytical methods for these compounds were analogous to that of the analysis of PCBs, namely, extraction, partitioning, chemi-

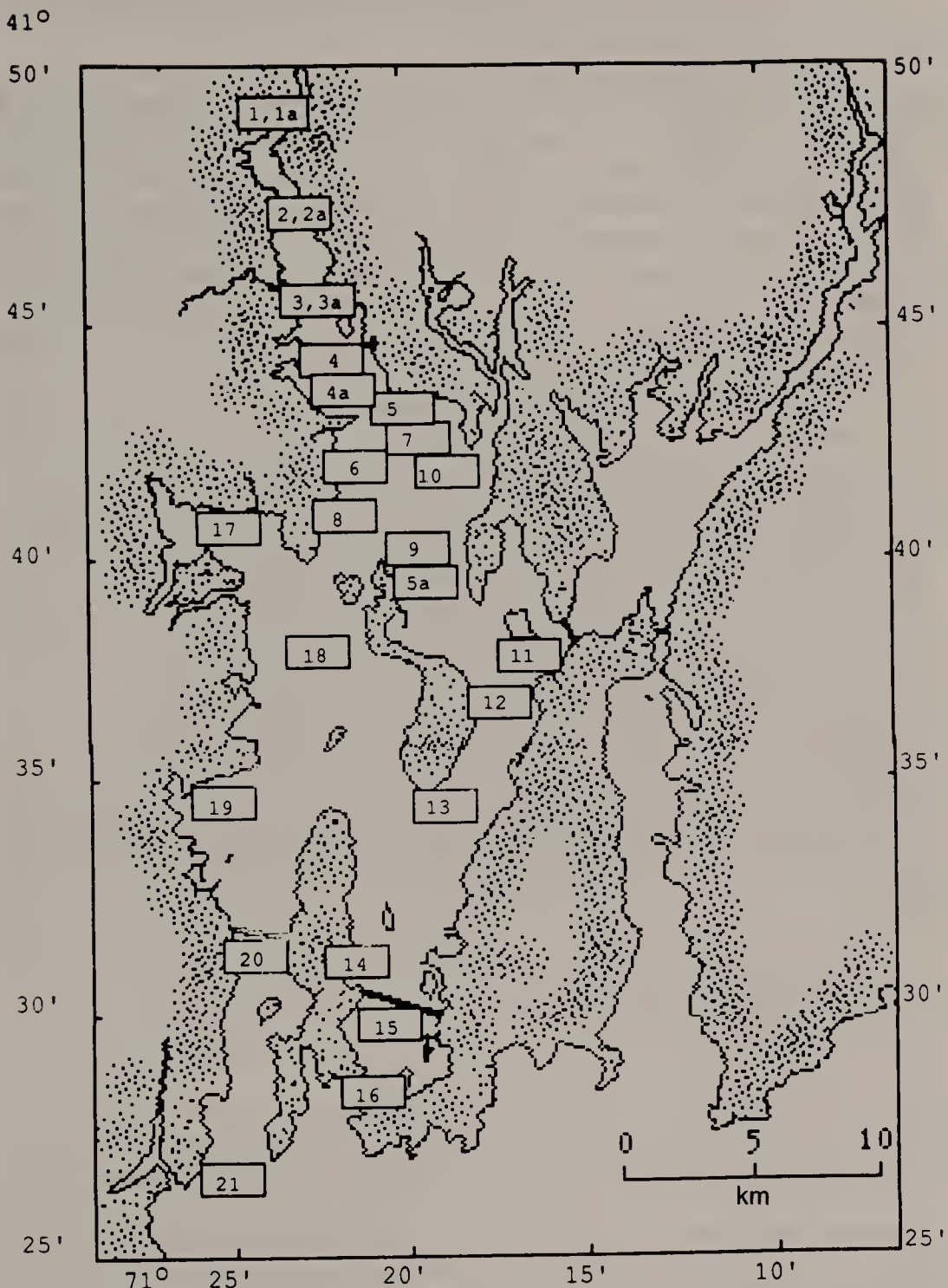


Figure 11.1. Surface sediment stations occupied during sample collection. When two numbers are reported, the second is labeled with a letter and represents samples collected one year later; for example, station 1 (1985); station 1a (1986).

cal fractionation, and gas chromatographic (GC) quantification, and details of these procedures can be found elsewhere.^{23,24}

The specific methodology used for the PCB analysis will be outlined. Initially, octachloronaphthalene (OCN), used as an internal standard, was added to the thawed sediment, followed by 100–200 mL of methanol. The slurry was then extracted, under reflux conditions, for 2 hr. Once refluxed, the PCBs associated with the methanol extract were partitioned against three successive hexane volumes (where hexane accounted for 10% of total methanol volume, or about 10–20 mL each). The isolated hexane layers were combined into another flask and reduced to a small volume (~1 mL) using vacuum rotary evaporation at room temperature (< 30°C). This hexane extract, containing PCBs and other neutral organics isolated from the sediment, was then fractionated using silica gel column chromatography. A 0.5 × 10 cm pasteur pipet filled with ~2 g of fully activated 200–325 mesh silica gel (Grace Grade 922) was used for the separation of PCBs from other organics during this step of the procedure. The hexane extract was charged onto the prepared column and the PCBs were eluted using a solution of 80:20 (hexane:methylene chloride) at a solvent flow rate of ~5 mL/min (facilitated with N₂ pressure). Under certain circumstances the extracts were eluted with a 98:2 solvent preparation in order to more fully remove interfering components from the PCBs. In addition, activated copper powder was routinely utilized, in the column chromatography step, to remove interfering inorganic sulfur from the extracts.

The PCB fraction derived from column chromatography was reduced to an appropriate volume (usually from 100–500 μL), and a 1 μL aliquot was injected into a Hewlett Packard 5710A gas chromatograph utilizing a high-resolution nonpolar phase fused silica capillary column (30 m, DB-5, J & W Scientific) and electron capture detection (⁶³Ni). The conditions of GC analysis were

- initial temperature, 100°C
- program rate, 8°C/min
- final temperature, 290°C
- final hold time, 8–32 min

The splitless injection port and detector temperatures were maintained at 300°C, and the carrier flow (He) was about 1.5 mL/min. Quantification was afforded by using response factors determined for OCN and standards of Aroclor mixtures and 10 chlorobiphenyl congeners obtained from the EPA chemical repository in North Carolina and the National Research Board of Canada. The PCB compounds determined in the study were three Aroclor formulations: Ar 1242, Ar 1254, Ar 1260; and ten individual chlorobiphenyl congeners (CB): CB101, CB151, CB153, CB138, CB180, CB170, CB201, CB195, CB194, CB209. Structural and chemical information for these compounds can be found in Table 11.1; further information can be obtained elsewhere.^{3,25}

This particular set of compounds was selected out of a possible 209 individ-

Table 11.1. PCB Compounds Evaluated in the Narragansett Bay Studies

Structure-(IUPAC No.)	Congener wt% ^a		
	Ar 1242	Ar 1254	Ar 1260
2,2',4,5,5'-(CB101)	<0.5	11.32	4.47
2,2',3,5,5',6-(CB151)	<0.5	<0.5	1.56
2,2',4,4',5,5'-(CB153)	<0.5	8.14	<0.5
2,2',3,4,4',5'- (CB138)	<0.5	9.49	11.68
2,2',3,4,4',5,5'-(CB180)	<0.5	<0.5	14.45
2,2',3,3',4,4',5-(CB170)	<0.5	<0.5	3.80
2,2',3,3',4,5',6,6'-(CB201)	<0.5	<0.5	1.50
2,2',3,3',4,4',5,6-(CB195)	<0.5	<0.5	<0.5
2,2',3,3',4,4',5,5'-(CB194)	<0.5	<0.5	0.83
2,2',3,3',4,4',5,5',6,6'-(CB209)	<0.5	<0.5	<0.5
Total wt %	<0.5	28.95	38.29

^aFrom Capel et al.⁴²

ual chlorobiphenyl congeners because of their association with the Aroclor formulations typically observed in Narragansett Bay and because they exhibit a wide range of chemical properties. It must be noted, however, that because the potential for coeluting congeners exists, their identification in the samples is considered tentative. A typical chromatogram of a sediment extract determined in Narragansett Bay is shown in Figure 11.2. It can be seen that a large number of peaks comprise the PCB fraction; those peaks labeled with numbers correspond to the congeners noted above. The peaks labeled with letters are those utilized for quantification of the PCBs as Aroclor equivalents; the details of the quantification can be found elsewhere.³ A comprehensive quality assurance/quality control program was used, including blank determinations, recovery experiments, and intercalibration analyses.³ Analytical determinations of blanks revealed undetectable levels of PCBs (i.e., < 1.0 ng Aroclor/g dry weight and < 0.05 ng congener/g dry weight). Recoveries of PCBs through the analytical protocol were from 73 to 112%. Precision, estimated by multiple extraction and analyses of the same sediment sample, was found to be usually within 10% of the mean. Accuracy, as determined from intercalibration and spiked samples, was typically found to be within 10% of the accepted values.

RESULTS AND DISCUSSION

Overall Concentration Levels

The concentration of total PCBs (i.e., Ar 1242 + Ar 1254 + Ar 1260) observed in the surface sediments of Narragansett Bay averaged 390 ng/g dry weight with a wide degree of spatial variability (range: 8–2410 ng/g). These values were similar to those observed in other estuaries that have industrial and municipal activity (Table 11.2). For example, Raritan Bay, Puget Sound, and Narragansett Bay all had values in the 300 to 500 ng/g range (Table 11.2).

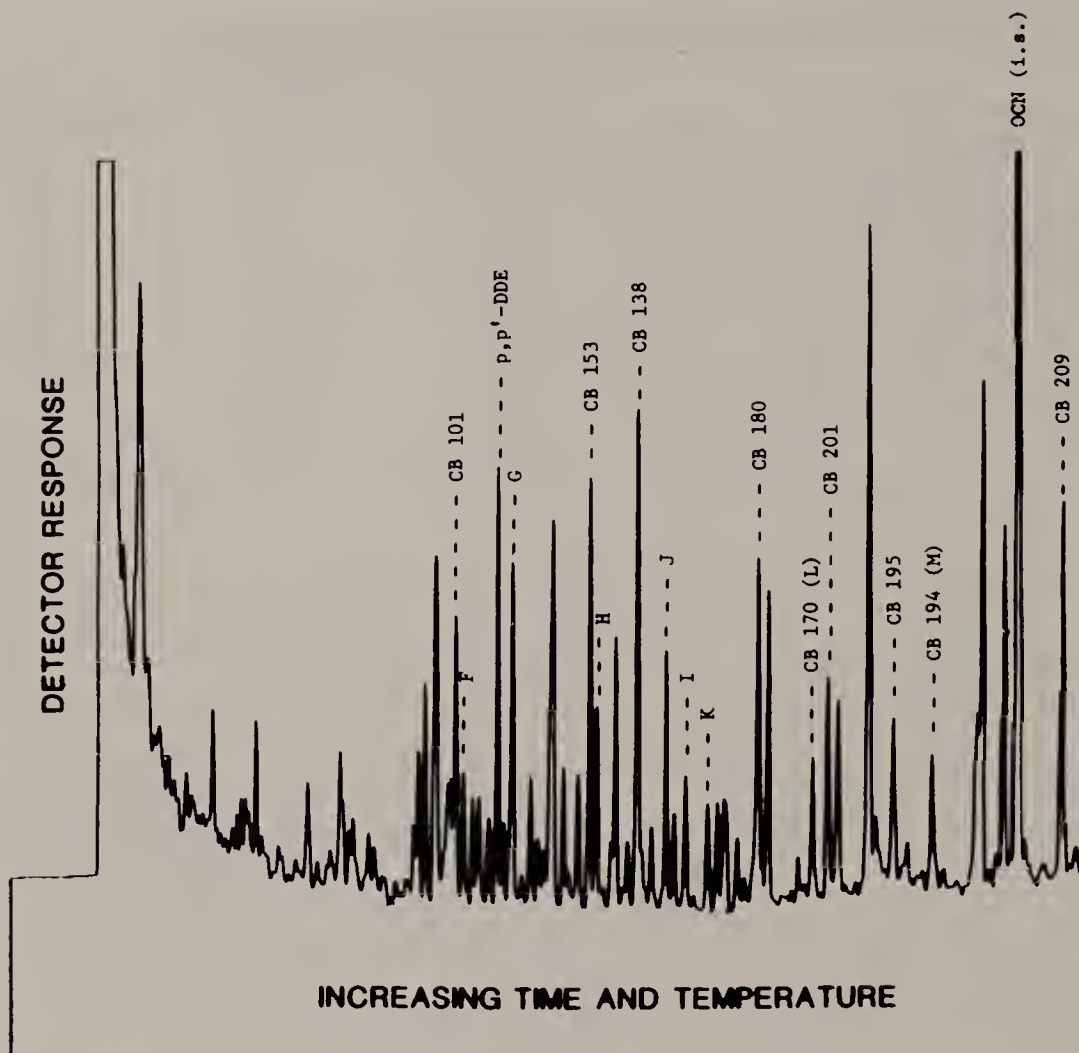


Figure 11.2. Chromatogram of a Narragansett Bay surface sediment extract using a high-resolution capillary column. See text for explanation of chlorobiphenyl (CB) designations. The letters F through M are used to calculate the Ar 1254 and Ar 1260 concentrations in the samples.

However, concentrations determined in the present study were significantly lower than in those areas that have been considered to be PCB "hot spots," that is, the Hudson River and New Bedford Harbor areas (e.g., concentrations greater than 3000 ng/g dry weight; Table 11.2).

Concentrations determined on suspended solids derived from rivers and municipal point sources in Narragansett Bay³ were found to exhibit mean values higher than those of the sediments (Table 11.3). For example, concentrations on the particles from the river and the wastewater inputs (1130 ± 333 and 862 ± 516 ng Ar 1254/g dry weight, respectively) were statistically greater ($P < 0.05$, Student's t-test) than the mean value for the surface sediments in the general vicinity (Providence River and upper bay: 376 ± 393 ng Ar 1254/g).

Table 11.2. The Concentrations of Total PCBs in Estuarine Surface Sediments from Different Regions

Location	Date	ng/g dry					
		Min.	Max.	Mean	SD	Notes	Reference
Tidal Hudson							
km 225-240	1981	1,600	140,000	30,000	—	Ar 1242	6
km 130-180	1981	4,100	29,000	10,000	—	Ar 1242	6
km 64-80	1981	500	26,000	6,000	—	Ar 1242	6
km 3-10	1981	700	5,800	3,000	—	Ar 1242	6
Raritan Bay	1981	40	1,400	400	—	Ar 1242	6
L.I. Sound	1984	<1	380	143	—	not spec.	43
Puget Sound	1981	33	1,630	500	579	not spec.	44
N. Bedford H.	< 1984	1,000	~10%w/w	—	—	not spec.	45
Chesapeake Bay	1984	1	160	49	—	not spec.	43
Narragansett Bay	1985-86	8	2,410	390	645	Ar 1242-60	This study

Note: not spec. = formulation not specified.

Within the water column itself, the PCB concentrations represent an interplay between dilution of source materials by autochthonous particles, degradation, resuspension-deposition, and the general hydrology of the system. The PCB levels for solids in the upper water column (mean = 838 ± 402 ng/g) were greater ($P < 0.05$, Student's t-test) than those at depth (mean = 464 ± 221 ng/g) (Table 11.3).³ The particulates with lower PCB levels may have been due to dilution of allochthonous particles (with higher PCB content) with planktonic particles (of lower PCB content). However, no direct chemical evidence for this, such as the concentration of n-C15 or n-C17, which has been shown to be associated with planktonic lipids,²⁶ was available. So other hypotheses are possible. These particulates, at depth in the water column, have similar PCB concentrations as the surface sediments, suggesting they are either resuspended from the active sediment layer or are the source material for the sediments.

Detailed scrutiny of the data, however, yielded a different view than the mean concentrations suggested. Specifically, the PCB concentrations in surficial sediments around Fox Point (1170 ± 66.5 ng Ar 1254/g dry weight) were statistically identical ($P < 0.05$, Student's t-test, 95% confidence limit) to those on the suspended solids from the Moshassuck (1200 ± 122 ng/g), Woonasquatucket (1620 ± 329 ng/g), and Blackstone (1740 ± 550 ng/g) Rivers, all of which discharge into the general vicinity of the Fox Point station (Table 11.3). In addition, the sedimentary concentrations in the area around the mouth of the Pawtuxet River suggested an influence from this river; that is, the Ar 1254 concentrations at sediment sites in the midportion of the Providence River (i.e., stations 2, 2a, 3, 3a) had a mean of 478 ± 104 ng/g, and this value was statistically equal to the mean loading of 648 ± 213 ng/g TSS determined for particles in the Pawtuxet River (Table 11.3). Thus, the sediments of the particular regions into which these freshwater inputs discharge generally reflect the PCB composition of the solids from the inputs.

Table 11.3. Mean PCB Concentrations (\pm SD) on Total Suspended Solids (TSS) in Rivers, Point Sources, Bay Water, and on Surficial Sediments from Throughout Narragansett Bay

	TSS or Sediment (ng/g)
<i>Freshwater^a</i>	
Pawtuxet River	648 ± 213
Moshassuck River	$1,200 \pm 122$
Woonasquatucket River	$1,620 \pm 329$
Blackstone River	$1,740 \pm 550$
Taunton River	434 ± 228
mean:	$1,130 \pm 333$
<i>Point Sources Effluents^a</i>	
Fields Point	930 ± 1090
Blackstone Valley	890 ± 160
All Others (n = 9)	767 ± 340
mean:	862 ± 516
<i>Marine Water^a</i>	
Surface (< 1 m)	
Fox Point	$1,092 \pm 534$
Conimicut Point	896 ± 187
West Passage	329 ± 321
East Passage	$1,036 \pm 253$
mean:	838 ± 402
Bottom (> 5m)	
Fox Point	809 ± 289
Conimicut Point	202 ± 156
West Passage	515 ± 169
East Passage	332 ± 158
mean:	464 ± 221
<i>Surface Sediments^b (top 0.5 cm)</i>	
Fox Point (st. 1,1a)	$1,170 \pm 66.5$
Mid Providence River (st. 2,2a,3,3a)	478 ± 104
Providence River/upper bay (st. 1-4,5a,11,18)	376 ± 393
mean: (entire bay):	217 ± 327

Note: PCBs are expressed as Ar 1254.

^aSamples taken under dry weather conditions only.⁴⁶

^bSee Figure 11.1 for station locations.

General Distribution of Sedimentary PCBs

Ar 1254 will be featured for discussion because it is the PCB formulation most consistently observed in sediments and other types of samples collected throughout the bay.³ Although the designation of PCBs as Aroclor equivalents is rather subjective, it is a framework suitable for the divulgence of information on spatial trends throughout the study area. Upon occasion, selected congeners will be utilized to make a point clearer due to their more exact analytical determination and/or their differing chemistries.

It should be noted at the outset that at least three types of Aroclors were discovered in the sediments of Narragansett Bay. Ar 1242 was found to be most prevalent in the upper Providence River, while Ar 1254 and Ar 1260 were typically found at all the sediment sites; generally, however, Ar 1254 was

detected in the highest concentrations. In addition, it was noted that chlorobiphenyl species in the nona- and decachlorinated range were consistently observed in the sediments of Narragansett Bay. These types of components are not found, in any appreciable concentrations, in the Aroclor formulations typically observed in the bay sediments. Furthermore, these constituents were encountered in samples from the fluvial inputs to the system, but not the wastewater inputs.³ It has been speculated that these highly chlorinated components may reflect a contribution from Aroclor 1268. This indeed may be the case; however, the distribution of the congeners is not quite what would be expected if Ar 1268 were involved (Latimer, unpublished data), although environmental alteration may be sufficient to cause the observed discrepancy. It is also possible that these constituents, especially the decachlorobiphenyl compound, may be derived from specialty formulations used in the die-casting industry or from atmospheric contributions.²⁷

The highest levels of PCBs in the surface sediments were observed in the Fox Point region (stations 1 and 1a) of the Providence River; in this vicinity, the concentration of Ar 1254 was over 1000 ng/g dry weight (Figure 11.3). The zone of the maxima is consistent with the mass transport conclusions derived from a study of the sources of PCBs to the bay. That investigation indicated the Blackstone River, which empties into Narragansett Bay at its northern terminus (via the Seekonk River), is the largest fluvial source of PCBs, at least under dry weather conditions.³ Samples of Seekonk River (estuary) sediment were evaluated in a later study and exhibited even greater PCB levels than at Fox Point (e.g., 1600 ng/g, in a 0–2 cm core section; Latimer, unpublished data). Higher concentrations would be expected in the Seekonk since many of the freshwater pollutant removal mechanisms take place by the time the salinity has reached 15–20 0/00.²⁸ The Blackstone River spills over a dam into the Seekonk River, where the average salinity ranges (based on data for 1986–1987) from less than 1 to 26.3 0/00.²⁹ Therefore, any dissolved or colloidally bound constituents will be destabilized and deposited, either by precipitation (salting out) or agglomeration, into the particulate pool, once the fresh and salt waters mix. In addition, the chemical nature of the colloids may be altered in this region, causing bound nonionic organics to desorb and become associated with settleable solids.

As Figure 11.3 illustrates, the PCBs showed a pattern of high levels in the Providence River, decreasing to lower values with increasing distance from this area. An exponential decrease in the sediment levels with distance from the highly industrialized Providence area was indicated. When the logarithm (base 10) of the concentration data were graphed with distance from station 1, a linear relationship with a negative slope was observed (Figure 11.4). The slope of this line can be used to estimate the half-distance ($D_{1/2}$) for a contaminant.¹⁹ Physically, $D_{1/2}$ is the distance, from the head of the bay, at which the concentration of a compound decreases to half its initial value. It was calculated by dividing log 2 by the slope of the semilog relationship. The half-distance can be used as a diagnostic parameter to gain information about the location of the

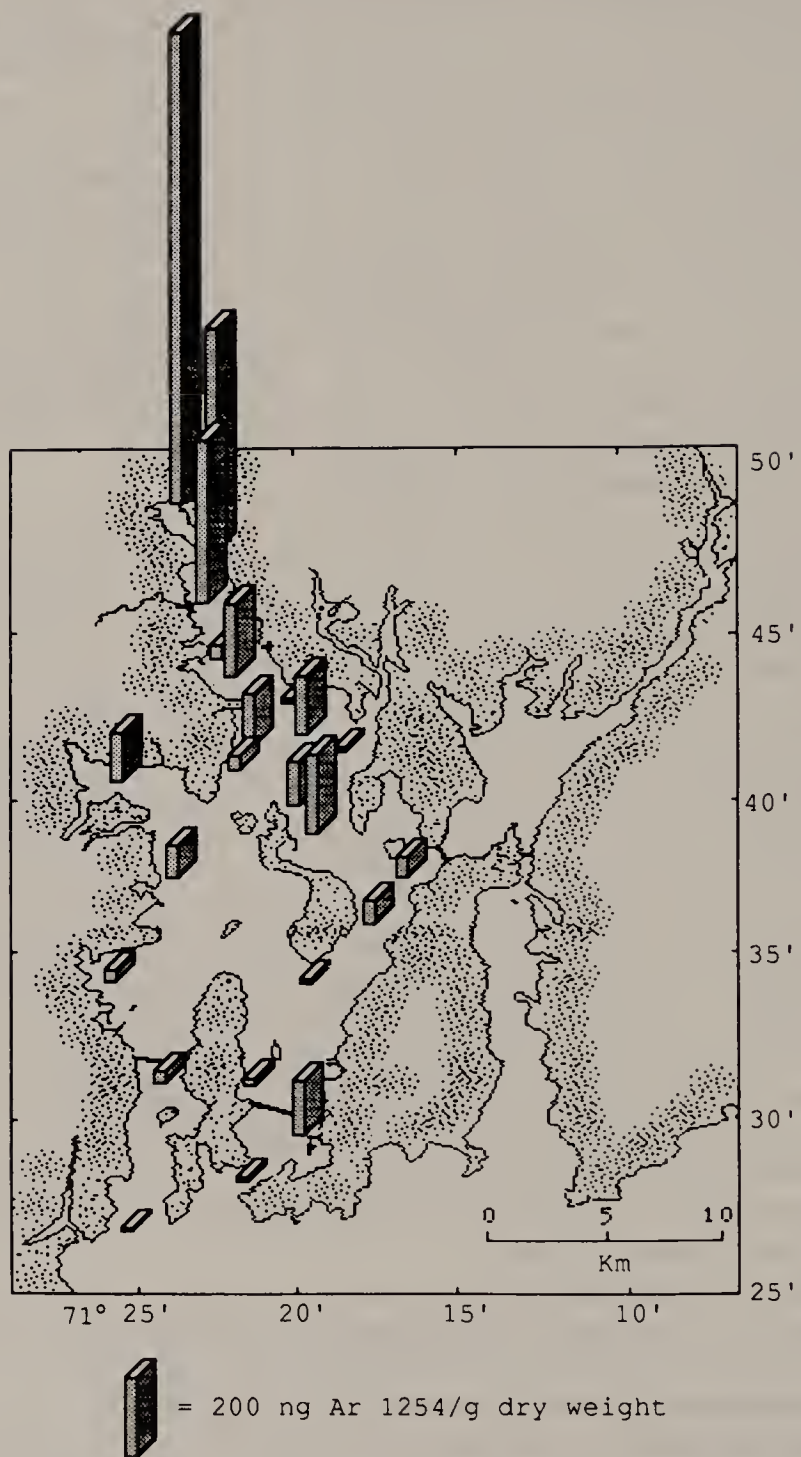


Figure 11.3. Ar 1254 concentrations in surface sediments expressed on a dry weight basis.

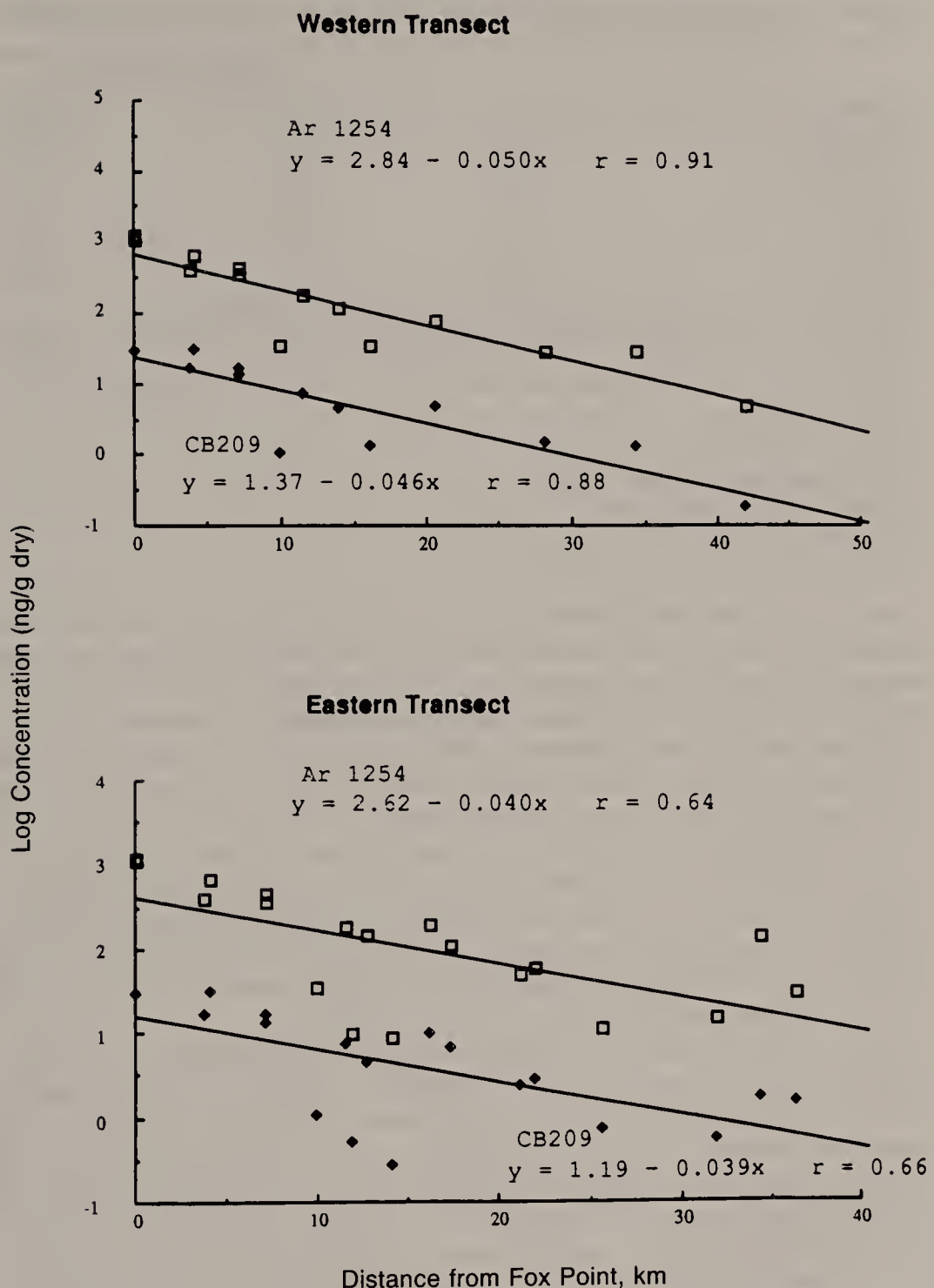


Figure 11.4. The log (10) concentration of PCBs (Ar 1254 and CB209) versus distance from the Fox Point station.

Table 11.4. Half-Distances Calculated for Selected Organic Contaminants in Narragansett Bay Surface Sediments

Constituent	$\log K_{ow}$	Half-Distance (km) ^a	
		W. Transect ^b	E. Transect ^c
Total organic carbon	—	13.7	15.8
Phenanthrene	4.64 ^d	9.6	13.1
Ar 1254	6.04 ^e	6.0	7.5
CB101	6.31 ^f	5.8	6.9
CB138	7.44 ^g	6.2	7.7
CB209	8.26 ^h	6.5	7.7

^aHalf-distance = $\log 2/\text{slope of semilog concentration-distance equation}$.

^bWest transect includes stations 1-4a, 6, 8, 18, 19, 20, 21 ($n = 14$). See Figure 11.1 for station locations.

^cEast transect includes stations 1-4a, 5, 5a, 7, 9, 10, 11-16 ($n = 19$). See Figure 11.1 for station locations.

^dFrom Mackay et al.⁴⁷

^eFrom Mabey et al.⁴⁸

^fFrom Kenaga and Goring.⁴⁹

^gFrom Rapaport and Eisenreich.⁵⁰

^hFrom Miller et al.⁵¹

source region and relative sedimentary desorption kinetics of a particular compound of interest. For example, the $D_{1/2}$ for Ar 1254 for the transect on the west side of the bay was calculated to be 6 km (Table 11.4). The slope of the line for the TOC was significantly lower than for the PCBs and gave a $D_{1/2}$ of 13.7 km for the western transect, which is similar to the value of 12.5 km calculated previously.¹⁹ A more diffuse source for organic carbon is consistent with these calculations since the organic carbon pool can be derived from both anthropogenic and natural sources, which are not necessarily dominated by the Providence River. Furthermore, correlational analysis indicated that the organic carbon varied in a manner that was more similar to the natural components of the sediments, such as the odd carbon number *n*-alkanes and *n*-aldehydes, rather than the anthropogenically derived petroleum hydrocarbons and PCBs (Latimer, unpublished data).

Once in the sediments, it has been proposed that compounds that exhibit a greater tendency to partition into the sediments are less likely to be desorbed and thus would be found at greater distances from the source regions than those that sorb less strongly.^{19,30} Therefore, it might be expected that constituents with high K_{ow} coefficients would be more likely to have greater half-distances than those with low values. Unfortunately, to test this hypothesis, the source functions (i.e., location and source strength) would need to be equal for the compounds of interest. In the case of the polycyclic aromatic hydrocarbons, as exemplified by phenanthrene in Table 11.4, which has a relatively long $D_{1/2}$, the sources were not localized and the longer half-distance may be due to nonpoint sources such as urban runoff and atmospheric inputs.³¹ The distributed inputs would tend to lengthen $D_{1/2}$, irrespective of the K_{ow} value. In contrast, the sources of PCBs have been shown to be principally from the Blackstone River (at the northernmost sector of the bay);³ therefore, the need

for a well-defined source function and differing K_{ow} coefficients was satisfied using three chlorobiphenyl congeners with different chemical properties. A longer half-distance with increasing K_{ow} 's was confirmed at least for the western transect (Table 11.4). The significance of the differences was not conclusive, however, suggesting that the chemical nature of the PCB contaminants is not an overriding determinant of the sedimentary distribution.

The chemical evidence implies that partitioning differences between the congeners were not the controlling factors in the overall PCB distribution in the sediment; in fact, all of these compounds are apparently sorbed strongly enough to merely represent the time-averaged sediment transport dynamics of the bay. Contrary to a physical/chemical explanation for the congener distribution, Figure 11.5 shows a similar chemical sequence for all 10 chlorobiphenyls studied in sediments, despite the geographic extremes of the sampling network and the widely different K_{ow} values for the congeners. This figure shows, quite convincingly, that the congener distributions for the surface sediments throughout the bay were relatively constant and were dominated by CB101, CB153, CB138, and CB180. The differences observed between the half-distances calculated for the western and eastern transects of the bay (Table 11.4) were, thus, a consequence of the general hydrology between these two areas, starting from the common source region—the Blackstone/upper Providence River. The half-distances calculated were a function of where the PCBs enter the bay and how the sediments are later distributed and were not primarily related to the sorptive properties of the compounds. A similar conclusion was reached by Pruell and Quinn.¹⁹ In addi-

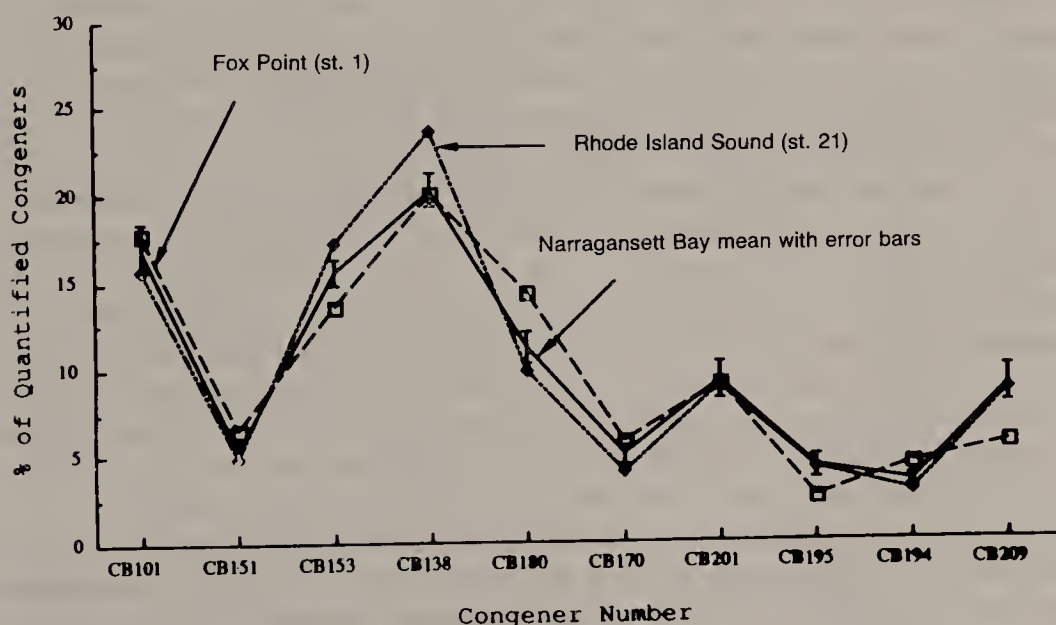


Figure 11.5. The congener distribution for station 1 (Fox Point), station 21 (Rhode Island Sound), and the mean (\pm SD) for all the Narragansett Bay surface sediment stations evaluated.

tion to these general characteristics, an elevated PCB concentration at station 15 was the reason for the slightly, but consistently, longer half-distances observed for the eastern transect of the bay. Moreover, the high PCB concentrations at station 15 and the low concentrations in some areas of the upper bay, together, contributed to the poorer correlations observed between the regression line variables in the eastern transect (Figure 11.4).

Localized Distribution of Sedimentary PCBs

There is a general attitude among organic geochemists that concentration data in sediments should be universally expressed on an organic carbon weight basis, since hydrophobic components such as PCBs are strongly associated with this fraction of the sediment.⁹ By expressing data in this manner, differences in sediment types can be normalized. The data would then be more reflective of the source strengths of the contaminants and less on the hydrodynamics, thereby disassociating the effects of the depositional regime. This is true because the organic carbon is associated to a greater extent with the fine-grained portion of the sediments; thus, organic carbon normalized data will also be a surrogate for fine-grained associated pollutants.³² It can be expected that during episodes of limited deposition—for example, during storms—only the larger grain size, sandy, low organic carbon type sediments would be deposited from the water column or would remain on the sediment surface. The smaller sized particles would be resuspended and swept away, only to be deposited elsewhere. The continuum of this resuspension-deposition situation will be reflected in the sedimentary reservoir.

Certain areas in the lower Providence River and upper bay (alluded to above) showed diminished levels of PCBs per unit dry weight of sediment. For example, the area just north of Conimicut Point (station 4a; see Figure 11.3; station locations are in Figure 11.1) was found to have a concentration of 182 ng Ar 1254/g dry weight; in contrast, the site just south, i.e., station 5, had only 10.3 ng Ar 1254/g dry weight. When these concentrations were expressed on a per weight organic carbon basis, the two stations showed nearly identical values (Figure 11.6; 3.88 and 3.51 ng Ar 1254/mg TOC, respectively, for stations 4a and 5). This indicated that the two sites were subject to sources of similar PCB character; however, because of the magnitude and direction of the bottom currents, station 5 appears to be in a nondepositional area, yielding lower organic carbon loadings and, presumably, more coarse sediments. Maps showing the distribution of sediments in this region indicate that the area from Nayatt to Rumstick Points (near stations 5 and 10) is mainly sand.³³

The bottom topography of a basin may also play an important role in the amounts of organic contaminants deposited. The low PCB concentration determined at station 10 (8.85 ng/g dry), although having low organic carbon levels, had PCB levels even lower than what would be expected when normalized to TOC (i.e., 0.89 ng Ar 1254/mg TOC), thus revealing that this area may be partially isolated from the higher PCB inputs coming from the Providence

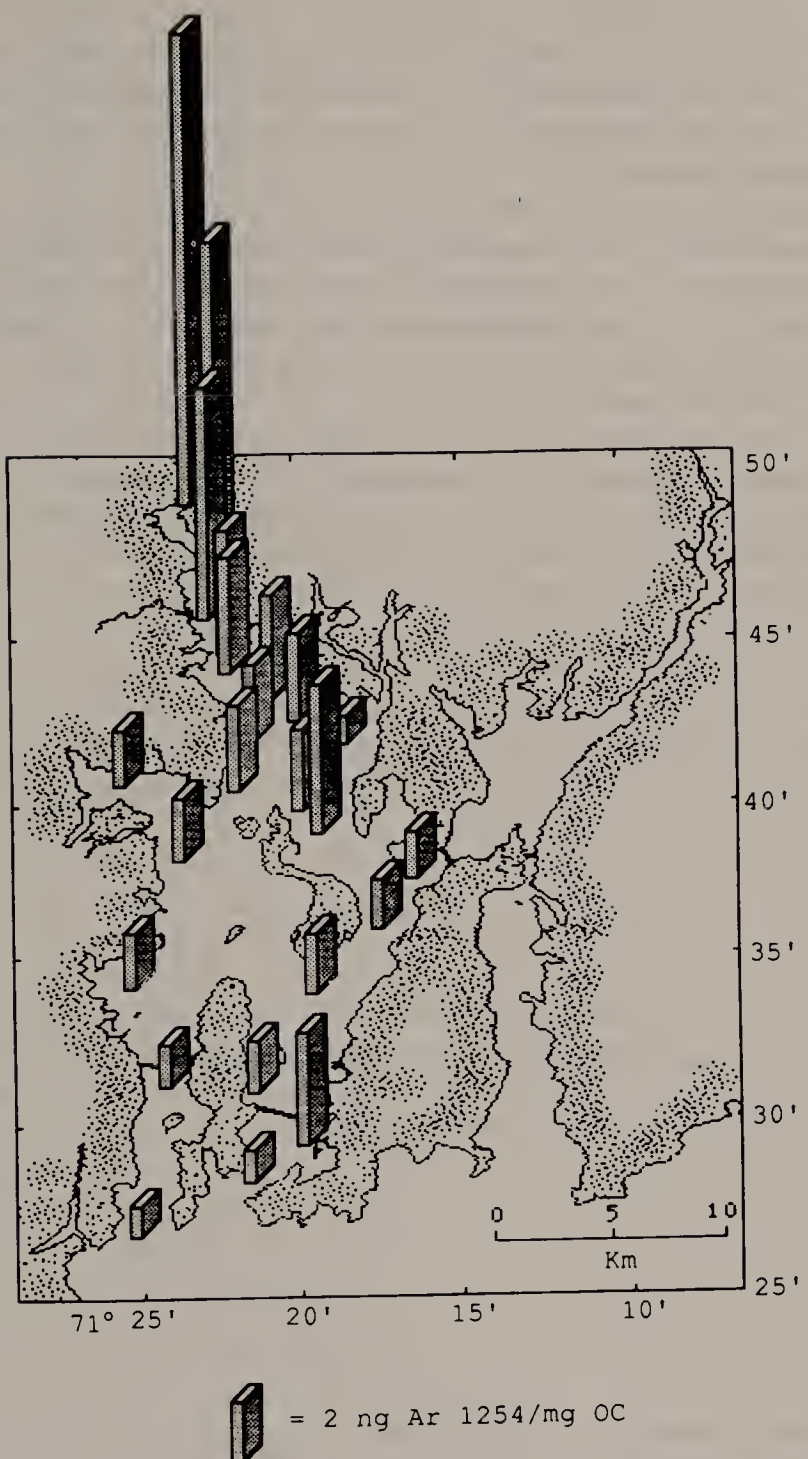


Figure 11.6. Ar 1254 concentrations in surface sediments expressed on an organic carbon weight basis.

River due to bottom contours. While the actual site was west of the topographic feature called Rumstick Shoal, it is possible that this area may be influenced by the shoal and derived its sediment and associated contaminants from the Warren River Basin (northeast of station 10), which may be less contaminated with PCBs.

Grain size analysis was undertaken for the majority of the sediment samples (King, unpublished data). In a general sense these data confirmed that organic carbon was most strongly associated with the silt ($r^2 = 0.557$) and even more so, the silt + clay ($r^2 = 0.568$) fractions of the sediments. As expected, there was a negative correlation in the concentration organic carbon with the sand content of the sediment.

A close examination of these data, however, indicated a more complicated system than first thought. The relationship between these bulk sediment characteristics (e.g., grain size and organic carbon content) and the PCB levels was revealing. Much of the PCB data, expressed in this case by CB180, were in the less than 10 ng/g concentration range (Figure 11.7). In this concentration

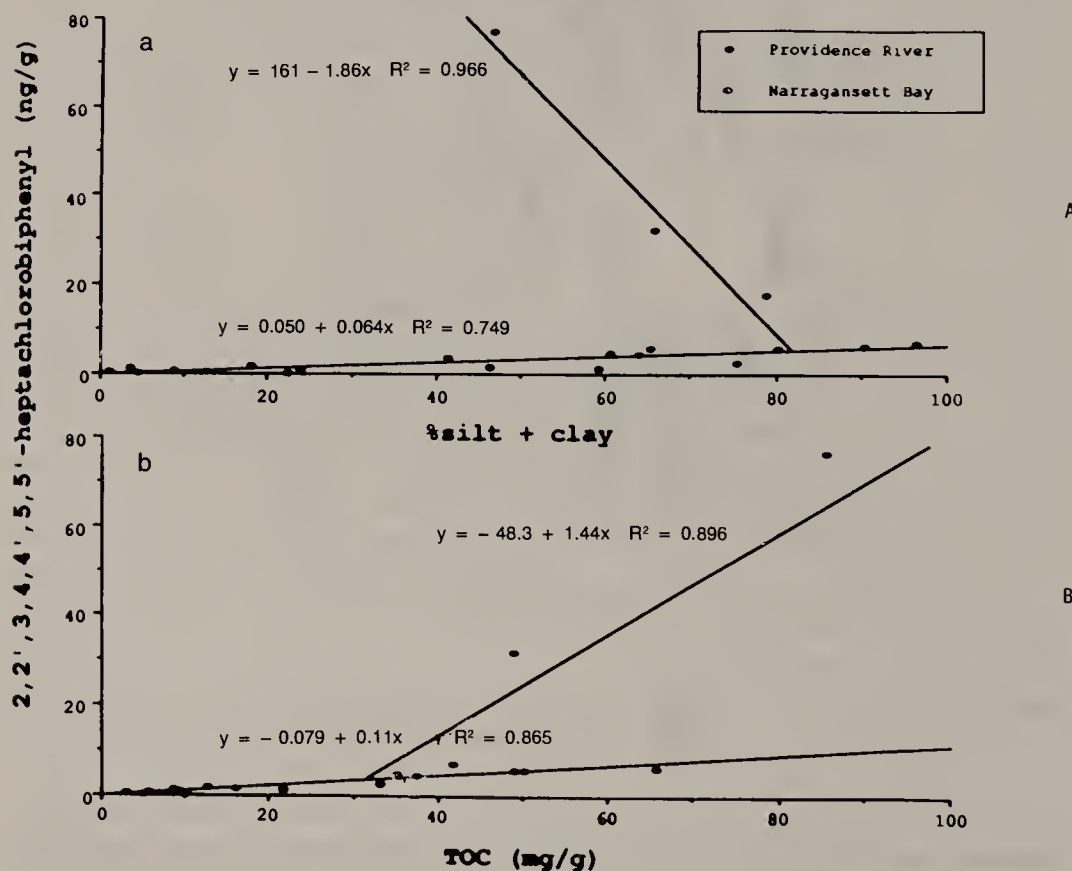


Figure 11.7. The concentration of CB180 (2,2',3,4,4',5,5'-heptachlorobiphenyl) versus bulk sediment properties for Narragansett Bay and upper Providence River sites: (a) percent silt + clay fraction of the sediments; (b) TOC concentration in the sediments.

realm, the fine-grained fractions and organic carbon content were directly proportional to the contaminant levels, i.e., organic carbon content ($r^2 = 0.865$) and the percent fine-grained (silt + clay, $r^2 = 0.749$).

In the relatively contaminated upper Providence River, however, the relationships are clearly different. This area appeared to follow a different regime than the remainder of the bay. The general functionality was independent of the PCB chemistry since all of the congeners showed similar behavior. In this region, the grain size properties were all in the 50–80% silt + clay category (Figure 11.7a), but, more importantly, the sediment had only slightly higher organic carbon content than areas outside of the upper Providence River (~4.5–8.5% TOC, Figure 11.7b). Contrary to conventional wisdom, in the upper Providence River, as the proportion of fine-grained material decreased (percent sand increased), the PCB levels increased markedly. The trends are identical even when the < 16 μm and the 16–62 μm size fractions are evaluated separately.

Various explanations are possible. One possible reason for this phenomenon is that the properties of the organic carbon in the upper portion of the Providence River are sufficiently different as to sorb or retain nonionic pollutants to a greater extent than organic carbon in the other areas, completely overriding the effects of grain size on PCB dynamics. The organic carbon content is important because it is not just the surface-to-volume ratio of the sediments (i.e., the grain size) that plays a role in the sequestering of contaminants, but the partitioning properties of the specific organic carbon coatings on the sediments themselves. Therefore, it is conceivable that the sediments from various areas may be expected to have different types of coatings (natural and anthropogenic) and differing sorption and retention affinities to organic contaminants. In this regard, it has been reported that the chemical character of humic materials will affect the degree of hydrophobic sorption.³⁴

Even more important, however, than natural humic materials, other phases are capable of sequestering PCBs. Anthropogenic substrates in soils, such as petroleum hydrocarbons (PHCs), have been shown to partition hydrophobic organics nearly 10 times more efficiently than natural organic materials.³⁵ Therefore, this may account for the observed trends since the Providence River has high levels of organic contaminants, including petroleum hydrocarbons.¹⁹ One way to test this hypothesis is to compare the PCB:PHC ratios in sediments from the upper Providence River with those for the remainder of the bay. If the petroleum is the active fraction of the TOC, then the ratio might be expected to be higher in the upper Providence River. This test was performed, and the results showed increased affinity of PCBs in this area, but not exceptionally so. Thus, the hypothesis cannot be confirmed.

Another plausible explanation of the behavior of PCBs is that the sediments are simply reflecting the fact that PCBs are entering the system on particles with the characteristic grain properties (i.e., very high PCB, higher sand content). Those sediments in the upper Providence River are nearest to the source regions with these peculiar grain properties. In order to test this deduction, one

would need PCB:TOC and PCB:percent sand ratios for TSSs in the source samples; unfortunately, these data are not available. Any other test would require further assumptions that begin to beg the question and as such would not be defensible. However, this latter proposition appears to be the most probable, and future studies should include grain size analyses for rivers discharging in this vicinity. Whatever the cause, the evidence indicates that the most highly contaminated sediments in Narragansett Bay are not associated with the smallest particle sizes and as such this region (the upper Providence River) would be less prone to down-bay transport of the contaminated materials; thus, it can be considered a sink.

Another area of interest is the sediment site in the vicinity of Newport (station 15). The outfalls of a primary wastewater treatment facility (WWTF) and combined sewer overflows (CSOs) are located in this general region. Station 15, which was in the same north-south direction as the tidal flow with the wastewater outfalls and CSOs, exhibited a PCB content that was similar (i.e., 136 ng Ar 1254/g dry, see Figure 11.3) to that of the upper bay. Station 14, which was across the bay in the vicinity of Conanicut Island near a secondary wastewater treatment facility, did not show elevated PCB concentrations on either a dry weight or an organic carbon weight basis (Figures 11.3 and 11.6). The concentration at station 16, southwest of station 15, was approximately what might be expected for this area of the bay.

The average PCB loadings on TSS from the Newport wastewater facility in 1985–1986 were 420 ± 330 ng Ar 1254/g TSS,³ which was somewhat higher than what was observed in the sediments. The suspended solids in the effluent, however, would be expected to be fractionated, once discharged into the marine environment, in such a way as to remove the more highly contaminated, smaller size fraction of the particles, leaving the less contaminated solids to settle to the bottom. The fact that the Newport plant is a primary treatment facility, in which the settling of in-flowing sewage is the only means of contaminant removal, suggests a possible link between it and the sediment levels. In addition, calculations indicated that this facility was one of the larger sources of PCBs to the bay relative to what would be expected from its typical effluent flow rate.³ However, it must be noted that, although there is circumstantial evidence that may implicate the Newport outfall, the entire Newport area has many pollution sources, including combined sewer overflows as well as industrial and shipping activities. These potential sources coupled with previous naval pollution in this region may have contributed to the elevated PCB levels in the sediment.

Sediment Quality Criteria

Sediment quality criteria research is a relatively new branch of applied environmental toxicology.³⁶ It is analogous in its application to the water quality criteria utilized by local and national environmental authorities in determining the degree of degradation of a water body. Water quality criteria are based on

the effects of contaminant levels in the water on various aquatic test organisms. Sediment quality criteria development is in the early stages, and several different methods of determining the detrimental contaminant levels are currently being explored. A detailed description of all of these methods is beyond the scope of this chapter; however, a few of the methods studied in the Puget Sound ecosystem will be mentioned and applied to Narragansett Bay.³⁷ The interested reader should consult an excellent review by Chapman.³⁸

Apparent Effects Threshold (AET)

In an effort to mitigate the limitations of other approaches, actual field bioeffects and chemical data are utilized in the AET methodology. This technique has the advantage of adaptability with respect to chemicals of concern and bioeffects utilized.³⁸ No assumptions are needed about the mechanisms of interactions between the pollutant and the fauna, so the AET has a wide appeal, partly because it yields noncontradictory evidence of sediment quality, an important attribute in a litigious society. However, the approach requires a large database of both chemical and biological information and suffers from a lack of standard methods for sediment toxicity testing. The Puget Sound study used four bioeffects testing parameters for comparative purposes: amphipod mortality level (e.g., *Rhepoxynius abronius*), oyster larvae abnormalities (e.g., *Crassostrea gigas*), benthic infaunal population depression (e.g., total abundances, polychaetes, mollusks, and crustaceans), and bacterial bioluminescence (Microtox bioassay) changes.³⁷ The benthic infaunal population and the oyster larvae bioindicators yielded the same criteria for the Puget Sound sediments ($1.1 \mu\text{g}$ total PCB/g sed.); the amphipod mortality indicator was significantly less sensitive ($2.5 \mu\text{g}$ total PCB/g sed.), whereas the bioluminescence indicator was extremely sensitive to low levels of PCBs ($0.13 \mu\text{g}$ total PCB/g sed.). The extreme sensitivity of the Microtox bioassay to the most nonpolar, neutral contaminants has been noted by others studying sediment toxicity.³⁹

The AET criteria was applied to Narragansett Bay sediments in order to compare PCB levels with possible biological effects. The criteria based on amphipod mortality suggested that only the very northern portion of the estuary had degraded sediment levels (Figure 11.8a), but the oyster larvae bioassay and the benthic infaunal abundance tests indicated that lower levels of PCBs were harmful; thus, the sediments in the vicinity of the Fields Point WWTF (near sediment stations 2 and 2a) were classified as degraded (Figure 11.8b). Due to the sensitivity of the Microtox bioassay, sediments throughout the Providence River and portions of the midbay as well as near Newport, RI, were deemed to be detrimental to organisms living in them (Figure 11.8c).

The applied AET sediment quality criteria were designed and intended for use in the Puget Sound only; its application should be strictly understood as an example of the utility of the technique in linking sediment PCB levels to adverse biological impacts in Narragansett Bay. Since the AET protocol is extremely site specific (e.g., total contaminant makeup of reference sites and

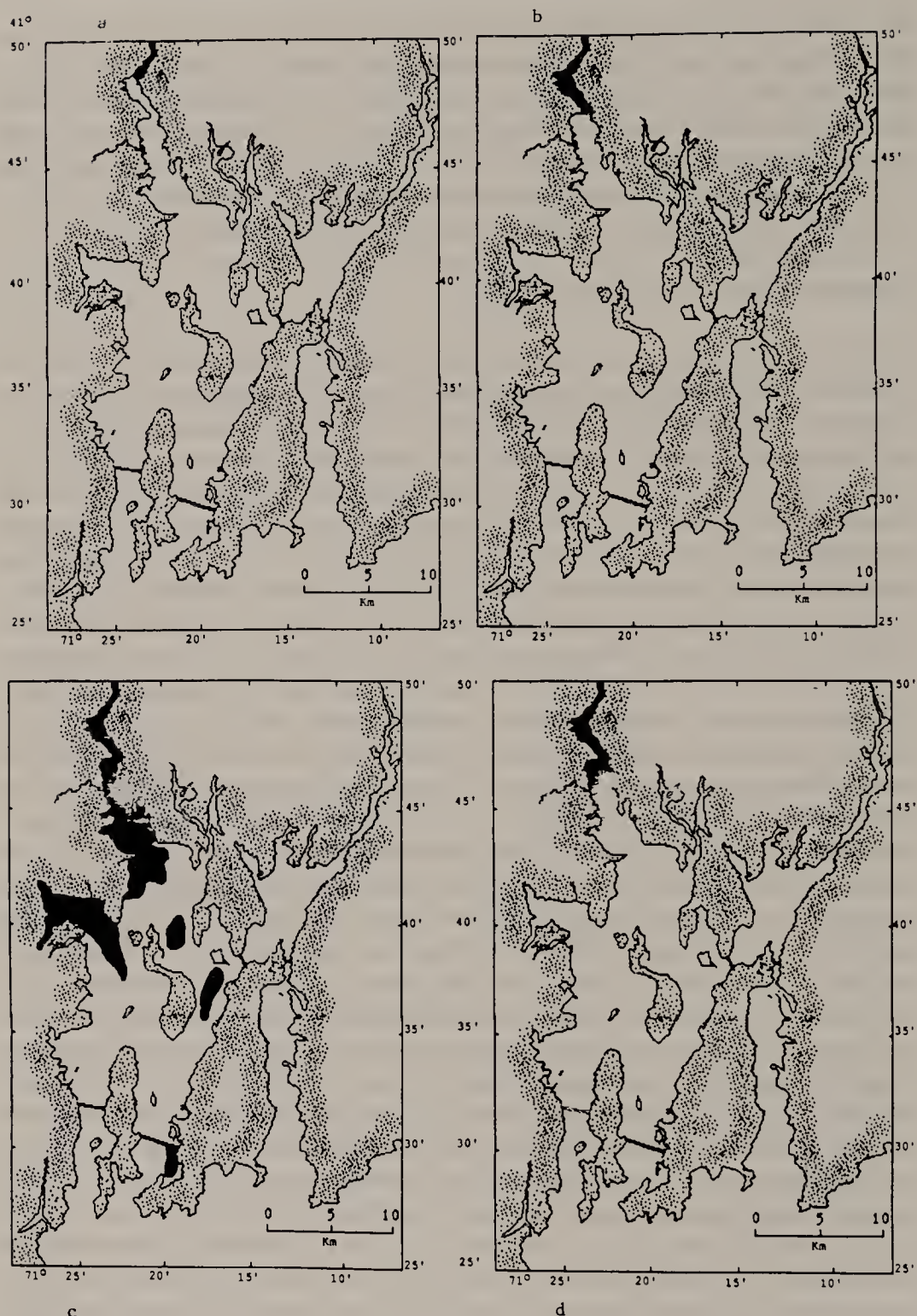


Figure 11.8. Map of Narragansett Bay showing that portion of the sediments that were characterized as degraded according to (a) the AET-amphipod mortality approach, (b) the AET-oyster larval abnormality and benthic infaunal population depression approaches, (c) the AET-Microtox approach, and (d) the EP-sediment/interstitial water approach.

polluted sites are employed), a similar study designed to categorize sediment levels of pollutants and adverse biological effects for Narragansett Bay sediments is essential in the absence of established sediment quality criteria.

Sediment-Water Equilibrium Partitioning (EP)

This method is framed on the premise that detrimental sedimentary levels of contaminants would be available to organisms if the interstitial water contained concentrations that are equal to, or greater than, the chronic water quality criteria as promulgated by the U.S. EPA. The criterion is based on the sedimentary contaminant concentration (organic carbon normalized) that would be in equilibrium with interstitial water contaminants. If this value is high enough, pore waters would acquire levels that meet or exceed the EPA water quality criterion of the contaminant of interest.

The method involves the calculation of an organic carbon normalized partition coefficient from the chemical characteristics of the pollutant—in this case, the octanol-water partition coefficient for PCBs. The general equation for this conversion is the standard

$$\log K_{TOC} = a \log K_{ow} + b$$

K_{TOC} is the organic carbon normalized partition coefficient defining the equilibrium of the compound between the interstitial water and sediment organic carbon phases. The regression parameters, a and b , can be obtained from the literature. Using values of 0.843 and 0.158 for these parameters, respectively, and a $\log K_{ow}$ value of 6.46 for PCBs,³⁷ the logarithmic organic carbon partition coefficient was calculated to be 5.60. Applying this value to the equation

$$K_{TOC} = C_{sed-TOC}/C_{water-criterion}$$

and solving for $C_{sed-TOC}$, a sedimentary concentration of 12.0 ng/mg TOC of PCBs would be required to yield 30 ng/L in the interstitial water.⁴⁰ In the case of Narragansett Bay, the northern and midsection of the Providence River (stations 1–3) would be suspected of being in a degraded state according to this criterion since the average concentration of PCBs was 22.5 ng/mg TOC (Figure 11.8d). It is entirely possible that the water quality criterion (WQC) published by EPA in 1987 for PCBs may be revised downward by regulatory agencies at the state level based on the reduction that the FDA promulgated in the late 1970s. The FDA tolerance level was reduced from 5 to 2 µg/g for saleable fish and shellfish based on more up-to-date information than the original EPA WQC data base.⁴¹ This reflects a criteria reduction of 60%. If extrapolated to WQC, this would translate into a revised 12 ng/L marine chronic criterion, which in turn would yield a sediment quality criterion (SQc) of 4.8 ng/mg TOC in the sediments. If this scenario were to be considered valid, then sediments of a much greater area in Narragansett Bay, similar to

the Microtox projections (see Figure 11.8c), would be above acceptable PCB levels.

The EP method has its strengths and weaknesses. One advantage is that it utilizes the toxicological database already in existence (i.e., U.S. EPA water quality criteria) and, as such, does not require any collection of biological data. Only the determination of contaminant concentrations along with the organic carbon content of the sediments is necessary. However, certain limitations exist—for example, the rather limited number of compounds for which water quality criteria exist restricts the applicability of the protocol. In addition, the application of toxicological data, determined in sediment-free test systems, to the field, may not be appropriate. Although uptake via partitioning is considered important, the method assumes bioaccumulation only through water partitioning and not from sediment ingestion. Furthermore, uncertainty due to interactive effects of chemicals in the environment must be addressed since most sediments have a myriad of organic and inorganic contaminants as well as a variety of physical and chemical characteristics that, taken together, may have a different influence on the infaunal organisms, not predicted with single chemical approaches.³⁸ In addition to these limitations, the validity of the assumption that equilibrium exists between the chemical sorbed to the sediment and that which is dissolved (or in colloidal suspension) in the interstitial waters is oftentimes questionable, especially in an area as dynamic as an estuary.³⁷

CONCLUSIONS

Concentrations of PCBs, as determined in the top 0.5 cm of surficial sediments throughout Narragansett Bay, generally reflected the various sources to the estuary. From the spatial concentration distribution, it was clear that the upper Providence River contained the highest sedimentary levels of PCBs. This pattern was consistent with the proximity of industrial and population centers in the region. The northern sector of the bay watershed can be characterized as a focal point of industrial/population enterprise, particularly in the Providence River area. The PCBs exhibited a significant concentration gradient with a maximum in the Fox Point region of the Providence River. In this area, levels of Ar 1254 were approximately 1000 ng/g dry weight; they decreased to around 100 ng/g in the upper bay. The southern portion of the bay has significantly less industrial activity, lower population density, and consequently, lower PCB levels. The concentrations were approximately 15–30 ng/g in the areas around Conanicut Island, and they finally reached < 10 ng/g levels near the mouth of the bay.

In some areas, the concentrations of PCBs in the sediments were relatively low due to decreased inputs of particulate organic material, as evidenced by the low organic carbon content of the sediment. The areas that showed the lower concentrations of organic carbon did so because of the nature of the

local circulation dynamics. Conversely, the upper segment of the Providence River contained PCB levels much higher than expected from the observed organic carbon content and other bulk sediment parameters relative to the other regions. This was perhaps due to either the anthropogenic nature of the sedimentary organic substrates capable of sequestering hydrophobic contaminants or from the particle characteristics of the sources of PCBs in this vicinity.

Other areas exhibited elevated levels of PCBs that were not necessarily due to the transport of contaminated sediment from Providence River sources, but were presumably due to inputs from local sources; the region near Newport, RI, was such an example.

The surficial concentrations of PCBs were categorized as to whether they would be deleterious to organisms in the sediment. The apparent effects threshold (AET) and equilibrium partitioning (EP) approaches were discussed; the EP technique was less site specific and, as such, more applicable to Narragansett Bay. Using this approach, it was determined that the upper and midregions of the Providence River were in a degraded state with respect to the ability of sediment to support thriving biological populations due to high PCB levels. It was further postulated that greater areas of the bay sediments would be considered to be in a degraded state if a more stringent regulatory standard were applied.

ACKNOWLEDGMENTS

We wish to thank Paul Heinmiller for collecting the sediments in less-than-ideal diving conditions. This study was principally supported by funds from the Narragansett Bay Project (URI Grant No. 5-39363) and the National Sea Grant Program; additional support was provided by a grant from the U.S. Environmental Protection Agency (CR-815992-01). This report has not been subjected to the EPA's review process and therefore does not necessarily reflect the views of the EPA, and no official endorsement should be inferred.

REFERENCES

1. Gibbs, R. J. "Effect of Natural Organic Coatings in the Coagulation of Particles," *Environ. Sci. Tech.* 17:237-240 (1983).
2. Gschwend, P. M., and S. Wu. "On the Constancy of Sediment-Water Partition Coefficients of Hydrophobic Organic Pollutants," *Environ. Sci. Technol.* 19:90-96 (1985).
3. Latimer, J. S. "The Sources, Transport, and Fate of Polychlorinated Biphenyls in Narragansett Bay," PhD Thesis, University of Rhode Island, Kingston, RI (1989).
4. Shaw, G. R., and D. W. Connell. "Physicochemical Properties Controlling Polychlorinated Biphenyl Concentrations in Aquatic Organisms," *Environ. Sci. Technol.* 18:18-23 (1984).
5. Eadie, B. J., and J. A. Robbins. "The Role of Particulate Matter in the Movement

- of Contaminants in the Great Lakes," *Advances in Chemistry Series 216*, R. A. Hites and S. J. Eisenreich, Eds. (Washington, DC: American Chemical Society, 1987).
6. Olsen, C. R., I. L. Larsen, R. H. Brewster, N. H. Cutshall, R. F. Bopp, and H. J. Simpson. "A Geochemical Assessment of Sedimentation and Contaminant Distributions in the Hudson-Raritan Estuary," Technical Report NOS OMS 2, National Oceanic and Atmospheric Administration (1984).
 7. Eisenreich, S. J. "The Chemical Limnology of Nonpolar Organic Contaminants: Polychlorinated Biphenyls in Lake Superior," in *Sources and Fates of Aquatic Pollutants*, R. A. Hites and S. J. Eisenreich, Eds. (Washington DC: American Chemical Society, 1987).
 8. Brownawell, B. J., and J. W. Farrington. "Biogeochemistry of PCBs in Interstitial Waters of a Coastal Marine Sediment," *Geochim. Cosmochim. Acta* 50:157-169 (1986).
 9. Brownawell, B. J. "The Role of Colloidal Organic Matter in the Marine Geochemistry of PCBs," PhD thesis, Woods Hole Oceanographic Institution, Woods Hole, MA (1986).
 10. O'Connor, D. J., and J. P. Connolly. "The Effect of Concentration of Adsorbing Solids on the Partition Coefficient," *Water Res.* 14:1517-1523 (1980).
 11. Hutzinger, O., S. Safe, and V. Zitko. "Introduction and Commercial PCB Preparations: Properties and Composition," in *The Chemistry of PCBs* (Cleveland, OH: CRC Press, 1974), pp. 1-39.
 12. Monsanto Company. "Polychlorinated Biphenyls. A Report on Uses, Environmental and Health Effects and Disposal," Public Relations Department, St. Louis, MO (1979).
 13. "Toxic Substances: EPA Has Made Limited Progress in Identifying PCB Users," Report to the Chairman, Subcommittee on Environment, Energy, and Natural Resources, Committee on Government Operations, House of Representatives, United States General Accounting Office, GAO/RCED-88-127 (1988).
 14. Tanabe, S. "PCB Problems in the Future: Foresight from Current Knowledge," *Environ. Poll.* 50:5-28 (1988).
 15. "Polychlorinated Biphenyls," National Research Council, National Academy of Sciences, Washington, DC (1979).
 16. Miller, S. "The Persistent PCB Problem," *Environ. Sci. Technol.* 16:98A-99A (1982).
 17. Wade, T. L., and J. G. Quinn. "Geochemical Distribution of Hydrocarbons in Sediments from Mid-Narragansett Bay, Rhode Island," *Org. Geochem.* 1:157-167 (1979).
 18. Hurtt, A. C., and J. G. Quinn. "Distribution of Hydrocarbons in Narragansett Bay Sediment Cores," *Environ. Sci. Technol.* 13:829-836 (1979).
 19. Pruell, R. J., and J. G. Quinn. "Geochemistry of Organic Contaminants in Narragansett Bay Sediments," *Est. Coastal Shelf Sci.* 21:295-312 (1985).
 20. Olney, C. E. "Transfer of Pesticides through Water, Sediments and Aquatic Life," Rhode Island Water Resource Res. 8th Annual Report, PL-88-379:26-32 (1972).
 21. Boehm, P. D., and J. G. Quinn. "Benthic Hydrocarbons of Rhode Island Sound," *Est. Coastal Mar. Sci.* 6:471-494 (1978).
 22. Paulson, A. J., and D. T. Brown. "PCBs: Their Environmental Significance and Distribution in Rhode Island," Technical Report 68, University of Rhode Island, Coastal Resources Center (1978).

23. LeBlanc, L. A. "The Geochemistry of Coprostanol in Narragansett Bay," MS thesis, University of Rhode Island, Kingston, RI (1989).
24. Quinn, J. G., J. S. Latimer, J. T. Ellis, L. A. LeBlanc, and J. Zheng. "Analysis of Archived Water Samples for Organic Pollutants. Final Report," NBP-88-04, Narragansett Bay Project, Providence, RI (1988).
25. Ballschmiter, K., and M. Zell. "Analysis of Polychlorinated Biphenyls (PCB) by Glass Capillary Gas Chromatography," *Fres. Z. Anal. Chem.* 302:20-31 (1980).
26. Saliot, A. "Natural Hydrocarbons in Sea Water," in *Marine Organic Chemistry*, E. K. Duursma and R. Dawson, Eds. (New York: Elsevier, 1981), Chapter 11.
27. Bumb, R. R., W. B. Crummett, S. S. Cutie, J. R. Gledhill, R. H. Hummel, R. O. Kagel, L. L. Lamparski, E. V. Luoma, D. L. Miller, T. J. Nestrick, L. A. Shadoff, R. H. Stehl, and J. S. Woods. "Trace Chemistries of Fire: A Source of Chlorinated Dioxins," *Science* 210:385-390 (1980).
28. Sholkovitz, E. R. "Flocculation of Dissolved Organic and Inorganic Matter During the Mixing of River Water and Seawater," *Geochim. Cosmochim. Acta* 40:831-845 (1976).
29. Doering, P. H., L. Weber, W. M. Warren, G. Hoffman, K. Sweitzer, M. E. Q. Pilson, C. A. Oviatt, J. D. Cullen, and C. W. Brown. "Monitoring of the Providence and Seekonk Rivers for Trace Metals and Associated Parameters. Final Report," NBP-89-16, Narragansett Bay Project, Providence, RI (1988).
30. Lopez-Avila, V., and R. A. Hites. "Organic Compounds in an Industrial Wastewater. Their Transport into Sediments," *Environ. Sci. Technol.* 14:1382-1390 (1980).
31. Hoffman, E. J., G. L. Mills, J. S. Latimer, and J. G. Quinn. "Urban Runoff as a Source of Polycyclic Aromatic Hydrocarbons to Coastal Waters," *Environ. Sci. Technol.* 18:580-586 (1984).
32. Boehm, P. D., and A. G. Requejo. "Overview of the Recent Sediment Hydrocarbon Geochemistry of Atlantic and Gulf Coast Outer Continental Shelf Environments," *Est. Coastal Shelf Sci.* 23:29-58 (1986).
33. McMaster, R. L. "Sediments of Narragansett Bay System and Rhode Island Sound, Rhode Island," *J. Sed. Petrol.* 30:249-274 (1960).
34. Gauthier, T. D., W. R. Seltz, and C. L. Grant. "Effects of Structural and Compositional Variations of Dissolved Humic Materials on Pyrene K_{oc} Values," *Environ. Sci. Technol.* 21:243-248 (1987).
35. Boyd, S. A., and S. Sun. "Residual Petroleum and Polychlorinated Oils as Sorptive Phases for Organic Contaminants in Soil," *Environ. Sci. Technol.* 24:142-144 (1990).
36. Shea, D. "Developing National Sediment Quality Criteria," *Environ. Sci. Technol.* 22:1256-1261 (1988).
37. Tetra Tech, I. "Development of Sediment Quality Values for Puget Sound. Final Report," TC3090-02, Resource Planning Associates for Puget Sound, Dredged Disposal Analysis and Puget Sound Estuary Program, Bellevue, WA (1986).
38. Chapman, P. M. "Current Approaches to Developing Sediment Quality Criteria," *Environ. Toxicol. Chem.* 8:589-599 (1989).
39. Ho, K. T. Y. University of Rhode Island student seminar, personal communication (1990).
40. "Quality Criteria for Water, 1986," U.S. EPA Report-440/5-86-001 (1987).
41. Hanson, D. Environmental Research Laboratory-Narragansett, personal communication (1990).

42. Capel, P. D., R. A. Rapaport, S. J. Eisenreich, and B. B. Looney. "PCBQ: Computerized Quantification of Total PCB and Congeners in Environmental Samples," *Chemosphere* 14(5):439-450 (1985).
43. Boehm, P. D., S. Freitas, E. Crecilius, R. Hillman, J. Payne, G. Farmer, A. Lissner, R. Sims, R. Shokes, J. Clayton, C. Peven, D. McGrath, H. Coasta, W. Steinhauer, and N. Young. "Collection of Bivalves and Surficial Sediments from Coastal U.S. Atlantic and Pacific Locations and Analysis for Organic Chemicals and Trace Elements. Phase 1 Final Report," National Oceanic and Atmospheric Administration, National Status and Trends Mussel Watch Program, Rockville, MA (1987).
44. Schults, D. W., S. P. Ferraro, G. R. Ditsworth, and K. A. Sercu. "Selected Chemical Contaminants in Surface Sediments of Commencement Bay and the Tacoma Waterways, Washington, USA," *Mar. Environ. Res.* 22:271-295 (1987).
45. Weaver, G. "PCB Contamination in and around New Bedford, MA," *Environ. Sci. Technol.* 18:22a-27a (1984).
46. Latimer, J. S., L. A. LeBlanc, J. T. Ellis, J. Zheng, and J. G. Quinn. "The Sources of PCBs to the Narragansett Bay Estuary," *Sci. Total Environ.* (in press).
47. Mackay, D., A. Bobra, and W. Y. Shiu. "Relationships between Aqueous Solubility and Octanol-Water Partition Coefficients," *Chemosphere* 9:701-711 (1980).
48. Mabey, W. R., J. H. Smith, R. T. Podoll, H. L. Johnson, T. Mill, T. W. Chou, J. Gates, I. W. Partridge, H. Jaber, and D. Vandenberg. "Aquatic Fate Process Data for Organic Priority Pollutants," U.S. EPA Report-440/4-81-014 (1982).
49. Kenaga, E. E., and C. A. I. Goring. "Relationship between Water Solubility, Soil Sorption, Octanol-Water Partitioning, and Concentration of Chemicals in Biota," *Aquatic Toxicology*, J. G. Eaton, P. R. Parrish, and H. C. Hendricks, Eds. (American Society for Testing and Materials, Philadelphia, 1980).
50. Rapaport, R. A., and S. J. Eisenreich. "Chromatographic Determination of Octanol-Water Partition Coefficients for 58 Polychlorinated Biphenyl Congeners," *Environ. Sci. Technol.* 18:163-170 (1984).
51. Miller, M. M., S. P. Waslk, G. L. Huang, W. Y. Shiu, and D. Mackay. "Relationships between Octanol-Water Partition Coefficients and Aqueous Solubility," *Environ. Sci. Technol.* 19:522-529 (1985).

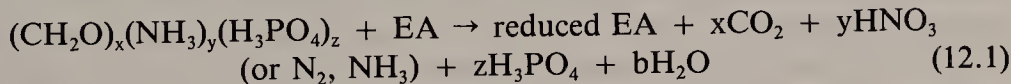
CHAPTER 12

Carbon Cycling in Coastal Sediments: 2. An Investigation of the Sources of ΣCO_2 to Pore Water Using Carbon Isotopes

Ann P. McNichol, Ellen R. M. Druffel, and Cindy Lee

INTRODUCTION

Oxidation of organic carbon during early diagenesis in coastal sediments is an important process which affects nutrient balances in coastal systems, the residence of pollutants in sediments, and the nature of the sediments themselves. Much of the organic matter that reaches the sediment-water interface in coastal regions is derived from organic matter produced in the surface waters; in many areas approximately 15–20% of the primary production reaches the sediment-water interface. A large percentage of the organic matter that reaches the sediments can be remineralized, i.e., oxidized to CO_2 . Oxidation of organic carbon in sediments proceeds with the use of electron acceptors (EA), available in seawater according to the following equation:



Electron acceptors are used in the order O_2 , NO_3^- and MnO_2 , Fe_2O_3 , SO_4^{2-} , and CO_2 and low-molecular-weight organic compounds.¹ Many of the compounds produced, and subsequently released to the sediment pore water, during the oxidation of organic carbon are important nutrients. Exchange between pore water and overlying water means that the oxidation of organic carbon in sediments can have an important effect on the amount of O_2 in overlying water, as well as the total amount of nutrients available for photosynthesis. Thus, it is important to understand the rates and mechanisms of oxidation in sediments.

It is generally recognized that hydrophobic organic pollutants are associated with the particulate organic matter in coastal systems. The exact nature of this association is still being studied, but it is likely that there are many types of associations possible and that the ultimate fate of pollutants will depend on the

type of association. Much of the organic matter that reaches the sediments is remineralized, a process which may alter the organic matrix in which pollutants reside. It is important to investigate not only the association of pollutants with organic matter, but any processes which may affect the associations. This chapter is concerned with the latter issue.

The oxidation of organic carbon in sediments can be traced by following the consumption or production of oxidants or decomposition products, respectively, in the pore water associated with sediments. In this study, we investigated the stable carbon isotope ratio— $\delta^{13}\text{C} = (\text{R}_{\text{sample}}/\text{R}_{\text{std}} - 1)10^3$, where $\text{R} = ^{13}\text{C}/^{12}\text{C}$ and $\text{R}_{\text{std}} = 0.0112372$ —of dissolved inorganic carbon (ΣCO_2) in order to investigate the processes affecting the production of dissolved inorganic carbon in coastal sediments.² Processes that have a major effect on pore-water inorganic carbon are the oxidation of organic carbon, exchange with bottom water, and the dissolution and precipitation of CaCO_3 . The $\delta^{13}\text{C}$ of ΣCO_2 is a sensitive indicator of the oxidation of organic matter within sediments because the $\delta^{13}\text{C}$ of sedimentary organic matter (approximately $-20.0\text{ }0/00$) is much less than that of bottom-water ΣCO_2 (approximately $0.0\text{ }0/00$) and CaCO_3 (approximately $+1.0\text{ }0/00$).³ The expected stoichiometric relationship between $\delta^{13}\text{C}-\Sigma\text{CO}_2$ and organic matter oxidants has been used to investigate a variety of processes in seawater and sediments. Deuser constructed a mass balance with the $\delta^{13}\text{C}$ of ΣCO_2 to determine the contribution of organic sulfur to the hydrogen sulfide pool in the Black Sea.⁴ Kroopnik has shown that the $\delta^{13}\text{C}$ of ΣCO_2 in deep ocean water is controlled mainly by the oxidation of organic carbon and the dissolution of CaCO_3 .⁵ Gradients in $\delta^{13}\text{C}$ of ΣCO_2 in pore water from sediment in the Pacific Ocean were used to calculate the organic carbon rain rate to sediments.⁶

In the studies discussed above, it was assumed that the organic matter had Redfield stoichiometry (C:N:P::106:16:1), a constant isotopic signature, and that oxidation occurred without isotopic fractionation. Other studies of the isotopic signature of ΣCO_2 in pore water suggest that these assumptions may not always be valid. Miller showed decreases with depth in the $\delta^{13}\text{C}$ of ΣCO_2 in pore water from sediments of the eastern equatorial Atlantic; he found that the ΣCO_2 added to the pore water was enriched in ^{13}C with respect to the organic matter in the sediments.⁷ Sayles and Curry found that the flux of ΣCO_2 from ocean sediments representing a wide range of redox conditions was enriched in ^{13}C over that expected from the stoichiometric oxidation of Redfield organic matter.⁸ In both studies, the enrichment was found even after CaCO_3 dissolution was accounted for. McArthur observed an enrichment of ^{13}C in pore water ΣCO_2 that he could not attribute to fractionation during the oxidation of organic matter or dissolution of CaCO_3 .⁹ In highly reducing sediments, it has been found that the $\delta^{13}\text{C}$ of ΣCO_2 can increase with depth in the sediment.¹⁰⁻¹³ This increase has been related to the production of highly ^{13}C -depleted CH_4 in these sediments.

In this study, we coupled an investigation of the $\delta^{13}\text{C}$ of ΣCO_2 in pore water with a comprehensive field study of pore-water chemistry and sediment envi-

ronment at a coastal site in order to define the sources of ΣCO_2 to pore water and to understand the observed variations in $\delta^{13}\text{C}$. We conducted the study at a coastal site to investigate the effect of seasonal changes in temperature and biological activity on the remineralization of organic carbon during early diagenesis in coastal sediments.

METHODS AND SITE DESCRIPTION

Site Description

Cores were collected at site M in Buzzards Bay, MA ($41^{\circ}31.25' \text{ N}$, $70^{\circ}45.7' \text{ W}$; Figure 12.1), previously described by McNichol et al.¹⁴ Briefly, the sampling site is in 15 m of water and has predominantly silty-clay sediments. The sediments contain approximately 20 mg C/g dry weight as organic carbon and are primarily sulfate reducing below 1 to 3 cm (Hobbie and Howarth, unpublished data). The overlying water is oxic throughout the year. There was no evidence, such as the exhaustion of dissolved sulfate in pore water or inflections in ΣCO_2 or $\delta^{13}\text{C}-\Sigma\text{CO}_2$ profiles, that the methane production zone was encountered in the sediments used in the studies described here.

The sampling strategy used to collect the cores and pore-water samples for the field study was described by McNichol et al.¹⁴ Briefly, five cores were collected between October 1983 and March 1985; the exact sampling dates and water temperature at the sampling time are listed in Table 12.1. Samples were collected for the analysis of ΣCO_2 , $\delta^{13}\text{C}-\Sigma\text{CO}_2$, alkalinity (Alk), Ca, PO_4^{3-} , H_2S , DOC, and SO_4^{2-} . In this chapter, we concentrate on the $\delta^{13}\text{C}-\Sigma\text{CO}_2$, ΣCO_2 , and Ca results; other results are discussed in McNichol¹⁵ and McNichol et al.¹⁴ The sediments were sectioned in a nitrogen atmosphere, and pore water was separated by centrifuging the sediment. Pore water was transferred to a 10-mL syringe and filtered through a 0.64- μm Nuclepore filter. A small portion of the sample was used to rinse the filter. Samples for ΣCO_2 analysis were collected first; a 1-mL sample of pore water was transferred directly into a 1-mL tuberculin syringe and analyzed within the hour. Samples for the analysis of $\delta^{13}\text{C}-\Sigma\text{CO}_2$ were taken immediately after collecting the ΣCO_2 sample. Water for isotopic analysis was filtered directly into a 3-mL syringe, transferred quickly into a 2-mL poisoned septum vial, and sealed with no headspace. A few crystals of HgCl_2 were used as the poison. Samples were stored in the dark at 4°C until analyzed for $\delta^{13}\text{C}$. Isotopic samples were always stripped and analyzed within 6 weeks of collection, and usually within 2 weeks. Recent laboratory work has shown that seawater samples can be stored up to 3 months without affecting the $\delta^{13}\text{C}-\Sigma\text{CO}_2$ (McNichol and Druffel, unpublished). The analytical methods used to analyze ΣCO_2 , $\delta^{13}\text{C}-\Sigma\text{CO}_2$, and Ca are discussed below. Subsequent samples were collected for Alk, Ca^{2+} , PO_4^{3-} , H_2S , DOC, and SO_4^{2-} . Sediment for solid-phase analyses was transferred to clean glass jars and stored at -40°C before being freeze-dried.

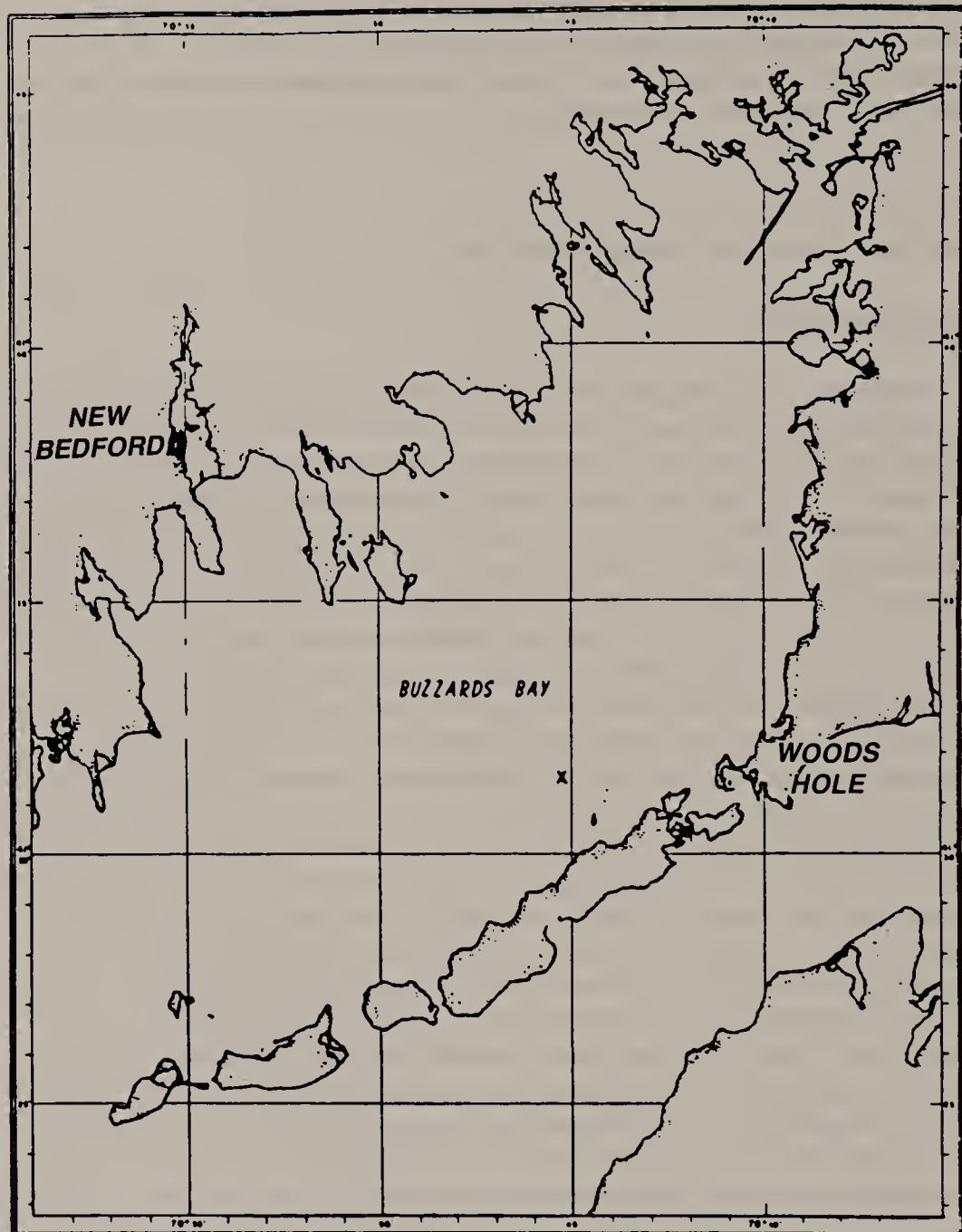


Figure 12.1. Sampling site in Buzzards Bay, MA: x, location of the site.

Chemical Analyses

Standard analytical methods were used for the analyses of ΣCO_2 and dissolved Ca^{2+} . ΣCO_2 samples were acidified with 2 N H_3PO_4 , stripped with helium, and measured by gas chromatography. This analysis was made immediately after sample collection; the precision of the analyses was $\pm 3\%$. Differ-

Table 12.1. Dates on Which the Cores for This Study Were Collected, the Water Temperature at the Time of Collection, and the Sediment Diffusion Coefficients for ΣCO_2 and Ca

Core Date	Temperature (°C)	$D_s \times 10^6 \text{ cm}^2/\text{sec}$	
		D_{HCO_3}	D_{Ca}
Oct. 17, 1983	15	6.4	4.1
Dec. 16, 1983	7	5.3	3.4
June 20, 1984	16	6.5	4.2
Aug. 30, 1984	21	7.1	4.6
March 26, 1985	4	5.0	3.2

ent analysis techniques were used for the measurement of ΣCO_2 during two months of the seasonal study. In October 1983, instead of measuring ΣCO_2 , pH was measured on the first aliquot of pore water collected. In March 1985, a different method was used to collect and analyze the ΣCO_2 samples because the gas chromatograph normally used was not available. For these samples, a 1-mL aliquot of the filtered sample was stored in a poisoned (HgCl_2) 2-mL septum vial. The samples were analyzed using a headspace technique within 10 hr of collection. The precision of the analyses was $\pm 10\%$. A high-precision EGTA (ethyleneglycol-bis(2-aminoethyl ether)-N,N,N',N'-tetra-acetic acid) titration described by Shiller and Gieskes was used to measure calcium.¹⁶ The precision of the Ca^{2+} titration was $\pm 0.2\%$.

Samples for the analysis of $\delta^{13}\text{C}-\Sigma\text{CO}_2$ were prepared in the following manner. Approximately 1 mL of the sample was introduced to an evacuated stripping chamber containing 1 mL of 100% H_3PO_4 . CO_2 -free nitrogen gas introduced through a glass frit underneath the sample was used to mix the acid and water and to strip CO_2 from the solution. The CO_2 collected was purified, and its isotopic ratio was measured on a VG-Micromass 602E mass spectrometer. Batches of local surface seawater were used to calculate the precision of the total analysis. Based on the analysis of 21 samples from two batches of seawater, the precision of the isotopic analysis is $\pm 0.2\text{‰}$. The $\delta^{13}\text{C}$ of solid-phase organic carbon (C_{org}) was measured on sediment samples prepared using a closed-tube combustion technique first reported by Sofer.¹⁷

RESULTS

Depth profiles of ΣCO_2 , $\delta^{13}\text{C}-\Sigma\text{CO}_2$, and Ca^{2+} in site M sediments are presented in Figure 12.2. The sediment profiles of $\delta^{13}\text{C}-\Sigma\text{CO}_2$ show an overall decrease with depth to a value of approximately -10.0‰ . In the October 1983 and June 1984 profiles, there is a minimum in the $\delta^{13}\text{C}$ profile between 4 and 10 cm. The relationship of $\delta^{13}\text{C}-\Sigma\text{CO}_2$ to ΣCO_2 is shown in Figure 12.3; a negative correlation is apparent. Data collected between 0 and 4 cm in June 1984 are represented separately because they appear to be enriched in ^{13}C . This anomaly will be discussed later. The concentrations of Ca^{2+} remained relatively constant over the depths sampled except in two months. In June 1984

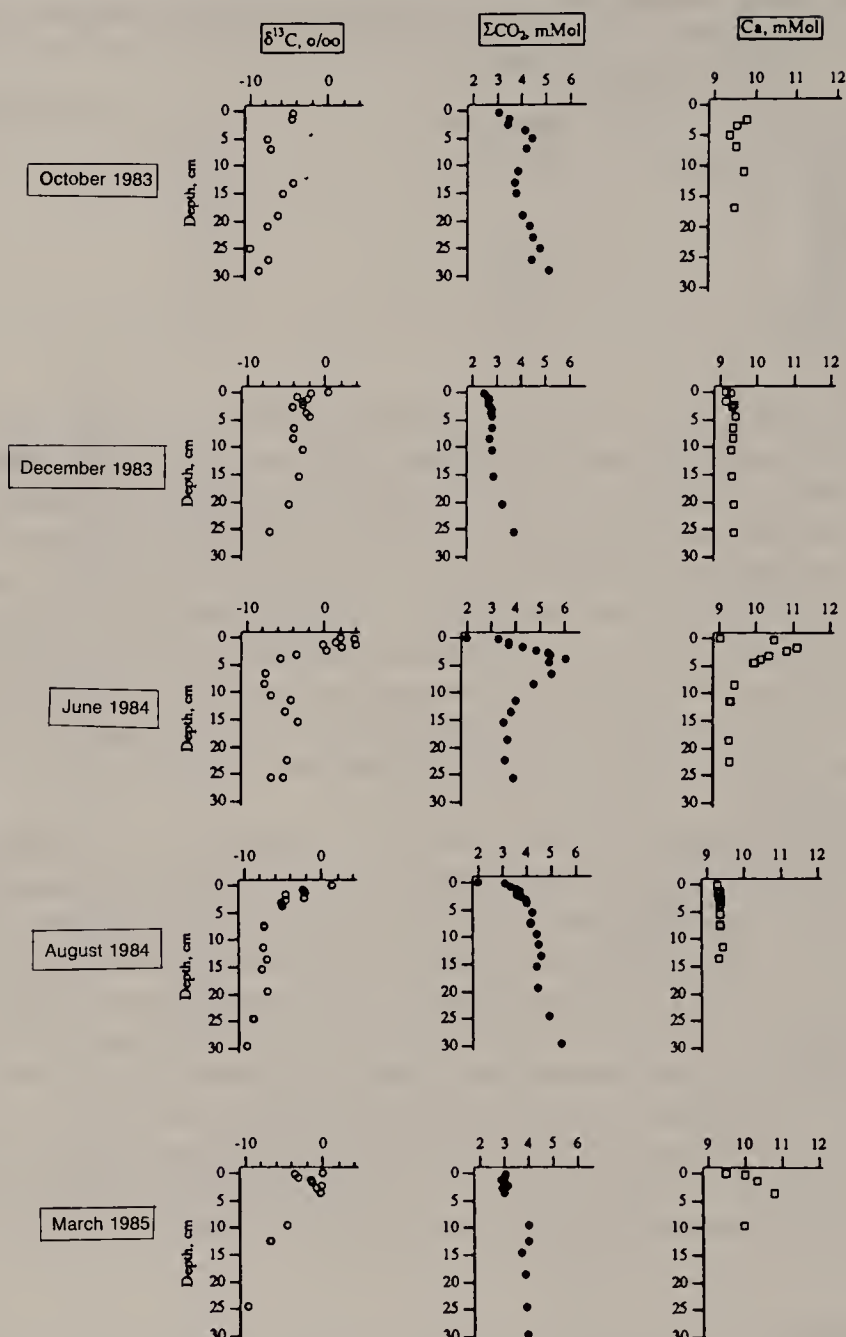


Figure 12.2. Depth profiles of $\delta^{13}\text{C}$ - ΣCO_2 , ΣCO_2 , and Ca^{2+} for the five cores that were collected as part of this study. The bottom water concentration is represented by the point that is centered on the x-axis. The sampling interval for these sediments was 0.5 cm in the upper 4 cm of the sediment column and 1.0 cm below 4 cm, except in October, when the interval was 1.0 cm above 4 cm and 2.0 cm below 4 cm.

and March 1985, the concentration of Ca^{2+} showed large maxima in the surface 4 cm. The $\delta^{13}\text{C}$ of C_{org} (Figure 12.4) changed little with depth and time; the average $\delta^{13}\text{C}$ of C_{org} is -20.6 ± 0.2 ‰.

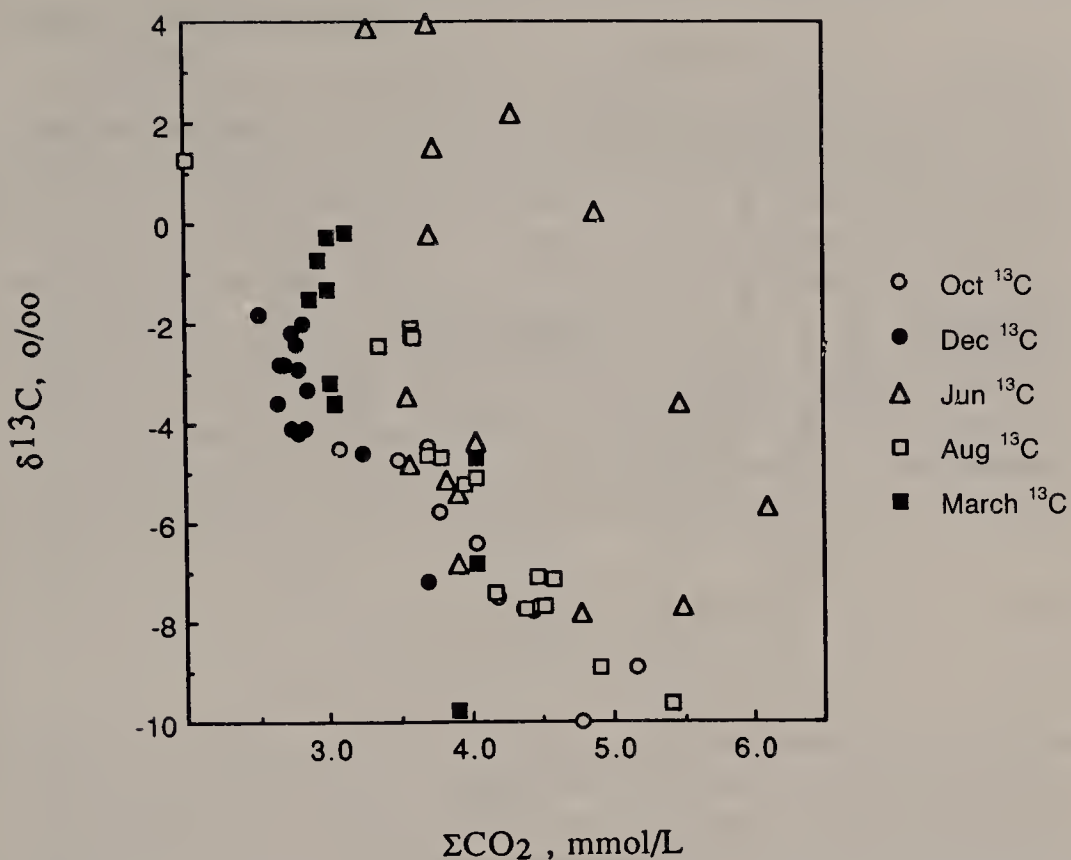


Figure 12.3. Variation of $\delta^{13}\text{C}$ with ΣCO_2 for the five cores sampled. The data from June 1984 which appear to lie on a different curve from the rest of the data are all from samples collected between 0 and 4 cm in the sediments.

DISCUSSION

The data collected in this study were used to investigate the sources of inorganic carbon to the pore water at site M. The oxidation of organic carbon in these sediments is an efficient process; 70–90% of the organic matter that reaches the sediment water interface is oxidized in the upper 30 cm of the sediments column.¹⁴ In general, the oxidation of organic matter will increase the concentration of carbon in the pore water and decrease $\delta^{13}\text{C}-\Sigma\text{CO}_2$. Exchange with bottom water will dilute the signal from oxidation by mixing in water with a relatively low carbon concentration and high isotopic ratio. The dissolution of CaCO_3 will increase the concentration of ΣCO_2 and have no effect or slightly increase the $\delta^{13}\text{C}-\Sigma\text{CO}_2$, and precipitation of CaCO_3 will have the opposite effect. The negative correlation between $\delta^{13}\text{C}$ and ΣCO_2 shown in Figure 12.3 indicates that the oxidation of organic carbon is an important process in these sediments. To fully understand the data, it is necessary to construct a model describing the processes affecting the $\delta^{13}\text{C}-\Sigma\text{CO}_2$ in coastal sediments. Physical disturbances such as mixing by tides and waves or biological activity can enhance the exchange between pore water and the overlying

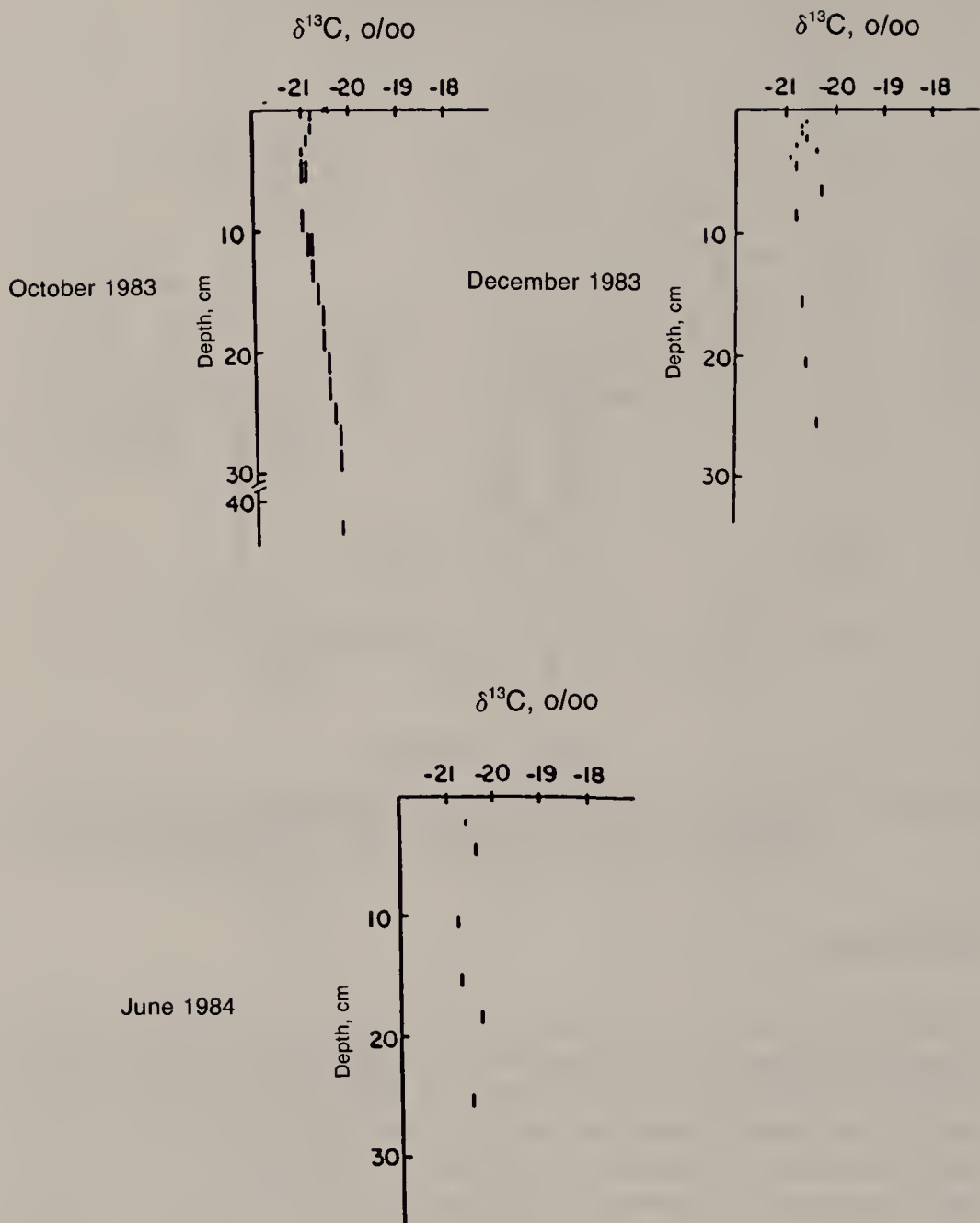


Figure 12.4. Measured values of $\delta^{13}\text{C-C}_{\text{org}}$ in the sediments at site M. The length of the symbol represents the sediment interval which was sampled.

water column. Microbial communities in the sediments oxidize organic matter at different rates depending on the availability and quality of the organic matter, the temperature, and location and size of the microbial population. We have constructed a model which accounts for the effects these factors will have on the $\delta^{13}\text{C-S}\Sigma\text{CO}_2$ profile in the sediments at site M.

Isotope Model Description

The model used to describe the profiles of $\delta^{13}\text{C}-\Sigma\text{CO}_2$ is a diffusion-advection-reaction model in which the reaction term encompasses the oxidation of organic carbon and the dissolution or precipitation of CaCO_3 , and a term which describes enhanced exchange with bottom water has been added. The model is shown in Figure 12.5. Changes in the concentration of ΣCO_2 due to oxidation of organic matter or equilibration with CaCO_3 are described by a CO_2 -production rate, $R_c(z)$. The function $R_c(z)$ is defined as two exponentially decreasing terms. The first term is used from the surface of the sediments to a depth, z_b and the second is used below z_b . This function was based on a study by Westrich and Berner, which showed that phytoplankton remains consist of two "metabolizable" fractions and a nondegradable fraction.¹⁸ The degradable fractions decompose at rates that decrease exponentially with time. The functions describing $R_c(z)$ are

$$R_c = R_o \exp(-\beta_1 z) \quad \text{from } 0 \text{ to } z_b \quad (12.2)$$

$$R_c = R_{zb} \exp(-\beta_2(z - z_b)) \quad \text{from } z_b \text{ to } \infty \quad (12.3)$$

where z_b is the depth at which the rapidly degradable material is exhausted and $R_{zb} = R_o \exp(-\beta_1 z_b)$. As defined, $R_c(z)$ also includes the net effects of equilibration with CaCO_3 . However, in these sediments, the shape of the profile is most likely dominated by oxidation because the profiles of dissolved Ca indicate that there is not a lot of dissolution or precipitation of CaCO_3 . The two months in which dissolution appear to be important are June 1984 and March 1985. McNichol et al. showed that in June 1984 the dissolution of CaCO_3 accounts for only 2% of the ΣCO_2 produced.¹⁴ As is discussed shortly, this model was not applied to the March 1985 data.

The enhanced transport of ΣCO_2 due to biological irrigation was described using the nonlocal source model of Emerson and Bender.¹⁹ In this model, an exchange parameter, $\alpha(z)$, is defined to allow direct exchange between bottom water and sediment pore water at any depth in the sediments, as indicated in Figure 12.5. Sediment diffusion coefficients (D_s) were calculated from the seawater molecular diffusion coefficients (D_{mol}) with the following equation:

$$D_s = D_{\text{mol}}/\theta^2 \quad (12.4)$$

where θ = tortuosity of the sediments, and

$$\theta = \phi(R/R_o) \quad (12.5)$$

where ϕ is porosity and R/R_o is the ratio of resistivity of bulk sediment to interstitial fluid. In these sediments, $D_s = 0.65 D_{\text{mol}}$. The values of D_{mol} reported in Li and Gregory were first corrected to the observed temperatures.²⁰ The calculated values of D_s are listed in Table 12.1.

To use the model to calculate the $\delta^{13}\text{C}$ of ΣCO_2 added to the pore water,

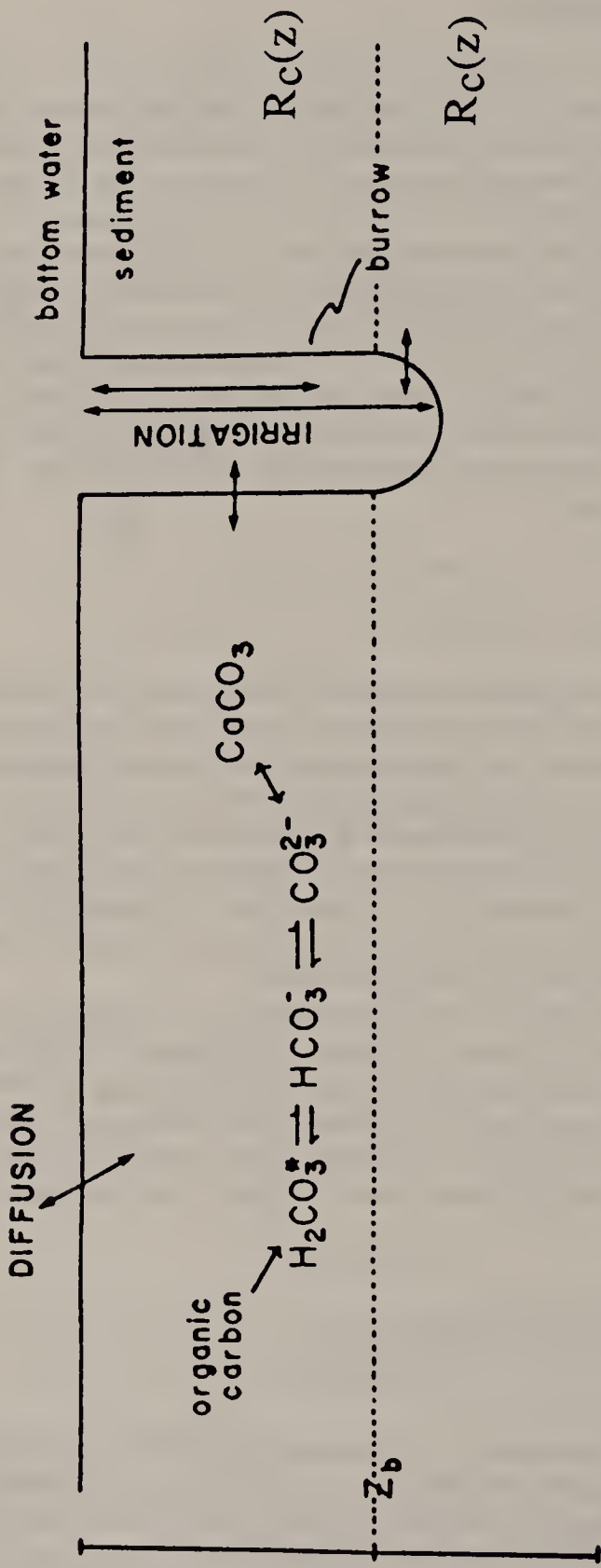


Figure 12.5. Model used to describe the profiles of $\delta^{13}\text{C}-\Sigma\text{CO}_2$ in the sediments.

Table 12.2. Parameters Used to Fit the Observed $\delta^{13}\text{C}$ - ΣCO_2 and ΣCO_2 Data

Date	$\delta^{13}\text{C}_{\text{add}}$	$R_c(z)$					$\alpha_{\text{Rn}}(z)$
		R_o ($\times 10^{-9}$)	β_1	β_2	z_b		
Oct. 1983	-14.6	5.8	0.19	4.80	5.4	$3.5 \times 10^{-6} \exp(-a)$	
June 1984	-6.3	5.1	0.14	0.20	3.3	3.7×10^{-7}	
						$5.6 \times 10^{-5} \exp(-b)$	
Aug. 1984	-10.8	7.5	0.30	0.32	0.3	$1.8 \times 10^{-6} \exp(-c)$	
Dec. 1983	-10.0						
March 1985	-10.4						

Notes: The model fits to the isotopic data shown in Figure 12.6. $\delta^{13}\text{C}_{\text{add}}$ is the value of $\delta^{13}\text{C}$ of ΣCO_2 added during early diagenesis; in December 1983 and March 1985, $\delta^{13}\text{C}_{\text{add}}$ was calculated using core-top gradients. $R_c(z)$ is the function $R_o \exp(-\beta_1 z)$ used to describe the CO_2 -production rate; if two exponential functions are used, the second is $R_2 \exp[-\beta_2(z - z_b)]$, where $R_2 = R_o \exp(-\beta_1 z_b)$. $\alpha_{\text{Rn}}(z)$ is the function used to describe the irrigation term. $a = z/2.63$; $b = z/4$; $c = z/4.34$.

equations must be written for each stable isotope of carbon, ^{13}C and ^{12}C . The equation describing the change of ΣCO_2 with time and depth is

$$\frac{\partial \Sigma^a\text{CO}_2}{\partial t} = D_{\text{HCO}_3}(d^2\Sigma^a\text{CO}_2/dz^2) - \alpha(z)(\Sigma^a\text{CO}_2 - \Sigma^a\text{CO}_{20}) + ^aR_c(z) \quad (12.6)$$

In this equation, the superscript a refers to the carbon atom under consideration (i.e., ^{12}C or ^{13}C), ΣCO_{20} is the bottom-water ΣCO_2 concentration, and the other parameters are discussed below. The concentrations of the individual isotopes in carbon reservoirs were calculated from measured values of $\delta^{13}\text{C}$ and the concentration of total carbon in each reservoir. The diffusion coefficient, D_{HCO_3} (cm^2/sec), is the sediment diffusion coefficient for HCO_3^- listed in Table 12.1. It is assumed that the diffusion coefficients of $\text{H}^{13}\text{CO}_3^-$ and $\text{H}^{12}\text{CO}_3^-$ are the same because the actual difference is inversely proportional to the ratio of the square root of the masses and thus is negligible.

The model is used to calculate the profiles of $\delta^{13}\text{C}-\Sigma\text{CO}_2$ expected at site M, where the seasonal rates of oxidation and nonlocal exchange are well known. In a study of the rates of oxidation of organic carbon at site M, values of $R_c(z)$ were defined using a model similar to the one described here to reproduce the profiles of ΣCO_2 observed in the same cores used in this study.¹⁴ The values reported by McNichol et al. are listed in Table 12.2 and are used in the isotope model.¹⁴ McNichol et al. found that the profiles of ΣCO_2 were fit well using these values and that changing $R_c(z)$ by a factor of two greatly changed the model-predicted profiles.¹⁴

The effects of biological irrigation on exchange between bottom water and pore water at site M have been studied extensively using ^{222}Rn .²¹ Martin and Sayles used ^{222}Rn profiles to define an irrigation parameter for ^{222}Rn , $\alpha_{\text{Rn}}(z)$, on cores collected seasonally at site M. We used the values of $\alpha_{\text{Rn}}(z)$ reported by Martin and Sayles for the months of October 1982, June 1984, and September 1983 to model carbon isotope data from October 1983, June 1984, and August 1984, respectively; the values are listed in Table 12.2.²¹ Martin and Sayles also

showed that irrigation was not an important exchange mechanism in the colder months.²¹ Martin has estimated that the calculated values of $\alpha_{Rn}(z)$ are known to $\pm 20\%$ (personal communication). We adjusted $\alpha_{Rn}(z)$ to $\alpha(z)$ using the diffusion coefficients of HCO_3^- and Rn .

To solve Equation 12.1, we assumed that the observed isotopic profiles were at steady-state concentrations, i.e., $\partial\Sigma^aCO_2/\partial t = 0$. McNichol used a non-steady-state model to show that, at reaction and irrigation rates typical of the sediments at site M, a steady-state approximation is only valid in warmer months.¹⁵ In these months, using an extreme assumption about initial conditions, it takes about 4 weeks for the sediments ΣCO_2 profile to reach 80% of its steady-state profile. Under more realistic conditions, the approach to steady state will be more rapid. Because of the steady-state assumption, it is only possible to apply this model to data from October 1983, June 1984, and August 1984.

Using the above-defined parameters, the only parameter necessary to define is a value for the $\delta^{13}C$ of the carbon added ($\delta^{13}C_{add}$) to the sediments during early diagenesis. We have approached the definition of $\delta^{13}C_{add}$ in two ways. First, we generated sediment profiles of $\delta^{13}C-\Sigma CO_2$ using values of $\delta^{13}C_{add}$ of -20 0/00 and -10 0/00. Second, we used a grid-search method to optimize the model fit to the data by varying the value of $\delta^{13}C_{add}$.²² The fits obtained for October 1983, June 1984, and August 1984 are shown in Figure 12.6 (*solid lines*); the best-fit value for $\delta^{13}C_{add}$ determined using the model is listed in Table 12.2.

Isotope Model Results

It is apparent from Figure 12.6 that, except in August 1984, the model does not describe the data well. The model does reproduce the general shape of the profile by indicating that there is a sharp gradient at the interface and a local minimum at approximately 4 cm. The model does not reproduce the magnitude of the maxima and/or minima observed in the data. As mentioned earlier, the isotope model is similar to the model that was used to accurately describe the ΣCO_2 profiles observed at this site.¹⁴ The inability of the isotope model to describe the observed isotopic data accurately when the ΣCO_2 profiles were well described with a similar model suggests that the latter model describing the ΣCO_2 profile does not take into account all the processes affecting ΣCO_2 in pore waters.

Although the model was not able to reproduce all the features of the observed profiles, there is a clear indication that $\delta^{13}C_{add}$ in the pore water was enriched in ^{13}C with respect to C_{org} ($\delta^{13}C = -20.6\ 0/00$). In each of the plots in Figure 12.6, the expected profile of $\delta^{13}C-\Sigma CO_2$ assuming that $\delta^{13}C_{add}$ is -20 0/00 (*dashed line*) consistently predicts values much lower than those observed in the field. Using a value of -10 0/00 for $\delta^{13}C_{add}$ (*dotted line*) generates a profile that more closely approximates the observed data in June 1984 and August 1984, but is too enriched in ^{13}C in October 1983. Even using a value of -10 0/00

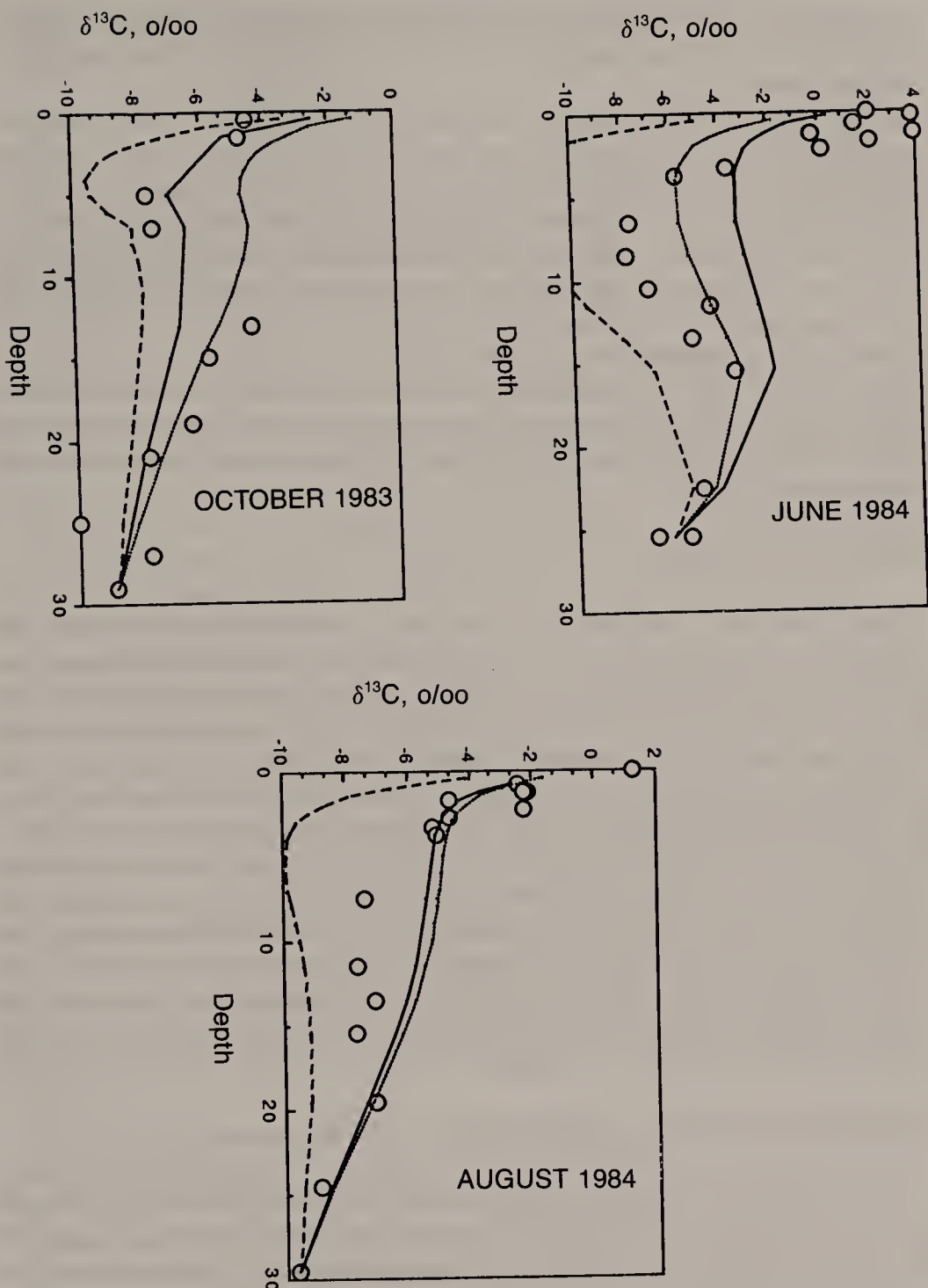


Figure 12.6. Model-derived profiles of $\delta^{13}\text{C}-\Sigma\text{CO}_2$ for October 1983, June 1984, and August 1984. The data are represented by the open symbols; the calculated best-fit is represented by the solid line. The model fit found using $\delta^{13}\text{C}_{\text{add}} = -10$ 0/‰ is shown with the dotted line, and the fit using $\delta^{13}\text{C}_{\text{add}} = -20$ 0/‰ is shown with the dashed line.

in June 1984, it is not possible to reproduce the data collected between 0 and 4 cm in June 1984. The anomalous $\delta^{13}\text{C}$ enrichment observed in these samples is discussed later.

Using the grid-search method to obtain the best fit, the model-predicted value for $\delta^{13}\text{C}_{\text{add}}$ is -14.6 ‰ in October 1983, -6.3 ‰ in June 1984, and -10.8 ‰ in August 1984. In the colder months, when this model is inappropriate, we used the core-top gradient in $\delta^{13}\text{C}-\Sigma\text{CO}_2$ to evaluate $\delta^{13}\text{C}_{\text{add}}$; $\delta^{13}\text{C}_{\text{add}}$ is -10.0 ‰ in December 1983 and -10.4 ‰ in March 1985. Thus, data from all the cores indicate that the inorganic carbon added to the pore water during early diagenesis is enriched in ^{13}C with respect to C_{org} ($\delta^{13}\text{C} = -20.6\text{ ‰}$). Several possible explanations could account for this enrichment. A significant amount of CO_2 may be produced from the dissolution of CaCO_3 , carbon isotopes may be fractionated during the oxidation of C_{org} , or there may be an unidentified source of ^{13}C -enriched carbon to the pore water. These hypotheses are discussed below.

Dissolution of CaCO_3

The concentration of Ca^{2+} in the pore water was measured to monitor the dissolution or precipitation of CaCO_3 . The only significant increases or decreases in dissolved Ca^{2+} were observed in June 1984 and March 1985. In these months, the magnitude of the dissolution is still too small to account for the isotopic differences between the added carbon and $\text{C}_{\text{org}}^{14}$ and can never account for values greater than 2.0 ‰ . In June 1984, McNichol et al. calculated that dissolution of CaCO_3 could account for 2% of the ΣCO_2 produced.¹⁴ If the $\delta^{13}\text{C}$ of the dissolving CaCO_3 is 1.7 ‰ , the average value measured on shells in these sediments,¹⁵ and the rest of the ΣCO_2 produced was from the oxidation of organic carbon, the value of $\delta^{13}\text{C}_{\text{add}}$ would change only from -20.6 ‰ to -20.1 ‰ . In March 1985, CaCO_3 dissolution has the largest effect, accounting for almost 25% of the diffusive carbon flux across the sediment-water interface, but even this large contribution will only change $\delta^{13}\text{C}_{\text{add}}$ from -20.6 ‰ to -15.2 ‰ .

Fractionation of Carbon Isotopes During the Oxidation of C_{org}

It is possible that the CO_2 produced during the oxidation of C_{org} is isotopically distinct from the bulk organic carbon. In a coastal environment it is difficult to evaluate this possibility using field data since extensive mixing of the sediments makes it unlikely that a significant gradient could be observed in the $\delta^{13}\text{C}$ of C_{org} . Also, it is difficult to define the $\delta^{13}\text{C}$ of the organic matter deposited at the sediment-water interface because of the difficulty in collecting a sample of sedimenting organic matter that has not been contaminated with resuspended matter.

In order to investigate the possibility of fractionation during organic carbon oxidation, we conducted laboratory studies to define the $\delta^{13}\text{C}$ of ΣCO_2 arising

Table 12.3. Values of $\delta^{13}\text{C}_{\text{exp}}$ (o/oo) Calculated from the Laboratory Experiments

t (days)	0–3 cm	12–15 cm	18–21 cm
2	-19.8 ± 4.8	*	*
8	-16.6 ± 2.5	*	*
19	-16.9 ± 1.7	n.s.	n.s.
31	n.s.	-16.6 ± 4.0	-26.3 ± 9.8
46	-21.2 ± 2.1	-20.9 ± 3.9	-23.6 ± 4.1

Note: The left-hand column indicates the length of the incubation, and the top row indicates the depth from which the sediment was collected.

n.s.—no sample taken.

*—Observed concentration changes too small for significant calculations.

from the oxidation of C_{org} in Buzzards Bay sediments.^{15,23} The experiments were conducted in a controlled environment, allowing us to observe organic carbon oxidation in these sediments without the complications of diffusion, irrigation, and mixing. The $\delta^{13}\text{C}$ of ΣCO_2 added over time in the pore water ($\delta^{13}\text{C}_{\text{exp}}$) during the experiments was calculated using a mass balance. Since there was little net dissolution or precipitation of CaCO_3 over the course of the experiment, we assume that the value of $\delta^{13}\text{C}_{\text{exp}}$ represents the average $\delta^{13}\text{C}$ of the total organic carbon that is oxidized in the sediments. Table 12.3 lists the values of $\delta^{13}\text{C}_{\text{exp}}$ that were calculated. In the surface sediments (0–3 cm interval), the results indicate that $\delta^{13}\text{C}_{\text{exp}}$ is greater than that of the organic carbon in the sediments (-20.6 o/oo). Most of the results from the deeper sediments (12–15 and 18–21 cm intervals) indicate that the $\delta^{13}\text{C}$ of the added carbon is equal to or more ^{13}C -depleted than the sediment organic carbon. In the surface interval, the rate of microbial activity is great enough for large changes to be observed in the values of $\delta^{13}\text{C}-\Sigma\text{CO}_2$ and ΣCO_2 over a short period of time. Thus, time-dependent artifacts resulting from long-term incubations of the sediment are minimized. Additionally, the values of $\delta^{13}\text{C}_{\text{exp}}$ calculated from the 0–3 cm interval are believed to represent most accurately the fractionation of C_{org} that would be observed in the field in the zone of rapid remineralization. Using all the data from 0–3 cm, we calculate that the weighted average value of $\delta^{13}\text{C}_{\text{exp}}$ is -18.6 ± 1.5 o/oo. This value is significantly (1σ) greater than the $\delta^{13}\text{C}$ of C_{org} .

These laboratory studies suggest that one reason modeling the field data produces an unexpected value for the $\delta^{13}\text{C}$ of added carbon is that there is fractionation during the oxidation of organic carbon in the sediments. Additionally, the apparent difference between $\delta^{13}\text{C}_{\text{exp}}$ in the surface and deep sediments may mean that the model assumption that $\delta^{13}\text{C}_{\text{add}}$ is constant with depth is an approximation, and a more realistic model might take this into account. It is also possible that these results are due to the exchange of CO_3^{2-} with CaCO_3 present in the sediments or to the uptake of CO_2 during chemosynthesis or other microbial processes (e.g., anaplerotic sequences). Isotopic exchange with CaCO_3 is not a likely explanation of the ^{13}C enrichment because the rates of exchange would have to be faster than reasonably expected. Based on the maximum amount of O_2 available, any microbially produced organic matter

would need a $\delta^{13}\text{C}$ of -100 ‰ or less to account for the results observed here; this is very unlikely. Further studies are needed to confirm that there is a fractionation occurring during the oxidation of organic matter in sediments.

The observed fractionation during the oxidation of organic carbon may be the result of selective remineralization of different compounds. At a molecular level, the microorganisms responsible for the oxidation of C_{org} may cleave carboxyl groups selectively from molecules. Carboxyl carbons are known to be enriched in ^{13}C with respect to the rest of the molecule.²⁴ Carbohydrates and amino acids, relatively labile compounds that are relatively enriched with ^{13}C ,²⁵ may also be degraded preferentially. Finally, the observed fractionation may be the result of the multiple sources of carbon to the sediment-water interface in coastal areas. The organic carbon is most likely a mixture of phytoplankton, terrestrial, and salt marsh carbon. Phytoplankton carbon is very reactive¹⁸ and is most likely the first fraction to be degraded. The calculated value of $\delta^{13}\text{C}_{\text{exp}}$, -18.5 ‰, is close to that measured on a plankton tow sample from Buzzards Bay (-17.7 ‰)¹⁵ and is within the range of values previously measured for plankton in the North Atlantic and Pacific.^{26,27} The isotopic similarity between phytoplankton carbon and $\delta^{13}\text{C}_{\text{exp}}$ implies that the oxidized carbon is phytoplankton derived and may reflect the reactivity of the planktonic organic matter.

The rate of carbon remineralization in Buzzards Bay sediments was calculated to be 69 g C/m² year.¹⁴ The postulation of fractionation during the oxidation of organic carbon appears inconsistent with the lack of a gradient in $\delta^{13}\text{C}-\text{C}_{\text{org}}$ with depth in the sediments (Figure 12.4); we would expect $\delta^{13}\text{C}-\text{C}_{\text{org}}$ to change from -19 ‰ to -21 ‰ with depth in the sediments. However, the results from the laboratory studies indicated that the fractionation is limited to the surface of the sediments, an area where the sediments are so rapidly mixed that a gradient would not be seen.

Role of Dissolved Organic Carbon (DOC) in Fractionation

At the surface of sediments, the concentration of DOC in pore water increases with depth because DOC is produced from either the oxidation or dissolution of C_{org} . If oxidation or dissolution occurs with fractionation which results in relatively ^{13}C -depleted DOC (i.e., $\delta^{13}\text{C}_{\text{DOC}} < \delta^{13}\text{C}_{\text{org}} < \delta^{13}\text{C}_{\text{add}}$), then production of DOC could explain the carbon isotope imbalance in the model studies. Isotopic studies of DOC in the ocean indicate that the $\delta^{13}\text{C}$ of DOC in the water column is either the same as or greater than that of particulate organic carbon (POC).²⁸⁻³⁰ In the pore waters of reducing sediment, the $\delta^{13}\text{C}$ of DOC was found to be the same as or less than that of the C_{org} .^{10,13} However, a recent study indicates that the methods commonly used to measure DOC may underestimate the concentration of DOC by a factor of two or three.³¹ The stable carbon isotopic content of the unmeasured DOC is unknown. DOC is composed of a variety of compounds, such as lipids and amino acids, of which only a small percentage have been characterized. These compounds have very

different reactivities, $\delta^{13}\text{C}$ signatures, and most likely have very different mobilities in pore water. However, there is little known about the rate of transfer of DOC from pore water to overlying water. This rate is dependent on the concentration of DOC and its diffusivity; the diffusivity is related to the size and reactivity of DOC. Observed DOC gradients suggest that DOC diffuses from pore water to overlying water at site M.^{15,32} Studies of the size of DOC in coastal pore water show that 50–90% of the DOC is in a high-molecular-weight fraction assumed to diffuse at such a slow rate that diffusion could not be an important source of this material to the overlying water.^{33,34} Questions about the reactivity of DOC further cloud the issue of the mobility of DOC. It is known that some fraction of DOC is adsorbed by aluminum and iron oxides,³⁵ but once the particles are coated, it is uncertain how they will react with the remaining DOC. Thus, DOC is a potentially important factor in the sedimentary carbon cycle, but at present too little is known to evaluate its significance.

Unidentified Sources of ^{13}C -Enriched Carbon to the Pore Water

The fractionation of carbon observed in the laboratory experiments is not large enough to explain fully the enrichment of ^{13}C observed in ΣCO_2 over that expected from the unfractionated oxidation of organic matter. Thus, other processes must be enriching ^{13}C in the pore waters. It is possible that the production of acid in pore water during early diagenesis creates conditions where exchange between ^{13}C and ^{12}C in overlying water and pore water is possible. Thus, one source of ^{13}C -enriched carbon may be carbonate ion from bottom water. Sayles and Curry have suggested this mechanism may be important in deep-sea sediments,⁸ although McArthur found that this process could not explain data from the Madeira Abyssal Plain.⁹ We used the measured values of Alk, ΣCO_2 , H_2S , and PO_4^{3-} concentrations in the pore water to calculate the concentrations of CO_3^{2-} , HCO_3^- , and H_2CO_3^* in bottom water and pore water. The concentration of CO_3^{2-} is much greater in bottom water than in pore water (155 $\mu\text{mol/L}$ vs 27 $\mu\text{mol/L}$). Because of the large concentration gradient, there could be a flux of CO_3^{2-} from bottom water to pore water, although there is a net flux of ΣCO_2 from pore water to bottom water. Most of the carbonate ion would become protonated in the pore water (pH 6.2–7.7) and would be transferred back across the interface. This exchange could also occur across burrow walls, thus enhancing transport in heavily bioturbated areas.

The magnitude of the proposed flux (J_{bw}) can be calculated in two ways. One method uses the calculated concentrations of CO_3^{2-} , and the other uses the measured isotopic ratios. In both calculations it is assumed that the flux of a species to and from bottom water is composed of the diffusive flux across the sediment-water interface (J_{dif}) and the flux due to irrigation (I), i.e., $J_t = J_{dif} + I$, where

Table 12.4. Values Calculated for J_{bw} , the Amount of the Total Flux of ΣCO_2 That Can Be Attributed to Recycled Bottom Water Carbonate Ion

Month	Concentration Used	$J_{bw} \times 10^{12}$	% J_t	$\delta^{13}C - J_t$
October 1983	CO_3^{2-}	0.5	2	
	$^{13}C (-20.6)$	3.1	14	-14.8
	$^{13}C (-18.5)$	1.3	6	
December 1983	CO_3^{2-}	2.2	22	
	$^{13}C (-20.6)$	3.4	34	-10.1
	$^{13}C (-18.5)$	2.9	29	
June 1984	CO_3^{2-}	1.2	15	
	$^{13}C (-20.6)$	1.7	23	-13.3
	$^{13}C (-18.5)$	1.2	16	
August 1984	CO_3^{2-}	5.2	11	
	$^{13}C (-20.6)$	13.5	28	-10.5
	$^{13}C (-18.5)$	1.1	23	
March 1985	CO_3^{2-}	1.6	8	
	$^{13}C (-20.6)$	3.0	16	-10.3
	$^{13}C (-18.5)$	1.8	10	

Notes: The fluxes were calculated using the concentrations of carbonate ion and again with the total dissolved concentrations of ^{13}C and ^{12}C . The values in parentheses represent the values of $\delta^{13}C$ of ΣCO_2 produced from the oxidation of organic carbon assumed for the calculation. The fluxes are reported in mol/cm² sec.

$$J_{dif} \equiv -\phi D_s \Delta C / \Delta z|_{z=0} \quad (12.7)$$

$$I = \int_0^{20} -\phi \alpha (C_z - C_o) dz \equiv \sum_o -\phi \alpha (C_z - C_o) \Delta z \quad (12.8)$$

Values calculated for the CO_3^{2-} concentration were used to make a direct calculation of the expected flux of bottom-water carbonate ion to pore water. These fluxes are poorly constrained because the concentrations of CO_3^{2-} are known only to within $\pm 25\%$. The values of J_{bw} calculated with this method are listed in Table 12.4.

The isotopic data were used to calculate the $\delta^{13}C$ of the flux of ΣCO_2 (J_t), and then the following mass balance was used to calculate the amount of the ΣCO_2 flux across the sediment-water interface that could be attributed to recycled bottom-water carbonate ion, J_{bw} :

$$J_t = J_{Ca} + J_{org} + J_{bw} \quad (12.9)$$

$$\delta^{13}C_{Jt} J_t = \delta^{13}C_{Ca} J_{Ca} + \delta^{13}C_{org} J_{org} + \delta^{13}C_{bw} J_{bw} \quad (12.10)$$

In this calculation it is assumed that $\delta^{13}C$ of CO_3^{2-} is the same as that of ΣCO_2 . The fractionation between CO_3^{2-} and HCO_3^- has never been measured. However, based on theoretical calculations, the $\delta^{13}C$ of CO_3^{2-} is approximately 1.5 ‰ less than the $\delta^{13}C$ of HCO_3^- .³⁶ Because this fractionation has been ignored here, the calculated values of J_{bw} are minimum values. The calculations were made first by assuming that the $\delta^{13}C$ of ΣCO_2 produced from the oxidation of organic carbon was the value determined from the laboratory experiments -18.5 ‰, and then by assuming that the oxidation of organic carbon occurred without fractionation ($\delta^{13}C = -20.6$ ‰). The values for J_{bw} calcu-

lated using the isotope data are listed in Table 12.4. Because the values of $\delta^{13}\text{C}$ - ΣCO_2 , ΣCO_2 , and Ca are known precisely (see "Methods" above), the values of J_{bw} calculated with the isotopic data are known with more certainty than those calculated using the carbonate ion concentration. This table also lists the $\delta^{13}\text{C}$ of J_t , and what percentage of the total flux across the sediment-water interface J_{bw} represents, i.e., $(J_{bw}/J_t)100$. The values for June 1984 represent the irrigation flux (I) between 6 and 16 cm. Data from the top 4 cm were not used because the isotopic values are much heavier than could be obtained in this sediment system by any of the processes described so far. These data are discussed later.

The flux calculations indicate that the fluxes calculated using the concentrations of the carbonate ion data are consistent with the isotopic data and that it is possible that the diffusion of bottom-water carbonate ion into the pore water is responsible in part for the isotopically heavy values calculated for $\delta^{13}\text{C}_{add}$ from the field data. If this is the only process adding heavy carbon to the pore water, then up to 30% of the ΣCO_2 flux to the bottom water must be recycled bottom-water carbonate ion. Emerson and Bender discussed the importance of bottom-water ΣCO_2 and the dissolution of CaCO_3 as sources of CO_3^{2-} which could neutralize the acid formed from the oxidation of organic carbon by oxygen in deep sea sediments.¹⁹ Based on their estimates of the relative rates of oxidation and dissolution, they concluded that bottom water was an unimportant source of carbonate ion. However, the sediments they discussed were CaCO_3 -rich—unlike the coastal sediments studied here—and the bottom water was not as supersaturated with respect to calcite as Buzzards Bay bottom water. Recent studies suggest that the dissolution rate of CaCO_3 is actually slower than previously reported,³⁷ indicating that diffusion of CO_3^{2-} may be more important than previously expected. In coastal sediments, a number of factors may create a situation where bottom-water ΣCO_2 could be an important source of CO_3^{2-} to pore water. Decomposition of a large quantity of organic matter leads to sulfate reduction and the production of solid-phase sulfides. The extensive mixing by organisms, particularly intense at certain times of the year, leads to the production of acid, not only from the aerobic oxidation of organic matter, but also from the oxidation of solid-phase sulfides. The relative lack of CaCO_3 in Buzzards Bay sediments, the increased diffusional area created by burrows in the bioturbated zones, and the large pH difference between the sediments and seawater create an environment where carbonate ion from bottom water is likely to be an important neutralizer of excess acid produced in the sediments.

The data from the June 1984 core suggest that diffusion of ^{13}C -depleted H_2CO_3^* from the pore water could also play a role in the enrichment of ^{13}C in pore water ΣCO_2 . The $\delta^{13}\text{C}$ of ΣCO_2 measured in pore water between 0 and 4 cm in the core collected in June 1984 is much greater than that observed in any other month (Figures 12.3 and 12.4). This core was different from other cores sampled at site M in many other aspects also.^{14,21,38} The dissolved iron concentration measured in the sediment interval 0.5–1.0 cm was the highest ever

observed in the sediments from site M.³⁸ The $^{222}\text{Rn}/^{226}\text{Ra}$ data could only be explained by assuming that irrigation was constant to 20 cm, although in other months the data could be modeled either with an exponentially decreasing irrigation term or by assuming no irrigation at all.²¹ The Alk measured between 0 and 0.5 cm is less than that in bottom water, unlike other months, where Alk was always greater in pore waters than in bottom water.¹⁴ These observations suggest that the oxidation of solid-phase iron sulfides is significant in this core, as has been discussed by Martin³⁸ and McNichol.¹⁵ Other researchers have discussed the importance of this process in near-shore sediments.^{39,40}

The production of strong acid by the oxidation of sulfides with oxygen may explain the isotopic data observed in this core. Using the Alk and ΣCO_2 data, the pH calculated for the 0–0.5 cm interval in June 1984 is 6.2. At this pH, H_2CO_3^* and HCO_3^- are present in approximately equal concentrations. Thus, the flux of ΣCO_2 from the sediments to bottom water in June 1984 must have contained a significant amount of H_2CO_3^* . Using the isotope equilibrium constants reported in Deines et al.,³⁶ the fractionation between H_2CO_3^* and HCO_3^- is approximately 8 0/00 with H_2CO_3^* enriched in ^{12}C . It is possible, then, that diffusion of H_2CO_3^* from the sediments preferentially removes ^{12}C from the sediments. This process might be important in other months to a lesser degree. For example, in August 1984, the pH of pore-water samples between 0 and 4 cm is also less than 7.0. In Table 12.4, the value calculated for J_{bw} in August 1984 using $\delta^{13}\text{C}-\Sigma\text{CO}_2$ does not agree well with that calculated using the carbonate ion concentration. In all other months the agreement is much better. Enrichment of ^{13}C in pore-water ΣCO_2 by the loss of ^{13}C -depleted H_2CO_3^* could explain this discrepancy.

SUMMARY AND CONCLUSIONS

In this study, the isotopic signature of ΣCO_2 was used as an indicator of the processes affecting ΣCO_2 in pore water. The $\delta^{13}\text{C}$ of ΣCO_2 provides a powerful tracer of the oxidation of organic matter because the $\delta^{13}\text{C}$ of organic carbon is so different from that of CaCO_3 and bottom-water carbonate species. An isotope model that accurately described the profiles of ΣCO_2 at this site¹⁴ could not be used to reproduce the observed isotopic profiles. The isotopic data indicate that the $\delta^{13}\text{C}$ of ΣCO_2 added to the sediment pore water was between -6.0 and -15.2 0/00, significantly greater than the $\delta^{13}\text{C}$ of C_{org} (-20.6 0/00). Calculations showed that the dissolution of CaCO_3 was not responsible for the ^{13}C -enrichment and that the enrichment must be due to fractionation during organic matter oxidation or to isotopic exchange with bottom water.

A laboratory study of the oxidation of organic carbon was performed to investigate the possibility of fractionation during oxidation. The results of the study showed that the $\delta^{13}\text{C}$ of the organic carbon oxidized was -18.5 ± 1.5 0/00, significantly greater than that of C_{org} , but not large enough to explain the enrichment observed in the field data. It was uncertain whether the fractiona-

tion was due to the variety of sources of organic matter to coastal sediments (e.g., terrestrial, salt marsh, or phytoplankton carbon) or the oxidation of specific organic compound classes, or whether the production of DOC played a role in the fractionation. The influence of DOC is a potentially important factor in the stable isotopic signature of sedimentary organic carbon which needs to be studied further.

This study suggests that both DOC and C_{org} are labile pools of carbon involved in early diagenesis and that they may have very different molecular structures. However, the actual effects that early diagenetic reactions have on the structure of organic matter associated with sediments and dissolved in pore water are not well known. The fate of contaminant organic matter will be affected by these reactions, structural alterations, and the molecular structures of organic matter; yet, the nature of the effect is difficult to predict without a better understanding of these processes.

Another source of ^{13}C -enriched carbon might be diffusion of bottom-water carbonate ion into the sediments, which would neutralize the acid produced during the oxidation of organic matter or the diffusion of ^{13}C -depleted H_2CO_3^* from pore water to bottom water. Further studies of these systems are necessary to distinguish between these two mechanisms. If isotopic exchange with bottom water by either of these mechanisms is important, it will have implications for the use of ΣCO_2 as an indicator of the amount of carbon oxidized in sediments and in the use of $\delta^{13}\text{C}$ as an indicator of past processes in the oceans.

ACKNOWLEDGMENTS

We wish to thank those who helped with the collection of the cores—in particular, Dick Colburn, captain of the *Asterias*, and the divers, Charlie Olson, Lary Ball, Stu Wakeham, and Hovey Clifford. Isotopic analyses were all performed on the VG Micromass 602E in Lloyd Keigwin's laboratory at Woods Hole Oceanographic Institution (WHOI). The manuscript benefited from reviews by Sharon Fitzgerald, Dan McCorkle, Bill Martin, and Brian Eadie. This research was supported in part by NSF-OCE83-15412, NSF-OCE84-2179, NSF-OCE84-16632, the Education Program at WHOI/MIT Joint Program, and the Coastal Research Center of WHOI.

REFERENCES

1. Froelich, P. N., G. P. Klinkhammer, M. L. Bender, N. A. Luedtke, G. R. Heath, D. Cullen, P. Dauphin, D. Hammond, B. Hartman, and V. Maynard. "Early Oxidation of Organic Matter in Pelagic Sediments of the Eastern Equatorial Atlantic: Suboxic Diagenesis," *Geochim. Cosmochim. Acta* 43:1075–1091 (1979).
2. Craig, H. "Isotopic Standards for Carbon and Oxygen and Correction Factors for

- Mass Spectrometric Analysis of Carbon Dioxide," *Geochim. Cosmochim. Acta* 12:133-149 (1957).
3. Deines, P. "The Isotopic Composition of Reduced Organic Carbon," in *Handbook of Environmental Isotope Geochemistry*, Vol. 1, P. Fritz and J. Fontes, Eds. (New York: Elsevier, 1980), pp. 329-406.
 4. Deuser, W. G. "Carbon-13 in Black Sea Waters and Implications for the Origin of Hydrogen Sulfide," *Science* 168:1575-1577 (1970).
 5. Kroopnik, P. "The Distribution of C-13 of CO₂ in the World Oceans," *Deep-Sea Res.* 32:57-84 (1985).
 6. McCorkle, D. C., S. R. Emerson, and P. D. Quay. "Stable Carbon Isotopes in Marine Porewaters," *Earth Planet. Sci. Lett.* 74:13-26 (1985).
 7. Miller, L. G. "Dissolved Inorganic Carbon Isotope Ratios in Reducing Marine Sediments," MS Thesis, University of Southern California, Los Angeles, CA (1980).
 8. Sayles, F. L., and W. B. Curry. "C-13, TCO₂, and the Metabolism of Organic Carbon in Deep-Sea Sediments," *Geochim. Cosmochim. Acta* 52:2963-2978 (1988).
 9. McArthur, J. M. "Carbon Isotopes in Pore Water, Calcite, and Organic Carbon from Distal Turbidites of the Madeira Abyssal Plain," *Geochim. Cosmochim. Acta* 53:2997-3004 (1989).
 10. Brown, F. S., M. J. Baedecker, A. Nissenbaum, and I. R. Kaplan. "Early Diagenesis in a Reducing Fjord, Saanich Inlet, British Columbia: III. Changes in Organic Constituents of Sediment," *Geochim. Cosmochim. Acta* 36:1185-1203 (1972).
 11. Nissenbaum, A., B. J. Presley, and I. R. Kaplan. "Early Diagenesis in a Reducing Fjord, Saanich Inlet, British Columbia: I. Chemical and Isotopic Changes in Major Components of Interstitial Waters," *Geochim. Cosmochim. Acta* 36:1007-1027 (1972).
 12. Alperin, M. J., and W. S. Reeburgh. "Geochemical Observations Supporting Anaerobic Methane Oxidation," in *Microbial Growth on C-1 Compounds*, R. L. Crawford and R. S. Hanson, Eds. (American Society for Microbiology, Washington, D.C., 1984), pp. 282-289.
 13. Alperin, M. J. "The Carbon Cycle in an Anoxic Marine Sediment: Concentrations, Rates, Isotope Ratios, and Diagenetic Models," PhD Thesis, University of Alaska, Fairbanks, AK (1988).
 14. McNichol, A. P., C. Lee, and E. R. M. Druffel. "Carbon Cycling in Coastal Sediments: 1. A Quantitative Estimate of the Remineralization of Organic Carbon in the Sediments of Buzzards Bay, MA," *Geochim. Cosmochim. Acta* 52:1531-1543 (1988).
 15. McNichol, A. P. "A Study of the Remineralization of Organic Carbon in Near-shore Sediments Using Carbon Isotopes," PhD Thesis, Woods Hole Oceanographic Institution, Woods Hole, MA, and Massachusetts Institute of Technology, Cambridge, MA (1986).
 16. Shiller, A. M., and J. M. Gieskes. "Processes Affecting the Oceanic Distribution of Dissolved A and Alkalinity," *J. Geophys. Res.* 85:2719-2727 (1980).
 17. Sofer, Z. "Preparation of Carbon Dioxide for Stable Carbon Isotope Analysis of Petroleum Fractions," *Anal. Chem.* 52:1389-1391 (1980).
 18. Westrich, J. T., and R. A. Berner. "The Role of Sedimentary Organic Matter in Bacterial Sulfate Reduction: The G Model Tested," *Limnol. Oceanog.* 29:236-249 (1984).

19. Emerson, S., and M. Bender. "Carbon Fluxes at the Sediment-Water Interface of the Deep-Sea: Calcium Carbonate Preservation," *J. Mar. Sci.* 39:139-162 (1981).
20. Li, Y. H., and S. Gregory. "Diffusion of Ions in Seawater and in Deep-Sea Sediments," *Geochim. Cosmochim. Acta* 38:703-714 (1974).
21. Martin, W. R., and F. L. Sayles. "Seasonal Cycles of Particle and Solute Transport Processes in Nearshore Sediments: Rn-222/Ra-226 and Th-234/U-238 Disequilibrium at a Site in Buzzards Bay, MA," *Geochim. Cosmochim. Acta* 51:927-943 (1987).
22. Bevington, P. R. *Data Reduction and Error Analysis for the Physical Sciences* (New York: McGraw-Hill, 1969).
23. McNichol, A. P., C. Lee, and E. R. M. Druffel. "The Effect of Sediment Handling on CO₂ Production Rates and Isotopic Fractionation Measured in the Laboratory: Results from Two Studies" (in preparation).
24. Abelson, P. H., and T. C. Hoering. "Carbon Isotope Fractionation in Formation of Amino Acids by Photosynthetic Organisms," *Proc. Nat. Acad. Sci.* 47:623-632 (1961).
25. Degens, E. T. "Biogeochemistry of Stable Carbon Isotopes," in *Organic Chemistry*, G. Eglington and M. T. J. Murphy, Eds. (New York: Springer-Verlag, 1969), pp. 304-329.
26. William, P. M., and T. W. Linick. "Cycling of Organic Carbon in the Ocean: Use of Naturally Occurring Radiocarbon as a Long and Short Term Tracer," in *Isotope Ratios as Pollutant Sources and Behavior Indicators* (Vienna: International Atomic Energy Agency, 1975), pp. 153-166.
27. Libes, S. M. "Stable Isotope Geochemistry of Nitrogen in Marine Particulates," PhD Thesis, Woods Hole Oceanographic Institution, Woods Hole, MA, and Massachusetts Institute of Technology, Cambridge, MA (1983).
28. Williams, P. M., and L. I. Gordon. "Carbon-13:Carbon-12 Ratios in Dissolved and Particulate Organic Matter in the Sea," *Deep-Sea Res.* 17:19-27 (1970).
29. Eadie, B. J., L. M. Jeffrey, and M. W. Sackett. "Some Observations on the Stable Carbon Isotope Composition of Dissolved and Particulate Organic Carbon in the Marine Environment," *Geochim. Cosmochim. Acta* 42:1265-1269 (1978).
30. Williams, P. M., and E. R. M. Druffel. "Radiocarbon in Dissolved Organic Matter in the Central North Pacific Ocean," *Nature* 330:246-248 (1987).
31. Sugimura, Y., and Y. Suzuki. "A High Temperature Catalytic Oxidation Method of Non-Volatile Dissolved Organic Carbon in Seawater by Direct Injection of Liquid Samples," *Mar. Chem.* 24:104-132 (1988).
32. Brownawell, B. J. "The Role of Colloidal Organic Matter in the Marine Geochemistry of PCBs," PhD Thesis, Massachusetts Institute of Technology, Cambridge, MA, and Woods Hole Oceanographic Institution, Woods Hole, MA (1986).
33. Krom, M. D., and E. R. Scholkovitz. "Nature and Reactions of Dissolved Organic Matter in the Interstitial Waters of Marine Sediments," *Geochim. Cosmochim. Acta* 41:1565-1573 (1977).
34. Elderfield, H. "Metal-Organic Associations in Interstitial Waters of Narragansett Bay Sediments," *Am. J. Sci.* 41:1565-1573 (1981).
35. Davis, J. A., and R. Gloor. "Adsorption of Dissolved Organic in Lake Water by Aluminum Oxide. Effect of Molecular Weight," *Environ. Sci. Technol.* 15:1223-1229 (1981).
36. Deines, P., D. Langmuir, and R. S. Harmon. "Stable Carbon Isotope Ratios and

- the Existence of a Gas Phase in the Evolution of Carbonate Ground Waters," *Geochim. Cosmochim. Acta* 38:1147-1164 (1974).
- 37. Archer, D., S. E. Emerson, and C. Reimers. "Dissolution of Calcite in Deep-Sea Sediments: pH and O₂ Microelectrode Results," *Geochim. Cosmochim. Acta* 53:2331-2345 (1990).
 - 38. Martin, W. R. "Transport of Trace Metals in Nearshore Sediments," Ph.D. Thesis, Woods Hole Oceanographic Institution, Woods Hole, MA, and Massachusetts Institute of Technology, Cambridge, MA (1985).
 - 39. Aller, R. C. "Diagenetic Processes near the Sediment Water Interface of Long Island Sound: I. Decomposition and Nutrient Element Geochemistry (S, N, P)," *Adv. in Geophys.* 22:237-350 (1980).
 - 40. Canfield, D. E. "Reactive Iron in Marine Sediments," *Geochim. Cosmochim. Acta* 53:619-632 (1989).

CHAPTER 13

Diffusive Rate Limitations in the Sorption of Organic Chemicals

William P. Ball and Paul V. Roberts

INTRODUCTION

It is becoming increasingly evident that the fate of organic contaminants in groundwater may be critically dependent upon rates of contaminant transfer between the aqueous and solid-bound (sorbed) phases. In the remediation of contaminated aquifers, for example, deviations from equilibrium can lead to situations where the majority of a contaminant is left in the solid phase long after aqueous concentrations are reduced to low levels,¹ and in situ bioremediation efforts may also be significantly hindered by desorption rate limitations.^{2,3}

In solute transport through porous media, the effects of solute diffusion to and from regions of immobilization (sorbing solid phases or “dead zones” of immobile water) have been extensively studied by chemical engineers, environmental engineers, and earth scientists. Where natural soils, sediments, and aquifer solids are involved, the nature of the immobile regions is often poorly understood, and the diffusive mechanism difficult to isolate and understand. It is clear, however, that the influence of diffusive rate limitations will be most important where (1) the capacity of the immobile regions for solute is high relative to the capacity of mobile regions, and (2) the rate of solute uptake and release by immobile regions is low relative to the rates of advective transport and hydrodynamic dispersion.⁴⁻⁹ Because of the often strong affinity of non-polar organics for the sorbed phase, the capacity of immobile regions for these solutes is potentially quite high, even at low porosity. Where transfer rates are sufficiently slow, large effects on transport are anticipated.

In this review, we consider the potential role of sorption rate limitations in the transport of organic solutes through natural solids, with emphasis on solute diffusion at the scale of individual particles of unconsolidated material. We begin with a brief review of field and column transport studies that have implied sorption or desorption rate limitations. This is followed by a review of

recent batch sorption/desorption experiments with organic chemicals and natural sorbents (soils, sediments, and aquifer solids). Emphasis is placed on recent studies which have either (1) suggested the presence of significant rate resistance or (2) provided insight into the mechanisms of rate limitation. In the context of understanding the potential sources of slow diffusion in sediments and aquifer solids, we also review literature describing diffusion in rock slabs, synthetic sorbents, and organic phases. Studies with these materials provide insight as to the potential magnitude of diffusive rate processes in media relevant to soil solids.

RATE IMPLICATIONS FROM TRANSPORT STUDIES

The Borden Field Experiment

A three-year field experiment was conducted by a team of researchers from Stanford University and the University of Waterloo, with the intent of evaluating field-scale groundwater transport of dissolved hazardous chemicals.¹⁰ Two tracers and five organic solutes were simultaneously injected, under natural gradient conditions, below the water table of an aquifer underlying an abandoned sand quarry in Borden, Ontario. The project involved extensive monitoring of solute movement over two years, together with concurrent modeling efforts and laboratory work using aquifer solids from the site. The study has been described in a series of articles.¹¹⁻¹⁵

Of the injected organic solutes, two—tetrachloroethene (PCE) and carbon tetrachloride (CCl_4)—exhibited an apparent conservation of mass, as calculated from the sum of aqueous mass and estimated sorbed mass, each calculated from spatial distributions of contaminant at several times. For the purposes of these mass balance calculations, aqueous mass was integrated directly from the plumes' zeroth moments¹² and sorbed mass was calculated using instantaneous velocity estimates (apparent retardation factors) inferred from the spatial first moment data.¹³ Centers of mass for all five of the organic plumes were observed to decrease in velocity over the course of the project, in contrast to chloride and bromide, which moved at a constant rate of roughly 9 cm/day (Figure 13.1). A number of possible explanations for the organic solute behavior have been investigated, including nonlinearity of isotherms, increasing sorption capacity downgradient, and mass transfer limitations. Isotherms have been shown to be sufficiently linear as to not cause the observed behavior^{14,16,17} and available sorption results with cored aquifer material show no significant increase in partitioning downgradient.¹⁸ As noted by Roberts et al.,¹³ the preponderance of evidence points toward a sorption rate limitation at the Borden site.

Goltz and Roberts have shown that spatial moment behavior of the type reflected in Figure 13.1 is a predictable result of nonequilibrium sorption.¹⁹ The same mass transfer parameters used to fit spatial data were also shown to

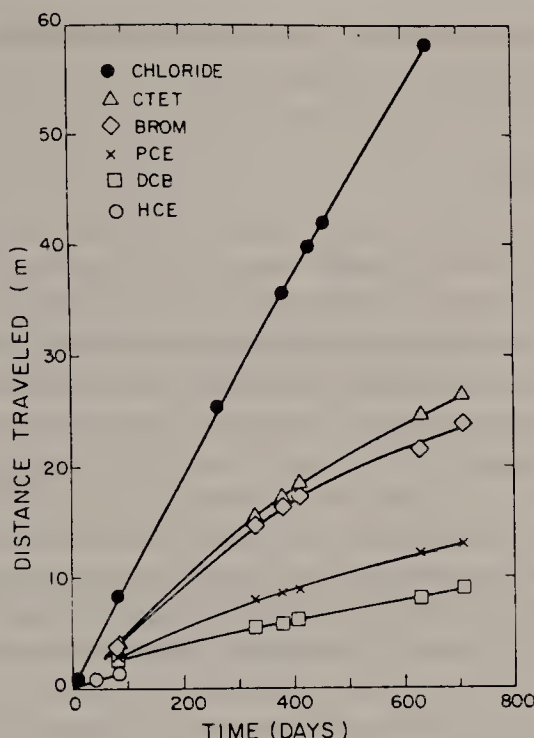


Figure 13.1. Distances traveled by plume centers of mass in the horizontal plane, as estimated from sampling data taken during the Borden transport experiment. From Roberts et al.¹³

qualitatively simulate the tailing observed in breakthrough data from near-field sampling points in the Borden field study.^{16,19,20} With regard to the apparent sorption nonequilibrium at the Borden site, it is important to note that the aquifer is unconfined and that the unconsolidated solids are comprised largely of sand-size grains which are almost devoid of clay minerals and very low in organic carbon content.²¹ Thus, diffusion through very thick organic layers or clay lenses can be ruled out. Pore diffusion into intraparticle regions or strongly sorbing zones of immobile water are thus implied. Interpretation is possible assuming either layered or spherical geometries for the regions of immobilized solute. In this regard, significant rate limitation has been found at the scale of the primary solid particles, but the very slow implied field transfer rates suggest that still greater resistance to mass transfer occurs in the field, possibly due to aggregation or layering of particles to create larger zones of low hydraulic conductivity. Specific rate constants implied by the field data are discussed later in this chapter, following review of the batch diffusion results with Borden solids.

Evidence of sorption and desorption mass transfer limitations has been extensively observed in other field studies as well, including numerous cases of slow elution during “pump and treat” remediation,²² as well as breakthrough curve tailing in controlled field studies. Some of the more controlled field

studies are briefly reviewed below, as evidence that field-scale nonequilibrium transport is not unique to the Borden site.

Other Field Studies

Roberts et al. have documented nonequilibrium trichloroethene (TCE) transport during a well-controlled field experiment of in situ bioremediation at Moffett Naval Air Station in Santa Clara County, CA.^{23,24} During the initial breakthrough experiments, significant tailing was observed in TCE's approach toward steady-state concentration, well beyond that observed for a nonsorbing tracer (bromide). During elution, low levels of TCE continued to leach from the system after more than 100 pore volumes, whereas 50% breakthrough of TCE was originally obtained after only about 7 pore volumes of contaminant feed. Laboratory work with well-mixed solids has demonstrated that intraparticle sorption continues to occur after 30 days, and nonequilibrium in the field is reasonably well described by intraparticle diffusion rates measured in the batch systems.²⁵

In another well-controlled field experiment in Ottawa, Canada,²⁶ Harrison and Barker observed that model fits for TCE breakthrough required 30 to 40 times more apparent dispersivity than for the nonsorbing tracer (iodide). The discrepancy was attributed to mass transfer limitations between dissolved solute and the aquifer solids.

Bahr has described a hazardous waste disposal site where transport of organic solutes (tetrahydrofuran and diethylether) deviated significantly from that anticipated on the basis of local equilibrium.²⁷ Using velocities and dispersivities estimated from a field-scale tracer test, Bahr used first-order numerical transport models to demonstrate that organic contaminant transport reflected a significant mass transfer resistance to sorption and desorption.

Pignatello et al. have described a field-scale study of EDB fate and transport, from which they conclude that nonequilibrium sorption and desorption were primary factors in the persistence of this chemical over several decades at the field site.²⁸ In this study, the "entrapment" of EDB molecules in micropores of soil particles or stable particle aggregates was believed to inhibit its biological degradation as well as its transport.

At a field site on Cape Cod, MA, Wood et al. have shown that a solute subject to ion exchange (lithium, Li⁺) underwent additional dispersive mechanisms beyond those affecting a conservative tracer (bromide, Br⁻).²⁹ The authors attribute the additional dispersion to mass transfer limitations associated with lithium diffusion into and out of the porous interiors of rock grains. Slow uptake at the grain scale was demonstrated through separate batch experiments with a sodium isotope (²²Na⁺) as penetrating solute. As discussed previously (and further elaborated later in this chapter), intragranular diffusion has also been proposed as an important source of sorption rate limitation in the Borden material. Although the mineralogical compositions of the Cape Cod

and Borden sites are significantly different, both aquifers contain fragments of clastic rock with low levels of porosity.^{21,29}

The potential significance of mass transfer limitations in field-scale transport is thus clear, but questions still abound about the most important domains of diffusion in real hydrogeologic environments. Distinction between large-scale rate limitations (as caused, for example, by sorbing layers of low permeability) and smaller (grain-) scale rate limitations is generally not possible from field data alone.¹⁹ Laboratory studies can serve to resolve some of these issues. As discussed in the sections which follow, however, long-term laboratory study may be needed to properly simulate field phenomena.

Laboratory Column Studies

Soil column experiments are often used to evaluate sorption equilibrium, rate, or both. Such columns are typically conducted in short columns and at flow rates ranging between 2 and 200 cm/hr. Because of the comparatively short soil-chemical contact time, column studies are prone to nonequilibrium effects at faster sorption and desorption rates than longer-term studies. Although this is a useful means of observing large effects, the studies may not accurately measure the capacity or rates associated with the most slowly addressed regions of solute sorption. Nonetheless, column experiments can provide useful data and have been a primary motivating force for the development of nonequilibrium solute transport models in soil systems. Numerous investigators have observed tailing in soil column breakthrough curves and, with varying degrees of success, have been able to model the observed behavior through nonequilibrium transport codes.^{9,30-37} Brusseau and Rao provide an overview of this literature and also discuss other processes which may lead to deviations from simple local equilibrium in organic solute transport.³⁸

As noted above, most column experiments performed to date would not be sensitive to very slow rate processes. In such columns, slowly addressed sorption capacity has little effect on transport and can be modeled simply by lowering the partitioning coefficient below the true, long-term value. Rate parameters, where fitted, will model some more rapid (and readily apparent) rate process. Estimates of partition coefficients for column transport studies have sometimes been estimated independently through batch study, but values have often required subsequent adjustment in order to fit column data at different velocities.^{34,35} Furthermore, separate batch partitioning measurements may be biased in a similar manner as the soil column data—i.e., taken over a similar time scale and also not at equilibrium—such that fortuitous agreement may be achieved using the “independent” K_d . If conducted under the proper conditions and for a sufficiently long time, however, batch studies can be a useful means of addressing long-term uptake. Although there is much variability with respect to reported equilibration times, carefully conducted soil sorption studies have demonstrated that organic solute equilibrium with

natural solids can take weeks, months, or even years to obtain. Some of these studies are reviewed in sections which follow.

SORPTION RATE IMPLICATIONS FROM BATCH STUDIES

Reported equilibrium times for sorption of organic chemicals by soils, sediments, and aquifer solids have shown great variability, as illustrated by Table 13.1. While many studies have reported equilibrium to be complete within hours or days, the number of studies reporting equilibrium times of "weeks to months" or "weeks to years" is steadily increasing. It is likely that true equilibrium may not have been attained in many of the early time cases, particularly since long-term samples (equilibrations on the order of weeks or months) were rarely evaluated for the possibility of slow but continuing uptake. The accurate determination of equilibrium uptake can be particularly difficult to measure where there are long-term continuing losses of chemical from the system and sorption occurs at comparatively slow rates. Sources of long-term solute loss include partitioning into, and diffusion through, septa or other sample seals¹⁴ and chemical or biological transformation.³⁹ On the other hand, bacterial inhibition must also be used with caution, since many treatments have been shown to change a soil's properties.⁴⁰⁻⁴³

The variability reflected in Table 13.1 inspired Karickhoff to make the following comment:⁴⁴

A great deal of confusion exists in the sorption literature regarding the speed of attainment of sorption equilibrium. . . . Current knowledge of this process (or processes) is incomplete or in some cases conflicting, but this author is very perplexed by the failure of most sorption reports to acknowledge any evidence of a "resistant" sorption component.

Additional, possibly related, confusion arises from the wide variety of potential sources of artifact in experimental sorption and desorption work.^{45,46} In addition to the problems of solute loss or transformation previously noted, artifacts can result from partitioning to unseparated colloidal material,⁴⁶⁻⁴⁸ or partitioning to solids filtration equipment.⁴⁶ In addition, where radiochemicals are used, radiochemical impurity can be an important source of error, requiring careful measurement and consideration.^{17,49}

These problems notwithstanding, batch sorption experiments have recently been successful in uncovering some very slow rates of organic solute sorption and desorption. In this review, we emphasize experimental work which has suggested a slowly sorbing component in the uptake or release of nonpolar organic chemicals. First, however, it is useful to review the theoretical framework and establish a consistent set of notation for intrasorbent diffusion.

Table 13.1. Reported Sorption Equilibration Times in Batch Sorption-Desorption Experiments

Reference	Solutes	Solid	Equilibration Time
Dao and Law, 1987 ³⁹ Hance, 1967 ^{40,*}	aniline, diuron atrazine, monuron, linuron, chloropharm diquat, prometone lindane	soils soils, bentonite, soil organic matter clay minerals	10 min to 5 hr 1 to 48 hr 1 hr 1.5 hr
Weber and Weed, 1968 ¹⁴¹	carbaryl, parathion atrazine, lindane phenolic compounds hexachlorobiphenyl maleic hydrazide polynaromatic hydrocarbons	soils sediments sediments soils sediments soil	2 hr 2 to 50 hr 3 hr 4 hr 4 to 24 hr 5 hr
Adams and Li, 1971 ¹⁴²	picloram hexazinone malathion benzene	soils sediment montmorillonite sediments, kaolinite	6 to 12 hr 12 hr 16 hr 18 hr
Leenheer and Ahrluchs, 1971 ^{143*}	substituted benzenes, PCE	soils	24 hr
Wauchope and Myers, 1985 ¹⁴⁴	2,4,5-T	soils	24 hr
Isaacson and Frink, 1984 ¹⁴⁵	various pesticides	soils	24 hr
Di Toro and Horzempa, 1982 ²²	diuron	soils	24 hr
Hermosin et al., 1987 ¹⁴⁶	diuron	soils	24 hr
Karickhoff et al., 1979 ⁸⁷	atrazine, aniline 2,4,5-T	soil	24 hr
van Genuchten et al., 1974 ³⁰	substituted benzenes, PCBs	soil	24 hr
Bouchard and Levy, 1985 ¹⁴⁷	bromacil, diquat	soil	2 days
Jaffe, 1986 ¹⁴⁸	nitrobenzene, lindane fluoridone	soil	2 days
Rogers et al., 1980 ¹⁴⁹	chlorinated benzenes, PCBs	soil	4 to 8 days
Schwarzenbach and Westall, 1981 ¹⁵⁰	bromacil, diquat	soil	6 days
Koskinen et al., 1979 ³⁹	nitrobenzene, PCBs	soil	>7 days
Bowman and Sans, 1985 ¹⁵¹	chlorinated benzenes	soils	weeks to months
Mustafa and Gamar, 1972 ¹⁵²	chlorinated benzenes	soils	8 days
Peck et al., 1980 ¹⁵³	tetrachloroethene (PCE)	soils	weeks to months
Nkedi-Kizza et al., 1987 ¹⁵⁴	chlorinated benzenes	soils	weeks to months
Koskinen and Cheng, 1983 ¹⁵⁵	chlorinated benzenes, PCBs	soils	months to years
Chiou et al., 1983 ¹⁵⁶	chlorinated benzenes	soils	months
Corwin and Farmer, 1984 ¹⁵⁷	organic pollutants	soils	months to years
Gschwend and Wu, 1985 ⁴⁸	chlorinated benzenes	soils	months to years
Weber and Miller, 1988 ⁶²	tetrachloroethene (PCE)	soils	months to years
McCloskey and Bayer, 1987 ¹⁵⁸	chlorinated benzenes	soils	months to years
Miller, 1984 ¹⁰¹	chlorinated benzenes	soils	months to years
Karickhoff, 1984 ⁴⁴	chlorinated benzenes	soils	months to years
Wu and Gschwend, 1986 ^{60,*}	chlorinated benzenes	soils	months to years
Ball and Roberts, 1985 ¹⁵⁹	chlorinated benzenes	soils	months to years
Karickhoff and Morris, 1985 ^{80,*}	chlorinated benzenes, PCBs	soils	months to years
Oliver, 1985 ^{90,*}	picloram	soils	months to years
McCall and Agin, 1985 ^{89,*}	diuron	soils	months to years
Chang, 1989 ^{98,*}	PCB congeners	soil	months to years
Coates and Elzerman, 1986 ^{91*}	PCB mixture	soil	months to years
Wikowski et al., 1987 ^{81,*}	PCE, tetrachlorobenzene	soils	months to years
Ball, 1989 ^{17,*}		soils	months to years

Note: Table adapted from Chang⁹⁸, with newly added citations where marked by asterisks.

Conceptual Framework for Intrasorbent Diffusion

Sorption of dissolved solute by a solid matrix, whether as adsorption to mineral surfaces or partitioning with nonaqueous organic phases, requires the transfer of solute from bulk solution to sites of immobilization. Resistance to such mass transfer may stem from transport across a fluid boundary layer external to the particle (external mass transfer), from diffusion to internal sites of the immobile phase (intrasorbent diffusion), or from rate limitations of the sorption process itself (chemical kinetics). For porous or solid sorbents, these processes are generally perceived as occurring in series, although the order of the last two processes will depend upon the nature of the diffusive process (i.e., aqueous- or sorbed-phase diffusion). For slow rates of observed uptake in batch systems, appropriate sample mixing will ensure that external mass transfer is rapid relative to the overall rate of uptake, except at very early times (when the driving force for intrasorbent diffusion is exceptionally high). For nonpolar organic chemicals, physical adsorption or partitioning to organic phases are the dominant processes and are believed to be sufficiently rapid as to not influence solute transport.⁵⁰

In the studies reviewed subsequently, investigators have usually assumed that resistance to solute uptake or release was due to some sort of diffusional limitation within the sorbing phase. Where first-order rate models have been used to describe sorption rate processes, either in transport experiments or batch study, it has usually been with the explicit understanding that the first-order coefficients are approximations for physical diffusion into regions of solute immobilization. In well-mixed batch systems, such diffusion must necessarily be associated with primary sorbent particles since significant regions of immobile water do not exist.

The driving force for intrasorbent diffusion may thus be either the concentration gradient of solute in the intraparticle pore water (pore diffusion), the concentration of sorbed solute on the pore walls (surface diffusion), or, for nonaqueous sorbing phases, the concentration of chemical in that phase. For transient conditions of uptake into a sorbent, mass balance considerations over a volume element of the porous sorbent can be combined with Fick's first law of diffusion to obtain

$$\epsilon_i(\partial C/\partial t) + \rho_a(\partial q/\partial t) = \epsilon_i D_p \nabla^2(C) + \rho_a D_s \nabla^2(q) \quad (13.1)$$

where C = solute concentration in intraparticle water, [(mass of solute in intraparticle water at radius r and time t)/(volume of intraparticle water)]

q = sorbed-phase solute concentration, [(mass of solute sorbed to intraparticle solids site at radius r and time t)/(mass of total aquifer solids)]

ϵ_i = internal porosity of the immobile phase, [(volume of immobile water)/(volume of immobile phase)]

- ρ_a = apparent density of the immobile phase, [(mass of immobile solids)/(volume of immobile phase)]
 D_p = the effective pore diffusion coefficient [L^2/T]
 D_s = the effective surface (or sorbed-phase) diffusion coefficient, [L^2/T]
 ∇^2 = the Laplacian operator

For the case of linear partitioning and reversible equilibrium within the pores, Equation 13.1 can be rewritten as

$$\partial C / \partial t = D_a \nabla^2(C) \quad (13.2)$$

where the apparent diffusion coefficient is defined as

$$D_a = \epsilon_i D_p / (\epsilon_i + \rho_a K_{di}) + \rho_a K_{di} D_s / (\epsilon_i + \rho_a K_{di}) \quad (13.3)$$

- where D_a = apparent diffusion coefficient [L/T^2]
 K_{di} = partitioning coefficient, considering only the diffusively limited (internal) sorbed phase, [mass solute sorbed to diffusively limited solids per unit mass of solids per unit intraparticle aqueous concentration]

For a spherical geometry, Equation 13.2 can be rewritten as

$$\partial C / \partial t = (D_a / r^2) \partial / \partial r [r^2 (\partial C / \partial r)] \quad (13.4)$$

Where diffusion of sorbed species is not believed to play an important role in the overall rate of uptake, a pore diffusion interpretation may be appropriate. The pore diffusion model has been well established in the chemical engineering literature.⁵¹⁻⁵³ With diffusion only in the aqueous phase, Equation 13.3 simplifies to

$$D_a = D_p / [1 + (\rho_a / \epsilon_i) K_{di}] \quad (13.5a)$$

where the denominator on the right hand side can be equated to an internal retardation factor for intraparticle diffusion, R_{int} , that is

$$D_a = D_p / R_{int} \quad (13.5b)$$

Some researchers have referred to D_p simply as the pore diffusion coefficient,⁵⁴ while others have designated it as an effective diffusion coefficient.^{33,34,55-59} However, this latter designation has been used by some authors to describe D_a .^{16,60} To avoid confusion, the term “effective pore diffusivity” will be used for D_p in this work.

In contrast to aqueous pore diffusion, some researchers have assumed that

diffusion occurs predominantly in the sorbed phase.^{61,62} The distinction can be important for sorbates with nonlinear isotherms. However, for sorbed-phase diffusion with linear partitioning, modeling is equivalent so long as intraparticle porosity is low ($\rho_a K_{di} > > \epsilon_i$), in which case D_a will be numerically identical to D_s . In the more specific case where diffusion is envisioned to occur through organic matter, the apparent (sorbed-phase) diffusivity will be related to an intraorganic matter diffusivity. For this mechanism, an accurate calculation of the intraorganic diffusivity would have to properly consider the geometry and size of the organic sorbing phase, and sorbed-phase concentrations (q) require conversion to reflect actual concentrations in the smaller volume of organic matter. For example, organic matter may exist only as an external layer (with poorly understood thickness and geometry), or it may exist throughout the intraparticle pore spaces of an aggregated particle. Intraorganic matter diffusion has been proposed as an important source of rate limitation by several investigators.^{38,63} For the reasons noted above, however, the quantitative estimation or prediction of intraorganic diffusion coefficients in natural material is still elusive. As discussed subsequently in this chapter, even the relationship between D_a and K_d is difficult to predict for intraorganic diffusion.

In the case of pore diffusion (Equations 13.5), the effect of K_d on diffusion rates is readily apparent, although D_p can be difficult to predict. In particular, it is important to recognize that D_p will be less than the bulk aqueous diffusivity in water (D_b), since the radial diffusion model assumes simple spherical geometry and straight diffusion paths, whereas real systems involve more tortuous pathways, dead-end pores, and variability in pore length and diameter. In addition, for very small pore diameters, pore constrictivity will play an important role.^{57,58,64} Following Satterfield et al.,⁵⁷ we write the following expression for D_p :

$$D_p = (D_b K_r) / \chi \quad (13.6)$$

where D_p = effective pore diffusivity [L^2/T]
 D_b = bulk aqueous diffusivity [L^2/T]
 K_r = constrictivity factor (≤ 1) [-]
 χ = tortuosity factor (≥ 1) [-]

In some works, τ^2 is used in lieu of χ , with τ representing the actual pore tortuosity, defined as the ratio of actual diffusion path length to the length in the assumed direction of diffusion—a good overview of the tortuosity concept is provided by van Brakel and Heertjes.⁶⁵ As used here, the tortuosity factor also accounts for decreases in effective diffusivity which arise due to dead-end pores and variabilities of pore diameter.^{66,67} Steric effects are separately accounted through K_r . Several theoretical models for determining the tortuosity (τ) have been proposed.⁶⁵ Theoretically and experimentally proposed values in unconsolidated material generally range between 1.3 and 3. However, con-

sideration of interconnectivity between random pores suggests a direct inverse relation between tortuosity and porosity,⁶⁸ such that much higher values are predicted for systems with very low porosities (e.g., $\chi = 100$ for porosity of 0.01).

Because it is often impractical to separate the effects of K_r and χ , it is sometimes useful to incorporate constrictivity through the use of an "effective" tortuosity factor, χ_e . Thus,

$$D_p = D_b/\chi_e \quad (13.7a)$$

$$\chi_e = \chi/K_r \quad (13.7b)$$

With respect to estimation of K_r , several investigators have related constrictivity effects to solute diameter and pore size.^{57,58,64,69,70} This work, describing restrictive diffusion in synthetic porous pellets, is reviewed later in this chapter.

When measuring diffusion from one bulk solution to another through a porous slab or membrane, researchers often report a diffusion coefficient based on the total cross-sectional area of the membrane and the aqueous concentration gradient across the membrane thickness. The diffusion coefficient, if determined under steady-state conditions, is the product of D_p and the porosity of the immobile region, ϵ_i . In the nomenclature of Bradbury and Green,⁵⁴ this steady-state diffusion coefficient is referred to as the intrinsic diffusion coefficient, D_i . Given that $D_i = \epsilon_i D_p$, the apparent diffusivity (D_a) can be redefined in terms of the measurable quantity, D_i ,

$$D_a = D_i / (\epsilon_i + \rho_a K_{di}) \quad (13.8)$$

Note that, in the context of solute transport through porous media, D_i/a^2 is the relevant parameter to determine when comparing plume or breakthrough curve spreading due to intrasorbent diffusion with that caused by hydrodynamic effects.⁸

Equations 13.1 through 13.8 provide a consistent framework and nomenclature for the discussion of diffusion through an immobile matrix. Under groundwater flow conditions, such diffusion may occur either at the scale of confining rock or clay matrices, at the scale of relatively large aggregated soil structures (so-called dead zones), or at the still finer scale of individual soil particles, which will include some combination of single mineral grains, clay particles, organic solids, clastic rock fragments, and other stable aggregates of finer material. Under conditions of batch uptake or release in well-mixed laboratory systems, it is the transport at the scale of these individual particles which is measured. Some experiments of this type are reviewed in the sections which follow.

Batch Rate Studies

Batch Studies with First-Order Interpretation

Karickhoff carried out batch experiments to observe sorption and desorption rates of several different organic compounds in river sediments.⁷¹ In both sorption and desorption experiments, the approach to equilibrium was described by a rapid component and a much slower component. Although the rate data for any specific soil/solute combination were limited, and desorption data suffered from mass balance problems, the overall results revealed a reciprocal variation of the slow rate constant with the partition coefficient for both a given chemical on different sediments, and for different chemicals on a given sediment. With this relationship, it was hypothesized that the slower process may be viewed as diffusive transfer to sorption sites inaccessible to the bulk water. In comparing the slow rate constants obtained from the sorption and desorption experiments, Karickhoff found no significant difference.

DiToro and Horzempa have also observed what they describe as a desorption resistant fraction in the sorption of hexachlorobiphenyl and other polychlorobiphenyls (PCBs) with natural lake sediment and clay mineral samples.⁷²⁻⁷⁴ They reported that the resistant component increases with incubation time and suggested that reversible sites are being converted to "strong binding sites" with time. DiToro and Horzempa did not attempt to address the temporal behavior of the resistant component of sorbed solute. Moreover, meaningful interpretation of the data has become extremely difficult due to conflicting hypotheses regarding a separate (but possibly related) particle concentration effect on sorption, with reduced sorptive capacity observed at higher solid-liquid ratios. Some have attributed observations of this kind to the effect of particle-particle interactions on sorption kinetics,⁷⁵⁻⁷⁷ while others have related it to the presence of solution-phase colloids or macromolecules which bind solute but are not separated by normal centrifugation or filtration.^{46-48,78,79} Other researchers have noted that particle concentration effects on desorption isotherms are a likely artifact of not attaining equilibrium during the uptake phase of the experiment.^{80,81}

In a study of diuron [N-(3,4-dichlorophenyl)-N,N-dimethylurea] desorption from soil, Rao and Nkedi-Kizza also observed apparent hysteresis (higher apparent K_d after desorption than adsorption), indicative of resistance to desorption.⁸² They noted that this effect was observed only for the larger size fractions. As previously noted, a number of investigators have discussed how such apparent hysteretic behavior can be expected if equilibrium is not attained during uptake, desorption, or both.^{38,81,83-86} Interestingly, Rao and Nkedi-Kizza also noted that carbon-normalized sorption (K_{oc}) for the larger sands was three times smaller than for the other fractions.⁸² Karickhoff et al. had observed a similar effect with sand (> 50 mm) compared with finer silts—8-to 24-hr K_{oc} values for polynuclear aromatics with the sands were between 15 and 50% of the silt values, and showed much less reproducibility from one

experiment to the next.⁸⁷ In both studies, it is possible that the apparently low K_{oc} values in the larger sands were the result of not attaining sorption equilibrium.

Karickhoff and Morris studied the desorption (and, to a lesser extent, the uptake) of pyrene, pentachlorobenzene, and hexachlorobenzene on eight sediments.⁸⁰ Although particle sizes were not reported, Karickhoff and Morris assumed 10- μm (0.01-mm) diameter particles to calculate diffusion coefficients implied by rate data taken during the first 9 days of desorptive release. The estimated apparent diffusion coefficients (D_a) were on the order of 10^{-11} to $10^{-13} \text{ cm}^2/\text{sec}$ and were compared with previous results for radionuclide uptake in sediments.⁸⁸ In describing the long-term desorption data (after the first 9 days), Karickhoff and Morris applied a two-compartment first-order model which assumed a fraction of labile sites. They stated that "no fixed geometry diffusion model . . . was found to be generally applicable" and attributed this to "sediment particle size and structural variability." As with the previous work of Karickhoff,⁷¹ the characteristic time for long-term desorption was found to vary inversely with K_d . Particle size effect was not studied, but aggregation was believed to be responsible for slowing the release of contaminant from cohesive soils at high sediment concentrations.

In unsaturated experiments with seven surface soils from different geographic regions, McCall and Agin estimated that picloram (an acidic organic pesticide) was still sorbing after over 200 days of incubation.⁸⁹ They also observed that desorption rates became increasingly slow as sorptive equilibrium time was increased. These researchers modeled the desorption process as a two-component process, characterized by fast and slow first-order rate constants.

Oliver studied the long-term desorption of three halogenated aromatics from contaminated sediments, but did not attempt to fit any rate models to the data.⁹⁰ He found that, after an initially rapid desorption over the first several days, the desorption rate decreased dramatically. Desorption was less than 80% complete after 40 days.

In a manner similar to Karickhoff and Morris, Coates and Elzerman conducted purge release experiments of chlorinated benzenes from sediments.⁹¹ As in the work of Karickhoff,^{71,80} the observed fractional release at a given point in time decreased in soils subjected to more prolonged prior equilibration. In one case, less than 50% of sorbed hexachlorobenzene was recovered after over 30 days of desorptive release (into presumably solute-free gas-purged solution), following 36 days of sorption. Nonattainment of equilibrium during the uptake portion of the experiment was suspected. Like Karickhoff and Morris, Coates and Elzerman observed lower rates of release for more hydrophobic compounds.

Witkowski et al. studied the sorption and desorption of Aroclor 1242 (a PCB mixture) from a lake sediment, using small batch reactors (centrifuge vials) as well as a completely stirred tank reactor (CSTR).⁸¹ Short-term experiments with the vials showed an apparent attainment of equilibrium after 3 to 4

days, based on negligible differences in aqueous concentration decreases between 3 and 7 days. Desorption experiments after these short times of equilibration showed an apparent hysteresis (which increased with solids concentration) similar to that observed by DiToro and Horzempa.⁷²⁻⁷⁴ However, longer-term desorption experiments showed continued gradual desorption for over 6 months (following an uptake period of 1 week). First-order rate coefficients were fitted to the desorption data, but nonequilibrium conditions probably existed when desorption was started. The reported long-term desorption constant ($k_2 = 0.003 \text{ day}^{-1} = 3.5 \times 10^{-8} \text{ sec}^{-1}$) was of the same order as those reported by Karickhoff and Morris⁸⁰ and Coates and Elzerman.⁹¹

The persistence of 1,2-dibromoethane (EDB) in soils has been extensively examined by Steinberg, Pignatello, Sawhney, and coworkers.^{28,92-96} Steinberg et al. found measurable desorption of EDB (to overlying water) from topsoils fumigated with EDB 13 years prior to sample collection.⁹⁵ Laboratory tests verified that field-applied EDB was extremely slow to desorb from soil, with the difficulty of extraction directly related to the length of time for the original soil-chemical equilibration. Extraction in reasonable time periods was achieved using water-miscible solvents (methanol, acetone, acetonitrile) at elevated temperature, whereas short periods of gas purge (11 min) and hexane extraction (24 hr) were only successful in recovering freshly applied EDB.⁹⁶ Results have shown the rate of release to increase with temperature and to decrease with particle size.⁹⁵ Under moist or water-saturated conditions, empirically estimated "immobile fractions" (based on fractions not extracted after a certain time period) were observed to increase with organic matter content of the soil,^{92,97} and decrease (significantly) with extent of soil pulverization.⁹⁵ In all of the above work, the authors have hypothesized the entrapment of EDB in soil micropores, and they make a strong case that the chemical's release is diffusion controlled. Although accurate calculation of diffusion coefficients was not possible (since the true equilibrium capacity of the soil was not known), this did not detract from the studies' fundamental conclusions: halogenated organic chemicals may persist for extremely long time periods at diffusively accessed locations within soil grains.

Slow sorption and significant resistance to desorption has also been observed by Chang.⁹⁸ In studies of diuron sorption and desorption by aquifer solids, Chang observed continuing uptake after 75 days of equilibration. In desorption experiments (conducted over 3 weeks following 44 days of sorption), no significant increases in aqueous concentration were observed beyond the first week, but the remaining sorbed concentrations greatly exceeded those achieved during sorption for equivalent aqueous concentration. Hysteretic isotherms were used to model the results.

Brusseau et al. have estimated desorption rate constants (k_2) by both column and gas purge techniques for several soil-organic solute systems and cite intra-sorbent diffusion as the most likely source of the rate limitation.⁹⁹ Column breakthrough results were shown to be reasonably well predicted from the batch results, which were obtained from 3- to 15-hr batch purge experiments.

The authors concluded that gas purge and miscible displacement techniques yield comparable results.

For intrasorbent diffusion with linear partitioning, first-order desorption rate coefficients defined in the manner of k_2 can be considered as approximations for a diffusion rate constant based on sorbed-phase concentration (D_a/a^2).^{80,81,91,99} Wu and Gschwend have described the relation between k_2 and D_a/a^2 for batch systems.⁶⁰ Inverse correlations of k_2 with K_d have been presented by Karickhoff and Morris⁸⁰ and Brusseau and coworkers.^{99,100} The correlations are useful means of presenting data trends and highlight the previously noted suggestion that D_a/a^2 may be inversely related to K_d in natural systems. However, the correlations themselves must be viewed with caution since most of the underlying rate constants were based on relatively short-term study; the correlations do not predict the very slow components of sorption uptake or release reflected by some studies.^{3,17,25,89,90} In addition, first-order rate constants do not include the effect of diffusive length scale, and thus cannot be expected to predict effects on rate which arise from differences in the size scale of diffusively limited regions, as due to differences in particle size or modification of aggregates by external forces (e.g., disaggregation, pulverization). In the following two sections, we review three sets of batch studies which have specifically considered intrasorbent diffusion. Two of these studies have demonstrated significant particle size effects on the rate of uptake, and one has uncovered continuing diffusion into sand-size particles for periods up to 3 years.

Batch Studies with Diffusive Interpretation

Miller and Weber have described studies of the partitioning of lindane (γ -hexachlorocyclohexane) with four soils and nitrobenzene with two of the same four soils.^{61,62,101} Bottle point rate studies and a CSTR were both used, and results showed a clear effect of increased sorption with time: concentration versus time curves showed continuing slightly negative slopes even after 7 days.¹⁰¹ Rate of uptake in the CSTR was simulated using a spherical diffusion model that also incorporated external mass transfer resistance. However, simulations were insensitive to the external transfer coefficient at all but the very earliest times.^{61,62} For the spherical diffusion model, D_s/a^2 values between 10^{-8} and 10^{-9} sec^{-1} were fitted to the data, and D_s was calculated assuming a particle radius (a) based on the median diameter of the particle size distribution. D_s values between 2.3×10^{-11} and $5.3 \times 10^{-7} \text{ cm}^2/\text{sec}$ were reported.⁶²

The rate data of Miller and Weber showed decreased D_s with strength of sorption, as in the previously cited work of Karickhoff and others. Another interesting result was that reported equilibrium capacities were higher for the CSTRs than for the bottle isotherms. This effect was tentatively attributed to particle breakup in the CSTR,⁶² possibly implying incomplete equilibration in the bottle point study.

Wu and Gschwend describe a study of sorption rate for chlorinated ben-

zenes with silt-sized river sediments and a surface soil using a closed-loop-stripping apparatus.⁶⁰ Sorptive uptake from the aqueous phase was monitored by tracking concentrations in a recycled gas stream for periods up to 1 week. Rate experiments were conducted with bulk sediments (having a distribution of particle sizes) and modeled using the radial diffusion approach. Computed values of D_a varied from 8×10^{-12} to $1 \times 10^{-9} \text{ cm}^2/\text{sec}$. These minimum and maximum values reflect pentachlorobenzene sorption on Charles River sediment (roughly 8% organic carbon content) and 1,4-dichlorobenzene sorption on Iowa soil (2.1% organic carbon), respectively. The apparent diffusion coefficients were found to vary inversely with K_d , an observation in agreement with the previous findings of Karickhoff.^{71,80} Using the same apparatus as for the sorption experiments, contaminated sediments were poured into clean water, and the desorptive release was monitored. These experiments, conducted with tetrachlorobenzene, showed that the sorption process was fully reversible, with desorption showing similar diffusive time scales as sorption. Experiments with finer size fractions and with disaggregated (sonicated) material showed an increased rate of sorption with decreased particle size.

By assuming the intraparticle tortuosity factor to be inversely proportional to particle porosity (and neglecting pore constrictivity), Wu and Gschwend obtained the following definition of D_a :⁶⁰

$$D_a = (D_b \epsilon_i^2) / (K_d (1 - \epsilon_i) \rho_s) \quad (13.9)$$

where ρ_s = solid density (specific gravity) of the sorbent = $\rho_a / (1 - \epsilon_i)$. Since D_b , ρ_s , and K_d were all known, Equation 13.9 allowed the rate information (D_a) to be interpreted as a fit of intraparticle porosity (ϵ_i), which was estimated to be roughly constant at 0.13 for all systems studied. Because of the assumed relation between porosity and tortuosity, a constant effective tortuosity was also implied. Although all of the experiments used to estimate D_a were conducted with a full size distribution of particles, the modeling effort admirably accounted for the complete size distribution.⁸⁶ However, independent characterization of size fractions was not conducted, and a constant K_d was assumed for all fractions of a given sediment.

In their concluding remarks, Wu and Gschwend optimistically suggested that their findings could allow *a priori* estimation of intraparticle diffusion rates.⁶⁰ However, the authors were careful to point out some limitations in the study. In particular, they noted that their apparatus did not allow longer-term study as required for larger aggregates and that more research was needed, "especially based on understanding the characteristics of natural particles." It is clear, for example, that the notion of intraparticle porosity being constant at 13% (as estimated by Wu and Gschwend for silt-sized aggregates) will not hold for all natural solids. As a case in point, the measured porosity in aquifer solids from Borden, Ontario, has been estimated at between 0.4% and 4.8%, depending on particle size.²¹ Furthermore, apparent diffusion coefficients in the Borden material were much lower than predicted by Equation 13.8, even

when this measured porosity was considered. These Borden results, reviewed below, suggest that additional tortuosity and/or steric hindrances may slow the diffusion process further.

Batch Studies with Borden Solids

Rates of sorption of tetrachloroethylene (PCE) and 1,2,4,5-tetrachlorobenzene (TeCB) by Borden solids were measured in the laboratory over long periods.^{17,102,103} To assure data reliability, special precautions were taken, including the use of prepurified ¹⁴C-labeled compounds, flame-sealed glass ampules for equilibration, and autoclaving of the solids. Continuing uptake beyond 3 days had previously been impossible to detect, owing to the slow rate of uptake and losses of comparable magnitude from blank samples containing no soil.¹⁴

Experiments were conducted with a homogenized bulk sample and sieved size fractions thereof, as well as with pulverized samples. The measured equilibrium distribution coefficients (K_d) were found to be linear within the concentration range of the batch rate experiments (0 to 50 $\mu\text{g/L}$), and differed greatly among the size fractions. In all cases K_d values were approximately 40 times greater for TeCB than for PCE. The data showed evidence of very slow approach to equilibrium, implying times as long as 1000 days for equilibrium between TeCB and a coarse size fraction (i.e., grain diameter = ca. 0.6 mm). For the slowly equilibrating samples, pulverization of the solids was found to be a judicious expedient for quantifying the equilibrium uptake, and comparisons with long-term equilibrium data from unpulverized samples were quite good.¹⁷

An internal diffusion model of the form previously described was used to interpret the rate data. The model fitting allowed for the possibility of instantaneous uptake with some fraction of the sorbing solids. For the coarse size fraction cited above, the single-parameter diffusion model (i.e., with no instantaneous fraction of sorption) provided a remarkably good fit to the data and suggested D_a values of 7.9×10^{-11} and $1.5 \times 10^{-12} \text{ cm}^2/\text{sec}$ for PCE and TeCB, respectively. Interpretation of these results with a pore diffusion model (using measured values for K_d and intraparticle porosity) yielded estimated effective pore diffusivities (D_p) of 3.5×10^{-8} and $2.4 \times 10^{-8} \text{ cm}^2/\text{sec}$ for PCE and TeCB, respectively. The good agreement between D_p for PCE and TeCB is consistent with the similarity of molecular diameter and aqueous diffusivity for the solutes and reflects the good inverse correlation between D_a and K_d . As previously noted, this dependence is predicted by the pore diffusion model, in which sorption acts to retard the approach to equilibrium. The effective pore diffusivity in the coarse size fractions was found to be approximately 200 times smaller than the bulk aqueous diffusivity. If pore diffusion is indeed the controlling mechanism, the very low rates may be explained by the combined effects of tortuosity, dead-end pores, and constrictions in the finest pores.

For finer size fractions, the same relationship between PCE and TeCB

uptake results were observed, but a simple diffusive interpretation was less successful in explaining results. However, good data fits were attained if 4 to 31% of the sorption was assumed to occur very rapidly. Figure 13.2 shows PCE uptake data for one of the intermediate size fractions, for which 4% instantaneous uptake provided the best fit. Apparent diffusivities in these finer fractions ($D_a = 2$ to 6×10^{-11} cm²/sec for PCE) were slightly lower than those in the coarser fractions, despite the considerably smaller distribution coefficients (K_d) for the finer solids. These data imply either (1) greater tortuosity or hindrance of diffusion in the fine-grained material or (2) aggregation of the finer material into larger aggregates in the isotherm bottles. Particle aggregation should have been minimal, however, since the material was comprised of well-defined rock fragments and mineral grains of low clay and organic content²¹ and samples were well mixed.^{17,102,103}

As previously noted, Goltz and Roberts have shown good simulation of near-field spatial and temporal plume behavior at the Borden site. These simulations were based on short-term (3-day) measures of PCE distribution (K_d), as estimated by Curtis et al.¹⁴ However, the revised (long-term) estimate of equilibrium partitioning obtained from the experiments described herein allows greatly improved simulation of the observed far-field retardation behavior. As evident from Figure 13.3, fitting of the spatial moment data using the 3-day K_d (Figure 13.3, solid line) successfully captures early-time behavior, but fails to model the long-term plume velocity. The higher PCE K_d values of the long-term batch experiments are necessary to model the long-term plume velocity—

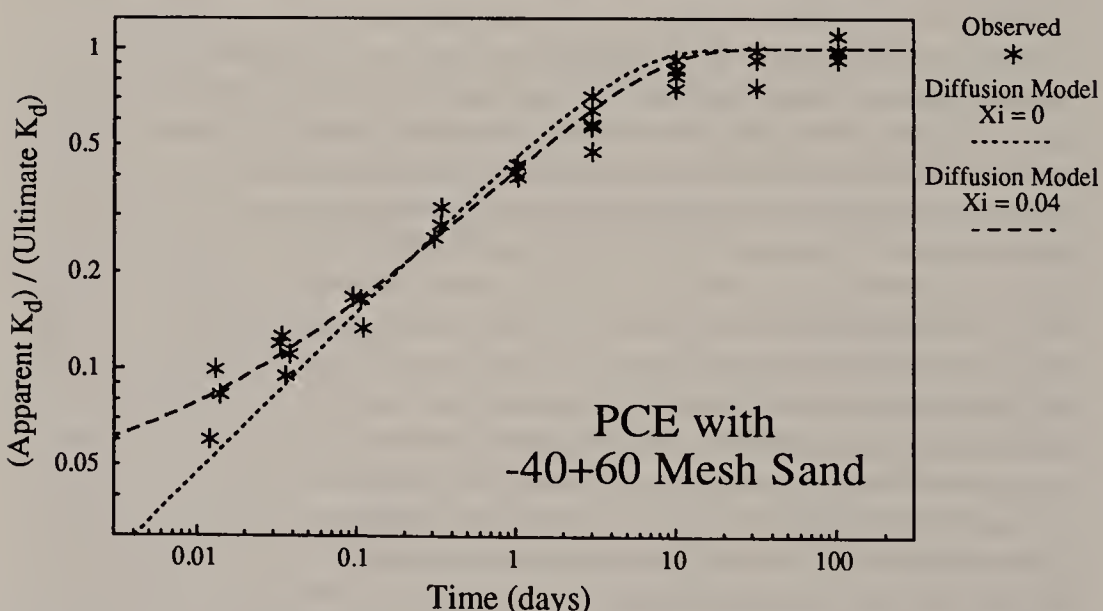


Figure 13.2. Normalized PCE distribution coefficient as a function of time for unaltered -40 + 60 mesh Borden aquifer material. Dotted line: one-parameter diffusion model fit ($D_a/a^2 = 2.3 \times 10^{-7}$ cm²/sec); dashed line: two-parameter diffusion fit ($D_a/a^2 = 1.6 \times 10^{-7}$ cm²/sec, instantaneous uptake estimated at 4%).

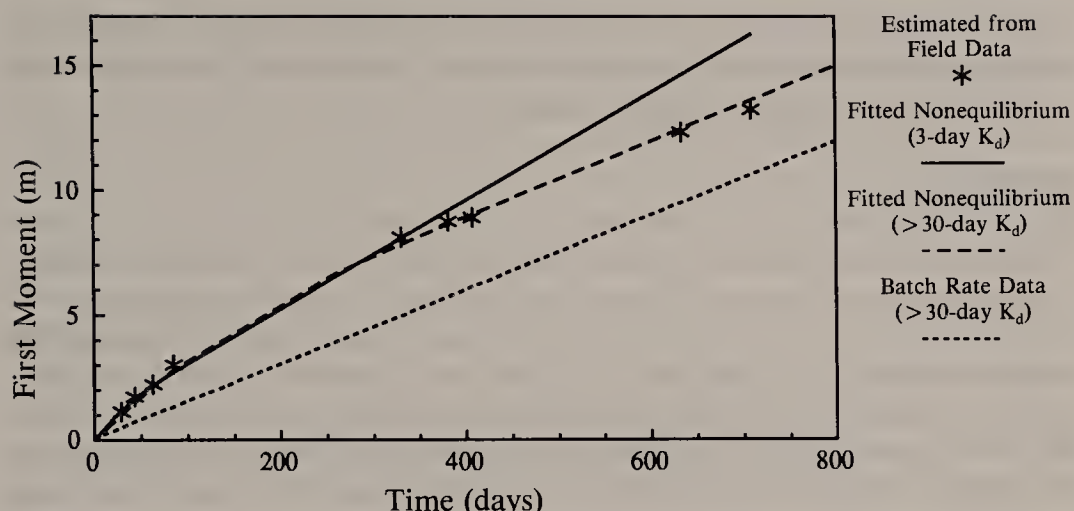


Figure 13.3. Distance traveled by PCE plume center of mass in the horizontal plane: *: as estimated from the Borden sampling data; dotted line: as simulated with independently measured long-term batch rate and equilibrium sorption parameters; dashed line: as simulated with best-fit rate parameters and using the measured long-term sorption equilibrium; solid line: as simulated with best-fit rate parameters but restricted to short-term equilibrium sorption.

revised PCE transport modeling with the 30-day K_d (bulk Borden solids) has been described elsewhere (Figure 13.3, *dashed line*).^{17,104} The results thus suggest that, unless the bulk Borden samples are pulverized to induce more rapid uptake in the laboratory, sorption experiments of 30 days or longer are required to predict the long-term (far-field) rate of transport.

It is also important to note that the fitted rate constants for the solid-and dashed-line simulations of Figure 13.3 are significantly lower than the batch estimate of D_a/a^2 , for which a simulation is shown as a dotted line in Figure 13.3; clearly, the rapid initial movement of the plume is not simulated using this rate constant. The fitted first-order rate constant (dashed line) corresponds to a D_a/a^2 value of $4.6 \times 10^{-9} \text{ sec}^{-1}$, or only one-fiftieth of the batch estimate with bulk solids. The fitted fraction of "instantaneous" sorption sites for the best-fit field estimate was 0.30, versus 0.07 estimated from the batch data.

Thus, despite the slow rate of uptake observed in the batch experiments, estimated diffusivities were not sufficiently low to explain the extent of non-equilibrium observed in the field. It appears certain that aquifer heterogeneity (e.g., solute diffusion into less permeable layers or aggregated dead zones^{19,105}) played a major role in the field experiment. In the unlikely case that batch measured D_a (which equals $3.4 \times 10^{-11} \text{ cm}^2/\text{sec}$ for bulk material) could be assumed to hold for the aggregates, a spherical aggregate diameter of roughly 0.8 mm would be needed to obtain the fitted rate constant.

Finally, the batch rate constants, while less than those expressed in the field, are sufficiently slow to be an important source of nonequilibrium under some conditions. For example, Ball and coworkers^{17,104} have shown that D_a/a^2 values

observed at the particle scale would lead to very significant nonequilibrium at conditions of laboratory soil column experiments or during field-scale ground-water extraction through radial pumping.

Summary

Recent evidence regarding organic partitioning with natural solids suggests that at least some fraction of the sorption capacity is subject to rate limitation. Field and column evidence suggests that it may be unrealistic to assume that sorption equilibrium is attained in contaminant transport, even at the relatively low velocities of natural gradient transport, and especially at the higher velocities of soil columns or groundwater remediation efforts. Although there have been a number of recent studies of sorption and desorption rates, very few of these have been conducted over the very long time periods (hundreds of days) over which very slow continuing rates of uptake have been shown to occur.

In many cases, first-order approximations have been used to describe rate-limited sorption, but often with the understanding that the first-order rates represent approximations to diffusive transport.^{20,106} An inverse correlation of rate constants with partitioning coefficient has been observed and is consistent with the concept of retarded intraparticle diffusion. Diffusive limitations have been extensively cited in transport studies and have begun to be investigated in more detail through direct batch assessment. Nonetheless, the diffusive process in natural solids is still poorly understood.

Since intraparticle diffusion is an important mechanism in determining sorption and desorption rates in aquifer solids, better understanding of the process is clearly desirable. In the following section, some studies are reviewed which specifically examine the nature of diffusion in different media which are—or may be—relevant to subsurface materials.

DIFFUSION STUDIES IN DEFINED MEDIA

Because of the extreme complexity and heterogeneity of soil solids, complete characterization of the diffusive medium is impossible. However, the nature of the medium will play a critical role in the diffusion process. For example, diffusion in pore space can be significantly affected by tortuosity, pore size (steric hindrance), and nature of the pore solvent (e.g., bulk water, surface-bound water, or organic gel phases). In this chapter, literature from three broad areas of diffusive transport research are reviewed, all of which have potential application to soil environments. First, we review recent studies of ion diffusion and light hydrocarbon diffusion in rock matrices. These studies, conducted under controlled conditions with rock slabs, should be directly applicable toward understanding diffusion in smaller-sized particles broken down from these same materials. Second, we review some of the vast literature

regarding diffusion into porous sorbent pellets. Because these sorbents are much better defined than soil solids, independent parameter estimation has been generally more feasible. Third, and finally, we review some theory regarding the diffusion of small organic molecules in larger organic structures. Although the nature of soil organics is highly variable and difficult to characterize, it may be possible to generalize from studies with more well-defined organic polymers.

Diffusion in Rock

Diffusion in rock matrices has received considerable recent attention, primarily in the context of radioactive waste disposal,^{54,66,107-111} but also in the context of hydrocarbon recovery from sedimentary rocks.¹¹²⁻¹¹⁴ In these contexts, investigators have studied diffusion across laboratory-scale rock slabs in bench-top diffusion cells. Parameters measured, in the notation defined previously, always include the intrinsic diffusion coefficient, D_i . In addition, the apparent (transient) diffusion coefficient, D_a (which equals $[\epsilon_i D_p]/[\epsilon_i + \rho_a K_d]$), is often estimated from early time data.^{54,113} The ratio of D_i/D_a provides an estimate of the "rock capacity factor" ($\epsilon_i + \rho_a K_d$). For the case where sorption is negligible, D_a also provides an estimate of the effective pore diffusivity, D_p . In cases where rock porosity has been independently measured,^{114,115} D_p can be estimated from the steady-state (intrinsic) diffusion coefficient ($D_p = D_i/\epsilon_i$).

Bradbury and coworkers^{54,66,108,110,116} and Neretnieks and coworkers^{107,111,115,117} have studied the diffusion of various ionic species in a variety of rock matrices, including granites and other crystalline rocks as well as sandstones and limestones. In these works, the reported steady-state diffusion coefficients (D_i) for iodide ranged from 2×10^{-10} cm²/sec (granite) to 3×10^{-7} cm²/sec (sandstone). With the given estimates for rock capacity factor, D_p , in the range of 2×10^{-7} cm²/sec to 4×10^{-6} cm²/sec were implied. Taking bulk iodide diffusivity to be 2×10^{-5} cm²/sec,¹⁰⁸ we calculate tortuosity factors to be in the range of 20 to 100 for these studies.

Similar tortuosities have been implied by a recent investigation of the diffusion of simple alkanes (primarily methane, ethane, and propane) through a wide variety of water-saturated rock samples at different temperatures by Krooss and Leythaeuser.¹¹⁴ Twenty-two different rock cores were studied, each with several hydrocarbons. Careful interpretation of the data of Krooss and Leythaeuser in the context of Equations 13.3-13.9 has been detailed elsewhere,¹⁷ and shows that χ_e values of between 10 and 100 are generally reflected by the data. This is in good agreement with the previously discussed data for iodide diffusion in crystalline rock. In addition, the data of Krooss and Leythaeuser reveal an important trend of increased tortuosity with solids of finer grain size (e.g., claystone versus sandstone).

Another interesting result of the hydrocarbon diffusion study was the comparison of diffusion rates among different alkanes. In general, ratios of diffusion coefficients (higher molecular weight compound:methane) were lower

than diffusivity in bulk water would suggest. In one shale, for example, the diffusion coefficient for ethane dropped almost two orders of magnitude below that of methane. Krooss and Leythaeuser suggest that "possibly a large fraction of pore diameters in this sample approaches molecular size and therefore acts as a sieve for larger molecules."¹¹⁴ The effective tortuosity values estimated for halogenated organic chemical diffusion in the Borden solids (200 to 1000) were similar to those found for ethane diffusion in shale by Krooss and Leythaeuser. The results suggest that similar effects of pore constrictivity may be at work in both studies. In the following sections, we review some studies with synthetic sorbents for which diffusion has been well studied and for which pore size is known to play an important role.

Diffusion in Microporous Sorbent Particles

Diffusively limited uptake and release of chemicals by synthetic sorbents has been investigated by chemical engineers for many years,^{118,119} and considerable research effort has been directed toward understanding rates of uptake by well-defined microporous particles. In some cases, diffusion of strongly adsorbed solutes is assumed to be augmented (surface diffusion), while other studies have shown restrictive or hindered diffusion in small pores. As an extreme case, diffusion in zeolites, which have pore diameters of approximately 0.3 to 0.8 nm, can be extremely slow. Because there are important conceptual differences between these related areas of research (surface diffusion, restricted diffusion in micropores, and zeolite diffusion), each is considered separately below.

Surface Diffusion

In some sorbents, solute uptake has been observed to progress more rapidly than can be predicted by pore diffusion alone, implying diffusion of sorbed species, presumably along an adsorption surface. For example, surface diffusion has been invoked in modeling the uptake of benzaldehyde from methanol and water into two different polymeric, porous Amberlite resins, XAD-4 and XAD-7.¹²⁰ Apparent diffusion coefficients calculated from the data were two times higher than pore diffusion would predict for XAD-7 and between 5 and 14 times higher for XAD-4, which sorbed benzaldehyde more strongly. This increased flux of solute was successfully simulated by incorporating surface diffusion into the uptake model. Assumptions of surface diffusion have also been extensively applied to modeling organic solute uptake and release by granular activated carbon, and a surface diffusion model has been extensively used to describe and design fixed-bed GAC adsorbers.¹²¹ Dobrezelewski,¹²² as cited by Crittenden et al.,¹²³ experimentally measured surface diffusivities for chlorinated alkanes, chlorinated alkenes, and aromatic compounds in batch rate experiments with granular activated carbon, for which observed uptake rates could not be accounted by pore diffusion alone. Estimated surface diffu-

sivities ranged between 10^{-10} and $10^{-7} \text{ cm}^2/\text{sec}$, or roughly one to four orders of magnitude lower than bulk aqueous diffusion coefficients. However, sorbed-phase concentrations were substantially higher than concentrations in the pore fluid, such that the large majority of the diffusive flux was estimated to occur in the adsorbed phase. Surface diffusion coefficients decreased with strength of sorption, such that the surface:pore diffusive flux ratio (calculated at the initial solute concentration) was relatively invariant for 31 GAC-solute systems (6.6 ± 2.0 ; 95% confidence).

Although mechanisms of surface diffusion are still poorly understood, one clear requirement of the process is continuity of adsorbing surface. In general, the surface diffusion process is only invoked when necessary to explain rates of uptake in excess of those explainable by pore diffusion alone. In the context of natural solids, particles are generally aggregates of different materials, with surfaces covered with a wide variety of coatings, including organic gels, humic substances, and polymeric oxides and hydroxides.⁴⁴ Such coatings are not likely to provide a continuous surface for diffusion of adsorbed species, and diffusion through the pore spaces and surface-associated gels is more likely to be important. These processes have also been addressed by studies in well-defined media, as described in the sections which follow.

Restrictive Pore Diffusion

In contrast to the surface diffusion model described above, diffusion in some commercial sorbents occurs at rates which are less than pore diffusion would predict. For example, results of this kind have been reported by Satterfield et al.,⁵⁷ who studied the effect of solute molecular diameter and pore size on liquid-phase diffusivity in silica-alumina catalyst beads (3 to 4 mm in diameter, median pore diameter of 3.2 nm). Twenty-two different solute-solvent systems were studied, including (1) sodium chloride and selected sugars in water, (2) substituted benzenes in iso-octane, and (3) selected alkanes, cycloalkanes, and 1-octene in hexane. Sorption was found to be fully reversible, and the authors reported that desorption experiments yielded identical diffusivities as the uptake studies. All solutes except the 1-octene and substituted benzenes were not sorbed beyond the extent expected for simple partitioning with pore water. Preferential adsorption of the aromatics and octene was attributed to the π -bonds found in these solutes.

For the sorbent studied, the effective tortuosity factor (i.e., $\chi_e = \chi/K_t$) was found to increase with the critical molecular diameter of the solute, defined as the diameter of the smallest cylinder through which a solute can pass without distortion. Effective pore diffusivities (D_p) ranged between 4 and 30% of bulk aqueous diffusivity. Data were regressed to the following equation:

$$\log(D_b/D_p) = \log(\chi_e) = 0.37 + 2.0 \lambda \quad (13.10)$$

where λ = ratio of critical molecular diameter to pore diameter [-], and the range of the regression was $0.09 < \lambda < 0.5$. Extrapolating to $\lambda = 0$ (where K_t

= 1 by definition), Satterfield et al. estimated a tortuosity factor ($\chi = K_r \chi_e$) of 2.3, which was cited as reasonable for these very porous sorbents. Assuming this value for χ , Equation 13.10 can be combined with Equation 13.7b to obtain:

$$\text{Log } (K_r) = -2.0 \lambda \quad (13.11)$$

Satterfield et al.⁵⁷ showed that this equation also described previous results for diffusion of nonelectrolytes through artificial mica membranes ($0.01 < \lambda < 0.2$).⁶⁹

Prasher and Ma conducted diffusion rate studies on a suite of 37 hydrocarbon solute-solvent pairs, using two types of cylindrical alumina pellets with mean pore diameters estimated at 11.4 and 13.3 nm.⁵⁸ χ_e was calculated for all solute-solvent pairs, using the measured apparent diffusion coefficient and an independently measured partitioning coefficient. Molecular sizes were much smaller than pore sizes in this study ($0.05 < \lambda < 0.09$), and λ was based on average molecular radius (calculated from molar volume) rather than critical diameter. For the systems studied, effective pore diffusion coefficients were estimated to be between 1.5 and 11% of D_b . In the midrange of their data ($\lambda = 0.07$), the reduction in effective diffusivity observed by Prasher and Ma was equivalent to that predicted by Equation 13.10.

Chantong and Massoth conducted experiments with a system of highly adsorbed polycyclic aromatic solutes and four γ -aluminas of differing pore size;^{64,70} λ values were > 0.09 and in the same range as those of Satterfield et al.⁵⁷ The four aluminas had average pore sizes between 5 and 15 nm, and pore size distributions (reported by the supplier) were roughly lognormal over a 10-fold range. Chantong and Massoth⁷⁰ follow Satterfield et al.⁵⁷ in using critical molecular diameter in calculating λ and found the same dependency of K_r to λ (Equation 13.11). Since some sorption isotherms were highly nonlinear ($1/n = 0.66$), Chantong and Massoth were able to use studies conducted at different concentrations to make a strong argument that surface diffusion did not play a role in their system.

The above studies firmly establish that the mobility of hydrocarbon molecules in restrictive pores is significantly less than in bulk solution, with decreasing mobility as the ratio of molecular size to pore size increases. All models assumed that there was retardation of pore diffusion due to sorption. Although there was some evidence for surface diffusion in the work of Satterfield et al.,⁵⁷ the other studies did not report similar evidence, and the effect was explicitly excluded by the interpretation of Chantong and Massoth.⁷⁰

Diffusion in Zeolites

Diffusion in zeolites represents an extreme form of hindered diffusion, for which the distinction between pore and surface diffusion is no longer important; because of the molecular dimensions involved, it is impossible to distin-

guish absorbed from adsorbed phases and the only meaningful diffusion coefficients are overall coefficients, numerically equivalent to D_a in our notation. Because zeolite diffusion represents the low end of potential diffusion rates in porous solids, it is briefly reviewed below.

Zeolites are highly porous crystalline chemical structures with molecular-sized pore openings of fixed dimension. Diffusion in these solids is quite sensitive to the molecular dimensions of the sorbing species relative to the size of the zeolite cavities and apertures. Reported diffusion coefficients at room temperature span over 10 orders of magnitude, with reported values as low as 10^{-18} cm²/sec (e.g., krypton in K-mordenite at room temperature).¹²⁴ In zeolite (5A) adsorption studies of straight-chained hydrocarbons out of benzene solution, Roberts noted that the zeolite diffusion rate constant decreased as the chain-length of the diffusing alkane was increased; a 500-fold decrease in rate constant was observed between hexane ($n = 6$) and octadecane ($n = 18$).¹²⁵ Zeolite diffusivity for hexane, measured at 25°C, was roughly 2×10^{-12} cm²/sec in this system. Satterfield and others have shown that counterdiffusion in the presence of solvent can be several orders of magnitude slower than diffusion into an initially empty pore structure.^{56,126,127}

The range of observed diffusion coefficients in zeolites serves to highlight the fact that extreme reductions of solute mobility are possible as pore sizes become small; apparent diffusion coefficients in small pore spaces can vary over many order of magnitudes, with a continuum of possible values down practically to the rates of solid diffusion (10⁻²⁰ cm²/sec). Although nonpolar zeolite surface sites will not play a role in the soil-water environment, similarly sized pores are conceivable; diffusion may occur in microcracks, or alternatively, intraparticle pore spaces of clastic rock fragments may be largely filled with organics or with clay weathering products. In such cases "pore" dimensions may approach the mean free travel distances found in zeolites, and diffusion rates may be similarly low. For the specific case of diffusion through an organic matrix, diffusion can be quite complex, as discussed in the following section.

Diffusion in Organic Polymers

Organic matter in the soil environment has been the subject of considerable research, including a growing body of work to chemically characterize extracted organic matter.¹²⁸⁻¹³⁰ Nonetheless, the precise nature and location of in situ organic phases is still poorly understood and will vary highly from one natural solid to the next. With regard to soils of low organic carbon content, such as Borden aquifer solids, it can be a difficult undertaking to determine the organic carbon content,²¹ much less understand its nature or location. It is possible that some of the organic matter has been incorporated into biogenic carbonate minerals (shells) as polysaccharides, or that it exists as an adsorbed phase on mineral surfaces, either external to soil particles or incorporated

within them via adsorption prior to aggregation and cementation. Ball et al. found good correlation of organic carbon content with inorganic carbon content in the Borden aquifer solids.²¹ In a study of organic carbon in marine sediments, Suess found a similar correlation and suggested that carbonate surfaces were covered by organic layers.¹³¹ If sorption sites for small organic molecules are uniformly distributed throughout the sorbed grains, access to those sites (whether organic or surface area related) may require diffusion through an organic phase. With this in mind, it is worthwhile to briefly consider such diffusion.

Although diffusion in soil organic matter has not been studied directly, some insight might be gained from the polymer literature, where diffusion into amorphous organic structures has been studied for many years.¹³² Diffusion in such systems can be quite complex, and no single mathematical model successfully predicts the various experimental observations. In general, diffusion of an organic molecule in a polymer will be dependent on the concentration of the diffusing molecule and on the rate of polymer relaxation relative to the rate of diffusion.

When relaxation times are quite rapid relative to the rate of diffusion, such as at temperatures above the polymer's glass transition temperature, the polymer is said to be rubbery, and diffusion will be Fickian: Fick's first and second laws will hold and the diffusion coefficient will be independent of the polymer's history.¹³³ Typically diffusion coefficients are strong functions of concentration—in regions of low weight fraction of penetrant (e.g., < 20%), the diffusion coefficient will typically increase exponentially with concentration of penetrant.¹³⁴ Duda et al. have used free volume theory to correlate the diffusivity of low-molecular-weight solvents in polymers to temperature and weight fraction of penetrant.¹³⁵ An interesting application of their model was for the system toluene-polyvinyl acetate, for which the diffusion coefficient at 35°C was estimated to be 10^{-16} cm²/sec at zero penetrant concentration but projected to increase rapidly to 10^{-10} cm²/sec at 5% weight fraction toluene.

At the other extreme, relaxation constants may be very much slower than diffusion rates, and penetration may be characterized by a constant velocity advancement of a diffusate front which represents the boundary between swollen gel and glassy core.¹³² This has been designated as Class II diffusion (with Fickian diffusion designated as Class I)¹³⁶ and has been found to apply, for example, to the swelling of coals by pyridine.¹³⁷

Intermediate cases (when relaxation rates and diffusion are comparable) are non-Fickian and are sometimes referred to as *anomalous diffusion*. Such non-Fickian diffusion has been the subject of a number of reviews^{133,138} and has recently been considered in the context of diffusion through soil organic solids.⁶³ The theoretical considerations for this type of diffusion can be quite complex and can involve components of swelling stress or strain, orientation of molecules, and swelling or dissolution kinetics.¹³³ As noted by Rogers, the

diffusivity of a penetrant will decrease with polymer density, rigidity, and degree of cross-linking.¹³⁸ Strong interactions between the penetrant and the polymer (e.g., hydrogen bonding) will also slow the diffusive process; non-Fickian diffusion is often associated with simple gas and hydrocarbon penetrants whose sorption appears to be described by both an absorption (solubility) component and a Langmuir contribution.¹³³ The latter contribution is thought to be related to immobilized penetrant at fixed sites (e.g., defects or cavities) in the medium.¹³³ Pignatello⁶³ has reviewed the data of Rogers¹³⁸ describing diffusion coefficients of small organic molecules in polymers near room temperature. The reported coefficients range from 10^{-13} cm²/sec (benzene in polystyrene) to 10^{-7} cm²/sec (methyl bromide in polyethylene).

In considering synthetic organic contaminants in natural organic matter, it is probably most reasonable to assume that the organic polymers will have relatively rapid relaxation rates, such that diffusion will be Fickian. Furthermore, if the chemical potential of the organic contaminant is sufficiently low (i.e., aqueous concentration well below solubility), the diffusion coefficient may be independent of contaminant concentration. With this scenario, the diffusion coefficient will be a function of molecular size of the penetrant, "tightness" of the polymer (as measured primarily by its molar density and viscosity), and, possibly, specific interactions between the penetrant and chemical moieties of the organic matter.

The role of natural organic matter in intrasorbent diffusion undoubtedly depends upon the geometry of the situation and the location of sorption capacity in the soil particles. If a sorbing organic phase is present as an adsorbed layer on the pore walls, for example, then retardation of pore diffusion will result. In this case, intraorganic diffusion could serve as a channel for surface (or solid) diffusion, and could thus enhance diffusive fluxes, but only if the organic sorbent layer is continuous. On the other hand, if a dilute organic phase fills the pore space (or a portion thereof), then the overall effect on rate of uptake is less clear—although reported diffusion coefficients in polymers are much less than bulk diffusivity (by two to eight orders of magnitude), the concentration driving force will also be much higher. Thus, in the case of intraorganic matter diffusion there is no straightforward mechanistic relation between apparent diffusivity and strength of sorption. In one sense, intraorganic matter diffusion might be viewed as diffusion through the open spaces within the organic matrix, and specific physicochemical interactions might be viewed as a source of retardation. Such reasoning leads to a conclusion that, as with retarded pore diffusion, intraorganic matter diffusion should decrease with greater sorptive interactions. Note that, in this case, greater sorptive interactions are required *within the organic phase*, such that reduced rates of intraorganic diffusion at higher organic contents are not necessarily predicted, except possibly through an effect of reduced diffusive length scale.

SUMMARY

Experimental work with nonpolar organic chemicals and natural solids has shown that sorption and desorption processes may be much slower than is generally recognized. Solute transport experiments have suggested non-equilibrium conditions, and laboratory sorption experiments have demonstrated that equilibrium can take weeks to years to attain, even in well-mixed systems with small particle sizes and low organic carbon content. Diffusion limitations seem the most likely explanation for such behavior. In the few studies which have explicitly explored this mechanism, there is strong indication that grain-scale processes are important and that diffusion rates are decreased for more strongly sorbing compounds. For river sediments with chlorinated benzenes,⁶⁰ and for Borden solids with halogenated organic chemicals,^{17,102,103} the effects of solute hydrophobicity on sorption rate suggested retarded pore diffusion. With both studies, a particle-scale process was implicated by findings that sorbent pulverization significantly decreased times to equilibrium.

Consideration of diffusive processes in more well-defined media (rock slabs, porous sorbents, and organic polymers) provides some useful insights with regard to both (1) the wide range of diffusivities which might be expressed in natural soil solids, and (2) potential complexities of modeling the process. Effective tortuosities on the order of 10 to 100 have been found for diffusion of small molecules and ions in a variety of rock types, with tortuosity increasing for finer pore structure. Limited study with a larger molecule (ethane) in shale suggested effects of pore constrictivity which were of similar magnitude to those estimated for halogenated chemical diffusion in Borden solids. Diffusion studies with porous alumina catalysts have shown that additional two-to twenty-fold reductions in diffusivity might be expected when solute size approaches 10 to 50% of pore diameter, while research into the diffusion of small organic molecules in polymers has elucidated some of the potential effects of the soil organic matrix on intrasorbent diffusion.

The discussions in this chapter highlight the difficulties in characterizing solute uptake by material as complex, diverse, and heterogeneous as soil, sediment, and subsurface aquifer solids. While recent advances provide important clues as to the nature and significance of the rate-limiting processes, accurate *a priori* estimation of sorption rates does not appear to be feasible at the present time. Further research is required to better understand the relevant diffusion media, length scales, and overall rates for different natural solids, and careful attention to experimental measurements is required. It is becoming increasingly apparent that short-term measurements with unaltered natural material, whether in column or batch study, may underestimate equilibrium sorption and overestimate sorption/desorption rate. This has been specifically demonstrated for Borden aquifer material and is almost assuredly true for other natural solids as well.

REFERENCES

1. Mackay, D. M., and J. A. Cherry. "Groundwater Contamination: Pump-and-Treat Remediation," *Environ. Sci. Technol.* 23(6):630-636 (1989).
2. Criddle, C. S., L. M. Alvarez, and P. L. McCarty. "Microbiological Processes in Porous Media," in *Fundamentals of Transport in Porous Media*, J. Bear and M. Y. Corapcioglu, Eds. (Dordrecht, The Netherlands: Kluwer Academic Publishers, in press).
3. Reijnaarts, H. H. M., A. Bachmann, J. C. Jumelet, and A. J. B. Zehnder. "Effect of Desorption and Intraparticle Mass Transfer on the Aerobic Biomineralization of α -Hexachlorocyclohexane in a Contaminated Calcareous Soil," *Environ. Sci. Technol.* 24(9):1349-1354 (1990).
4. van Genuchten, M. T., and P. J. Wierenga. "Mass Transfer Studies in Sorbing Porous Media: I. Analytical Solutions," *Soil Sci. Soc. Am. J.* 40(4):473-480 (1976).
5. Rao, P. S. C., R. E. Jessup, and T. M. Addiscott. "Experimental and Mathematical Aspects of Solute Diffusion in Spherical and Non-Spherical Aggregates," *Soil Sci.* 133(6):342-349 (1982).
6. Valocchi, A. J. "Validity of the Local Equilibrium Assumption for Modeling Sorbing Solute Transport through Homogeneous Soils," *Water Resour. Res.* 21(6):808-820 (1985).
7. Bahr, J. M., and J. Rubin. "Direct Comparison of Kinetic and Local Equilibrium Formulations for Solute Transport Affected by Surface Reactions," *Water Resour. Res.* 23(3):438-452 (1987).
8. Roberts, P. V., M. N. Goltz, R. S. Summers, J. S. Crittenden, and P. Nkedi-Kizza. "The Influence of Mass Transfer on Solute Transport in Column Experiments with an Aggregated Soil," *J. Contam. Hydrol.* 1(4):375-393 (1987).
9. Brusseau, M. L., R. E. Jessup, and P. S. C. Rao. "Modeling the Transport of Solutes Influenced by Multi-Process Nonequilibrium," *Water Resour. Res.* 25(9):1971-1988 (1989).
10. Roberts, P. V., and D. M. Mackay. "A Natural Gradient Experiment on Solute Transport in a Sand Aquifer," Stanford University Technical Report No. 292, Department of Civil Engineering, Stanford University, Stanford, CA (1986).
11. Mackay, D. M., D. L. Freyberg, P. V. Roberts, and J. A. Cherry. "A Natural Gradient Experiment on Solute Transport in a Sand Aquifer: 1. Approach and Overview of Plume Movement," *Water Resour. Res.* 22(13):2017-2029 (1986).
12. Freyberg, D. L. "A Natural Gradient Experiment on Solute Transport in a Sand Aquifer: 2. Spatial Moments and the Advection and Dispersion of Non-Reactive Tracers," *Water Resour. Res.* 22(13):2031-2046 (1986).
13. Roberts, P. V., M. N. Goltz, and D. M. Mackay. "A Natural Gradient Experiment on Solute Transport in a Sand Aquifer: 3. Retardation Estimates and Mass Balances for Organic Solutes," *Water Resour. Res.* 22(13):2047-2058 (1986).
14. Curtis, G. P., M. Reinhard, and P. V. Roberts. "Sorption of Hydrophobic Organic Compounds by Sediments," in *Geochemical Processes at Mineral Surfaces*, ACS Symposium Series 323, J. A. Davis and K. F. Hayes, Eds. (Washington, DC: American Chemical Society, 1986), pp. 191-216.
15. Sudicky, E. A. "A Natural Gradient Experiment on Solute Transport in a Sand Aquifer: 5. Spatial Variability of Hydraulic Conductivity and Its Role in the Dispersion Process," *Water Resour. Res.* 22(13):2069-2082 (1986).

16. Goltz, M. N. "Three-Dimensional Analytical Modeling of Diffusion-Limited Solute Transport," PhD Dissertation, Stanford University, Stanford, CA (1986).
17. Ball, W. P. "Equilibrium Partitioning and Diffusion Rate Studies with Halogenated Organic Chemicals and Sandy Aquifer Material," PhD Dissertation, Stanford University, Stanford, CA (1989).
18. Durant, M. G. "Spatial Variability of Organic Solute Sorption in the Borden Aquifer," MS Thesis and Technical Report No. 303, Stanford University, Stanford, CA (1986).
19. Goltz, M. N., and P. V. Roberts. "Simulations of Physical Solute Transport Models: Application to a Large-Scale Field Experiment," *J. Contam. Hydrol.* 3(1):37-63 (1988).
20. Goltz, M. N., and P. V. Roberts. "Interpreting Organic Solute Transport Data from a Field Experiment Using Physical Nonequilibrium Models," *J. Contam. Hydrol.* 1(1):77-93 (1986).
21. Ball, W. P., C. Buehler, T. C. Harmon, D. M. Mackay, and P. V. Roberts. "Characterization of a Sandy Aquifer Material at the Grain Scale," *J. Contam. Hydrol.* 5(3):253-295 (1990).
22. Travis, C. C., and C. B. Doty. "Can Contaminated Aquifers at Superfund Sites Be Remediated?" *Environ. Sci. Technol.* 24(10):1464-1465 (1990).
23. Roberts, P. V., L. Semprini, G. D. Hopkins, D. Grbic-Galic, P. L. McCarty, and M. Reinhard. "In-Situ Aquifer Restoration of Chlorinated Aliphatics by Methanotrophic Bacteria," U.S. EPA Report-600/2-89/033, R. S. Kerr Environmental Research Laboratory, Ada, OK (1989).
24. Semprini, L., G. D. Hopkins, P. V. Roberts, and P. L. McCarty. "A Field Evaluation of In-Situ Biodegradation of Chlorinated Ethenes: Part 3, Studies of Competitive Inhibition," *Ground Water* 29(2):239-250 (1991).
25. Harmon, T. C., L. Semprini, and P. V. Roberts. "Investigating the Validity of the Local Equilibrium Assumption at an Experimental Aquifer Restoration Site Using Laboratory-Scale Parameter Estimates," in *Proceedings of the 1990 Specialty Conference on Environmental Engineering*, C. R. O'Melia, Ed. (New York: American Society of Civil Engineers, 1990), pp. 298-306.
26. Harrison, E. M., and J. F. Barker. "Sorption and Enhanced Biodegradation of Trace Organics in a Groundwater Reclamation Scheme—Gloucester Site, Ottawa, Canada," *J. Contam. Hydrol.* 1(4):349-373 (1987).
27. Bahr, J. M. "Analysis of Nonequilibrium Desorption of Volatile Organics During Field Test of Aquifer Decontamination," *J. Contam. Hydrol.* 4(3):205-222 (1989).
28. Pignatello, J. J., C. R. Frink, P. A. Marin, and E. X. Droste. "Field-Observed Ethylene Dibromide in an Aquifer after Two Decades," *J. Contam. Hydrol.* 5(2):195-214 (1990).
29. Wood, W. W., T. F. Kraemer, and P. Hearn, Jr. "Intragranular Diffusion: An Important Mechanism Influencing Solute Transport in Clastic Aquifers?" *Science* 247:1569-1572 (1990).
30. van Genuchten, M. T., J. M. Davidson, and P. J. Wierenga. "An Evaluation of Kinetic and Equilibrium Equations for the Prediction of Pesticide Movement through Porous Media," *Soil Sci. Soc. Am. Proc.* 38(1):29-35 (1974).
31. van Genuchten, M. T., and P. J. Wierenga. "Mass Transfer Studies in Sorbing Porous Media: II. Experimental Evaluation with Tritium," *Soil Sci. Soc. Am. J.* 41(2):272-278 (1977).

32. Rao, P. S. C., J. M. Davidson, R. E. Jessup, and H. M. Selim. "Evaluation of Conceptual Models for Describing Nonequilibrium Adsorption-Desorption of Pesticides During Steady-Flow in Soils," *Soil Sci. Soc. Am. J.* 43(1):22-28 (1979).
33. Rao, P. S. C., D. E. Rolston, R. E. Jessup, and J. M. Davidson. "Solute Transport in Aggregated Porous Media: Theoretical and Experimental Evaluation," *Soil Sci. Soc. Am. J.* 44(6):1139-1146 (1980).
34. Nkedi-Kizza, P., P. S. C. Rao, R. E. Jessup, and J. M. Davidson. "Ion Exchange and Diffusive Mass Transfer During Miscible Displacement through an Aggregated Oxisol," *Soil Sci. Soc. Am. J.* 46(3):471-476 (1982).
35. Hutzler, N. J., J. C. Crittenden, and J. S. Gierke. "Transport of Organic Compounds with Saturated Groundwater Flow: Experimental Results," *Water Resour. Res.* 22(3):285-295 (1986).
36. Miller, C. T., and W. J. Weber, Jr. "Modeling the Sorption of Hydrophobic Contaminants by Aquifer Materials—II. Column Reactor Systems," *Water Res.* 22(4):465-474 (1988).
37. Lee, L. S., P. S. C. Rao, M. L. Brusseau, and R. A. Ogwaday. "Nonequilibrium Sorption of Organic Contaminants During Flow through Columns of Aquifer Materials," *Environ. Toxicol. Chem.* 7:779-793 (1988).
38. Brusseau, M. L., and P. S. C. Rao. "Sorption Nonideality During Organic Contaminant Transport in Porous Media," *CRC Crit. Rev. Environ. Control* 19(1):33-99 (1989).
39. Koskinen, W. C., G. A. O'Connor, and H. H. Cheng. "Characterization of Hysteresis in the Desorption of 2,4,5-T from Soils," *Soil Sci. Soc. Am. J.* 43(5):871-874 (1979).
40. Saloni, P. O., J. B. Robinson, and F. E. Chase. "A Comparison of Autoclaved and Gamma-Irradiated Soils as Media for Microbial Colonization Experiments," *Plant and Soil* 27(2):239-248 (1967).
41. Skipper, H. D., and D. T. Westermann. "Comparative Effects of Propylene Oxide, Sodium Azide, and Autoclaving on Selected Soil Properties," *Soil Biol. Biochem.* 5:409-414 (1973).
42. Boyd, S. A., and R. King. "Adsorption of Labile Organic Compounds by Soil," *Soil Sci.* 137(2):115-119 (1984).
43. Mackay, D. M., W. P. Ball, and M. G. Durant. "Variability of Aquifer Sorption Properties in a Field Experiment on Groundwater Transport of Organic Solutes: Methods and Preliminary Results," *J. Contam. Hydrol.* 1(1):119-132 (1986).
44. Karickhoff, S. W. "Organic Pollutant Sorption in Aquatic Systems," *J. Hydraul. Eng. Div., ASCE* 110(6):707-735 (1984).
45. Rao, P. S. C., and J. M. Davidson. "Estimation of Pesticide Retention and Transformation Parameters Required in Nonpoint Source Pollution Models," in *Environmental Impact of Nonpoint Source Pollution*, M. R. Overcash and J. M. Davidson, Eds. (Ann Arbor, MI: Ann Arbor Science, 1980), pp. 23-67.
46. Morel, F. M. M., and P. M. Gschwend. "The Role of Colloids in the Partitioning of Solutes in Natural Waters," in *Aquatic Surface Chemistry*, W. Stumm, Ed. (New York: John Wiley and Sons, 1987), pp. 405-422.
47. Voice, T. C., C. P. Rice, and W. J. Weber, Jr. "Effect of Solids Concentration on the Sorptive Partitioning of Hydrophobic Pollutants in Aquatic Systems," *Environ. Sci. Technol.* 17(9):513-518 (1983).
48. Gschwend, P. M., and S.-C. Wu. "On the Constancy of Sediment-Water Partition

- Coefficients of Hydrophobic Organic Pollutants," *Environ. Sci. Technol.* 19(1):90-96 (1985).
49. McCarthy, J. F., B. D. Jimenez, G. R. Southworth, D. M. DiToro, and M. C. Black. "Anomalous Binding of Organic Contaminants May Be Artifactual Due to Radiochemical Impurities," *Water Res.* 20(10):1251-1254 (1986).
50. Weber, W. J., Jr. *Physicochemical Processes for Water Quality Control* (New York: John Wiley and Sons, 1972).
51. Kasten, P. R., and N. R. Amundson. "An Elementary Theory of Adsorption in Fluidized Beds—Mathematics of Adsorption in Beds," *Ind. Eng. Chem.* 42(7):1341-1346 (1952).
52. Masamune, S., and J. M. Smith. "Adsorption Rate Studies—Interaction of Diffusion and Surface Processes," *Am. Inst. Chem. Eng. J.* 11(1):34-40 (1965).
53. Lee, R. G., and T. W. Weber. "Isothermal Adsorption in Fixed Beds," *Can. J. Chem. Eng.* 47(1):54-59 (1969).
54. Bradbury, M. H., and A. Green. "Measurement of Important Parameters Determining Aqueous Phase Diffusion Rates through Crystalline Rock Matrices," *J. Hydrol.* 82(1/2):39-55 (1985).
55. Roberts, P. V., and R. York. "Adsorption of Normal Paraffins from Binary Liquid Solutions by 5A Molecular Sieve Adsorbent," *Ind. Eng. Chem. Process Design Develop.* 6(4):516-525 (1967).
56. Moore, R. M., and J. R. Katzer. "Counterdiffusion of Liquid Hydrocarbons in Type Y Zeolite: Effect of Molecular Size, Molecular Type, and Direction of Diffusion," *Am. Inst. Chem. Eng. J.* 18(4):816-824 (1972).
57. Satterfield, C. N., C. K. Colton, and W. H., Pitcher, Jr. "Restricted Diffusion in Liquids within Fine Pores," *Am. Inst. Chem. Eng. J.* 19(3):628-635 (1973).
58. Prasher, B. D., and Y. H. Ma. "Liquid Diffusion in Microporous Alumina Pellets," *Am. Inst. Chem. Eng. J.* 23(3):303-311 (1977).
59. Bouchard, D. C., A. L. Wood, M. L. Campbell, P. Nkedi-Kizza, and P. S. C. Rao. "Sorption Nonequilibrium During Solute Transport," *J. Contam. Hydrol.* 3(1):209-223 (1988).
60. Wu, S.-C., and P. M. Gschwend. "Sorption Kinetics of Hydrophobic Organic Compounds to Natural Sediments and Soils," *Environ. Sci. Technol.* 20(7):717-725 (1986).
61. Miller, C. T., and W. J. Weber, Jr. "Sorption of Hydrophobic Organic Pollutants in Saturated Soil Systems," *J. Contam. Hydrol.* 1(1/2):243-261 (1986).
62. Weber, W. J., Jr., and C. T. Miller. "Modeling the Sorption of Hydrophobic Contaminants by Aquifer Materials: I. Rates and Equilibria," *Water Res.* 22(4):457-464 (1988).
63. Pignatello, J. J. "Sorption Dynamics of Organic Compounds in Soils and Sediments," in *Reactions and Movements of Organic Chemicals in Soils*, B. L. Sawhney and K. Brown, Eds. (Madison, WI: Soil Science Society of America and American Society of Agronomy, 1989), pp. 45-80.
64. Chantong, A. "Diffusion of Polyaromatic Compounds in Amorphous Catalyst Supports," PhD Dissertation, University of Utah, Logan, UT (1982).
65. van Brakel, J., and P. M. Heertjes. "Analysis of Diffusion in Macroporous Media in Terms of a Porosity, a Tortuosity and a Constrictivity Factor," *Int. J. Heat Mass Transfer* 17(9):1093-1103 (1974).
66. Lever, D. A., M. H. Bradbury, and S. J. Hemingway. "The Effect of Dead-End Porosity on Rock-Matrix Diffusion," *J. Hydrol.* 80(1/2):45-76 (1985).

67. Burganos, V. N., and S. V. Sotirchos. "Diffusion in Pore Networks: Effective Medium Theory and Smooth Field Approximation," *Am. Inst. Chem. Eng. J.* 33(10):1678-1689 (1987).
68. Wakao, N., and J. M. Smith. "Diffusion in Catalyst Pellets," *Chem. Eng. Sci.* 17(11):825-834 (1962).
69. Beck, R. E., and J. S. Schultz. "Hindrance of Solute Diffusion within Membranes as Measured with Microporous Membranes of Known Pore Geometry," *Biochim. Biophys. Acta* 255:273-303 (1972).
70. Chantong, A., and F. E. Massoth. "Restrictive Diffusion in Aluminas," *Am. Inst. Chem. Eng. J.* 29(5):725-731 (1983).
71. Karickhoff, S. W. "Sorption Kinetics of Hydrophobic Pollutants in Natural Sediments," in *Contaminants and Sediments, Vol. 2: Analysis, Chemistry, and Biology*, R. A. Baker, Ed. (Ann Arbor, MI: Ann Arbor Science, 1980), pp. 193-205.
72. DiToro, D. M., and L. M. Horzempa. "Reversible and Resistant Components of PCB Adsorption-Desorption," *Environ. Sci. Technol.* 16(9):594-602 (1982).
73. Horzempa, L. M., and D. M. DiToro. "The Extent of Reversibility of Polychlorinated Biphenyl Adsorption," *Water Res.* 17(8):851-859 (1983).
74. DiToro, D. M., and L. M. Horzempa. "Reversible and Resistant Component Model of Hexachlorobiphenyl Adsorption-Desorption Resuspension and Dilution," in *Physical Behavior of PCBs in the Great Lakes*, D. Mackay, S. Peterson, S. J. Eisenreich, and M. S. Simmons, Eds. (Ann Arbor, MI: Ann Arbor Science, 1983), pp. 89-113.
75. DiToro, D. M. "A Particle Interaction Model of Reversible Organic Chemical Sorption," *Chemosphere* 14(10):1503-1538 (1985).
76. DiToro, D. M., J. D. Mahony, P. R. Kirchgraber, A. L. O'Byrne, L. R. Pasquale, and D. C. Piccirilli. "The Effects of Nonreversibility, Particle Concentration, and Ionic Strength on Heavy Metal Sorption," *Environ. Sci. Technol.* 20(1):55-61 (1986).
77. Mackay, D., and B. Powers. "Sorption of Hydrophobic Chemicals from Water: A Hypothesis for the Mechanism of the Particle Concentration Effect," *Chemosphere* 16(4):745-757 (1987).
78. Voice, T. C., and W. J. Weber, Jr. "Sorbent Concentration Effects in Liquid/Solid Partitioning," *Environ. Sci. Technol.* 19(9):789-796 (1985).
79. Honeyman, B. D., L. S. Balistrieri, and J. W. Murray. "Oceanic Trace Metal Scavenging: The Importance of Particle Concentration," *Deep-Sea Res.* 35(2):227-246 (1988).
80. Karickhoff, S. W., and K. R. Morris. "Sorption Dynamics of Hydrophobic Pollutants in Sediment Suspensions," *Environ. Toxicol. Chem.* 4:469-479 (1985).
81. Witkowski, P. J., P. R. Jaffe, and R. A. Ferrara. "Sorption and Desorption Dynamics of Aroclor 1242 to Natural Sediment," *J. Contam. Hydrol.* 2(3):249-269 (1987).
82. Rao, P. S. C., and P. Nkedi-Kizza. "Pesticide Sorption on Whole Soils and Soil Size-Separates," in *Estimation of Parameters for Modeling the Behavior of Selected Pesticides and Orthophosphate*, NTIS PB84-148774, P. S. C. Rao, V. E. Berkheisen, and L. T. Ou, Eds., prepared for U.S. EPA, Office of Research and Development, Environmental Research Laboratory, Athens, GA (1984), pp. 5-47.
83. Selim, H. M., J. M. Davidson, and R. S. Mansell. "Evaluation of a Two-Site Adsorption-Desorption Model for Describing Solute Transport in Soils," in *Pro-*

- ceedings of the Summer Computer Simulation Conference* (Washington, D.C., 1976), Simulations, Councils Inc., LaJolla, CA, pp. 444-448.
- 84. Jaffe, P. R., and D. M. Tuck. "Theoretical Study of Partitioning of Organic Solutes on Soil," paper presented at Ground Water Geochemistry Conference, Association of Ground Water Scientists and Engineers, Denver, CO, Feb. 16-18, 1988.
 - 85. Miller, C. T., J. A. Pedit, and W. J. Weber, Jr. "Modeling Sorption, Desorption and Hydrolysis Processes in Groundwater Systems," *EOS* 69(44):1196 (1988).
 - 86. Wu, S.-C., and P. M. Gschwend. "Numerical Modeling of Sorption Kinetics of Organic Compounds to Soil and Sediment Particles," *Water Resour. Res.* 24(8):1373-1383 (1988).
 - 87. Karickhoff, S. W., D. S. Brown, and T. A. Scott. "Sorption of Hydrophobic Pollutants on Natural Sediments," *Water Res.* 13(3):241-248 (1979).
 - 88. Duursma, E. K., and C. J. Bosch. "Theoretical, Experimental and Field Studies Concerning Diffusion of Radioisotopes in Sediments and Suspended Solid Particles of the Sea: Part B, Methods and Experiments," *Neth. J. Sea Res.* 3(3):423-457 (1970).
 - 89. McCall, P. J., and G. L. Agin. "Desorption Kinetics of Picloram as Affected by Residence Time in the Soil," *Environ. Toxicol. Chem.* 4(1):37-44 (1985).
 - 90. Oliver, B. G. "Desorption of Chlorinated Hydrocarbons from Spiked and Anthropogenically Contaminated Sediments," *Chemosphere* 15(8):1087-1106 (1985).
 - 91. Coates, J. T., and A. W. Elzerman. "Desorption Kinetics for Selected PCB Congeners from River Sediments," *J. Contam. Hydrol.* 1(1):191-210 (1986).
 - 92. Steinberg, S. M., and B. L. Sawhney. "Sorption and Desorption of 1,2-Dibromoethane by Soils," paper presented at 78th Annual Meeting, American Society of Agronomy, New Orleans, LA, Nov. 30-Dec. 5, 1986 (Agron. Abstr. 172-173).
 - 93. Pignatello, J. J. "Ethylene Dibromide Mineralization in Soils under Aerobic Conditions," *Appl. Environ. Microbiol.* 51:588-592 (1986).
 - 94. Pignatello, J. J., B. L. Sawhney, and C. R. Frink. "EDB: Persistence in Soil," *Science* 236:898 (1987).
 - 95. Steinberg, S. M., J. J. Pignatello, and B. L. Sawhney. "Persistence of 1,2-Dibromoethane in Soils: Entrapment in Intraparticle Micropores," *Environ. Sci. Technol.* 21(12):1201-1208 (1987).
 - 96. Sawhney, B. L., J. J. Pignatello, and S. M. Steinberg. "Determination of 1,2-Dibromoethane (EDB) in Field Soils: Implications for Volatile Organic Compounds," *J. Environ. Qual.* 17(1):149-152 (1988).
 - 97. Pignatello, J. J. "Slow Desorption of Halogenated Aliphatic Hydrocarbons in Soils," paper presented at 194th National Meeting of the American Chemical Society, Denver, CO, September 1988.
 - 98. Chang, S.-L. "Sorption-Desorption of Diuron in Subsurface Systems: An Investigation of Desorption Hysteresis," Master's Thesis, Technical Report, University of North Carolina, Chapel Hill, NC (1989).
 - 99. Brusseau, M. L., R. E. Jessup, and P. S. C. Rao. "Sorption Kinetics of Organic Chemicals: Evaluation of Gas-Purge and Miscible-Displacement Techniques," *Environ. Sci. Technol.* 24(5):727-735 (1990).
 - 100. Brusseau, M. L., and P. S. C. Rao. "The Influence of Sorbate-Organic Matter

- Interactions on Sorption Nonequilibrium," *Chemosphere* 18(9/10):1691-1706 (1989).
101. Miller, C. T. "Modeling of Sorption and Desorption Phenomena for Hydrophobic Organic Contaminants in Saturated Soil Environments," PhD Dissertation, University of Michigan, Ann Arbor, MI (1984).
 102. Ball, W. P., and P. V. Roberts. "Long-Term Sorption of Halogenated Organic Chemicals: Part 1, Equilibrium" *Environ. Sci. Techol.* (in press, 1991).
 103. Ball, W. P., and P. V. Roberts. "Long-Term Sorption of Halogenated Organic Chemicals: Part 2, Intraparticle Diffusion" *Environ. Sci. Techol.* (in press, 1991).
 104. Ball, W. P., M. N. Goltz, and P. V. Roberts. "Sorption Rate Studies with Halogenated Organic Chemicals and Sandy Aquifer Material—Implications for Solute Transport and Groundwater Remediation," in *Proceedings of the 1990 Specialty Conference on Environmental Engineering*, C. R. O'Melia, Eds. (New York: American Society of Civil Engineers, 1990), pp. 307-313.
 105. Valocchi, A. J. "Spatial Moment Analysis of the Transport of Kinetically Adsorbing Solutes through Stratified Aquifers," *Water Resour. Res.* 25(2):273-279 (1989).
 106. van Genuchten, M. T. "A General Approach for Modeling Solute Transport in Structured Soils," in *Proceedings of the 17th International Congress, International Association of Hydrogeologists, Tucson, AZ: Hydrogeology of Rocks of Low Permeability* (Tucson, AZ: IAH Press, 1985), pp. 513-526.
 107. Skagius, K., and I. Neretnieks. "Diffusion in Crystalline Rocks," in *Scientific Basis for Radioactive Waste Management*, Vol. 5, W. Lutze, Ed. (Amsterdam: Elsevier Science, 1982), pp. 509-518.
 108. Bradbury, M. H., D. Lever, and D. Kinsey. "Aqueous Phase Diffusion in Crystalline Rock," in *Scientific Basis for Radioactive Waste Management*, Vol. 5, W. Lutze, Ed. (Amsterdam: Elsevier Science, 1982), pp. 569-578.
 109. Feenstra, S., J. A. Cherry, E. A. Sudicky, and Z. Haq. "Matrix Diffusion Effects on Contaminant Migration from an Injection Well in Fractured Sandstone," *Ground Water* 22(3):307-316 (1984).
 110. Bradbury, M. H., and A. Green. "Investigations into the Factors Influencing Long Range Matrix Diffusion Rates and Pore Space Accessibility at Depth in Granite," *J. Hydrol.* 89(1/2):123-139 (1986).
 111. Skagius, K., and I. Neretnieks. "Measurements of Cesium and Strontium Diffusion in Biotite Gneiss," *Water Resour. Res.* 24(1):75-84 (1988).
 112. Leythaeuser, D., R. G. Schaefer, and A. Yukler. "Diffusion of Light Hydrocarbons through Near-Surface Rocks," *Nature* 284:522-525 (1980).
 113. Krooss, B. M., and R. G. Schaefer. "Experimental Measurements of the Diffusion Parameters of Light Hydrocarbons in Water-Saturated Sedimentary Rocks: I. A New Experimental Procedure," *Org. Geochem.* 11(3):193-199 (1987).
 114. Krooss, B. M., and D. Leythaeuser. "Experimental Measurements of the Diffusion Parameters of Light Hydrocarbons in Water-Saturated Sedimentary Rocks: II. Results and Geochemical Significance," *Org. Geochem.* 12(2):91-108 (1988).
 115. Skagius, K., and I. Neretnieks. "Porosities and Diffusivities of Some Nonsorbing Species in Crystalline Rocks," *Water Resour. Res.* 22(3):389-398 (1986).
 116. Bradbury, M. H., and I. G. Stephen. "Diffusion and Permeability Based Sorption Measurements in Intact Rock Samples," *Mat. Res. Soc. Symp. Proc.* 50:81-90 (1985).

117. Birgersson, L., and I. Neretnieks. "Diffusion in the Matrix of Granitic Rock. Field Test in the Stripa Mine," in *Scientific Basis for Radioactive Waste Management*, Vol. 5, W. Lutze, Ed. (Amsterdam: Elsevier Science, 1982), pp. 519–528.
118. Satterfield, C. N. *Mass Transfer in Heterogeneous Catalysis* (Cambridge, MA: MIT Press, 1970).
119. Ruthven, D. M. *Principles of Adsorption and Adsorption Processes* (New York: John Wiley and Sons, 1984).
120. Komiyama, H., and J. M. Smith. "Intraparticle Mass Transport in Liquid-Filled Pores," *Am. Inst. Chem. Eng. J.* 20(4):728–734 (1974).
121. Crittenden, J. C., and W. J. Weber, Jr. "Predictive Model for Design of Fixed-Bed Adsorbers: Parameter Estimation and Model Development," *J. Environ. Eng. Div., ASCE* 104(EE2):185–197 (1978).
122. Dobrezelewski, M. "Determination and Prediction of Surface Diffusivities of Volatile Organic Compounds Found in Drinking Water," Master's Thesis, Michigan Technological University, Houghton, MI (1985).
123. Crittenden, J. C., D. W. Hand, H. Arora, and B. W. Lykins, Jr. "Design Considerations for GAC Treatment of Organic Chemicals," *Journal AWWA* 79(1):74–82 (1987).
124. Barrer, R. M. "Sorption Kinetics and Diffusivities in Porous Crystals," in *The Properties and Applications of Zeolites*, R. P. Townsend, Ed. (London: The Chemical Society, 1980), pp. 3–25.
125. Roberts, P. V. "The Adsorption of Normal Paraffins from Binary Liquid Solutions by Molecular Sieve 5A Adsorbent," PhD Dissertation, UMI #66-7842, Cornell University, Ithaca, NY (1966).
126. Satterfield, C. N., and J. R. Katzer. "Counterdiffusion of Liquid Hydrocarbons in Type Y Zeolite," in *Molecular Sieve Zeolites*, Vol. 2, Advances in Chemistry Series 102, E. M. Flanigen and L. B. Sand, Eds. (Washington, DC: American Chemical Society, 1971), pp. 193–208.
127. Satterfield, C. N., and C. S. Cheng. "Liquid Counterdiffusion of Selected Aromatic and Naphthenic Hydrocarbons in Type Y Zeolites," *Am. Inst. Chem. Eng. J.* 18(4):724–728 (1972).
128. Schnitzer, M., and S. U. Khan, Eds. *Soil Organic Matter* (Amsterdam: Elsevier Science, 1978).
129. Theng, B. K. G. *Formation and Properties of Clay-Polymer Complexes* (Amsterdam: Elsevier Science, 1979).
130. Schnitzer, M. "Binding of Humic Substances by Soil Mineral Colloids," in *Interactions of Soil Minerals with Natural Organics and Microbes*, SSSA Spec. Pub. No. 17 (Madison, WI: Soil Science Society of America, 1986), pp. 77–101.
131. Suess, E. "Interaction of Organic Compounds with Calcium Carbonate: II. Organo-Carbonate Association in Recent Sediments," *Geochim. Cosmochim. Acta* 37:2435–2447 (1973).
132. Crank, J. *The Mathematics of Diffusion*, 2nd ed. (Oxford: Oxford University Press, 1975).
133. Frisch, H. L. "Sorption and Transport in Glassy Polymers—A Review," *Polymer Eng. Sci.* 20(1):2–13 (1980).
134. Petropoulos, J. H., and P. P. Roussis. "A Discussion of Theoretical Models of Anomalous Diffusion of Vapors in Polymers," in *Permeability of Plastic Films and Coatings to Gases, Vapors and Liquids; Borden Award Symposium*, Los

- Angeles, CA, H. B. Hopfenberg, Ed. (New York: Plenum Press, 1974), pp. 207-218.
135. Duda, J. L., J. S. Vrentas, S. T. Ju, and H. T. Liu. "Prediction of Diffusion Coefficients for Polymer-Solvent Systems," *Am. Inst. Chem. Eng. J.* 28(2):279-285 (1982).
136. Alfrey, T., Jr., E. F. Gurnee, and W. G. Lloyd. "Diffusion in Glassy Polymers," *J. Polymer Sci.*, Part C 12:249-261 (1966).
137. Barr-Howell, B. D., N. A. Peppas, and D. N. Winslow. "Transport of Penetrants in the Macromolecular Structure of Coals: II. Effect of Porous Structure on Pyridine Transport Mechanisms," *Chem. Eng. Comm.* 43(4-6):301-315 (1986).
138. Rogers, C. E. "Solubility and Diffusivity," in *Physics and Chemistry of the Organic Solid State*, D. Fox et al., Eds. (New York: John Wiley and Sons, 1965).
139. Dao, T. H., and T. L. Lavy. "A Kinetic Study of Adsorption and Desorption of Diquat, Paraquat, Aniline, Benzoic Acid, Phenol, and Diuron in Soil Suspensions," *Soil Sci.* 144:66-71 (1987).
140. Hance, R. J. "The Speed of Attainment of Sorption Equilibria in Some Systems Involving Herbicides," *Weed Res.* 7:29-36 (1967).
141. Weber, J. B., and S. B. Weed. "Adsorption and Desorption of Diquat, Paraquat, and Prometone by Montmorillonitic and Kaolinitic Clay Minerals," *Soil Sci. Soc. Am. Proc.* 32:485-487 (1968).
142. Adams, R. S., and P. Li. "Soil Properties Influencing Sorption and Desorption of Lindane," *Soil Sci. Soc. Am. Proc.* 35(1):78-81 (1971).
143. Leenheer, J. A., and J. L. Ahlrichs. "A Kinetic and Equilibrium Study of the Adsorption of Carbaryl and Parathion upon Soil Organic Matter Surfaces," *Soil Sci. Soc. Am. Proc.* 35(5):700-705 (1971).
144. Wauchope, R. D., and R. S. Myers. "Adsorption-Desorption Kinetics of Atrazine and Linuron in Freshwater-Sediment Aqueous Slurries," *J. Environ. Qual.* 14(1):132-136 (1985).
145. Isaacson, P. J., and C. R. Frink. "Nonreversible Sorption of Phenolic Compounds by Sediment Fractions: The Role of Sediment Organic Matter," *Environ. Sci. Technol.* 18:43-48 (1984).
146. Hermosin, M. C., J. C. Perez, and J. L. Rodriguez. "Adsorption and Desorption of Maleic Hydrazide as a Function of Soil Properties," *Soil Sci.* 144:250-256 (1987).
147. Bouchard, D. C., and T. L. Lavy. "Hexazinone Adsorption-Desorption Studies with Soil and Organic Adsorbents," *J. Environ. Qual.* 14(2):181-186 (1985).
148. Jaffe, P. R. "Modeling Sorbing Chemicals: Considering the Nonsingular Adsorption-Desorption Isotherm," *J. Environ. Sci. Health* A21(1):55-69 (1986).
149. Rogers, R. D., J. C. McFarlane, and A. J. Cross. "Adsorption and Desorption of Benzene in Two Soils and Montmorillonite Clay," *Environ. Sci. Technol.* 14(4):457-460 (1980).
150. Schwarzenbach, R. P., and J. Westall. "Transport of Nonpolar Organic Compounds from Surface Water to Groundwater: Laboratory Sorption Studies," *Environ. Sci. Technol.* 15(11):1360-1367 (1981).
151. Bowman, B. T., and W. W. Sans. "Partitioning Behavior of Insecticides in Soil-Water Systems: II. Desorption Hysteresis Effects," *J. Environ. Qual.* 14(2):270-273 (1985).
152. Mustafa, M. A., and Y. Gamar. "Adsorption and Desorption of Diuron as a Function of Soil Properties," *Soil Sci. Soc. Am. Proc.* 36:561-564 (1972).

153. Peck, D. E., D. L. Corwin, and W. J. Farmer. "Adsorption-Desorption of Diuron by Freshwater Sediments," *J. Environ. Qual.* 9(1):101-106 (1980).
154. Nkedi-Kizza, P., P. S. C. Rao, and A. G. Hornsby. "Influence of Organic Cosolvents on Leaching of Hydrophobic Organic Chemicals through Soils," *Environ. Sci. Technol.* 21(11):1107-1111 (1987).
155. Koskinen, W. C., and H. H. Cheng. "Effects of Experimental Variables on 2,4,5-T Adsorption-Desorption from Soils," *J. Environ. Qual.* 12(3):325-330 (1983).
156. Chiou, C. T., P. E. Porter, and D. W. Schmedding. "Partition Equilibria of Nonionic Organic Compounds between Soil Organic Matter and Water," *Environ. Sci. Technol.* 17(4):227-231 (1983).
157. Corwin, D. L., and W. J. Farmer. "Nonsingle-Valued Adsorption-Desorption of Bromacil and Diquat by Freshwater Sediments," *Environ. Sci. Technol.* 18:507-514 (1984).
158. McCloskey, W. B., and D. E. Bayer. "Thermodynamics of Fluridone Adsorption and Desorption as a Function of Soil Properties," *Soil Sci. Soc. Am. Proc.* 51:605-611 (1987).
159. Ball, W. P., and P. V. Roberts. "Rate Limited Sorption of Halogenated Aliphatics onto Sandy Aquifer Material: Experimental Results and Implications for Solute Transport," *EOS* 66(46):894 (1985).

CHAPTER 14

Investigation of the Distribution of Natural Organic Compounds in the Sediments of Estuaries with Indication of Their Likely Sources

Brian J. Harland, Malcolm J. Hetheridge, and Simon J. Molloy

INTRODUCTION

Estuarine sediments accumulate persistent and hydrophobic chemicals from the overlying water, and often these chemicals can be used as marker chemicals of biogenic and anthropogenic discharges to the river system. Some of the more common of the biogenic markers are the constituents of higher plant waxes. These include long-chain normal alkanes from C₂₇-C₃₃,¹ in which odd carbon numbers predominate over even, and long-chain normal alcohols from C₂₂-C₃₀, in which even carbon numbers predominate over odd. Such components are frequently found in both estuarine and marine sediments.² Additionally, the corresponding aldehydes to the alcohols have also been postulated as leaf wax constituents.³ These three constituents (alkanes, aldehydes, and alcohols) were found in estuarine sediments from three river systems in southwest England in a previous study by this laboratory.⁴ The particular homologues identified in this work were a range of normal alkanes from C₂₇-C₃₁ exhibiting odd over even preference and long-chain primary alcohols and aldehydes of C₂₆ and C₂₈ carbon number. Other components found in these sediments were a number of sterols, of which the sewage markers,⁵ coprostanol and cholesterol, were identified. All three of the rivers investigated—Teign, Dart, and Exe—receive only low volumes of industrial and domestic waste and consequently are relatively unpolluted.

Although the plant waxes are considered to be the major source of the long-chain alkanes, alcohols, and aldehydes found in sediments, other sources for these components have been postulated. For example, a marine origin has been claimed for some long-chain alcohols,⁶ and the possibility of forming the long-chain aldehydes by diagenesis of other sediment constituents has also been raised.^{7,8}

In this chapter, we present the results of an investigation to provide further information on the sources of these long-chain substances and, in particular, to determine whether they are of marine or terrigenous origin. This investigation was based on analysis of long-chain plant wax components in both riverine and estuarine sediments from the River Teign, one of the rivers previously studied.

SAMPLING SITES

Sediment samples were taken from the River Teign in southwest England. The river, which is fast flowing in its upper reaches, rises on peat moorland (Dartmoor) and flows for 56 km through mixed agricultural and wooded land until it reaches the sea at Teignmouth. The estuarine part of the river accounts for approximately 9 km of this length. Industrial presence in the vicinity of the river is limited; therefore, the only major anthropogenic discharges arise from domestic sewage inputs. Sediment samples were taken on March 8, 1989 at 10 sites over the course of the river, as shown in Figure 14.1. Samples numbered 1 to 3 are estuarine samples and 4 to 10 are riverine.

SAMPLING AND ANALYSIS

All sediment extracts, produced by Soxhlet extraction of the freeze-dried sediment, were examined without prior fractionation by capillary gas chroma-



Figure 14.1. Location of sampling sites (1–10) on the River Teign. The length of the river is 56 km.

tography or gas chromatography-mass spectrometry (GC-MS). This direct method of analysis was chosen because it avoids losses or contamination which can be introduced during the fractionation procedure, even though it does suffer from some disadvantages. For example, the injection of the neat sample directly onto the column rapidly degrades its performance, and there is also much more chance of coelution occurring during the analysis, making interpretation of the data more difficult.

Sampling Procedure

Sediments (0–4 cm) were collected using a metal scoop, placed in glass bottles fitted with polypropylene tops, and held at the laboratory at 4°C until analyzed.

Extraction

Sediment samples (20 g) were freeze-dried for 24 hr (Edwards EF4 Modulyo freeze-drier) and ground to a fine powder. The powdered residue was then extracted with 100 mL dichloromethane (Rathburn HPLC grade) in a Soxhlet apparatus for 6 hr. The resultant dichloromethane extract was reduced to smaller volume (4 mL) using a Kuderna-Danish concentrator (Kontes Glass Co.).

Gas Chromatography Analysis

The concentrated extract was subjected to gas chromatography analysis using a Varian 3500 gas chromatograph fitted with flame ionization detection. A 25-m CP-Sil8 CB (Chrompack) bonded phase FSOT column of 0.32-mm internal diameter and 0.25- μ m film thickness was used for the separation of components. The temperature program used for the analysis was the following: initial temperature of 50°C, held for 5 min, followed by a ramp of 8°C/min to a final temperature of 280°C, held for 15 min, using helium carrier gas (2.5 mL/min). Samples (1 μ L) were injected using the Varian on-column injector in conjunction with the Varian 8035 autosampler. All gas chromatographic data were collected on a Trilab 2000 data station (Trivector Ltd.) for further processing.

Gas Chromatography-Mass Spectrometry Analysis

Gas chromatography-mass spectrometry analysis of selected samples was performed using the Finnigan TSQ-70 tandem mass spectrometer in conventional (i.e., single quadrupole) mode. The gas chromatographic conditions were similar to those used for GC-FID analysis with the following differences. The gas chromatograph was a Varian 3400, and a split-splitless injector was used in the Grob splitless mode for injection of the samples. Additionally, the

final column temperature was reduced to 250°C. The mass spectrometry conditions used were electron impact ionization at 70 eV with an emission current of 200 μA and multiplier voltage of 1.1 kV. The scan range was 30–500 amu in 0.5 sec. One sample (station 3) was analyzed by chemical ionization mass spectrometry using methane as the reagent gas.

Particle Size Analysis/Organic Content

Particle size analysis of the sediment was obtained using a 3600E Laser Particle Sizer (Malvern Instruments). The organic content of the sediment was determined from the weight loss after heating oven-dried sediments (110°C) to 600°C until constant weight was achieved.

Gas Chromatography–Fourier Transform Infrared

One sample was analyzed by gas chromatography–Fourier transform infrared using a Mattson Cryolect 4800 system. Gas chromatography conditions were as described previously.

RESULTS AND DISCUSSION

The gas chromatogram obtained from analysis of one of the Teign estuarine sediment samples (sample 3) is illustrated in Figure 14.2. Only the relevant latter part of the chromatogram is shown (27 to 40 min) since the earlier part was devoid of any significant peaks. The main components identified and indicated on the figure are a range of long-chain normal alkanes from C21–C33 of predominantly odd distribution, and a range of long-chain normal aldehydes and alcohols from C22–C30 of predominantly even distribution. A number of sterols were also present from approximately the retention time of hentriacontane (C31) onwards, but of these only the sewage markers, coprostanol and cholesterol, were positively identified. Although most of this information was generated using electron impact (EI) ionization conditions, some other confirmatory work was considered necessary because of the tendency of the aldehydes and alcohols to dehydrate in the mass spectrometer source under the conditions used. Consequently, further confirmation of these components was obtained by use of chemical ionization (CI) mass spectrometry, to indicate their molecular weight, and gas chromatography–Fourier transform infrared (GC-FTIR), which showed the presence of the carbonyl band in the more abundant of the aldehyde homologues.

The results obtained for sample 3 are in good agreement with those found in the previous investigation of estuarine sediments from the Teign and other nearby rivers,⁴ although the long-chain aldehydes in the latter were not identified until after publication.⁹ The source of these long-chain components—alkanes, alcohols, and aldehydes—has been postulated as the waxes of higher

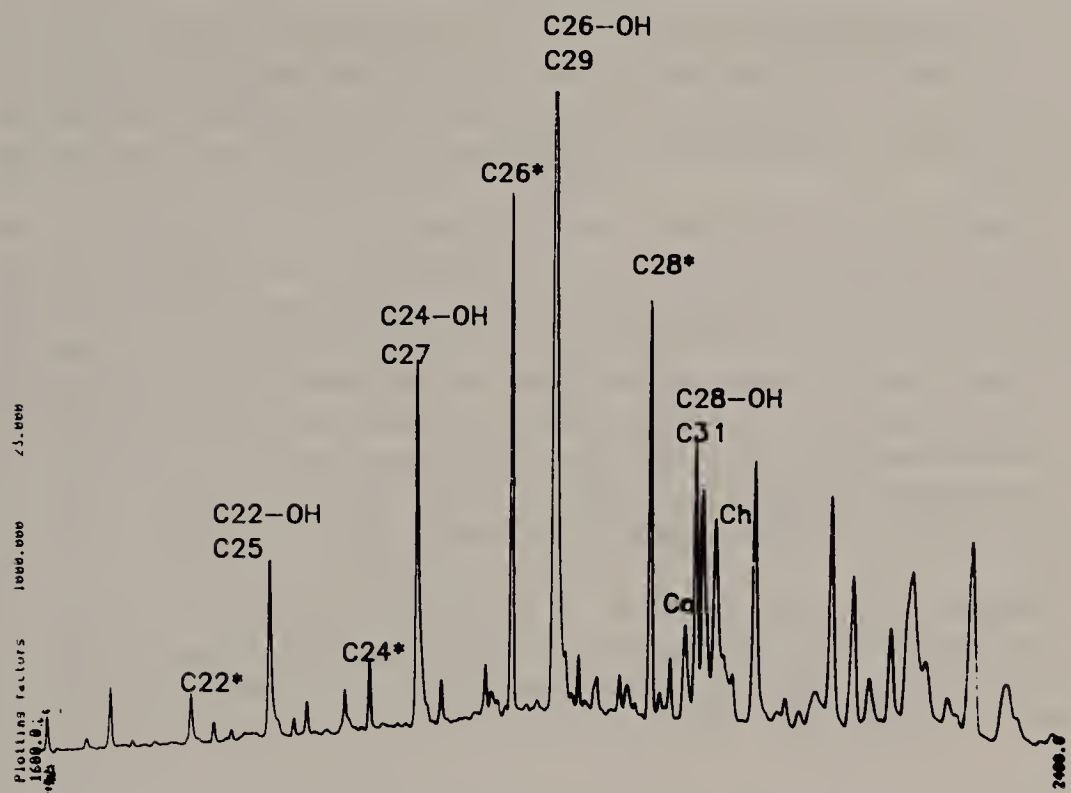


Figure 14.2. Expanded part (27–40 min) of the chromatogram of estuarine sediment sample 3. The *n*-alkanes are identified by carbon number (*C*#), the *n*-alcohols by carbon number with –OH suffix (*C*#-OH), and the *n*-aldehydes by carbon number with asterisk suffix (*C*#*). Coprostanol and cholesterol are indicated by *Co* and *Ch*, respectively.

plants,^{1–3} and the chemistry and morphology of this latter material has been reviewed by Baker.¹⁰ He has summarized information on the homologue distribution of these three types of substances in epicuticular plant waxes as shown in Table 14.1.

The homologue distributions given for these substances in the Table 14.1 agree well with those found in the estuarine sediment, supporting a plant wax source for these components. Nevertheless, further evidence on the origin of

Table 14.1. Homologue Distribution of Hydrocarbons, Primary Alcohols, and Aldehydes in Epicuticular Plant Waxes

Component Class	Homologue Range	Most Common Constituent	Distribution (Carbon Number)
Hydrocarbons	C17–C35	C29, C31, C33	predominantly odd
Primary alcohols	C22–C32	C26, C28, C30	predominantly even
Aldehydes	C22–C32	C26, C28, C30	predominantly even

Source: Baker.¹⁰

these substances in sediments is necessary to confirm their terrigenous nature and, if possible, to determine their exact source. It was anticipated that analysis of the series of sediments taken along the freshwater (riverine) and brackish water (estuarine) stretches of the Teign would provide information on this matter.

Results of GC examination of the 10 sediments taken over the length of the Teign are presented in Figures 14.3, 14.4, and 14.5. As for Figure 14.2, only the later part of the chromatogram is shown in each case (10.5–48 min for Figure 14.3 and 11.5–49 min for Figures 14.4 and 14.5) since the early part is virtually devoid of peaks. In the figures the individual gas chromatograms have been aligned and, for most samples, the nonacosane (C₂₉)/hexacosanol (C₂₆-OH) doublet has been marked with the symbol ●. The intensity of the chromatograms has been scaled (Table 14.2) to make peaks more visible in weaker samples. A higher scaling factor means greater magnification of the data.

Generally, the scaling factor used is inversely related to the silt content or organic content of the sediment (Table 14.3). For example, sample 10, which is a very coarse sediment since it was taken close to the river source, has the weakest chromatogram, while samples 1–3, which were taken from the silty

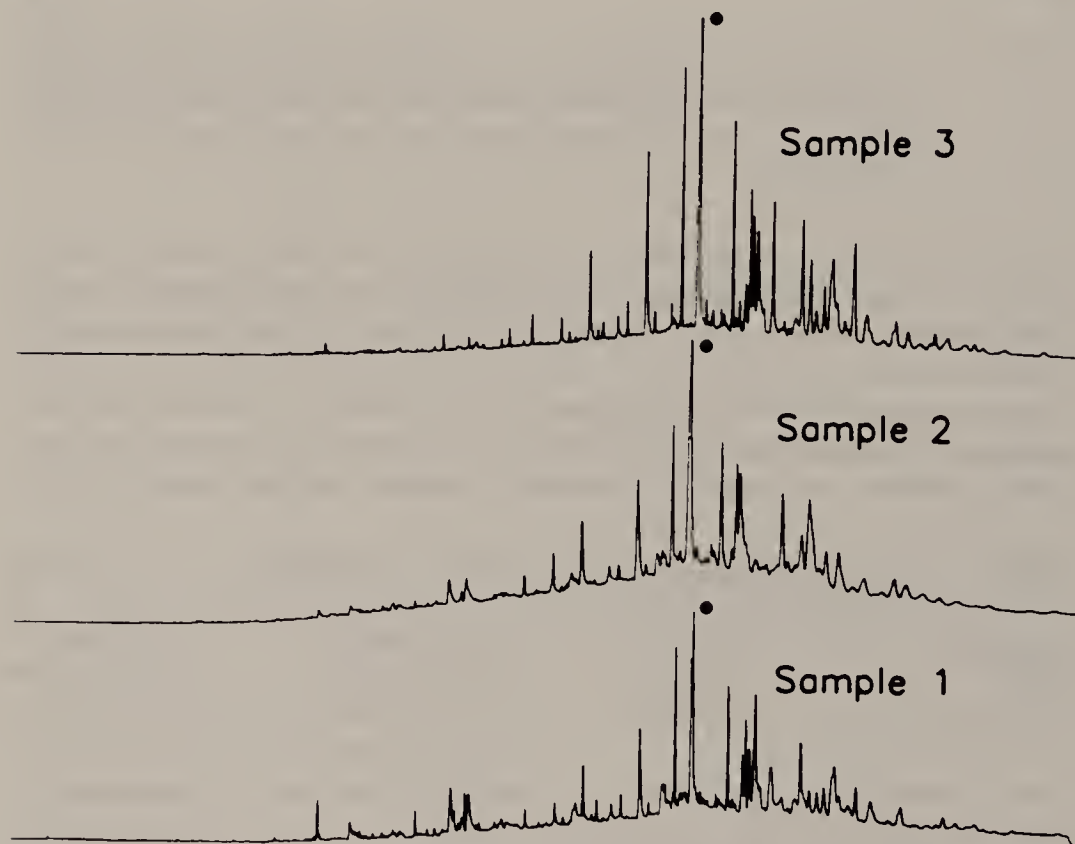
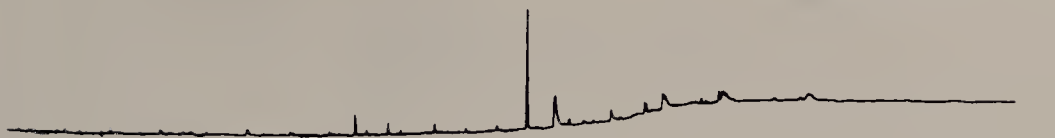
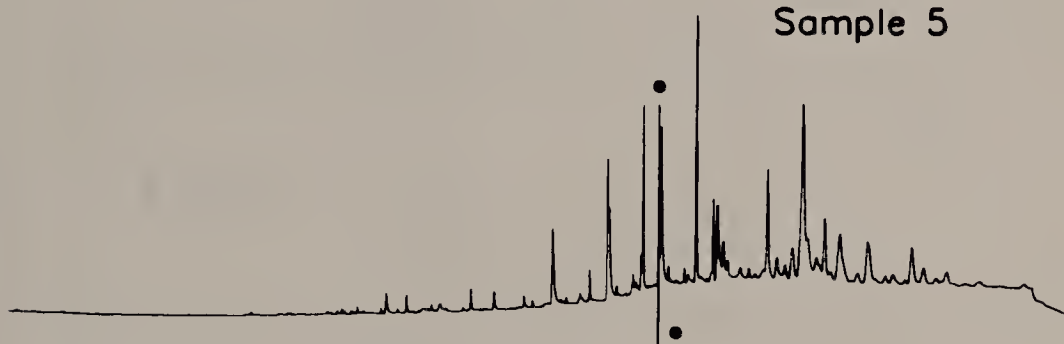


Figure 14.3. Part (10.5–48 min) of the chromatograms of estuarine sediment samples from the River Teign showing samples 1, 2, and 3. The peak corresponding to *n*-nonacosane/*n*-hexacosanol is marked by the symbol ●.

Sample 6



Sample 5



Sample 4

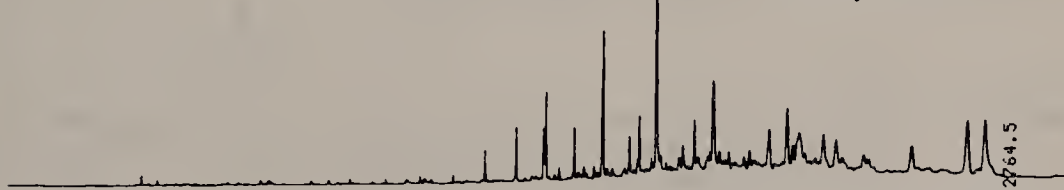


Figure 14.4. Part (11.5–49 min) of the chromatograms of riverine sediment samples from the River Teign showing samples 4, 5, and 6. The peak corresponding to *n*-nonacosane/*n*-hexacosanol is marked by the symbol ●.

estuarine mud, give the strongest chromatograms. There are, however, some anomalies, the reasons for which are not well understood. The chromatograms for samples 6 and 7 are relatively weak, yet their organic contents are only slightly less than that of sample 8.

Inspection of Figures 14.4 and 14.5 indicates that the stronger chromatograms for the riverine sediments exhibit similar patterns for the long-chain alkanes, alcohols, and aldehydes to those found in the estuarine sediments (Figure 14.3). Confirmation of this observation has been obtained by GC-MS analysis of selected sediments (samples 5, 8, and 9). Furthermore, this analysis showed that the difference in peak height for the nonacosane (C₂₉)/hexacosanol (C₂₆-OH) doublet in samples 8 and 9 was the result of a slight change in the resolution of these components during the chromatographic analysis. This reason could also account for the similar difference noted between samples 4 and 5.

Since the River Teign receives little industrial waste and only a relatively small amount of sewage commensurate with the low population living in its catchment, the most likely inputs of organic matter to the sediments are those

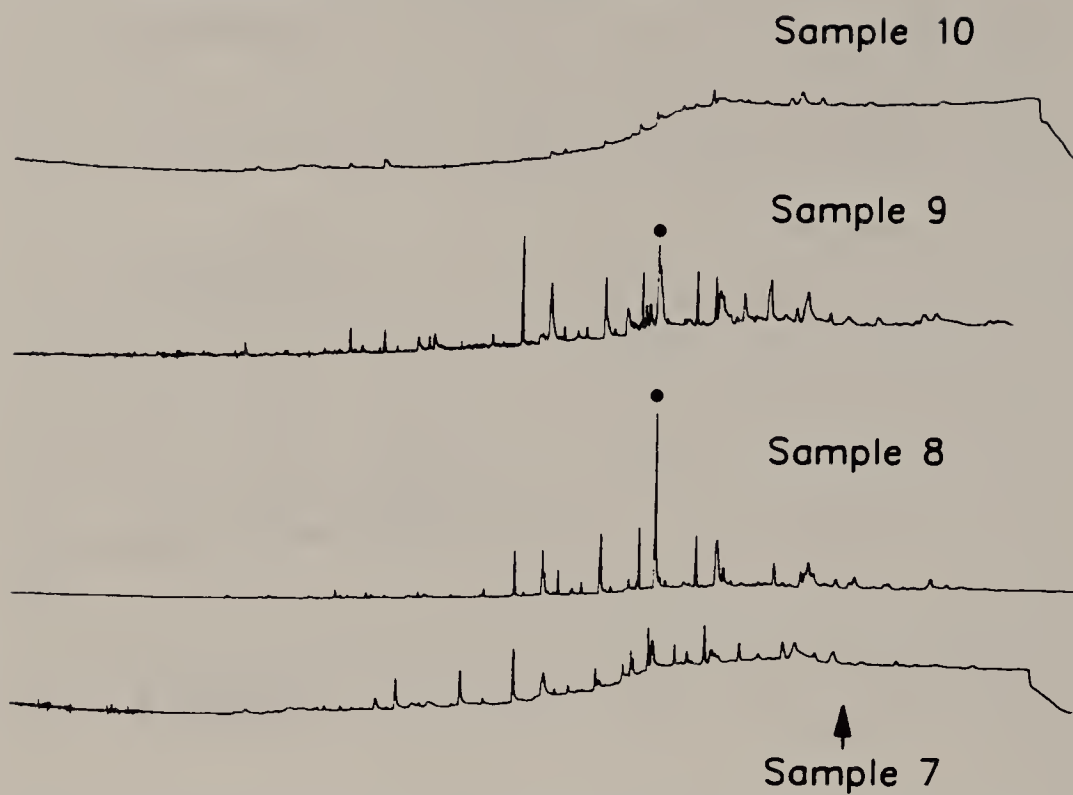


Figure 14.5. Part (11.5–49 min) of the chromatograms of riverine sediment samples from the River Teign showing samples 7, 8, 9, and 10. The peak corresponding to *n*-nonacosane/*n*-hexacosanol is marked by the symbol ●.

from natural sources. The river source lies in open moorland (Dartmoor), but the lower and middle reaches of the estuary flow through agricultural land, primarily grassland. Stretches of the river are also heavily wooded, with pine woods predominating near the source and mixed woodland (i.e., broad-leaved and pine) being commoner downstream.

The presence of the plant wax components—alkanes, aldehydes, and alcohols—throughout the length of the river points to a terrigenous origin for this material. Additionally, the somewhat irregular distribution, although largely the result of the differing particle size distributions of the sediments,

Table 14.2. Scaling of Chromatograms

Sediment No.	Scaling Factor
1	1000
2	1000
3	400
4	1000
5	2000
6	5000
7	4000
8	2000
9	4000
10	5000

Table 14.3. Teign River Sediments: Particle Size and Organic Content (%)

Sediment Number	Pebbles 4-64 mm	Granules 2-4 mm	S-V. Coarse 1-2 mm	S-Coarse 0.5-1 mm	S-Med./Fine 125-500 μm	S-V. Fine 65-125 μm	Silt/Clay 0-65 μm	% Organic Content
1			1.9	7.5	28.6	23.4	48.0	4.2
2					28.8	13.4	48.4	5.0
3			14.5	47.5	2.2	8.7	89.1	11.7
4	1.3	0.5	0.5	12.2	29.8	1.7	5.2	2.6
5	3.2		24.3	71.5	74.7	3.1	6.3	3.1
6			5.8	20.5	71.5	3.8		1.1
7			2.0	0.2	40.6	30.6	0.2	2.1
8			10.3	36.3	6.7	83.6	4.4	1.4
9	1.2	4.3	19.9	46.8	38.5	12.8	0.2	0.8
10					23.2	4.6	0.4	0.6

points to a diffuse, rather than a point, source. The most likely diffuse natural sources would appear to be either the leaves of the broad-leaved trees, which are transported into the river during autumn, or some form of agricultural runoff from grassland (or crops). The possibility of either aquatic plants in the river or peat, which surrounds the headwaters, being the source would appear unlikely. The river is fast flowing in its upper reaches, and the amount of aquatic plant matter is consequently very small, although there are sizable reed beds in the area of the upper estuary. Additionally, the greater presence of the plant wax components in the sediments taken from the lower part of the river and the estuary would suggest that the more significant sources are located in this area rather than several kilometers away in the peat moorland of the headwaters.

Differentiation between the two more likely sources, leaf litter and agricultural runoff, cannot, however, be accomplished from the composition of the components identified in the sediments. According to Baker,¹⁰ long-chain primary alcohols are probably the most dominant components of epicuticular plant waxes, even though only three homologues constitute major wax components. Hydrocarbons are also ubiquitous, although they rarely comprise a large proportion of the wax deposit. Only the aldehydes of the three identified plant wax components in these sediments are less common. Consequently, it might be expected that they would provide more indication of the origins of these waxes than the alkanes and alcohols. However, aldehydes are found in a diverse variety of plants, their appearance correlating strongly with rodlike wax structures.¹⁰

Prahl and Pinto, in recent work on Washington coastal sediments, have investigated the origin of long-chain aldehydes to ascertain whether they are of terrigenous origin or whether they are formed by diagenesis of other components in the sediments.³ Their investigations point to these compounds coming "preformed" out of the Columbia River into the Washington coastal sediments. This conclusion is in agreement with our results on the Teign. However, identification of the precise source of these plant wax components—leaf litter or agricultural runoff—will need to await investigation of sediment samples taken from a location in this environment for which only one of these sources is possible.

SUMMARY

Results from the Teign estuarine and riverine sediments have identified a number of long-chain normal alkanes, ranging in carbon number from C21 to C33 with predominantly odd distribution, and long-chain aldehydes and primary alcohols, of C22 to C30 carbon number and predominantly even distribution. The occurrence of these components in both the estuarine and riverine sediments indicates a terrigenous source. However, the precise origin of these

higher plant wax components—leaf litter or agricultural runoff—cannot yet be established.

REFERENCES

1. Eglinton, G., R. J. Hamilton, R. A. Raphael, and A. G. Gonzalez. "Hydrocarbon Constituents of the Wax Coatings of Plant Leaves: A Taxonomic Survey," *Nature* 193:739 (1962).
2. Simoneit, B. R. T. "The Organic Chemistry of Marine Sediments," in *Chemical Oceanography*, Vol. 7, J. P. Riley and R. Chester, Eds. (London: Academic Press, 1978).
3. Prahl, F. G., and L. A. Pinto. "A Geochemical Study of Long Chain *n*-Aldehydes in Washington Coastal Sediments," *Geochim. Cosmochim. Acta* 51:1573-1582 (1987).
4. Harland, B. J., and R. W. Gowling. "Determination of Organic Chemicals in Sediments Taken from Three Unpolluted Estuaries in South West England," in *Proceedings of the 5th European Symposium on Organic Micropollutants in the Aquatic Environment* (Dordrecht: Kluwer Academic, 1988), pp. 103-107.
5. Hatcher, P. G., L. E. Keister, and P. A. McGillivray. "Steroids as Sewage Specific Indicators in New York Bight Sediments," *Bull. Environ. Contam. Toxicol.* 17:491-498 (1977).
6. Shaw, P. M., and R. B. Johns. "The Identification of Organic Input Sources of Sediments from the Santa Catalina Basin Using Factor Analysis," *Org. Geochem.* 10:951-958 (1986).
7. Cardoso, J. N., and M. I. Chicarelli. "The Organic Geochemistry of the Paraiba Valley and Marau Oil Shales," in *Advances in Organic Geochemistry*, M. Bjoroy et al., Eds. (New York: John Wiley and Sons, 1981), pp. 828-833.
8. Albaiages, J., J. Algaba, and J. Grimalt. "Extractable and Bound Neutral Lipids in Some Lacustrine Sediments," *Org. Geochem.* 6:223-236 (1985).
9. Giger, W., and E. Stephanou. Personal communication, Rome (1987).
10. Baker, E. A. "Chemistry and Morphology of Plant Epicuticular Waxes," in *Proceedings of the Linnean Society Symposium Series No. 10: The Plant Cuticle*, D. F. Cutler et al., Eds. (London: Academic Press, 1982), pp. 139-165.

CHAPTER 15

Environmental Response to Hazardous Chemicals

R. E. Speece, N. Nirmalakhandan, and Diane J. W. Blum

INTRODUCTION

The environmental fate of hazardous chemicals is an important issue because accidental spills and industrial processes and products result in their introduction to the air, soil, or water environment. The partitioning of hazardous chemicals in these various environmental compartments and their relative half-lives, food-chain transmission, and bioconcentration effects are key elements in a risk assessment of such chemicals. Quantitative structure-activity relationships (QSAR) are correlations between the chemical structure of a compound and a characteristic of that compound, such as its toxicity to an organism, aqueous solubility, or Henry's constant. Because partitioning of hazardous chemicals in the environment is directly related to their physical properties, this chapter will briefly address some of the QSAR techniques used to model parameters describing the environmental fate of chemicals: Henry's constant (H), aqueous solubility, soil sorption, and toxicity to selected environmentally relevant organisms.

The physical and biological properties of hazardous chemicals have been commonly modeled using log P—the octanol water partitioning coefficient. This technique is widely used and technically simple. Log P can be calculated as a “lumped” parameter that consists of about 35 components, which are the contribution values for various possible constituents of the molecule. The computer program C Log P by Leo et al. calculates log P for any molecule.¹ This approach works well for many chemicals and is grandfathered into many environmental fate models. However, for more complicated molecules, specifically dyes, the calculated log P can be off by a factor of 100 or more.

This chapter will present two less-used QSAR techniques for environmental fate modeling: the molecular connectivity system of Kier and Hall² and the solvatochromatic parameters approach of Kamlet et al.³

RATIONALE OF QSAR MODEL FOR H

A QSAR model for H was derived by Pierotti using a semitheoretical analysis by considering the chemical potential of a solute in the aqueous and gaseous phases.⁴ In very dilute solutions, the potential of a nonelectrolytic solute, μ_2^L , is given by

$$\mu_2^L = G_c + G_i + kT \ln(x_2/v_1) - kT \ln\lambda \quad (15.1)$$

where G_c and G_i are the energies associated with the formation of a cavity in the solvent to accommodate a solute molecule and solute-solvent interaction, respectively. The third term is a measure of the internal energy, and the last term is a measure of the pure solvent effect; x_2 is the mole fraction of the solute in the solvent, v_1 the molar volume of the solvent, T the temperature, and the subscripts 1 and 2 denote the solvent and solute, respectively. Similarly, the potential of the solute in the gaseous phase is given by

$$\mu_2^G = -kT \ln\lambda + kT \ln(p_2/kT) \quad (15.2)$$

where λ = measure of the internal degrees of freedom of solute, and p_2 is the partial pressure of the solute in the gaseous phase. Equating these two potentials in an air-water system in equilibrium results in

$$kT \ln(p_2/kT) = G_c + G_i + kT \ln(x_2/v_1) \quad (15.3)$$

or, rearranging,

$$\ln(p_2/x_2) = G_c/kT + G_i/kT + \ln(kT/v_1) \quad (15.4)$$

Now, substituting $H = (p_2/x_2)$, an expression for Henry's constant can be obtained as

$$\ln H = G_c/kT + G_i/kT + \ln(kT/v_1) \quad (15.5)$$

which provides a means of modeling H of various solutes at a given temperature in terms of G_c and G_i , or of a given solute at various temperatures, assuming constant G_c and G_i over a small range of T, as encountered in environmental applications.

MODELING H OF DIFFERENT SOLUTES

In order to use Equation 15.5 in modeling H of different solutes, the first two terms, G_c and G_i , have to be evaluated. The cavity term, G_c , has been theoretically modeled and experimentally verified by the scale particle theory

for simple molecules. In an analysis by Pierotti^{4,5}, this term has been derived as a complex function of the molecule's hard-core diameter. The interaction energy term, G_c , can be considered to be a result of polarizability.^{5,6} Following these concepts, we have used the QSAR approach to quantify the two energy terms, in terms of molecular descriptors, that encode information relating to molecular size and polarizability.

The cavity term is modeled by using the solute's molar volume, which in turn is modeled by using topological molecular descriptors called connectivity indexes, χ . These indexes can be easily calculated by considering the hydrogen-suppressed molecular skeleton as discussed by Kier and Hall.² The X indexes have been shown to correlate well with many geometrical and physicochemical properties of organic chemicals. For instance, the molar volume, V, of 48 chemicals was well correlated with zero-, first-, and fourth-order connectivity indexes:²

$$V = 19.60 - 32.58^0X^v + 4.867^1X^v - 3.814^4X^{pc} \quad (15.6)$$

$$n = 48; r^2 = 0.998; SE = 1.51$$

where r^2 is the correlation coefficient and SE is the standard error.

Connectivity indexes have also been shown to correlate with polarizability, Φ :²

$$\Phi = 0.864 + 2.36^0X + 5.49^1X \quad (15.7)$$

$$n = 36; r = 0.998; SE = 1.85$$

However, when the connectivity indexes were tried in QSAR studies to predict H, the results were not satisfactory, explaining only 78% of the variation in H data. This may be due to the fact that the 0X and 1X indexes cannot differentiate between heteroatoms, even though they are rich in structural information content. Therefore, an alternate method to relate polarizability to molecular structure as proposed by Ketelaar was used.⁷ In this method, Φ is estimated by an additive scheme using atomic contribution factors:

$$\Phi = A(\text{no. of H}) + B(\text{no. of C}) + C(\text{no. of Cl}) + \dots + A_1(\text{no. of double bonds}) \quad (15.8)$$

where A, B, C, etc. are constants.

In this study, we have used a combination of connectivity indexes X and Φ to model the energy terms G_c and G_i and thus derived a QSAR model for Henry's constant. Since the X indexes encode information relating to molar volume as well as polarizability, the coefficients in Ketelaar's equation were kept variable, and a modified Φ was derived by statistically optimizing the coefficients so that, in combination, they could yield the best predictive equation for H.

Henry's constant data reported by Hine and Mookerjee were used to formulate the QSAR model for H° .⁸ A "training set" consisting of 183 compounds was formed by selecting all the hydrocarbons, halohydrocarbons, esters, and alcohols from their data set. The hydrocarbons included saturated and unsaturated aliphatics and aromatics with alkyl substitutions. The halogens included bromine, iodine, chlorine, and fluorine. The five halogenated alcohols from their data set were placed in a "testing set" because the halogens and the hydroxyl groups are individually represented by other members of the set. Similarly, cyclohexanol and the four PAH in the original set were also placed in the testing set.

Because the functional groups in amines, ethers, aldehydes, and ketones are known to behave in a mechanistically different manner from the rest of the compounds, they were excluded from this study. For instance, the amines are more soluble in water than the alcohols of corresponding molecular weight. The carbonyl group $> C=O$: in aldehydes and ketones behaves for the most part as though the functional group is "ionized" as represented by $>C^+-\ddot{O}^-$.

The fitted values agreed satisfactorily with the experimental values, except in the case of alkanes and the fluorinated compounds in particular, where the model generally underestimated, with residues ranging up to 1.11 log units.

It appeared that the systematic error of certain classes of compounds and the unexplained variance could be due to the effect of hydrogen bonding. To account for this effect, we followed the approach of Hansch et al.,⁹ where an indicator variable, I, is used to differentiate between compounds on the basis of their ability to take part in hydrogen bonding. This indicator, I, is assigned a value of 1 for all compounds containing an electronegative element (oxygen, nitrogen, halogen, etc.) attached directly to a carbon atom holding a hydrogen atom.

Acetylinic compounds and aromatic compounds with partially substituted hydrogen atoms were also assigned 1. For the remaining compounds, I was set equal to zero. With this indicator variable, the following model was obtained:

$$\log H = 1.29 + 1.005 \Phi - 0.468^1X^v - 1.258I \quad (15.9)$$

$$n = 180; r = 0.99; r^2 = 0.98; SE = 0.262$$

The optimized contributions of the atoms to Φ are summarized in Table 15.1. This model explains over 98% of the variance in the data, leaving only 2% for inadequacy of the model and the experimental errors in the data. The standard error is superior to that in other estimation methods, and comparable to that in experimental results. The experimental and calculated $\log H$ values are shown in Figure 15.1. For the QSAR model derived in this study, the absence of collinearity among the descriptors was positively confirmed.

Another criterion for a sound QSAR model is that the general model should be valid for smaller subsets of the training set. This ensures that the general model is not unduly biased by any influential sets of points. Validation by

Table 15.1. Optimized Contributions to Polarizability

Atom/Bond	Contribution
Carbon	0.577
Hydrogen ^a	-0.120
Oxygen	-0.825
Hydroxyl	-3.701
Chlorine	-0.187
Bromine	-0.222
Iodine	0.407
Fluorine	-0.570
Cycle	-0.952
Double bond	-0.859
Triple bond	-0.109

^aAttached to carbon atoms only.

subsets also increases the utility of the general model and its applicability to compounds not included in the training set. In this study, various congeneric subsets were deleted from the main set, and regression runs were done on the remaining members. The results of these runs are shown in Table 15.2. The fact that the same descriptors were chosen by the stepwise procedure and that the quality of the model and its coefficients are essentially the same for all the subsets strongly supports the general QSAR model given by Equation 15.9.

Next, we used a testing set to demonstrate the predictive ability of this model. In addition to the 10 chemicals indicated previously, 10 more, obtained from other sources, were added to the testing set. The experimental and predicted log H values of these 20 compounds are compared in Table 15.3. In the

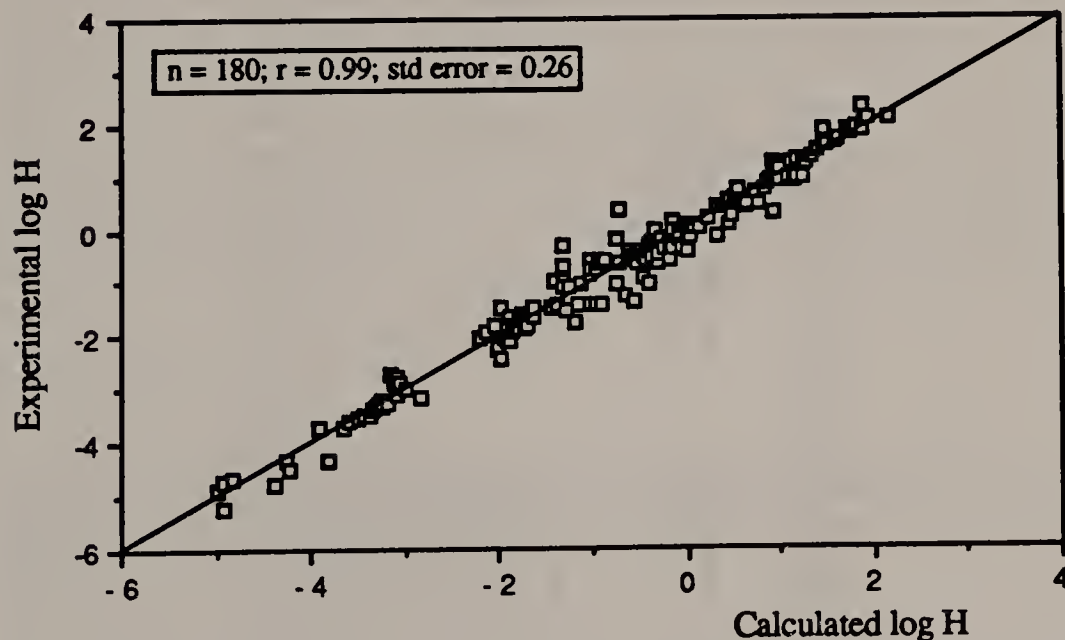


Figure 15.1. Comparison between experimental and fitted log H-refined model with indicator variable.

Table 15.2. Results of Regression Runs for Subsets

Run No.	Compounds Deleted	Number Deleted	Number Included	r	Std. Error	Constant	Model Parameters		
							Φ	oX	${}^1X'$
1	None	—	180	0.988	0.262	1.298	0.971(—)	-0.518(—)	-1.354(—)
2	All alkanes	14	166	0.985	0.272	1.277	1.005 1.035(+)	-0.468 -0.434(+)	-1.258 -1.258(+)
3	All alcohols	25	155	0.981	0.274	1.314	0.999(✓)	-0.479(✓)	-1.215(✓)
4	All esters	24	156	0.988	0.272	1.310	1.004(✓)	-0.476(✓)	-1.260(✓)
5	All aromatics	25	155	0.988	0.268	1.318	0.991(✓)	-0.477(✓)	-1.252(✓)
6	Halogenated compounds	25	155	0.992	0.234	1.272	1.002(✓)	-0.475(✓)	-1.272(✓)
7	All alcohols and esters	49	131	0.977	0.286	1.317	0.997(✓)	-0.477(✓)	-1.268(✓)

Note: (—) denotes lower limit and (+) denotes upper limit of estimates of coefficients at 95% confidence level.

(✓) denotes coefficient lying within lower and upper limits of the coefficients of the general model.

Table 15.3. Comparison Between Observed and Predicted Log H Values for Testing Set (H in Nondimensional Form)

No.	Chemical	Ref.	Φ	${}^1X^v$	I	Observed log H	Predicted log H	Residue
1	2,2,2-Trifluoroethanol	12	-2.96	0.32	1	-3.15	-3.09	-0.06
2	1,1,1-Trifluoro-2-propanol	12	-2.62	1.08	1	-3.05	-3.11	0.06
3	2,2,3,3-Tetrafluoropropanol	12	-2.56	0.89	1	-3.59	-2.96	-0.63
4	2,2,3,3,3-Pentafluoropropane	12	-2.50	0.85	1	-3.04	-2.87	-0.17
5	Hexafluoro-2-propanol	12	-2.43	0.73	1	-2.76	-2.75	-0.01
6	Cyclohexanol	12	-2.51	3.05	1	-3.63	-3.92	0.29
7	Naphthalene	12	-0.34	3.39	1	-1.77	-1.90	0.13
8	Acenaphthene	12	-0.38	4.43	1	-2.49	-2.42	-0.07
9	Anthracene	12	0.86	4.81	1	-3.14	-1.35	-1.79 ^a
10	Phenanthrene	12	-0.86	4.81	1	-2.98	-3.08	0.10
11	Fluorene	2	-0.57	4.60	1	-2.37	-2.69	0.32
12	Pyrene	2	-0.56	5.55	1	-3.33	-3.13	-0.20
13	Biphenyl	2	0.57	4.07	1	-1.77	-1.30	-0.47
14	1-Methyl naphthalene	2	0.00	3.80	1	-1.96	-1.75	-0.21
15	1,5-Dimethyl naphthalene	24	-0.48	4.24	1	-1.82	-2.43	0.61
16	1-Chloronaphthalene	24	-0.41	3.91	1	-1.84	-2.21	0.37
17	2-Chloronaphthalene	24	-0.41	3.91	1	-1.88	-2.21	0.33
18	1,2,3-Trichlorobenzene	24	-0.04	3.51	1	-1.30	-1.65	0.35
19	1,2,3,5-Tetrachlorobenzene	24	-0.10	3.65	1	-1.19	-1.78	0.59
20	Hexachlorobenzene	25	-0.24	5.08	0	-1.27	-1.33	0.06

^aIf alternate experimental value of -1.52 is used, error = -0.17. See discussion in text.

case of anthracene, the experimental value reported by Hine and Mookerjee is -3.14,⁸ whereas the value predicted by our model is -1.35. A literature search revealed two other experimental values: -1.52 and -0.55.¹⁰ While the last value appears to be out of line, it is premature to comment on the other two experimental values. Apart from this compound, the QSAR model appears to predict reasonably well—particularly so in the case of PAH, when one considers the fact that the training set contained none. Even though some members of the testing set contain “multiple features” (e.g., the halogen and hydroxyl groups in hexa-fluoro-2-propanol), which were represented in the training set individually (e.g., by the halogenated compounds and the alcohols), the agreement between their experimental and predicted log H values shows the utility of the model in predicting H for compounds without any experimental data.

SOLUBILITY

Aqueous solubility data were collected from the literature for 470 organic chemicals. A basic solubility model was developed from a training set of 144 chemicals using molecular connectivity coupled with Ketelaar's polarizability concept:

$$\log S = 1.465 + 1.758^{\circ}X - 1.465^{\circ}X^v + 1.01 \Phi \quad (15.10)$$

$$n = 144; r^2 = 0.949; SE = 0.281$$

where S = moles/L

$^{\circ}X$ = zero-order molecular connectivity term

$^{\circ}X^v$ = zero-order volume molecular connectivity term

Φ = modified polarizability parameter

This basic model was then extended to include all the available solubility data for 107 PNAs, PCBs, and PCDDs.

Connectivity indexes alone were not sufficient to account for all the variance in the solubility data of a diverse set, and the modified polarizability parameter had to be included to explain a substantial portion of the variance. For Equation 15.10, $\Phi = -0.963$ (no. of Cl) - 0.361 (no. of H) - 0.767 (no. of double bonds). Subsequently, when compounds with structures and substituents vastly differing from those employed in the training set were modeled, appropriate terms were added to this Φ expression.

To illustrate the generality of this approach, additional chemicals with additional atoms and classes were added (e.g., F., I, alkanes, alkenes, and multiple structural and heteroatom features, amines, aldehydes, ketones, nitro compounds, polychlorinated dibenzo-p-dioxins). The basic model for these 365 chemicals was

$$\log S = 1.464 + 1.662^{\circ}X - 1.367^{\circ}X^v + 1.001 \Phi \quad (15.11)$$

$$n = 365; r^2 = 0.967; SE = 0.306$$

$$\begin{aligned} \Phi = & -0.963(\text{no. of Cl}) - 0.361(\text{no. of H}) - 0.767(\text{no. of double bonds}) \\ & - 2.620(\text{no. of F}) + 1.474(\text{no. of I}) + 0.0(\text{no. of B}) \\ & - 1.24(\text{hydrogen bonding ability}) + 1.014(\text{ketone}) + \\ & 0.636(\text{no. of NH}_2) + 0.833(\text{no. of NH}) - 1.695(\text{no. of NO}_2) \\ & - 1.823(\text{dioxin}) \end{aligned}$$

It is to be noted that this equation covering 365 chemicals is essentially the same in form and quality as that obtained originally from the basic training set of 145 chemicals. Φ is a lumped parameter containing 12 terms, which are used only when the chemical contains those appropriate terms. This does not in any way violate any statistical standards because of the large database of 365 chemicals. The observed vs calculated results are shown in Figure 15.2.

PREDICTIVE ABILITY OF THE GENERAL MODEL

The validity of our approach and the predictive ability of our general model are demonstrated below on various sets of a congeneric series and miscellaneous compounds such as PCBs, PNAs, PCDDs, phenols, etc., which are of considerable importance in environmental contamination. Even though many of these compounds are not directly represented per se in the training set, their

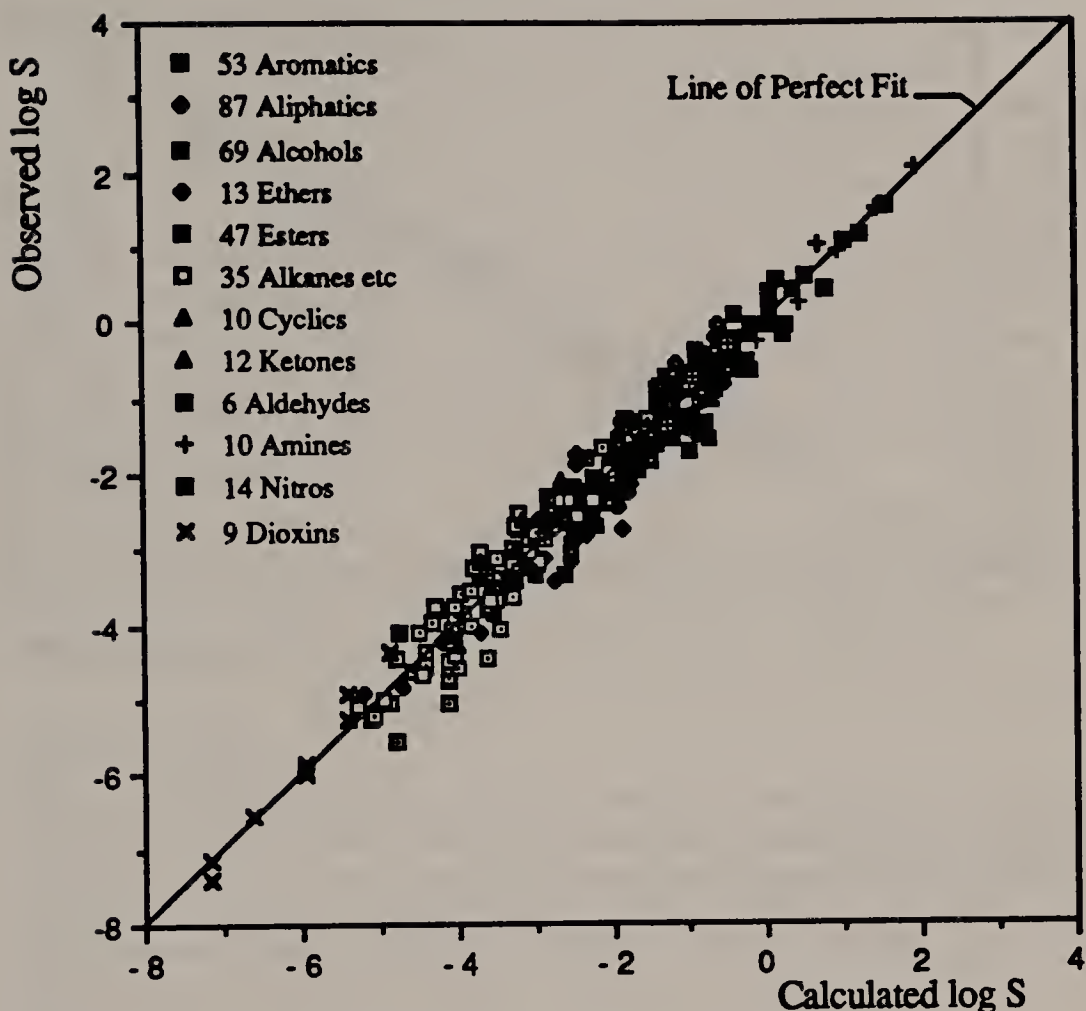


Figure 15.2. Comparison between observed and calculated log S (S in moles/L).

basic structural features are adequately represented, and therefore, the model could be expected to predict satisfactorily without any parameter adjustment. All the reported solubility data for 45 PCBs¹¹ containing up to 10 chlorine substitutions were tested, and the agreement between the observations and predictions was found to be quite satisfactory, with an r of 0.955 and standard error of 0.287. Further, 38 PNAs containing up to six fused rings were tested, and again the agreement was found to be reasonable. Figure 15.3 illustrates the quality of the prediction, from which the agreement between the observed and predicted log S can be seen to be very good, with $r = 0.987$ and SE = 0.382.

The validity of our approach is amply demonstrated by the results of this predictive test. The fact that the original training set did not contain any PCBs or PNAs adds further credence to our model. This also shows that our model parameters are richer in information content relating to aqueous solubility when compared to others such as $\log P^{9,12}$ and total surface area,^{11,13,14} which have been used by many researchers in deriving QSAR models for selected congeneric sets of compounds. The robustness of the general model is further

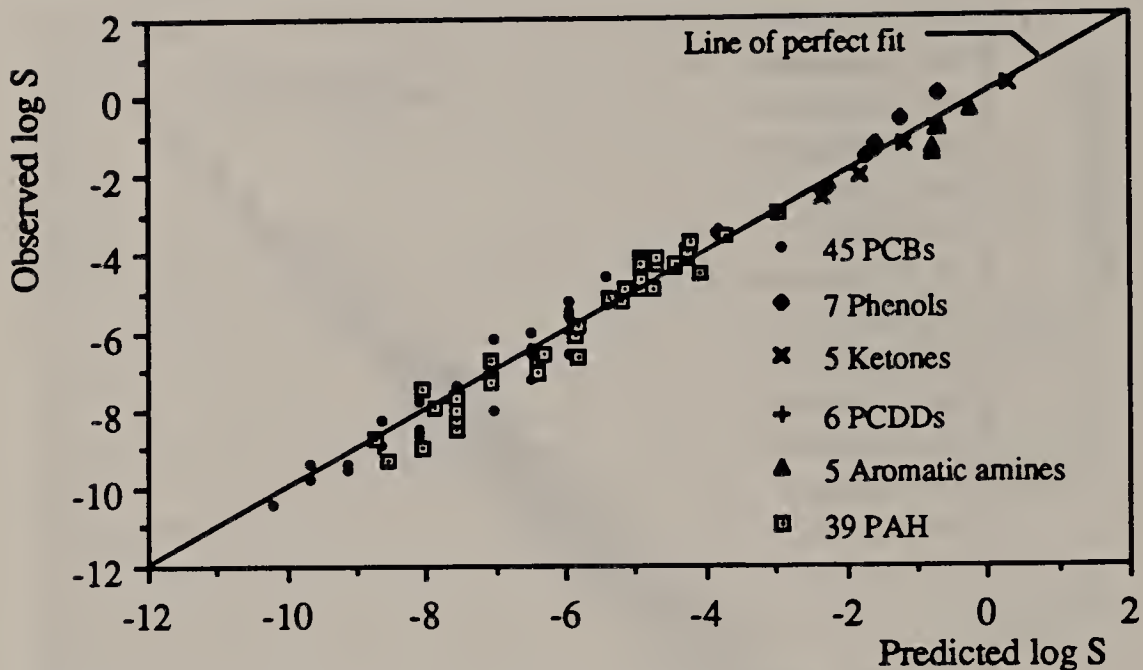


Figure 15.3. Comparison between observed and predicted log S (S in moles/L).

validated when this testing data set is merged with the previous set of 365 miscellaneous compounds; the same basic model fitted all the 470 chemicals with an r of 0.99 and a standard error of 0.332:

$$\log S = 1.543 + 1.638^{\circ}X - 1.374^{\circ}X^v + 1.003 \Phi \quad (15.12)$$

$$n = 470; r = 0.990; r^2 = 0.980; SE = 0.332$$

TOXICITY TO ENVIRONMENTAL ORGANISMS

We tested or collected data for the toxicity of a broad range of chemicals, including substituted benzenes, substituted phenols, chlorinated aliphatic hydrocarbons, and alcohols.¹⁵ Each of the chemicals was tested individually. Although most toxic wastes include a combination of toxicants, evaluating individual constituents is a first step in assessing the toxicity of a mixture.

We collected laboratory data for three groups of bacteria of central interest in the natural environment and in wastewater treatment systems: aerobic heterotrophs, Nitrosomonas, and methanogens. Aerobic heterotrophs predominate in activated sludge systems and natural aerobic environments, converting organic material to carbon dioxide and water. Nitrosomonas convert ammonia nitrogen to nitrite as the first and more sensitive step in the biological oxidation of inorganic nitrogen. Methanogens are a key organism in the conversion of organic matter to carbon dioxide and methane in anaerobic environments. Data were also collected from the literature for the fathead minnow and the Microtox test. We collected toxicity data for 50–130 chemicals

per species to compare the toxicity of the same chemicals to five organisms. We then used the data to develop QSARs for nonreactive toxicants.

We found highly successful QSARs covering a broad range of chemical toxicants for all species tested. Our work identifies the advantages and disadvantages of three QSAR methods: octanol-water partitioning ($\log P$), linear solvation energy relationships (LSERs), and molecular connectivity. LSER QSARs were more accurate and covered the greatest range of chemicals. Parameters are more readily available for $\log P$ and molecular connectivity QSARs. Molecular connectivity indices can be computed with no knowledge of chemical properties, simply from structural formulas. It is therefore easy to see how changes in structure affect predicted toxicity. However, $\log P$ and LSER QSARs afford a more intuitive understanding of the properties affecting toxicity.

Our QSARs are valuable to practicing engineers for predicting the toxicity of untested chemicals to the species considered, provided the chemicals are related to our test chemicals. The QSAR equations can be interpreted to find clues about the relationship between toxicity and chemical structure.

QSAR METHODS

The three QSAR methods mentioned previously – octanol-water partitioning, LSERs, and molecular connectivity – were used in our research of toxicity of chemicals to environmental bacteria. Each method is described with examples from our research and others' to indicate its strengths and weaknesses.

Log P

The octanol-water partition coefficient used as $\log P$ is the most common parameter used in toxicity QSARs. It models the relative partitioning between the aqueous phase and the more nonpolar, lipidlike biophase. As $\log P$ increases, toxicity increases. At high values of $\log P$, the low aqueous solubility will begin to decrease the toxicity of a compound. For this reason, a second-order P term or a bilinear term is often introduced.

Lyman et al. show how $\log P$ is obtained by adding fragment constants and correction factors.¹⁶ $\log P$ can be estimated by a computer-based expert system (CLOGP3) developed by Hansch and Leo at Pomona College.¹ The availability of accurate methods for computation of $\log P$ make this parameter easy to use.

We found $\log P$ to be quite successful at correlating toxicity. For instance, for a training set of 53 chemicals tested for aerobic heterotrophs, we found an adjusted r^2 of 0.82 and a root mean square error of 0.39 (see Figure 15.4). $\log P$ was sometimes more successful in correlations for chemicals separated by chemical class. For instance, for Microtox bacteria, a QSAR covering a wide

$$\log IC_{50} = 5.12 - 0.76 \log P$$

$$n = 53 \quad s = 0.39 \quad adj r^2 = 0.82$$

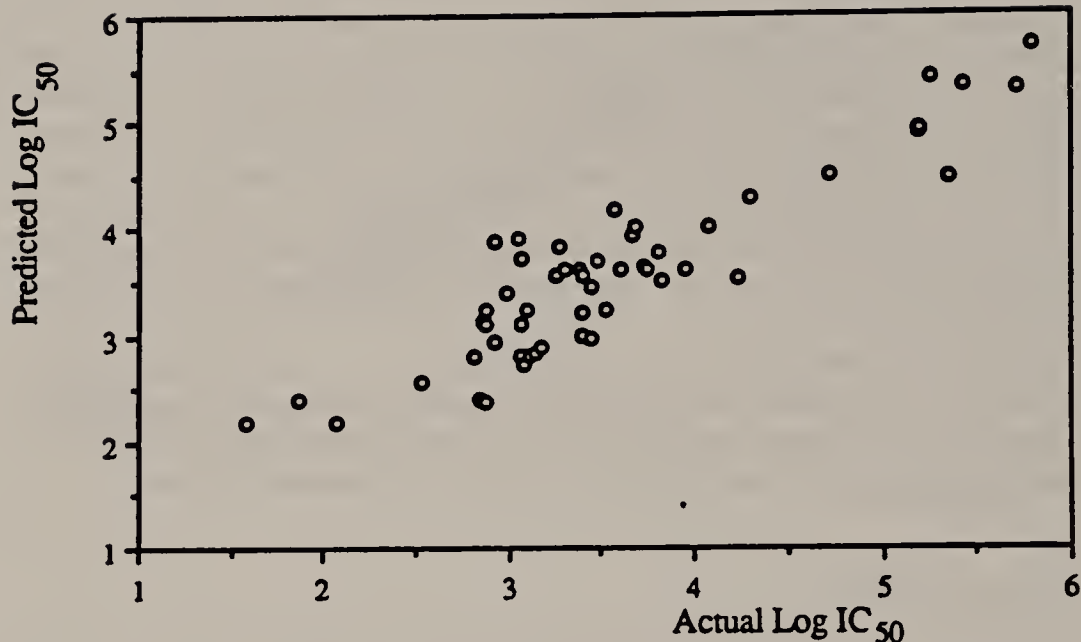


Figure 15.4. Aerobic heterotroph log P QSAR.

range of chemical classes had an adjusted r^2 of 0.68 and a root mean square error of 0.80. However, a QSAR covering just substituted benzenes achieved an adjusted r^2 of 0.77 and a root mean square error of 0.29.

Many previous studies have found very successful QSARs using log P in the field of aquatic toxicology. Konemann related the toxicity to guppies of industrial pollutants to log P in a linear relationship ($n = 50$, $s = 0.237$, $r^2 = 0.976$).¹⁷ Veith et al. used a two-term log P relationship to describe the toxicity of a variety of industrial chemicals to the fathead minnow.¹⁸ Even more common than log P QSARs for diverse chemical sets is the application of this method to smaller congeneric series of chemicals.

LSER

LSERs developed by Kamlet and coworkers have successfully correlated many diverse chemical properties, including toxicity, that depend on solute-solvent interactions. They are based on four molecular characteristics, called solvatochromic parameters: V_i , the intrinsic molecular volume; π , a measure of polarity or polarizability; and α_m and β_m , measures of the ability to participate in hydrogen bonding as a hydrogen donor or acceptor, respectively. A particularly good overview of the LSER method is found in Kamlet et al.³

A limitation of the LSER method is that the parameters are only available

for a finite number of chemicals. V_i can be computed using a number of molecular modeling systems based on structural fragments and standard bond lengths and angles such as those described in Leahy et al.¹⁹ In addition, V_i can be estimated with sufficient accuracy by the McGowan method.²⁰ Values for the remaining solvatochromic parameters were originally determined from solvent effects on ultraviolet and visible spectra. There are now a number of high-quality correlations, particularly with chromatographic data, that can be used to find additional parameters. The parameters also have clear chemical interpretations. Therefore, it is possible to estimate parameters from closely related chemicals. A number of rules are available to help make these estimates. In spite of these options, obtaining parameters for the LSER method is more difficult than for other methods (notably for phenols).

Of the three methods we considered, LSER produced the most accurate QSARs covering the widest range of chemical classes. For example, a QSAR for aerobic heterotrophs that included 52 compounds in the training set achieved an adjusted r^2 of 0.92 and a root mean square error of 0.27 (see Figure 15.5).

Other successful toxicity QSARs for nonreactive toxicity have been established for a number of organisms, including Microtox bacteria,²¹ Golden Orfe fish,²² and *Daphnia pulex*.²³ Chemicals acting by a reactive toxicity mechanism

$$\log IC_{50} = 5.24 - 4.15 V_i/100 + 3.71 \beta_m - 0.41 \alpha_m$$

$$n = 52 \quad s = 0.27 \quad \text{adj } r^2 = 0.92$$

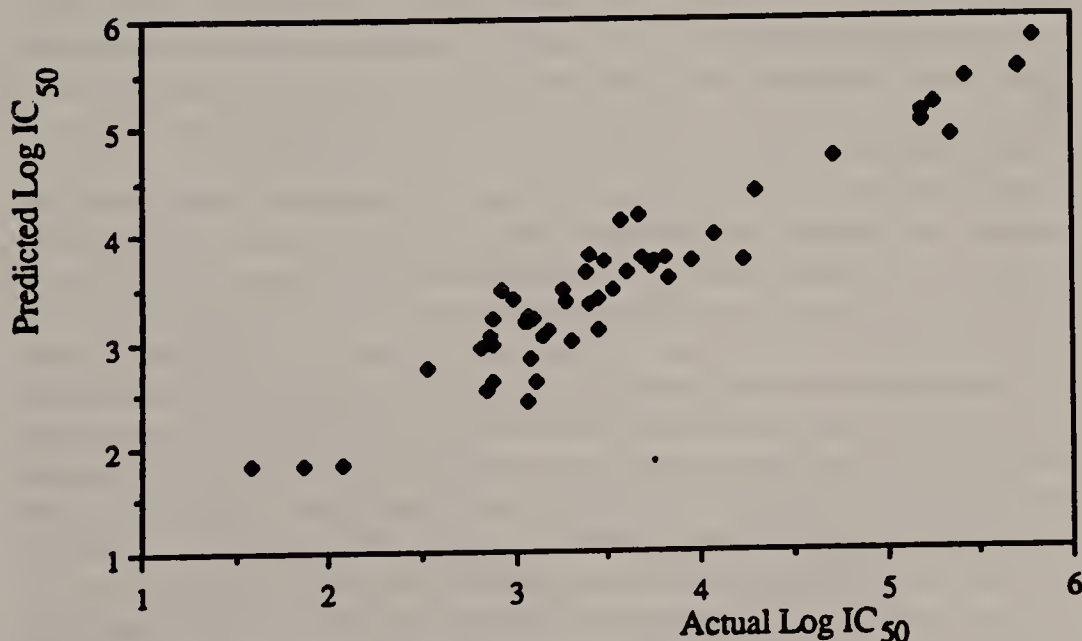


Figure 15.5. Aerobic heterotroph LSER QSAR.

are outliers from these relationships. Identification of outliers can provide information and impetus for identifying reactive toxicity mechanisms.

For instance, the differences between the observed and predicted toxicities of the carboxylic acid esters for the Golden Orfe fish²² were compared to the rate constants for hydrolysis of these compounds and found to correlate with an r^2 of 0.950. Thus, esters that hydrolyze rapidly showed enhanced toxicity, and those that hydrolyze slowly showed lesser toxicity and, in the extreme, followed a nonreactive toxicity mechanism.

The toxicity QSARs using LSER are all similar in form and relate to the physical meaning of the parameters. As the intrinsic molar volume or the hydrogen bond donor acidity increases, aqueous solubility decreases and toxicity increases. As the hydrogen bond donor acceptor basicity increases, aqueous solubility increases and toxicity decreases. The only term that runs counter to the trend expected on the basis of solubility is polarity-polarizability. As polarity increases, aqueous solubility increases and so does toxicity. Kamlet et al. hypothesized that this effect may relate to the mechanism of nonreactive toxicity.²²

Molecular Connectivity

Molecular connectivity uses graph theory techniques to calculate indexes by treating the hydrogen-suppressed chemical structures as linear and star graphs and identifying the various connected paths and clusters or subgraphs. Further details on the definitions and calculations of these indexes can be found in Kier and Hall.²

We found very accurate QSARs using molecular connectivity. For example, for aerobic heterotroph data including 46 compounds, a correlation using two indices yielded an adjusted r^2 of 0.78 and a root mean square error of 0.43 (see Figure 15.6). Although we found molecular connectivity QSARs covering many classes of compounds, the accuracy was sometimes improved by separating compounds by class.

The valence index, ${}^1X^v$, carries information relating to both volume and electronic character. Higher-order indices, based on larger substructures, encode more complex aspects of structure and often appear in multivariate regression analyses of molecules for physical and biological properties.²⁴ Additional information is contained in terms derived from the addition of valence and nonvalence indices and subtraction of valence and nonvalence indices for a given order.²⁵ Other researchers have tried to relate indices to known physical qualities with limited success.^{26,27} Therefore, although some molecular connectivity indices have been correlated with—or hypothesized to describe—specific characteristics, they are not defined well enough to be selected *a priori* for use in correlations. They are selected to optimize the correlation statistically.

In our work, the indices most often selected for inclusion in toxicity QSARs were a zero-order or first-order index. The second index selected was often a “difference index,” derived from the subtraction of a valence from a nonva-

$$\log IC_{50} = 6.09 - 0.59^0X + 2.29(1X^{-1}X^V) + 0.37^3X^C$$

$$n = 46 \quad s = 0.43 \quad adj r^2 = 0.78$$

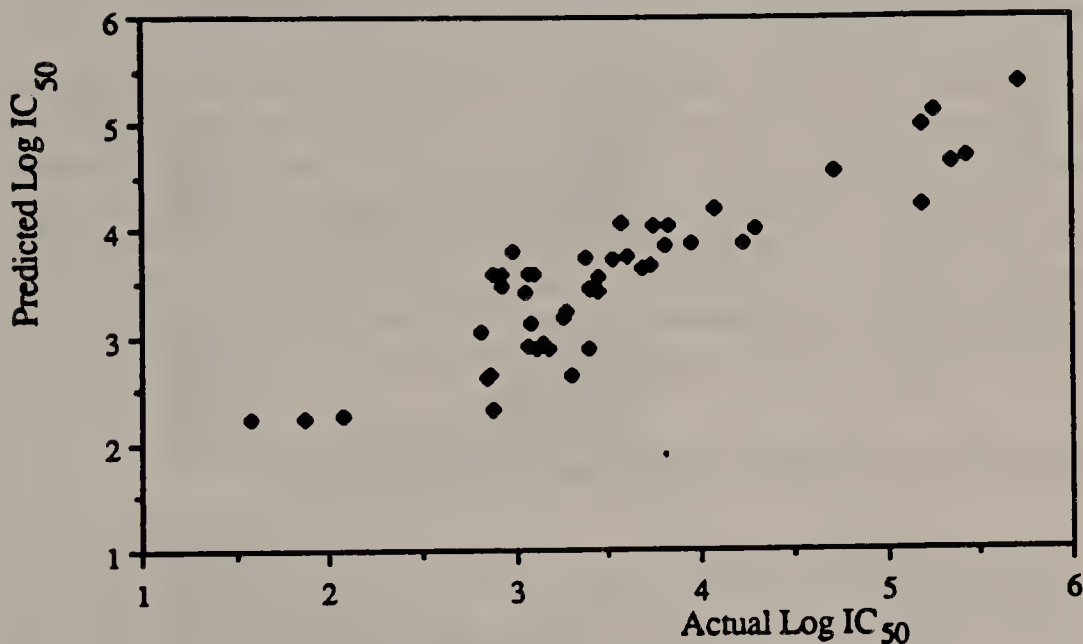


Figure 15.6. Aerobic heterotroph molecular connectivity QSAR.

lence index. The similarities found between the indices used in our different toxicity QSARs support the presumption that these indices are describing fundamental aspects of toxicity.

Other researchers have used molecular connectivity in environmental toxicology. Murray et al. used molecular connectivity to correlate biological activity that had previously been described in QSARs using log P.²⁸ Hall and Kier derived equations describing the antimicrobial action of halogenated phenols in an inverse relationship to 0X and a hyperbolic relationship with 1X .²⁹ Schultz et al. developed a structure-activity relationship for the toxicity of nitrogenous heterocyclic compounds to the freshwater ciliate *Tetrahymena pyriformis*.³⁰ This correlation showed an improvement in r^2 over a previous correlation of the data using log P.

Koch used first- and second-order valence connectivity indices to correlate toxicological data.^{31,32} He found that the accuracy of the linear relationships depended on the test organism and the similarity of the structure of chemical compounds. Better correlations were found for homologous series of chemicals rather than for more diverse sets. Koch developed QSARs for bioconcentration, sorption, and toxicity to guppies of a wide variety of environmental pollutants. All QSARs showed a linear dependence on $^1X^V$.³²

Sabljic and Protic showed the bioconcentration of a variety of halogenated environmental contaminants to be well correlated by a parabolic relationship

with ${}^2X^v$.³³ Sabljic demonstrated a correlation of toxicity to sheepshead minnows of chlorinated compounds with 0X .³⁴

Boyd et al. looked at a congeneric series of antimicrobial chemicals that had been previously correlated with $\log P$.³⁵ They found that higher-order (third-, fourth-, and fifth-order) connectivity indices provided improved correlations over $\log P$.

Molecular connectivity relationships are often used to make structural interpretations of toxicity.^{24,29,30} For instance, Hall and Kier developed a QSAR for toxicity of substituted phenols to fathead minnows.²⁴ They were able to show that an increase in molecular size (and hence 1X) results in increased toxicity. The inclusion of ${}^3X_p^v$ in the equations showed that valence definition of the indices is influential in describing toxicity. Hall and Kier pointed out that similar structural interpretations of toxicity are not possible in correlations based on physicochemical properties such as $\log P$.²⁹

EFFECT OF HALOGEN ADDITIONS ON A MOLECULE

It is worthwhile to visually note the relative effect of halogen additions to a molecule on Henry's constant, aqueous solubility, soil sorption, and environmental organism toxicity. The trend of a chemical property can abruptly change with additional halogenation in some cases, as will be noted below. In the following figures, experimental data are plotted for solubility, Henry's constant, and toxicity to the four organisms. The soil sorption data are the results of Sabljic's model.³⁶

With the two to six chlorinated ethanes, Henry's constant declines up to tetra and increases for penta and hexa (Figure 15.7). Aqueous solubility shows a decline with additional chlorination. Sabljic correlated molecular structure and soil sorption, and soil sorption shows a regular increase with chlorination.³⁶ Heterotrophic and Microtox toxicity show a general decline in IC_{50} with chlorination, i.e., more toxic with addition of chlorines. However, methanogen toxicity shows an abrupt decrease in IC_{50} for tri vs di chlorination, followed by an increase in IC_{50} from tri to hexa. Nitrosomonas also shows di and hexa to be least toxic and tri, tetra, and penta chlorination to show more severe toxicity, i.e., reduced IC_{50} . Conversely, Microtox shows additional chlorination of the ethane molecule to yield progressively increased toxicity.

Figure 15.8 shows the response of single chlorine substitution on propane, butane, pentane, hexane, octane, and decane. Solubility declines in a regular manner with carbon chain length, and soil sorption increases regularly with chain length. Heterotrophic toxicity increases generally with chain length, with a slight exception for hexane. Methanogen toxicity shows little regular pattern with increasing chain length; Nitrosomonas shows an abrupt toxicity reduction for the chlorinated octane and a slight decrease in IC_{50} for propane to hexane. Microtox shows reduced tolerance as chain length increases except for octane.

Figure 15.9 shows the exceptional predictability of the alcohol congeners.

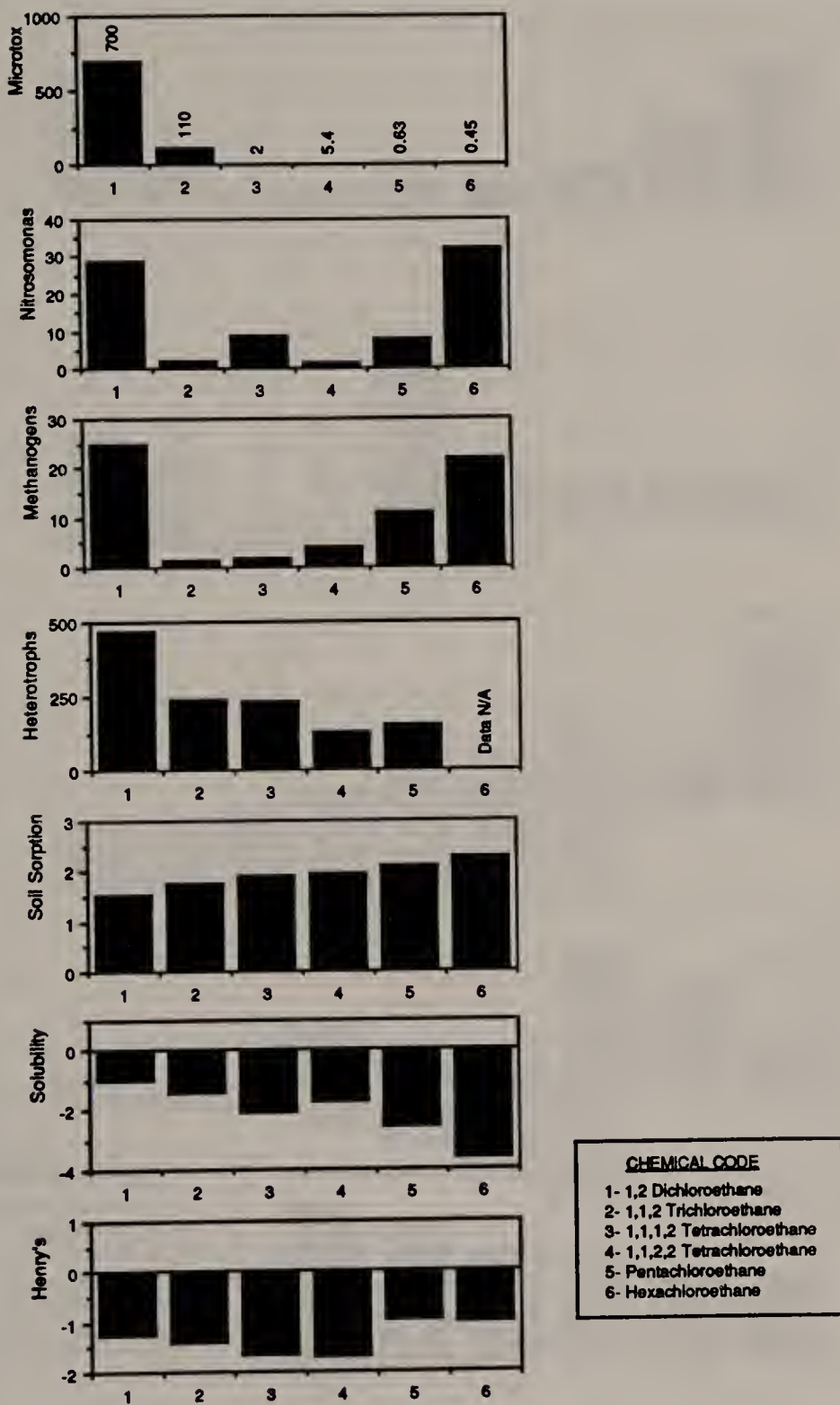


Figure 15.7. Effect of halogenation on ethane.

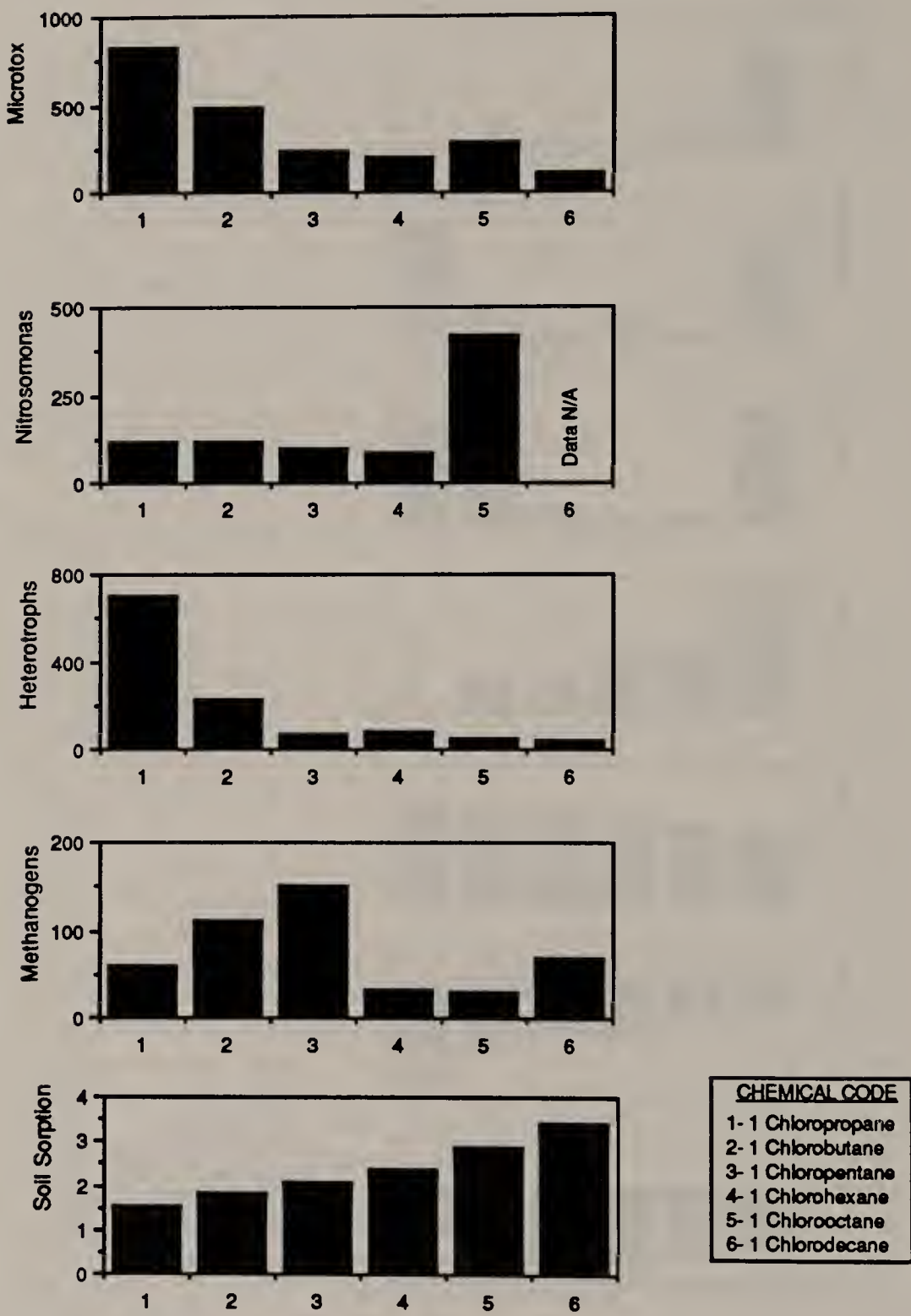


Figure 15.8. Effect of single chlorine on alkanes.

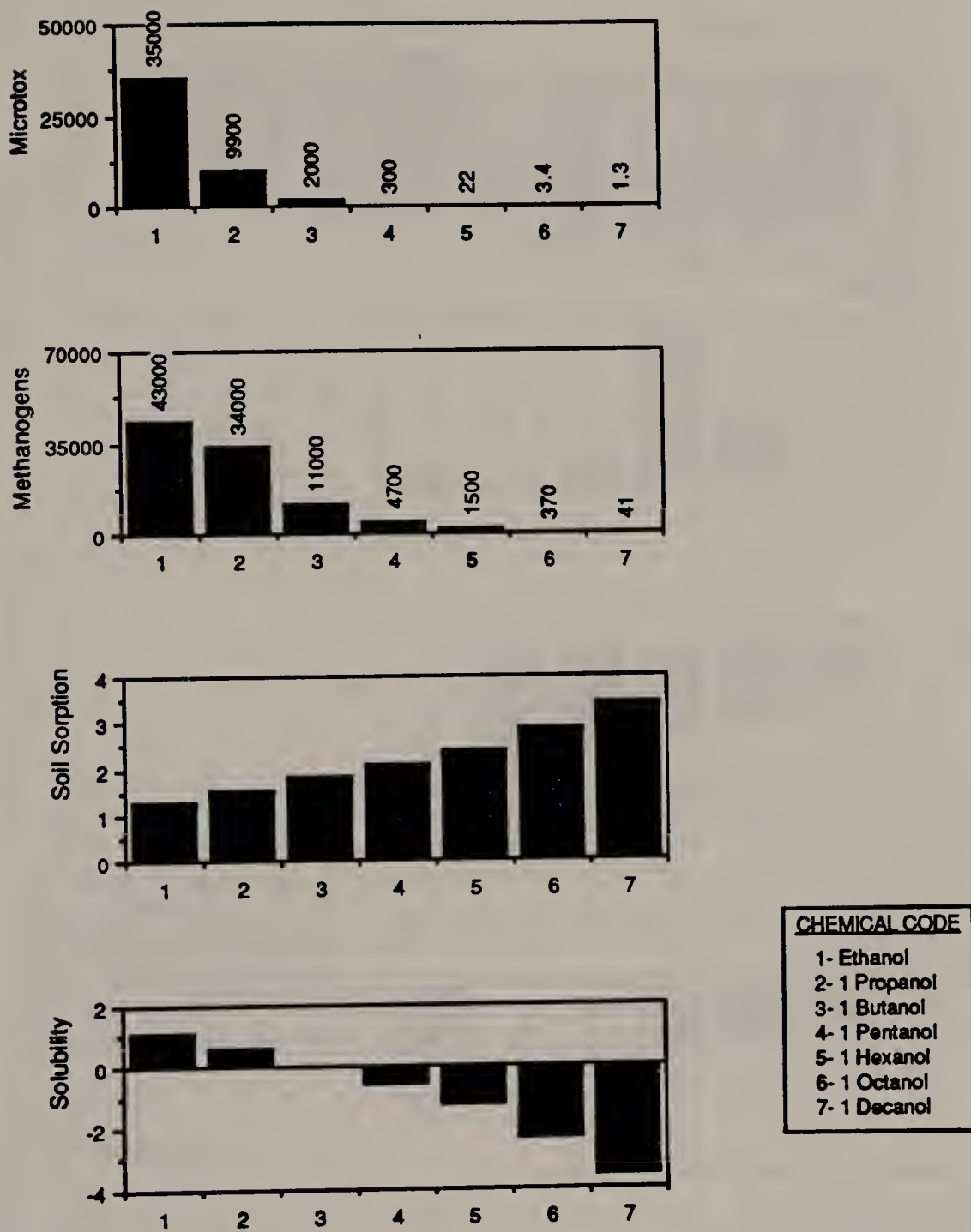
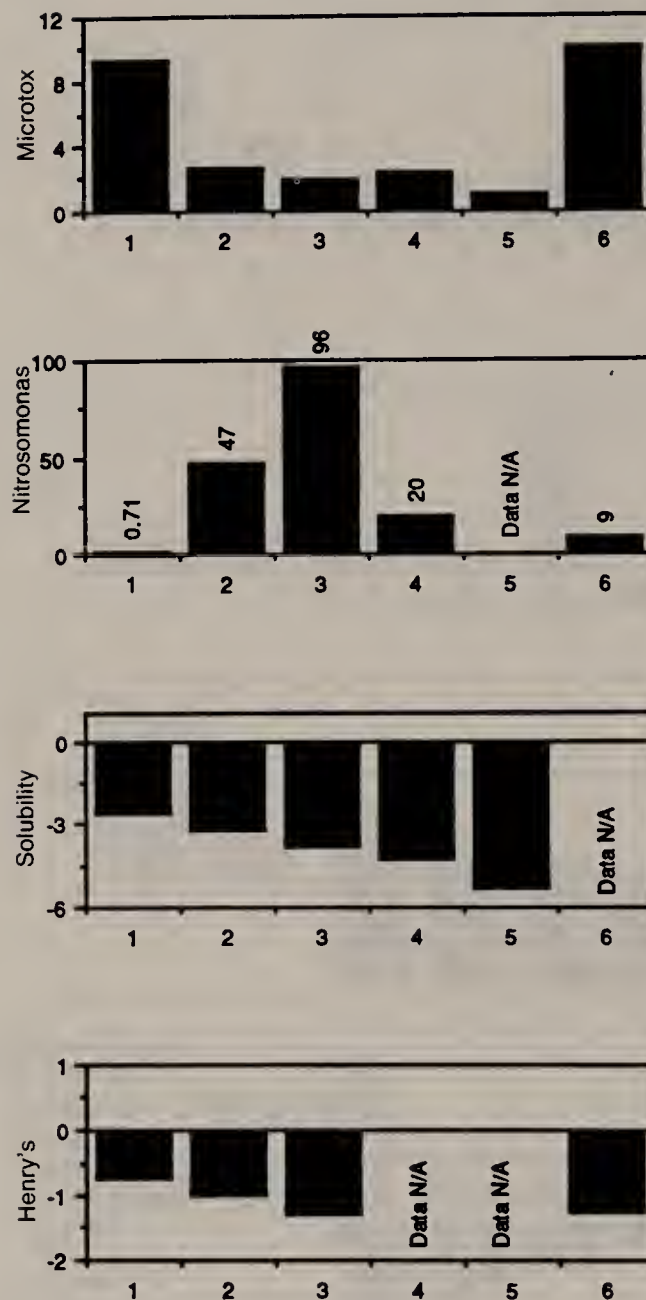


Figure 15.9. Predictability for alcohol congeners.

Figure 15.10 shows the patterns for chlorobenzenes, which yield irregular toxicity response with Nitrosomonas and Microtox. Figure 15.11 shows a general trend of reduced solubility of dioxins with increased chlorination.



<u>CHEMICAL CODE</u>	
1-	Chlorobenzene
2-	1,2 Dichlorobenzene
3-	1,2,3 Trichlorobenzene
4-	1,2,3,4 Tetrachlorobenzene
5-	Pentachlorobenzene
6-	Hexachlorobenzene

Figure 15.10. Effect of chlorination on benzene.

SUMMARY

The environmental fate of organic chemicals is directly related to their physical and chemical characteristics. Aqueous solubility, soil sorption, gas liquid partitioning, and toxicity to relevant environmental organisms are reviewed with particular emphasis on the quantitative structure-activity relationships which have been developed. These models are based upon four approaches to QSAR modeling—log P, linear solvation energy relationships,

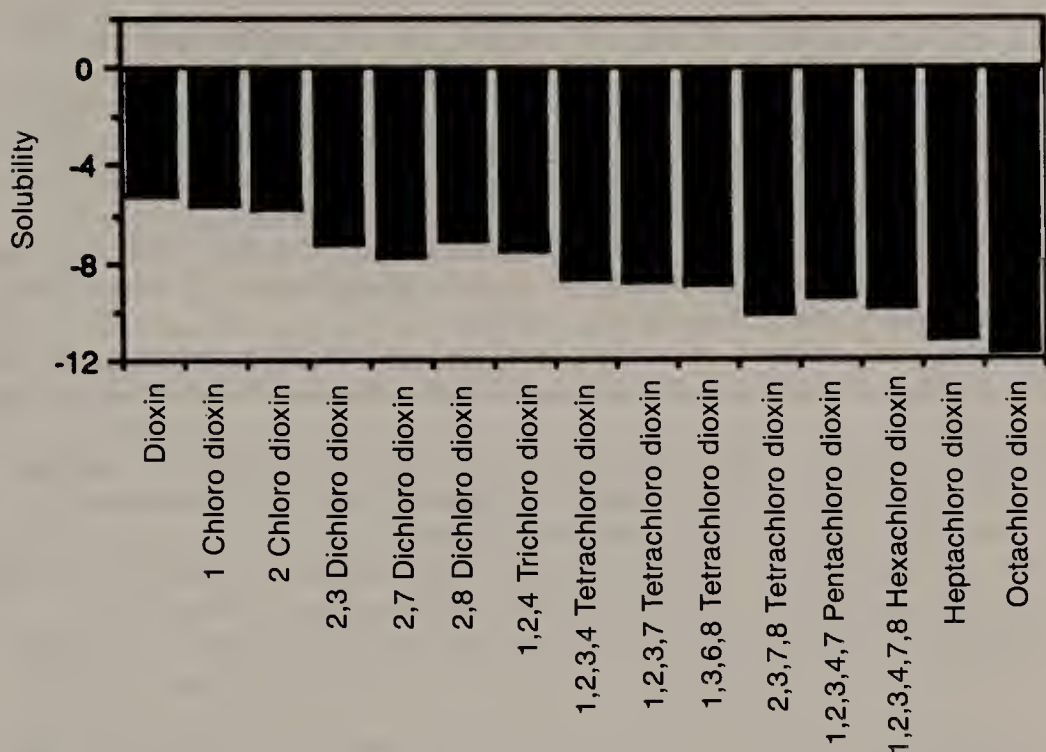


Figure 15.11. Solubility variation of chlorinated dioxins.

molecular connectivity, and a modification that incorporates polarizability of the molecule. Large data sets have been successfully modeled. All organic chemicals (470) with aqueous solubilities reported in the literature were successfully incorporated into one model with $r^2 = 0.98$. Likewise, all organic chemicals (180) with Henry's constants reported in the literature were incorporated into another model with $r^2 = 0.98$. IC₅₀ on a large set of organic chemicals which caused 50% inhibition to aerobic heterotrophs, methanogens, Nitrosomonas, Microtox, and fathead minnows was modeled by QSAR methods, and the correlations between the various organisms were determined.

REFERENCES

1. Leo, A., P. Y. C. Jow, C. Silipo, and C. Hansch. "Calculation of Hydrophobic Constant (Log P) from Pi and f Constants," *J. Med. Chem.* 18(9):865–868 (1975).
2. Kier, L. B., and L. H. Hall. *Molecular Connectivity in Structure-Activity Analysis* (Hertfordshire, Eng.: Research Studies Press, 1986).
3. Kamlet, M. J., R. M. Doherty, J. M. Abboud, M. H. Abraham, and R. W. Taft. "Solubility, A New Look," *Chemtech* 9:566 (1986).
4. Pierotti, R. A. "The Solubility of Gases in Liquids," *J. Phys. Chem.* 67:1840–1845 (1963).
5. Pierotti, R. A. "Aqueous Solutions of Non-Polar Gases," *J. Phys. Chem.* 69:281–288 (1965).

6. Wilhelm, E. and R. Battino. "On Solvophobic Interaction," *J. Chem. Phys.* 56:563-566 (1972).
7. Horvath, A. L. *Halogenated Hydrocarbons* (New York: Marcel Dekker, 1982).
8. Hine, J. and P. K. Mookerjee. "The Intrinsic Hydrophilic Character of Organic Compounds: Correlations in Terms of Structural Contributions," *J. Org. Chem.* 40:292-298 (1975).
9. Hansch, C., A. Vittoria, C. Silipo, and P. Y. C. Jow. "Partition Coefficient and Structure Activity Relationship of the Anaesthetic Gases," *J. Med. Chem.* 18:546-548 (1975).
10. Mackay, D. and W. Y. Shiu. "A Critical Review of Henry's Law Constants for Chemicals of Environmental Concern," *J. Phys. Chem. Ref. Data* 10:1175-1199 (1981).
11. Opperhulzen, A., F. A. P. C. Gobas, J. M. D. Van der Steen, and O. Hutzinger. "Aqueous Solubility of Polychlorinated Biphenyls Related to Molecular Structure," *Environ. Sci. Technol.* 22:638-646 (1988).
12. Yalkowski, S. H., S. C. Valvani, and D. Mackay. "Estimation of Aqueous Solubility of Some Aromatic Compounds," *Residue Rev.* 85:43-55 (1983).
13. Baker, R. J., B. J. Donelan, L. J. Peterson, W. E. Acree, Jr., and C. Tsai. "Correlation and Estimation of Aqueous Solubilities of Halogenated Benzenes," *Phys. Chem. Liq.* 16:279-292 (1987).
14. Hansch, C., J. E. Quinlan, and G. L. Lawrence. "The Linear Free Energy Relationship Between Partition Coefficient and the Aqueous Solubility of Organic Liquids," *J. Org. Chem.* 33:347-350 (1968).
15. Sabljic, A. "On the Prediction of Soil System Coefficients of Organic Pollutants from Molecular Structure: Application of Molecular Topology Model," *Environ. Sci. Tech.* 21:358-366 (1987).
16. Lyman, W. J., W. F., Reehl, and D. H., Rosenblatt. *Handbook of Chemical Property Estimation Methods*, (New York: McGraw-Hill, 1982), pp. 1.1-1.54.
17. Konemann, H. "Quantitative Structure-Activity Relationships in Fish Toxicity Studies, Part 1: Relationship for 50 Industrial Pollutants," *Toxicol.* 19:209-221 (1981).
18. Veith, G. D., D. J. Call, and L. T. Brooke. "Structure Toxicity Relationships for Fathead Minnows: Narcotic Industrial Chemicals," *Can. J. Fish. Aquat. Sci.* 40:743-748 (1983).
19. Leahy, D. E., P. W. Carr, R. S. Pearlman, R. W. Taft, and M. J. Kamlet. "Linear Solvation Energy Relationships: A Comparison Between Molar Volume and Intrinsic Molecular Volume as Measures of the Cavity Term in RPLC," *Chromatographia* 21:473-478 (1986).
20. Kamlet, M. J., R. M. Doherty, M. H. Abraham, P. W. Carr, R. F. Doherty, and R. W. Taft. "Linear Solvation Energy Relationships: Important Differences Between Aqueous Solubility Relationships for Aliphatic and Aromatic Solutes," *J. Phys. Chem.* 91(7): 1996-2004 (1987).
21. Kamlet, M.J., R. M. Doherty, G. D. Veith, R. W. Taft, and M. H. Abraham. "Solubility Properties in Polymers and Biological Media: 7. An Analysis of Toxicant Properties That Influence Inhibition of Bioluminescence in Microtox," *Environ. Sci. Technol.* 20(7):690-695 (1986).
22. Kamlet, M. J., R. Doherty, R. W. Taft, M. H. Abraham, G. D. Veith, and D. J. Abraham. "Solubility Properties in Polymers and Biological Media: 8. An Analysis

- of the Factors That Influence Toxicities of Organic Non-Electrolytes to Golden Orfe Fish," *Environ. Sci. Technol.* 21(2):149-155 (1987).
- 23. Passino, D. R. M., J. P. Hickey, and A. M. Frank. "Linear Solvation Energy Relationships for Toxicity of Selected Organic Chemicals to *Daphnia pulex* and *Daphnia magna*," Third International Workshop on Quantitative Structure-Activity Relationships in Environmental Toxicology, Knoxville, TN, May 1988.
 - 24. Hall, L. H., and L. B. Kier. "Molecular Connectivity of Phenols and Their Toxicity to Fish," *Bull. Environ. Contam. Toxicol.* 32:354-362 (1984).
 - 25. Kier, L. B., and L. H. Hall. "Derivation and Significance of Valence Molecular Connectivity," *J. Pharm. Sci.* 70:583-589 (1981).
 - 26. Murray, W. J. "Molecular Connectivity and Steric Parameters," *J. Pharm. Sci.* 66:1352-1354 (1977).
 - 27. Dearden, J. C. "The Physical Significance of Molecular Connectivity Indices," Third International Workshop on Quantitative Structure-Activity Relationships in Environmental Toxicology, Knoxville, TN, May 1988.
 - 28. Murray, W. J., L. H. Hall, and L. B. Kier. "Molecular Connectivity:III. Relationship to Partition Coefficient," *J. Pharm. Sci.* 64:1978-1981 (1975).
 - 29. Hall, L. H., and L. B. Kier. "A Comparative Analysis of Molecular Connectivity, Hansch, Free Wilson, and Darc Pelco Methods in Structure Activity Relationship of Halogenated Phenols," *Eur. J. Med. Chem.* 13(1):89-92 (1978).
 - 30. Schultz, T. W., L. B. Kier and L. H. Hall. "Structure-Toxicity Relationships of Selected Nitrogenous Heterocyclic Compounds:III. Relationships Using Molecular Connectivity," *Bull. Environ. Contam. Toxicol.* 28:373-378 (1982).
 - 31. Koch, R. "Molecular Connectivity and Acute Toxicity of Environmental Pollutants," *Chemosphere* 11:925-931 (1982).
 - 32. Koch, R. "Molecular Connectivity Index for Assessing Ecotoxicological Behavior of Organic Compounds," *Toxicol. Environ. Chem.* 6:87-96 (1983).
 - 33. Sabljic, A. and M. Protic. "Molecular Connectivity: A Novel Method for Prediction of Bioconcentration Factor of Hazardous Chemicals," *Chem. Biol. Interactions* 42:301-310 (1982).
 - 34. Sabljic, A. "Quantitative Structure-Toxicity Relationship of Chlorinated Compounds: A Molecular Connectivity Investigation," *Bull. Environ. Contam. Toxicol.* 30:80-83 (1983).
 - 35. Boyd, J. C., J. S. Millership, and A. D. Woolfson. "A Comparison of Log P and Molecular Connectivity in the Structure Activity Analysis of Some Antimicrobial Agents," *J. Pharm. Pharmacol.* 34:158-161 (1982).
 - 36. Sabljic, A. "On the Prediction of Soil Sorption Coefficient of Organic Pollutants from Molecular Structure: Application of Molecular Topology Model," *Environ. Sci. Technol.* 21:358-366 (1987).

PART III

INTERFACIAL AND ORGANIC-INORGANIC PROCESSES

CHAPTER 16

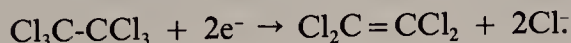
Reduction of Hexachloroethane and Carbon Tetrachloride at Surfaces of Biotite, Vermiculite, Pyrite, and Marcasite

Michelle R. Kriegman-King and Martin Reinhard

INTRODUCTION

Contamination of groundwater resources by halogenated compounds spurred the formation of a national program to clean up hazardous waste sites across the United States. Compounds such as carbon tetrachloride (CTET), chloroform (CF), and hexachloroethane (HCA) are a few of the chemicals which have been proposed to be “characteristic” hazardous wastes to be included in the toxic contaminant leachate potential (TCLP) test.¹ Consequently, chemical and biological transformation pathways are being studied to aid in understanding the fate of these contaminants in groundwater environments and to apply the processes occurring naturally in groundwater environments to remediation technologies. This chapter shows the importance of mineral surfaces and common environmental reductants such as sulfide in abiotic transformations of HCA and CTET and summarizes pertinent literature.

Halogenated aliphatic compounds can be chemically transformed by reductive dehalogenation (hydrogenolysis) and reductive elimination (dihaloelimination) in sediment-water systems.²⁻⁴ Hydrogenolysis and dihaloelimination are electron transfer reactions that remove (one and two, respectively) halogens from haloaliphatics forming halides, radical intermediates, and reduced organic products. An example of reductive elimination is the transformation of HCA to tetrachloroethylene (PCE):



In this reaction, two electrons need to be donated for every HCA that is reduced. In groundwater environments, ferrous iron or hydrogen sulfide in the aqueous or solid phase could provide these electrons. Both ferrous iron and sulfide (HS^-) tend to be stable under reducing conditions. In homogeneous

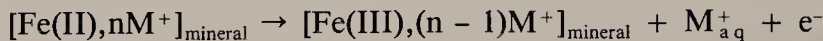
solution, they may act as electron donors according to the following reactions:



and



where HSSH is hydrogendisulfide. At circumneutral pH, once the ferrous iron becomes oxidized, it forms an amorphous precipitate which crystallizes with age.⁵ In the solid phase, Fe(II) commonly occurs in minerals found in crystal rocks, such as biotite, amphibole, pyroxene, magnetite, ilmenite, and clays.⁶ The heterogeneous oxidation of ferrous iron present in these silicate and oxide minerals could be formulated as follows:



where M⁺ is a cation released to solution to maintain a charge balance in the mineral.^{7,8} Farmer et al.⁷ and Veith and Jackson⁸ indicated that the electroneutrality of micaceous vermiculite during oxidation of structural Fe(II) is maintained by a reversible deprotonation of octahedral hydroxyl groups or an irreversible expulsion of octahedral metal cations.

Surface sulfide groups in sulfide minerals such as pyrite can act as electron donors and can be oxidized to polysulfides, elemental sulfur, thiosulfate, and ultimately to sulfate.^{9,10} In the presence of sheet silicates, sulfide can adsorb at Al-OH and Mg-OH edge sites. These sites are protonated below pH 9 and 12, respectively. Katser and Ropot studied the adsorption of HS⁻ on natural sheet silicates and showed that 0.1 g/L slurries of bentonite, hydromica, and palygorskite adsorbed more than 90% of 0.6 mM HS⁻ within 4 hr.¹¹ No information is available in the literature on the redox properties of sulfide sorbed by mica surfaces.

In this chapter, we report that the transformation rates of HCA and CTET are significantly faster in mineral systems than homogeneous systems, particularly when sulfide is present. HCA was chosen as a model compound because it is a fully halogenated ethane whose dehalogenation product, PCE, is formed nearly quantitatively and is easy to monitor. Transformation of CTET, a common environmental contaminant, was also studied. CF, the expected hydrogenolysis product of CTET transformation, was the only CTET transformation product identified, and most of the products (> 80%) remain unidentified.

The minerals that were used in this study were biotite, vermiculite, pyrite, and marcasite. Biotite and vermiculite are 2:1 sheet silicates with iron predominantly in the octahedral layer. Biotite is characterized by a relatively high ferrous iron content (3.41 weight percent) and an interlayer spacing of 9.8 Å.

Since vermiculite is a weathering product of biotite, its ferrous iron content is considerably lower (0.89 weight percent) than that in biotite, and its interlayer spacing is approximately 14 Å. The interlayer spacing is much larger in vermiculite because the potassium interlayer cations in biotite are exchanged for sodium, calcium, or magnesium, which become hydrated. The expandable sheets of vermiculite provide additional internal surface area. Pyrite and marcasite are iron sulfides with the chemical formula FeS₂. The structural difference between them is that pyrite is a cubic mineral and marcasite is orthorhombic. Although pyrite is much more common than marcasite, both minerals are found in anoxic sedimentary environments.⁶

MATERIALS AND METHODS

Biotite and vermiculite were obtained from Ward's Scientific Establishment, Inc. (Rochester, NY). The minerals were wet ground with an Osterizer blender (using deoxygenated Milli-Q water) in an anaerobic glove box, which had a 90% N₂/10% H₂ atmosphere. After grinding, the minerals were freeze-dried, dry-sieved to three size fractions (< 200, 200–50, > 50 mesh U.S. Standard), and stored in the anaerobic glove box. The 50–200 mesh (75–300 µm) size fraction was used for the experiments. Pyrite and marcasite were also obtained from Ward's Scientific Establishment. The pyrite, from Custer, South Dakota, contained lead, copper, and zinc as minor impurities. The marcasite, from Dundas, Ontario, contained lead, cadmium, copper, nickel, and zinc as minor impurities.¹² The pyrite and marcasite were ground in a ball-mill and dry-sieved to three size fractions, as above. The 75–300 µm size fractions of pyrite and marcasite were cleaned to remove any oxidized coating. The cleaning method was based on "method 3" described by Moses et al.¹⁰ A 15-g sample of the mineral was placed in 250 mL of boiling 6 N HCl for 15 min. The mineral was allowed to settle for 5 min, decanted, rinsed twice with 150–200 mL of boiling 6 N HCl, which was allowed to settle for 5 min before decanting. The mineral was then rinsed with warm acetone according to the same procedure. The cleaned mineral was transferred to a preweighed vial and placed in the glove box to dry for 24 hr. After drying, the vial was weighed so a known amount of mineral was added to the slurry for the transformation experiments.

All transformation experiments were conducted in flame-sealed glass ampules because the reaction times were on the order of weeks to months at elevated temperature. To minimize oxidation in the autoclave, the biotite- or vermiculite-filled ampules were autoclaved under a nitrogen atmosphere. The method of filling the ampules was similar to that described by Barbash and Reinhard.¹³ After autoclaving, ampules were placed in the anaerobic glove box and were filled with Tris buffer (Sigma Chemical Co., St. Louis, MO) that was cold-sterilized with a 0.2-µm polysulfone membrane filter (Gelman Sciences, Ann Arbor, MI). Pyrite and marcasite were added to the ampules as slurries

because the minerals could not be removed from the glove box once they were cleaned. The buffer solutions were made outside the glove box and were autoclaved and deoxygenated. Once the buffers were in the glove box and deoxygenated by bubbling glove box atmosphere through the buffer solutions, the cleaned pyrite or marcasite was added. The ampules were filled with a sterilized syringe and needle, which was fitted to the slurry with sterilized PTFE tubing and a three-way valve. Ampules were covered with polyvinylidene chloride (Saran) sheets, secured with rubber O-rings, and removed from the glove box. Ampules were immediately spiked with an aqueous or methanolic spike and flame-sealed with an oxygen/propane flame.

Sealed ampules were held in the dark in a 50°C ($\pm 0.1^\circ\text{C}$) water bath for the duration of the experiment. Samples were regularly removed from the bath, manually mixed, and returned to the bath within 5 min. At each sampling time, two ampules for each experimental condition were removed from the constant temperature bath, centrifuged, extracted, and analyzed for CTET or HCA and their products (PCE or CF) using a gas chromatograph equipped with an electron capture detector.

Adsorption of 1 μM HCA onto biotite was measured over 165 days under the same experimental conditions as the transformation studies, except the reaction temperature was 25°C to prevent transformation of the HCA. Sorption remained constant at $7 \pm 1.3\%$ (99% confidence interval) over the time scale of the experiment. The biotite used in these experiments has a BET surface area (determined by krypton adsorption) of $1.44 \text{ m}^2/\text{g}$. Thus, the amount of HCA adsorbed onto biotite at a given time during an experiment is $7.6 \times 10^{-4} \text{ molecules/nm}^2$.

EVALUATION OF KINETIC DATA

The reaction between haloaliphatics (RX) and the reductants (ferrous iron or sulfide complexes) in solution or at mineral surfaces was evaluated to see if a pseudo-first-order rate model with respect to RX could be applied. The data were evaluated using the rate law:

$$\frac{-d[\text{RX}]}{dt} = k'_{\text{obs}} [\text{RX}]_{\text{total}}$$

because the reductants (ferrous iron or sulfide in solution or in the solid phase) were always at least two orders of magnitude in excess. $[\text{RX}]_{\text{total}}$ corresponds to the sum of the dissolved and sorbed RX per volume.

In both homogeneous and heterogeneous systems k'_{obs} may be comprised of several pseudo-first order reaction constants. In homogeneous solutions, k'_{obs} may be the sum of the rates due to reaction with water and with the reductant:

$$(k'_{\text{obs}})_{\text{homo}} = k'_{\text{water}} + k'_{\text{HS-}}$$

Table 16.1. Observed Rate Constants for the Disappearance of 1 μM HCA at 50°C and [Tris(hydroxymethyl)aminomethane (Tris Buffer)] = 0.01 M

Exper. ^a Name	Mineral	Solids Conc (g/L)	pH	[Sulfide] (mM)	k'_{obs} (days ⁻¹) ^b	$t_{1/2}$ (days)
H	—	—	8	0	0.0019 \pm 0.0006	365
HB	biotite	38.5	8	0	0.0036 ^c \pm 0.001	190
HV	vermiculite	38.5	8	0	0.012 ^c \pm 0.005	57
HS	—	—	7.8	4	0.046 \pm 0.028	15
HBS	biotite	38.5	7.8	4	1.06 ^c \pm 0.36	0.65
HVS	vermiculite	38.5	7.8	4	1.53 ^c \pm 0.45	0.45

^aH = HCA, B = biotite, V = vermiculite, S = sulfide.

^b95% confidence interval around k'_{obs} .

^cRate constants in the presence of solids.

In heterogeneous systems, k'_{obs} would include the homogeneous rate constants in addition to several heterogeneous rate constants, such as

$$(k'_{\text{obs}})_{\text{hetero}} = (k'_{\text{obs}})_{\text{homo}} + k'_{\text{primary mineral}} + k'_{\text{secondary mineral}} + k'_{\text{adsorbed reductant}}$$

In this case $(k'_{\text{obs}})_{\text{homo}}$ would include terms for water, sulfide, and aqueous reductants formed by mineral dissolution. For our sheet silicate/sulfide experiments, the primary mineral rate constant ($k'_{\text{primary mineral}}$) would be for reaction with the sheet silicate; the secondary mineral rate constant ($k'_{\text{secondary mineral}}$) would be for reaction with precipitated iron sulfides, if formed; and the adsorbed reductant rate constant ($k'_{\text{adsorbed reductant}}$) would be for reaction with sulfide adsorbed onto the sheet silicate surface. These rate constants are likely to be a function of pH, surface area, reductant concentration, and temperature.

Rate constants (k'_{obs}) were calculated from the slope of plots of $\ln(C_t/C_0)$ versus time, where C_0 is the concentration at time = 0 and C_t is the concentration of the sample at time t. Linear regressions were calculated by allowing the intercept to float and by forcing the intercept through zero. The difference between the intercepts was tested by comparing the 95% confidence intervals based on the standard error of the estimates. The rate constants calculated with the floating intercept are presented in this chapter. The 95% confidence interval of k'_{obs} was calculated using the standard error of the slope.

RESULTS

The experimental conditions for the transformation of HCA and CTET are summarized in Tables 16.1 and 16.2. In experiments conducted with sulfide, the pH was at 7.7–7.8. Because the pK_a of the first dissociation of hydrogen sulfide at 50°C is 6.73 ± 0.02 ,¹⁴ ninety percent of the total sulfide in these experiments was present as HS^- , which is probably the reactive sulfur species. In the experiment with 0.1 mM ferrous iron in solution, HYDRAQL, a chemical equilibrium program,¹⁵ predicted that 95% of the iron was present as aquo-iron ($\text{Fe}^{2+}_{\text{aq}}$). The remaining iron was complexed with chloride and sulfate.

Table 16.2. Observed Rate Constants for Disappearance of 1 μM CTET at 50°C, [Tris] = 0.01 or 0.05 M (Pyrite, Marcasite Experiments)

Exper. ^a Name	Mineral	Solids Conc (g/L)	pH	[Sulfide] (mM)	[Fe] (mM)	k'_{obs} (days ⁻¹) ^b	$t_{1/2}$ (days)
C ^c	—	—	—	0	0	0.0018	380
CS	—	—	7.7	4	0	0.005 \pm 0.004	130
CBS	biotite	38.5	7.7	4	0	0.15 ^d \pm 0.012	4.5
CVS	vermiculite	38.5	7.7	4	0	0.24 ^d \pm 0.012	2.9
CFe	—	—	6.6	0	0.1	0.0066 \pm 0.003	100
CP	pyrite	18.1	7.5	0	0	1.59 ^d \pm 0.27	0.44
CM	marcasite	17.3	7.6	0	0	0.82 ^d \pm 0.16	0.85

^aC = CTET, S = sulfide, B = biotite, V = vermiculite, Fe = ferrous iron, P = pyrite, and M = marcasite.

^b95% confidence interval around k'_{obs} .

^cCalculated from Jeffers et al.¹⁶

^dRate constants in the presence of solids.

In Table 16.1, the overall rate constants (k'_{obs}) and calculated half-lives at 50°C are summarized for the disappearance of HCA in homogeneous solution with and without 4 mM HS⁻ (experiments HS and H, respectively), and in heterogeneous systems with biotite and vermiculite with and without HS⁻. As shown in Figures 16.1 and 16.2, HCA is slowly reduced to PCE in the presence of biotite and vermiculite. The HCA and PCE data were fitted using a first-order model. The scatter in the Day 190 data is unexplained. By adding HS⁻, the half-lives of HCA to PCE were shortened to 0.65 and 0.45 days, respec-

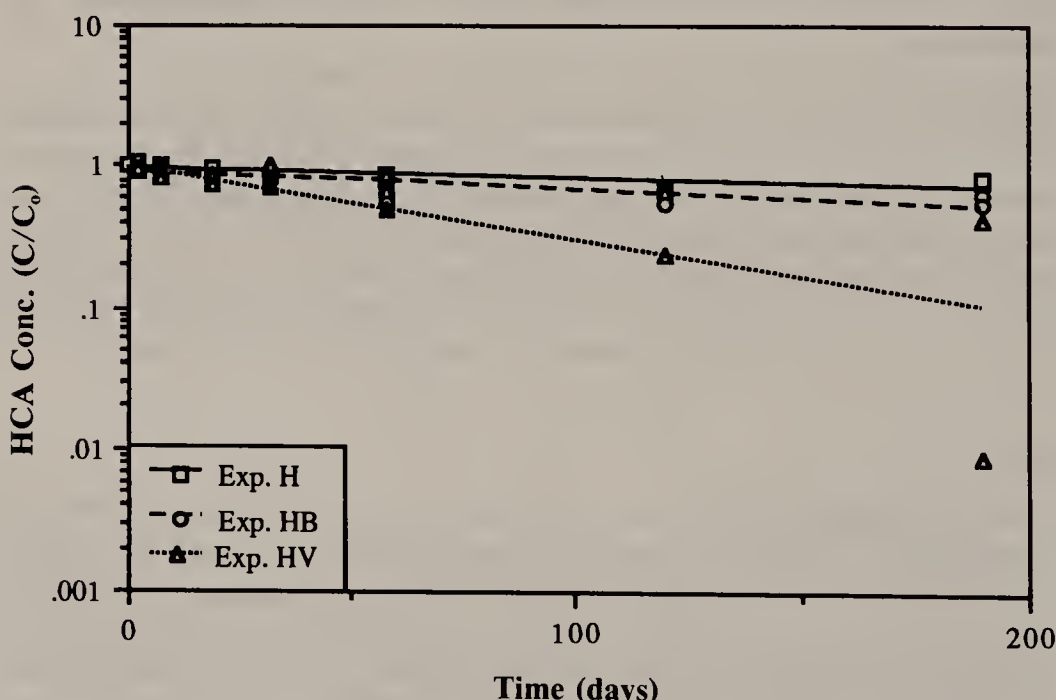


Figure 16.1. HCA transformation in the presence of biotite and vermiculite at 50°C and pH 8. H = HCA, B = biotite, V = vermiculite.

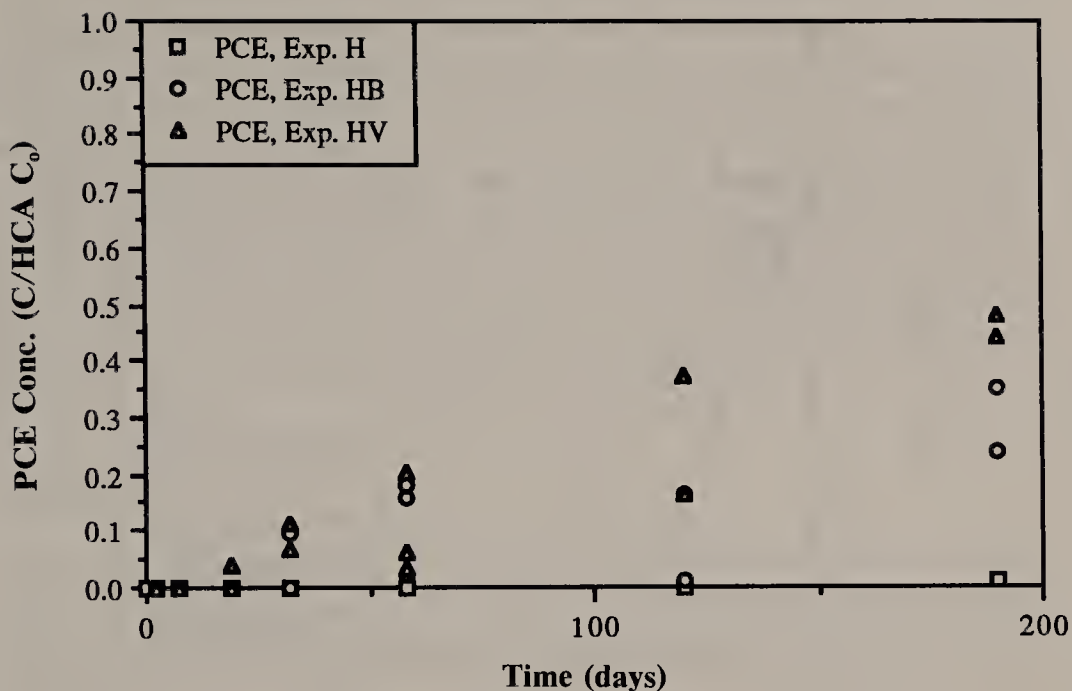


Figure 16.2. PCE appearance in the presence of biotite and vermiculite at 50°C and pH 8. H = HCA, B = biotite, V = vermiculite.

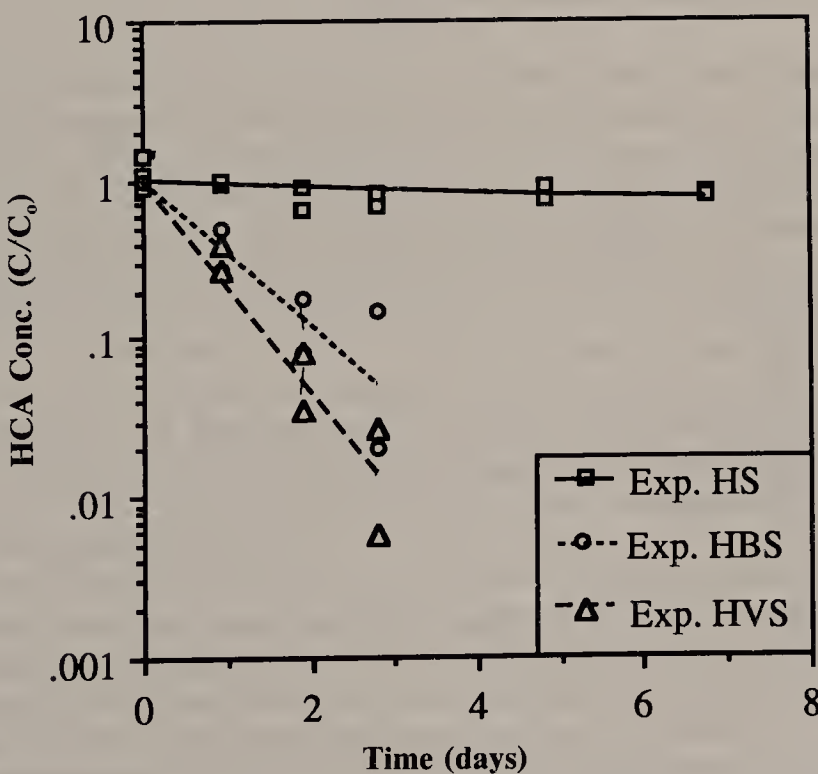


Figure 16.3. HCA transformation in the presence of HS^- , biotite, and vermiculite at 50°C and pH 7.8. H = HCA, S = sulfide, B = biotite, and V = vermiculite.

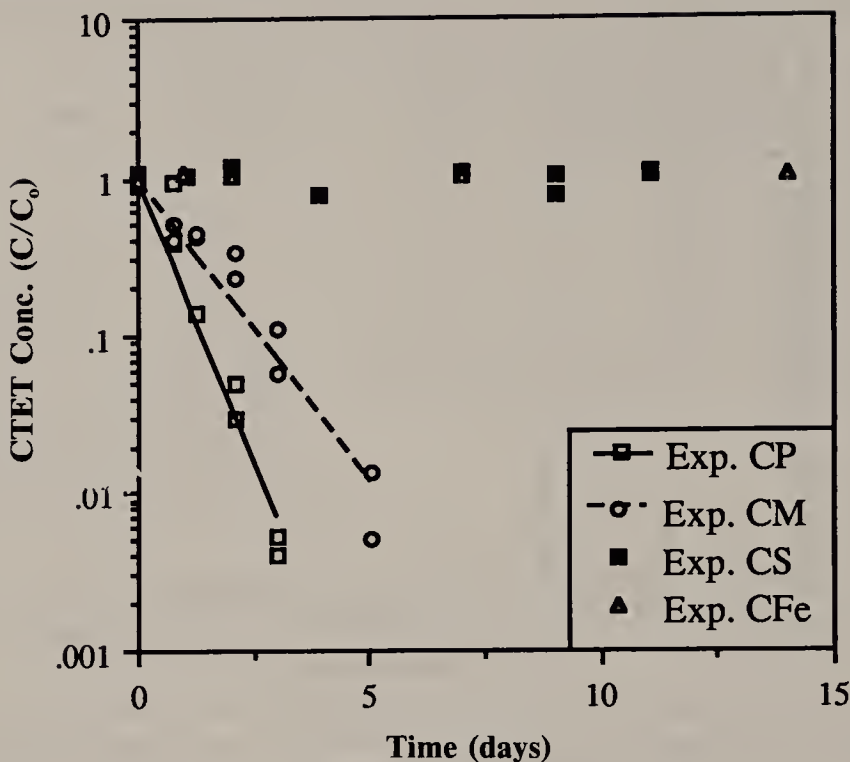


Figure 16.4. CTET transformation in the presence of pyrite and marcasite at 50°C. C = CTET, M = marcasite, P = pyrite.

tively (Figure 16.3). These data demonstrate that the combination of minerals and sulfide increases the transformation rate of HCA compared to its transformation rate in water or in mineral systems without sulfide. The heterogeneous disappearance of HCA in the presence of HS^- also adhered to a first-order model over more than three half-lives. In the homogeneous systems, adherence to first-order kinetics was not clear because of the low conversions.

The transformation of CTET was studied in homogeneous solution with 4 mM HS^- and in heterogeneous systems with HS^- and biotite or vermiculite. Table 16.2 shows the observed rate constants for these systems. The calculated hydrolysis rate of CTET at 50°C is included in Table 16.2 for comparison.¹⁶ CTET transformation was also studied with natural iron sulfides (pyrite and marcasite) because they react readily with oxygen and ferric iron, and they are suspected to form as secondary minerals at the surface of biotite and vermiculite immersed in sulfide solutions. Although the 18 g/L of pyrite and marcasite used in these experiments is higher than amounts expected to form at the surface of the sheet silicate systems, the levels of iron sulfides used in this study can be compared to levels found in salt marsh and coastal marine sediments.¹⁷⁻¹⁹ As shown in Table 16.2 and Figure 16.4, both pyrite and marcasite reacted very quickly with CTET. The data for CTET disappearance in the presence of iron sulfide minerals also adhered to a first-order model over more than five half-lives.

Addition of 18 g/L of pyrite or marcasite increased the reaction rate with CTET by two orders of magnitude above the rate with 4 mM sulfide or 0.1 mM ferrous iron in solution. These rate increases support a heterogeneous mechanism because iron sulfides are extremely insoluble (with the pK_{so} on the order of 18). In experiments CS and CFe, sulfide or ferrous iron in solution (at concentrations much higher than could be achieved by pyrite dissolution) could not account for the fast reaction with pyrite or marcasite. Furthermore, the slow reaction in the CS and CFe experiments also show that the transformation rate in the sheet silicate/sulfide systems is due to a heterogeneous mechanism, possibly from secondary iron sulfide formation.

DISCUSSION

Our study of the reactions of HCA and CTET with environmental reductants and mineral surfaces demonstrated that transformation of halogenated aliphatic compounds can be promoted by heterogeneous processes. To gain insight into the mechanism of these heterogeneous transformations, we compared the organic reactions studied herein with studies of heterogeneous reactions between the Fe(II)-bearing minerals and inorganic redox agents. Studies of heterogeneous processes of hydrophobic organics which might serve as an analog are electrode processes.²⁰ Studies of mineral oxidation by inorganic compounds, such as ferric iron, oxygen, and hydrogen peroxide, and speculated reaction mechanisms are described below.

The literature discussed below shows that minerals can promote heterogeneous transformations of organic and inorganic compounds by

1. concentrating the reactants at the surface, which increases the proximity of the reactants, thereby increasing the probability of reaction,
2. placing the reactants in a more favorable redox environment, and
3. altering the reactant's configuration at the mineral surface, causing the reactivity to increase.

The types of heterogeneous redox reactions that have been studied are summarized in Table 16.3. The table includes sheet silicates and iron sulfides as the mineral surfaces and considers both organic and inorganic redox agents.

Oxidation of Sheet Silicates

Biotite and vermiculite significantly increased the transformation rate of HCA compared to the rate in water. The heterogeneous electron transfer reaction which could describe the observed reaction between HCA and the sheet silicates could be of the form:

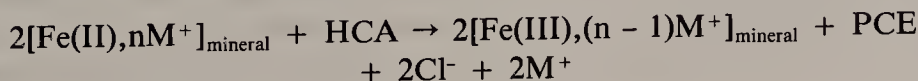


Table 16.3. Heterogeneous Oxidation of Sheet Silicates and Pyrite

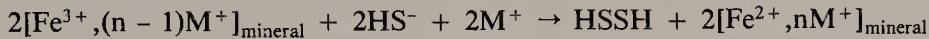
System	Reference	Proposed Surface Site
Sheet Silicates:		
O ₂	(21) White and Yee, 1985	not proposed
H ₂ O ₂	(7) Farmer et al., 1971 (8) Veith and Jackson, 1974 (22) Amonette et al., 1985	interlayer not proposed interlayer
HOCl	(22) Amonette et al., 1985	not proposed
Br ₂ , HOBr	(7) Farmer et al., 1971 (22) Amonette et al., 1985	interlayer interlayer
Fe ³⁺	(21) White and Yee, 1985 (24) Graf von Reichenbach and Beyme, 1988	not proposed interlayer
Cu ²⁺	(23) Sayin, 1982	interlayer
HCA	This chapter	interlayer
CTET, HCA (with HS ⁻)	This chapter	edges? iron sulfide precipitates?
Pyrite:		
O ₂	(25) Singer and Stumm, 1970 (26) Goldhaber, 1983 (28) McKibben and Barnes, 1986 (10) Moses et al., 1987 (29) Nicholson et al., 1988	indirect oxidant ^a sulfur sites not proposed indirect oxidant ^a sulfur sites
H ₂ O ₂	(28) McKibben and Barnes, 1986	not proposed
Fe ³⁺	(25) Singer and Stumm, 1970 (27) Wiersma and Rimstidt, 1984 (28) McKibben and Barnes, 1986 (10) Moses et al., 1987	sulfur sites not proposed edges, pits, defects sulfur sites
Pd ²⁺	(31) Hyland and Bancroft, 1990 (32) Bancroft and Hyland, 1990	sulfur sites; edges, pits, defects same
Electrochemical	(30) Mycroft et al., 1990	sulfur sites
OCI ⁻	(12) Umaña, 1979	sulfur sites
CTET	This chapter	not proposed

^aOxygen acts to oxidize Fe²⁺ to Fe³⁺, and the Fe³⁺ sustains pyrite oxidation.

The stoichiometry of this reaction is difficult to verify because we can not measure iron speciation accurately enough. The addition of sulfide to the biotite and vermiculite systems made the reactions much faster; the transformation rate of HCA in the presence of HS⁻ and biotite or vermiculite increased by more than an order of magnitude over the rate observed in the absence of HS⁻. The sheet silicate surfaces with sulfide increased the transformation rate compared to that of HCA in solution with sulfide by approximately an order

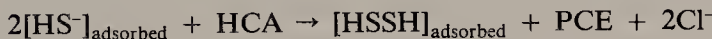
of magnitude. In homogeneous solution there was an absence of significant reaction between the haloaliphatics and HS^- , suggesting that the reaction with HS^- is heterogeneous. Although the exact mechanism is not known, it appears that HS^- can influence the reaction rate in the following three ways:

1. HS^- can regenerate Fe(II) sites, in particular the most accessible ones, as shown in the reaction



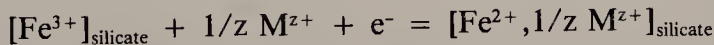
where HSSH is a disulfide which can become further oxidized to polysulfides and sulfate.

2. HS^- can transfer electrons to the haloaliphatic via a surface reaction which does not include surface or structural ferrous iron according to the reaction



3. HS^- can react with ferrous iron which has dissolved from the minerals to form an iron sulfide precipitate. This iron sulfide precipitate can act as an electron donor, as was shown for CTET using iron sulfide minerals.

Our data do not allow us to evaluate which of the above mechanisms is most likely. In order to look for analogies, we have summarized the literature which discusses oxidation of ferrous iron in sheet silicates. Oxidation of structural ferrous iron can occur while the iron remains in the sheet silicate lattice. In 1985, White and Yee showed that the oxidation of structural ferrous iron in augite, biotite, and hornblende by either ferric iron or oxygen was a surface reaction.²¹ Electron transfer occurred between structural ferrous iron and the aqueous oxidants. In experiments with ${}^{59}\text{Fe}^{3+}_{\text{aq}}$ as the oxidant, White and Yee observed that the ${}^{59}\text{Fe}^{3+}_{\text{aq}}$ was reduced to ${}^{59}\text{Fe}^{2+}$, which remained in solution.²¹ Thus, the reaction could not be explained by dissolution of structural Fe^{2+} and subsequent oxidation in solution. In addition, they bracketed the standard potential for the reduction of ferric iron silicates to be between +0.33 and 0.52 V, according to the reaction:



since the standard electrode potential for the reduction of ferric iron in solution is +0.77 V, ferrous iron in the silicates is a stronger reductant than ferrous iron in solution. Because the standard potential of iron in the silicates is lower than iron in solution, the reduction of HCA by biotite and vermiculite is thermodynamically more favorable than the reduction in solution.

The interlayers of sheet silicates are the suggested site for oxidants which react with ferrous iron in the octahedral layers. Amonette et al. studied the effectiveness of H_2O_2 , Br_2 (and HOBr), and OCl^- as oxidants of ferrous iron in biotite.²² When the biotite was expanded by pretreatment with sodium tetraphenylborate (NaBPh_4), hydrogen peroxide (H_2O_2) and bromine (Br_2) oxidized more of the ferrous iron more quickly than without the NaBPh_4 .

pretreatment. The Br_2 experiments were conducted at low pH, which could have induced dissolution and dehydroxylation of the mica. The relative effects of H_2O_2 and Br_2 were not conclusive because of the low pH of the Br_2 solution, decomposition of H_2O_2 , and interactions with NaBPh_4 . Hypochlorite (OCl^-), on the other hand, was an ineffective oxidant whether or not the biotite was expanded. The ineffectiveness of OCl^- as an oxidant of biotite may be due to anion exclusion of OCl^- from the interlayers.²² Their work suggests that the interlayers are the preferred site for the oxidation of biotite. In our experiments the oxidant is hydrophobic and will not undergo site-specific adsorption. However, vermiculite can absorb organic liquids in its interlayers,⁶ suggesting that the haloaliphatics could adsorb in the interlayers.

Transition metal cations exchanged within the interlayers may also promote oxidation of structural metal cations. Cupric ions (Cu^{2+}) can catalyze the oxidation of structural Fe^{2+} in vermiculitized biotite.²³ Since cuprous ions (Cu^{1+}) are not stable under oxic conditions, Sayin proposed that Cu^{2+} in the interlayer position oxidizes the Fe^{2+} to Fe^{3+} , and the Cu^{1+} is subsequently oxidized by O_2 to form Cu^{2+} . In this reaction scheme, Cu^{2+} acts as a catalyst since the Cu^{2+} concentration is regenerated. In experiments conducted at pH = 2.8 and at a fixed $\text{Fe}^{2+}_{\text{aq}}/\text{Fe}^{3+}_{\text{aq}}$ activity ratio, the oxidation rate of structural Fe^{2+} by Fe^{3+} was closely related to the cation exchange rate of Fe^{3+} into the interlayer exchange sites.²⁴ The rate of oxidation increased at higher redox potentials because (1) the Fe^{3+} activity in solution was higher, and (2) Fe^{3+} preferentially adsorbs in the interlayer positions relative to Fe^{2+} . Therefore, an increase in redox potential causes an increase in interlayer Fe^{3+} , which promotes structural Fe^{2+} oxidation. These studies show that the interlayers provide a favorable environment for electron transfer, and the electron transfer can occur across the sheet silicate lattice.

The studies reviewed above suggest that the oxidation of structural Fe^{2+} in sheet silicates by inorganic oxidants probably occurs by the following reaction sequence:

1. exchange of the oxidants into the interlayers
2. electron transfer across the octahedral oxygen or hydroxyl
3. release of a cation or proton to maintain the charge balance in the mineral.

Using the above studies as an analog, it seems possible that in systems without HS^- , HCA diffuses into the interlayers before it can undergo electron transfer. In systems with HS^- , the HS^- will be adsorbed to the Al-OH and Mg-OH edge sites, and excluded from the interlayers. The accessibility of HS^- at the edges is a possible cause of the increased reaction rate of the haloaliphatics in the presence of HS^- and sheet silicates as compared with the sheet silicates alone. The reactivity of pyrite and marcasite with CTET suggest that if iron sulfide precipitates are forming in the sheet silicate systems, these secondary minerals may also be reacting with CTET.

Oxidation of Pyrite

The experiments with pyrite and marcasite showed that CTET can be reduced by iron sulfide surfaces, but the mechanism of electron transfer is unknown. Inferences may be possible from studies involving aqueous pyrite oxidation by oxygen and metal ions. In the initial work by Singer and Stumm, a pyrite oxidation model was proposed in which ferric iron was the direct oxidant of pyrite.²⁵ The reduced Fe(II) was recycled (reoxidized) to Fe(III) by molecular oxygen, which further propagated pyrite oxidation. In abiotic systems, the rate limiting step is the oxidation of Fe(II) by oxygen.⁹ Goldhaber,²⁶ Wiersma and Rimstidt,²⁷ McKibben and Barnes,²⁸ Moses et al.,¹⁰ and Nicholson et al.²⁹ all suggest that abiotic pyrite oxidation is controlled by a surface process. McKibben and Barnes' SEM micrographs of cleaned pyrite and oxidized pyrite indicated that pyrite oxidation occurred at edges, corners, and other defects (high energy sites).²⁸ If oxidation occurs at defects, then the oxidation rates will be very sensitive to mineral pretreatment.

Measurements of aqueous pyrite oxidation intermediates and consideration of molecular orbital theory have led to a better understanding of the mechanism for pyrite oxidation. X-ray photoelectron spectroscopy (XPS) was used to study electrochemical oxidation of pyrite, and galena and sphalerite oxidation by palladium(I) and gold(III).^{30,31} XPS analysis of the oxidized metal sulfides showed the formation of polysulfides at the surface but did not provide evidence of S-O species formation.^{31,32} Bancroft and coworkers also used in situ Raman spectroscopy to study pyrite oxidation upon electrochemical oxidation.³² Their data show strong evidence for polysulfide and elemental sulfur formation. Sulfate was observed in solution in all of these experiments, but no evidence of sulfoxyl species were observed on the mineral surfaces.^{31,32} These studies show that metal sulfide S is the primary electron donor and that metal sulfide oxidation occurs via formation of polysulfide intermediates on the mineral surface.

Moses et al. studied pyrite oxidation by ferric iron and oxygen by measuring aqueous intermediates and products of sulfide oxidation.¹⁰ Since thiosulfate ($S_2O_3^{2-}$) was a significant aqueous intermediate, it was suggested that the Fe-S bond must break before the S-S bond. Luther's molecular orbital analysis indicates that if Fe^{3+}_{aq} loses a hydroxyl group, it can bind to the sulfur in FeS_2 and strengthen the S-S bond by forming a Fe-S-S-Fe bridge.³³ Molecular oxygen, on the other hand, cannot form a strong bond to FeS_2 because O_2 bonding to FeS_2 strengthens the S-S bond while weakening the O-O bond. Ferric iron is expected to be a more likely oxidant than O_2 .

With these considerations, Moses et al.¹⁰ expanded the Singer and Stumm²⁵ pyrite oxidation model to include the transfer of the hydroxyl radical to pyrite S upon adsorption of Fe^{3+}_{aq} . A sequence of hydroxylation of sulfide groups is proposed to occur until the Fe-S bond is weakened and thiosulfate is released to solution. Since CTET is similar to oxygen in that it is hydrophobic and paramagnetic, it would seem possible that CTET could act as an indirect

oxidant like molecular oxygen. However, oxygen sustains pyrite oxidation by reoxidizing ferrous iron to ferric iron. We have shown that CTET and ferrous iron react much more slowly than CTET and pyrite, making this mechanism unlikely. CTET most likely acts as a direct oxidant of iron sulfide surfaces, although the mechanism of this oxidation remains to be investigated.

SUMMARY AND CONCLUSIONS

We have studied some of the environmental factors which affect the abiotic fate of chlorinated hydrocarbons under simulated groundwater conditions. Specifically, we have studied the capability of biotite, vermiculite, pyrite, and marcasite to promote the transformation of HCA and CTET. In all systems studied, the rate of disappearance of 1 μM CTET and HCA was fitted to a first-order model with respect to substrate concentration. Addition of 4 mM sulfide to sheet silicate (38 g/L) systems increased the transformation rate of HCA and CTET by approximately an order of magnitude compared with the rates in solution with sulfide. The literature on oxidation of sheet silicates by Fe^{3+} , H_2O_2 , Br_2 , and Cu^{2+} suggests that the interlayers are the most likely location for electron transfer to occur. We suspect that HCA oxidation by biotite and vermiculite also occurs in the interlayers. Since HS^- is probably excluded from sorption in the interlayers, the rate increase observed upon HS^- addition is likely due to surface complexes formed at the edges of the silicates or from secondary formation of iron sulfide minerals.

Iron sulfide particles (18 g/L) significantly increased the rate of CTET degradation above the rate observed in sulfide or ferrous iron solutions. The reaction rates were measured at 50°C, but transformation rates may be appreciable relative to groundwater residence times. Using O_2 and Fe^{3+} as analogs for CTET, it is suggested that CTET acts as a direct oxidant of the pyrite surface. In light of the significance of CTET and halogenated hydrocarbons as environmental contaminants, further research to better understand the mechanistic details of heterogeneous transformation processes is essential.

ACKNOWLEDGMENT

This work was supported by the R. S. Kerr Environmental Research Laboratory of the U.S. Environmental Protection Agency through Agreement CR 814823 (Stephen R. Hutchins, project officer) with Stanford University. This publication has not been subjected to the EPA's peer and administrative review and therefore does not necessarily reflect the views of the EPA, and no official endorsement should be inferred.

REFERENCES

1. Daley, P. S. "Cleaning Up Sites with On-Site Process Plants," *Environ. Sci. Technol.* 23:912-916 (1989).
2. Criddle, C. S., P. L. McCarty, M. C. Elliot, and J. F. Barker. "Reduction of Hexachloroethane to Tetrachloroethylene in Groundwater," *J. Contam. Hydrol.* 1:133-142 (1986).
3. Jafvert, C. T., and N. L. Wolfe. "Degradation of Selected Halogenated Ethanes in Anoxic Sediment-Water Systems," *Environ. Toxicol. Chem.* 6:827-837 (1987).
4. Curtis, G. P. "Reductive Dehalogenation of Hexachloroethane and Carbon Tetrachloride by Aquifer Sand and Humic Acid," PhD Thesis, Stanford University, Stanford, CA (1991).
5. Stumm, W., and J. J. Morgan. *Aquatic Chemistry* (New York: John Wiley and Sons, 1981).
6. Deer, W. A., R. A. Howie, and J. Zussman. *An Introduction to the Rock Forming Minerals* (Essex, England: Longman Group Limited, 1982).
7. Farmer, V. C., J. D. Russell, W. J. McHardy, A. C. D. Newman, J. L. Ahlrichs, and J. Y. H. Rimsaite. "Evidence for Loss of Protons and Octahedral Iron from Oxidized Biotites and Vermiculites," *Mineral. Mag.* 38:121-137 (1971).
8. Veith, J. A., and M. L. Jackson. "Iron Oxidation and Reduction Effects on Structural Hydroxyl and Layer Charge in Aqueous Suspensions of Micaceous Vermiculites," *Clays Clay Min.* 22:345-353 (1974).
9. Nordstrom, D. K. "Aqueous Pyrite Oxidation and the Consequent Formation of Secondary Iron Minerals," in *Acid Sulfate Weathering*, L. R. Hossaer, J. A. Kittrick, and D. F. Faming, Eds. (Madison, WI: Soil Science Society of America, 1982).
10. Moses, C. O., D. K. Nordstrom, J. S. Herman, and A. L. Mills. "Aqueous Pyrite Oxidation by Dissolved Oxygen and by Ferric Iron," *Geochim. Cosmochim. Acta* 51:1561-1571 (1987).
11. Katser, R. P., and V. M. Ropot. "A Study of Hydrosulfide Ion Sorption on Natural Sorbents," *Khim. Teckhnol. Vody*. 8:81-82 (1986).
12. Umaña, A. F. "Kinetics of Oxidative Dissolution of Pyrite by Aqueous Chlorine Species," PhD Dissertation, Department of Civil Engineering, Stanford University, Stanford, CA (1979).
13. Barlash, J. E., and M. Reinhard. "Abiotic Dehalogenation of 1,2-Dichloroethane and 1,2-Dibromoethane in Aqueous Solution Containing Hydrogen Sulfide," *Environ. Sci. Technol.* 23:1349-1358 (1989).
14. Millero, F. J. "The Thermodynamics and Kinetics of the Hydrogen Sulfide System in Natural Waters," *Mar. Chem.* 18:121-147 (1986).
15. Papelis, C., K. F. Hayes, and J. O. Leckie. "HYDRAQL: A Program for the Computation of Chemical Equilibrium Composition of Aqueous Batch Systems Including Surface-Complexation Modeling of Ion Adsorption at the Oxide/Solution Interface," Department of Civil Engineering Tech. Report No. 306, Stanford University, Stanford, CA (1988).
16. Jeffers, P. M., L. M. Ward, L. M. Woytowitch, and N. L. Wolfe. "Homogeneous Hydrolysis Rate Constants for Selected Chlorinated Methanes, Ethanes, Ethenes, and Propanes," *Environ. Sci. Technol.* 23:965-969 (1989).
17. Jørgensen, B. B. "The Sulfur Cycle of a Coastal Marine Sediment (Limfjorden, Denmark)," *Limnol. Oceanogr.* 22:814-832 (1977).

18. Kriegman, M. R. "The Sulfur Redox System in a Salt Marsh, Tuckerton Meadows, NJ," BSE Thesis, Princeton University, Princeton, NJ (1985).
19. Swider, K. T., and J. E. Mackin. "Transformations of Sulfur Compounds in Marsh-Flat Sediments," *Geochim. Cosmochim. Acta* 53:2311-2323 (1989).
20. Criddle, C. S. "Reductive Dehalogenation in Microbial and Electrolytic Model Systems," PhD Thesis, Stanford University, Stanford, CA (1989).
21. White, A. F., and A. Yee. "Aqueous Oxidation-Reduction Kinetics Associated with Coupled Electron-Cation Transfer from Iron-Containing Silicates at 25°C," *Geochim. Cosmochim. Acta* 49:1263-1275 (1985).
22. Amonette, J., F. T. Ismail, and A. D. Scott. "Oxidation of Biotite by Different Oxidizing Solutions at Room Temperature," *Soil Sci. Soc. Am. J.* 49:772-777 (1985).
23. Sayin, M. "Catalytic Action of Copper on the Oxidation of Structural Iron in Vermiculitized Biotite," *Clays Clay Min.* 30:287-290 (1982).
24. Graf von Reichenbach, H., and B. Beyme. "Oxidation of Structural Ferrous Iron in Vermiculites: 1. Oxidation by Fe^{3+} ," *Clay Min.* 23:261-270 (1988).
25. Singer, P. C., and W. Stumm. "Acid Mine Drainage—The Rate Limiting Step," *Science* 167:1121-1123 (1970).
26. Goldhaber, M. B. "Experimental Study of Metastable Sulfur Oxyanion Formation During Pyrite Oxidation at pH 6-9 and 30°C," *Am. J. Sci.* 283:193-217 (1983).
27. Wiersma, C. L., and J. D. Rimstidt. "Rates of Reaction of Pyrite and Marcasite with Ferric Iron at pH 2," *Geochim. Cosmochim. Acta* 48:85-92 (1984).
28. McKibben, M. A., and H. L. Barnes. "Oxidation of Pyrite in Low Temperature Acidic Solutions: Rate Laws and Surface Textures," *Geochim. Cosmochim. Acta* 50:1509-1520 (1986).
29. Nicholson, R. V., R. W. Gillham, and E. J. Reardon. "Pyrite Oxidation in Carbonate-Buffered Solution: 1. Experimental Kinetics," *Geochim. Cosmochim. Acta* 52:1077-1085 (1988).
30. Mycroft, J. R., G. M. Bancroft, N. S. McIntyre, J. W. Lorimer, and I. R. Hill. "Detection of Sulphur and Polysulfides on Electrochemically Oxidized Surfaces by X-ray Photoelectron Spectroscopy and Raman Spectroscopy," *J. Electroanalyt. Chem. Interfacial. Electrochem.* 292:139-152 (1990).
31. Hyland, M. M., and G. M. Bancroft. "Palladium Sorption and Reduction on Sulphide Mineral Surfaces: An XPS and AES Study," *Geochim. Cosmochim. Acta* 54:117-130 (1990).
32. Bancroft, G. M., and M. M. Hyland. "Spectroscopic Studies of Adsorption/Reduction Reactions of Aqueous Metal Complexes on Sulphide Surfaces," in *Mineral-Water Interface Geochemistry*, M. F. Hochella and A. F. White, Eds. (Washington, DC: Mineralogical Society of America, 1990), pp. 511-558.
33. Luther, G. W., III. "Pyrite Oxidation and Reduction: Molecular Orbital Theory Considerations," *Geochim. Cosmochim. Acta* 51:3193-3199 (1987).

CHAPTER 17

The Effect of pH and Anions on the Solubility and Sorption Behavior of Acridine

Robert A. Matzner, Douglas R. Hunter, and Roger C. Bales

INTRODUCTION

A better understanding of the mechanisms controlling the sorption of hydrophobic ionizable organic compounds (HIOCs) is needed to improve our ability to evaluate and model the fate of these compounds in natural waters. The class of HIOCs contains many compounds of environmental concern, including phenols, anilines, and nitrogen-heterocyclic compounds. Acridine and quinoline are nitrogen-heterocyclic compounds that have been found in groundwater contaminated with wastes from wood-treatment processes.¹ They are also present in high boiling point petroleum distillates and constitute a substantial fraction of shale oil, coal tar, and coal liquefaction products.²⁻⁵ Both compounds are weak bases (Table 17.1) whose aqueous solubility is a function of pH.

The sorption of acridine to soils and sediments increases with the organic carbon content of the soil.⁶ Quinoline sorption to subsurface materials is dominated by ion exchange of the quinolinium ion even at pH values two units above the compound's pK_a .⁷ Weak solvophobic forces are thought to be responsible for adsorption of the neutral molecule, with Ca^{2+} competing with quinolinium for exchange sites. Similar results are found for acridine and pyridine, with acridine sorption the greatest, then quinoline, and finally, pyridine.⁸ The greater acridine cation sorption is attributed to increased van der Waals interactions and increased delocalization of acridinium's positive charge. Quinolinium sorption is observed to release H^+ in a 1:1 ratio up to a limiting surface density, after which more quinolinium is adsorbed than H^+ is released.⁹ The maximum sorption of quinoline to amorphous silica occurs near the compound's pK_a .¹⁰ The increase in deprotonated surface-hydroxyl groups with increasing pH has no apparent effect on sorption. The small effect of electrolyte composition and ionic strength suggests that surface complexes are either strong and inner sphere or are dominated by interactions with neutral sites where competition with electrolyte cations is minimal. Hydrogen bonding

Table 17.1. Selected Properties of Quinoline and Acridine

Compound	Structure	MW	mp (°C)	bp (°C)	solubility (mM)	K _{ow}	pK _a
quinoline		129.2	-15	238	46.4 ^a	~110 ^a	4.9 ^a
acridine		179.2	107-110	346	0.320 ^b 0.214 ^c	2500 ^b 4200 ^c	5.6 ^b

^aFrom Zachara et al.⁸^bFrom Albert.¹¹^cFrom Banwart et al.⁶

is the apparent sorption mechanism for the neutral molecule, and ion exchange for the cation.

The purpose of the work described here was to determine the effects of anion type and concentration on the aqueous solubility of acridine and quinoline. The effect of anion type and concentration, pH, average interstitial velocity (μ_e), and solute concentration (C_0) on the rate and extent of acridine sorption were also investigated. Silica was chosen as the sorbent due to its well-defined surface properties and because it is a common constituent of soil materials.

METHODS AND MATERIALS

Aqueous batch experiments were used to study the aqueous solubility of quinoline and acridine. The sorption of acridine onto silica was then investigated in continuous-flow column experiments; the primary variables were anion type (phosphate, bicarbonate), solute concentration (5.58 nM, 55.8 nM), average interstitial velocity (0.136, 0.058 cm/sec), and pH (4.0 and 7.0) of the system.

Solubility Experiments

Batch experiments with acridine were performed over a pH range of 2 to 8 with three different buffers (phosphate, phosphate-acetate, phthalate). Quinoline batch experiments were performed with a phosphate-citrate buffer over a pH range of 4.6 to 8.2. Solutions containing the desired buffer concentration were prepared in glass vials with distilled-deionized water and then saturated by adding solid acridine or quinoline. Using a rotating rack, the solutions were agitated for a minimum of 24 hr, or until equilibration was reached. After equilibration, the pH of each vial was measured, and the vials were centrifuged for 15-25 min at ca. 2400 RCF (Relative Centrifugal Field) and the supernatant removed. Dilutions of the supernatant were made and then analyzed using high-performance liquid chromatography (HPLC).

The octanol batch experiments were run by saturating octanol with acridine in a glass vial. One batch experiment was run with a saturated solution of phosphate in octanol. The remainder of the procedure was the same as for the aqueous batch experiments.

The solubility of acridine at pH 4 and in the presence of 2 and 10 μM phosphate at pH 6 and 8 was measured using a pH stat. A jacketed beaker with a circulating temperature bath was used to maintain the temperature of the solution at 25°C. The solutions were agitated slowly using a magnetic stir bar, and an N₂ atmosphere maintained. For the pH 6 and 8 experiments, a buffer solution was placed in the reaction beaker and saturated with acridine. The solution for the pH 4 experiments was prepared by saturating distilled-deionized water with acridine and then adding the desired volume of buffer. Aliquots were taken from the beaker after equilibration and centrifuged. The supernatant was diluted and analyzed using HPLC.

The HPLC assay for acridine consisted of injecting 0.46 cm i.d. 20 μL of the diluted supernatant onto a stainless-steel column (15 cm length \times 0.46 cm i.d.) packed with a C₁-bonded phase (Analytichem International). The mobile phase, a 95% methanol, 5% dichloromethane mixture, was pumped through the column at a rate of 1.2 mL/min. A Schoeffel Instruments model FS970 spectrofluorometer was used for detection and was set at an excitation wavelength of 250 nm. Each dilution was injected five times, and the average was used for the total acridine concentration. Five acridine standards were run to develop the calibration curve each day. Standard solutions, and the stock solution from which they were made, were prepared fresh when the correlation of the calibration curve began to drop significantly.

The quinoline HPLC assay consisted of injecting 20 μL of the dilution onto a fully encapped RSIL C₁₈ HL column (Alltech Associates, Inc.). The mobile-phase, 85% acetonitrile, 5% water, was pumped at a flow rate of 1.0 mL/min. A Kratos Analytical Spectroflow 750 UV detector was used set at 225 nm. The standards and duplicate samples were injected three times. If the difference between the duplicates was greater than 10%, additional samples were analyzed.

Column Experiments

All column experiments were performed with porous unbonded silica (PQ Corporation). The average particle diameter was 125 μm , with an average pore diameter of 20 nm. The silica was washed in a suction filter apparatus, first with methanol, then pentane, then again with methanol. The silica was then rinsed twice with HCl (1.0 M) and once with distilled-deionized water and dried overnight at 105°C. The resultant porosity of the packed columns was between 0.83 and 0.85, with dry bulk densities of 0.34 to 0.37 g/cm³, respectively.

The acridine-free solution (1 mM Na₂HPO₄ or NaHCO₃, 10 mM KClO₄ or NaCl) was pumped through the column until a stable conductivity reading was

achieved. The acridine-containing solution (5.58 nM or 55.8 nM acridine, 1 mM Na₂HPO₄ or NaHCO₃, 20 mM KClO₄ or NaCl) was then pumped at a constant flow rate through the column until the detector response equaled that of the influent solution. The column was then flushed with the acridine-free solution until the initial baseline of the solute detector was achieved. The solutions and column were equilibrated at the experimental temperature (25°C) at least one day prior to the experiment. The solutions were prepared in distilled-deionized water and were degassed with N₂ prior to and during the experiments. The effluent flow rate was measured continuously during the experiment. The column apparatus (Figure 17.1) consisted of a packed stainless-steel column (0.46 cm i.d. by 5.0 cm length); glass solution reservoirs and appropriate valves located in a thermostatted chamber; HPLC pumps (Beckman 110A); and a flow-through conductivity meter (Wescan 213505), fluorometer (Schoeffel Instruments FS970), and pH electrode cell for the continuous detection of the conservative tracer and solute concentrations, and pH, respectively.

RESULTS

Solubility

Acridine solubility was independent of buffer type and concentration at pH's above the pK_a (5.6) (Figure 17.2.a-c). The apparent solubility of acridine increased with pH until the formation of a precipitate when the phosphate or phosphate-acetate buffer concentration reached 10 mM. The decrease in apparent acridine solubility when the buffer concentration was changed from 10 mM to 100 mM was about one order of magnitude. The solubility of quinoline (Figure 17.2d) showed no dependence on phosphate-citrate concentration.

The acridine-octanol solubility was 0.895 M. The solubility of acridine in octanol saturated with phosphate was slightly lower, 0.856 M. A K_{ow} value was calculated for each pH and buffer by dividing the apparent acridine solubility by the octanol solubility. The values ranged from 3600 to 80, decreasing with pH.

Column Experiments

Column experiments with acridine were performed at pH 7 and 4 with phosphate and bicarbonate as anions. Two conservative tracers, NaCl and KClO₄, were used to investigate the effect of Cl⁻ and ClO₄⁻ on acridine sorption. Acridine sorption was less at pH 7 than at pH 4. The results for all 12 column experiments are listed in Table 17.2.

Experiments 1, 5, 9, and 11 (Figure 17.3) show the results of changing C₀ and μ_e on acridine sorption at pH 7 with a Na₂HPO₄ buffer and NaCl salt

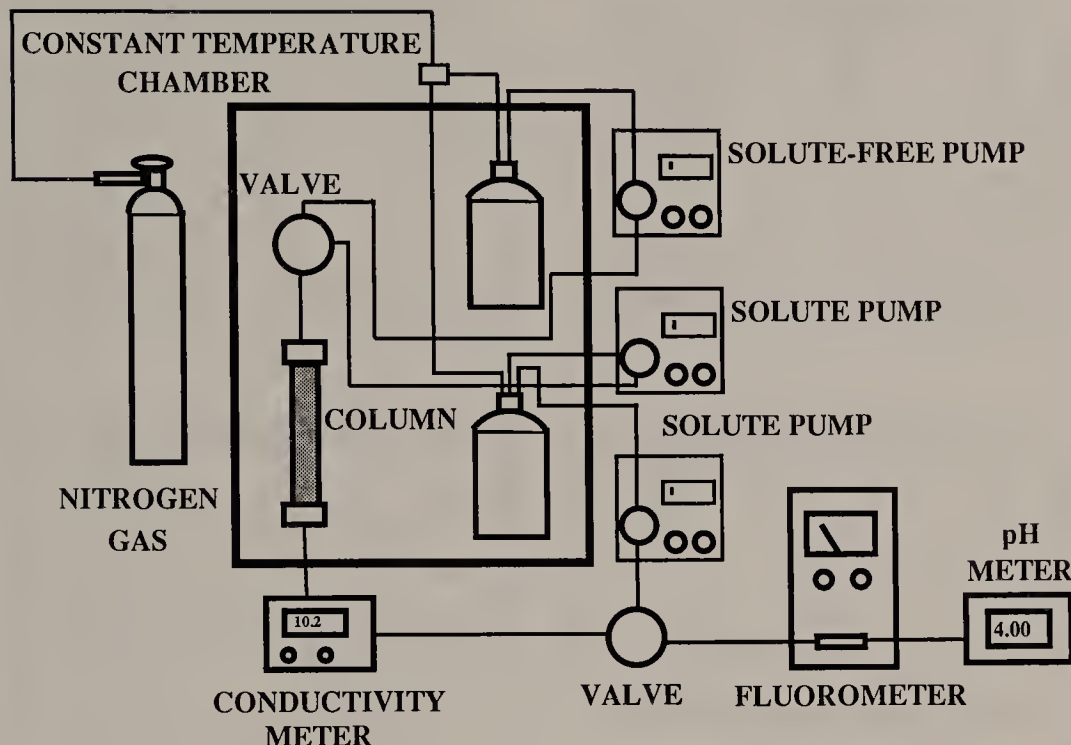


Figure 17.1. Apparatus for column experiments.

tracer. Experiments 1 and 5 were run under the same conditions, but the average of the sorption and desorption K_d 's differed by 4 units, 28 vs 32 cm^3/g . The breakthrough for experiment 5 had more retardation and approached equilibrium slower than did that of experiment 1. The difference in the K_d 's represents variability inherent in the experimental procedure. C_0 was increased by an order of magnitude for experiment 9, with an average K_d of 29 cm^3/g . Experiment 11 was run at about one-half the μ_e of experiments 1, 5, and 11 to investigate the possibility of kinetic effects on acridine sorption. The average K_d for experiment 11 was 30 cm^3/g . The average K_d for all four experiments was $30 \pm 2 \text{ cm}^3/\text{g}$; the changes in C_0 and μ_e had no effect on acridine sorption. The close agreement of the K_d values and the good mass balances (0.98 ± 0.07) indicate the reproducibility of the experimental procedure.

The effects of changes in C_0 and μ_e on acridine sorption at pH 4 were investigated in experiments 2, 10, and 12 (Figure 17.4). Experiment 10 was run under the same conditions as experiment 2 except that C_0 was increased by a factor of 10. The K_d 's were 39 and 40 cm^3/g , respectively. μ_e was reduced by approximately one-half for experiment 12. The K_d for experiment 12 was 45 cm^3/g , compared to 40 cm^3/g for experiment 2. The initial breakthrough of experiments 2 and 12 was identical, but as they approached equilibrium the curve for experiment 12 showed considerably more tailing. However, the desorption tailing for the two experiments was identical, suggesting that the

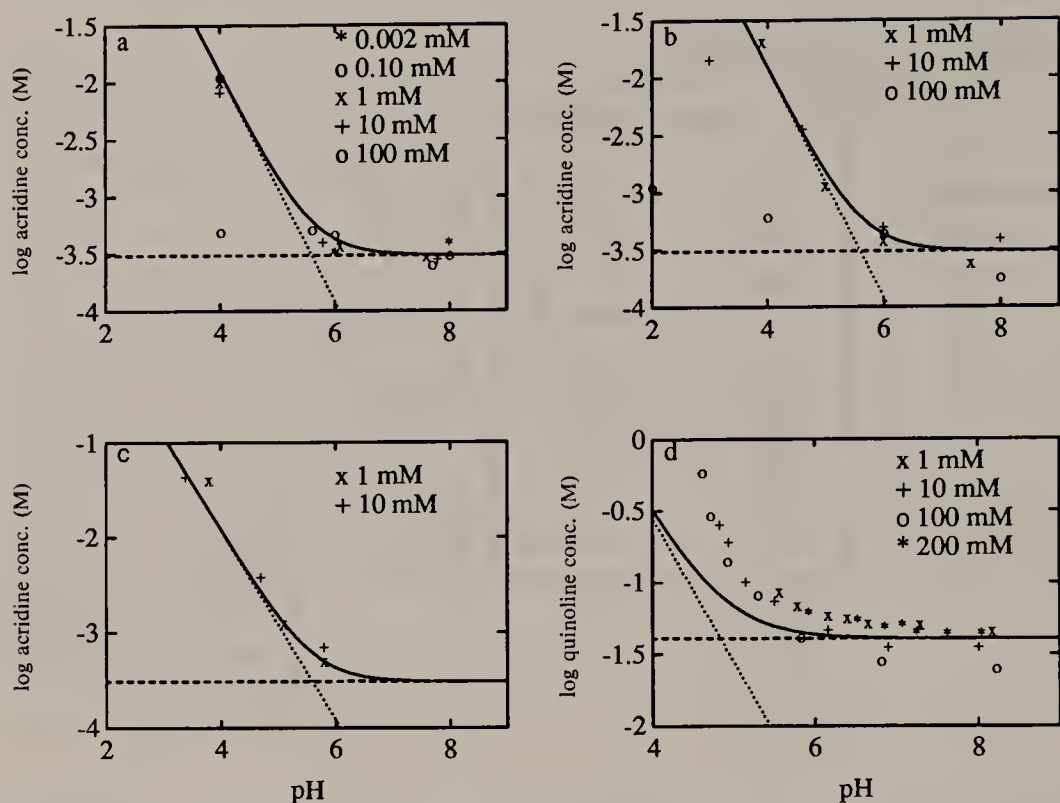


Figure 17.2. Acridine solubility as a function of pH in the presence of different concentrations of (a) phosphate, (b) phosphate-acetate, (c) phthalate; (d) Quinoline solubility in the presence of phosphate-citrate. Dashed lines are neutral compound conc., dotted lines are cation conc., based on Henderson-Hasselbach equation, and the average neutral compound conc. for these experiments; solid line is the sum of the two.

Table 17.2. Experimental Conditions and Mass Balance Results for Breakthrough Curves

Exp.	pH	Buffer	u_e (cm/sec)	Mass Balance ^a	K_d ^b (cm ³ /g)			Pulse ^c
					Sorption	Desorption	Average	
1	7	Na ₂ HPO ₄	0.136	1.08	27.0	29.1	28	50.3
2	4	Na ₂ HPO ₄	0.131	0.90	42.2	37.8	40	84.1
3	7	NaHCO ₃	0.122	0.96	41.6	39.6	41	77.9
4	4	NaHCO ₃	0.121	1.01	42.8	43.1	43	93.0
5	7	Na ₂ HPO ₄	0.120	0.91	33.0	30.0	32	67.5
6	7	NaHCO ₃	0.120	0.93	36.9	34.4	36	51.7
7	4	NaHCO ₃	0.123	1.09	50.0	53.8	52	88.1
8	7	NaHCO ₃	0.125	0.86	30.4	25.9	28	50.3
9	7	Na ₂ HPO ₄	0.123	0.99	29.6	29.3	29	57.5
10	4	Na ₂ HPO ₄	0.122	1.01	36.9	40.5	39	56.6
11	7	Na ₂ HPO ₄	0.057	0.94	31.0	29.1	30	54.1
12	4	Na ₂ HPO ₄	0.058	0.93	46.9	43.8	45	57.0

Note: Acridine concentration = 55.8 nM in experiments 9 and 10, 5.58 nM in all other experiments; KClO₄ used to fix ionic strength in experiments 7 and 8, NaCl in other experiments.

^aRatio of the solute mass desorbed to the solute mass sorbed.

^b K_d from dividing S (mass sorbed, from curves, divided by sorbent mass) by C.

^cPore volumes of solute fed into the column.

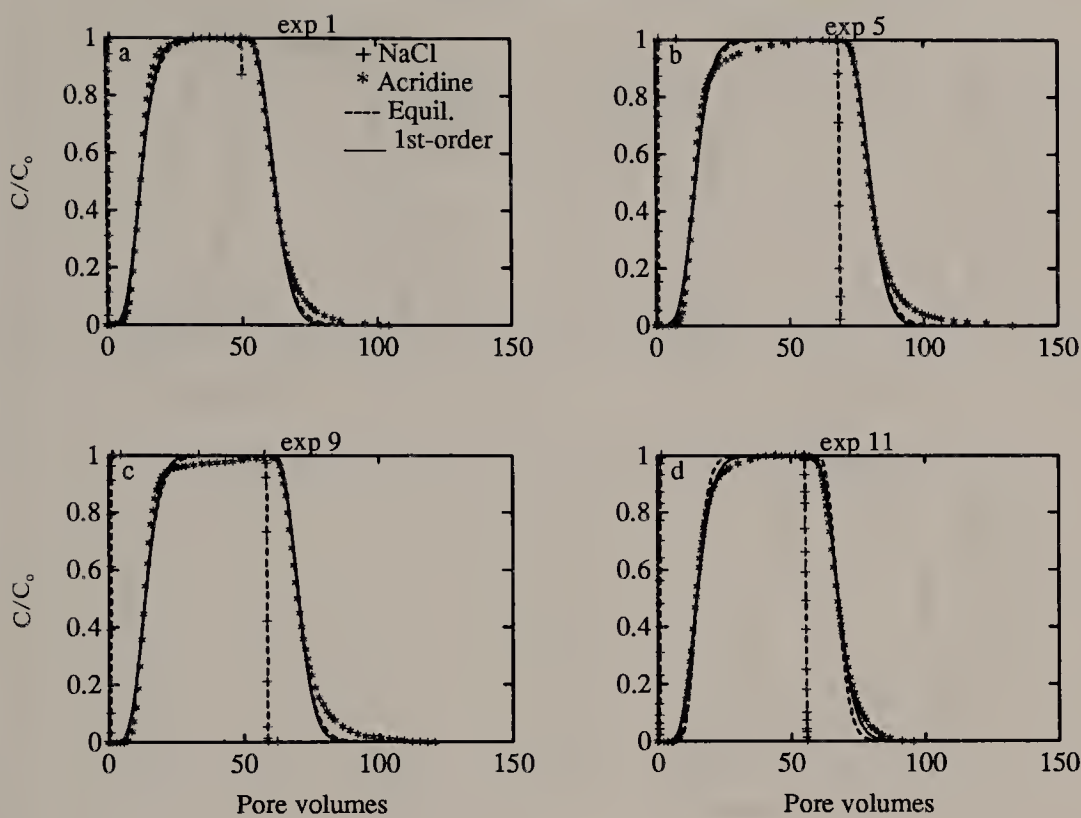


Figure 17.3. Breakthrough curves for salt tracer and acridine at pH 7 and Na_2HPO_4 buffer: (a) experiment 1, (b) experiment 5, (c) experiment 9, (d) experiment 11; conditions noted in Table 17.2.

desorption rates at the two μ_e^3 's were the same. The average K_d for experiments 2, 10, and 12 was $41 \pm 3 \text{ cm}^3/\text{g}$, and the average mass balance was 0.95 ± 0.06 . There is apparently no significant effect on acridine sorption as a result of the changes in C_0 and μ_e . Also, the reproducibility of experiments was good.

The anion was changed for experiments 3, 6, and 8 (Figure 17.5). Experiments 3 and 6 were run under the same conditions, using NaHCO_3 instead of Na_2HPO_4 . The average K_d 's were 41 and $36 \text{ cm}^3/\text{g}$, respectively. The breakthrough curves have similar shapes, but experiment 6 shows slightly less retardation. The average K_d and mass balance for experiments 3 and 6 were $38 \pm 3.5 \text{ cm}^3/\text{g}$ and 0.94 ± 0.02 , respectively. The reproducibility of these experiments was good. Experiment 8 was run with a KClO_4 tracer instead of NaCl . The average K_d for experiment 8 was lower, $28 \text{ cm}^3/\text{g}$, close to the average for the phosphate-buffered experiments.

Experiments 4 and 7 investigated the effect of different anions at pH 4. The average K_d for experiment 4 ($43 \text{ cm}^3/\text{g}$) was similar to that when phosphate was used ($41 \pm 3 \text{ cm}^3/\text{g}$) (Figures 17.6a and b). However, in experiment 7, when both bicarbonate and KClO_4 were used instead of phosphate and NaCl , the K_d was much larger, 52 vs $41 \pm 3 \text{ cm}^3/\text{g}$.

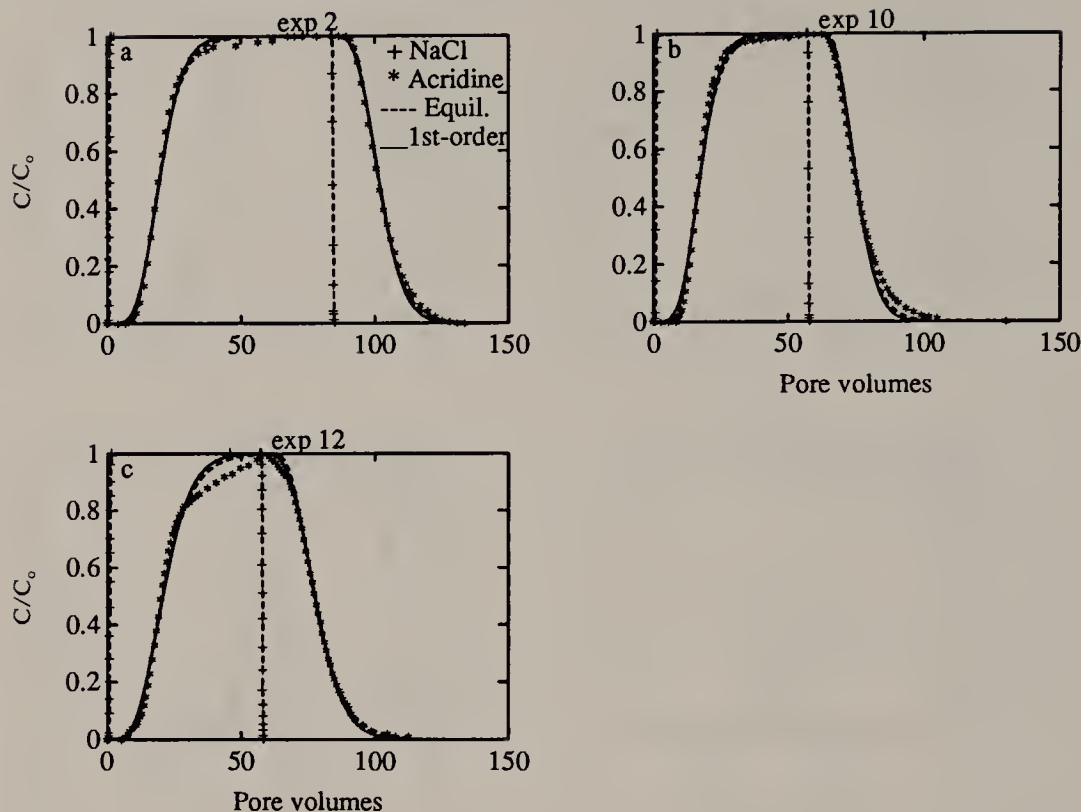


Figure 17.4. Breakthrough curves for salt tracer and acridine at pH 4 and Na_2HPO_4 buffer: (a) experiment 2, (b) experiment 10, (c) experiment 12; conditions noted in Table 17.2.

Comparison of the sorption and desorption limbs for each experiment indicates that the breakthrough curves are not mirror images. In experiment 1 (pH 7), 39.4 pore volumes were required during solute desorption to reduce the dimensionless concentration (C/C_0) from 0.5 to <0.01 . By comparison, only 23.1 pore volumes were required during solute sorption to increase C/C_0 from 0.5 to >0.99 . This trend of more pore volumes required for desorption than sorption was also observed in the other pH 7 experiments (experiments 3, 5, 6, 8, and 11). In direct contrast to the pH 7 results, the breakthrough data for experiment 2 (pH 4) show that only 30.3 pore volumes were required during desorption to reduce C/C_0 from 0.5 to <0.01 , compared to 48.2 pore volumes required during sorption to increase C/C_0 from 0.5 to >0.99 . Experiment 12 (pH 4) displayed similar behavior.

Sorption and desorption partition coefficients for each of the 12 experiments agreed well (Table 17.2). The average K_d value for acridine sorption in all 7 experiments at pH 7 was $32.8 \pm 5.0 \text{ cm}^3/\text{g}$, compared to the average desorption K_d of $31.1 \pm 4.5 \text{ cm}^3/\text{g}$. At pH 4, the average sorption K_d in all five experiments ($43.8 \pm 5.0 \text{ cm}^3/\text{g}$) was identical to the average desorption value ($43.8 \pm 6.1 \text{ cm}^3/\text{g}$).

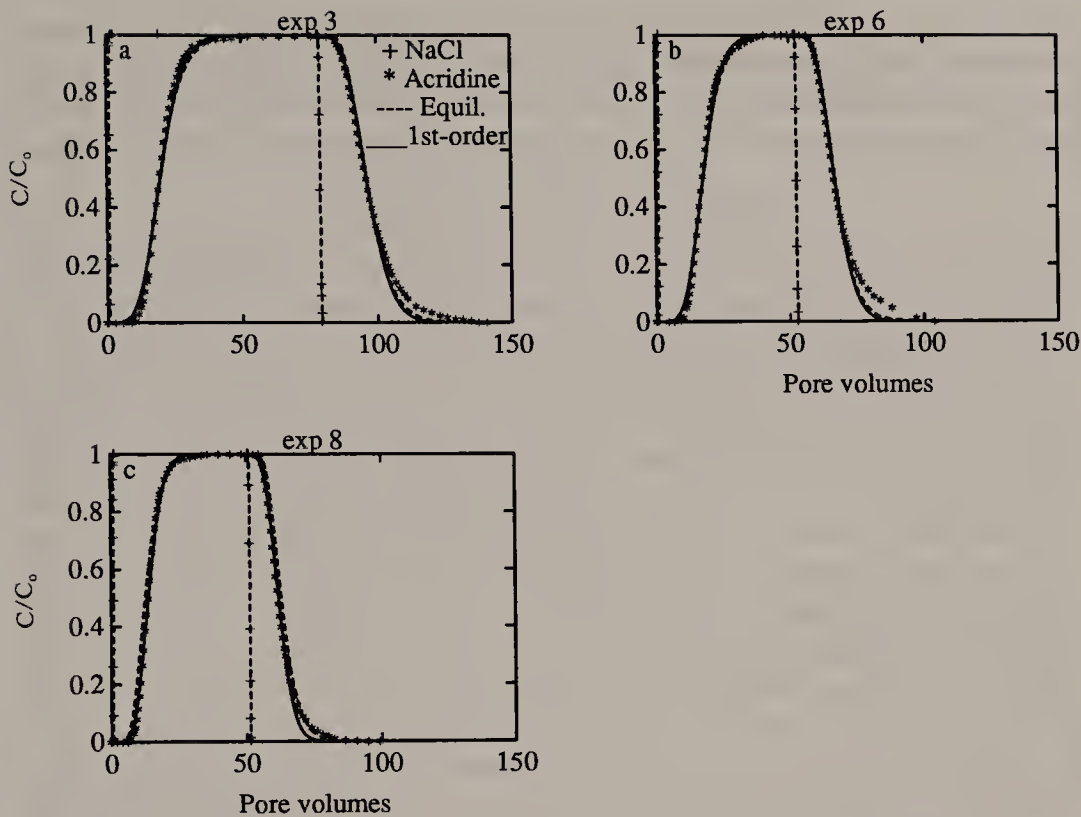


Figure 17.5. Breakthrough curves for salt tracer and acridine at pH 7 and NaHCO_3 buffer: (a) experiment 3, (b) experiment 6, (c) experiment 8; conditions noted in Table 17.2.

DISCUSSION

Acridine Solubility

The average aqueous solubility of neutral acridine was $3.06 \pm 0.06 \times 10^{-4}$ M, based on the phosphate-acridine pH-8 results. The value for the phosphate-

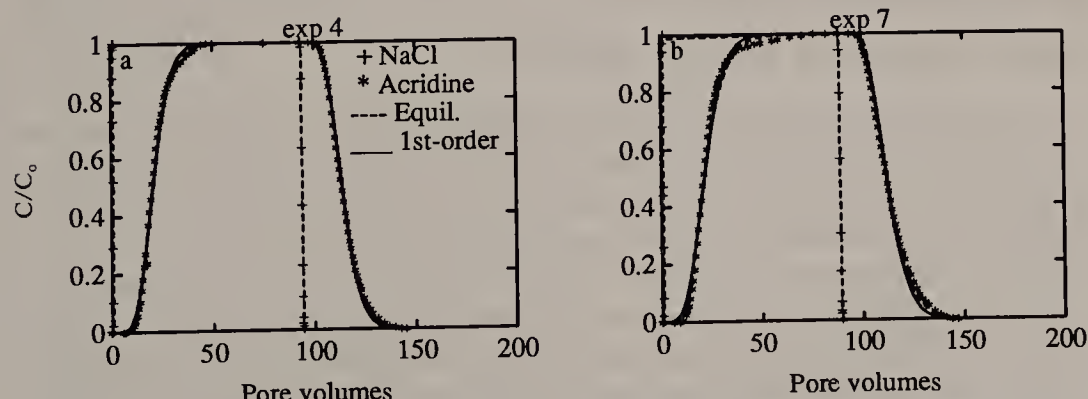


Figure 17.6. Breakthrough curves for salt tracer and acridine at pH 4 and NaHCO_3 buffer: (a) experiment 4, (b) experiment 7; conditions noted in Table 17.2.

acetate-acridine pH-8 results was $2.65 \pm 0.10 \times 10^{-4}$ M. Both of these values are within the range reported previously of 2.14×10^{-4} M and 3.20×10^{-4} M.^{6,11} The predicted increase in total acridine solubility with decreasing pH in Figure 17.2 is in good agreement with the Henderson-Hasselbach equation:

$$\log[AH^+] = pK_a - pH + \log[A] \quad (17.1)$$

where $pK_a = 5.6$ and $\log [A] = -3.51$. The sum of acridinium ($[AH^+]$), acridine ($[A]$) and acridinium-anion complex ($[AH^+L^-]$) gives the total acridine concentration in the aqueous phase.

In the range between pH 8 and pH 5, the observed solubilities for all three buffer concentrations correspond well with the calculated values. As the pH drops below 6.5, acridine solubility depends on both the degree of protonation of the compound and the extent of acridine/buffer complexation. Equation 17.1 accounts for changes in $[AH^+]$ due solely to compound speciation and thus provides no limit on acridine solubility with decreasing pH. Therefore, the maximum solubility of acridine in this system depends, in part, on the solubility of acridinium-anion complexes formed in solution. The deviation from the calculated solubility curve observed for the 1.0 M phosphate and phosphate-acetate results is due to the precipitation of an acridinium-anion salt, resulting in the depletion of all the acridine solid and most of the acridine in solution. There was no apparent decrease in acridine solubility for the acridine-phthalate system, suggesting no precipitate.

Quinoline Solubility

The average aqueous solubility of neutral quinoline was $4.2 \pm 0.8 \times 10^{-2}$ M, based on the phosphate-acetate-quinoline pH-8 and pH-7 results. This is within the range of a previously reported value of 4.6×10^{-2} M.¹⁰ The experimental data do not follow the calculated curve determined from the Henderson-Hasselbach equation ($pK_a = 4.96$). The deviations increase as the pH decreases. This may be a result of changes in the pK_a with changes in the ionic strength of the solutions. A pK_a of 5.55 would be needed to fit the experimental data to Equation 17.1.

Effect of Anions on Sorption Equilibria

The effect of anion type on acridine sorption can be recognized by changes in K_d with variation in anion. Changing electrolyte ($NaCl$ to $KClO_4$) and buffer (Na_2HPO_4 to $NaHCO_3$) together had no effect on K_d at pH 7. The same changes at pH 4 resulted in a 27% increase in K_d . This greater K_d at pH 4 was influenced by the pH of experiment 7 being 4.7 rather than 4.0. The maximum sorption for quinoline to amorphous silica was shown to occur at the pK_a ,¹⁰ so a larger K_d for acridine at pH 4.7 vs pH 4.0 is consistent with the same trend. When changing Na_2HPO_4 to $NaHCO_3$ with an $NaCl$ electrolyte, a 27% increase in K_d resulted at pH 7, but no change in K_d at pH 4.

Hydrogen bonding was probably the dominant acridine sorption mechanism

at pH 7, similar to that suggested for quinoline.¹⁰ Therefore, for the increase in K_d at pH 7 to occur, bicarbonate must have enhanced hydrogen bonding relative to phosphate. Hydrogen bonding can occur at surface hydroxyl groups and/or to water adsorbed to the surface. Phosphate may be a stronger ligand for silanol sites than bicarbonate, thus reducing the number of potential hydrogen bonding sites. The same effect is not observed when KClO_4 replaces NaCl because ClO_4^- interacts with OH sites more readily than Cl^- because of its greater polarizability and more effectively reduces the number of potential hydrogen bonding sites. Steric hindrance may also reduce acridine sorption because ClO_4^- is larger than Cl^- , more effectively blocking adjacent OH sites than Cl^- . It is also possible there is no effect on acridine sorption from bicarbonate, and the larger K_d value is a result of the experimental pH being lower than 7.0, similar to what was observed at pH 4. However, this seems unlikely because the experiment was duplicated when the anomalous results were observed. The results were comparable for the second experiment.

The acridinium-anion ion pair was the dominant species adsorbed at pH 4 because $>\text{SiO}^-$ is a stronger base than acridine. Ion exchange of acridinium with H^+ at $>\text{SiOH}$ sites or adsorption of acridinium at $>\text{SiO}^-$ sites would produce aqueous acridine and $>\text{SiOH}$. Changing Cl^- to ClO_4^- had no effect on K_d because both anions will form ion pairs with acridinium and associate with the surface. There was no effect on acridine adsorption at pH 4 from changing Na_2HPO_4 to NaHCO_3 because their concentration is 20 times less than Cl^- and ClO_4^- . Therefore, ion pairs formed with either buffer would be insignificant compared to those formed with the electrolyte anions. Anion effects on $>\text{SiOH}$ sites at pH 7 were not important at pH 4 because ion pairs may interact with one another at the surface, whereas molecular acridine adsorbs to individual $>\text{SiOH}$ sites.

Advection-Dispersion Model Fits to Breakthrough Curves

The conservative tracer and solute data for each breakthrough curve were modeled using the one-dimensional advection-dispersion equation. For the case of pseudo-first-order, kinetically limited sorption and desorption, the equations are:¹²

$$\theta \frac{\partial C}{\partial t} + \rho_b \frac{\partial S}{\partial t} = \theta D \frac{\partial^2 C}{\partial z^2} - \mu_e \theta \frac{\partial C}{\partial z} \quad (17.2)$$

$$\rho_b \frac{\partial S}{\partial t} = k_f \theta C - \rho_b k_b S \quad (17.3)$$

where C is the aqueous-phase solute concentration ($\mu\text{g}/\text{cm}^3$); S is the sorbed concentration ($\mu\text{g}/\text{g}$); θ is the volume fraction of water; ρ_b is the dry bulk density (g/cm^3) of the porous media; D is the longitudinal hydrodynamic dispersion coefficient (cm^2/sec); μ_e is the average interstitial velocity (cm/sec);

and k_f and k_b are the pseudo-first-order forward and reverse rate coefficients (sec^{-1}), respectively. Dimensionless equations can be defined:

$$\frac{\partial C_1}{\partial T} + (R - 1) \frac{\partial C_2}{\partial T} = \frac{1}{P} \frac{\partial^2 C_1}{\partial Z^2} - \frac{\partial C_1}{\partial Z} \quad (17.4)$$

$$(R - 1) \frac{\partial C_2}{\partial T} = \omega(C_1 - C_2) \quad (17.5)$$

having four parameters, solute pulse, or duration of solute injection (included in boundary condition); retardation factor ($R = 1 + \rho_b K_d / \theta$); Peclet number ($P = \mu_e L / D$); and the dimensionless rate coefficient ($\omega = k_b K_d L \rho_b / \theta \mu_e$). The dimensionless variables are ($Z = z / L$, $T = t u_e / L$, $C_1 = C / C_0$, and $C_2 = S / K_d C_0$, where L is column length and C_0 is the solute concentration in the column inlet). Both the conservative tracer and solute data were first fit assuming local equilibrium (ω large). The solute data were also fit to the first-order model. A nonlinear least-squares method was used for parameter estimation.¹³

The good equilibrium model fits (Table 17.3) to the conservative tracer data with R near 1.0 suggests that most of the pore space is accessible to transport. The sum of squared errors (ssq) was less than 2% in all cases. Allowing the pulse to be fit rather than fixed improved the overall model fits significantly; the difference between observed and fitted pulse values was less than 0.5 pore volumes and is most likely due to small fluctuations in flow velocity during an experiment.

Because of the limited range of velocities in the experiments, five additional NaCl breakthrough curves were run to determine the effect of μ_e on D (0.059 to 0.152 cm/sec). The best-fit equation for the results was

$$D = 0.055 u_e^{1.3} \quad r^2 = 0.99 \quad (17.6)$$

Although the slope of the line is greater than one, it falls within the range of 1.0 to 1.5 observed for a variety of porous particles.¹⁴ A best linear fit gives $D/\mu_e = 0.036$ cm.

D 's estimated from the equilibrium model for acridine (Table 17.3) were an order of magnitude greater than the D values for NaCl (Figure 17.7), suggesting that intraaggregate diffusion or slow sorption and desorption contribute to the apparent dispersion. Diffusion time for the particle size used in this study (0.0125 cm) is on the order of seconds to minutes. In the absence of slow sorption and desorption, the fitted D 's for the salt tracer and acridine should differ only due to their different molecular sizes. The average K_d 's (Table 17.2) agreed well with the equilibrium model values. The average difference for all 12 experiments was 5.6%. The pulse value was fitted by the equilibrium model instead of being fixed. This resulted in an average difference of 2.3% from the experimental values.

Table 17.3. Equilibrium Model Fits to Breakthrough Curves

Exp.	Salt Tracer			ssq ^a	Acridine					
	R	P	D(cm ² /sec)		Pulse ^b	R	P	K _d (cm ³ /g)	D(cm ² /sec)	ssq ^a
<i>Sodium-Phosphate Buffer</i>										
1	1.01	95.5	0.0071	0.001	49.4	12.5	13.5	28	0.050	0.077
2	1.02	83.8	0.0078	0.015	81.9	19.4	14.7	45	0.034	0.018
5	1.01	151	0.0040	0.009	65.4	14.6	17.1	33	0.041	0.100
9	1.02	144	0.0043	0.009	56.6	13.4	17.2	30	0.046	0.110
10	1.01	121	0.0050	0.001	57.7	17.0	14.8	39	0.041	0.009
11	1.02	59.8	0.0048	0.009	52.9	14.4	17.9	33	0.016	0.030
12	1.01	66.5	0.0044	0.008	56.8	20.4	11.7	47	0.025	0.060
<i>Sodium-Bicarbonate Buffer</i>										
3	1.02	126	0.0048	0.019	76.4	18.5	16.3	42	0.037	0.080
4	1.01	117	0.0052	0.002	93.0	20.2	17.6	47	0.034	0.020
6	1.01	186	0.0032	0.006	49.2	17.5	18.4	40	0.033	0.066
7	1.00	108	0.0057	0.003	90.4	21.1	13.5	49	0.046	0.066
8	1.01	222	0.0028	0.008	47.9	13.7	20.7	31	0.030	0.031

^aSum of squared errors.^bPulse value fitted by the model.

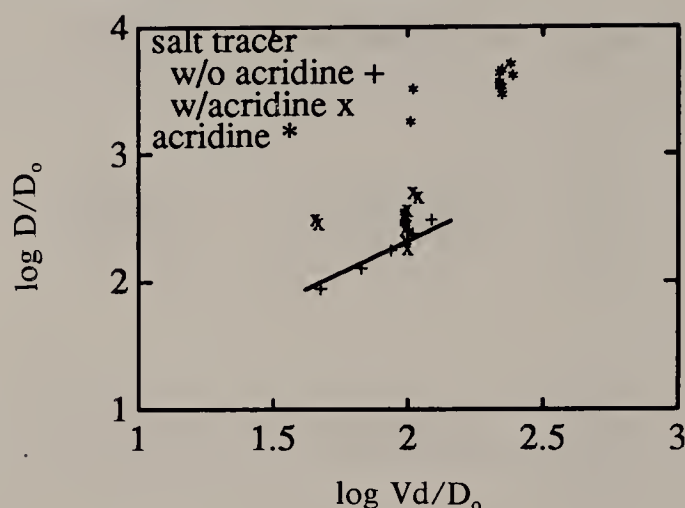


Figure 17.7. Dispersion versus Peclet number for salt tracer and acridine. D values are noted in Table 17.2. $D_0 = 1.55 \times 10^{-5} \text{ cm}^2/\text{sec}$ for NaCl and $6.90 \times 10^{-6} \text{ cm}^2/\text{sec}$ for acridine; $d = 125 \mu\text{m}$; $v (\mu_e)$ values are noted in Table 17.2.

In order to separate slow sorption and desorption from dispersion, an independent estimate of acridine dispersion was made,¹⁵ which is based on an empirical equation^{16,17} that accounts for differences in molecular size. The ratio of the calculated acridine dispersion coefficient to that of sodium chloride was 1.6, suggesting that slow kinetics rather than physical dispersion account for the 10-fold greater dispersion of the solute breakthrough curve.

A D value that was 1.6 times that estimated from the NaCl breakthrough curves was then used to fix P for a first-order model fit of the acridine breakthrough curves. The difference in apparent dispersion, or tailing, is then

Table 17.4. First-Order Model Fits to Acridine Breakthrough Curves

Exp.	Pulse ^a	R	P ^b	ω	$K_d(\text{cm}^3/\text{g})$	$D(\text{cm}^2/\text{sec})$	$k_b(\text{sec})$	ssq
<i>Sodium-Phosphate Buffer</i>								
1	49.5	12.9	59.7	17.3	29	0.011	0.040	0.094
2	81.9	19.9	56.4	20.9	46	0.012	0.029	0.032
5	65.5	15.0	94.4	21.1	34	0.006	0.036	0.140
9	56.7	13.7	90.0	20.8	31	0.007	0.040	0.131
10	57.8	17.6	75.9	19.0	40	0.008	0.028	0.108
11	52.9	14.7	37.4	35.8	33	0.008	0.030	0.044
12	56.9	21.1	41.6	17.6	49	0.007	0.010	0.064
<i>Sodium-Bicarbonate Buffer</i>								
3	76.5	20.1	78.8	21.0	46	0.008	0.027	0.097
4	93.1	20.8	72.8	23.8	48	0.008	0.029	0.038
6	49.3	18.0	116	22.0	41	0.005	0.031	0.090
7	90.6	21.9	67.2	18.1	51	0.009	0.021	0.086
8	47.9	14.1	139	23.4	32	0.004	0.045	0.051

^aPulse value fitted by the model.

^bPeclet value fixed at $0.625 \times$ the salt tracer value.

reflected in the fitted ω value. Transport parameters obtained from the first-order model fits are listed in Table 17.4. The K_d values from the first-order model were an average of 8.1% different than the average K_d values (Table 17.2) and were 2.5% different than those from the equilibrium model. The fitted pulse values were 2.3% different than the experimental values and the same as those from the equilibrium model. These differences are slightly larger than experimental variations, but are not significant. Overall, the first-order model provided nearly as good a fit to the data as did the equilibrium model.

Breakthrough curves were also modeled using a mobile-immobile region model,^{18,19} which has one more parameter that accounts for diffusion through internal pores. The fit provided by the mobile-immobile region model was only slightly better ($\leq 2\%$) than the fit to the first-order model, consistent with prior results.¹⁵

In the first-order model, ω is directly proportional to the first-order rate coefficient k_b and is a measure of how close the system is to equilibrium. ω values greater than 100 are characteristic of equilibrium systems, whereas ω values less than 0.1 are characteristic of sorption processes too slow to observe. The average k_b values observed at pH 7 ($0.032 \pm 0.006 \text{ sec}^{-1}$) and pH 4 ($0.023 \pm 0.008 \text{ sec}^{-1}$) were not significantly different, indicating that sorption reactions between acridine and the silica surface were equally fast at both pH values. However, the tendency of the first-order model to underestimate the observed desorption tailing suggests that the experiments were further from equilibrium than the model indicated (experiments 1, 3, 5, 6, 8, 9, 10).

The first-order model's underestimate of the desorption tailing of the breakthrough curves was the primary concern in the curve-fitting results. The breakthrough curve for experiment 4 was nearly symmetrical; consequently it gave a very good fit. The most asymmetric curves had the greatest ssq (experiments 5, 6, and 8). Breakthrough curve symmetry was found to be directly proportional to the observed fluctuations in pore-water velocity measured during the course of the experiment. For example, the fluctuation in pore-water velocity for experiment 4 was approximately 3%, the lowest of any experiment. The most asymmetric breakthrough curves (experiments 5, 6, and 8) had the highest percent fluctuations in pore-water velocity, ranging from 7 to 10%. The fluctuations in pore-water velocity for the remaining experiments ranged between 4 and 6%.

Interpretation of similar experiments with chlorinated-benzene compounds invoked bonding mechanisms indicative of van der Waals interactions. The chlorinated-benzene experiments were carried out under the same conditions, but with a patchy hydrophobic coating applied to the silica to give 0.015 mass fraction organic carbon.¹⁵ Time scales on the order of hours to days were needed to achieve sorption equilibrium, with the mass transfer coefficient inversely related to K_d for the different compounds. Sorption and desorption limbs of the breakthrough curves were mirror images, indicating good reversibility, however. Acridine sorption experiments with C_{18} bonded silica resulted in extremely long times to equilibrium.

CONCLUSIONS

Acridine sorption to porous silica is 71% greater at pH 4 than at pH 7. There appears to be a trend of increasing sorption as the pK_a is approached. Bicarbonate enhances acridine sorption relative to phosphate at pH 7. The reason may be a smaller reduction in hydrogen bonding sites because HCO_3^- is a weaker liquid for silanol sites than phosphate. Changes in C_0 and μ_e had no effect on K_d . There was no anion effect at pH 4, indicating that ion pair adsorption is independent of anion type.

The first-order kinetic model provided a good fit to the experimental data. The equilibrium model fit the data, but gave dispersion values an order of magnitude greater than the salt tracer. The k_b^{-1} values were in the range of 25–100 sec, indicating that sorption/desorption rates were relatively fast. Anion effects on sorption may be neglected except when HCO_3^- is the major anion.

Acridine aqueous solubility was reduced by salt precipitation at low pH and high phosphate concentrations. Otherwise, there are no anion corrections on acridine and quinoline solubility.

ACKNOWLEDGMENTS

We would like to thank M. T. Cavajal-Figueroa for running the quinoline solubility experiments and S. H. Yalkowsky for valuable advice throughout the work. Financial support for this research was provided by U.S. Environmental Protection Agency (EPA) grant R813179010. The contents of this chapter do not necessarily reflect the views and policies of the EPA.

REFERENCES

1. Rostad, C. E., W. E. Pereira, and S. M. Ratcliff. "Bonded-Phase Extraction Column Isolation of Organic Compounds in Ground-Water at a Hazardous Waste Site," *Anal. Chem.* 56:2856–2860 (1984).
2. McKay, J. F., J. H. Weber, and D. R. Latham. "Characterization of Nitrogen Bases in High-Boiling Point Petroleum Distillates," *Anal. Chem.* 48:891–898 (1976).
3. Uden, P. C., and S. Siggia. "Composition and Analysis of Oil Shale and Shale Oil," Centennial Meeting of the American Chemical Society, New York, NY, April 7, 1976.
4. Lang, K. F., and I. Eigen. "Organic Compounds in Coal Tar," *Forts. Chem. Forsch.* 8:91–170 (1969).
5. Aczel, T., and H. E. Lumpkin. "Mass Spectrometric Characterization of Coal Liquefaction Products and Related Materials," Centennial Meeting of the American Chemical Society, New York, NY, April 7, 1976.
6. Banwart, W. L., J. J. Hassett, S. G. Wood, and J. C. Means. "Sorption of Nitrogen-Heterocyclic Compounds by Soils and Sediments," *Soil Sci.* 133:42–47 (1982).

7. Zachara, J. M., C. C. Ainsworth, L. J. Felice, and C. T. Resch. "Quinoline Sorption to Subsurface Materials: Role of pH and Retention of the Organic Carbon," *Environ. Sci. Technol.* 20:620-627 (1986).
8. Zachara, J. M., C. C. Ainsworth, C. E. Cowan, and B. L. Thomas. "Sorption of Binary Mixtures of Aromatic Nitrogen Heterocyclic Compounds on Subsurface Materials," *Environ. Sci. Technol.* 21:397-402 (1987).
9. Ainsworth, C. C., J. M. Zachara, and R. L. Schmidt. "Quinoline Sorption on Na-Montmorillonite: Contributions of the Protonated and Neutral Species," *Clays Clay Min.* 35:121-128 (1987).
10. Zachara, J. M., C. C. Ainsworth, C. E. Cowan, and R. L. Schmidt. "The Effect of Nitrogen on the Sorption of Ionizable N-Containing Aromatic Compounds by Amorphous Silica," *Environ. Sci. Technol.* 24:118-126 (1990).
11. Albert, A. *The Acridines* (London: Edward Arnold, 1966).
12. VanGenuchten, M., J. Davidson, and P. Wierenga. "An Evaluation of Kinetic and Equilibrium Equations for the Prediction of Pesticide Movement through Porous Media," *Soil Sci. Soc. Am. Proc.* 38:29-35 (1974).
13. VanGenuchten, M. T. "Non-Equilibrium Transport Parameters from Miscible Displacement Experiments," Research Report 119, U.S. Salinity Lab, Riverside, CA (1981).
14. Rose, D. "Hydrodynamic Dispersion in Porous Materials," *Soil Sci.* 123:277-283 (1977).
15. Szecsody, J. E., and R. C. Bales. "Sorption Kinetics of Low-Molecular-Weight Hydrophobic Organic Compounds on Surface-Modified Silica," *J. Contam. Hydrol.* 4:181-203 (1989).
16. Horvath, C., and H. Lin. "Movement and Band Spreading of Unsorbed Solutes in Liquid Chromatography," *J. Chromatog.* 126:401-420 (1976).
17. Horvath, C., and H. Lin. "Band Spreading in Liquid Chromatography," *J. Chromatog.* 149:43-70 (1978).
18. Crittenden, J. C., N. J. Hutzler, D. G. Geyer, J. L. Oravitz, and G. Friedman. "Transport of Organic Compounds with Saturated Groundwater Flow: Model Development and Parameter Sensitivity," *Water Resour. Res.* 22:271-284 (1986).
19. Roberts, P. V., M. Goltz, R. Summers, J. C. Crittenden, and P. Nkedi-Kizza. "The Influence of Mass Transfer on Solute Transport in Column Experiments with an Aggregate Soil," *J. Contam. Hydrol.* 1:375-393 (1987).

CHAPTER 18

Surfactant-Enhanced Solubility of Hydrophobic Organic Compounds in Water and in Soil-Water Systems

David A. Edwards, Zhongbao Liu, and Richard G. Luthy

INTRODUCTION

This chapter discusses surfactant solubilization of hydrophobic organic compounds (HOCs) in systems that consist of soil and micellar nonionic surfactant solution. Surfactant solubilization of HOCs in such systems involves a number of physicochemical processes, including partitioning of surfactant and HOC between soil and solution, micelle formation, and HOC partitioning between micelles and the aqueous pseudophase. The amount and type of surfactant present in a system can affect these processes significantly.

As separate processes, soil-water partitioning and micelle-water partitioning of either HOCs or surfactants have been investigated for many years. The partitioning of organic solutes between solids and water in soil-water systems and aquifers has been the topic of numerous research papers over the last three decades, beginning with studies of sorption of organic pesticides (e.g., Lambert et al.¹). Sorption of surfactants onto soil likewise has received attention, although most of the studies have focused on anionic surfactants.²⁻⁵ The process of amphiphilic molecules aggregating to form micelles has long been a topic of investigation, and studies of solubilization of hydrophobic compounds in colloidal solutions of surfactant micelles have been undertaken since the 1930s. Until recently, however, published research relating to the partitioning behavior of HOCs in systems of soil or aquifer solids in contact with micellar surfactant solution has been exiguous and largely qualitative. Detailed physical and chemical characterization of the mechanisms of partitioning of hydrophobic organic solutes in such systems is necessary in order to properly describe and predict hydrophobic contaminant behavior in natural porous media in the presence of micellar surfactant solution, whether such a solution is present by accident or by design.

Engineering applications of surfactant solutions for the purpose of reme-

inating contaminated soils or aquifers can result in HOC desorption from solid media and enhancement of HOC solubilities; at present, however, there are various technical problems with injection and separation operations that must be resolved before surfactant remediation can be implemented successfully on a general basis.⁶⁻¹⁰ While inadvertent transfer of micellar surfactant solutions to soils or aquifers conceivably could cause desorption of toxic hydrophobic contaminants from the solid phase, resulting in high bulk-aqueous-phase concentrations and rapid contaminant transport,¹¹⁻¹³ there are, to our knowledge, no reports in the literature relating to the actual occurrence of incidental micellar surfactant plumes. On the other hand, contamination by surfactant at monomeric concentrations, that is, below the threshold concentration at which micellar aggregates of surfactant molecules form, has been described by several researchers.^{2,14} In monomeric surfactant solutions, the solubility of highly hydrophobic compounds, such as DDT or polycyclic aromatic hydrocarbons (PAH), may be enhanced relative to solubility in water.^{15,16} Monomeric surfactant solutions in the subsurface could thus result in increased desorption and mobility of HOCs.

After a brief review of fundamental surfactant properties, this chapter addresses several aspects of nonionic surfactant solubilization of HOCs in both aqueous and soil-aqueous systems. The first four sections review and interpret experimental results dealing with the solubilization of naphthalene, phenanthrene, and pyrene by four alkyl or alkylphenol polyoxyethylene (POE) surfactants: $C_{12}H_{25}O(CH_2CH_2O)_4H$; $C_8H_{17}-C_6H_4-O(CH_2CH_2O)_{9.5}H$; $C_8H_{17}-C_6H_4-O(CH_2CH_2O)_{12}H$; and $C_9H_{19}-C_6H_4O(CH_2CH_2O)_{10.5}H$.¹⁶ The remaining sections discuss the development and experimental validation of a model for solubilization of HOCs in systems of soil and micellar nonionic surfactant solution.¹⁷ Although the concepts described in this chapter are relevant to the design of surfactant remediation of HOC-contaminated soil or sediment, many of the physical, chemical, and biological processes potentially impacting this technology are beyond the scope of this chapter.

MONOMERIC AND MICELLAR SURFACTANT SOLUTION PROPERTIES

An individual surfactant molecule, or *monomer*, possesses two or more structural moieties of varying polarity—typically one that is polar, and a second that is nonpolar. When sufficient numbers of surfactant molecules are present in solution to attain a critical micelle concentration (CMC), the surfactant molecules representing the differential increase in surfactant concentration above the CMC spontaneously associate to form multimeric structures called *micelles*. The nonpolar portions of the surfactant molecules constituting a micelle are hydrophobic and are directed inward toward the center of the micelle, away from monomeric solution. The polar portions of the micellar molecules are hydrophilic and are directed outward from the micelle into

monomeric solution. The hydrophobic interiors of the micelles in solution collectively function as what may be conceptualized as a micellar pseudophase, being distinct in terms of its chemical properties from the aqueous pseudophase,¹³ and, in a system with soil, from the sorbed phase. The micelle interiors of this pseudophase, being hydrophobic, have the capacity to solubilize slightly-soluble HOCs,¹⁸ a process that often results in greatly-increased apparent aqueous solubilities of the organic compounds. Hydrocarbons (e.g., PAH) are generally solubilized within the micelle core, whereas more polar organic compounds may be solubilized in portions of the micelle closer to its interface with the aqueous pseudophase.¹⁹ The aqueous and micellar pseudophases in bulk solution can be treated in modeling as two compartments for the distribution of HOCs. In a system in which the bulk-liquid phase is a monomeric surfactant solution, the concentration of surfactant in the aqueous phase increases with increasing amounts of surfactant added to the system until surfactant solubility in the aqueous phase is attained at the CMC. Upon further addition of surfactant, the concentration of surfactant in the aqueous pseudophase remains constant at the CMC, while the excess surfactant is incorporated in the system in the form of micelles.²⁰ The value of the CMC depends on surfactant structure and composition, temperature, ionic strength, and the amount and type of organic additives in the solution.¹⁹

HOC PARTITIONING BETWEEN PSEUDOPHASES IN BULK AQUEOUS SOLUTION

In a system consisting of micellar surfactant solution and HOC, the degree to which a hydrophobic organic compound is distributed between the micellar and aqueous pseudophases can be quantified by employing either one of two parameters, the molar solubilization ratio (MSR) or the mole fraction micelle-aqueous-pseudophase partition coefficient (K_m).

In an aqueous system in the presence of a separate phase of HOC (e.g., solid phenanthrene), the MSR represents the number of moles of HOC solubilized within the micellar pseudophase per mole of surfactant monomers forming this pseudophase. Both the MSR and K_m in this type of system have constant values over a wide range of surfactant concentrations. Although the value of K_m is constant in a system in which HOC is not present as a separate phase, the value of the MSR in such a system decreases as the volume of the micellar pseudophase is increased.¹⁶ For aqueous systems in which HOC does exist as a separate phase, the MSR can be evaluated by calculating the slope of the relationship between the molar concentration of the solubilized HOC and the molar concentration of the micellar surfactant.

In order to introduce nomenclature that will be useful later in the chapter, the molar concentration of the micellar surfactant is here defined for a micellar surfactant system at any surfactant dose as the difference between C_{surf} , the bulk solution molar surfactant concentration, and the CMC, the surfactant

monomer molar solubility. Similarly, the molar concentration of the solubilized HOC is expressed as the difference between S_{mic} and S_{cmc} , where S_{mic} is the apparent molar solubility of HOC in dissolved and micellar form in surfactant solution at C_{surf} , and S_{cmc} is the molar HOC solubility in a solution in contact with separate-phase HOC and with a surfactant concentration equal to the CMC. Since S_{mic} represents the solubility of HOC in both dissolved and solubilized forms, the value of S_{mic} varies as a function of surfactant dose. S_{cmc} , on the other hand, is a constant, representing the maximum equilibrium concentration of dissolved HOC in a solution saturated with surfactant monomers.

In a plot of apparent molar HOC solubility as a function of total molar surfactant concentration in an aqueous system in the presence of pure-phase HOC, the slope of the linear, post-CMC portion of the solubilization curve is identical to the slope of a plot of the molar concentration of the solubilized HOC versus the molar concentration of the micellar surfactant, thus providing a value for the MSR directly from experimental data, as exemplified in Figure 18.1. The data in this figure are obtained from experiments described later in this chapter.

In contrast to the MSR, the parameter K_m represents, in a thermodynamically rigorous manner, the equilibrium partitioning of a specific HOC between the micelle pseudophase and the aqueous pseudophase in a solution of water and a given surfactant. K_m is defined for a given system as the ratio of the

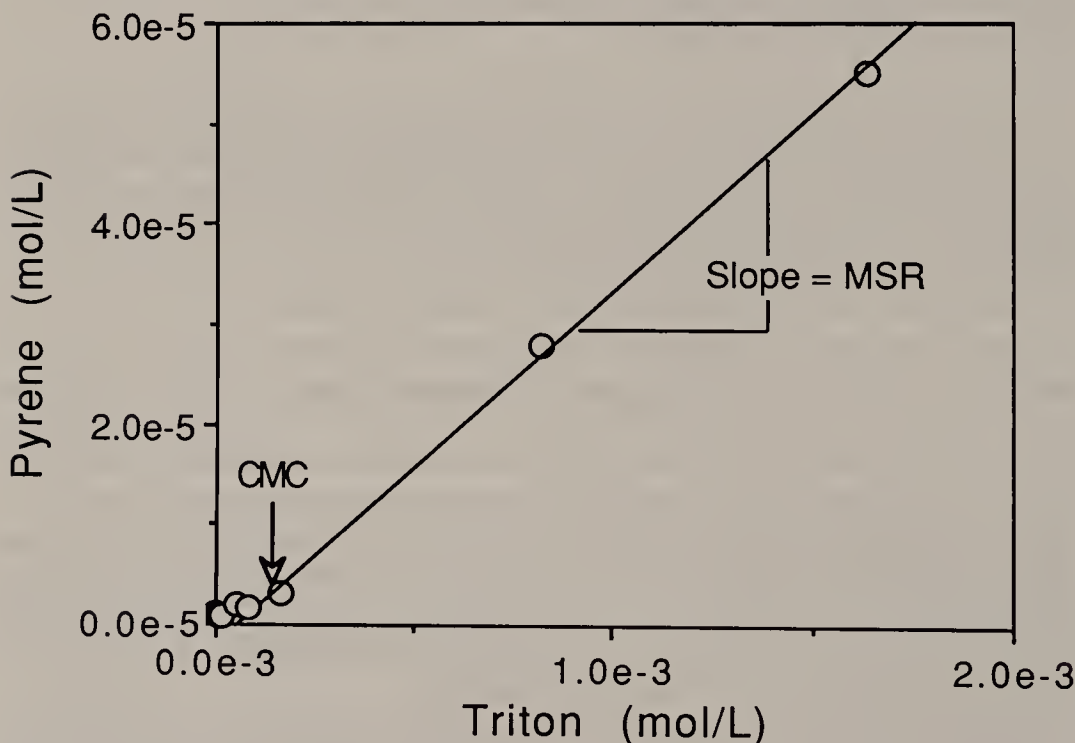


Figure 18.1. Solubilization of pyrene by $\text{C}_8\text{PE}_{9.5}$ nonionic surfactant. The slope of the post-CMC solubilization relationship is equal to the molar solubilization ratio. Notation denotes base ten exponentiation.

micellar-pseudophase mole fraction of the organic compound, X_m , to X_a , the aqueous-pseudophase mole fraction of the organic compound:²¹

$$K_m = \frac{X_m}{X_a} \quad (18.1)$$

In experiments in which a separate phase of HOC is present in the system (e.g., the experiments described in the methods section), the aqueous-pseudophase HOC concentration has a constant value equal to the HOC solubility in monomeric surfactant solution at the CMC, and K_m can be determined from experimental data for such a system by either one of two methods.

In the first method, the micellar-pseudophase mole fraction of hydrophobic organic compound can be assessed using the following equation:

$$X_m = \frac{(S_{\text{mic}} - S_{\text{cmc}})}{(S_{\text{mic}} - S_{\text{cmc}} + C_{\text{surf}} - \text{CMC})} \quad (18.2)$$

while the aqueous-pseudophase mole fraction of HOC in a dilute solution is approximately

$$X_a = S_{\text{cmc}} V_w \quad (18.3)$$

where V_w denotes the molar volume of water, that is, 0.01805 L/mole at 25°C, so that K_m is given as

$$K_m = \frac{(S_{\text{mic}} - S_{\text{cmc}})}{\{(C_{\text{surf}} - \text{CMC} + S_{\text{mic}} - S_{\text{cmc}})(S_{\text{cmc}} V_w)\}} \quad (18.4)$$

The values of S_{mic} , S_{cmc} , C_{surf} , and CMC can be evaluated individually by experiment.

In the second method, a value for K_m is computed by employing the following equation and a measured value of the MSR, obtained as the post-CMC slope of a plot of HOC apparent solubility versus surfactant dose in aqueous solution:¹⁶

$$K_m = [1/(S_{\text{cmc}} V_w)][\text{MSR}/(1 + \text{MSR})] \quad (18.5)$$

It is apparent from Equation 18.5 that if the aqueous pseudophase HOC concentration in a micellar surfactant system remains constant at S_{cmc} due to aqueous contact with pure-phase HOC, experimental findings of constancy of either K_m or the MSR over a given surfactant concentration range would imply constancy of the other parameter. By rearrangement of Equation 18.5, the number of moles of organic compound solubilized per unit increase in moles of surfactant in micelle form in solution in the presence of pure organic compound can be expressed in terms of K_m :

$$\text{MSR} = \frac{[K_m V_w S_{\text{cmc}}]}{[1 - K_m V_w S_{\text{cmc}}]} \quad (18.6)$$

The value of K_m is invariant with respect to increasing micellar surfactant concentration, since it represents equilibrium partitioning between two pseudophases, in which there is a fixed ratio of the value of X_m to the value of X_a . In this respect, K_m is analogous to K_{ow} , the octanol-water partition coefficient. The value of the MSR, however, may be either constant or variable, depending on the conditions of the system. It has been shown for aqueous batch tests with PAH compounds, as illustrated in Figure 18.1, that the value of the MSR does not change with respect to increasing micellar nonionic surfactant dose when the bulk solution remains in contact with the pure-phase HOC, resulting in the aqueous-pseudophase HOC concentration being constant at S_{cmc} .¹⁶ In systems not in contact with pure-phase HOC, the addition of sufficient surfactant to create micelles results in an aqueous-pseudophase organic compound concentration, C_{aq} , which is less than S_{cmc} , and which varies as a function of the amount of micellar surfactant in the system.¹⁷ In this case Equation 18.5 is modified to

$$K_m = [1/(C_{aq} V_w)][MSR/(1 + MSR)] \quad (18.7)$$

and Equation 18.6 is changed to

$$MSR = \frac{[K_m V_w C_{aq}]}{[1 - K_m V_w C_{aq}]} \quad (18.8)$$

The value of K_m for a given surfactant-HOC combination can be determined in a micellar surfactant system in which separate-phase HOC is present by employing Equation 18.5 and the constant value of the MSR for the system as obtained from experimental data. With this value of K_m , Equations 18.7 and 18.8 then permit calculation of the MSR as it varies as a function of C_{aq} for systems in which HOC is not present as a separate phase.

EXPERIMENTAL METHODS FOR AQUEOUS SYSTEMS

Batch tests designed to assess solubilization of PAH in surfactant solution were conducted at 25°C for 12 surfactant-PAH systems.¹⁶ The surfactants of this study, used as received from suppliers, are listed in Table 18.1; the PAH compounds, obtained from Aldrich Chemical Company, are listed in Table 18.2.^{22,23} ¹⁴C-labeled PAH compounds were acquired from Amersham Corporation.

Experiments were conducted with a duplicate series of eight to ten samples, with each sample representing a different aqueous surfactant concentration. Each 5 mL sample, consisting of a measured amount of surfactant and a given volume of PAH stock in deionized water, was placed in an 8-mL glass vial. The PAH stock was a mixture in methanol of both nonlabeled and ¹⁴C-labeled solutions of an individual PAH compound. A Beckman LS 500 TD liquid

Table 18.1. Selected Commercial Surfactants

Notation	Trade Name	Avg. Molecular Formula	CMC (mol/L) ^a	Avg. MW (g/mol)
C ₁₂ E ₄	Brij 30	C ₁₂ H ₂₅ O(CH ₂ CH ₂ O) ₄ H	2.3 × 10 ⁻⁵	363
C ₈ PE ₁₂	Igepal CA-720	C ₈ H ₁₇ -C ₆ H ₄ -O(CH ₂ CH ₂ O) ₁₂ H	2.3 × 10 ⁻⁴	735
C ₉ PE _{10.5}	Tergitol NP-10	C ₉ H ₁₉ -C ₆ H ₄ -O(CH ₂ CH ₂ O) _{10.5} H	5.4 × 10 ⁻⁵	686
C ₈ PE _{9.5}	Triton X-100	C ₈ H ₁₇ -C ₆ H ₄ -O(CH ₂ CH ₂ O) _{9.5} H	1.7 × 10 ⁻⁴	628

^aObtained by surface tension measurement.

scintillation counter (LSC) was employed to measure the radioactivity of the ¹⁴C-labeled PAH solution. The mass ratio of nonlabeled PAH compound to ¹⁴C-labeled PAH compound had been selected previously so that each sample would have a decay rate sufficiently high relative to the background decay rate in order to insure accuracy. The total mass of PAH added to each sample was 20 to 80 times the mass needed for a solution to attain solubility in water, so as to permit observation of the amount of solubilization that would occur as a function of bulk solution surfactant concentration. The methanol carrier solvent from the PAH stock solution resulted in approximately 1% methanol by volume in the sample and did not affect the solubilization relationship.¹⁶ The seal of each sample vial consisted of a Teflon-lined septum and an open-port screw cap. The samples were submerged in a water bath at 25°C and reciprocated at 80 cycles/min for approximately 24 hr. Measured portions of each sample were removed by glass syringe and filtered through preconditioned Teflon membrane filters having pore diameters of 0.22 µm in order to restrict passage of solid-phase PAH compound. A given sample portion, with a volume of 0.5 to 2.0 mL depending on the experiment, was mixed with 10 mL liquid scintillation cocktail (Scintiverse II, Fisher Scientific), and the cocktail was placed in the LSC for counting. Decay rates of duplicate samples were counted using the quench monitoring and automatic quench compensation technique. Background decay rate corrections were made preparatory to calculating conversion from sample disintegrations per minute (DPM) to bulk solution apparent solubility.

A second series of tests involved measuring the surface tensions of aqueous solutions as a function of bulk solution surfactant concentration in order to obtain values of the CMC for individual surfactants. The surface tension of each solution was measured with a Fisher Tensiomat Model 21 duNuoy tensiometer. The data showed a characteristic pattern of a substantial decrease in surface tension per unit increase in the logarithm of surfactant concentration

Table 18.2. Properties of the PAH Compounds of This Study

Name	Molecular Formula	Solubility (mol/L) ^a	Log K _{ow} ^b	MW (g/mol)
naphthalene	C ₁₀ H ₈	2.5 × 10 ⁻⁴	3.36	128
phenanthrene	C ₁₄ H ₁₀	7.2 × 10 ⁻⁶	4.57	178
pyrene	C ₁₆ H ₁₀	6.8 × 10 ⁻⁷	5.18	202

^aFrom Mackay and Shiu.²²

^bFrom Karickhoff et al.²³

at surfactant concentrations less than the CMC, but little or no change at surfactant concentrations greater than the CMC.

RESULTS OF AQUEOUS SYSTEM SOLUBILIZATION EXPERIMENTS

The apparent solubility of a PAH compound in a given surfactant solution was calculated by dividing the sample DPM value, corrected for background decay rate, by the sample volume, and then converting this quotient to an equivalent solution concentration by employing the following: the conversion factor of 2.22×10^6 DPM per microcurie, the mass ratio of radiolabeled to nonlabeled compound, and the specific activity of the radiolabeled PAH.

Solubilization Relationships

In Figure 18.1 the apparent solubility of pyrene is plotted as a function of surfactant dose for a solution of the nonionic surfactant $C_8PE_{9.5}$. This plot shows the linearity of the micellar surfactant solubilization relationship, with a constant slope of the solubilization relationship being observed for surfactant doses greater than the CMC.

CMC values for the surfactants of this study were determined through independent surface tension measurements. Surface tension data for CMC determination of $C_8PE_{9.5}$ in water are shown in Figure 18.2. Although certain types of solubilizates can greatly affect CMC values, hydrocarbons, such as PAH, are solubilized in micelle interiors and generally exert only a slight influence on CMC values.¹⁹ On an expanded scale, the data in Figure 18.1 show a break in slope for solubilization of phenanthrene by $C_8PE_{9.5}$ surfactant at a surfactant dose in the vicinity of the CMC. The value of the CMC was determined independently by surface tension measurements of the type illustrated in Figure 18.2 as 1.7×10^{-4} mol/L.²⁴ Similar solubilization phenomena are observed for the 12 surfactant-PAH systems for which experiments were performed, though often the break in slope is more evident, in contrast to the situation in Figure 18.1. The value of the CMC for the surfactants employed in this work actually represents a composite of CMC values of a number of Poisson-distributed homologues due to the heterogeneous composition of the commercial $C_8PE_{9.5}$ surfactant. The averaged CMC value for heterogeneous surfactants is obtained from surface tension graphs and is estimated in solubilization plots by taking the intersection of the projection of the linear, post-CMC apparent solubility curve segment with the projection of the linear pre-CMC segment. Examples are shown in Figures 18.1 and 18.2.

An increase in the apparent solubility of phenanthrene as a function of $C_8PE_{9.5}$ pre-CMC surfactant concentrations is about 30%. The increases in pre-CMC apparent solubility for this and the other 11 PAH-surfactant combinations are shown in Table 18.3. The maximum value of the ratio between PAH solubility in monomeric surfactant solution at the CMC and PAH solu-

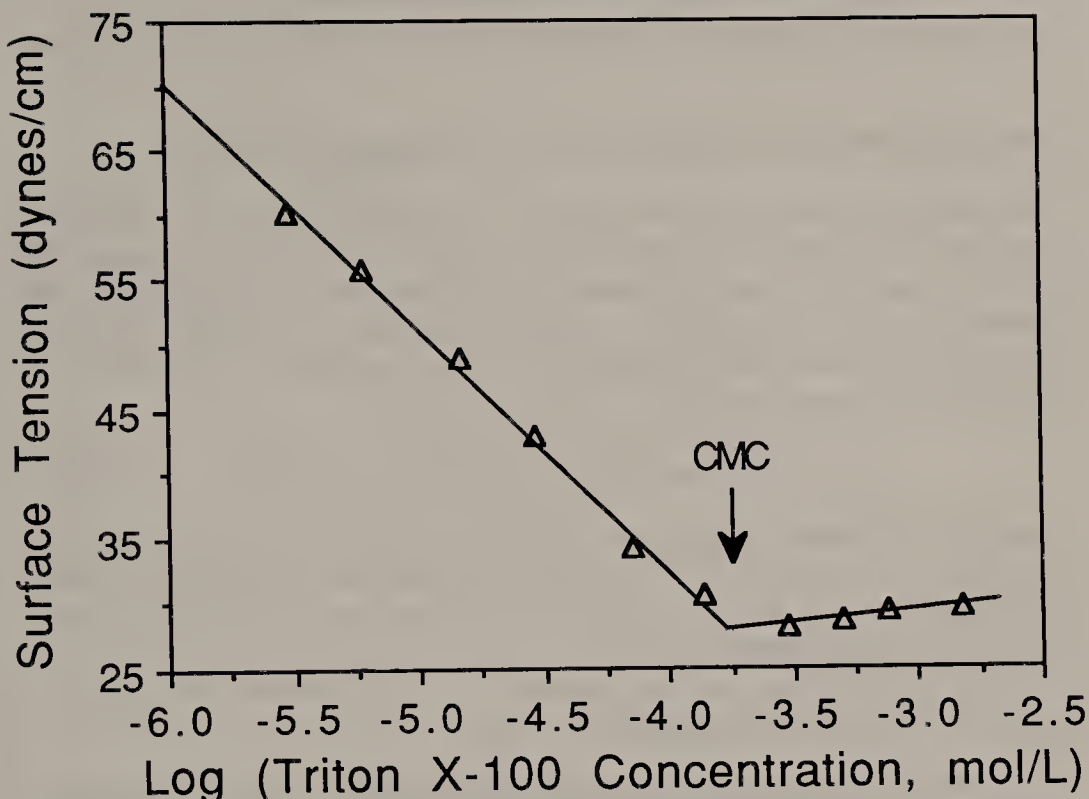


Figure 18.2. Determination of CMC by surface tension measurement for $C_8PE_{9.5}$ nonionic surfactant.

Table 18.3. Experimental PAH Solubilities and Mole Fraction Micelle-Aqueous-Pseudophase Partition Coefficients

PAH Compound	Surfactant	Notation	MSR	Log K_m	PAH Solubility (mol/L) ^a	
					No Surfactant	$C_{surf} = CMC$
naphthalene	Brij 30	$C_{12}E_4$	3.17×10^{-1}	4.59	3×10^{-4}	3.4×10^{-4}
naphthalene	Igepal CA-720	C_8PE_{12}	3.23×10^{-1}	4.63	3×10^{-4}	3.2×10^{-4}
naphthalene	Tergitol NP-10	$C_9PE_{10.5}$	3.68×10^{-1}	4.57	3×10^{-4}	4.0×10^{-4}
naphthalene	Triton X-100	$C_8PE_{9.5}$	3.38×10^{-1}	4.64	3×10^{-4}	3.2×10^{-4}
phenanthrene	Brij 30	$C_{12}E_4$	1.52×10^{-1}	5.57	9×10^{-6}	2.0×10^{-5}
phenanthrene	Igepal CA-720	C_8PE_{12}	1.04×10^{-1}	5.68	1×10^{-5}	1.1×10^{-5}
phenanthrene	Tergitol NP-10	$C_9PE_{10.5}$	1.60×10^{-1}	5.72	1×10^{-5}	1.5×10^{-5}
phenanthrene	Triton X-100	$C_8PE_{9.5}$	1.11×10^{-1}	5.70	1×10^{-5}	1.3×10^{-5}
pyrene	Brij 30	$C_{12}E_4$	7.15×10^{-2}	6.53	1×10^{-6}	1.1×10^{-6}
pyrene	Igepal CA-720	C_8PE_{12}	4.25×10^{-2}	6.01	8×10^{-7}	2.1×10^{-6}
pyrene	Tergitol NP-10	$C_9PE_{10.5}$	5.76×10^{-2}	6.41	8×10^{-7}	1.2×10^{-6}
pyrene	Triton X-100	$C_8PE_{9.5}$	3.52×10^{-2}	6.03	1×10^{-6}	1.9×10^{-6}

^aWith 1% by volume methanol.

bility in pure water was found for the compounds of this study to be about 2.5.

Partitioning Between Micelles and the Aqueous Pseudophase

The MSR is a measure of the ability of a given surfactant in solution to solubilize nonpolar organic compounds within the micellar pseudophase. The product of the MSR and the aggregation number of the micelle gives the number of molecules of organic compound solubilized per micelle. The MSR is related to the mole fraction micelle/aqueous-pseudophase partition coefficient, K_m , from Equation 18.5:

$$K_m = ((55.4 \text{ moles/L})/S_{cmc})(MSR/(1 + MSR)) \quad (18.9)$$

Table 18.3 displays values of S , the measured PAH solubility in water before the addition of surfactant; S_{cmc} , the PAH solubility at the surfactant CMC; MSR; and $\log K_m$ for each of the 12 systems of nonionic surfactant and PAH that were studied by Edwards et al.¹⁶

Log K_m /Log Solubility Correlations

The parameter K_m characterizes the distribution of organic compound between the nonpolar micellar pseudophase and the polar aqueous pseudophase in a system containing micellar surfactant solution. K_m can be considered to be analogous to the octanol-water partition coefficient, K_{ow} , where the micellar pseudophase represents the octanol phase, and water saturated with surfactant monomers represents the aqueous phase saturated with octanol. In fact, $\log K_m$ values are linearly correlated with the logarithm of the PAH octanol-water partition coefficient.^{13,16} Since $\log K_m$ values in general have linear correlations with log water solubility values for HOC compounds,²⁵ it follows that $\log K_m$ should be linearly related to log water solubility for the HOC compounds of this study. Figure 18.3 shows the relationship between $\log K_m$ and $\log S$ for five HOCs solubilized by $C_8PE_{9.5}$ at 25°C. Two of the HOCs are DDT and 1,2,3-trichlorobenzene. Log S values for DDT and 1,2,3-trichlorobenzene are taken from Kile and Chiou.¹⁵ Kile and Chiou also provide solubilization data that allow computation of the $\log K_m$ values for these two compounds in $C_8PE_{9.5}$ solution.¹⁵ The other three organic compounds in Figure 18.3 are PAH compounds for which $\log S$ values are obtained from Mackay and Shiu,²² and $\log K_m$ values are given in Table 18.3. It is seen from Figure 18.3 that $\log K_m$ for a $C_8PE_{9.5}$ solution has a negative, linear correlation with $\log S$. Similar relationships exist for $C_{12}E_4$, C_8PE_{12} , and $C_9PE_{10.5}$ surfactants.

X_m -Molecular Weight Correlations

In a micellar surfactant system in which PAH is present as a separate phase, the mole fraction of PAH in the micelle pseudophase can be expressed as

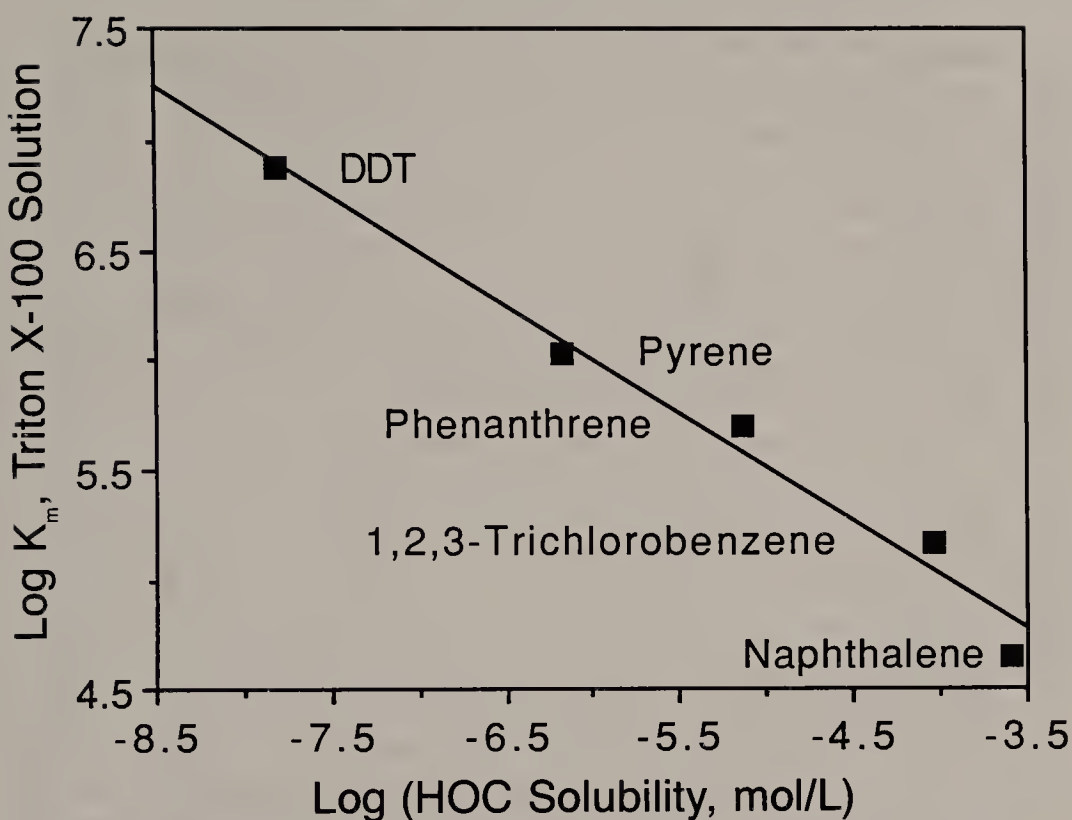


Figure 18.3. Relationship of $\log K_m$ and \log PAH solubility in $C_8PE_{9.5}$ nonionic surfactant solution.

$$X_m = K_m V_w S_{cmc} \quad (18.10)$$

Figure 18.4 shows a graph of X_m versus the molecular weight of the PAH molecule for naphthalene, phenanthrene, and pyrene in $C_{12}E_4$, C_8PE_{12} , $C_9PE_{10.5}$, and $C_8PE_{9.5}$ surfactant solutions. Based on this limited amount of data, X_m appears to be a nearly linear, monotonically decreasing function of the PAH molecular weight over the range of experimental values. For this particular homologous series of HOC compounds, X_m seems to be less dependent on the chemistry of the nonionic surfactants than on the molecular weight of the PAH solubilizate.

NONIONIC SURFACTANT SORPTION ONTO SOIL

In systems of surfactant solution and either soil or sediment, a fraction of the surfactant present in the system sorbs onto the solids that are in contact with the surfactant solution.^{3,5,17,24} Little research has been done specifically with regard to nonionic surfactant sorption onto soil. Urano et al. studied sorption behavior for two nonionic surfactants sorbed onto different soils at aqueous-phase surfactant concentrations covering a range of about an order of magnitude close to, but less than, the CMC.³ The data were analyzed in

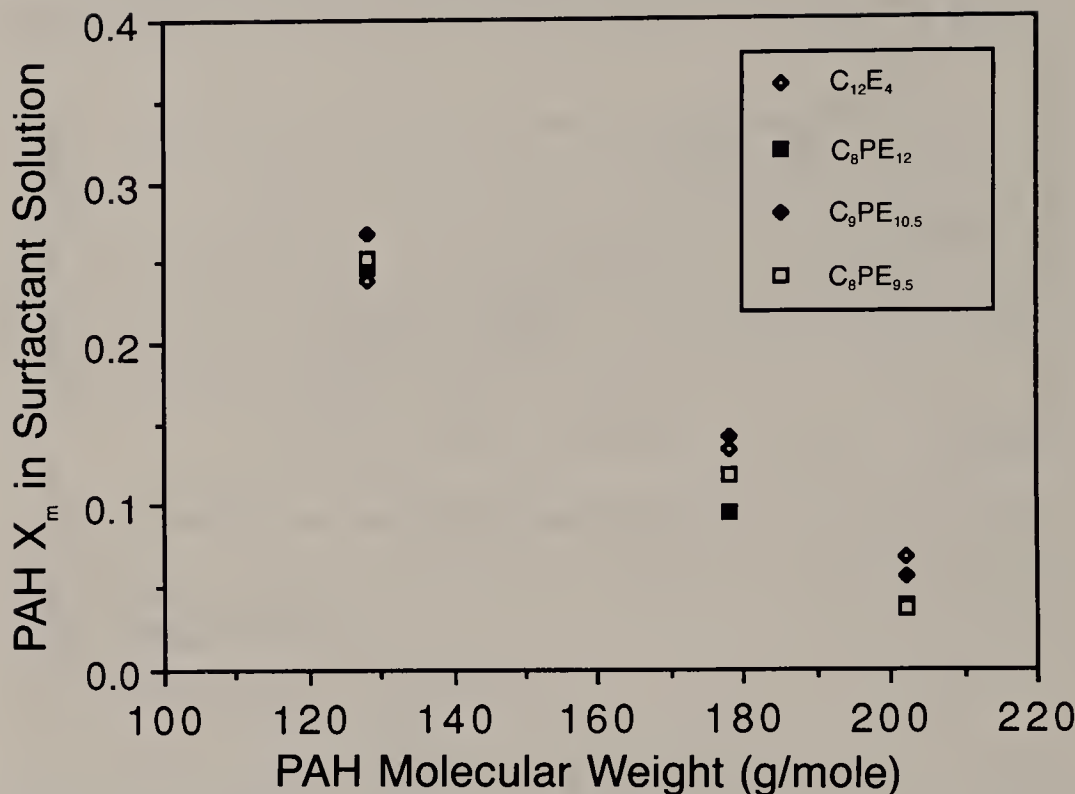


Figure 18.4. Mole fraction of PAH in nonionic surfactant micelles as a function of PAH molecular weight.

Freundlich isotherm form. It was found that the amount of nonionic surfactant sorbed onto soil at a given aqueous-phase surfactant concentration was proportional to the fractional organic carbon content of the soil. When normalized for organic carbon content, the sorption isotherms for three soils having organic carbon contents of 1.7, 2.5, and 6.0% were nearly identical. This is significant since it implies that in this range of percent organic carbon, most of the sorbed surfactant may be associated with the organic matter of the soil. That the amount of sorption of a particular surfactant onto soil is largely a function of the fraction of organic carbon present is consistent with the finding that the extent of sorption of a nonionic surfactant onto hydrophobic sorbents is generally greater than the extent of sorption onto hydrophilic sorbents.²⁶

Liu and Luthy also report nonionic surfactant sorption onto soil, characterizing the sorption data for aqueous-phase surfactant concentrations less than the CMC with Freundlich isotherms.²⁴ The surfactant sorption isotherms for certain nonionic surfactants plateau at or near the aqueous-phase CMC for surfactant doses of up to about 10^{-3} moles of surfactant per liter of solution in the system, i.e., one to two orders of magnitude greater than the CMC.

Although quantitative studies relating to nonionic surfactant sorption saturation are in the process of being conducted for soil, some inferences can be drawn from currently available information. Soil generally consists of a heter-

ogeneous assemblage of silica and clay minerals, which are predominantly negatively charged, as well as organic matter, which contains hydrophobic regions as well as polar hydrophilic and negatively charged sites. In experiments with systems of silica particles and surfactant solution, nonionic surfactant sorption has generally been reported as attaining a maximum plateau value at or near the aqueous CMC.^{19,26,27} For octylphenol and nonylphenol POE surfactants, sorption increases with decreasing number of oxyethylene (OE) units.^{26,27} When silica is chemically modified with methyl groups attached to silica silanol sites, making the surface hydrophobic, nonionic surfactant exhibits maximum plateau sorption at or near the aqueous CMC on this surface as well, although to a greater extent.²⁶ The behavior of the sorption isotherm for nonionic surfactant sorption onto clay minerals depends on the clay mineralogy, but at least in some cases, maximum sorption onto clay minerals appears to be achieved at aqueous-phase surfactant concentrations approximately twice as great as the CMC.²⁸ However, sorption of nonionic surfactant onto the mineral surfaces of soil having at least 1% organic matter appears to be relatively minor in comparison to surfactant sorption onto the organic matter of the soil. Over an experimental range of aqueous-phase surfactant concentrations ranging from about one-tenth the CMC to slightly less than the CMC, Urano et al. show that the bulk of the surfactant that sorbs onto such soils associates with the organic component.³ It follows that isotherm behavior for nonionic surfactant sorption onto soils of moderate organic content is predominantly a function of the affinity of nonionic surfactant toward organic matter, rather than toward mineral surfaces.

Nonionic surfactant may interact with soil organic matter in three ways:

1. hydrophobic surface interaction between the hydrocarbon chains of the surfactant molecules and hydrophobic regions of the humic matter
2. hydrogen bonding between surfactant oxyethylene groups and polar groups of the humic matter, such as hydroxyl and phenolic groups
3. partitioning of the nonionic surfactant into the bulk organic matter in a manner analogous to solute partitioning into an organic liquid such as octanol

If partitioning into organic matter is the predominant mechanism of nonionic surfactant sorption onto soil, as has been proposed for sorption of nonpolar organic solutes,²⁹ or if hydrophobic surface interactions prevail, resulting in monolayer surface coverage of hydrophobic regions on soil organic matter, then maximum equilibrium nonionic surfactant sorption onto soil organic matter should occur concomitantly with attainment of maximum aqueous-phase surfactant concentration. Aqueous-phase surfactant monomer solubility, attained at the aqueous-phase CMC, is constant at greater surfactant doses since the addition of surfactant to a system beyond that required to attain aqueous-phase surfactant solubility results in the formation of micelles.²⁰ Since sorption of micelles onto surfaces directly from bulk solution has been reported to be insignificant,^{19,28} it seems likely that the maximum mass of

surfactant sorbed per unit weight of soil at any micellar surfactant dose would have a value nearly equal to that attained at the aqueous-phase CMC. This is in agreement with the results of Liu and Luthy for a limited set of nonionic surfactants.²⁴ The model for nonionic surfactant solubilization of HOC in soil-aqueous systems as proposed by Edwards et al. is based on this assumption,¹⁷ but the model can easily be modified to treat a soil-aqueous system in which surfactant sorption reaches a plateau value at some surfactant concentration greater than the CMC, or one in which surfactant sorption is any identifiable function of the amount of surfactant added to the system.

Nonionic surfactant sorption to soil increases the fractional organic carbon content of the soil, with the effect of tending to increase the value of the HOC soil-water partitioning coefficient. This effect is the opposite of that produced by the presence of surfactant monomers in solution, the latter slightly enhancing HOC solubility and tending to decrease the partition coefficient.

As a result of surfactant sorption to soil, a much greater amount of surfactant must be added to a soil-water system than to an aqueous system having the identical water volume in order for the aqueous-phase CMC to be attained. Once the aqueous-phase CMC is attained, a given amount of surfactant incrementally supplied to either system will result in the same increase in micellar surfactant concentration. Values of parameters related to surfactant sorption to soil can be obtained through experiments involving solubilization or surface tension.^{24,30}

Calculation of the number of moles of surfactant sorbed per unit weight of a given soil can be performed using surface tension measurements of a number of systems comprising soil and surfactant solution, each having a different soil-water weight-to-volume ratio.²⁴ For each system with a unique soil-water weight-to-volume ratio, the surface tension of a soil-monomeric solution system is plotted against the log of the surfactant dose. Figure 18.5 shows a graph of surface tension plotted against the log of the surfactant dose for a system consisting of water, Morton grassland soil having a fractional carbon content of 0.0096, and C₈PE_{9.5} surfactant.²⁴ As is similarly observed in Figure 18.2 for the system without soil, a linear decrease in surface tension is evident up to the point at which there is an abrupt change in slope, this point denoting attainment of the CMC in the aqueous pseudophase. At greater surfactant doses, there is no significant change in surface tension inasmuch as monomeric surfactant solubility in the aqueous pseudophase and a plateau value of surfactant sorption onto soil are attained. The number of moles of surfactant sorbed onto soil is equal to m_{cmc} , the total number of moles of surfactant required to be added to the system for the CMC to be attained in the aqueous phase, less the product of the aqueous CMC and v_a , the volume of the aqueous solution in liters.

In view of the preceding discussion, the equilibrium amount of nonionic surfactant sorbed onto soil may remain constant in a given system for bulk solution surfactant concentrations equal to or greater than the CMC. Q_{surf} is defined as the number of moles of surfactant sorbed on soil divided by the

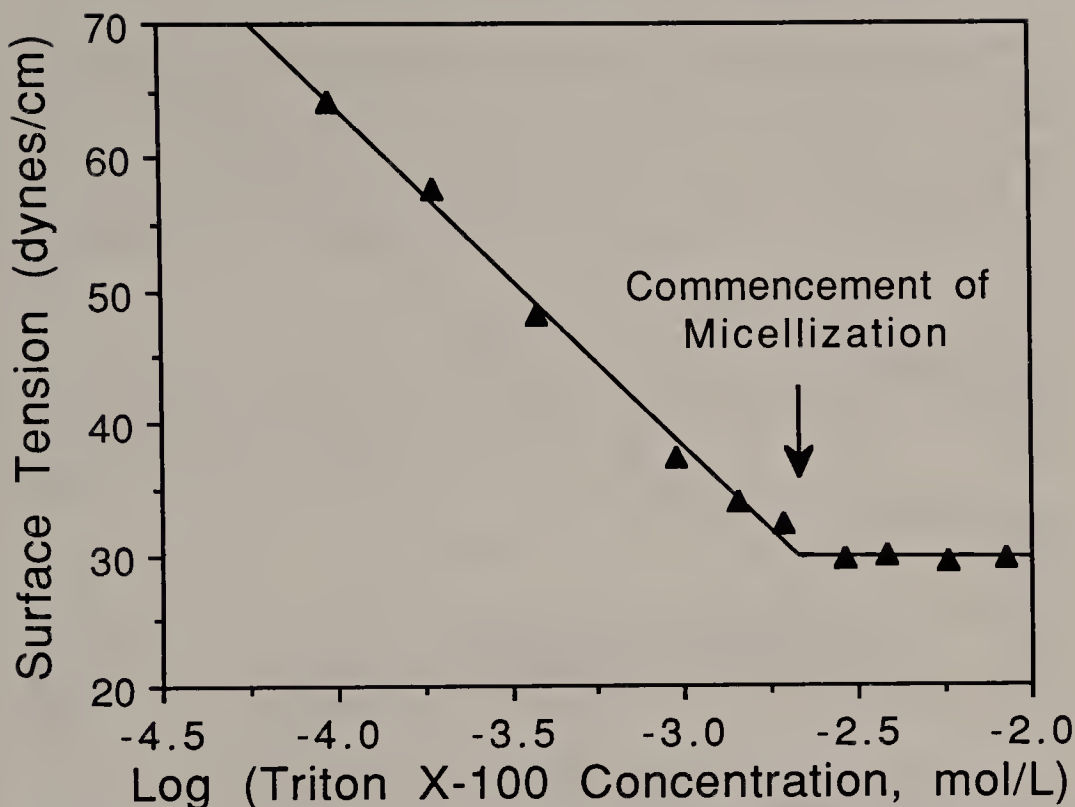


Figure 18.5. Measurement of $C_8PE_{9.5}$ nonionic surfactant surface tension in the presence of soil. The point at which there is an abrupt change of slope of the surface tension measurements signifies attainment of the aqueous-phase CMC after surfactant sorption onto soil has occurred.

weight of the soil for a given micellar surfactant system. Experiments by Liu and Luthy have shown that Q_{surf} is constant over a wide range of soil-aqueous-phase weight-to-volume ratios for certain nonionic surfactants. Figure 18.6 illustrates this principle for the previously described system of $C_8PE_{9.5}$ surfactant and Morton grassland soil.²⁴ The number of moles of surfactant sorbed in a system of soil and micellar surfactant solution can be calculated as

$$m_{\text{sorb}} = Q_{\text{surf}} w_{\text{soil}} \quad (18.11)$$

while the number of moles of surfactant in micelle form, m_{mic} is given by

$$m_{\text{mic}} = m_{\text{tot}} - Q_{\text{surf}} w_{\text{soil}} - v_a \text{CMC} \quad (18.12)$$

where m_{tot} is the total number of moles of nonionic surfactant added to the system.

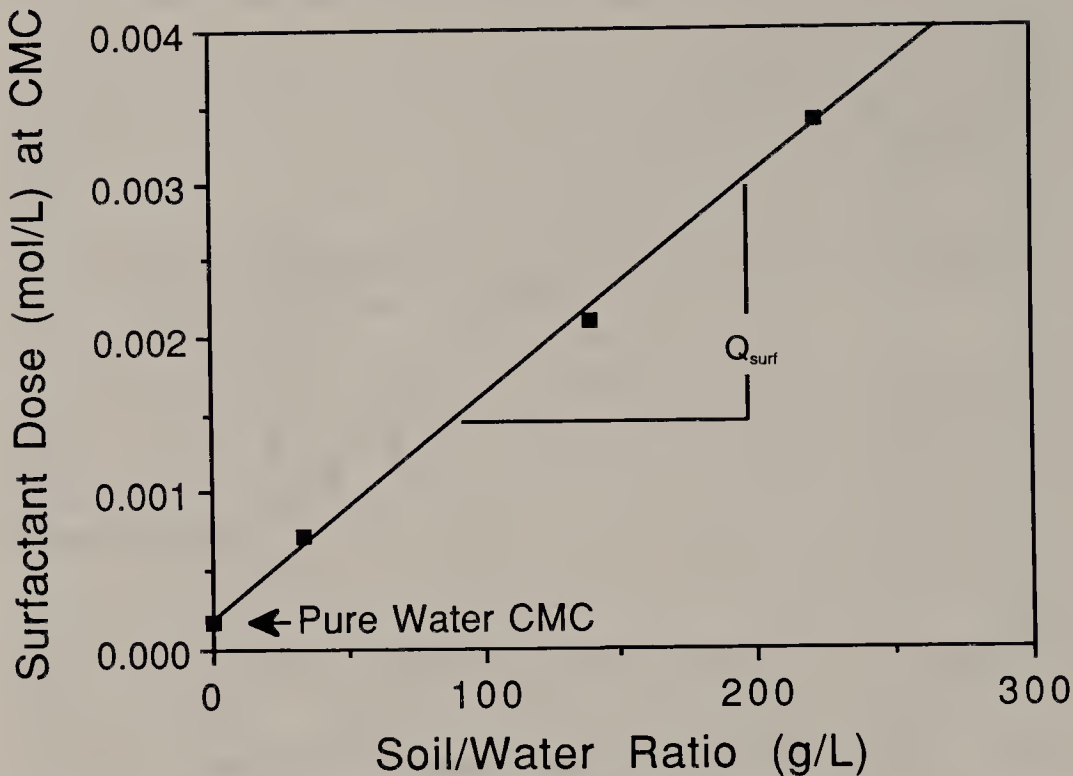


Figure 18.6. The surfactant dose associated with the abrupt change in slope of the surface tension relationship, as exemplified in Figure 18.5, is plotted here as a function of the soil-water weight-to-volume ratio. Q_{surf} , the number of moles of $\text{C}_8\text{PE}_{9.5}$ nonionic surfactant sorbed onto soil per unit gram of soil, is obtained by taking the slope of this plot.

HOC PARTITIONING BETWEEN SOIL AND MONOMERIC SURFACTANT SOLUTION

For a system of soil and surfactant solution in which the aqueous-phase CMC has been attained, the value of the HOC sorption coefficient differs from the value of the HOC sorption coefficient for a system of soil and water. The modified HOC sorption coefficient should be a constant at micellar surfactant concentrations for systems in which surfactant sorption saturation is attained at the CMC. The value of the modified HOC sorption coefficient can be determined directly by experiment or estimated from other data.

In a system of soil and micellar surfactant solution, the equilibrium number of moles of HOC in the aqueous pseudophase, n_{aq} , is given by

$$n_{\text{aq}} = C_{\text{aq}} v_a \quad (18.13)$$

while the number of moles of HOC in the sorbed phase at equilibrium is

$$n_{\text{sorb}} = K_{d,\text{cmc}} C_{\text{aq}} w_{\text{soil}} \quad (18.14)$$

where $K_{d,cmc}$ is a linear soil-aqueous-phase partition coefficient that characterizes the equilibrium distribution of the HOC between soil and monomeric surfactant solution at the CMC over a specified organic compound concentration range.³⁰ This coefficient is defined as the ratio of the number of moles of HOC sorbed per gram of soil to the number of moles of HOC dissolved per liter of monomeric surfactant solution at the CMC:

$$K_{d,cmc} = (n_{sorb}/w_{soil})/(n_{aq}/v_a) \quad (18.15)$$

$K_{d,cmc}$ has nominal units of liters per gram. The value of $K_{d,cmc}$ can be obtained experimentally for a system of soil, water, surfactant, and HOC. Alternatively, $K_{d,cmc}$ may be estimated as¹⁷

$$K_{d,cmc} = K_d(S/S_{cmc})(f'_{oc}/f_{oc}) = K_{oc}(S/S_{cmc})(f'_{oc}) \quad (18.16)$$

where K_d = a linear soil-water partition coefficient in the absence of surfactant in nominal units of liters per gram

S = the solubility of the HOC in pure water in moles per liter

S_{cmc} = the enhanced solubility of the HOC in surfactant solution at the CMC, also in units of moles per liter

f_{oc} = the fractional natural organic carbon content of the soil

f'_{oc} = the fractional organic carbon content of the soil after sorption of surfactant

K_{oc} = the linear soil-water partition coefficient in the absence of surfactant, normalized for soil organic carbon content, in nominal units of liters per gram

Experimental or estimated values for S and K_{oc} often are available from the literature. Experiments with soil alone permit determination of f_{oc} . The value of f'_{oc} can be calculated with a knowledge of f_{oc} , the molecular weight of the surfactant, the weight fraction of organic carbon in the surfactant, and Q_{surf} . S_{cmc} can be evaluated through measurement of organic solute concentration in monomeric surfactant solution at the CMC.

MODELING HOC PARTITIONING IN SYSTEMS OF SOIL AND MICELLAR SURFACTANT SOLUTION

Edwards et al. describe a model that permits characterization of solubilization behavior in systems of soil, micellar surfactant solution, and HOC.¹⁷ F , the fraction of HOC in bulk solution, is defined as

$$F = (n_{aq} + n_{mic})/(n_{aq} + n_{mic} + n_{sorb}) \quad (18.17)$$

where n_{mic} is the number of moles of HOC solubilized in the micellar pseudophase, given by the product of the MSR and the number of moles of micellar surfactant in solution:

$$n_{\text{mic}} = \{[K_m V_w C_{\text{aq}}]/[1 - K_m V_w C_{\text{aq}}]\} [m_{\text{tot}} - Q_{\text{surf}} w_{\text{soil}} - v_a \text{CMC}] \quad (18.18)$$

Substitution of Equations 18.13, 18.14, and 18.18 into Equation 18.17 and division of both numerator and denominator by C_{aq} yields an equation which permits modeling of the mole fraction of HOC present in the bulk solution:¹⁷

$$F = \frac{v_a + \{[K_m V_w][m_{\text{tot}} - Q_{\text{surf}} w_{\text{soil}} - v_a \text{CMC}]/[1 - K_m V_w C_{\text{aq}}]\}}{v_a + \{[K_m V_w][m_{\text{tot}} - Q_{\text{surf}} w_{\text{soil}} - v_a \text{CMC}]/[1 - K_m V_w C_{\text{aq}}]\} + w_{\text{soil}} K_{d,\text{cmc}}} \quad (18.19)$$

where C_{aq} is given by the following expression:

$$c_{\text{aq}} = \frac{-b + \sqrt{b^2 - 4ac}}{2a} \quad (18.20)$$

$$\begin{aligned} \text{where } a &= \{-K_m V_w(1 + K_{d,\text{cmc}} w_{\text{soil}}/v_a)\} \\ b &= \{[C_{\text{init}} K_m V_w(1 + K_d w_{\text{soil}}/v_a)] + [1 + K_{d,\text{cmc}} w_{\text{soil}}/v_a] + \\ &\quad [K_m V_w(m_{\text{tot}} - Q_{\text{surf}} w_{\text{soil}} - v_a \text{CMC})/v_a]\} \\ c &= \{-C_{\text{init}}[1 + K_d w_{\text{soil}}/v_a]\} \end{aligned}$$

and where C_{init} represents the original aqueous-phase organic compound concentration before the addition of surfactant to the soil-aqueous-phase system. Equation 18.20 can also be expressed in terms of the initial total mass of PAH in the system.

Figure 18.7 shows the results of modeling $C_8\text{PE}_{9.5}$ surfactant solubilization of pyrene in a system of 0.045 L of water and 6.25 g of soil with Equations 18.19 and 18.20 using parameter values obtained from independent experimental tests and shown in Table 18.4.^{16,22-24,30,31} Calculated values of percent pyrene in bulk solution ($F \times 100\%$) are plotted as a function of surfactant dose and compared with the experimental data of Liu et al.³⁰ The agreement appears to be reasonable and illustrates the utility of the model as a predictor of HOC partitioning in systems of soil and micellar surfactant solution of uniform concentration.

CONCLUSION

The apparent solubility of certain PAH compounds can be enhanced by as much as a factor of two in nonionic surfactant solutions having surfactant concentrations less than the CMC. The apparent solubility of PAH compounds in general can be enhanced to a much greater extent, however, through solubilization in nonionic surfactant micelles. Micellar solubilization commences at the CMC and is a linear function of micellar surfactant concentration. PAH partitioning between micellar and aqueous pseudophases can be

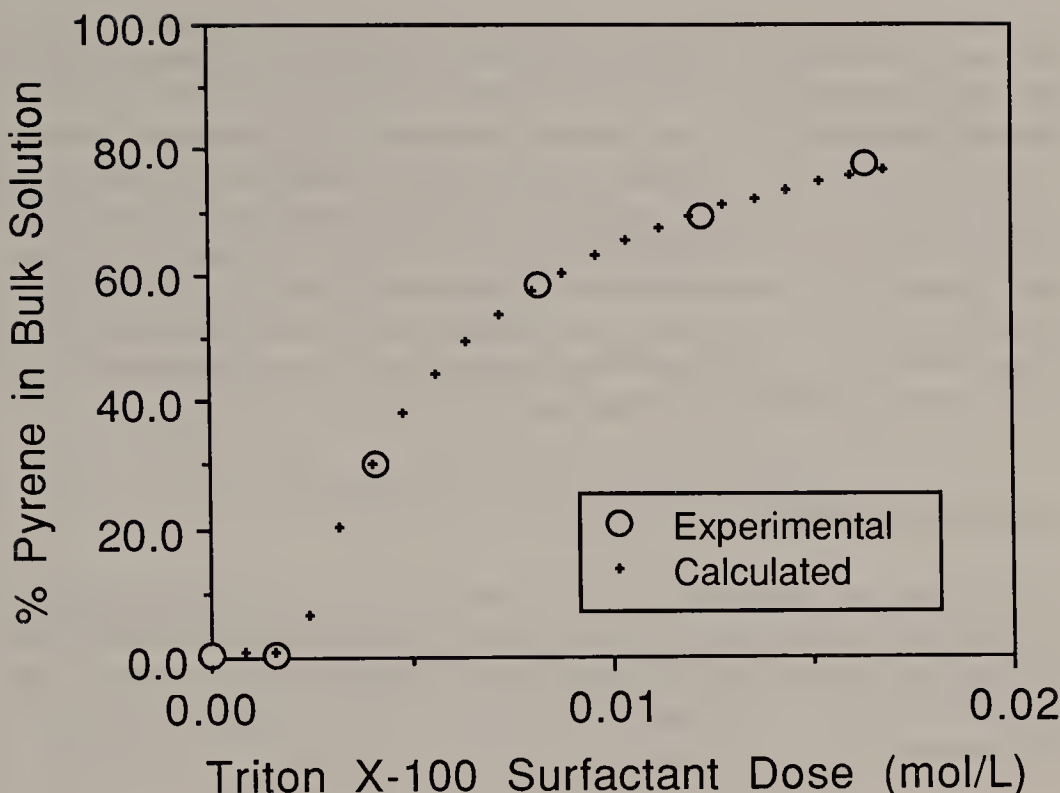


Figure 18.7. Percent pyrene in the bulk aqueous phase as a function of $C_8PE_{9.5}$ nonionic surfactant dose. This nonlinear relationship is modeled with Equations 18.19 and 18.20 and is shown accompanied by experimental data from Liu et al.³⁰

characterized by a mole fraction micelle-aqueous-pseudophase partition coefficient, K_m . For a given surfactant solution, $\log K_m$ is a linearly decreasing function of the logarithm of the PAH solubility, S ; the mole fraction of PAH solubilized in the micellar pseudophase is a decreasing function of PAH molecular weight.

The dose of nonionic surfactant required to attain the aqueous-phase CMC in a soil-water system is significantly larger than that for clean water owing to sorption of surfactant onto soil. Nonionic surfactant sorption onto soil

Table 18.4. Model Parameter Values for Figure 18.7

Parameter	Value	Reference
pyrene C_{init}	S in pure water	30
pyrene S in pure water	6.8×10^{-7} mol/L	22
(S/S_{cmc}) in experimental solution	0.42	31
pyrene $\log K_{ow}$	5.18	23
soil f_{oc}	0.0096	30
Q_{surf} for soil- $C_8PE_{9.5}$ solution	1.431×10^{-5} mol/g	24
pyrene K_{oc}	$6.3 \times 10^{-4} K_{ow}$	23
$\log K_m$ for pyrene- $C_8PE_{9.5}$ solution	6.03	16
$C_8PE_{9.5}$ aqueous-phase CMC	1.7×10^{-4} mol/L	24

increases the fractional organic carbon content of the soil, which tends to increase HOC sorption. Nonionic surfactant monomers in solution, on the other hand, enhance HOC apparent solubility and tend to decrease HOC sorption. The net effect is a change in the value of the soil-water partition coefficient, the sign and magnitude of the change depending on the relative contributions of the sorption and solubility effects. An estimate for a modified HOC soil-water partition coefficient can be calculated, as can the aqueous-pseudophase HOC concentration. A mathematical model for estimating the fraction of HOC in bulk solution is presented that incorporates parameters whose values can be obtained from independent tests. The model results appear to fit experimental data reasonably well.

ACKNOWLEDGMENT

We express our appreciation to Annette Jacobson and Shonali Laha of Carnegie Mellon University for their helpful comments. Appreciation is also extended to the two reviewers of this chapter. This work was sponsored by the U.S. EPA, Office of Exploratory Research, under grant number R-816113-01-0.

NOTATION AND UNITS USED IN THIS CHAPTER

- C_{aq} = HOC concentration in the aqueous pseudophase in a micellar surfactant system (mol/L)
- C_{surf} = bulk solution surfactant concentration (mol/L)
- CMC = critical micelle concentration of surfactant (mol/L)
- f_{carbon} = weight fraction of carbon in the surfactant (dimensionless)
- f_{oc} = weight fraction of natural organic carbon in the soil (dimensionless)
- f'_{oc} = weight fraction of organic carbon content in the soil after surfactant is sorbed (dimensionless)
- F = fraction of HOC mass in bulk solution by weight (dimensionless)
- K_d = HOC soil-water partition coefficient (L/g)
- K_{oc} = organic carbon normalized HOC soil-water partition coefficient (L/g)
- $K_{d,cmc}$ = HOC soil-aqueous-pseudophase partition coefficient for a system of soil and solution having an aqueous-pseudophase surfactant concentration equal to the CMC (L/g)
- K_{ow} = HOC octanol-water partition coefficient (dimensionless)
- K_m = HOC mole fraction micelle-aqueous-pseudophase partition coefficient (dimensionless)
- m_{mic} = mass of surfactant in micelles in the system (moles)
- m_{sorb} = mass of surfactant sorbed onto soil in the system at the CMC (moles)

- m_{tot} = total mass of surfactant in the system (moles)
 MSR = molar solubilization ratio (dimensionless)
 n_{aq} = mass of HOC in the aqueous phase of the soil-water system (moles)
 n_{sorb} = mass of HOC in the sorbed phase of the soil-water system (moles)
 Q_{surf} = mass of surfactant sorbed per unit weight of soil (mol/g)
 S = HOC solubility in water (mol/L)
 S_{cmc} = HOC solubility as enhanced by surfactant monomers in a solution having an aqueous-phase surfactant concentration equal to the CMC (mol/L)
 V_w = molar volume of water in the system (L/mol)
 v_a = volume of the aqueous phase or pseudophase in a system (L)
 w_{soil} = weight of soil (g)
 X_a = mole fraction of HOC in the aqueous pseudophase
 X_m = mole fraction of HOC in the micellar pseudophase

REFERENCES

1. Lambert, S. M., P. E. Porter, and H. Schieferstein. "Movement and Sorption of Chemicals Applied to the Soil," *Weeds* 13:185-190 (1965).
2. Fink, D. H., G. W. Thomas, and W. J. Meyer. "Adsorption of Anionic Detergents by Soils," *J. Water Poll. Control Fed.* 42(2):265-271 (1970).
3. Urano, K., M. Saito, and C. Murata. "Adsorption of Surfactants on Sediments," *Chemosphere* 13(2):293-300 (1984).
4. Hand, V. C., and G. K. Williams. "Structure-Activity Relationships for Sorption of Linear Alkylbenzenesulfonates," *Environ. Sci. Technol.* 21(4):370-373 (1987).
5. DiToro, D. D., L. J. Dodge, and Y. C. Hand. "A Model for Anionic Surfactant Sorption," *Environ. Sci. Technol.* 24(7):1013-1020 (1990).
6. Ellis, W. D., J. R. Payne, and G. D. McNabb. "Treatment of Contaminated Soils with Aqueous Surfactants," U.S. EPA Final Report-600/2-85/129, NTIS PB86-122561 (1986).
7. Nash, J. H., and R. P. Traver. "Field Evaluation of In-Situ Washing of Contaminated Soils with Water/Surfactants," in *Land Disposal, Remedial Action, Incineration and Treatment of Hazardous Wastes: Proc. of 12th Ann. Res. Symp.*, U.S. EPA Report-600/9-86/022 (1986), pp. 208-217.
8. Rickabaugh, J., S. Clement, and R. F. Lewis. "Surfactant Scrubbing of Hazardous Chemicals from Soil," in *Proc. 41st Purdue Ind. Waste Conf.* (Ann Arbor, MI: Lewis Publishers, 1986), pp. 377-382.
9. Rajput, V. S., S. Pilapitiya, M. E. Singley, and A. J. Higgins. "Detoxification of Hazardous Waste Contaminated Soils and Residues by Washing and Biodegradation," in *Proc. Intl. Conf. on Physicochemical and Biol. Detox. of Haz. Wastes*, Y. C. Wu, Ed. (Lancaster, PA: Technomic, 1989), pp. 409-417.
10. Vignon, B. W., and A. J. Rubin. "Practical Considerations in the Surfactant-Aided Mobilization of Contaminants in Aquifers," *J. Water Poll. Control Fed.* 61(7):1233-1240 (1989).
11. Huling, S. G. "Facilitated Transport," Robert S. Kerr Environmental Laboratory, U. S. EPA Report-540/4-89/003 (1989).
12. Kan, A. T., and M. B. Thompson. "Facilitated Transport of Naphthalene and

- Phenanthrene in a Sandy Soil Column with Dissolved Organic Matter-Macromolecules and Micelles," in *Proc. of the NWWA/API Conf. Pet. Hyd. Org. Chem. Grd. Wat. - Prevention, Detection and Restoration* (Dublin, OH: Water Well Jour. Pub. Co., 1986), pp. 93-105.
13. Valsaraj, K. T., and L. J. Thibodeaux. "Relationship between Micelle-Water and Octanol-Water Partition Constants for Hydrophobic Organics of Environmental Interest," *Water Res.* 23(2):183-189 (1989).
 14. Thurman, E. M., L. B. Barber, Jr., and D. LeBlanc. "Movement and Fate of Detergents in Groundwater: A Field Study," *J. Contam. Hydrol.* 1(2):143-161 (1986).
 15. Kile, D. E., and C. T. Chiou. "Water Solubility Enhancements of DDT and Trichlorobenzene by Some Surfactants Below and Above the Critical Micelle Concentration," *Environ. Sci. Technol.* 23(7):832-838 (1989).
 16. Edwards, D. A., R. G. Luthy, and Z. Liu. "Solubilization of Polycyclic Aromatic Hydrocarbons in Micellar Nonionic Surfactant Solutions," *Environ. Sci. Technol.* 25(1):127-133 (1991).
 17. Edwards, D. A., Z. Liu, and R. G. Luthy. "Nonionic Surfactant Solubilization of Hydrophobic Organic Compounds in Soil/Aqueous Systems," Dept. of Civil Engineering, Carnegie Mellon University (in publication).
 18. Attwood, D., and A. T. Florence. *Surfactant Systems: Their Chemistry, Pharmacy and Biology* (New York: Chapman and Hall, 1983).
 19. Rosen, M. J. *Surfactants and Interfacial Phenomena*, 2nd ed. (New York: John Wiley and Sons, 1989).
 20. Martin, A. N., J. Swarbrick, and A. Cammarata. *Physical Pharmacy* (Philadelphia: Lea and Febiger, 1969).
 21. Hayase, K., and S. Hayano. "The Distribution of Higher Alcohols in Aqueous Micellar Solutions," *Bull. Chem. Soc. Japan* 50(1):83-85 (1977).
 22. Mackay, D., and W. Y. Shiu. "A Critical Review of Henry's Law Constants for Chemicals of Environmental Interest," *J. Phys. Chem. Ref. Data* 10(4):1175-1199 (1981).
 23. Karickhoff, S. W., D. S. Brown, and T. A. Scott. "Sorption of Hydrophobic Pollutants on Natural Sediments," *Water Res.* 13(3):241-248 (1979).
 24. Liu, Z., D. A. Edwards, and R. G. Luthy. "Sorption of Nonionic Surfactants onto Soil," Dept. of Civil Engineering, Carnegie Mellon University (in publication).
 25. Chiou, C. T., V. H. Freed, D. W. Schmedding, and R. L. Kohnert. "Partition Coefficient and Bioaccumulation of Selected Organic Chemicals," *Environ. Sci. Technol.* 11(5):475-477 (1977).
 26. Aston, J. R., J. E. Lane, and T. W. Healy. "The Solution and Interfacial Chemistry of Nonionic Surfactants Used in Coal Flotation," *Mineral Proc. Extr. Metal. Rev.* 5(4):229-256 (1989).
 27. Partyka, S., S. Zaina, M. Lindheimer, and B. Brun. "The Adsorption of Non-Ionic Surfactants on a Silica Gel," *Colloid Surf.* 12(5):255-270 (1984).
 28. Clunie, J. S., and B. T. Ingram. "Adsorption of Nonionic Surfactants," in *Adsorption from Solution at the Solid/Liquid Interface*, G. D. Parfitt and C. H. Rochester, Eds. (London: Academic Press, 1983), pp. 105-152.
 29. Chiou, C. T., P. E. Porter, and D. W. Schmedding. "Partition Equilibria of Non-ionic Organic Compounds between Soil Organic Matter and Water," *Environ. Sci. Technol.* 17(4):227-231 (1983).
 30. Liu, Z., S. Laha, and R. G. Luthy. "Surfactant Solubilization of Polycyclic Aro-

- matic Hydrocarbons in Soil/Water Suspensions," *Water Sci. Tech.* 23:475-485 (1991).
31. Edwards, D. A., Z. Liu, and R. G. Luthy. "Comparison of Experimental Data with Model Results for Nonionic-Surfactant Solubilization of Polycyclic Aromatic Hydrocarbons in Soil/Water Systems," Dept. of Civil Engineering, Carnegie Mellon University (in publication).

PART IV

ANALYTICAL

CHAPTER 19

Determination of Anthropogenic Organic Compounds Associated with Fixed or Suspended Solids/Sediments: An Overview

Martha J. M. Wells and V. Dean Adams

INTRODUCTION

The role of aquatic sediments in the fate and transport of pollutants is the focus of substantial current interest. Contaminants, in particular anthropogenic organic compounds (AOC), are potentially adsorbed by sediments from natural waters. Concentrations of AOC in sedimentary material may be greater than those observed in the water.

The heterogeneous nature of sedimentary materials complicates analytical protocol development for anthropogenic organic compounds. Suspended solids/sediments in natural waters are chemically intricate systems of water immiscible mineral particulates, colloidal materials, and living or decaying organisms. They are composed of inorganics, such as kaolin, bentonite, illite, and silica, and naturally occurring organic materials, such as amino acids, peptides, monosaccharides, carbohydrates, and tannic, humic, and fulvic acids. These autochthonous materials originate from geological detritus as well as animal and vegetative biomass remains.

Complex equilibria govern partitioning of organic pollutants in natural waters among the aqueous phase, dissolved organic carbon, and fixed or suspended sedimentary materials, and are not well understood. Most studies to date concentrate on the relationship between the partition coefficient of the organic contaminant, and the organic carbon content of the sediment. Research in this area has demonstrated that, in general, the accumulation potential of foreign organics in sediments is greater for organic solutes having large octanol-water partition coefficients, and for sediments containing a high proportion of naturally occurring organic matter. The influence of this "associated" state on the ultimate degradation of such organic compounds, or their bioavailability to the food chain, is unclear. Ongoing studies of these issues call for the continual development of rapid, yet reliable, analytical protocols for

the determination of organics associated with fixed or suspended solids and sediments.

OBJECTIVES AND METHODS

A discussion of the current status and unresolved issues related to the analysis of anthropogenic organic compounds associated with fixed or suspended solids or sediments is provided. The research of two decades, 1969–1989, is summarized. Although a literature search revealed that much research on this subject has been published by German and Japanese scientists in those languages, the articles reviewed are limited to those published in English. This overview includes only the analysis of sedimentary material. Related research on soils is omitted. Differences in the quantity and quality of naturally occurring aquatic and terrestrial humic materials, which can require different purification procedures, and differences in sample handling procedures resulting from the disparity in moisture content between sediments and soils, justify the omission of references to protocol with soils from this effort.

Research on sample collection procedures for fixed or suspended solids and sediments is reviewed in Table 19.1.^{1–44} [Editor's Note: All tables are at the end of the chapter.] Analytical methodology for anthropogenic organic compounds is outlined in a tabular format presenting a historical perspective on method development (Tables 19.2–19.14). This overview includes procedures for the determination of petroleum-derived compounds,^{45–88} polychlorinated biphenyls,^{85,89–99} dioxins and dibenzofurans,^{100–103} pesticides,^{104–131} miscellaneous chlorinated compounds,^{132–141} phenolic compounds,^{142–146} surfactants,^{147–151} phthalates,^{152–156} alkyl and aryl phosphates,^{157–159} organometallic compounds,^{160–177} miscellaneous anthropogenic organic compounds,^{178–183} and multiclass anthropogenic organic compounds^{184–203} associated with fixed or suspended solids or sediments.

The majority of published papers on anthropogenic organics associated with sediments are concentrated in four chemical categories: petroleum-derived compounds, polychlorinated biphenyls (PCBs), pesticides, and organometallic compounds. Environmental problems caused by polychlorinated biphenyls were identified by the late 1960s. By 1969, research on the analysis of petroleum-derived compounds—particularly polycyclic aromatic hydrocarbons (PAHs)—associated with sediments was under way, and extensive research on pesticides had been published. Other factors that produce the high publication rate for PAHs, PCBs, pesticides, and organometallics are (1) the usage rate and extent of commercial distribution that govern introduction into the environment and (2) the highly hydrophobic nature of these compounds, which mediates the degree of association with the sediment once introduced into the environment. Because sediments function not only as sinks but also sources of organic substrates,²⁰⁴ analysts are still concerned with the determi-

nation of some contaminants long after their commercial usage has been curtailed by environmental regulation.

As in any review of this type, in spite of precautions taken to assure completeness, some research will doubtless be inadvertently overlooked. For the most part, the articles included are publications that concentrated on analytical research. Equally valid are analytical protocols presented in extensive fate and transport studies. However, analytical methodology imbedded in these types of references was difficult to locate, and/or the details of analysis were often sketchy or published separately. Some references to protocol contained within more extensive environmental studies are included, however. In a few instances, publications were omitted from this review because they contained insufficient analytical detail, did not add substantial new information to references already cited, or were not readily available.

Related reviews of analytical methodology for certain categories of anthropogenic organic compounds associated with various environmental media, including sediments, have been published. Only a review by Zitko is dedicated solely to the analysis of aquatic sediments for organic compounds.²⁰⁵ Lichtenthaler²⁰⁶ and Clark²⁰⁷ discussed petroleum-derived compounds, and chlorinated dioxins and dibenzofurans were reviewed by Donnelly et al.²⁰⁸ Pesticide analyses were reviewed by Chesters et al.,²⁰⁹ Hylin,²¹⁰ and Nash et al.,²¹¹ organochlorine analyses, by Wells;²¹² and organometallic compounds by Ashby et al.²¹³ The publications of Chesters et al.²⁰⁹ and Ashby et al.²¹³ were presented in a tabular fashion similar to this overview. Articles reviewed in those papers on pesticides and organometallics, overlapping the time period presented here, are not included in Tables 19.6 or 19.12. State-of-the-art methods addressing sampling; analytical methods; aquatic biological, microbiological, and virological methods; QA/QC; and risk assessment of sediment, sludge, and waste streams were presented by Lichtenberg et al.²¹⁴ This overview is designed to supplement, rather than repeat, information previously published.

DISCUSSION

Analyzing for trace organic contaminants in the presence of the complex background of organic and inorganic components found naturally in sediments is a complicated, tedious, and expensive task. Chau and Lee itemize a generalized, seven-step scheme for residue analysis that will form the outline of this discussion:²¹⁵

1. sampling, sample handling, preservation, and storage
2. sample preparation
3. extraction
4. cleanup
5. determination
6. confirmation of identity

7. confirmation of quantity

No single step in this scheme is more important than another. Improper procedure at any stage leads to inappropriate results.

Sampling, Sample Handling, Preservation, and Storage

A sample is a part intended to show the nature of the whole. Most environmental studies are sampled in both space and time. The importance of planning a statistically sound sampling schedule prior to collection cannot be overemphasized. Obtaining a homogeneous sample of a heterogeneous system is certainly a challenge, and the resulting analytical data are only as reliable as the sample collection procedure.

Sampling techniques for sediments and suspended particulate matter were recently discussed by Norris.²¹⁶ Grab sampling as well as more sophisticated instream composite sampling are used to collect suspended solids and sediments (Table 19.1). Sampling bottom materials is done manually, or by using various types of dredges, coring devices, or cryogenic samplers. Sampling in deeper waters may require divers. Cryogenic samplers are especially appropriate for preserving stratified sample layers. Sampling for suspended particulate matter can involve filtration, the use of sediment traps, or continuous-flow centrifugation techniques.

If the sample cannot be analyzed immediately, it is stored under chilled or frozen conditions. Depending on the desired analysis, the presence or absence of atmospheric oxygen may be controlled to preserve sample integrity. "EPA Test Methods for Evaluating Solid Waste," commonly known as "SW-846," presents sampling considerations and recommends widemouthed glass containers with Teflon liners, maintained at 4°C.²¹⁷ Sediment samples should be held no longer than 14 days prior to analysis.

Sample Preparation

Various techniques used to prepare sediment samples for extraction are reported in Tables 19.3–19.14 (Table 19.2 assigns the chemical categories presented in Tables 19.3–19.14). Sediments were extracted either in the moist state after centrifuging or decanting excess water, after addition of sodium sulfate to complex water present in the sample, or were air-dried, oven-dried, or freeze-dried. In some cases, moisture is refortified to known levels prior to extraction. When sodium sulfate is added, the reported sediment-to-sodium sulfate ratios ranged from 1:1 to 1:5. The "EPA Test Methods for Evaluating Solid Waste" recommends the addition of sodium sulfate at one to two times the weight of sediment.²¹⁷

One problem with air-drying is that microbial activity is still ongoing in the sample after collection, and biological degradation of the organic contaminant may continue. Some researchers overcome this difficulty by adding biocides, such as formaldehyde or sodium azide, to reduce microbial activity. Oven-

drying or freeze-drying can selectively diminish the levels of volatile organic chemicals in the sediment sample. The effect of moisture content on extraction procedures continues to be debated in the literature and may indeed be more pronounced in the analysis of certain chemical categories. However, a growing number of authors appear to have reached the conclusion, as have Dunnivant and Elzerman,⁹⁸ that "drying of samples prior to extraction is probably undesirable."

As originally designed, Tables 19.3–19.14 included a column detailing the method of fortification of the sedimentary sample matrix for sample spikes. So few of the articles provided this information that the category was eventually dropped from the format. However, this omission does not diminish the importance of preparing laboratory-fortified samples representative of environmentally contaminated samples. Fortification procedures are the foundation on which our conclusions regarding environmental contamination are built. Errors at this stage of the scheme may lead to gross under-or overestimation of environmental impacts. Lee and Chau found less reliable results (i.e., a larger coefficient of variation) for the determination of PCBs extracted from naturally contaminated dry sediments as compared to spiked wet sediment.^{218,219} In 1980, Bellar et al. demonstrated, in research comparing the Soxhlet, sonification, and steam distillation extraction of PCBs and pesticides from environmentally contaminated sediments and from laboratory-fortified sediments, that each of the three extraction procedures gave near quantitative recoveries for the spiked samples, while Soxhlet extraction gave significantly greater recoveries from environmentally contaminated sediments than sonification or steam distillation.¹⁸⁸

The fortification procedures cited most often by those authors providing this information are (1) spiking into the liquid organic sediment extract or (2) spiking directly onto the sediment with contaminants contained in either an organic (water-miscible or immiscible) or aqueous solvent, followed by either immediate extraction or extraction after a specified aging period. All are reasonable procedures as long as the meaning of the extraction efficiency represented by the data is clear. For example, spiking into the organic sediment extract is valid as long as it is understood that this recovery value reflects the procedural error only from that point forward in the extraction scheme. Spiking with organic solvents, even if allowed to evaporate before proceeding with the extraction, may not adequately distribute the contaminants in the sediment or reflect the natural binding processes occurring in the environment. There is not yet enough data in the literature to conclusively compare fortification procedures. However, spiking organic contaminants from aqueous solutions or aqueous mixtures with polar, water-miscible, organic solvents onto sediments under conditions of controlled moisture content, followed by thorough mixing and aging for a specified period of time, should most closely represent an environmentally contaminated sample.

Providing an answer to the question of what the specified period of time should be, is difficult. Ozretich and Schroeder report that storage time and/or

temperature had significant effects on the recovery of organic compounds from spiked sediment.¹⁹⁵ Karickhoff states that "sorbed chemicals become increasingly difficult to extract with increased incubation time in the sorbed state."²²⁰ Organics appear to form both "reversible" and "irreversible" associations with sediments that may directly affect environmental fate and certainly influence analytical recovery. Research on appropriate methods of fortification is still needed.

Extraction

Chemical treatments are used to separate anthropogenic organic contaminants from sediments and suspended solids. Frequently, a miscible, sometimes azeotropic, combination of polar and nonpolar solvents is selected for the extraction. Such solvent combinations overcome the difficulty of wetting the surface of the sediment and are an appropriate compromise for extracting both polar and nonpolar organic contaminants.

The four most commonly used extraction techniques are stirring/shaking, sonication, Soxhlet, and steam distillation. Reported recoveries obtained with steam distillation are usually less than those reported for Soxhlet or sonication techniques, but extracts may require little or no further purification. Other, less commonly used, extraction or desorption techniques reported in Tables 19.3–19.14 include static headspace or dynamic headspace (i.e., purge-and-trap), pyrolysis, or supercritical fluid extractions. The "EPA Test Methods for Evaluating Solid Waste" includes standard procedures for Soxhlet (Method 3540), sonication (Method 3550), and purge-and-trap (Method 5030) extraction.²¹⁷

Cleanup: Purification/Fractionation

Extraction of contaminants from sedimentary materials is usually followed by purification or fractionation of the extract using liquid-liquid and/or chromatographic extraction. Depending on the method of preparation of the sediment (e.g., extracted moist, dried, sodium sulfate added, etc.), choosing the next step in the analytical scheme may be dictated by the presence of water and/or water-miscible organic solvents.

For partitioning the sediment extract by liquid-liquid extraction, a water-immiscible solvent such as hexane or methylene chloride is often selected. Organic components may be separated into hydrophilic and hydrophobic acid, base, and neutral fractions (SW-846 Method 3650).²¹⁷

Chromatographic extractions can likewise be used to produce purification and fractionation of sediment extracts. Those cited in Tables 19.3–19.14 utilize a variety of sorbent materials, such as silica gel, alumina, carbon, Florisil, synthetic polymeric resins, and bonded silicas, and various chromatographic techniques, including thin-layer chromatography, linear and nonlinear column chromatography, gel permeation chromatography, and high-performance liq-

uid chromatography. The "EPA Test Methods for Evaluating Solid Waste" details procedures for cleanup with alumina (Methods 3610, 3611), Florisil (Method 3620), silica gel (Method 3630), and gel permeation (Method 3640).²¹⁷

One particularly ubiquitous interferant in sediment extracts is sulfur.^{186,221-223} If not removed, the presence of sulfur in the extract will interfere with the final determination of many compounds, particularly chlorinated organic contaminants. Approaches to removing sulfur from the extract include treatment with copper, nickel, mercury, or tetrabutylammonium sulfite, or separation by gas chromatography or gel permeation chromatography. The "EPA Test Methods for Evaluating Solid Waste" procedure for sulfur cleanup (Method 3660) utilizes copper, mercury, or tetrabutylammonium sulfite.²¹⁷

Comparison of Sample Preparation Technologies

Table 19.15 is a subset of the articles cited in Tables 19.3-19.14. It outlines those references in which studies were performed to compare various procedures for sediment preparation, extraction, purification, and fractionation. The variants compared include many of those discussed to this point. Comparisons of field wet, sodium sulfate added, freeze-dried, air-dried, and oven-dried sediment preparation methods; stirring/shaking, Soxhlet, sonication, supercritical fluid, purging, and steam distillation extraction techniques; non-polar solvents alone and in combination with miscible polar solvents, and supercritical fluids as extraction solvents; and alumina, silica gel, and gel permeation sediment extract purification procedures are cited in Table 19.15. The techniques that produce the best results, as concluded by the authors, are given. Extraction efficiency alone was not the only criterion used by these authors to determine the "best technique." When high recovery is accompanied by high variability, a more reproducible technique may be preferred even if extraction efficiency is lower. Some authors selected the "best" procedure based on simplicity, or time and/or solvent consumption.

Inspection of Table 19.15 leads to the conclusion that, at the current state-of-the-art in sediment analysis for organic contaminants, it is not possible to definitively recommend any single method for sediment preparation, extraction, purification, and fractionation. Obviously, as for many other sample matrices, advances in sample preparation technology for sediments have lagged behind improvements in analytical instrumentation. Further research is warranted.

Final Determination

Virtually every appropriate type of analytical instrumentation has been tested for the final determination of organics associated with sediments. The chronological order in which Tables 19.3-19.14 are arranged reveals the increased sophistication of analytical techniques applied to the analysis of organics associated with sedimentary material during the past 20 years.

Gas chromatography is indeed the analytical workhorse of environmental analyses; however, liquid chromatography is preferred for nonvolatile compounds and for those compounds that are labile under conditions required by gas chromatography. For the determination of very complicated samples, such as the multiclass anthropogenic organic compounds in Table 19.14, researchers have employed fractionation of sediment extracts by high-performance liquid chromatography, using nondestructive modes of detection, followed by gas chromatographic analysis of the fractions.²⁰⁰⁻²⁰³

Some research on development of field measurement methods of extraction and final determination for detecting the presence of organic contaminants in sediments was reported.²²⁴⁻²²⁶ The "8000 Series" of the "EPA Test Methods for Evaluating Solid Waste" provides gas chromatographic, gas chromatographic/mass spectrometric, and high-performance liquid chromatographic methods for the determination of organic analytes.²¹⁷

Confirmation of Identity

While some instrumental methods allow confirmation of quantity only, others provide confirmation of identity as well, depending on whether the detector senses specific or bulk properties of the organic compound. Truly confirmatory tests are those based upon some unique chemical property of a substance, leaving no doubt as to the structure producing the given results. Two categories of such tests exist: those involving chemical reaction and those involving spectroscopic and spectrometric analysis. Chemical modification of the sample, or derivatization, is one solution to achieving improved detectability or improved chromatographic conditions.

Confirmation of Quantity

Standard Reference Materials

Standard reference materials (SRMs) for organics associated with sediments have been developed in this country by the National Institute of Standards and Technology (NIST), formerly the National Bureau of Standards, and by comparable institutions in other countries. At least one commercial vendor currently offers an SRM for organics in sediments. Several authors have published research on the development of standard reference materials for sediments.^{85,89,90} Epstein et al. recently commented that the ideal sediment reference material should be certified for both inorganic and organic constituents, noting the problem with that approach to be the equipment used to collect and process the sediment for organics is a source of contamination for metals, and vice versa.²²⁷ Wells identified the need for reference materials for which low levels of contaminants are established, to be used for method blanks or spiked addition.²²⁸

The difficulties in developing SRMs for sediments involve many of the same

analytical quandaries alluded to earlier in this discussion. Four possible permutations of types of sediment reference materials exist: natural or spiked samples can be supplied either wet or dry.⁹⁰ Although the need for standardized wet sediment homogenates is recognized,²²⁸ and some researchers have prepared fortified wet sediment reference materials,^{89,90} most sediment SRMs are supplied as dried powders. Certainly, dried materials are easier to handle and are less subject to microbial change. However, volatile compounds may be lost during drying procedures, and uncertainty regarding the effects of moisture content on extraction leads researchers to question whether analytical reference materials should be prepared and supplied in a dry or wet state.

The method of fortification of standard reference materials, as with laboratory-fortified samples, is also at issue. Should these materials be derived from sources of environmental contamination or prepared by spiking? Environmentally contaminated sediments represent the "natural" situation, but establishing the true pollutant level is difficult and involves analysis by two or more methods in more than one laboratory. The levels of laboratory-fortified samples can be known more precisely, but the fortification method and the aging process are complicating factors.

Interlaboratory Method Validation

Several interlaboratory studies, most commonly comparing recovery of petroleum-derived contaminants^{78,195,229-232} or PCBs,^{95,218,219} have been conducted, although one interlaboratory study of polychlorinated dibenzofurans and dioxins analyses¹⁰⁰ and two studies of multiclass contaminated sediments^{199,203} were reported. Interlaboratory variability is usually reported as the coefficient of variation or relative standard deviation and ranged about 30% or less.

Errors in the preparation of analytical standard calibration solutions were identified as contributing to the variability in intercomparison experiments.²²⁸ Albaiges and Grimalt confirmed that the extraction-partition step was the main source of error in the interlaboratory survey they conducted.⁷⁸

From interlaboratory validation studies involving PCBs, some research groups have concluded that most of the variability is due to the complex quantitation methods required for the determination of polychlorinated biphenyls.^{95,218,219} The problems of quantitating PCBs are worth noting even though the difficulty is not confined to the analysis of sediments. Some researchers have solved this problem by converting all PCBs to a single compound, either by perchlorination or dechlorination.^{184,233} Others have quantified these compounds by comparison with commercial formulations (e.g., Aroclors),²³⁴ by grouping isomers according to level of chlorination,²³⁵⁻²³⁸ by grouping congeners exhibiting similar response factors,^{237,239} or as individual constituents.²⁴⁰

CONCLUSIONS

Our knowledge of the distribution of organics in the aquatic environment grows in direct correlation to the development of improved analytical methods for the determination of contaminants associated with suspended solids and sediments. A historical perspective of analytical method development in tabularized format is presented to provide easy access to published protocol for a wide variety of anthropogenic organic contaminants. The major unresolved issues in analytical method development for organics associated with sedimentary materials appear to include sampling equipment and overall sampling strategies, determination of the appropriate moisture content comprising samples and standard reference materials at the time of extraction, and fortification procedures for preparation of representative sample spikes and standard reference materials. Continuing research in these areas is needed.

ACKNOWLEDGMENTS

The authors wish to express their appreciation to Laura Buenning, Tami Fish, Dodd Galbreath, Barbara Goodson, Linda Mulder, and Mary Williford for their assistance in the preparation of this manuscript.

REFERENCES

Sample Collection Procedures

1. Little, J. A., J. H. Finger, and R. W. Knight. "Regional and State Needs in Sampling and Analytical Methodology," in *Chemical and Biological Characterization of Sludges, Sediments, Dredge Spoils, and Drilling Muds, ASTM STP 976*, J. J. Lichtenberg, J. A. Winter, C. I. Weber, and L. Fradkin, Eds. (Philadelphia: American Society for Testing and Materials, 1988), pp. 18-24.
2. Pitard, F. F. "The Variographic Experiment: An Essential Test for Optimizing Sampling Methodology in Monitoring Streams," in *Chemical and Biological Characterization of Sludges, Sediments, Dredge Spoils, and Drilling Muds, ASTM STP 976*, J. J. Lichtenberg, J. A. Winter, C. I. Weber, and L. Fradkin, Eds. (Philadelphia: American Society for Testing and Materials, 1988), pp. 44-58.
3. Håkanson, L. "Sediment Sampling in Different Aquatic Environments: Statistical Aspects," *Water Resour. Res.* 20(1):41-46 (1984).
4. Plumb, R. H., Jr. "Sampling, Preservation, and Analysis of Sediment Samples: State-of-the-Art Limitations," in *Management of Bottom Sediments Containing Toxic Substances, Proceedings of the Fifth United States-Japan Experts Meeting*, U.S. EPA Report-600/9-80-044 (1980).
5. Parr, J. F., G. H. Willis, L. L. McDowell, C. E. Murphree, and S. Smith. "An Automatic Pumping Sampler for Evaluating the Transport of Pesticides in Suspended Sediments," *J. Environ. Qual.* 3(3):292-294 (1974).

6. Miller, C. R. "Sediment Sampling: Instrumentation and Techniques," *Trans. Am. Soc. Agric. Eng.* 8(2):267-270, 274 (1965).
7. Honsaker, J. L., I. A. Campbell, and R. B. Bryan. "Remote Semiautomatic Instrumentation for Intermittent Streamflow Measurements and Suspended Sediment Sampling," *Can. J. Civ. Eng.* 11(4):993-996 (December 1984).
8. Suffet, I. H., K. Hunchak, and T. Belton. "Trace Organic Analysis of Suspended Sediments Collected with an In-Stream Composite Sampler: The Need for a Standard Method," in *Chemical and Biological Characterization of Sludges, Sediments, Dredge Spoils, and Drilling Muds, ASTM STP 976*, J. J. Lichtenberg, J. A. Winter, C. I. Weber, and L. Fradkin, Eds. (Philadelphia: American Society for Testing and Materials, 1988), pp. 184-203.
9. Analytical Quality Control (Harmonised Monitoring) Committee. "Accuracy of Determination of Total Suspended Solids in River Waters: Analytical Quality Control in the Harmonised Monitoring Scheme," *Analyst* 108:1365-1373 (November 1983).
10. Becchi, I., P. Billi, and P. Tacconi. "Analysis of a Simple Suspended Load Integrating Sampler," in *Proceedings of the Florence Symposium, Erosion and Sediment Transport Measurement*, IAHs Publication No. 133 (Washington, DC: International Association of Hydrological Sciences, 1981), pp. 115-122.
11. Bennett, J. P. "At-Stream-Velocity Pumping Sediment Sampling System," *J. Hydraul. Div., ASCE*, Paper 9801, 99(HY6):873-887 (1973).
12. Bryant, R., D. J. A. Williams, and A. E. James. "A Sampler for Cohesive Sediment in the Benthic Boundary Layer," *Limnol. Oceanogr.* 25(3):572-576 (1980).
13. Bates, T. S., S. E. Hamilton, and J. D. Cline. "Collection of Suspended Particulate Matter for Hydrocarbon Analyses: Continuous Flow Centrifugation Versus Filtration," *Estuar. Coastal Shelf Sci.* 16:107-112 (1983).
14. Burrus, D., R. L. Thomas, J. Dominik, and J. P. Vernet. "Recovery and Concentration of Suspended Solids in the Upper Rhone River by Continuous Flow Centrifugation," *Hydrol. Proc. HYPRE3* 3(1):65-74 (1989).
15. Dressing, S. A., J. Spooner, J. M. Kreglow, E. O. Beasley, and P. W. Westerman. "Water and Sediment Sampler for Plot and Field Studies," *J. Environ. Qual.* 16(1):59-64 (1987).
16. Guy, H. P. "Laboratory Theory and Methods for Sediment Analysis," in *Techniques of Water-Resources Investigations of the United States Geological Survey*, USGS, Arlington, VA (1969).
17. Hansen, E. "Field Test on an Automatic Suspended Sediment Pumping Sampler," *Trans. Am. Soc. Agric. Eng.* 9(5):739-743 (1966).
18. Jackson, R. E. "Development of Methods for Sampling, Preserving and Analyzing Contaminated Ground Waters and Aquifer Sediments," in *Hydrology Research Division, Annual Progress Reports and Short Research Notes, 1977-78*, Report Series No. 64 HR 75-1 (Ottawa: Environment Canada Inland Waters Directorate, 1979), pp. 32-42.
19. Jones, B. L. "Simplified Pumping Sampler for Suspended Sediments," *Geol. Surv. Res. 1969, Prof. Pap. 650-C* (1969), pp. 212-214.
20. Walling, D. E., and A. Teed. "A Simple Pumping Sampler for Research into Suspended Sediment Transport in Small Catchments," *J. Hydrol.* 13:325-337 (1971).

21. King, E. W., and D. A. Everett. "A Remote Sampling Device for Under-Ice Water, Bottom Biota and Sediments," *Limnol. Oceanog.* 25(5):935-938 (1980).
22. Melcher, R. G., T. L. Peters, and H. W. Emmel. "Sampling and Sampling Preparation of Environmental Material," *Top. Curr. Chem.* 134(Anal. Probl.):59-123 (1986).
23. Reed, G. D. "Evaluation of the Standard Sampling Technique for Suspended Solids," U.S. EPA Report-907/9-77-001 (1977).
24. Simpson, W. R. "Particulate Matter in the Oceans—Sampling Methods, Concentration, Size Distribution and Particle Dynamics," *Oceanog. Mar. Biol. Ann. Rev.* 20:119-172 (1982).
25. Fleming, G. "Suspended Solids Monitoring: A Comparison Between Three Instruments," *Water Water Eng.* 73(883):366-382 (1969).
26. Busatti, G., A. Magagnoli, M. Mengol, and S. Guerzoni. "A Sediment-Water Core Sampler for Coastal Pollution Studies," *Environ. Technol. Lett.* 9:375-378 (1988).
27. Baker, E. T., H. B. Milburn, and D. A. Tennant. "Field Assessment of Sediment Trap Efficiency under Varying Flow Conditions," *J. Mar. Res.* 46:573-592 (1988).
28. Scrudato, R. J., G. Yogis, and G. Hocutt. "In-Situ Integrated Suspended Sediment Stream Sampler (IS3)," *Environ. Geol. Water Sci.* 12:177-179 (1988).
29. Kimmel, B. L., R. P. Axler, and C. R. Goldman. "A Closing, Replicate-Sample, Sediment Trap," *Limnol. Oceanog.* 22(4):768-772 (1977).
30. Kellerhals, R., and D. I. Bray. "Sampling Procedures for Coarse Fluvial Sediments," *J. Hydraul. Div., ASCE Proc.*, Paper 8279, 97(HY8):1165-1180 (1971).
31. John, P. H., M. A. Lock, and M. M. Gibbs. "Two New Methods for Obtaining Water Samples from Shallow Aquifers and Littoral Sediments," *J. Environ. Qual.* 6(3):322-324 (1977).
32. Straughan, D. "Field Sampling Methods and Techniques for Marine Organisms and Sediments," NBS Spec. Publ. 409, Marine Pollution Monitoring (Petroleum), Proceedings of a Symposium and Workshop, Gaithersburg, MD (1974), pp. 183-187.
33. Bruce, H. E., and S. P. Cram. "Sampling Marine Organisms and Sediments for High Precision Gas Chromatographic Analysis of Aromatic Hydrocarbons," NBS Spec. Pub. 409, Marine Pollution Monitoring (Petroleum), Proceedings of a Symposium and Workshop, Gaithersburg, MD (1974), pp. 181-182.
34. Daniel, T. C., and G. Chesters. "Design and Construction of a Shallow Water Sediment Core Sampler," *Environ. Lett.* 1(3):225-228 (1971).
35. Satake, K. "Handy Impact Corer for Sampling Lake Surface Sediment," *Hydrobiologia* 169:259-264 (1988).
36. Fukuhara, H., and M. Sakamoto. "Improved Ekman-Birge Grab for Sampling an Undisturbed Bottom Sediment Core Sample," *Japan. J. Limnol. RIZAA* 48(2):127-132 (1987).
37. Heinemann, W. H., and M. J. Brown. "Fractional Water-Sediment Sampler," *Soil Sci. Soc. Am. Proc.* 36(2):376-377 (1972).
38. Knaus, R. M. "Cryogenic Coring Device for Sampling Loose, Unconsolidated Sediments Near the Water Sediment Interface," *J. Sed. Petrol.* 56(4):551-553 (1986).
39. Moshiri, G. A., D. P. Brown, and W. G. Crumpton. "An Inexpensive and Easily

- Fabricated Sampler for Collecting Sediment Cores to Measure EH Potentials," *Florida Scientist* 40(2):203-205 (1977).
40. Noble, M., P. C. Oloffs, R. So, J. Yee, and F. Yuen. "A Device for Sampling the Mud-Water Interface in Eutrophic Lakes and Bogs for Residue Analysis," *J. Environ. Sci. Health* B21(5):359-373 (1986).
 41. Hairr, L. M., and M. E. Wrenn. "Environmental Sampling for River Sediments Around a Nuclear Power Station," *Trans. Am. Nucl. Soc.* 15:82-83 (1972).
 42. Reeburgh, W. S., and R. E. Erickson. "A 'Dipstick' Sampler for Rapid, Continuous Chemical Profiles in Sediments," *Limnol. Oceanog.* 27(3):556-559 (1982).
 43. Williams, J. D. H., and A. E. Pashley. "Lightweight Corer Designed for Sampling Very Soft Sediments," *J. Fish. Res. Bd. Can.* 36:241-246 (1979).
 44. Stevens, H. H., Jr., and G. A. Lutz. "Collapsible-Bag Suspended Sediment Sampler," *J. Hydraul. Div., ASCE Proc.* 106:608-615 (1980).

Petroleum-Derived Compounds

45. Scarratt, D. J., and V. Zitko. "Bunker C Oil in Sediments and Benthic Animals from Shallow Depths in Chedabucto Bay, N.S.," *J. Fish. Res. Bd. Can.* 29:1347-1350 (1972).
46. Zafiriou, O. C. "Petroleum Hydrocarbons in Narragansett Bay: II. Chemical and Isotopic Analysis," *Estuar. Coastal Mar. Sci.* 1(1):81-87 (1973).
47. Bean, R. M., J. W. Blaylock, E. A. Sutton, R. E. Wildung, and F. M. Davidson. "Characterization of Sediments in the Vicinity of Offshore Petroleum Production," *Div. Pet. Chem., ACS* 19(4):726-35 (1974).
48. Giger, W., and M. Blumer. "Polycyclic Aromatic Hydrocarbons in the Environment: Isolation and Characterization by Chromatography, Visible, Ultraviolet, and Mass Spectrometry," *Anal. Chem.* 46:1663-1671 (1974).
49. Hunter, L., H. E. Guard, and L. H. DiSalvo. "Determination of Hydrocarbons in Marine Organisms and Sediments by Thin Layer Chromatography," NBS Special Publication 409, Marine Pollution Monitoring (Petroleum), Proceedings of a Symposium and Workshop, Gaithersburg, MD (1974), pp. 213-216.
50. Hargrave, B. T., and G. A. Phillips. "Estimates of Oil in Aquatic Sediments by Fluorescence Spectroscopy," *Environ. Poll.* 8:193-215 (1975).
51. Hertz, H. S., W. E. May, S. N. Chesler, and B. H. Gump. "Analysis of Microgram/kg (ppb) Level Hydrocarbons in Intertidal Zone Sediments and Water by Gas Chromatography-Mass Spectrometry," in *Proceedings of 23rd Annual Conference on Mass Spectrometry and Allied Topics* (Springfield, VA: National Technical Information Service, 1975), pp. 663-665.
52. May, W. E., S. N. Chesler, S. P. Cram, B. H. Gump, H. S. Hertz, D. P. Enagonio, and S. M. Dyszel. "Chromatographic Analysis of Hydrocarbons in Marine Sediments and Seawater," *J. Chromatog. Sci.* 13(11):535-540 (1975).
53. Chesler, S. N., B. H. Gump, H. S. Hertz, W. E. May, S. M. Dyszel, and D. P. Enagonio. "Trace Hydrocarbon Analysis: The National Bureau of Standards Prince William Sound/Northeastern Gulf of Alaska Baseline Study," National Bureau of Standards Technical Note 889 (1976).
54. Chesler, S. N., B. H. Gump, H. S. Hertz, W. E. May, and S. A. Wise. "Methods for Analysis of Trace Levels ($\mu\text{g}/\text{kg}$) of Hydrocarbons in the Marine Environment," NBS Special Publication 464 (1977), pp. 81-85.
55. Strosher, M. T., and G. W. Hodgson. "Polycyclic Aromatic Hydrocarbons in

- Lake Waters and Associated Sediments: Analytical Determination by Gas Chromatography-Mass Spectrometry," in *Water Quality Parameters, ASTM STP 573* (Philadelphia: American Society for Testing and Materials, 1975), pp. 259-270.
- 56. Walker, J. D., R. R. Colwell, M. C. Hamming, and H. T. Ford. "Extraction of Petroleum Hydrocarbons from Oil-Contaminated Sediments," *Bull. Environ. Contam. Toxicol.* 13(2):245-248 (1975).
 - 57. Miles, D. H., M. J. Coign, and L. R. Brown. "A Liquid Chromatographic Fluorescence Technique for Estimating Crude Oil in Water, Sediment, and Biological Material," *API Publ. 4284* (1977), pp. 179-182.
 - 58. Wise, S. A., S. N. Chesler, H. S. Hertz, L. R. Hilpert, and W. E. May. "Chemically-Bonded Aminosilane Stationary Phase for the High-Performance Liquid Chromatographic Separation of Polynuclear Aromatic Compounds," *Anal. Chem.* 49:2306-2310 (1977).
 - 59. Giger, W., and C. Schaffner. "Determination of Polycyclic Aromatic Hydrocarbons in the Environment by Glass Capillary Gas Chromatography," *Anal. Chem.* 50(2):243-249 (1978).
 - 60. Black, J. J., P. P. Dymerski, and W. F. Zapisek. "Routine Liquid Chromatographic Method for Assessing Polynuclear Aromatic Hydrocarbon Pollution in Fresh Water Environments," *Bull. Environ. Contam. Toxicol.* 22:278-284 (1979).
 - 61. Meuser, J. M., F. R. Moore, P. E. Strup, and J. E. Wilkinson. "Analysis of Polycyclic Aromatic Hydrocarbons in Air and Water," in *Spec. Conf.: Control Specific (Toxic) Pollut., [Proc.]*, E. R. Frederick, Ed. (Pittsburgh, PA: Air Pollution Control Association, 1979), pp. 109-117.
 - 62. Griest, W. H. "Multicomponent Polycyclic Aromatic Hydrocarbon Analysis of Inland Water and Sediment," *Environ. Sci. Res.* 16:173-183 (1980).
 - 63. Tjessem, K. "On the Importance of Fractionation of Environmental Samples Prior to Analysis by High Resolution Gas Chromatography," *Chem. Scr.* 15(4-5):189-92 (1980).
 - 64. Whelan, J. K., J. M. Hunt, and A. Y. Huc. "Applications of Thermal Distillation-Pyrolysis to Petroleum Source Rock Studies and Marine Pollution," *J. Anal. Appl. Pyrolysis* 2(1):79-96 (1980).
 - 65. Obana, H., S. Hori, and T. Kashimoto. "Determination of Polycyclic Aromatic Hydrocarbons in Marine Samples by High-Performance Liquid Chromatography," *Bull. Environ. Contam. Toxicol.* 26:613-620 (1981).
 - 66. Ramos, L. S., and P. G. Prohaska. "Sephadex LH-20 Chromatography of Extracts of Marine Sediment and Biological Samples for the Isolation of Polynuclear Aromatic Hydrocarbons," *J. Chromatog.* 211:284-289 (1981).
 - 67. Santoni, B., and C. Mandon. "Determination of PAH in Water and Sediments by Low Temperature Fluorimetry," *Analisis* 9(6):259-264 (1981).
 - 68. Steinheimer, T. R., W. E. Pereira, and S. M. Johnson. "Application of Capillary Gas Chromatography Mass Spectrometry/Computer Techniques to Synoptic Survey of Organic Material in Bed Sediment," *Anal. Chim. Acta* 129:57-67 (1981).
 - 69. Belisle, A. A., and M. L. Gay. "Isolation of Hydrocarbon Residues from Sediment by Steam Distillation," *Bull. Environ. Contam. Toxicol.* 29:539-543 (1982).
 - 70. Matsumoto, G. "Comparative Study on Organic Constituents in Polluted and Unpolluted Inland Aquatic Environments: V. Organic Carbons and Hydrocarbons in Sediments," *Water Res.* 17(7):823-830 (1983).
 - 71. Eganhouse, R. P. "Long-Chain Alkylbenzenes: Their Analytical Chemistry, Envi-

- ronmental Occurrence and Fate," *Int. J. Environ. Anal. Chem.* 26:241–263 (1986).
72. Hagenmaier, H., H. Kaut, and P. Krauss. "Analysis of Polycyclic Aromatic Hydrocarbons in Sediments, Sewage Sludges and Composts from Municipal Refuse by HPLC," *Int. J. Environ. Anal. Chem.* 23:331–345 (1986).
73. Killops, S. D. "Identification of Petrogenic Contamination in Recent Sediments by HPLC Monitoring of Aromatic Components: A Preliminary Investigation," *Chemosphere* 15(3):229–241 (1986).
74. Lebo, J. A., and L. M. Smith. "Determination of Fluorene in Fish, Sediment, and Plants," *J. Assoc. Off. Anal. Chem.* 69(6):944–951 (1986).
75. de Leeuw, J. W., E. W. B. de Leer, J. S. Sinninghe Damste, and P. J. W. Schuyt. "Screening of Anthropogenic Compounds in Polluted Sediments and Soils by Flash Evaporation/Pyrolysis Gas Chromatography–Mass Spectrometry," *Anal. Chem.* 58:1852–1857 (1986).
76. Marcomini, A., B. Pavoni, R. Donazzolo, and A. A. Orio. "Combined Preparative and Analytical Use of Normal-Phase and Reversed-Phase High-Performance Liquid Chromatography for the Determination of Aliphatic and Polycyclic Aromatic Hydrocarbons in Sediments of the Adriatic Sea," *Mar. Chem.* 18:71–84 (1986).
77. West, W. R., P. A. Smith, G. M. Booth, S. A. Wise, and M. L. Lee. "Determination of Genotoxic Polycyclic Aromatic Hydrocarbons in a Sediment from the Black River (Ohio)," *Arch. Environ. Contam. Toxicol.* 15:241–249 (1986).
78. Albaiges, J., and J. Grimalt. "A Quality Assurance Study for the Analysis of Hydrocarbons in Sediments," *Int. J. Environ. Anal. Chem.* 31:281–293 (1987).
79. Garrigues, P., and M. Ewald. "High Resolution Emission Spectroscopy (Shpol'skii Effect): A New Analytical Technique for the Analysis of Polycyclic Aromatic Hydrocarbons (PAH) in the Environmental Samples," *Chemosphere* 16(2/3):485–494 (1987).
80. Hawthorne, S. B., and D. J. Miller. "Extraction and Recovery of Polycyclic Aromatic Hydrocarbons from Environmental Solids Using Supercritical Fluids," *Anal. Chem.* 59:1705–1708 (1987).
81. Morel, G., and P. Courtot. "A Study of an Extraction Procedure for Organic Trace Levels: Some Results Concerning Hydrocarbons in Marine Sediments," *Int. J. Environ. Anal. Chem.* 30:105–133 (1987).
82. Poole, S. K., T. A. Dean, and C. F. Poole. "Preparation of Environmental Samples for the Determination of Polycyclic Aromatic Hydrocarbons by Thin-Layer Chromatography," *J. Chromatog.* 400:323–341 (1987).
83. Saber, A., J. Jarosz, M. Martin-Bouyer, L. Paturel, and M. Vial. "Analysis of Polycyclic Aromatic Hydrocarbons in Lacustral Sediments by High Resolution Shpol'skii Spectrofluorimetry at 10 K," *Int. J. Environ. Anal. Chem.* 28:171–184 (1987).
84. Fernández, P., C. Porte, D. Barceló, J. M. Bayona, and J. Albaiges. "Selective Enrichment Procedures for the Determination of Polychlorinated Biphenyls and Polycyclic Aromatic Hydrocarbons in Environmental Samples by Gel Permeation Chromatography," *J. Chromatog.* 456:155–164 (1988).
85. Sim, P. G., W. D. Jamieson, S. S. Berman, and V. J. Boyko. "Sediment Reference Materials and the Canadian Marine Analytical Chemistry Standards Program," in *Chemical and Biological Characterization of Sludges, Sediments, Dredge Spoils, and Drilling Muds, ASTM STP 976*, J. J. Lichtenberg, J. A.

- Winter, C. I. Weber, and L. Fradkin, Eds. (Philadelphia: American Society for Testing and Materials, 1988), pp. 27-34.
- 86. Quilliam, M. A., and P. G. Sim. "Determination of Polycyclic Aromatic Compounds by High-Performance Liquid Chromatography with Simultaneous Mass Spectrometry and Ultraviolet Diode Array Detection," *J. Chromatog. Sci.* 26:160-167 (1988).
 - 87. Bianchi, A., and M. S. Varney. "Determination of Volatile Aromatic Hydrocarbons in Estuarine and Coastal Sediments Using Gas Syringe Injection of Head-space Vapours and Gas Chromatography With Flame-Ionisation Detection," *Analyst* 114:47-51 (1989).
 - 88. Giuliano, M., P. Doumenq, A. Jawad, and G. Mille. "Structural Characterization of Aromatic Isomers in Marine Sediments by Combined Gas Chromatography/Fourier Transform Infrared Spectroscopy," *Appl. Spect.* 43(3):571-573 (1989).

PCBs

- 89. Chau, A. S. Y., J. Carron, and H.-B. Lee. "Analytical Reference Materials. II. Preparation and Sample Integrity of Homogeneous Fortified Wet Sediment for Polychlorinated Biphenyl Quality Control Studies," *J. Assoc. Off. Anal. Chem.* 62(6):1312-1314 (1979).
- 90. Chau, A. S. Y., and H.-B. Lee. "Analytical Reference Materials. III. Preparation and Homogeneity Test of Large Quantities of Wet and Dry Sediment Reference Materials for Long Term Polychlorinated Biphenyl Quality Control Studies," *J. Assoc. Off. Anal. Chem.* 63(5):947-951 (1980).
- 91. Kerkhoff, M. A. T., A. de Vries, R. C. C. Wegman, and A. W. M. Hofstee. "Analysis of PCBs in Sediments by Glass Capillary Gas Chromatography," *Chemosphere* 11(2):165-174 (1982).
- 92. Oliver, B. G., and K. D. Nicol. "Gas Chromatographic Determination of Chlorobenzenes and Other Chlorinated Hydrocarbons in Environmental Samples Using Fused Silica Capillary Columns," *Chromatographia* 16:336-340 (1982).
- 93. Oliver, B. G., and A. J. Niimi. "Trophodynamic Analysis of Polychlorinated Biphenyl Congeners and Other Chlorinated Hydrocarbons in the Lake Ontario Ecosystem," *Environ. Sci. Technol.* 22(4):388-397 (1988).
- 94. McMurtrey, K. D., N. J. Wildman, and H. Tai. "Pyrolysis Gas Chromatography-Mass Spectrometry of Polychlorinated Biphenyls on Sediment," *Bull. Environ. Contam. Toxicol.* 31:734-737 (1983).
- 95. Alford-Stevens, A. L., W. L. Budde, and T. A. Bellar. "Interlaboratory Study on Determination of Polychlorinated Biphenyls in Environmentally Contaminated Sediments," *Anal. Chem.* 57:2452-2457 (1985).
- 96. Brownawell, B. J., and J. W. Farrington. "Partitioning of PCBs in Marine Sediments," in *Marine and Estuarine Geochemistry*, A. C. Sigleo and A. Hattori, Eds. (Chelsea, MI: Lewis Publishers, 1985), pp. 97-120.
- 97. Eisenreich, S. J. "The Chemical Limnology of Nonpolar Organic Contaminants: Polychlorinated Biphenyls in Lake Superior," in *Sources and Fates of Aquatic Pollutants*, Advances in Chemistry Series 216, R. A. Hites and S. J. Eisenreich, Eds. (Washington, DC: American Chemical Society, 1987), pp. 393-469.
- 98. Dunnivant, F. M., and A. W. Elzerman. "Determination of Polychlorinated Biphenyls in Sediments, Using Sonication Extraction and Capillary Column Gas

- Chromatography-Electron Capture Detection with Internal Standard Calibration," *J. Assoc. Off. Anal. Chem.* 71(3):551-556 (1988).
99. Huckins, J. N., T. R. Schwartz, J. D. Petty, and L. M. Smith. "Determination, Fate, and Potential Significance of PCBs in Fish and Sediment Samples with Emphasis on Selected AHH-Inducing Congeners," *Chemosphere* 17(10):1995-2016 (1988).

Dioxins and Dibenzofurans

100. Smith, L. M., D. L. Stalling, and J. L. Johnson. "Determination of Part-per-Trillion Levels of Polychlorinated Dibenzofurans and Dioxins in Environmental Samples," *Anal. Chem.* 56:1830-1842 (1984).
101. Cattabeni, F., A. di Domenico, and F. Merli. "Analytical Procedures to Detect 2,3,7,8-TCDD at Seveso after the Industrial Accident of July 10, 1976," *Ecotoxicol. Environ. Safety* 12:35-52 (1986).
102. Afghan, B. K., J. Carron, P. D. Goulden, J. Lawrence, D. Leger, F. Onuska, J. Sherry, and R. Wilkinson. "Recent Advances in Ultratrace Analysis of Dioxins and Related Halogenated Hydrocarbons," *Can. J. Chem.* 65:1086-1097 (1987).
103. Simon, N., J. Guzzetta, and D. Thielen. "GC/MS and GC/MS/MS: Complementary Techniques for the Quantitation of Tetrachlorodibenzo-*p*-dioxin in Soils and Sediments from Industrial Sites," *Chemosphere* 18:163-168 (1989).

Pesticides

104. Pfister, R. M., P. R. Dugan, and J. I. Frear. "Microparticulates: Isolation from Water and Identification of Associated Chlorinated Pesticides," *Science* 166:878-879 (1969).
105. Chau, A. S. Y. "Confirmation of Pesticide Residue Identity. V. Alternative Procedure for Derivative Formation in Solid Matrix for the Confirmation of α - and β -Endosulfan by Gas Chromatography," *J. Assoc. Off. Anal. Chem.* 55(6):1232-1238 (1972).
106. Lyons, E. T., and H. A. Salman. "Development of Analytical Procedures for Determining Chlorinated Hydrocarbon Residues in Waters and Sediments from Storage Reservoirs," Bureau of Reclamation, Denver, CO, Report No. REC-ERC-72-15 (1972).
107. Routh, J. D. "DDT Residues in Salinas River Sediments," *Bull. Environ. Contam. Toxicol.* 7(2/3):168-176 (1972).
108. Woodham, D. W., C. D. Loftis, C. W. Collier. "Identification of the Gas Chromatographic Dieldrin and Endrin Peaks by Chemical Conversion," *J. Agric. Food Chem.* 20(1):163-165 (1972).
109. Saleh, F. Y., and G. F. Lee. "Analytical Methodology for Kepone in Water and Sediment," *Environ. Sci. Technol.* 12(3):297-301 (1978).
110. Muir, D. C. G., and N. P. Grift. "Determination of Niclosamide (Bayer 2353) in Water and Sediment Samples," *Int. J. Environ. Anal. Chem.* 8:1-14 (1980).
111. Wegman, R. C. C., and A. W. M. Hofstee. "Determination of Organochlorines in River Sediment by Capillary Gas Chromatography. Application to Dutch River Sediment," *Water Res.* 16:1265-1272 (1982).
112. Gambrell, R. P., C. N. Reddy, V. Collard, G. Green, and W. H. Patrick, Jr. "The Recovery of DDT, Kepone, and Permethrin Added to Soil and Sediment Suspensions," *Environ. Sci. Technol.* 16(10):1030-1035 (1982).

- sions Incubated under Controlled Redox Potential and pH Conditions," *J. Water Poll. Control Fed.* 56(2):174-182 (1984).
113. Grift, N., and W. L. Lockhart. "Gas-Liquid Chromatographic Determination of Fenitrothion in Fish, Water, and Sediment," *J. Assoc. Off. Anal. Chem.* 57(6):1282-1284 (1974).
114. Kjølholt, J. "Determination of Trace Amounts of Organophosphorus Pesticides and Related Compounds in Soils and Sediments Using Capillary Gas Chromatography and a Nitrogen-Phosphorus Detector," *J. Chromatog.* 325:231-238 (1985a).
115. Kjølholt, J. "Determination of Dimethoate in Waste Water, Soil and Sediment Using Gel Permeation Chromatography for Sample Clean-up," *Int. J. Environ. Anal. Chem.* 20:161-166 (1985b).
116. Muir, D. C. G. "Determination of Terbutryn and Its Degradation Products in Water, Sediments, Aquatic Plants, and Fish," *J. Agric. Food Chem.* 28:714-719 (1980).
117. Janda, V., G. Steenbeke, and P. Sandra. "Supercritical Fluid Extraction of s-Triazine Herbicides from Sediment," *J. Chromatog.* 479:200-205 (1989).
118. Scott, B. F., E. Nagy, J. Hart, and B. K. Afghan. "New Extraction/GC Technique Finds Traces of Water Pollutants," *Ind. Res. Dev.* 24(4):130-134 (1982).
119. Lee, H.-B., and A. S. Y. Chau. "Analysis of Pesticide Residues by Chemical Derivatization. VI. Analysis of Ten Acid Herbicides in Sediment," *J. Assoc. Off. Anal. Chem.* 66(4):1023-1028 (1983).
120. Westlake, W. E., M. Ittig, and F. A. Gunther. "Determination of *m*-sec-Butylphenyl *N*-Methyl-*N*-thiophenylcarbamate (RE-11775) in Water, Soil and Vegetation," *Bull. Environ. Contam. Toxicol.* 8(2):109-112 (1972).
121. Reeves, R. G., and D. W. Woodham. "Gas Chromatographic Analysis of Methomyl Residues in Soil, Sediment, Water, and Tobacco Utilizing the Flame Photometric Detector," *J. Agric. Food Chem.* 22(1):76-78 (1974).
122. West, S. D., and S. J. Parka. "Determination of the Aquatic Herbicide Fluridone in Water and Hydrosoil: Effect of Application Method on Dissipation," *J. Agric. Food Chem.* 29:223-226 (1981).
123. Lee, H.-B., and A. S. Y. Chau. "Gas Chromatographic Determination of Trifluralin, Diallate, Triallate, Atrazine, Barban, Diclofop-Methyl, and Benzoylprop-Ethyl in Sediments at Parts Per Billion Levels," *J. Assoc. Off. Anal. Chem.* 66(6):1322-1326 (1983).
124. Dawson, V. K., and J. L. Allen. "Liquid Chromatographic Determination of Rotenone in Fish, Crayfish, Mussels, and Sediments," *J. Assoc. Off. Anal. Chem.* 71(6):1094-1096 (1988).
125. Hale, J. R., M. D. Walla, and T. A. Bryson. "Determination of Fenvalerate in Seawater and Sediment Utilizing Isotopic Dilution and GC/MS," *J. Agric. Food Chem.* 37:70-74 (1989).
126. Thompson, D. G., J. E. Cowell, R. J. Daniels, B. Staznik, and L. M. MacDonald. "Liquid Chromatographic Method for Quantitation of Glyphosate and Metabolite Residues in Organic and Mineral Soils, Stream Sediments, and Hardwood Foliage," *J. Assoc. Off. Anal. Chem.* 72(2):355-360 (1989).
127. Schutzmann, K. L., D. W. Woodham, and C. W. Collier. "Removal of Sulfur in Environmental Samples Prior to Gas Chromatographic Analysis for Pesticide Residues," *J. Assoc. Off. Anal. Chem.* 54(5):1117-1119 (1971).
128. Amore, F. "Analysis of Soil and Sediment to Determine Potential Pesticide Con-

- tamination of a Water Supply Impoundment," NBS, Special Publication 519 (1979), pp. 191-203.
129. Belisle, A. A., and D. M. Swineford. "Simple, Specific Analysis of Organophosphorus and Carbamate Pesticides in Sediments Using Column Extraction and Gas Chromatography," *Environ. Toxicol. Chem.* 7:749-752 (1988).
130. Marble, L. K., and J. J. Delfino. "Extraction and Solid Phase Cleanup Methods for Pesticides in Sediment and Fish," *Am. Lab.* 20:23-32 (1988).
131. Barceló, D., and J. Albaigés. "Characterization of Organophosphorus Compounds and Phenylurea Herbicides by Positive and Negative Ion Thermospray Liquid Chromatography-Mass Spectrometry," *J. Chromatog.* 474:163-173 (1989).

Miscellaneous Chlorinated Compounds

132. Murray, A. J., and J. P. Riley. "The Determination of Chlorinated Aliphatic Hydrocarbons in Air, Natural Waters, Marine Organisms, and Sediments," *Anal. Chim. Acta* 65:261-270 (1973).
133. Erickson, M. D., R. A. Zweidinger, L. C. Michael, and E. D. Pellizzari. "Environmental Monitoring Near Industrial Sites: Polychloronaphthalenes," U.S. EPA Report-560/6-77-019 (1978), pp. 1-267.
134. Hollies, J. I., D. F. Pinnington, A. J. Handley, M. K. Baldwin, and D. Bennett. "The Determination of Chlorinated Long-Chain Paraffins in Water, Sediment and Biological Samples," *Anal. Chim. Acta* 111:201-213 (1979).
135. Ellington, J. "Analysis of Volatile Organics on Sediments and in Associated Water," in *Advances in the Identification and Analysis of Organic Pollutants in Water*, Volume 2, L. H. Keith, Ed. (Ann Arbor, MI: Ann Arbor Science, 1981), pp. 729-746.
136. Hiatt, M. H. "Analysis of Fish and Sediment for Volatile Priority Pollutants," *Anal. Chem.* 53:1541-1543 (1981).
137. Amin, T. A., and R. S. Narang. "Determination of Volatile Organics in Sediment at Nanogram-per-Gram Concentrations by Gas Chromatography," *Anal. Chem.* 57:648-651 (1985).
138. Onuska, F. I., and K. A. Terry. "Determination of Chlorinated Benzenes in Bottom Sediment Samples by WCOT Column Gas Chromatography," *Anal. Chem.* 57:801-805 (1985).
139. Charles, M. J., and M. S. Simmons. "Recovery Studies of Volatile Organics in Sediments Using Purge/Trap Methods," *Anal. Chem.* 59:1217-1221 (1987).
140. Lee, H.-B. "Determination of Twenty-One Chloroanisoles in Water and Sediment Samples," *J. Assoc. Off. Anal. Chem.* 71(4):803-807 (1988).
141. Scholz, B., and N. Palauschek. "The Determination of Substituted Aromatic Amines in Water and Sediment Samples," *Fres. Z. Anal. Chem.* 331:282-289 (1988).

Phenolics

142. Goldberg, M. C., and E. R. Weiner. "Extraction and Concentration of Phenolic Compounds from Water and Sediment," *Anal. Chim. Acta* 115:373-378 (1980).
143. Pierce, R. H., Jr., S. A. Gower, and D. M. Victor. "Pentachlorophenol and Degradation Products in Lake Sediment," in *Contaminants and Sediments, Vol-*

- ume 2: *Analysis, Chemistry, Biology*, R. A. Baker, Ed. (Ann Arbor, MI: Ann Arbor Science, 1980), pp. 43–56.
- 144. Lee, H.-B., Y. D. Stokker, and A. S. Y. Chau. "Analysis of Phenols by Chemical Derivatization. V. Determination of Pentachlorophenol and 19 Other Chlorinated Phenols in Sediments," *J. Assoc. Off. Anal. Chem.* 70(6):1003–1008 (1987).
 - 145. Cardwell, T. J., I. C. Hamilton, M. J. McCormick, and R. K. Symons. "Determination of 2-Phenylphenol and 4-Chloro-3-Methylphenol in Water and Sediments by Liquid Chromatography Using Electrochemical Detection," *Int. J. Environ. Anal. Chem.* 34:167–178 (1988).
 - 146. Shiraishi, H., D. S. Carter, and R. A. Hites. "Identification and Determination of *tert*-Alkylphenols in Carp from the Trenton Channel of the Detroit River, Michigan, USA," *Biomed. Environ. Mass Spect.* 18:478–483 (1989).

Surfactants

- 147. Uchiyama, M. "Separation and Determination of Fluorescent Whitening Agent and Alkyl Benzenesulfonate in Water," *Water Res.* 13:847–853 (1979).
- 148. De Henau, H., E. Mathijs, and W. D. Hopping. "Linear Alkylbenzene Sulfonates (LAS) in Sewage Sludges, Soils and Sediments: Analytical Determination and Environmental Safety Considerations," *Int. J. Environ. Anal. Chem.* 26:279–293 (1986).
- 149. Matthijs, E., and H. De Henau. "Determination of LAS. Determination of Linear Alkylbenzene Sulfonates in Aqueous Samples, Sediments, Sludges and Soils Using HPLC," *Tenside Surfactants Detergents* 24:193–199 (1987).
- 150. Marcomini, A., and W. Giger. "Simultaneous Determination of Linear Alkylbenzenesulfonates, Alkylphenol Polyethoxylates, and Nonylphenol by High-Performance Liquid Chromatography," *Anal. Chem.* 59:1709–1715 (1987).
- 151. Inaba, K., and K. Amano. "HPLC Determination of Linear Alkylbenzenesulfonate (LAS) in Aquatic Environment. Seasonal Changes in LAS Concentration in Polluted Lake Water and Sediment," *Int. J. Environ. Anal. Chem.* 34:203–213 (1988).

Phthalates

- 152. Webster, R. D. J., and G. Nickless. "Problems in the Environmental Analysis of Phthalate Esters," *Proc. Analyt. Div. Chem. Soc.* 13(11):333–335 (1976).
- 153. Payne, W. R., Jr., and J. E. Benner. "Liquid and Gas Chromatographic Analysis of Diethyl Phthalate in Water and Sediment," *J. Assoc. Off. Anal. Chem.* 64(6):1403–1407 (1981).
- 154. Waldock, M. J. "Determination of Phthalate Esters in Samples from the Marine Environment Using Gas Chromatography Mass Spectrometry," *Chemistry in Ecology* 1:261–277 (1983).
- 155. Thurén, A. "Determination of Phthalates in Aquatic Environments," *Bull. Environ. Contam. Toxicol.* 36:33–40 (1986).
- 156. Thurén, A., and A. Södergren. "Clean-Up with Sulphuric Acid Prior to the Gas Chromatographic Determination of Phthalate Esters," *Int. J. Environ. Anal. Chem.* 28:309–315 (1987).

Alkyl and Aryl Phosphates

157. Muir, D. C. G., N. P. Grift, and J. Solomon. "Extraction and Cleanup of Fish, Sediment, and Water for Determination of Triaryl Phosphates by Gas-Liquid Chromatography," *J. Assoc. Off. Anal. Chem.* 64(1):79–84 (1981).
158. Muir, D. C. G., and N. P. Grift. "Extraction and Cleanup Procedures for Determination of Diarylphosphates in Fish, Sediment, and Water Samples," *J. Assoc. Off. Anal. Chem.* 66(3):684–690 (1983).
159. Ishikawa, S., M. Taketomi, and R. Shinohara. "Determination of Trialkyl and Triaryl Phosphates in Environmental Samples," *Water Res.* 19(1):119–125 (1985).

Organometallics

Organometallic Lead

160. Chau, Y. K., P. T. S. Wong, G. A. Bengert, and O. Kramar. "Determination of Tetraalkyllead Compounds in Water, Sediment, and Fish Samples," *Anal. Chem.* 51(2):186–188 (1979).
161. Tiravanti, G., A. Rozzi, M. Dall'Aglio, W. Delaney, and A. Dadone. "The Cavtat Accident: Evaluation of Alkyl Lead Pollution by Simulation and Analytical Studies," *Prog. Wat. Technol.* 12(1):49–65 (1980).
162. Chau, Y. K., P. T. S. Wong, G. A. Bengert, and J. L. Dunn. "Determination of Dialkyllead, Trialkyllead, Tetraalkyllead, and Lead(II) Compounds in Sediment and Biological Samples," *Anal. Chem.* 56:271–274 (1984).
163. Wong, P. T. S., Y. K. Chau, J. Yaromich, P. Hodson, and M. Whittle. "The Analyses of Alkyllead Compounds in Fish and Environmental Samples in Ontario, Canada," *Appl. Organomet. Chem.* 3:59–70 (1989).

Organometallic Mercury

164. Ealy, J. A., W. D. Shults, and J. A. Dean. "Extraction and Gas Chromatographic Determination of Methyl-, Ethyl-, and Methoxyethylmercury(II) Halides," *Anal. Chim. Acta* 64:235–241 (1973).
165. Longbottom, J. E., R. C. Dressman, and J. J. Lichtenberg. "Gas Chromatographic Determination of Methyl Mercury in Fish, Sediment, and Water," *J. Assoc. Off. Anal. Chem.* 56(6):1297–1303 (1973).
166. Floyd, M., and L. E. Sommers. "Determination of Alkylmercury Compounds in Lake Sediments by Steam Distillation-Flameless Atomic Absorption," *Anal. Lett.* 8(8):525–535 (1975).
167. Shariat, M. "Determination of Dialkyl Mercury Compounds by Gas Chromatography," *J. Chromatog. Sci.* 17:527–530 (1979).

Organometallic Nickel

168. Nakamura, A., and T. Kashimoto. "Determination of Total Organic Nitrogen and Organometallic Nickel in Oil, Sediments and Marine Products," *Bull. Environ. Contam. Toxicol.* 22:345–349 (1979).

Organometallic Tin

169. Gilmour, C. C., J. H. Tuttle, and J. C. Means. "Determination of Picogram Quantities of Methyltins in Sediment," *Anal. Chem.* 58:1848-1852 (1986).
170. Tsuda, T., H. Nakanishi, T. Morita, and J. Takebayashi. "Simultaneous Gas Chromatographic Determination of Dibutyltin and Tributyltin Compounds in Biological and Sediment Samples," *J. Assoc. Off. Anal. Chem.* 69(6):981-984 (1986).
171. Epler, K. S., T. C. O'Haver, G. C. Turk, and W. A. MacCrehan. "Laser-Enhanced Ionization as a Selective Detector for the Liquid Chromatographic Determination of Alkyltins in Sediment," *Anal. Chem.* 60:2062-2066 (1988).
172. Turk, G. C., W. A. MacCrehan, K. S. Epler, T. C. O'Haver. "Laser-Enhanced Ionization as an Element Specific Detector for Liquid Chromatography," in *Proceedings of the Fourth International Symposium on Resonance Ionization Spectroscopy, and Its Applications: Resonance Ionization Spectroscopy NBS Institute of Physics Conference Series No. 94: Section 9*, T.B. Lucatorto and J.E. Parks, Eds. (Bristol and Philadelphia: Institute of Physics, 1989), pp. 327-330.
173. Huggett, R. G., M. A. Unger, F. A. Espourteille, and C. D. Rice. "Determination of Tributyltin in the Marine Environment," *J. Res. NBS* 93(3):277-279 (1988).
174. Stephenson, M. D., and D. R. Smith. "Determination of Tributyltin in Tissues and Sediments by Graphite Furnace Atomic Absorption Spectrometry," *Anal. Chem.* 60:696-698 (1988).
175. Matthias, C. L. "A Gas Chromatographic Determination of Tributyltin Species in Estuarine Water and Sediment Using Hydride Derivatization and Flame Photometric Detection," *Diss. Abstr. Int. B*. 49(8):3150 (1989).
176. Siu, K. W. M., G. J. Gardner, and S. S. Berman. "Ionspray Mass Spectrometry/Mass Spectrometry: Quantitation of Tributyltin in a Sediment Reference Material for Trace Metals," *Anal. Chem.* 61:2320-2322 (1989).

Multiclass Organometallic Tin and Lead Analyses

177. Donard, O. F. X., L. Randall, S. Rapsomanikis, and J. H. Weber. "Developments in the Speciation and Determination of Alkylmetals (Sn, Pb) Using Volatilization Techniques and Chromatography-Atomic Absorption Spectroscopy," *Int. J. Environ. Anal. Chem.* 27:55-67 (1986).

Miscellaneous Anthropogenic Organic Compounds

178. Jaffe, R., and R. A. Hites. "Fate of Hazardous Waste Derived Organic Compounds in Lake Ontario," *Environ. Sci. Technol.* 20(3):267-274 (1986).
179. Epstein, P. S., T. Mauer, M. Wagner, S. Chase, and B. Giles. "Determination of Parts-per-Billion Concentrations of Dioxane in Water and Soil by Purge and Trap Gas Chromatography/Mass Spectrometry or Charcoal Tube Enrichment Gas Chromatography," *Anal. Chem.* 59:1987-1990 (1987).
180. Headley, J. V. "GC/MS Identification of Organosulphur Compounds in Environmental Samples," *Biomed. Environ. Mass Spect.* 14:275-280 (1987).
181. Tsukioka, T., and T. Murakami. "Capillary Gas Chromatographic-Mass Spectrometric Determination of Pyridine Bases in Environmental Samples," *J. Chromatog.* 396:319-326 (1987).

182. Breitung, V., B. Packebusch, and O. Hutzinger. "Analysis of Disperse Yellow 42 in Environmental Samples," *Int. J. Environ. Anal. Chem.* 32:135-144 (1988).
183. Watanabe, N., H. Nagase, and Y. Ose. "Distribution of Silicones in Water, Sediment and Fish in Japanese Rivers," *Sci. Total Environ.* 73:1-9 (1988).

Multiclass Anthropogenic Organics

184. Berg, O. W., P. L. Diosady, and G. A. V. Rees. "Column Chromatographic Separation of Polychlorinated Biphenyls from Chlorinated Hydrocarbon Pesticides, and Their Subsequent Gas Chromatographic Quantitation in Terms of Derivatives," *Bull. Environ. Contam. Toxicol.* 7(6):338-347 (1972).
185. Goerlitz, D. F., and L. M. Law. "Determination of Chlorinated Insecticides in Suspended Sediment and Bottom Material," *J. Assoc. Off. Anal. Chem.* 57(1):176-181 (1974).
186. Jensen, S., L. Renberg, and L. Reutergardh. "Residue Analysis of Sediment and Sewage Sludge for Organochlorines in the Presence of Elemental Sulfur," *Anal. Chem.* 49:316-318 (1977).
187. Veith, G. D., and L. M. Kiwus. "An Exhaustive Steam-Distillation and Solvent-Extraction Unit for Pesticides and Industrial Chemicals," *Bull. Environ. Contam. Toxicol.* 17(6):631-636 (1977).
188. Bellar, T. A., J. T. Lichtenberg, and S. C. Lonneman. "Recovery of Organic Compounds from Environmentally Contaminated Bottom Materials," in *Contaminants and Sediments, Volume 2: Analysis, Chemistry, Biology*, R. A. Baker, Ed. (Ann Arbor, MI: Ann Arbor Science, 1980), pp. 57-70.
189. Buchert, H., S. Bihler, P. Schott, H. P. Röper, H.-J. Pachur, and K. Ballschmiter. "Organochlorine Pollutant Analysis of Contaminated and Uncontaminated Lake Sediments by High Resolution Gas Chromatography," *Chemosphere* 10(8):945-956 (1981).
190. Murray, H. E., L. E. Ray, and C. S. Giam. "Analysis of Marine Sediment, Water and Biota for Selected Organic Pollutants," *Chemosphere* 10(11/12):1327-1334 (1981).
191. Ray, L. E., H. E. Murray, and C. S. Giam. "Analysis of Water and Sediment from the Nueces Estuary/Corpus Christi Bay (Texas) for Selected Organic Pollutants," *Chemosphere* 12(7/8):1039-1045 (1983).
192. Chang-Yen, I., and M. Sampath. "Oxalic Acid Enhancement of Recoveries of Organochlorine Insecticides and Polychlorobiphenyls in Estuarine Sediment Using Cyclic Steam Distillation," *Bull. Environ. Contam. Toxicol.* 32:657-660 (1984).
193. Grimalt, J., C. Marfil, and J. Albaigés. "Analysis of Hydrocarbons in Aquatic Sediments. I. Sample Handling and Extraction," *Int. J. Environ. Anal. Chem.* 18:183-194 (1984).
194. Bahnick, D. A., and T. P. Markee. "Occurrence and Transport of Organic Micro-contaminants in the Duluth-Superior Harbor," *J. Great Lakes Res.* 11(2):143-155 (1985).
195. Ozretich, R. J., and W. P. Schroeder. "Determination of Selected Neutral Priority Organic Pollutants in Marine Sediment, Tissue, and Reference Materials Utilizing Bonded-Phase Sorbents," *Anal. Chem.* 58:2041-2048 (1986).
196. Japenga, J., W. J. Wagenaar, F. Smedes, and W. Salomons. "New, Rapid Clean-Up Procedure for the Simultaneous Determination of Different Groups of

- Organic Micropollutants in Sediments; Application in Two European Estuarine Sediment Studies," *Environ. Technol. Lett.* 8(1):9-20 (1987).
- 197. Lopez-Avila, V., S. Schoen, and J. Milanes. "Single-Laboratory Evaluation of Method 8080—Organochlorine Pesticides and PCBs," U.S. EPA Report-600/4-87/022 (1987).
 - 198. Aceves, M., J. Grimalt, J. Albaigés, F. Broto, L. Comellas, and M. Gassiot. "Analysis of Hydrocarbons in Aquatic Sediments. II. Evaluation of Common Preparative Procedures for Petroleum and Chlorinated Hydrocarbons," *J. Chromatog.* 436:503-509 (1988).
 - 199. Alford-Stevens, A. L., J. W. Eichelberger, and W. L. Budde. "Multilaboratory Study of Automated Determinations of Polychlorinated Biphenyls and Chlorinated Pesticides in Water, Soil, and Sediment by Gas Chromatography/Mass Spectrometry," *Environ. Sci. Technol.* 22(3):304-312 (1988).
 - 200. Krahn, M. M., L. K. Moore, R. G. Bogar, C. A. Wigren, S.-L. Chan, and D. W. Brown. "High-Performance Liquid Chromatographic Method for Isolating Organic Contaminants from Tissue and Sediment Extracts," *J. Chromatog.* 437:161-175 (1988).
 - 201. Petrick, G., D. E. Schulz, and J. C. Duinker. "Clean-Up of Environmental Samples by High-Performance Liquid Chromatography for Analysis of Organochlorine Compounds by Gas Chromatography with Electron-Capture Detection," *J. Chromatog.* 435:241-248 (1988).
 - 202. Schantz, M. M., S. N. Chesler, B. J. Koster, and S. A. Wise. "Analytical Methods for the Determination of Organic Contaminants in Marine Sediments and Tissues," NBS, Special Publication 740 (1988), pp. 40-52.
 - 203. Czuczwa, J. M., and A. Alford-Stevens. "Optimized Gel Permeation Chromatographic Cleanup for Soil, Sediment, Wastes, and Oily Waste Extracts for Determination of Semivolatile Organic Pollutants and PCBs," *J. Assoc. Off. Anal. Chem.* 72(5):752-759 (1989).

Narrative

- 204. Lindeboom, H. J., H. A. J. De Clerk, and A. J. J. Sandee. "Mineralization of Organic Carbon on and in the Sediment of Lake Grevelingen," *Neth. J. Sea Res.* 18:492-510 (1984).
- 205. Zitko, V. "The Analysis of Aquatic Sediments for Organic Compounds," in *Contaminants and Sediments, Volume 2: Analysis, Chemistry, Biology*, R. A. Baker, Ed. (Ann Arbor, MI: Ann Arbor Science, 1980), pp. 89-100.
- 206. Lichtenthaler, R. G. "Instrumental Analysis of Petroleum Hydrocarbons," in *Analysis of Organic Micropollutants in Water*, G. Angeletti and A. Bjorseth, Eds. (Dordrecht: D. Reidel Publishing Company, 1983), pp. 225-233.
- 207. Clark, R. C., Jr. "Methods for Establishing Levels of Petroleum Contamination in Organisms and Sediment as Related to Marine Pollution Monitoring," NBS, Special Publication 409 (1974), pp. 189-194.
- 208. Donnelly, J. R., G. W. Sovocool, Y. Tondeur, S. Billets, and R. K. Mitchum. "Some Analytical Considerations Relating to the Development of a High-Resolution Mass Spectrometric Dioxin Analytical Protocol," in *Chlorinated Dioxins and Dibenzofurans in Perspective*, C. Rappe, G. Choudhary, and L. H. Keith, Eds. (Chelsea, MI: Lewis Publishers, 1986), pp. 381-398.
- 209. Chesters, G., H. G. Pionke, and T. C. Daniel. "Extraction and Analytical Tech-

- niques for Pesticides in Soil, Sediment, and Water," in *Pesticides in Soil and Water*, W.D. Guenzi, Ed. (Madison, WI: Soil Science Society of America, 1974), pp. 451-549.
210. Hylin, J. W. "Pesticide Residue Analysis of Water and Sediments: Potential Problems and Some Philosophy," *Residue Rev.* 76:203-210 (1980).
211. Nash, R. G., M. J. M. Wells, A. E. Smith, and E. Van Wambeke. "Pesticide Residues in Environmental Samples," in *Analytical Methods for Pesticides and Plant Growth Regulators*, Vol. 15, G. Zweig and J. Sherma, Eds. (Orlando, FL: Academic Press, 1986), pp. 247-286.
212. Wells, D. E. "Extraction, Clean-Up and Group Separation Techniques in Organochlorine Trace Analysis," *Pure Appl. Chem.* 60:1437-1448 (1988).
213. Ashby, J., S. Clark, and P. J. Craig. "The Analysis of Organotin Compounds from Environmental Matrices," in *The Biological Alkylation of Heavy Elements*, Special Publication No. 66, P. J. Craig and F. Glockling, Eds. (London: Royal Society of Chemistry, 1988), pp. 263-290.
214. Lichtenberg, J. J., J. A. Winter, C. I. Weber, and L. Fradkin, Eds. *Chemical and Biological Characterization of Municipal Sludges, Sediments, Dredge Spoils, and Drilling Muds, ASTM STP 976* (Philadelphia: American Society for Testing and Materials, 1988).
215. Chau, A. S. Y., and H.-B. Lee. "Basic Principles and Practices on the Analysis of Pesticides," in *Analysis of Pesticides in Water*, Vol. 1, A. S. Y. Chau and B. K. Afghan, Eds. (Boca Raton, FL: CRC Press, 1982), pp. 25-81.
216. Norris, J. E. "Techniques for Sampling Surface and Industrial Waters. Special Considerations and Choices," in *Principles of Environmental Sampling*, L. H. Keith, Ed. (Washington, DC: American Chemical Society, 1988), pp. 247-253.
217. "Test Methods for Evaluating Solid Waste. Volume 1B: Laboratory Manual Physical/Chemical Methods," U.S. Environmental Protection Agency, SW-846, 3rd ed. (November 1986).
218. Lee, H.-B., and A. S. Y. Chau. "National Interlaboratory Quality Control Study No. 25: PCBs in Wet Sediments," National Water Research Institute, Report Series No. 71 (1981).
219. Lee, H.-B., and A. S. Y. Chau. "National Interlaboratory Quality Control Study No. 27: PCBs in Naturally Contaminated Dry Sediments," National Water Research Institute, Report Series No. 72 (1981).
220. Karickhoff, S. W. "Sorption Kinetics of Hydrophobic Pollutants in Natural Sediments," in *Contaminants and Sediments, Volume 2: Analysis, Chemistry, Biology*, R. A. Baker, Ed. (Ann Arbor, MI: Ann Arbor Science, 1980), pp. 193-205.
221. Goerlitz, D. F., and L. M. Law. "Note on Removal of Sulfur Interferences from Sediment Extracts for Pesticide Analysis," *Bull. Environ. Contam. Toxicol.* 6(1):9-10 (1971).
222. Lester, J. F., and J. W. Smiley. "Rapid Method for Identifying Aldrin in the Presence of Sulfur by Electron Capture Gas Chromatography," *Bull. Environ. Contam. Toxicol.* 7:43-44 (1972).
223. Baird, R. B., L. G. Carmona, and C. L. Kuo. "Gas-Liquid Chromatographic Separation of Sulfur from Chlorinated Pesticide Residues in Wastewater Samples," *Bull. Environ. Contam. Toxicol.* 9(2):108-115 (1973).
224. Brown, L. R. "Development of a Simple, Rapid Field Technique for Estimating Oil Concentrations in the Sediments," Report to Coast Guard Office of Research and Development, Report No. CG-D-27-77 (April 1977).

225. Spittler, T. M. "Field Measurement of PCBs in Soil and Sediment Using a Portable Gas Chromatograph," in *Management of Uncontrolled Hazardous Waste Sites* (Silver Spring, MD: Hazardous Materials Control Research Institute, 1983), pp. 105-107.
226. Spittler, T. M. "Field Measurement of Polychlorinated Biphenyls in Soil and Sediment Using a Portable Gas Chromatograph," in *Environmental Sampling for Hazardous Wastes*, G.E. Schweitzer and J.A. Santolucito, Eds. (Washington, DC: American Chemical Society, 1984), pp. 37-42.
227. Epstein, M. S., B. I. Diamondstone, and T. E. Gills. "A New River Sediment Standard Reference Material," *Talanta* 36(1/2):141-150 (1989).
228. Wells, D. E. "The Need for Organic Reference Materials in Marine Science," *Fres. Z. Anal. Chem.* 332:583-590 (1988).
229. Wise, S. A., S. N. Chesler, B. H. Gump, H. S. Hertz, and W. E. May. "Interlaboratory Calibration for the Analysis of Petroleum Levels in Sediment," in *Fate and Effects of Petroleum Hydrocarbons in Marine Organisms and Ecosystems*, D. A. Wolfe, Ed. (Elmsford, NY: Pergamon Press, 1977), pp. 345-350.
230. Chesler, S. N., H. S. Hertz, W. E. May, and S. A. Wise. "Quality Assurance Program for Trace Hydrocarbon Analysis," in *Environmental Assessment of the Alaskan Continental Shelf. Principal Investigators' Reports for the Year Ending March 1977, Vol. 13. Contaminant Baselines* (Washington, DC: National Bureau of Standards, 1977), pp. 1-14.
231. Hilpert, L. R., W. E. May, S. A. Wise, S. N. Chesler, and H. S. Hertz. "Interlaboratory Comparison of Analyses for Trace Level Petroleum Hydrocarbons in Marine Sediments," in *Environmental Assessment of the Alaskan Continental Shelf. Principal Investigators' Reports for the Year Ending March 1977, Vol. 13. Contaminant Baselines* (Washington, DC: National Bureau of Standards, 1977), pp. 15-39.
232. MacLeod, W. D., Jr., P. G. Prohaska, D. D. Gennero, and D. W. Brown. "Interlaboratory Comparisons of Selected Trace Hydrocarbons from Marine Sediments," *Anal. Chem.* 54:386-392 (1982).
233. De Kok, A., R. B. Geerdink, R. W. Frei, and U. A. T. Brinkman. "The Use of Dechlorination in the Analysis of Polychlorinated Biphenyls and Related Classes of Compounds," *Int. J. Environ. Anal. Chem.* 9(4):301-318 (1981).
234. Webb, R. G., and A. C. McCall. "Quantitative PCB [Polychlorinated Biphenyl] Standards for Electron Capture Gas Chromatography," *J. Chromatog. Sci.* 11(7):366-373 (1973).
235. Gebhart, J. E., T. L. Hayes, A. L. Alford-Stevens, and W. L. Budde. "Mass Spectrometric Determination of Polychlorinated Biphenyls as Isomer Groups," *Anal. Chem.* 57:2458-2463 (1985).
236. Slivon, L. E., J. E. Gebhart, T. L. Hayes, A. L. Alford-Stevens, and W. L. Budde. "Automated Procedures for Mass Spectrometric Determination of Polychlorinated Biphenyls as Isomer Groups," *Anal. Chem.* 57:2464-2469 (1985).
237. Voyksner, R. D., J. T. Bursey, T. W. Pack, and R. L. Porch. "Development of Methane Positive Chemical Ionization Gas Chromatography/Mass Spectrometry Procedures to Determine Polychlorinated Biphenyls," *Anal. Chem.* 58:621-626 (1986).
238. Alford-Stevens, A. L., and W. L. Budde. "Determination of Polychlorinated Compounds (Dioxins, Furans, and Biphenyls) by Level of Chlorination with

- Automated Interpretation of Mass Spectrometric Data," in *Chemical and Biological Characterization of Sludges, Sediments, Dredge Spoils, and Drilling Muds, ASTM STP 976*, J. J. Lichtenberg, J. A. Winter, C. I. Weber, and L. Fradkin, Eds. (Philadelphia: American Society for Testing and Materials, 1988), pp. 204-212.
239. Onuska, F. I., R. J. Kominar, and K. A. Terry. "Identification and Determination of Polychlorinated Biphenyls by High-Resolution Gas Chromatography," *J. Chromatog.* 279:111-118 (1983).
240. Mullin, M. D., C. M. Pochini, S. McCrindle, M. Romkes, S. H. Safe, and L. M. Safe. "High-Resolution PCB Analysis: Synthesis and Chromatographic Properties of All 209 PCB Congeners," *Environ. Sci. Technol.* 18:468-476 (1984).

Table 19.1. Fixed or Suspended Solids/Sediments Sampling

Reference	Type of Sample	Sampling Methods	Comments
1 Little et al. (1988)	Sediments, sludge, and dredge spoils	Demonstrated need for standardization of environmental monitoring programs	Recommendations are made with regard to sampling and analysis.
2 Pitard (1988)	Streams, sediments, dredge spoils, etc.	Variographic techniques were used to optimize sampling methodology	Methods were given to determine if a systematic sample scheme is appropriate or not.
3 Håkanson (1984)	Suspended sediment and bottom sediment	Statistical aspects of sample representativity	Wet sieving through a 63- μm mesh seemed to give the best information.
4 Plumb (1980)	Sediment	Procedure for preparing sediment sampling programs	Testing procedures are to be selected based upon the sample property they measure and specific need.
5 Parr et al. (1974)	Suspended sediment	Automatic pumping sampler	The results indicated that the sampler was suitable for evaluating the transport of relatively water-insoluble pesticides.
6 Miller (1965)	Sediment	USDA sediment sampling procedures	A variety of methods to improve and automate sediment sampling were discussed.
7 Honsaker et al. (1984)	Suspended sediment	Automatic sequential sampler	Solar cell panels were used to provide power to the sampler in collecting ephemeral stream samples during rainfall events.
8 Suffet et al. (1988)	Suspended sediments	In-stream composite sampler	A scheme was developed to simultaneously examine the aqueous and suspended phases.

Table 19.1, continued

Reference	Type of Sample	Sampling Methods	Comments
9 Analytical Quality Control Committee (1983)	Suspended solids	Filtration	Eleven categories participated in an accuracy-of-determination quality control scheme.
10 Beccuti et al. (1981)	Suspended sediment	Filtering bag integrating sampler	Filtering efficiency of two filters were compared. Relationships were developed between filtering efficiency and sediment diameter.
11 Bennett (1973)	Suspended sediment	Pitot tube velocity sensor/sampler nozzle, siphon sampler, and a US DH-48 sampler	The performances of the samplers were compared.
12 Bryant et al. (1980)	Sediment suspension	Evacuated pressure-resistant bottles	The sampling apparatus was developed and tested at a depth of 30 m in water velocities of 1-2 m/sec.
13 Bates et al. (1983)	Suspended particulate matter	Flow centrifugation versus filtration	Both methods collected equivalent weights of suspended matter and similar particle size distributions. The glass-fiber filters retained more lipid-extractable organic matter and saturated hydrocarbons.
14 Burrus et al. (1989)	Suspended solids (SS)	Continuous-flow centrifugation	Six river system stations were sampled quarterly for two years. SS did not vary as a function of depth or location across the river but did vary with time, flow, and location.
15 Dressing et al. (1987)	Water and suspended sediments	Flush-type sampler	Design and performance characteristics for the sampling device were described.

16 Guy (1969)	Suspended sediment	Filtration and evaporation	Several methods are presented for sample collection and particle size analysis.
17 Hansen (1966)	Suspended sediment	Automatic pump	Three intake level samples were obtained under a variety of stream flow conditions and compared to average SS concentration in the stream.
18 Jackson (1979)	Aquifer sediments	Sediment sampler and separation of the interstitial water	The equipment used, field sampling, preservation, and the analyses were discussed.
19 Jones (1969)	Suspended sediment	Pumping sampler	A simplified pumping sampler was developed which allowed varied intervals between samples collected.
20 Walling and Teed (1971)	Suspended sediment	Pumping sampler	A large number of samples can be provided automatically during storm events.
21 King and Everett (1980)	Bottom sediment	Remote mechanical suction	The sampler was used to collect sediments samples under ice cover.
22 Melcher et al. (1986)	Various	General sampling methods for environmental material	Equipment and procedures are discussed.
23 Reed (1977)	Suspended solids	Various	Methods for sample collection were evaluated.
24 Simpson (1982)	Particulate matter	Various	Review of existing sampling methods in oceans.
25 Fleming (1969)	Suspended solids	Davall siltmeter, Southern analytical suspended solids monitor, and the Fleming siltmeter	The instruments yielded similar results when used for stream samples.
26 Busatti et al. (1988)	Sediment	Sediment-water gravity corer	Sediment cores from 5 to 40 cm with accompanying overlying water were obtained with little disturbance.

Table 19.1, continued

Reference	Type of Sample	Sampling Methods	Comments
27 Baker et al. (1988)	Aqueous/suspended sediment	Sediment trap	The study indicated that consideration must be given to both scaling trap diameter and aspect ratio according to the expected flow conditions.
28 Scrudato et al. (1988)	Suspended sediment	Sedimentation trap	A lightweight stream sampler provided a continuous collection of suspended stream sediments.
29 Kimmel et al. (1977)	Sedimenting seston	Sediment trap	The device permits remote closure, replication correction for attached growth and use in vertical series.
30 Kellerhals and Bray (1971)	Fluvial sediments	Densely paired cubes and geometric conversions	Several procedures were compared.
31 John et al. (1977)	Littoral sediments and shallow aquifers	Two types of sampling probes	Two different sampling procedures were compared and were shown to have considerable application.
32 Straughan (1974)	Marine organisms and sediments	Box core (21 x 29 cm)	Difficulties in obtaining representative data for petroleum contaminant in sediments and organisms were described.
33 Bruce and Cram (1974)	Sediments and marine organisms	Circular core	Sediment cores were taken to develop a baseline data set for aromatic hydrocarbons at the ppt to ppm levels.
34 Daniel and Chesters (1971)	Sediment	Sediment core sampler	A low-cost sampler was constructed. It was easy to operate and can be used for sediments ranging from sand to highly organic clayey material.

35	Satake (1988)	Bottom sediment	Corer	A new impact corer was described.
36	Fukuhara and Sakamoto (1987)	Bottom sediment	Ekman-Birge bottom mud sampler (core)	The devised sampler proved successful for sampling undisturbed sediment.
37	Heinemann and Brown (1972)	Suspended sediment	Fractional water-sediment	Samples can be split to 50 or 25% of original sampled flow before being put in containers.
38	Knaus (1986)	Sediment	Cryogenic coring	The device was used to sample flocculent material at and below the water-sediment interface in shallow waters.
39	Moshiri et al. (1977)	Sediment cores	Coring device	A new sampler was described for the purpose of collecting single and multiple cores.
40	Noble et al. (1986)	Sediment	Tubular coring device	The performance and operation of the sampler were described.
41	Hairr and Wrenn (1972)	River sediments	Dredge oil corer	Dredge and core samples were compared in evaluating sediments near a nuclear power station.
42	Reeburgh and Erickson (1982)	Sediments	"Dipstick"	The procedure, with appropriate reagents, gave rapid, continuous, and semiquantitative measurements.
43	Williams and Pasley (1979)	Soft sediments	Corer	A corer was developed to take a sample 10 cm in diameter, up to 1 m long.
44	Stevens and Lutz (1980)	Suspended sediments	Collapsible-bag sampler	The sampler is easy to use and maintain.

Table 19.2. Tabular Assignment of Anthropogenic Organic Compounds by Chemical Category

Chemical Category	Table #
Petroleum-Derived Compounds	3
Polychlorinated Biphenyls	4
Chlorinated Dioxins and Dibenzofurans	5
Pesticides	6
Miscellaneous Chlorinated Compounds	7
Phenolic Compounds	8
Surfactants	9
Phthalates	10
Alkyl and Aryl Phosphates	11
Organometallic Compounds	12
Miscellaneous Anthropogenic Organic Compounds	13
Multiclass Anthropogenic Organic Compounds	14

Table 19.3. Determination of Petroleum-Derived Compounds (Including Aliphatic and Aromatic Hydrocarbons, PAHs, and Related Oxygenated Compounds) Associated with Fixed or Suspended Solids/Sediments

Reference	Sampling, Sample Handling, Preservation, and Storage	Sample Preparation		Final Determination
		Extraction, Purification, Fractionation	UV	
45 Scarratt and Zifko (1972)	Sediment cores, frozen	Hexane extracted		
46 Zafiriou (1973)	Grab frozen, coarse-sieved	Soxhlet, benzene-methanol (1:2); water wash; benzene concentrated; chilled to precipitate sulfur Activated Cu sulfur removal Fractionated on silica gel over alumina; pentane/benzene eluant	IR, UV, GC-FID (capillary column), MS	
47 Bean et al. (1974)		Fractionated by solvent extraction, solvent precipitation, and liquid chromatography to yield saturated, aromatic, polar, and asphaltic fractions	Gravimetric	
48 Giger and Blumer (1974)	Van Veen grab sealed in stainless steel, frozen	Soxhlet, methanol-benzene; partitioned with pentane Sulfur removed on Cu column Gel permeation/adsorption chromatography on Sephadex LH-20 Purified on alumina/silica gel Charge transfer complexation Fractionated on alumina	UV, Visible, MS	
49 Hunter et al. (1974)		Mortar and pestle; ground with hexane, sand, and magnesium sulfate Silica gel; hexane eluant	TLC (silica gel; hexane), fluorescence, densitometry	
50 Hargrave and Phillips (1975)	Grab, Ekman sampler, excess water removed over vacuum	Shaker/centrifuge	Fluorescence	

Table 19.3, continued

Reference	Sampling, Sample Handling, Preservation, and Storage		Sample Preparation	Extraction, Purification, Fractionation	Final Determination
51 Hertz et al. (1975)	Sediment corer, frozen at -10°C		Thawed (4°C); water added; dynamic headspace sampling using nitrogen	Volatile components concentrated on Tenax GC; nonvolatile components in aqueous extract of sediment concentrated on C ₁₈ sorbent	Tenax-GC columns analyzed by GC-FID, -MS (capillary column)
52 May et al. (1975)					C ₁₈ columns analyzed by HPLC-UV with fraction collector for subsequent UV, FD, MS
53 Chesler et al. (1976)					
54 Chesler et al. (1977)					
55 Strosher and Hodgson (1975)	Plastic coring tubes, refrigerated near freezing		Wet sediment; Polytron homogenizer/disintegrator: (1) acetone, (2) benzene-methanol (3:1)	Fractionated on alumina; hexane, benzene, methanol eluants	GC-MS (packed column)
56 Walker et al. (1975)	Grab, Ponar sampler		Various extraction methods: (1) Soxhlet, (2) stirring, (3) sonication, (4) shaking and solvents: (1) hexane, (2) benzene, (3) chloroform were compared	MS	
57 Miles et al. (1977)					HPLC-FD
58 Wise et al. (1977)			Ultrasonic; ether; solvent exchanged to pentane		HPLC-UV, -FD
59 Giger and Schaffner (1978)	Gravity coring device or grab sampler, frozen, subsequently freeze-dried, particulates by filtration of water		Fractionated by HPLC-aminosilane column; solvent exchanged to acetonitrile Soxhlet; methylene chloride Activated Cu sulfur removal Fractionated on Sephadex LH-20 (gel permeation/adsorption chromatography); benzene-methanol (1:1) eluant Each fraction further fractionated on silica gel; pentane/methylene chloride eluant		GC-FID, -MS (capillary column)

60	Black et al. (1979)	Wet sediment; methanol/potassium hydroxide; reflux	HPLC-UV
61	Meuser et al. (1979)	Liquid-liquid extracted with cyclohexane Fractionated on Florisil; cyclohexane/ methylene chloride eluant; fluorescent PAH fraction located by UV light source	
62	Griest (1980)	Extracted by liquid chromatography or liquid-liquid extraction	GC-MS
63	Tjessem (1980)	Fractionated by two-step adsorption column chromatography	GC-MS
64	Whelan et al. (1980)	Extracted with toluene/methanol; methylated Fractionated by TLC; methylene chloride eluant Fractionated by Sephadex LH-20; isopropyl alcohol eluant	GC-MS (capillary column)
65	Obama et al. (1981)	Wet sediment; thermal distillation-pyrolysis	GC-MS (capillary column)
66	Ramos and Prohaska (1981)	Saponified; ethanol/potassium hydroxide; refluxed Liquid-liquid extracted with hexane; water wash; extracted with dimethyl sulfoxide; extracted with hexane; water wash Fractionated on silica gel over alumina; hexane/diethyl ether eluant Sulfur removed on column of granular Cu and silica gel Fractionated on silica gel; hexane eluant Fractionated on Sephadex LH-20; cyclohexane- methanol-methylene chloride (6:4:3) or cyclohexane-isopropanol (2:1) eluant	HPLC-FD
67	Santoni and Mandon (1981)	Ultrasonic extracted/dimethyl sulfoxide Hexane reextracted; silica gel	Low-temperature fluorometry/ Shpol'skii effect

Table 19.3, continued

Reference	Sampling, Sample Handling, Preservation, and Storage	Sample Preparation		Final Determination
		Extraction, Purification, Fractionation		
68 Steinheimer et al. (1981)	Bed material dredge, chilled in ice, mixed, lyophilized	Extracted (1) ultrasonically with benzene-methanol (2:1) and (2) Soxhlet; concentrated Fractionated on silica gel; hexane/methylene chloride/methylene chloride-methanol (1:1)	GC-MS (capillary column)	
69 Belisle and Gay (1982)		Nielson-Kryger steam distilled; water/isooctane Fractionated on silica gel; petroleum ether/methylene chloride	GC-FID (capillary column)	
70 Matsumoto (1983)	Ekman-Birge dredge, stored below 0°C	Wet sediment; saponified; methanol/potassium hydroxide; refluxed; residue acidified and further extracted with ethyl acetate; water wash Silica gel	GC-MS (packed column)	
71 Eganhouse (1986)		Wet sediment; ambient temperature extracted with methylene chloride Activated Cu sulfur removal TLC on silica gel with methylene chloride or silver nitrate-impregnated silica gel with hexane	GC-FID, HRGC-MS	
72 Hagenmaier et al. (1986)		Various extraction methods and solvents: (1) Wet sediment extraction-acetone/liquid-liquid extraction petroleum ether-water (2) Lyophilized sediment/hot Soxhlet acetone-hexane (1:1); (3) Wet sediment-sodium sulfate (1:4)/hot Soxhlet hexane; (4) Wet sediment-sodium sulfate (1:4)/hot Soxhlet hexane-acetone (1:1); (5) Lyophilized sediment/hot Soxhlet hexane; (6) Lyophilized sediment/ultrasonic-2X acetone, 1X hexane were compared	HPLC-FD	

73 Kilops (1986)	Ultrasonic extracted/isopropyl alcohol-light petroleum ether (4:1); partitioned with water-hexane (2:3) Hydrolyzed-aqueous potassium hydroxide; extracted hexane Fractionated by HPLC: normal phase cyano/amino bonded phase—in series with a silica column; hexane/methylene chloride	GC-FID (capillary column)
74 Lebo and Smith (1986)	Core sampler, frozen, air-dried Extracted with methylene chloride in chromatography column Cu turnings submerged in extract for sulfur removal Tandem silica gel/potassium silicate/carbon columns; cyclopentane-methylene chloride eluant; solvent exchanged to acetonitrile	HPLC-UV, -FD
75 de Leeuw et al. (1986)	Ekman-Birge sampler, homogenized by sonication Wet sediment; serially extracted with ultrasonication and centrifugation: (1) methanol-methylene chloride (3:1); (2) methanol-methylene chloride (1:1); (3) methanol-methylene chloride (1:3); (4) methylene chloride; methylene chloride layer separated	GC-FID (capillary column), direct evaporation, pyrolysis, GC-MS
76 Marcomini et al. (1986)	Box corer, frozen at -20°C, lyophilized, stored in aluminum-lined glass jars Soxhlet hexane; saponified methanol/potassium hydroxide, sodium chloride added; partitioned hexane Fractionated on activated Cu/Florisil Fractionated by HPLC: normal-phase silica; hexane	HPLC-UV, GC-FID, -MS
77 West et al. (1986)	Extracted benzene-methanol (3:2)/methylene chloride Extract adsorbed on neutral alumina/added to alumina column; hexane/benzene eluant Fractionated by HPLC: normal-phase aminosilane; methylene chloride/pentane	GC-FID, -MS (capillary column)

Table 19.3, continued

Reference	Sampling, Sample Handling, Preservation, and Storage	Sample Preparation		Final Determination
		Extraction, Purification, Fractionation		
78 Albaiges and Grimalt (1987)		Refluxed with potassium hydroxide-methanol solution (saponification); water added; partitioned with pentane; concentrated fractionated on alumina; pentane/pentane-methylene chloride/methylene chloride eluants		GC (capillary column), Uv-fluorometry
79 Garrigues and Ewald (1987)	Air-dried	Fractionated by HPLC		Low-temperature fluorometry/ Shpol'skii effect
80 Hawthorne and Miller (1987)		Supercritical fluid extractions with (1) carbon dioxide; (2) carbon dioxide-5% methanol modifier; (3) nitrous oxide; (4) nitrous oxide-5% methanol modifier; or (5) ethane were collected into methylene chloride and compared with Soxhlet and sonication extractions with benzene or methylene chloride		GC-MS (capillary column)
81 Morel and Courtot (1987)	Glass coring device	Extracted by mechanical tumbling or Soxhlet with FREON 113 or carbon tetrachloride Various sample pretreatments: (1) freeze-drying; (2) pestle pulverization; (3) manual screening; and (4) homogenization were compared		IR
82 Poole et al. (1987)	River sediment sample, NBS 1645	Ultrasonically extracted with acetonitrile; evaporated; redissolved in hexane Fractionated by liquid-liquid extraction with hexane/dimethyl sulfoxide followed by silica gel; cyclohexane eluant		Reversed-phase HPLC with fluorescence scanning densitometry
83 Saber et al. (1987)		Acidified; ultrasonically extracted; toluene/methanol (80:20) Hexane extracted; saponified; toluene/methanol (50:50); refluxed; hexane extracted; solid-phase extraction C ₁₈ sorbent; hexane eluant		High-resolution Shpol'skii spectrofluorometry

84	Fernandez et al. (1988)	Sample wrapped in aluminum foil, frozen at -20°C, freeze-dried	Sonication extracted using methylene chloride-methanol (2:1) Concentrated extract adsorbed onto alumina; transferred to a column of alumina over silica gel; 20% methylene chloride in hexane eluant	GC-FID, -FPD, -ECD, -MS (capillary column)
85	Sim et al. (1988)	Van Veen grab, freeze-dried, sieved, homogenized	Soxhlet; methylene chloride or hexane Fractionated on granular copper over silica gel; methylene chloride/diethyl ether eluant	GC-FID, -MS, HPLC-UV, -FD, -MS
86	Quilliam and Sim (1988)		Fractionated on Sephadex LH 20; cyclohexane-methanol-methylene chloride (6:4:3) eluant	
87	Bianchi and Varney (1989)	Van Veen sediment grabs, sodium azide	Thawed Static equilibrium headspace/solid phase dispersed into water; equilibrate in 80°C bath	GC-FID (capillary column)
88	Guiliano et al. (1989)		Soxhlet extracted Fractionated on silica-alumina; toluene-hexane (1:3) eluants	GC-MS, FTIR (capillary column)

Table 19.4. Determination of Polychlorinated Biphenyls Associated with Fixed or Suspended Solids/Sediments

Reference	Sampling, Sample Handling, Preservation, and Storage	Sample Preparation		Final Determination
		Extraction, Purification, Fractionation		
89 Chau et al. (1979)		Wet sediment: extracted with acetone-hexane (1:1); purified on Florisil; hexane eluant; isoctane added; concentrated	GC-ECD (capillary and packed columns)	
90 Chau and Lee (1980)		Dry sediment: water and activated copper powder added; extracted and purified as for wet sediment; treated with mercury for sulfur removal		
91 Kerkhoff et al. (1982)	Dredge	Wet sediment extracted with acetone; allowed to stand overnight; partitioned into petroleum ether after the addition of water; elemental sulfur removed; concentrated extract shaken with tetrabutyl ammonium hydrogen sulfate and sodium sulfite Fractionation/purification by column chromatography: (1) anhydrous sodium sulfate over alumina; pentane eluant; and (2) silica; hexane eluant Analyzed at this point and after perchlorination to dechlorobiphenyl	GC-ECD (capillary and packed columns)	
92 Oliver and Nicol (1982)		Wet sediment combined with approximately equal amount of celite; Soxhlet; hexane/acetone (4:1:59); back-extracted with water to remove acetone	GC-ECD (capillary columns)	
93 Oliver and Niimi (1988)		Purified on column of sodium sulfate over sulfuric acid treated silica gel and Florisil; hexane eluant Extract agitated with triple distilled mercury to remove sulfur		
94 McMurtrey et al. (1983)	Grab sampler, excess water drained, dried for two days under flowing air in a fume hood	Continuous extractor; acetone/hexane; dried extract spiked with PCBs; pyrolyzed	PY-GC-MS	

95 Alford-Stevens et al. (1985)	Wet sediment mixed, placed in glass jars with Teflon-lined screw caps, packed in ice to transport, refrigerated until used	Comparison of three extraction procedures: (1) Wet sediment; air-dried; Soxhlet; acetone-hexane (1:1); dried with sodium sulfate; concentrated; (2) Wet sediment; Soxhlet; first, 2-propanol; second, methylene chloride; extracts combined; washed with aqueous sodium sulfate solution; organic extracts combined; dried with sodium sulfate; concentrated; (3) Wet sediment extracted ultrasonically; acetone; acetone extract combined with aqueous sodium sulfate; partitioned with hexane; concentrated All extracts purified on Florisil; ethyl ether-hexane eluant Sulfur removed with tetrabutylammonium sulfite reagent	GC-ECD, -MS (packed or capillary column)
96 Brownawell and Farrington (1985)	Soutar box corer, Sandia-Hessler type MK3 sediment corer, pore water removed, sediment frozen	Soxhlet (wet sediment); hexane-acetone (1:1) Purified on silica gel columns layered with activated copper (to remove reduced and elemental sulfur); hexane or toluene in hexane eluant	GC-ECD (capillary column)
97 Eisenreich (1987)		Wet sediment extracted with hexane-acetone (1:1); back-extracted with hexane; dried over anhydrous sodium sulfate; concentrated Fractionated on Florisil; hexane/hexane-diethyl ether eluants	GC-ECD (capillary column)
98 Dunnivant and Elzerman (1988)	Freeze-dried EPA sediments, field sediments homogenized, stored at 4 °C	Comparison of three extraction procedures: (1) Soxhlet (dried or field-wet sediments mixed with sand); acetone-hexane (1:1) Extracted with water-acetone-sodium chloride solution; aqueous phase discarded; dried sodium sulfate Purified by chromatography on layered sodium sulfate-alumina column; isoctane eluant;	GC-ECD (capillary column)

Table 19.4. Determination of Polychlorinated Biphenyls Associated with Fixed or Suspended Solids/Sediments

Reference	Sampling, Sample Handling, Preservation, and Storage	Sample Preparation	Extraction, Purification, Fractionation	Final Determination
99 Huckins et al. (1988)	Frozen		(2) Steam distilled (dried or field-wet sediments added to 12 N sulfuric acid and potassium dichromate) Extract concentrated in Dean-Stark trap containing hexane Hexane layers composited—aqueous layer separated and discarded; dried sodium sulfate Purified as for Soxhlet procedure; (3) Sonicated (dried or field-wet sediments added to acetone) Filtrate extracted with isoctane-water-sodium chloride solution; isoctane extracts dried sodium sulfate Purified as for Soxhlet procedure	GC-ECD (capillary column)
85 Sim et al. (1988)	Van Veen grab, freeze-dried, steel cans		Soxhlet; hexane Extract treated with copper amalgam to remove sulfur; concentrated Purified on Florisil; hexane eluant; concentrated	GC-ECD, -MS (packed and capillary columns)

Table 19.5. Determination of Chlorinated Dioxins and Dibenzofurans Associated with Fixed or Suspended Solids/Sediments

Reference	Sampling, Sample Handling, Preservation, and Storage	Extraction, Purification, Fractionation	Sample Preparation	Final Determination
100 Smith et al. (1984)	Sediment-sodium sulfate (1:4) placed in a chromatographic column; column contents solvent extracted; cyclohexane-methylene chloride (50:50) Extract passed through a series of sorbents: (1) potassium silicate; (2) silica gel; (3) potassium silicate; (4) silica gel; and (5) carbon with glass fibers; toluene eluant Solvent exchanged to hexane and charged to a second series of sorbents: (1) cesium silicate; (2) sulfuric acid impregnated silica gel; and (3) alumina; fractionated elution from alumina column by methylene chloride in hexane gradient	Pretreatment: desiccated; acid or alkaline treated Extracted: manual or mechanical shaking; ultrasonic Purified: acid treated; Florisil and alumina column chromatography	GC-ECD, -MS	HRGC-LRMS, GC-ECD
101 Cattabeni et al. (1986)	Grab-scooping	Acid treated (hydrochloric acid); filtrate extracted; toluene Solids mixed with sodium sulfate and Soxhlet extracted; toluene	GC-MSD, -MS (capillary columns)	
102 Afghan et al. (1987)		Purified by (1) liquid-liquid extraction with trisodium phosphate; water wash; (2) treated with mercury; (3) gel permeation chromatography; chloroform eluant; (4) liquid-liquid extracted with sulfuric acid Fractionated by (1) basic alumina chromatography; methylene chloride-hexane eluants; (2) activated carbon-glass fiber sorbent; methylene chloride-cyclohexane/ethyl acetate/benzene-ethyl acetate/toluene eluants		
103 Simon et al. (1989)		Soxhlet; concentrated Purified: basic silica, acidic silica, and alumina; methylene chloride-hexane eluants Further purified on silver nitrate silica or 2,3,7,8-TCDD-specific alumina	GC-MS, -MS-MS	

Table 19.6. Determination of Pesticides Associated with Fixed or Suspended Solids/Sediments

Reference	Analyte	Sampling, Sample Handling, Preservation, and Storage		Sample Preparation	Extraction, Purification, Fractionation	Final Determination
		ORGANOCHLORINE COMPOUNDS				
104	Pfister et al. (1969)	Lindane, endrin, heptachlor, aldrin	Continuous centrifugation	Particulates fractionated by centrifugation on a linear sucrose gradient; divided into four fractions; each fraction extracted with hexane	GC-ECD (packed column), TLC	
105	Chau (1972)	α - and β -endosulfan	Extracted; partitioned; Florisil column preseparated	Derivative formation on alumina-sulfuric acid solid matrix	GC-ECD (packed column)	
106	Lyons and Salman (1972)	Lindane	Soxhlet; diethyl ether in petroleum ether (6:94) Purified on Florisil		GC	
107	Routh (1972)	DDT and related derivatives	Shaken with acetone-hexane (20:80) in glass collection bottle; extract combined with acid washed Nuchar Attaclay; separated; concentrated Purified by chromatography on Nuchar Attaclay-silica gel (1:25) Treated with metallic mercury for sulfur removal		GC-ECD (packed column)	
108	Woodham et al. (1972)	Dieldrin and endrin	Sediment extracts treated with 10% boron trichloride in 2-chloroethanol; reacted by heating in water bath Partitioned with hexane-aqueous sodium sulfate		GC-ECD (packed column)	
109	Saleh and Lee (1978)	Kepone	Soxhlet (air-dried sediment); ethyl ether-hexane (35:65) Purified on Florisil; ethyl ether-hexane/hexane/methanol-benzene-hexane eluants		GC-ECD (packed column)	

110	Muir and Griff (1980)	Niclosamide	Filtration	Direct analysis of extract by HPLC-UV, analysis of derivative by GC-AFD, -ECD
111	Wegman and Höstee (1982)	α -, β -, and δ -HCH, aldrin, dieldrin, endrin, isodrin, telodrin, heptachlor, β -heptachlorepoxyde, DDT	Water added to sediment shaken with acetone; kept overnight; extract concentrated; water added; partitioned with petroleum ether Fractionated on basic alumina; petroleum ether/diethyl ether-petroleum ether eluants Petroleum ether fraction further fractionated on silica gel; petroleum ether/petroleum ether-methylene chloride eluants Sulfur removed by propanol/tetrabutylammonium hydrogen sulfate/sodium sulfite treatment	GC-ECD (capillary column)
112	Gambrell et al. (1984)	DDT, kepone	Stored in glass or plastic-lined metal containers at 4°C in natural moist or saturated conditions	GC-ECD (packed column)
113	Griff and Lockhart (1974)	Fenitrothion	Shaken with ethyl acetate; centrifuged; partitioned with acetonitrile-hexane Concentrated ethyl acetate-acetonitrile layer purified on Florisil layered between sodium sulfate; benzene-ethyl acetate eluant	GC-phosphorus, sulfur detectors (packed column)

ORGANOPHOSPHORUS COMPOUNDS

Table 19.6, continued

Reference	Analyte	Sampling, Sample Handling, Preservation, and Storage		Sample Preparation	Extraction, Purification, Fractionation	Final Determination
114 Kjølholt (1985a)	Triethyl phosphate, O,O-diethyl-s-methyl thiophosphate, O,O,s-triethyl thiophosphate, O,O,s-triethyl dithiophosphate, sulfotep, malathion, parathion, dimethoate	Sediment acidified with hydrochloric acid Soxhlet; acetone-hexane (4:1) Elemental sulfur removed by treatment with tetrabutylammonium hydrogen sulfate-sodium sulfite			GC-NPD (capillary column)	
115 Kjølholt (1985b)		Extract partitioned with water and methylene chloride at pH 6; methylene chloride extract dried with anhydrous sodium sulfate Purified by either of two methods depending on analyte:		(1) Extract evaporated to near dryness; propylene glycol solution and ethyl acetate added; chromatographed on a column of activated carbon-magnesium oxide-Celite 545 (1:4:8); ethyl acetate-acetone-toluene (1:1:2); eluate evaporated to dryness; residue dissolved in cyclohexane; (2) Extract evaporated to dryness; redissolved in cyclohexane; fractionated by gel permeation chromatography		
TRIAZINE COMPOUNDS						
116 Muir (1980)	Terbutryn and degradation products	Ekman dredge		Extracted wet by refluxing with acetonitrile-water (4:1); filtered and residual sediment shaken with acetonitrile-water-ammonium hydroxide; extracts combined and concentrated; water added, and partitioned with methylene chloride Organic phase dried with sodium sulfate and purified on basic alumina; hexane-ethyl acetate eluant	GC-AFD (packed column), HPLC-UV	

		Aqueous phase evaporated to remove methylene chloride; diluted with methanol; purified by chromatography on cationic exchange resin; ammonium hydroxide-methanol eluant; evaporated to dryness; dissolved in methanol and purified on acidic alumina; methanol-propionic acid eluant Additional fractionation by HPLC	GC-FID (capillary column), HPLC-UV
117	Janda et al. (1989)	Simazine, atrazine, propazine, terbutylazine, cyanazine	Sediment dried through lyophilization
118	Scott et al. (1982)	2,4-D and 2,4-DCP	Acrylic corer, stored at -20°C, particulate matter collected on 0.45-μm filter
119	Lee and Chau (1983)	Dicamba, 2,3,6-TBA, 2,4-DP, MCPA, silver, 2,4-D, MCPB, 2,4,5-T, 2,4-DB, picloram	<p>PHENOXYALKANOIC ACID COMPOUNDS</p> <p>Shaken with trisodium phosphate; centrifuged; filtered; acidified to pH 2 with sulfuric acid; partitioned with diethyl ether; ether extracts combined with petroleum ether and anhydrous sodium sulfate</p> <p>Solution concentrated and diazomethane derivatizing agent in methanol added and allowed to stand overnight</p> <p>Wet sediment acidified to pH ≤ 1 with sulfuric acid solution; extracted ultrasonically with acetone-hexane (1:1); extract passed through Celite column; water wash; aqueous layer extracted with methylene chloride; combined organic extracts evaporated; benzene added and evaporation repeated just to dryness; residue dissolved in acetone</p> <p>Pentafluorobenzyl bromide derivatizing agent in acetone and potassium carbonate solution were added and heated; reaction mixture evaporated; hexane added and evaporation repeated just to dryness; residue dissolved in benzene-hexane (1:9)</p> <p>Purified on deactivated silica topped with anhydrous sodium sulfate; benzene-hexane and ether-benzene eluants</p>

Table 19.6, continued

Reference	Analyte	Sampling, Sample Handling, Preservation, and Storage	Sample Preparation	Extraction, Purification, Fractionation	Final Determination
MISCELLANEOUS PESTICIDES					
120 Westlake et al. (1972)	<i>m</i> -sec-Butylphenyl- <i>N</i> -methyl- <i>N</i> -thiophenylcarbamate	Blended with acetonitrile; filtered through filtering aid; water added; partitioned with hexane; hexane extract evaporated and redissolved in ethyl acetate Purified by chromatography on Nuchar-Attaclay over silica gel; ethyl acetate eluant	GC-FPD (sulfur), -ECD (packed column)		
121 Reeves and Woodham (1974)	Methomyl	Sodium sulfate added (1:1); extracted with methylene chloride; filtered; nujol-in-hexane solution added and the solvent concentrated by evaporation Purified on Florisil; diethyl ether-methylene chloride/methylene chloride acetone eluants; nujol-in-hexane solution added and solvent evaporated to dryness; residues redissolved in benzene	GC-FPD (packed column)		
122 West and Parka (1981)	Fluridone	Soil sampler containing removable plastic tube, filtered, blended, air-dried, stored at 4°C	Boiled in water bath with 2 N sodium hydroxide/methanol (50:50); filtered Purified by chromatography on XAD-2 resin; sodium hydroxide-methanol stepwise gradient eluants Methanol eluate combined with sodium chloride solution and partitioned with methylene chloride; dried sodium sulfate; evaporated; redissolved in hexane-methylene chloride (70:30) Purified by chromatography on alumina topped with sodium sulfate; hexane-methylene chloride stepwise gradient eluants; evaporated; redissolved in methanol-water (60:40)	HPLC-UV	

123	Lee and Chau (1983)	Trifluralin, diallate, triallate, atrazine, barban, diclofop-methyl, benzoylprop-ethyl	Stored frozen, in dark, in metal cans	GC-ECD, -NPD Extracted ultrasonically wet sediment; acetone; extract filtered through Celite 545; volume reduced; combined with potassium hydrogen carbonate solution; partitioned with methylene chloride; extract dried with anhydrous sodium sulfate; isoctane added; solvent exchanged to hexane Fractionated on Florisil topped with anhydrous sodium sulfate; benzene-hexane (fraction A)/ methanol-benzene (fraction B) eluants Purified (fraction A) on Florisil topped with anhydrous sodium sulfate; methylene chloride-hexane/methylene chloride eluants; shaken with mercury to remove sulfur compounds Purified (fraction B) on Florisil topped with anhydrous sodium sulfate; benzene-hexane/acetone-benzene eluants	GC-ECD (packed column)
112	Gambrell et al. (1984)	Permethrin	Stored in glass or plastic-lined metal containers at 4°C in natural moist or saturated conditions	Thawed; centrifuged; aqueous phase discarded; sediment extracted with acetone to remove excess water; extract retained Residual sediment Soxhlet extracted; hexane-acetone (60:40) Extracts combined and aqueous-acetone layer was discarded after separation in a separatory funnel Dried sodium sulfate	HPLC-UV
124	Dawson and Allen (1988)	Rotenone	Mixed with methanol; centrifuged; filtered; concentrated by evaporation; combined with hydrochloric acid solution; partitioned with hexane; evaporated to dryness; redissolved in benzene Purified on silica gel; benzene/benzene-acetone eluants; evaporated to dryness; redissolved in methanol		

Table 19.6, continued

Reference	Analyte	Sampling, Sample Handling, Preservation, and Storage		Extraction, Purification, Fractionation	Sample Preparation	Final Determination
125 Hale et al. (1989)	Fenvalerate			Extracted ultrasonically; acetone-hexane (1:1); filtered; extract concentrated, hexane added; evaporated to dryness; redissolved in hexane Purified on Florisil (solid-phase extraction column); hexane/diethyl ether-hexane eluants; evaporated to dryness; redissolved in isoctane	GC-MS (capillary column)	
126 Thompson et al. (1989)	Glyphosate and metabolite			Shaken with ammonium hydroxide solution; centrifuged, filtered Treated with batch and column anion-exchange resin; ammonium hydrogen carbonate eluant; repetitive dissolution and evaporation with water to eliminate bicarbonate Purified on cation-exchange resin; water eluant; evaporated; redissolved in potassium dihydrogen phosphate buffer solution; filtered	HPLC-visible (postcolumn derivatization with ninhydrin)	
127 Schutzmann et al. (1971)	Organochlorine and organophosphorus			Anhydrous sodium sulfate added; shaken with hexane-isopropanol (3:1); extract washed with water; dried over anhydrous sodium sulfate Desulfurized with Raney copper powder	GC-ECD (packed column)	
128 Amore (1979)	Organochlorine, organophosphorus, carbamate			Air-dried sediment wetted with ethyl alcohol; extracted by acetone by allowing to set at room temperature with occasional swirling for 24 hr; filtered; acetone extract combined with water and sodium chloride and partitioned with diethyl ether-petroleum ether (10:90); water wash; extract concentrated; anhydrous sodium sulfate added; diluted with hexane Fractionated on Florisil; diethyl ether-petroleum ether stepwise gradient eluants; mercury treated to remove sulfur	GC-ECD, -FPD	

MULTI-CLASS PESTICIDE ANALYSES

129	Belisle and Swineford (1988)	Organophosphorus and carbamate	Stored in glass at 4°C	GC-NPD, -FPD (capillary column)
130	Marble and Delfino (1988)	Organochlorine and organophosphorus	Wet sediment extracted by blending with sodium chloride and acetonitrile and shaking; dried over sodium sulfate; concentrated by evaporation Extracts diluted with water and purified by chromatography (solid-phase extraction) on reversed-phase C ₁₈ sorbent; methylene chloride-acetonitrile-hexane (50:3:47) eluant; solvent exchanged to isoctane	GC-ECD (capillary column)
131	Barceló and Albaiges (1989)	Organophosphorus, trialkyl phosphates, and phenylurea	Soxhlet wet sediment; methanol-water (9:1); concentrated by evaporation	HPLC-MS (thermospray)

Table 19.7. Determination of Miscellaneous Chlorinated Compounds Associated with Fixed or Suspended Solids/Sediments

Reference	Analyte	Sampling, Sample Handling, Preservation, and Storage	Sample Preparation		Final Determination
			Extraction, Purification, Fractionation		
132 Murray and Riley (1973)	Chloroform, carbon tetrachloride, and other chlorinated aliphatic hydrocarbons	Wet sediments heated while purged with nitrogen; extract cryogenically trapped on sorbent; argon gas flushed sample onto GC column			GC-ECD (packed column)
133 Erickson et al. (1978)	Polychloronaphthalenes	Extracts collected on polyurethane foam plugs recovered by extraction with toluene			GC-MS
134 Hollies et al. (1979)	Chloro- <i>n</i> -paraffins	Purified on silica gel			TLC
135 Ellington (1981)	Chloroalkanes and other aliphatic and aromatic hydrocarbons	Metal spatula or scoop, stored in jars at ambient temperature less than one month; at time of analysis, sediment dried in vacuum oven	Comparison of desorption methods Purging: (1) conventional purge-and-trap; (2) Grob closed-loop stripping analysis Solvent extractions: (1) sonication; (2) sonication-homogenization; (3) Soxhlet; (4) hypovial extraction		GC-FID, -Hall, -MS (capillary column)
136 Hiatt (1981)	28 Volatile organic priority pollutants	Sediments placed in liter bottles with 200 mL water stored at 18°C	Vacuum extracted with ultrasonic agitation; cryogenic concentration		Purge and trap
137 Amin and Narang (1985)	16 Volatile organics		Closed-loop stripping (with addition of water at room temperature, without additional water at 120°C) onto Porapak N sorbent; methanol eluant		GC-ECD, -PID (packed column)
138 Onuska and Terry (1985)	Chlorinated benzenes	Air-dried, manually ground	Comparison of extraction methods: (1) Soxhlet; Celite added to sediment; hexane-acetone-isooctane (43:43:14); water wash; water extracted with benzene; organic layers combined; dried sodium sulfate; purified on Florisil; hexane eluant; treated with mercury as needed;		GC-ECD (capillary column)

139	Charles and Simmons (1987)	Chloroform, trichloroethylene, and chlorobenzene	Ekman dredge, stored at 4°C
140	Lee (1988)	Chloranisoles and chloromethyl anisoles	Soxhlet; sediment over Celite; acetone-hexane (59:41) Purified by liquid-liquid extraction with potassium hydrogen carbonate; organic layer dried on sodium sulfate column; aqueous layer extracted with petroleum ether; dried on same sodium sulfate column Fractionated on column of sodium sulfate over Florisil; petroleum ether/methylene chloride-petroleum ether eluants
141	Sholz and Palauschek (1988)	Chlorinated anilines and benzidines	Purified by GC-ECD, -MSD (capillary columns) GC-NFID, -MS (capillary column) Sediment homogenized with sodium sulfate and toluene-pyridine (95:5); shaken; filtered; concentrated Purified by (1) Fractionation with gel permeation chromatography; cyclohexane-ethyl acetate (50:50) eluant; or (2) Hydrochloric acid solution added; partitioned with methylene chloride; aqueous fraction converted to basic pH; partitioned again with methylene chloride

Table 19.8. Determination of Phenolic Compounds Associated with Fixed or Suspended Solids/Sediments

Reference	Analyte	Sampling, Sample Handling, Preservation, and Storage	Sample Preparation		Final Determination
			Extraction, Purification, Fractionation		
142 Goldberg and Weiner (1980)	Phenol, o, m-, p-chlorophenol, 2,4-dichlorophenol, 2,4,5-trichlorophenol, 1-2-naphthol, o-methoxyphenol, o-aminopheno, o-nitrophenol, o- and m-cresol, 2,6-dimethylphenol	Batch sampling Soxhlet system; methylene chloride			GC-FID (packed column)
143 Pierce et al. (1980)	Pentachlorophenol	Ekman dredge stored frozen in aluminum foil-lined freezer containers	Two extraction methods compared: (1) Wet sediment washed with hydrochloric acid; refluxed in acetone-hexane (60:40); (2) Air-dried sediment Soxhlet extracted with hexane-acetone-acetic acid (59:40:1)	Purified by liquid-liquid extraction; acetone removed by water wash; hexane extracted by basic solution; acidified; partitioned into hexane	GC-ECD, -MS (packed column)
144 Lee et al. (1987)	Pentachlorophenol and 19 other chlorinated phenols	Celite 545 added; acidified to pH < 1; Soxhlet; acetone-hexane (59:41); partitioned into potassium hydrogen carbonate	Extractive acetylation with acetic anhydride and petroleum ether	Purified on deactivated silica gel; hexane/toluene eluant	GC-ECD, -MSD (capillary columns)
145 Cardwell et al. (1988)	2-Phenylphenol and 4-chloro-3-methylphenol	Stainless-steel sampling spatula, glass bottles, storage at -18°C	Distillation following addition of water, copper sulfate, and sulfuric acid	HPLC-EC	
146 Shiraishi et al. (1989)	Tertiary alkyl phenols	Ponar grab sampler, homogenized, stored in glass at 4°C	Mixed with anhydrous sodium sulfate; Soxhlet; (1) isopropanol; (2) methylene chloride; solvent-exchanged to hexane	Fractionated on columns of sodium sulfate/ deactivated silica gel/hydrochloric acid-rinsed copper; hexane/methylene chloride/methanol eluants	GC-MS (capillary column)

Table 19.9. Determination of Surfactants Associated with Fixed or Suspended Solids/Sediments

Reference	Analyte	Sampling, Sample Handling, and Preservation, and Storage		Extraction, Purification, Fractionation	Sample Preparation	Final Determination
		Sample Preparation	Extraction, Purification, Fractionation			
147 Uchiyama (1979)	FWA, LAS	Ekman-Birge sampler, filtered under vacuum, frozen	Extracted by refluxing; methanol/benzene (1:1); organic solvents evaporated; residue dissolved in hot water			UV, fluorometry
148 De Henau et al. (1986)	LAS	Grab samples, air-dried, sieved	Extracted by refluxing; methanol Purified by solid-phase extraction on anion exchange sorbent; methanol/hydrochloric acid eluant	HPLC-UV		
149 Matthijs and De Henau (1987)			Purified by solid-phase extraction on C ₈ sorbent; water/methanol eluant			
150 Marcomini and Giger (1987)	LAS, OPEO, NPEO		Soxhlet; methanol Extract diluted to a final composition of methanol/sodium dodecyl sulfate in water/acetone (1:1:2) Analyzed at this stage by reversed-phase HPLC Partitioned into hexane for analysis by normal-phase HPLC		HPLC-UV, -FD	
151 Inaba and Amano (1988)	LAS	Core sampler, freeze-dried	Sonicated; methanol; extract diluted to 10% in water; partitioned with 4-methyl-2-pentanone; back-extracted into water		HPLC-UV	

Table 19.10. Determination of Phthalates Associated with Fixed or Suspended Solids/Sediments

Reference	Analyte	Sampling, Sample Handling, and Preservation, and Storage		Sample Preparation Extraction, Purification, Fractionation	Final Determination
152 Webster and Nickless (1976)	DEHP, BBP, DCHP, DBP, DIBP, DNP, DAP, DMEP	Extracted by organic solvent Fractionated on deactivated alumina; hexane/diethyl ether eluant Further fractionated by TLC on silica gel G; ethyl acetate/hexane developing solvent			GC-ECD (packed column)
153 Payne and Benner (1981)	DEP	Soxhlet, acetonitrile; acetonitrile extract diluted with water; partitioned into hexane			GC-ECD, HPLC-UV
154 Waldock (1983)	DMP, DEP, DIBP, DBP, DEHP, DNP, Di-heptylphthalate	Grab sample Purified on deactivated alumina; methylene chloride eluant		Equivalent weight of anhydrous sodium sulfate added; left overnight at 4°C; Soxhlet; methylene chloride	GC-MS (capillary column)
155 Thurén (1986)	DMP, DBP, BBP, DEHP	Excess water removed by centrifugation		Liquid-solid extracted with acetonitrile/methylene chloride/petroleum ether Fractionated on deactivated Florisil; petroleum ether/diethyl ether eluant	GC-ECD (capillary column)
156 Thurén and Södergren (1987)	DBP, DEHP			Extracted as in reference 155 Purified by partitioning between sulfuric acid/hexane/hydrated sulfuric acid	GC-FID (capillary column)

Table 19.11. Determination of Alkyl and Aryl Phosphates Associated with Fixed or Suspended Solids/Sediments

Reference	Analyte	Sampling, Sample Handling, Preservation, and Storage	Sample Preparation		Final Determination
			Extraction, Purification, Fractionation		
157 Muir et al. (1981)	Triphenyl phosphate, cresyl diphenyl phosphate, and <i>o</i> -, <i>m</i> -, and <i>p</i> -tricresyl phosphates	Ekman dredge, stored in polyethylene containers at -50°C	Comparison of three extraction methods: (1) Wet sediment refluxed with methanol-water (9:1); filtered; concentrated; (2) Wet sediment refluxed with methylene chloride-methanol (1:1); concentrated; (3) Soxhlet; air-dried sediment; acetone-hexane (1:1), concentrated	Extracts diluted with water; adjusted to pH 3 with hydrochloric acid Partitioned with methylene chloride; organic extract dried with sodium sulfate; evaporated; redissolved in hexane-diethyl ether (7:3) Purified on acid alumina; hexane-diethyl ether eluent	GC-NPD (packed column)
158 Muir and Griff (1983)	Diphenyl phosphate, <i>o</i> -, <i>m</i> -, and <i>p</i> -dicesyl phosphates, triphenyl phosphate, and 2-ethylhexyl-diphenylphosphate	Ekman dredge, stored -50°C	Wet sediment refluxed with methanol-water (9:1); extract diluted with sulfuric acid solution Purified on XAD-2 resin; acetone eluant; eluate combined with sulfuric acid solution and sodium chloride; partitioned with ethyl acetate; dried over anhydrous sodium sulfate; concentrated Derivatized by diazobutane; excess reagent removed by evaporation; diluted with hexane Purified on acid alumina topped with anhydrous sodium sulfate; hexane-diethyl ether eluent	GC (packed column)	
159 Ishikawa et al. (1985)	Tributyl phosphate, tris (3-chloropropyl) phosphate, tris (2-chloroethyl) phosphate, trioctyl phosphate, tris (2,3-dichloropropyl) phosphate, triphenyl phosphate, and tricresyl phosphate	Ekman-Birge dredge	Extracted by shaking with acetone; filtered; diluted with water; partitioned with methylene chloride; concentrated; redissolved in pentane Purified on Florisil topped with anhydrous sodium sulfate; methylene chloride-pentane (1:9)ethyl alcohol-methylene chloride (1:99) eluants; concentrated	GC-FPD, -MS (packed column)	

Table 19.12. Determination of Organometallic Compounds Associated with Fixed or Suspended Solids/Sediments

Reference	Sampling, Sample Handling, Preservation, and Storage	Sample Preparation		Final Determination
		Extraction, Purification, Fractionation		
ORGANOMETALLIC LEAD COMPOUNDS				
160 Chau et al. (1979)		Wet sediment combined with ethylenediamine-tetraacetic acid solution and hexane and shaken; centrifuged		GC-AAS
161 Tiravanti et al. (1980)	Sampler consisted of outer stainless-steel tube and an inner PVC tube	Autoclaved; nitric acid and bromine oxidation		AA (graphite furnace)
162 Chau et al. (1984) 163 Wong et al. (1989)	Ekman grab sampler or scoop, frozen immediately	Dried or wet sediment combined with benzene, water, sodium chloride, potassium iodide, sodium benzoate, glass beads and sodium diethyldithiocarbamate for chelation extraction during mechanical shaking; centrifuged; butylation with Grignard reagent; washed with sulfuric acid solution; organic layer separated and dried with anhydrous sodium sulfate	GC-AAS (packed column)	
ORGANOMETALLIC MERCURY COMPOUNDS				
164 Ealy et al. (1973)		Extracted with sodium iodide; partitioned with benzene	GC-ECD (packed column)	
165 Longbottom et al. (1973)	Shake, stir, or blend to homogenize	Wet sediment combined with water and copper sulfate reagent; shaken; bromide reagent (sulfuric acid and potassium bromide) added; shaken; toluene added; shaken; centrifuged; layers separated Sodium thiosulfate reagent added; shaken; repeated; aqueous layer retained Combined with potassium iodide reagent and benzene; dried with sodium sulfate; concentrated	GC-ECD (packed column)	

166	Floyd and Sommers (1975)	Ekman dredge, stored in glass at 4°C, air-dried, ground	Wet sediment combined with cysteine-borate buffer solution and steam distilled; distillate collected in saturated potassium peroxydisulfate	Treated with reducing solution (consisting of sodium chloride, hydroxylamine hydrochloride, hydrazine sulfate, stannous chloride, and sulfuric acid)	Flameless-AA
167	Shariat (1979)		Extracted with pentane-ether (80:20); combined with a solution of potassium bromide and mercuric bromide and shaken; sodium thiosulfate added	Potassium iodide added to aqueous layer and extracted with benzene	GC-ECD (packed column)
168	Nakamura and Kashimoto (1979)		Saponified with potassium hydroxide/ethanol; water added; extracted with hexane; concentrated		AAS
169	Gilmour et al. (1986)	Van Veen grab or Lexan core tubes, core samples subsampled by removing minicores, frozen	Sample combined with sodium borate buffer; adjusted to pH 8; added to purge tube Derivatization solution of sodium borohydride, sodium hydroxide, and water Purged components cryogenically trapped at the head of a gas chromatographic column		GC-MS (packed column), Hydride generator, purge-and-trap sampler
170	Tsuda et al. (1986)		Wet sediment extracted with hexane after addition of water and hydrochloric acid; centrifuged; organic layer concentrated; ethanol and hydrogenation reagent (sodium borohydride in ethanol) added; shaken; water and sodium chloride added; extracted with hexane Purified on silica gel; hexane eluant		GC-ECD (packed column)

Table 19.12 continued

Reference	Sampling, Sample Handling, Preservation, and Storage		Sample Preparation		Final Determination
			Extraction, Purification, Fractionation		
1171 Epler et al. (1988)	Ponar grab sampler, frozen in polycarbonate bottles		Wet sediment combined with 1-butanol; vortexed; extracted ultrasonically; centrifuged; filtered		HPLC-LEI
1172 Turk et al. (1988)					
1173 Huggett et al. (1989)			Wet sediment combined with anhydrous sodium sulfate and precipitated silica; Soxhlet; hexane	GC-FPD, -MS (capillary column)	
1174 Stephenson et al. (1988)			Derivatized with <i>n</i> -hexyl magnesium bromide Purified on Florisil		
1175 Matthias (1989)			Sample acidified with hydrochloric acid solution; mixed; extracted with methylene chloride; centrifuged; evaporated; redissolved in hexane; sodium hydroxide wash; back-extracted with nitric acid	GFAA	
1176 Siu et al. (1989)	Sediment reference material		Refluxed in acidified methanol; methanolic layer extracted with cyclohexane	GC-FPD	
			Derivatized using sodium borohydride		
1177 Donard et al. (1986)	Schipeck sampler, dried at 60°C, ground before storage		Sample combined with hydrochloric acid solution and methanol; extracted ultrasonically; isooctane added; shaken; centrifuged; aliquot of extract diluted with methanol containing ammonium acetate solution; alternative procedure produced equivalent results with 1-butanol extractant	ISMS-MS	
MULTICLASS ORGANOMETALLIC TIN AND LEAD ANALYSES					
			Comparison of three digestion methods: (1) nitric acid solution; (2) hydrochloric acid solution; (3) sodium hydroxide solution Sonicated; shaken in the dark; water added and centrifuged; volatilization by hydride generation (derivatization)	GC-AAS	
			Cryogenic trapping on chromatographic sorbent; mild thermal desorption		

Table 19.13. Determination of Miscellaneous Anthropogenic Organic Compounds Associated with Fixed or Suspended Solids/Sediments

Reference	Analyte	Sampling, Sample Handling, and Preservation, and Storage	Sample Preparation		Final Determination
			Extraction, Purification, Fractionation		
178 Jaffe and Hites (1986)	Fluorinated aromatic compounds	Subcores of box-core samples or grab samples, frozen	Soxhlet; (1) isopropyl alcohol; (2) methylene chloride Sulfur removal with activated copper Purified on silica gel; hexane/hexane-methylene chloride (9:1)/methylene chloride/methanol; concentrated		GC-MS (capillary column)
179 Epstein et al. (1987)	1,4-Dioxane		Sediment mixed with aqueous sodium sulfate solution; heated purge and trap		GC-MS (packed column)
180 Headley (1987)	Organosulfur compounds		Shaken with methylene chloride-hexane; concentrated		GC-MS (capillary column)
181 Tsukioka and Murakami (1987)	Pyridine bases		Moist sediment combined with distilled water; sodium hydroxide solution, and silicone oil; distilled into sulfuric acid solution; concentrated; diluted with water; hexane and sodium hydroxide added with cooling; after shaking, hexane layer removed; dried with anhydrous sodium sulfate		GC-MS (capillary column)
182 Breitburg et al. (1988)	Disperse yellow 42 dyestuff	Frozen	Shaken with methanol; dried over anhydrous sodium sulfate; concentrated	HPLC-Visible	
183 Watanabe et al. (1988)	Silicones		Purified on Florisil; methylene chloride eluant; evaporated; redissolved in acetonitrile-water (3:1); filtered Samples combined with petroleum ether; allowed to stand overnight; extracted ultrasonically; dried with anhydrous sodium sulfate; evaporated; redissolved in methyl isobutyl ketone		ICP

Table 19.14. Determination of Multiclass Anthropogenic Organic Compounds Associated with Fixed or Suspended Solids/Sediments

Reference	Analyte	Sampling, Sample Handling, Preservation, and Storage		Extraction, Purification, Fractionation	Sample Preparation	Final Determination
184 Berg et al. (1972)	PCBs, organochlorine pesticides			Extraction from solids unspecified Fractionated on charcoal; pesticides eluted with acetone-diethyl ether (25:75); PCBs eluted with cold benzene; further cleanup on Florisil for heavily contaminated eluates		GC/FID as bicyclohexyl, GC/ECD as decachlorobiphenyl (packed column)
185 Goerlitz and Law (1974)	PCBs, organochlorine pesticides, polychlorinated naphthalenes			Water separated from sediment by centrifugation Moist solid with equivalent weight of sodium sulfate added extracted with acetone-hexane on wrist-action shaker Suspended sediment separated by filtration/water wash of organic extract/back-extracted water wash with hexane; combine; water wash again Hexane extract fractionated on alumina with hexane eluant; treated with mercury to remove sulfur interferences; further fractionated on silica gel with hexane/benzene eluant		GC-ECD, -MS (packed column)
186 Jensen et al. (1977)	PCBs, organochlorine pesticides, chlorophenols			Wet sediment extracted with (1) acetone; (2) acetone-hexane (1:3); centrifuged; extracts combined with sodium chloride solution in phosphoric acid; partitioned with (1) hexane-diethyl ether-undecane (90:10:2); (2) diethyl ether; combined organic phases shaken with sodium hydroxide solution Aqueous phase; acidified with phosphoric acid solution; partitioned with trimethylpentane; derivatized Organic phase: evaporated; redissolved in trimethyl pentane; shaken with 2-propanol and tetrabutylammonium hydrogen sulfite reagent; water added and shaken; organic phase recovered and shaken with sulfuric acid monohydrate; centrifuged		GC-ECD (packed column)

187	Veith and Kiwus (1977)	PCBs, organochlorine pesticides	GC
188	Bellar et al. (1980)	PCBs, organochlorine pesticides	GC-ECD
189	Buchert et al. (1981)	PCBs, organochlorine pesticides, polychlorotrophenyls	Freezing technique for sediment cores
190	Murray et al. (1981)	PCBs, organochlorine pesticides, chlorinated aromatics, phthalates	Glass jars, refrigerated
191	Ray et al. (1983)		
			Dried sediment; Soxhlet extracted with hexane-acetone-toluene (60:30:10) Fractionated on (1) Florisil; (2) activated silver on silica to remove elemental sulfur; (3) sulfuric acid-treated silica
			Refluxed with acetone-acetonitrile; filtered; combined with aqueous sodium chloride; extracted under basic then acidic conditions with petroleum ether
			Basic extract purified on Florisil; petroleum ether-diethyl ether eluant
			Acidic extract derivatized with diazomethane and purified on acid alumina; hexane-benzene eluant
			GC-FID, -ECD (capillary column)
			HPLC-FD

GC

Sediments blended with water; extracted by exhaustive steam distillation
Sulfur interference removed by refluxing with Raney copper

Free water decanted; sediment air-dried, 10% water added

Three extraction procedures were compared:

- (1) Soxhlet with acetone-hexane (10:90); extract dried, concentrated;
- (2) Sonicated with acetone; water added; partitioned with methylene chloride-hexane (15:85);
- (3) Nielson-Kryger steam distilled into hexane; aqueous phase discarded; organic phase dried, concentrated

Cleanup on Florisil of Soxhlet and sonicated extracts; sulfur removed by shaking with (1) mercury; (2) tetrabutylammonium sulfite Extracts by steam distillation required only removal of sulfur

Dried sediment; Soxhlet extracted with hexane-acetone-toluene (60:30:10)
Fractionated on (1) Florisil; (2) activated silver on silica to remove elemental sulfur; (3) sulfuric acid-treated silica

Refluxed with acetone-acetonitrile; filtered;
combined with aqueous sodium chloride; extracted under basic then acidic conditions with petroleum ether

Basic extract purified on Florisil;
petroleum ether-diethyl ether eluant
Acidic extract derivatized with diazomethane and purified on acid alumina; hexane-benzene eluant

GC-FID, -ECD
(packed and capillary columns),
HPLC-FD

Table 19.14, continued

Reference	Analyte	Sampling, Sample Handling, Preservation, and Storage	Sample Preparation	Extraction, Purification, Fractionation	Final Determination
192 Chang-Yen and Sampath (1984)	PCBs, organochlorine pesticides			Sediments blended with water (0.1 M oxalic acid)-hexane (15:1); extracted by cyclic steam distillation Acid-washed copper powder added to hexane extract to remove sulfur	GC-ECD (packed column)
193 Grimalt et al. (1984)	PCBs, organochlorine pesticides, aliphatic and aromatic hydrocarbons	Grab sampler, frozen at -20°C	Sediment analyzed (1) as such; (2) freeze-dried; (3) oven-dried 50°C Soxhlet, or sonication with (1) hexane; (2) chloroform; or (3) methylene chloride-methanol (2:1)	Purified on column of copper powder Fractionated on column of silica gel over alumina; hexane-methylene chloride eluant	GC-FID, -ECD (capillary or packed column), UV-fluorometry
194 Bahnick and Markee (1985)	PCBs, pentachlorophenol, PAHs	Ponar dredge, gravity corer, amber glass bottles, continuous-flow centrifugation	Soxhlet; (1) acetone-hexane (1:1); (2) benzene; partitioned with sodium hydroxide solution to separate basic-neutral and acidic components Basic-neutral fraction purified by gel permeation chromatography (methylene chloride eluant) and cesium silicate fractionation, steam distillation collected in isoctane, or Florisil chromatography (hexane/benzene eluants) Acidic fraction purified by addition of sulfuric acid and partitioned with methylene chloride; dried with sodium sulfate; gel permeation chromatography (methylene chloride eluant) and cesium silicate fractionation	GC-FID, -ECD, -MS (capillary column)	Alternatively, acid fraction extracted from isoctane with sodium borate, acidified, back-extracted with hexane; derivatized with diazoethane

195	Ozretich and Schroeder (1986)	PCBs, organochlorine pesticides, phthalates, PAHs	Reference, contaminated, and spiked sediments	Wet sediment combined with anhydrous sodium sulfate (1:5); extracted ultrasonically with acetonitrile; concentrated Purified on C ₁₈ sorbent by solid-phase extraction Copper powder over the C ₁₈ sorbent used for sulfur removal	GC-FID, -MS (capillary column)
196	Japenga et al. (1987)	PCBs, organochlorine pesticides, PAHs		Pretreated with acid; mixed with silica; Soxhlet; benzene-hexane Purified on sodium sulfite/sodium hydroxide- treated basic alumina Fractionated on silica	GC
197	Lopez-Avila et al. (1987)	PCBs, organochlorine pesticides		SW-846 Method 8080: Extracted by Soxhlet (Method 3540) or sonication (Method 3550); concentrated Fractionated on Florisil or silica gel Treated with tetrabutylammonium sulfite to remove sulfur	GC (capillary column)
198	Aceves et al. (1988)	PCBs, organochlorine pesticides, PAHs		Fractionations by chromatography were compared: (1) Alumina/silica column (1:1); methylene chloride-hexane eluant; (2) Florisil column; diethyl ether-hexane eluant	GC-FID, -ECD (capillary column)
199	Alford- Stevens et al. (1988)	PCBs, organochlorine pesticides	Stored at 4°C, sieved, placed in glass bottles with Teflon-lined screw caps	Four combinations of extraction/purification procedures were compared: (1) Shaker/Florisil chromatography; (2) Shaker/gel permeation chromatography; (3) Sonication/Florisil chromatography; (4) Sonication/gel permeation chromatography Shaker procedure: extracted by shaking with (1) methanol; (2) methylene chloride-methanol (9:1)	GC-MS (capillary column)
				Sonicator procedure: sample mixed with anhydrous sodium sulfate; extracted ultrasonically with methylene chloride-acetone (1:1) Extracts from either shaker or sonicator procedures combined with aqueous sodium sulfate solution; organic layer separated after shaking; dried with anhydrous sodium sulfate; concentrated	

Table 19.14, continued

Reference	Analyte	Sampling, Sample Handling, Sample Preservation, and Storage		Sample Preparation		Final Determination
				Extraction, Purification, Fractionation		
200	Krahn et al. (1988)	Mixed in small cement mixer, glass jars, stored at -20°C		Extracted by tumbling wet sediment with sodium sulfate, methylene chloride, and activated copper; centrifuged; decanted; concentrated by evaporation; filtered Fractionated by HPLC preparative size-exclusion column; solvent exchanged each fraction to hexane	GC-FID, -ECD, -MS (capillary column)	
201	Petrick et al. (1988)	PCBs, organochlorine pesticides, aromatic hydrocarbons, PAHs		Extracted with hexane Purified on alumina; concentrated by evaporation Fractionated by HPLC analytical-scale normal-phase column	GC-FID, -ECD (capillary column)	
202	Schantz et al. (1988)	PCBs, organochlorine pesticides, PAHs		Wet sediment mixed with sodium sulfate; Soxhlet; methylene chloride; concentrated by evaporation Purified on silica gel by solid-phase extraction Fractionated by HPLC normal-phase semipreparative aminosilane column; evaporatively concentrated	GC-FID, -ECD (capillary column), HPLC-FD	
203	Czuczwa and Alford-Stevens (1989)	PCBs, organochlorine and organophosphorus pesticides, substituted phenols and benzenes, nitroaniline, DEHP, PAHs	Air-dried, sieved, glass bottles with Teflon-lined screw caps	Sediment mixed with anhydrous sodium sulfate (1:2); extracted ultrasonically; methylene chloride-acetone (1:1); extracts combined; centrifuged; concentrated; diluted with methylene chloride (compared with dilution by butyl chloride-methylene chloride [1:1]); filtered Fractionated by preparative-scale gel permeation chromatography; methylene chloride eluant	GC-ECD, -MS (capillary column)	

Table 19.15. Research on Comparisons of Sediment Preparation, Extraction, Purification, or Fractionation Techniques for the Determination of Anthropogenic Organic Compounds

Reference	Analyte	Sediment Preparation Methods Compared	Sediment Extraction Techniques Compared	Sediment Extraction Solvents Studied	Extract Purification Comparisons	Conclusions/Best Results
56 Walker et al. (1975)	Petroleum-derived	Soxhlet, stirring, sonication, shaking	Hexane, benzene, chloroform, benzene-methanol			Shaking/benzene or benzene-methanol
72 Hagenmaier et al. (1986)	PAHs	Wet, lyophilized, sediment-sodium sulfate (1:4)	Shaking, hot Soxhlet, sonication	Acetone, hexane, acetone-hexane (1:1), acetone followed by hexane		Lyophilized/ hot Soxhlet/ acetone-hexane (1:1)
80 Hawthorne and Miller (1987)	PAHs		Supercritical fluid extraction, Soxhlet, sonication	Five supercritical fluids: ethane, carbon dioxide, nitrous oxide, carbon dioxide-5% methanol, and nitrous oxide-5% methanol; benzene, methylene chloride		Supercritical fluid extraction/nitrous oxide-5% methanol
81 Morel and Courtois (1987)	Petroleum-derived	Freeze-dried, pestle pulverization, manual screening, homogenization	Mechanical tumbling, Soxhlet	Freon 113, carbon tetrachloride		Mechanical tumbling
95 Alford-Stevens et al. (1985)	PCBs		Two Soxhlet procedures, sonication			Soxhlet procedures equivalent and had lower RSD than sonication

Table 19.15, continued

Reference	Analyte	Sediment Preparation Methods Compared	Sediment Extraction Techniques Compared	Sediment Extraction Solvents Studied	Extract Purification Comparisons	Conclusions/Best Results
98 Dunnivant and Elzerman (1988)	PCBs	Freeze-dried, field-wet	Soxhlet, steam distillation, sonication	Acetone, acetone-hexane (1:1)		Field-wet/sonication equivalent to or better than Soxhlet
135 Ellington (1981)	Misc. chlorinated compounds		Purge-and-trap, Grob closed-loop stripping analysis, sonication, sonication-homogenization, Soxhlet, hypovial extraction	Hexane, acetone-hexane (1:1)		Grob closed-loop stripping analysis
138 Onuska and Terry (1985)	Misc. chlorinated compounds		Soxhlet, sonication, steam distillation	Acetone-hexane-isooctane (43:43:14), acetone-hexane (1:1)		Steam distillation
143 Pierce et al. (1980)	Phenolic compounds	Wet, air-dried	Reflux, Soxhlet	Acetone-hexane (60:40), hexane-acetone-acetic acid (59:40:1)		Extraction efficiency greater (but more variable) for reflux method compared to Soxhlet extraction
157 Muir et al. (1981)	Alkyl and aryl phosphates					Refluxing with methanol-water (9:1)

188	Bellar et al. (1980)	Multiclass compounds	Soxhlet, sonication, steam distillation	Acetone-hexane (10:90), acetone	Soxhlet best for environmentally contaminated sediments; all three procedures equivalent for spiked sediments
193	Grimalt et al. (1984)	Multiclass compounds	Field-wet, freeze-dried, oven-dried	Soxhlet, sonication	Sonication/ methylene chloride-methanol (2:1)
197	Lopez-Avila et al. (1987)	Multiclass compounds		Hexane, chloroform, methylene chloride-methanol (2:1)	Silica gel/ best when both organochlorine pesticides and PCBs are present
198	Aceves et al. (1988)	Multiclass compounds		Silica gel, Florisil	Alumina-silica fractionations better; Florisil recommended in presence of lipids
199	Alford-Stevens et al. (1988)	Multiclass compounds		Shaking, sonication	Florisil, gel permeation No definitive conclusion could be reached
				Methanol, methylene chloride-methanol (9:1), methylene chloride-acetone (1:1)	

CHAPTER 20

Determination of Polyvinyl Alcohol in Sewage

C. Ellen Gonter, Lorraine C. Guyette, and Thomas G. Stevens

The use of individual septic tank systems for the disposal of household wastewater has increased dramatically over the past 20 years. The 1980 census found about 21.9 million residences in the United States relying on septic tanks, a 31.9% increase over the 16.6 million residences noted in the 1970 census.¹ This trend continued into the 1980s, as about 25% of the new homes constructed utilized septic tank systems prior to disposal of wastewater.² Various consumer products commonly discharged to residential septic tank systems have been alleged to be the source of system upset or failure. Upset of the system can result in unacceptable discharge of pollutants to the subsurface soil absorption system, resulting in the complete failure of the system. These facts indicate the importance of demonstrating that products, which are intended for disposal and treatment in residential septic tanks, will not adversely impact the systems.

In order to study the disposability characteristics of products containing polyvinyl alcohol (PVA) in residential septic tanks, a procedure had to be developed that would determine low concentrations of the PVA in wastewater discharged from the tanks.

Since 1851, when Grange reported the use of starch for the determination of iodine,³ many studies of the iodo-starch complex have been carried out. West and others studied the reaction of PVA–boric acid–iodine in aqueous solutions in which chromogens, similar to those formed with iodine and starch, were produced.^{4–7}

Depending upon the concentration of the components, PVA in the presence of borates and iodine produced colors ranging from red to blue. This property was utilized as the basis for the identification of borates and PVA. Under certain conditions, fully hydrolyzed (deacetylated) PVA will produce red to blue colors in the absence of borate.

Commercially produced grades of PVA, used in paper coatings and personal products, contain various concentrations of residual partially hydrolyzed polyvinyl acetate and starch, added to enhance the product's biodegradability. Due

to the presence of these materials, Finley used the PVA-boric acid-iodine reaction to quantitate the PVA in paper coatings.⁸ Yamatani and Ishikawa used the method for the determination of PVA used as a water-soluble marker in studies of the gastrointestinal system of rats.⁹

EXPERIMENTAL

Reagents and Apparatus

- boric acid solution, 3.8%—40 g of reagent-grade boric acid dissolved in 1 L of deionized (DI) water
- iodine solution, 0.1 N—13.8 g of resublimed iodine dissolved in 25 mL of a concentrated solution of potassium iodide (40 g) and diluted to 1.0 L with DI water
- standard polyvinyl alcohol stock solution— 1.0000 ± 0.0002 g of fully hydrolyzed PVA (99% from Eastman Kodak Co.) previously washed with pure methanol to pH 7 and dried to constant weight, dissolved in 100 mL of DI water on a steam bath, and after cooling to ambient temperature, diluted to 1.0 L with DI water. The solution is stable for 1 month stored under refrigeration.
- homogenizer—Tekmar, SDT Tissumizer
- spectrophotometer—IBM, UV/Visible, 9420/9430, equipped with a Quick Flow Sampler
- cylinders—50-mL, graduated, S/T stoppers

PROCEDURE

The sample of acid-preserved (2 mL 5 N H_2SO_4 /L, pH < 2) sewage was homogenized for 15–20 sec, 100 mL poured into a 200-mL Berzelius beaker, heated to 90–95°C, and evaporated to a volume of approximately 70 mL. The sample was cooled to ambient temperature and filtered through a MSI 47-mm plain white, cellulosic, 5-μm membrane filter with the aid of vacuum. The filtrate was quantitatively transferred into a 100-mL volumetric flask, diluted to volume with DI water, and mixed thoroughly. Two 20-mL aliquots were pipetted into each of two 50-mL S/T stoppered graduated cylinders. To the first cylinder, 5 mL of DI water was added, and to the second, 20 mL of DI water was added (sample blank). Then 15 mL of 3.8% boric acid solution was pipetted into the first cylinder, and both cylinders inverted twice to mix. Into each cylinder, 3 mL of 0.1 N iodine was pipetted; the solutions were diluted to 50.0 mL, mixed thoroughly, and allowed to stand at ambient temperature for 25 min. The absorbance of each solution was determined at 650 nm versus a blank solution containing the same amounts of reagent solutions and domestic tap water. The difference between the absorbance readings of the solutions in the first and second cylinders was used to calculate the concentration of PVA in the sample.

STANDARDIZATION

A working standard solution containing 0.1 g PVA/L was prepared from the stock solution by diluting 10.0 mL to 100 mL in a volumetric flask. Acidified tap water from the Village of Chelsea, Michigan, was used for the dilution. Aliquots up to 10.0 mL were pipetted into 50-mL S/T stoppered cylinders and diluted to 25 mL with the acidified tap water, followed by the addition of 15.0 mL of boric acid solution, 3.0 mL of iodine solution, and dilution to volume with DI water. The solutions were mixed thoroughly after each addition. The absorbance of each solution was determined at 650 nm versus the blank. The slope, intercept, and correlation coefficient were calculated by linear regression; Beer's law was followed (Figure 20.1)

DISCUSSION

The samples to be examined were effluents collected from septic tanks, seeded with septage from an active septic tank and dosed with wastewater from the main interceptor sewer to the Village of Chelsea, Michigan, wastewater treatment plant. The products under evaluation were added to the wastewater dosed to the septic tanks. The wastewater contained starch and cellulosic materials, as well as a high concentration of suspended solids.

Starch, under the conditions of the test, was reported to exhibit absorption

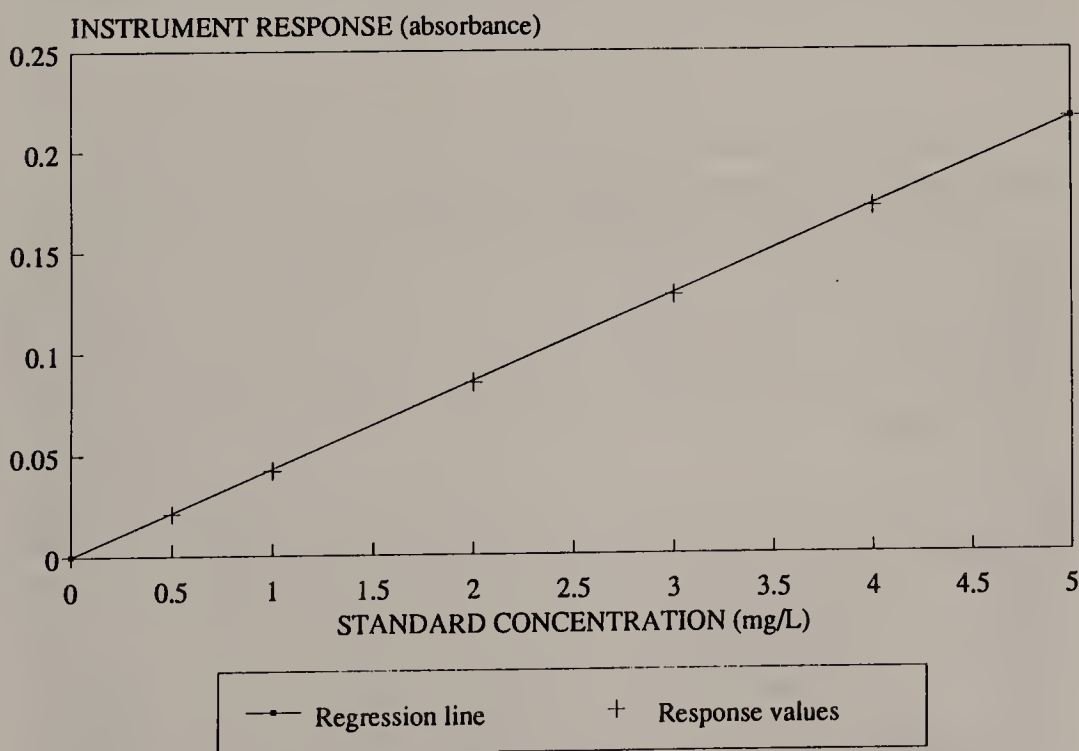


Figure 20.1. Calibration curve, PVA standards (650 nm).

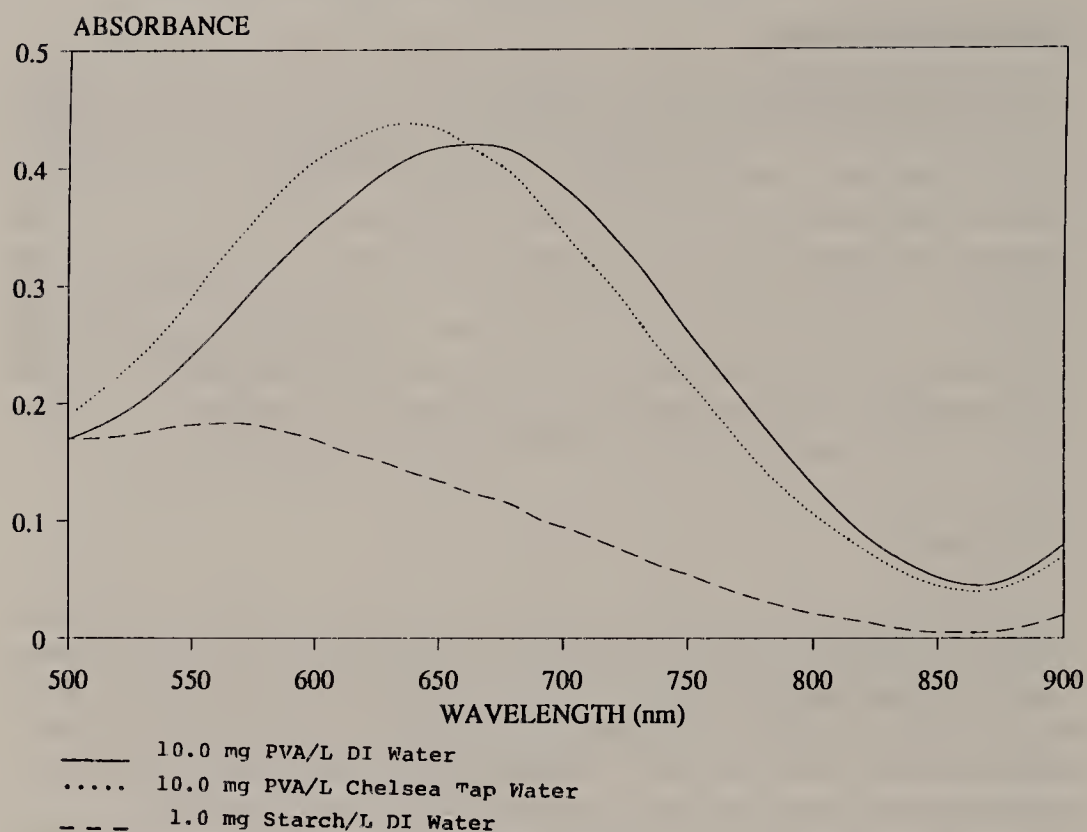


Figure 20.2. Absorption of boric acid-iodine systems of PVA and starch.

Table 20.1. Analysis of Chelsea, MI, Tap Water—1987

	mg/L
Barium	0.25
Cadmium	0.0012
Calcium	118
Inorganic carbon	72
Organic carbon	1.9
Chloride	46.1
Chromium, total	<0.001
Fluoride	1.4
Iron, total	0.001
Lead	0.003
Magnesium	34
Nitrate	0.4
Phosphate	0.2
Potassium	1.8
Sodium	22
Sulfate	105
Alkalinity (CaCO_3)	315
Hardness (CaCO_3)	433
Total dissolved solids	525

between 500 and 700 nm. This was confirmed by treating a solution containing 1.0 mg starch/L with boric acid and iodine (Figure 20.2). The presence of titanium dioxide, clays, calcium carbonate, and rosin has been reported to seriously affect the recovery of PVA.⁸ The exact nature of the interference is not known, but it is believed that adsorption of PVA may occur on substances that have a very large surface area and known adsorptive properties.

At the beginning of the study, samples were taken directly from the septic tanks. Various procedures were tried for the removal of the solids and colloidal material (e.g., filtration, centrifugation). It had been assumed that by treating duplicate aliquots in an identical manner except for the addition of boric acid to one aliquot, that the concentrations of PVA and starch could be obtained by difference; this approach appeared successful with solutions of test material only. Due to the differences in color produced by iodine with various types of starch, and due to the apparent adsorption of PVA on solids and the presence of other unknown components in the sewage samples, this approach had to be abandoned. The recovery of PVA in these instances was low or negative. This preliminary work indicated the necessity for eliminating the interference caused by the presence of starch by acid hydrolysis to noninterfering substances, as well as the removal of interfering suspended material.

Chelsea tap water contains high concentrations of calcium, magnesium, sulfate, and carbonate (Table 20.1). In order to reduce or eliminate the effect of these constituents in the wastewater, Chelsea tap water was used for the preparation and dilution of the standards. Samples preserved with sulfuric acid to pH < 2 were used because of the potential that there would be sufficient acid present to hydrolyze the starch, precipitate the calcium, and inhibit further bacterial action at ambient temperature.

Absorption curves of solutions of standard with and without sulfuric acid were identical. Curves prepared with the Chelsea tap water show a shift of the maximum absorbance wavelength to a lower value (635 nm) than those obtained in DI water (665 nm) or those reported in the literature (670 and 690 nm) (see Figure 20.2). All curves obtained with solutions containing from 0.5 to 5.0 mg PVA/L in acidified tap water indicated a slight shift of the maximum absorbance to longer wavelengths as the concentration of PVA was decreased. For the range of concentrations expected in the samples, 650 nm was selected.

Sample temperatures between 20 and 25°C did not appear to affect the color development. However, below 20°C there was a tendency for the PVA-borate-iodine to coagulate. For very accurate work, constant temperature is recommended for color development in both samples and standards.

Known amounts of PVA stock standard solution were added to samples taken from the wastewater and effluents from the test and control tanks. The applicability of the procedure is illustrated in Table 20.2. Recoveries from additional samples treated in a similar manner ranged from 90 to 102%.

Several of the acidified samples, stored for several days at ambient tempera-

Table 20.2. Determination of PVA in Spiked Samples

Sample Source	mg PVA/L		
	Added	Recovered	% Recovery
Influent	0.0	0.0	
	2.5	2.24	90
	5.0	4.66	93
Treatment tank	0.0	2.00	
	2.5	4.38	95
	5.0	6.52	90
Control tank	0.0	0.52	
	2.5	2.90	95
	5.0	5.51	100

ture, were analyzed with and without the heating step. The results were nearly identical with the results obtained from analysis completed within 24 hr after sampling. The unpreserved samples, which had been stored under refrigeration and acidified prior to heating and analysis, yielded much lower results. This was an indication that adsorption and/or bacterial action did not take place in the presence of acid. Therefore, the samples should be acid-preserved as described.

Small pieces of the test material found in the treatment tanks were dried on an aluminum sheet, and an infrared spectrum of the material was obtained. Infrared spectra were obtained on the original material and film prepared from the Eastman product (Figure 20.3). These spectra indicate that the original test PVA was not completely deacetylated and contained an appreciable amount of starch, determined to be approximately 10%. The spectrum of the material taken from the tank indicates that the starch had either dissolved or was removed by bacterial action while in the septic tank.

In order to determine the expected detection limit, a series of synthetic samples was prepared by adding various amounts of PVA to a composite of acidified samples from the control tank. The concentrations ranged from 0.04 to 2.0 mg PVA/L. The PVA content in these samples was determined each day for 5 days. Using these data, plus the results from 10 daily standardizations, the method detection limit (MDL) calculated by the EPA method¹⁰ was 0.08 mg PVA/L at a concentration of 0.16 mg PVA/L. At the same concentration, the limit of detection (LOD) and the limit of quantitation (LOQ) were 0.06 and 0.19 mg PVA/L, respectively, applying the ACS method.¹¹

The overall method reporting limit (MRL), calculated by the practice under consideration by ASTM D-19.06—a combination of the methods proposed by Hubaux and Vos¹² and the U.S. Army Toxic and Hazardous Materials Agency¹³—was determined to be 0.12 mg PVA/L at the 95% confidence limit, and 0.15 at the 99% confidence limit (Table 20.3 and Figures 20.4 and 20.5).

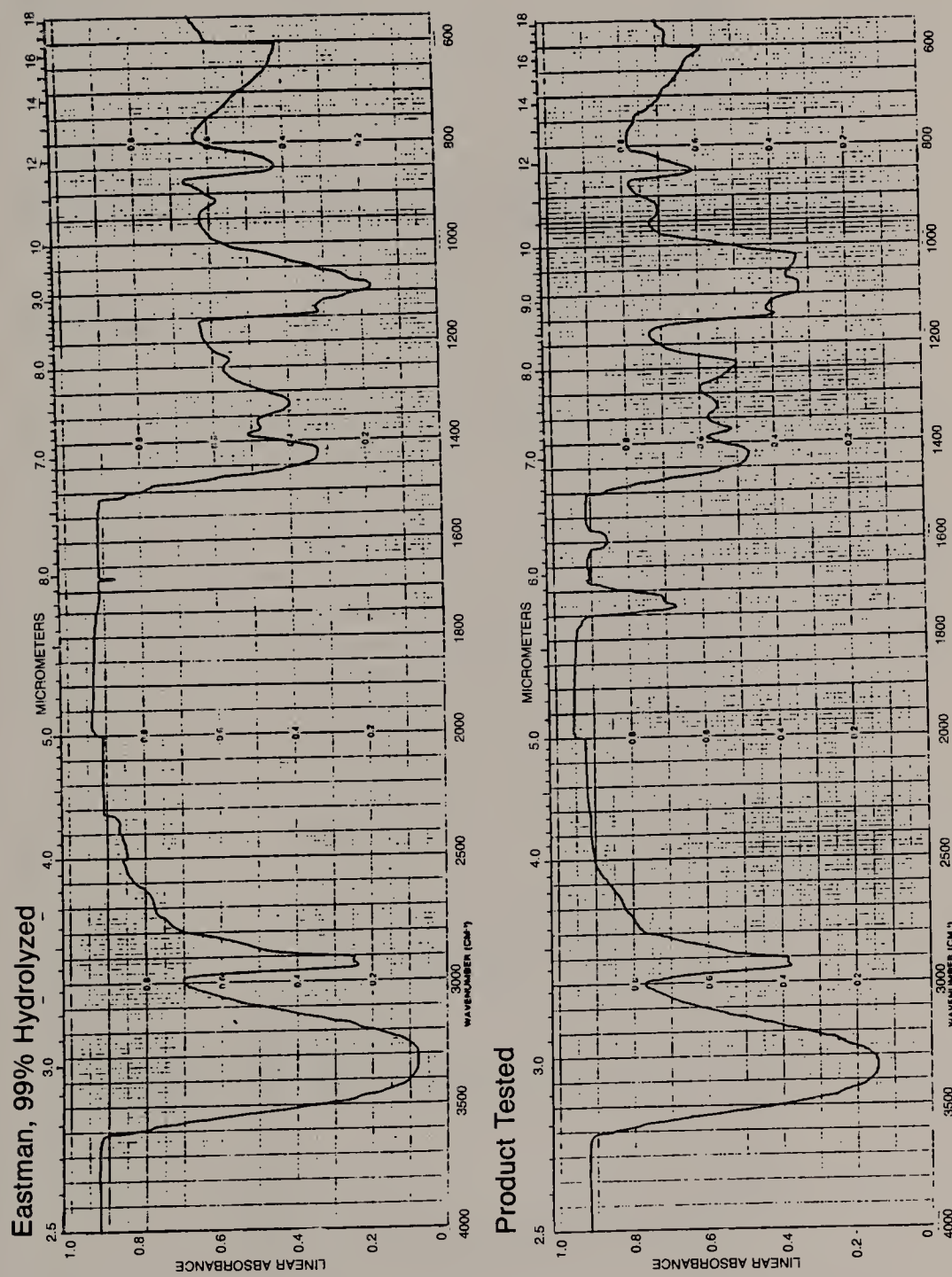


Figure 20.3. Infrared spectra of PVA films.

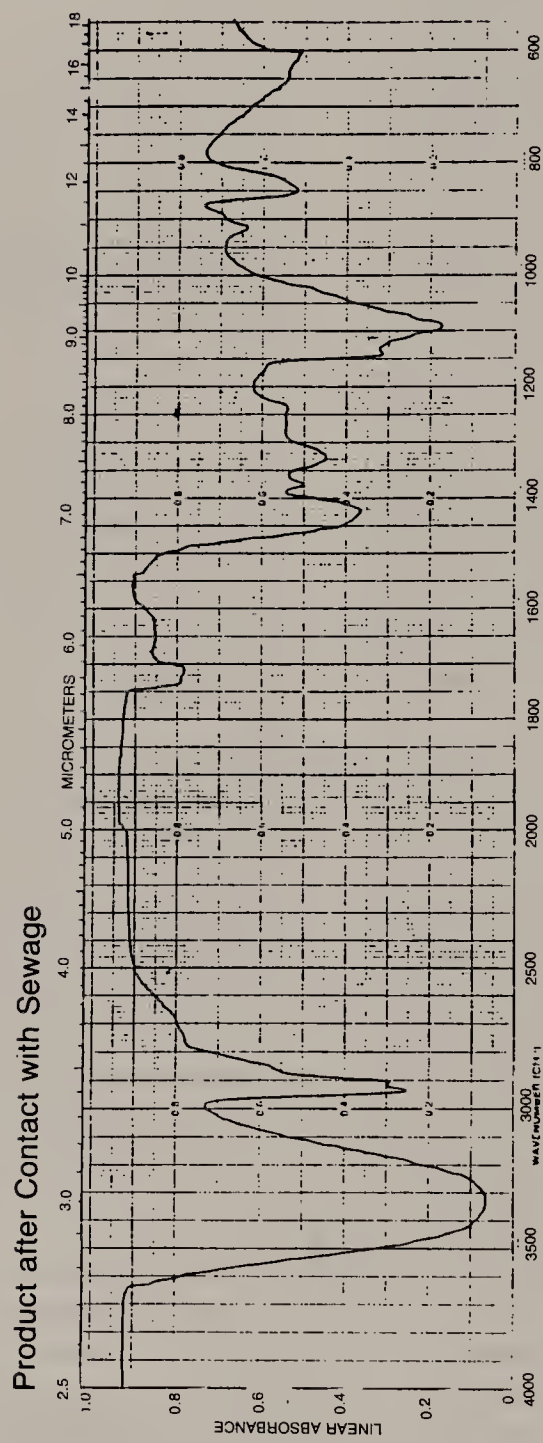


Figure 20.3., continued.

Table 20.3. Detection of PVA

	Standard	Conc. mg PVA/L	Sample	Spike Conc. mg PVA/L
MDL-EPA	0.15	0.5	0.08	0.16
LOD-ACS	0.15	0.5	0.06	0.16
LOQ-ACS	0.53	0.5	0.19	0.16
MRL			0.12 (95%) 0.15 (99%)	
Procedure Variability				
ASTM D4210	0.15	0.5		

Note: 6 standards + blank, run each day for 10 days.

7 spiked samples + blank, run each day for 5 days.

SUMMARY

For the project described, the procedure yielded satisfactory results. Samples analyzed over a period of 7 months contained an average of 2 mg PVA/L. The results were reported to the nearest 0.1 mg PVA/L.

However, the procedure could be refined to produce more sensitive and accurate results. It is known that the color reaction is sensitive to the conditions used to produce the PVA, the degree of polymerization of PVA, its crystallinity and tacticity, as well as the concentrations of boric acid and iodine used.¹⁴ In order to optimize conditions the techniques should be tried on both influent water and sewage before data are generated.

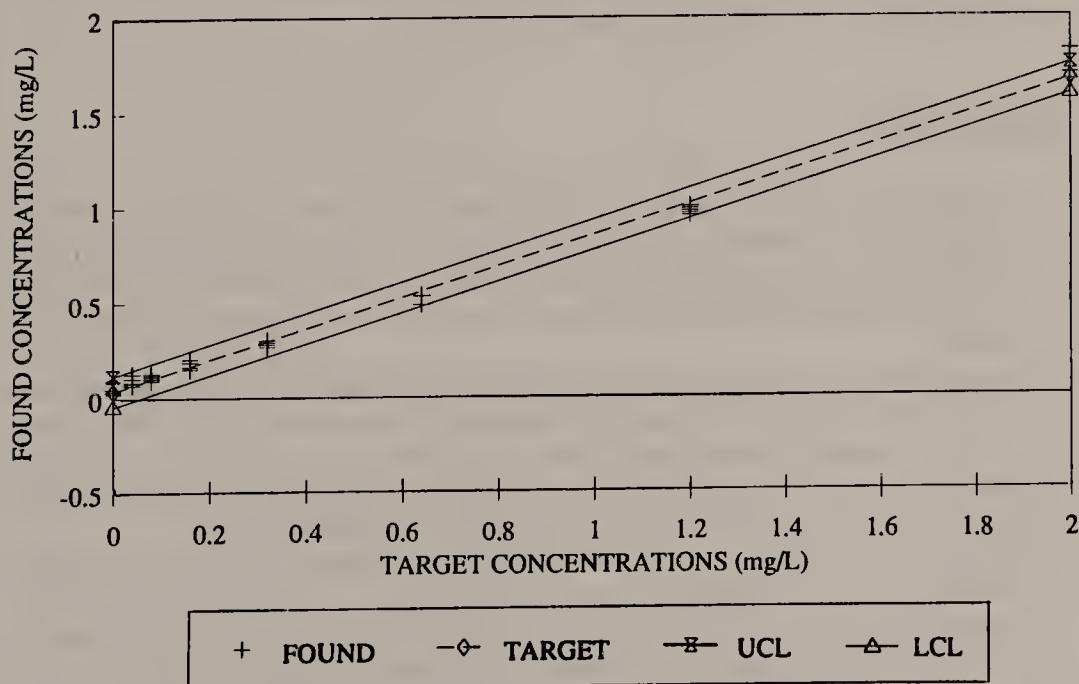


Figure 20.4. MRL graph, all target concentration levels.

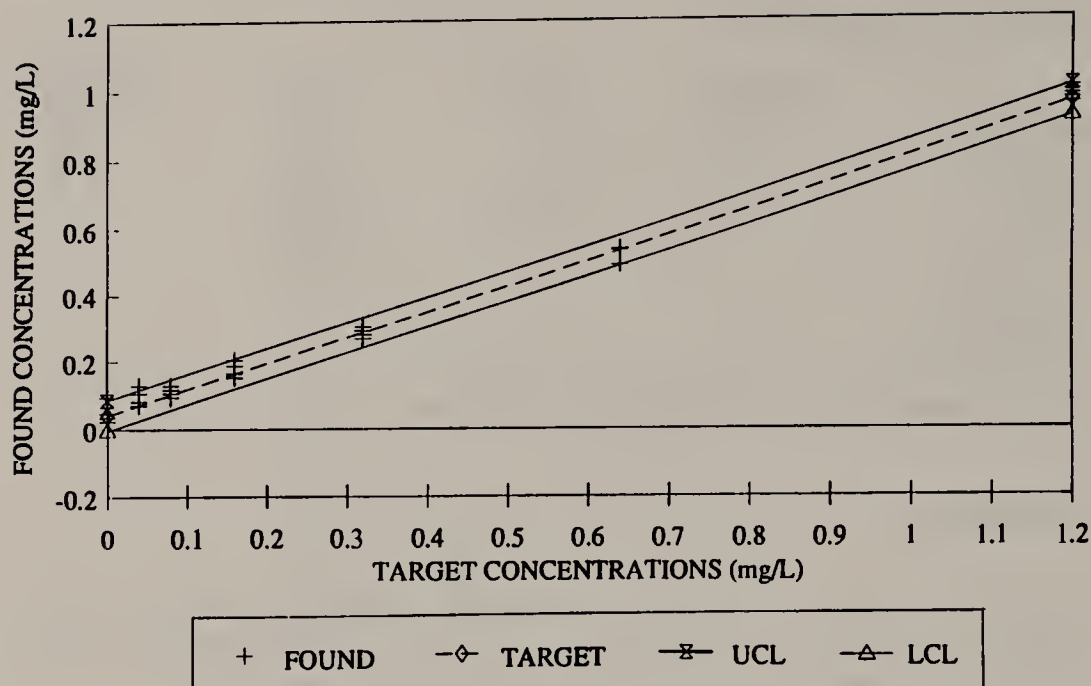


Figure 20.5. MRL graph, reduced target data.

ACKNOWLEDGMENTS

This chapter is based upon work funded by ConvaTec, 200 Headquarters Park, Skillman, NJ 08558. The authors express their gratitude to J. W. Koehn for calculation of the minimum reporting limits.

REFERENCES

1. "Handbook of Septage Treatment and Disposal," U.S. EPA Report-625/6-84-009, Municipal Environmental Research Laboratory, Cincinnati, OH (October 1984).
2. "Design Manual—Onsite Wastewater Treatment and Disposal Systems," U.S. EPA, Municipal Environmental Research Laboratory, Cincinnati, OH (October 1980).
3. Grange, M. "Nouveau Moyen de reconnaître La Presence des plus jaibles traces d'iode et d'iodures, et de separer les bromures de l'iode ou des iode ou des iodures qui y sont meles," *Compt. Rend.* 33:627-629 (1851).
4. West, C. D. "I. X-Ray Diffraction by Addition Compounds of Halogens with Hydrophilic Organic Polymers," *J. Chem. Phys.* 15:689 (1947).
5. West, C. D. "II. Aqueous Dispersion of Polyvinyl Borate—Iodine and Its Heat of Formation," *J. Chem. Phys.* 17:219-220 (1949).
6. Monti-Bovi, A. J., J. J. Sciarra, and D. Montorana. "The Qualitative Determination of Borates by Polyvinyl Alcohol," *Drug Stand.* 27:15-17 (1959).
7. Monti-Bovi, A. J. and J. J. Sciarra. "A Study of the Polyvinyl Alcohol-Borate-Iodine Complex I.," *Drug Stand.* 27:136-140 (1959).

8. Finley, J. H. "Spectrophotometric Determination of Polyvinyl Alcohol in Paper Coatings," *Anal. Chem.* 33:1925-1927 (1961).
9. Yamatani, Y., and S. Ishikawa. "Polyvinyl Alcohol as a Water-Soluble Marker," *Agr. Biol. Chem. (Japan)* 32:474-478 (1968).
10. "Methods for the Chemical Analysis of Water and Wastes," U.S. EPA Report-600/4-79-020, Environmental Monitoring and Support Laboratory, Cincinnati, OH (March 1979; revised March 1983).
11. ACS Committee on Environmental Improvement, "Guidelines for Data Acquisition and Data Quality Evaluation in Environmental Chemistry," *Anal. Chem.* 52:2242-2249 (1980).
12. Hubaux, A., and G. Vos. "Decision and Detection Limits for Linear Calibration Curves," *Anal. Chem.* 42:849-855 (1970).
13. U.S. Army Toxic and Hazardous Materials Agency, *Installation and Restoration Program, Quality Assurance Program* (December 1985).
14. Finch, C. A., Ed. *Polyvinyl Alcohol Properties and Applications* (New York: John Wiley and Sons, 1973).

CHAPTER 21

Use of ^{14}C Label to Study Fine Particulate Organic Matter Dynamics in Flowing Water

J. Denis Newbold, Colbert E. Cushing, and G. Wayne Minshall

INTRODUCTION

Particulate organic matter (POM) in streams and rivers is an important energy source for microbes and invertebrates.^{1,2} POM is also important in controlling the dynamics of contaminants because of its affinity for hydrophobic organic compounds.³ Understanding the relationships between downstream transport and sedimentary storage of POM is therefore critical to studies of ecosystem processes, as well as to characterizing the fate and effects of contaminants.

Flow fluctuations clearly play an important role in suspending and transporting POM,⁴ but very little is known about the magnitude of deposition and suspension during steady flows. Budgetary studies of stream ecosystems have shown that base flow transport of POM is often quite large relative to POM storage.⁵⁻⁸ Minshall et al. made this comparison by dividing daily transport of POM (g/day) by the standing stock per meter length of stream (g/m), which yields a theoretical velocity at which the stock of POM would migrate downstream if all particles exchanged frequently between the suspended and sedimentary pools.⁷ Among a number of streams, they calculated velocities ranging from 0.19 m/day in a very small stream to about 1000 m/day in a medium-size river. These figures suggest that even modest exchanges between suspended and sedimentary pools would have a large impact on sedimentary POM dynamics. Models for contaminant transport that require parameter values for deposition and resuspension generally determine these parameters indirectly through data fitting, and in some circumstances use the quiescent water fall velocity to describe deposition.⁹⁻¹¹ Use of fall velocity is suggested by theoretical approaches to sediment transport^{12,13} and particle deposition through laminar sublayers,¹⁴ but has not been verified by field studies.

Direct measurement of deposition and resuspension rates of natural POM in streams or rivers has been hampered by the difficulty of distinguishing experi-

mentally introduced natural particles from the pool of particles already present in the stream. This chapter presents a method for estimating the flux of particles from the water column to the streambed using POM collected directly from the water column and labeled with ^{14}C according to methods developed for marine detritus. We compare the resulting deposition velocity with laboratory-measured fall velocities and discuss implications regarding resuspension rates.

METHODS

Study Site

The study was conducted in a 1-km reach of Smiley Creek, a tributary to the main stem of the Salmon River in central Idaho. At the time of the field experiment (July 7, 1989), discharge was $0.68 \text{ m}^3/\text{sec}$, and the mean width, depth, and velocity were 7.7 m, 0.33 m, and 0.26 m/sec , respectively. Water temperature was approximately 15°C . The stream meanders through a broad meadow valley through a series of pools and riffles, with stream width varying between 3.9 and 10.8 m (based on 20 transects). Inorganic sediment sizes range from sand to cobble.

POM Collection and Labeling

Suspended particles were collected from Smiley Creek by suspending a $100\text{-}\mu\text{m}$ net within a $50\text{-}\mu\text{m}$ net for approximately 30 min. Particles collected in the $50\text{-}\mu\text{m}$ net (i.e., 50-to $100\text{-}\mu\text{m}$ size range) were stored cold, but not frozen (to minimize both microbial and physical effects on particle size), and shipped to Pacific Northwest Laboratory for labeling. Particles were batch-soaked in [^{14}C]acetic anhydride over a period of 2.5 hr, following the method described by Banks and Wolfenbarger,¹⁵ who found that this method acetylates the primary amines in the detrital material, forming covalent bonds stable to environmental extremes of pH, temperature, and salt concentration. After washing with distilled water and centrifugation, the detritus was batch-soaked in [^{14}C]dimethyl sulfate (in acetone) for 100 min, as described by Wolfenbarger and Crosby,¹⁶ who showed that this procedure methylates hydroxyl groups in cellulose.

The concentration of POM ($50\text{--}100\text{ }\mu\text{m}$) in the water column was estimated by pumping 318 L of stream water through nested 50-and $100\text{-}\mu\text{m}$ nets, and obtaining ash-free dry mass (AFDM). Additional samples of suspended particles were analyzed for density and fall velocity by methods of Webster et al.¹⁷ Mean particle size (as nominal diameter, or that of a sphere of equivalent volume) was determined by microscopic examination of 600 particles. POM on the surface of the stream bottom was estimated by suction-cleaning areas within a 1-m^2 quadrat and passing collected material through nested 50-and $100\text{-}\mu\text{m}$ nets.

Field Release of Labeled Particles

The labeled POM was transported to Smiley Creek, where 1.5 g wet mass (approximately 0.7 g dry mass or 0.1 g AFDM) of labeled detritus was suspended in a 4-L jar containing 18.4 g rhodamine WT dye, which served as a hydrodynamic tracer. Sixteen transects were established at 10-to 250-m intervals over a 1000-m reach. A plank bridge was constructed at each transect to provide access for sampling the water. A device holding three quart (0.95-L) jars was used to dip samples. The center sample was taken from the thalweg (point of maximum velocity), with the lateral samples 1 m to each side. The mixture of rhodamine and labeled POM was poured into the stream at the head of the experimental reach, following which samples were taken from each transect according to a schedule established from a previous dye release. Within 8 hr of collection, a 20-mL subsample was removed from each jar for determination of rhodamine concentration by fluorescence, and each sample was filtered (1.2- μm membrane filter). The filters were placed in scintillation vials, combining the sets of three lateral samples, and returned to the laboratory, where liquid scintillation cocktail was added and the samples were radioassayed.

Data Analysis

Rhodamine concentrations from each set of three lateral samples were averaged for comparability with the POM analysis. We computed the area under the concentration-vs-time curve for both labeled POM and rhodamine from each sampling transect, and the ratio (POM:rhodamine) of these areas at each transect. This ratio, $R(x)$, represents the quantity of labeled POM observed passing a transect x meters downstream from the injection relative to the quantity of rhodamine introduced to the stream, provided that rhodamine was not sorbed to sediments or degraded within the stream. A comparison between rhodamine WT and chloride transport in a 700-m reach of similar stream nearby showed no significant loss of rhodamine, and a maximum loss (i.e., 95% confidence limit) of 12% (unpublished data). If it is assumed that

1. all the POM particles behaved identically and were well mixed throughout the depth of the stream
2. the stream was longitudinally uniform
3. resuspension of deposited particles did not measurably affect the POM curves

(the validity of these assumptions is addressed below), then a constant fraction, k_L , of the suspended particles are deposited per longitudinal meter of stream, that is,

$$\frac{\partial R(x)}{\partial x} = -k_L R(x) \quad (21.1)$$

The solution to this equation is

$$R(x) = R_0 \exp(-k_L x) \quad (21.2)$$

in which R_0 represents the POM:rhodamine ratio injected (at $x = 0$). Values of $R(x)$ were fitted to the exponential function by linear regression of $\log[R(x)]$ versus x .

Under the assumptions given above, deposition can be described from the frame of reference of a moving parcel of water as a pseudohomogeneous first-order reaction. Letting $\partial x = v_w \partial t$, in which v_w is the average water velocity, and substituting for ∂x in Equation 21.1 yields

$$R(t) = R_0 \exp(-k_T t) \quad (21.3)$$

in which $k_T = v_w k_L$ and is the reaction rate. The deposition velocity of particles then is analogous to a mass transfer coefficient and is given by

$$v_{dep} = k_T d = k_L v_w d \quad (21.4)$$

in which d is the water depth.

RESULTS

Figure 21.1 illustrates the passage of the pulse of rhodamine dye and labeled POM at three of the fifteen sampling transects. Based on the travel time of the rhodamine dye, the water velocity averaged 0.26 m/sec. At 540 m, POM peaked at 1.8 pCi/L, which was near the limit of detection of our assay (the 95% confidence interval for 2 pCi/L was ± 1.6 pCi/L). Therefore, data from only the first fourteen transects ($x \leq 540$ m) were used in estimating deposition. The regression of $\log[R(x)]$ on x (Figure 21.2) explained 64% of the variance ($P < 0.001$) and yielded an estimate for R_0 of 0.096 pCi/(\mu g rhodamine), with 95% confidence interval of 0.082–0.114. Based on R_0 , and the known input of 18.4 g rhodamine, an estimated 1.8 μ Ci of 14 C were injected into the stream. The estimate for k_L was 0.0014 m^{-1} (95% confidence interval, 0.0007–0.0020), which yields an estimate of $1.2 \times 10^{-4} \text{ m/sec}$ for v_{dep} , the mean deposition velocity of particles (see Table 21.1).

The mean fall velocity from laboratory measurements of 100 particles was $3.4 \times 10^{-3} \text{ m/sec}$ (95% confidence interval, $3.1\text{--}3.8 \times 10^{-3}$), or more than one order of magnitude greater than the field deposition velocity. The mean particle specific gravity was 2.04, and the mean particle size was 0.74 μm . From these values, the theoretical (Stoke's law) fall velocity for a sphere¹⁸ is $2.8 \times 10^{-3} \text{ m/sec}$, which is much closer to the laboratory fall velocity than to the field deposition velocity.

The mean suspended POM concentration (50–100 μm) was 0.11 g/m^3 (95%

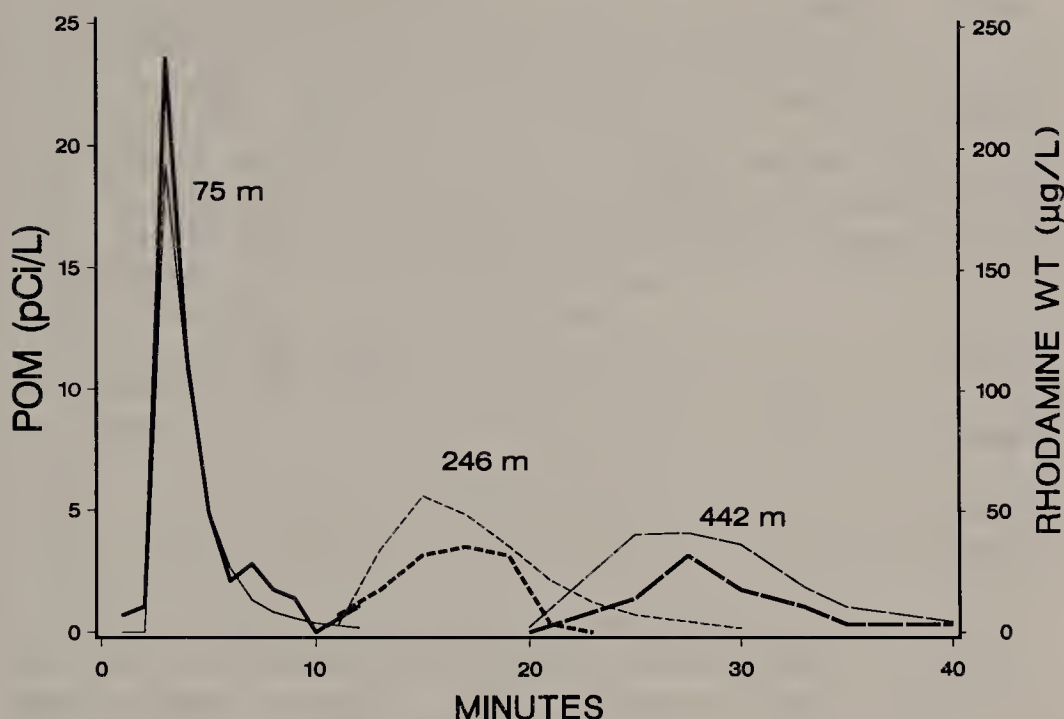


Figure 21.1. Concentrations of ^{14}C -labeled POM (thick lines) and rhodamine (thin lines) at three locations downstream from the point of release: 75 m (solid lines), 246 m (short-dashed lines), and 442 m (long-dashed lines).

confidence interval, 0.06–0.17) and comprised 16–22% of the dry mass of particles in this size range. Multiplying this by v_{dep} yields an estimated deposition flux of 0.05 g/m² hr. Sedimentary POM in the 50–100 μm size range exposed to the surface averaged 0.8 g/m² (95% confidence interval, 0.4–1.2), equivalent to approximately 16 hr of deposition.

DISCUSSION

The longitudinal pattern of loss conformed to the exponential model reasonably well (Figure 21.2), suggesting that the assumptions underlying this model were not seriously violated. Visual observations of the dye indicated the assumption of complete vertical mixing was achieved within the first 40 m, or about 2–3 min of travel time. On theoretical grounds, Denny and Shibata calculated that vertical turbulent transport under velocity and depth conditions similar to Smiley Creek is sufficient to mix particles throughout the water column within approximately 1 min.¹⁹ The assumption of a longitudinally uniform stream channel is clearly violated over distances of tens of meters by the stream's pool/riffle structure. However, the average particle traveled a distance of 710 m (i.e., $1/k_L$), and on this scale there were no significant longitudinal gradients in stream flow, width, or depth ($P > 0.05$). Our final assumption was that resuspended particles did not contribute to the POM

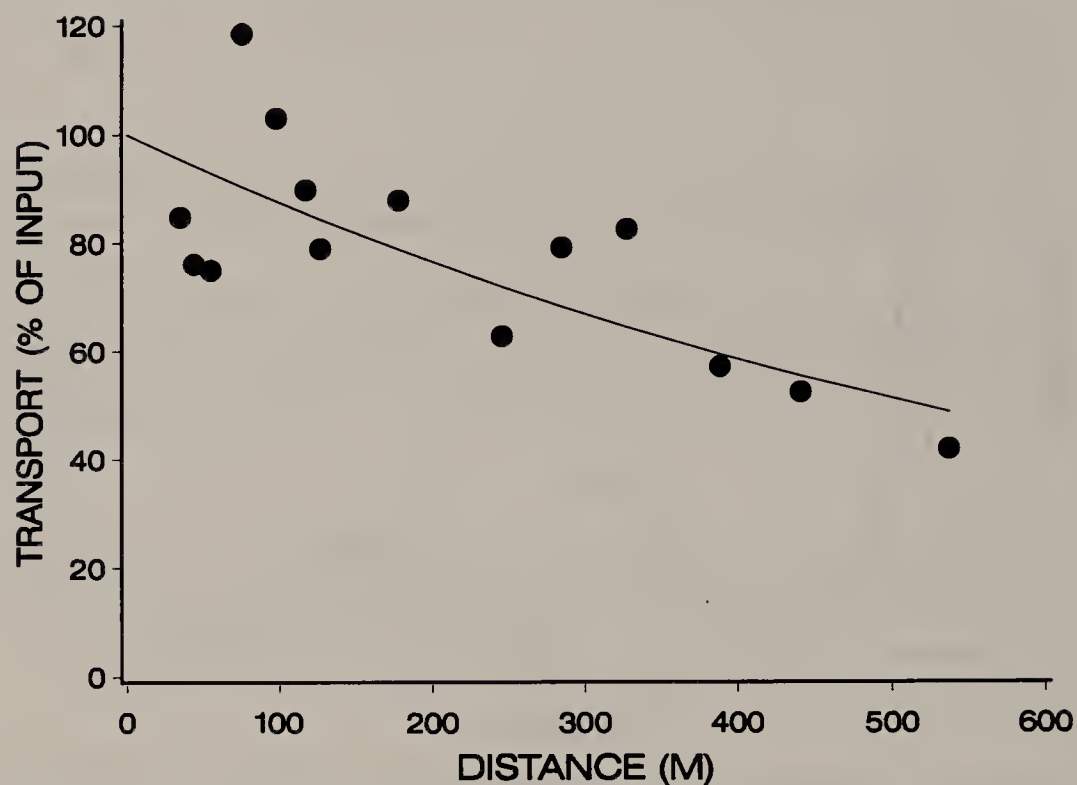


Figure 21.2. Transport of ^{14}C -labeled POM in Smiley Creek, July 7, 1989. The fitted line is given by $100 \exp(-0.0014x)$, where x is distance.

Table 21.1. Summary of Results and Calculations

Stream Characteristics	
Water velocity, v_w	0.26 m/sec
Depth, d	0.33 m
Width, w	7.7 m
Temperature	15°C
Particle Characteristics	
Mean diameter	0.75 μm
Specific gravity	2.04
Laboratory fall velocity	3.4×10^{-3} m/sec
Theoretical fall velocity	2.8×10^{-3} m/sec
Particle Deposition	
Longitudinal deposition rate, k_L	0.0014 m^{-1}
Temporal deposition rate, $k_T = v_w k_L$	$3.6 \times 10^{-4} \text{ sec}^{-1}$
Deposition velocity, $v_{dep} = k_T d$	1.2×10^{-4} m/sec
Suspended POM concentration, C	0.11 g/m ³
Deposition flux, $F_{dep} = v_{dep} C$	0.05 g/m ² hr
Stock of POM (50–100 μm) in surficial sediments, B	0.8 g/m ²
Turnover time of POM in sediments, $T_B = B/F_{dep}$	16 hr

curves. If deposited labeled particles were resuspended within a few minutes in sufficient numbers to affect the magnitude of the POM curve, they would also—because of the brief immobilization—affect the shape of the POM curve, producing a lag relative to the rhodamine and an extended tail. However, the shape and timing of the POM curves at downstream transects (e.g., see Figure 21.1, 440 m) did not differ noticeably from the respective rhodamine curves. Particles that contact the bottom but are immediately resuspended would not affect the curves and would not have contributed to the estimated deposition.

The theoretical and laboratory-derived fall velocities exceeded field deposition velocities by more than one order of magnitude. Webster et al. measured fall velocities of 1.0×10^{-3} to 2.0×10^{-3} m/sec for suspended particles in the 43–105 μm range from several North Carolina streams.¹⁷ These values are 30–60% of those of Smiley Creek particles, but still 8–16 times higher than the field deposition velocity. In theory, the deposition and fall velocities are equal if deposition occurs from a fully mixed free stream, through a laminar sublayer onto a surface,¹⁴ where passage through the laminar layer is governed by fall velocity. However, if particles reaching the stream bottom in this manner were immediately returned to suspension, they would not have been observed as “deposited” in the experiment (as discussed above). The average current velocity of 0.3 m/sec well exceeds that required to suspend particles in the 50–100 μm size range from a uniform bed.²⁰ But the streambed and flow patterns in Smiley Creek are highly heterogeneous, with many sites, such as sediment interstices within riffle areas and lateral zones with slack current, where resuspension may be unlikely. Thus, particles contacting the stream bottom may fall into two distinct populations, one being immediately returned to suspension, the other entering the pool of sedimentary POM. If this is the case, a predictive model for deposition velocity might involve the product of fall velocity and a measure representing the proportion of streambed area on which particles can be deposited. Such a measure would undoubtedly be related to streambed roughness, which has been shown in flume studies to influence strongly the rate of POM deposition.⁴

Resuspension of deposited POM was not observed directly. The quantity of tracer deposited (approximately 1 nCi/m²) was too low to detect in the sediments, and no tracer was observed in the water column after the passage of the injected pulse. In general, suspension in streams must equal or exceed deposition in order to produce any transport at all and to maintain particle concentrations against downstream dilution. If it is assumed that suspension was equal to deposition at 0.05 g/m² hr and that these exchanges involved the pool of 0.8 g/m² in surface sediments, then particles in this pool would be suspended on the average once every 16 hr, and migrate downstream at about 1 km per day. However, a portion of the deposited materials may be transported into deeper sediments via intragravel flow, and much of the suspension may derive from particles newly generated by biological activity.²¹ More research is needed to distinguish among these possibilities. However, our results demon-

strate that, regardless of their ultimate fate, particles are deposited on the stream bottom at a rate sufficient to have a major influence on sedimentary pools of POM.

REFERENCES

1. Cole, J. J., S. Findlay, and M. L. Pace. "Bacterial Production in Fresh and Saltwater Ecosystems: A Cross-System Overview," *Mar. Ecol. Progr. Ser.* 43:1-10 (1988).
2. Cummins, K. W., and M. J. Klug. "Feeding Ecology of Stream Invertebrates," *Ann. Rev. Ecol. Syst.* 10:147-172 (1979).
3. Karichhoff, S. "Organic Pollutant Sorption in Aquatic Systems," *J. Hydraulic Eng.* 110:707-735 (1984).
4. Webster, J. R., E. F. Benfield, S. W. Golladay, B. H. Hill, L. E. Hornick, R. F. Kazmierczak, Jr., and W. B. Perry. "Experimental Studies of Physical Factors Affecting Seston Transport in Streams," *Limnol. Oceanogr.* 32:848-863 (1987).
5. Fisher, S. G., and G. E. Likens. "Energy Flow in Bear Brook, New Hampshire: An Integrative Approach to Stream Ecosystem Metabolism," *Ecol. Monog.* 43:421-439 (1973).
6. Fisher, S. G. "Organic Matter Processing by a Stream-Segment Ecosystem: Fort River, Massachusetts, U.S.A.," *Int. Rev. Ges. Hydrobiol.* 62:701-727 (1977).
7. Minshall, G. W., R. C. Petersen, K. W. Cummins, T. L. Bott, J. R. Sedell, C. E. Cushing, and R. L. Vannote. "Interbiome Comparison of Stream Ecosystem Dynamics," *Ecol. Monog.* 53:1-25 (1983).
8. Naiman, R. J., J. M. Melillo, M. A. Lock, and T. E. Ford. "Longitudinal Patterns of Ecosystem Processes and Community Structure in a Subarctic River Continuum," *Ecology* 68:1139-1156 (1987).
9. O'Connor, D. J. "Models of Sorptive Toxic Substances in Freshwater Systems. I. Basic Equations," *J. Environ. Engin.* 114:507-532 (1988).
10. O'Connor, D. J. "Models of Sorptive Toxic Substances in Freshwater Systems. III. Streams and Rivers," *J. Environ. Engin.* 114:552-574 (1988).
11. Thomann, R. V., J. A. Mueller, R. P. Winfield, and C.-R. Huang. "Mathematical Model of the Long-Term Behavior of PCBs in the Hudson River Estuary," prepared for the Hudson River Foundation, Environmental Engineering and Sciences Program, Manhattan College, Riverdale, NY (1989).
12. Bagnold, R. A. "Physiographic and Hydraulic Studies of Rivers. An Approach to the Sediment Transport Problem from General Physics," U.S. Geological Survey Prof. Paper 422-I (1966).
13. Yalin, M. S. *Mechanics of Sediment Transport* (New York: Pergamon Press, 1977).
14. O'Melia, C. R. "Aquasols: The Behavior of Small Particles in Aquatic Systems," *Environ. Sci. Technol.* 14:1052-1060 (1980).
15. Banks, C. W., and L. Wolfinbarger, Jr. "A Rapid and Convenient Method for Radiolabeling Detritus with [¹⁴C]Acetic Anhydride," *J. Exp. Mar. Biol. Ecol.* 53:115-123 (1981).
16. Wolfinbarger, L., Jr., and M. P. Crosby. "A Convenient Procedure for Radiolabeling Detritus with [¹⁴C]Dimethylsulfate," *J. Exp. Mar. Biol. Ecol.* 67:185-198 (1983.)

17. Webster, J. R., E. F. Benfield, S. W. Golladay, R. F. Kazmierczak, Jr., W. B. Perry, and G. T. Peters. "Effects of Watershed Disturbance on Stream Seston Characteristics," in *Forest Hydrology and Ecology at Coweeta*, W. T. Swank and D. A. Crosley, Jr., Eds. (New York: Springer-Verlag), pp. 279-294.
18. Dietrich, W. E. "Settling Velocity of Natural Particles," *Water Resour. Res.* 18:1615-1626 (1982).
19. Denny, M. W., and M. F. Shibata. "Consequences of Surf-Zone Turbulence for Settlement and External Fertilization," *Am. Nat.* 134:859-889 (1989).
20. Richards, K. *Rivers: Form and Process in Alluvial Channels* (New York: Methuen, 1982).
21. Webster, J. R. "The Role of Benthic Macroinvertebrates in Detritus Dynamics of Streams: A Computer Simulation," *Ecol. Monog.* 53:383-404 (1983).

CHAPTER 22

Synchronous Fluorescence Spectra of Dissolved Organic Matter

Stephen E. Cabaniss

FLUORESCENCE OF DISSOLVED ORGANIC MATTER

The intrinsic fluorescence of dissolved organic matter (DOM) has been noted for some time.^{1–3} Fluorescence measurements can provide a wealth of information about molecular size, shape, association, structure, and the kinetics and equilibrium of binding.⁴ However, use of DOM fluorescence as an analytical tool has been complicated by the presence of many overlapping fluorescence peaks that combine to form broad, indistinct spectra. Interpretation of these spectra is often difficult. Synchronous excitation can often separate overlapping bands in mixtures of fluorophores. This chapter discusses synchronous excitation spectra of DOM and use of this technique as an environmental tracer and as a method for probing metal binding sites.

Features

The fluorescence of DOM, including humic acid (HA) and fulvic acid (FA), has been measured as a function of wavelength^{5–7} and time^{7–11} by several research groups. Maximum fluorescence intensity is typically quoted with excitation wavelength 330–360 nm and emission wavelength 420–460 nm. Excitation spectra (emission 450–500) show a broad peak near 350 nm and sometimes a shoulder or separate peak at lower wavelengths. Emission spectra (excitation 300–350) typically show a broad peak near 450 nm, often with a small shoulder. Fluorescence decay curves of terrestrially derived FA samples require two or three decay components (fluorophores) to fit the data;^{7–9} curves from marine sources require only one component.^{10,11} Decay is rapid; most fluorophores exhibit fluorescence lifetimes < 2 ns.

These results are consistent with the idea that DOM is a mixture of a number of different fluorophores. Evidence supporting this hypothesis includes the very broad excitation and emission peaks, red shifts in emission maxima as excitation wavelengths increase (and vice versa), and the multicomponent fluo-

rescence decay curves. This mixture model for the fluorescence of DOM is reasonable in light of the diverse origins and degradation patterns of the organic molecules in DOM.¹²

Uses

DOM fluorescence has been used as a surrogate measure for dissolved organic carbon (DOC),¹³⁻¹⁶ as a tracer for different water bodies,^{17,18} as an indicator of DOM size,^{8,9} and as an indicator of metal binding.¹⁹⁻²⁷ In general, the excitation and emission wavelengths used have corresponded to the peak intensity of the excitation-emission matrix. These peak intensity measurements are therefore quite sensitive even with relatively simple equipment.

DOC analysis typically uses combustion or oxidation to convert the DOM into CO₂ and water, and then quantifies the CO₂ generated by infrared (IR) absorption.²⁸ This analysis requires special equipment and is often times consuming. It is fraught with experimental difficulties in marine systems due to the presence of chloride, which can poison the combustion catalyst or attack the silver coating on the IR detection cell.

Fluorescence measurements, on the other hand, are highly sensitive and largely unaffected by a high-salt matrix. Consequently, several groups have investigated the use of DOM peak fluorescence intensity as a surrogate for DOC measurements in marine and coastal waters.^{13-16,29} Fluorescence intensity is proportional to DOC at low concentrations (< 5 mg DOC/L) of DOM, and the coefficient of proportionality is roughly constant in some water bodies.^{16,30} The chief drawback to the method is that the coefficient cannot be assumed to be constant, but must be calibrated with a more conventional method. Fluorescence can provide a quantitative estimate of DOC in these systems, providing the coefficient is checked periodically.

Peak fluorescence intensity may also be used as a tracer for DOM from different sources without determining this coefficient. Willey and others showed that the relative contributions of two rivers to a coastal water can be determined by measuring salinity and fluorescence of each end member.^{14,15,17} DOM fluorescence intensities of the rivers must be significantly different from each other and from the ocean water. Hayase et al. measured DOM fluorescence in the north Pacific Ocean to examine organic matter cycling as a function of depth.³¹

Depolarization of peak intensity can be used to estimate molecular rotation time in solution; provided the temperature and viscosity are known, hydrodynamic radii of the fluorescing molecules can be calculated from this data.⁴ Lapan and Seitz found a rotational relaxation time (RRT) of 2.0 ns and a hydrodynamic radius of 10.6 Å for a soil fulvic acid at 20°C using steady-state depolarization.⁸ Lochmuller and Saavedra measured time-dependent depolarization of Contech FA and found RRTs varied from 2.2 ns at pH 2 to 4.4 ns at pH 8.⁹ Both studies were complicated by the presence of several decay compo-

nents and by the extremely fast relaxation times, which required the use of a glycerol–water solvent to enhance viscosity.

The quenching of DOM fluorescence (FQ) by bound metal ions has been used as the basis for quantitative metal binding measurements by Weber and coworkers.^{22,23,25,26} Paramagnetic metal ions like Cu(II) and heavy metals like Pb(II) cause static quenching of the peak fluorescence upon binding. FQ can be used in solutions of very low DOC and is the only method currently used to observe the free ligand in metal-FA titrations.^{20,32} A consequence of this unique ability is the relative insensitivity of FQ to low metal concentrations, which only slightly perturb the free ligand concentration.^{20,27}

DOM fluorescence measurements would be still more useful if they provided qualitative information about the source of DOM or about the nature of the metal-binding sites. Fluorescence spectra can be used to distinguish between fulvic and humic acids.^{33,34} Unfortunately, emission spectra of DOM from different sources are generally featureless and often similar. Researchers in Europe⁵ and the United States¹⁸ found that emission maxima varied little (< 5 nm) from an average position of 448 nm in spectra of DOM from a series of rivers. Emission spectra and peak fluorescence measurements are consequently of limited value in distinguishing different sources of DOM. Similarly, measurements of peak fluorescence intensity are poorly suited to distinguishing among different metal-binding sites. Although different metals quench peak DOM fluorescence to different extents,^{22,25} this may be due to one of several effects:

1. different degrees of binding (different equilibrium K values)
2. different quenching efficiencies of bound metal
3. different metal ions occupying different sites

The first two possibilities can be tested by simultaneously measuring free metal concentration. The possibility that the binding sites differ can be examined through more detailed studies of the DOM fluorescence.

EXPERIMENTAL

Fulvic acids were isolated by the procedure of Thurman and Malcolm.³⁵ Suwannee River FA (SRFA) was isolated from the Suwannee River in the Okefenokee Swamp, GA, and a standard sample was obtained from the International Humic Substances Society. SRFA has been characterized and described in numerous publications.¹² White Oak River FA (WORFA) was isolated from a coastal river in North Carolina; its interactions with Cu(II) and Ni(II) have been described previously.^{36,37} Lake Drummond FA (LDFA) was isolated from Lake Drummond, VA, by Yeung-Hua Seo and Russell Christman (personal communication). Stock solutions of FA contained 10 mg DOC/L and were kept in dark refrigeration for less than 6 weeks before use; during

that time no significant change in the fluorescence spectra occurred. All chemicals used were reagent grade from Aldrich Chemical.

Fluorescence spectra were recorded using a Photon Technology International Alphascan photon-counting spectrofluorometer equipped with a 150-watt xenon arc lamp and 0.25-m excitation and emission monochromators. Spectra were collected with 0.5-sec integration time and 5-nm entrance and exit slits for both monochromators. Emission spectra were collected with the excitation wavelength set to 350 nm. Synchronous spectra were collected with a constant 20-nm offset between excitation and emission wavelengths. Spectra were stored on the Alphascan data system for later analysis.

SYNCHRONOUS EXCITATION SPECTRA

General Properties

Steady-state fluorescence can be viewed as a three-dimensional measurement, with excitation and emission wavelengths the independent variables and emission intensity as the dependent variable. As such, fluorescence has a higher potential information content for resolving mixtures than a two-dimensional technique such as UV-VIS absorbance. This potential is often not realized in excitation or emission scans because of two drawbacks: (1) broad excitation and emission peaks and (2) symmetry in the excitation-emission matrix.³⁸ Measuring the entire excitation-emission matrix (EEM) provides high information content, but requires either a specialized vidicon detector or long acquisition times. In addition, EEMs are often acquired at relatively low resolution along one axis.^{7,39}

Synchronous excitation spectra, acquired by scanning both monochromators simultaneously, contain information from a diagonal cut across the excitation-emission matrix.^{40,41} These spectra are collected with a constant wavelength offset (monochromators scanned at same speed) or a constant energy offset (different speeds) between the excitation and emission wavelengths. Constant wavelength offset spectra place fewer demands on the instrumentation, but constant energy offset spectra are more easily interpreted in terms of 0-0 electronic transitions.⁴² Typical experiments use wavelength offsets of 3 to 25 nm.^{40,41}

Peaks in the synchronous spectra are generally less intense but better resolved than those from excitation or emission spectra.^{41,43} Model calculations suggest a decrease in peak width of $1/\sqrt{2}$ is possible.⁴⁴ The spectra are also simplified by the elimination of weak bands.⁴³ Synchronous spectra are often relatively simple to interpret and can be acquired quickly with good resolution using a standard PMT detector. Chief disadvantages are low signal due to the narrow slit widths employed⁴³ and increased probability of internal quenching in concentrated solutions.⁴⁵

Synchronous spectra are particularly useful for resolving mixtures of

fluorophores, since by cutting a diagonal across the EEM, symmetrical parts of the EEM are avoided. Synchronous scans have been used to resolve mixtures of polycyclic aromatic hydrocarbons,^{39,42,43} to "fingerprint" petroleum,^{46,47} and to distinguish fluorescence of different amino acids.³⁸

DOM Excitation, Emission, and Synchronous Spectra

Synchronous spectra of a mixture of fluorophores like DOM should have narrower, better-resolved peaks than either excitation or emission spectra. Spectra of White Oak River FA show that this expectation is partly realized (Figure 22.1). The emission spectrum (excited at 350 nm) is a single broad peak near 455 nm, while the excitation spectrum (emission 450 nm) shows a single peak at 345 nm and at < 250 nm. The synchronous spectrum, on the other hand, shows peaks at excitation 440 and 470 nm with shoulders at 350 nm, 395 nm, and 520 nm. The observed bands are not fully resolved, but can be detected. Knowledge of band shape may permit statistical analysis to isolate distinct bands in the mixture that may correspond to distinct groups of fluorophores.⁴⁴

Previous work with aquatic FA,³³ soil FA and HA,^{33,48} leaf litter extracts,^{18,49} and raw river water¹⁸ confirm that synchronous spectra are more highly structured than excitation or emission spectra for several types of DOM. Cabaniss

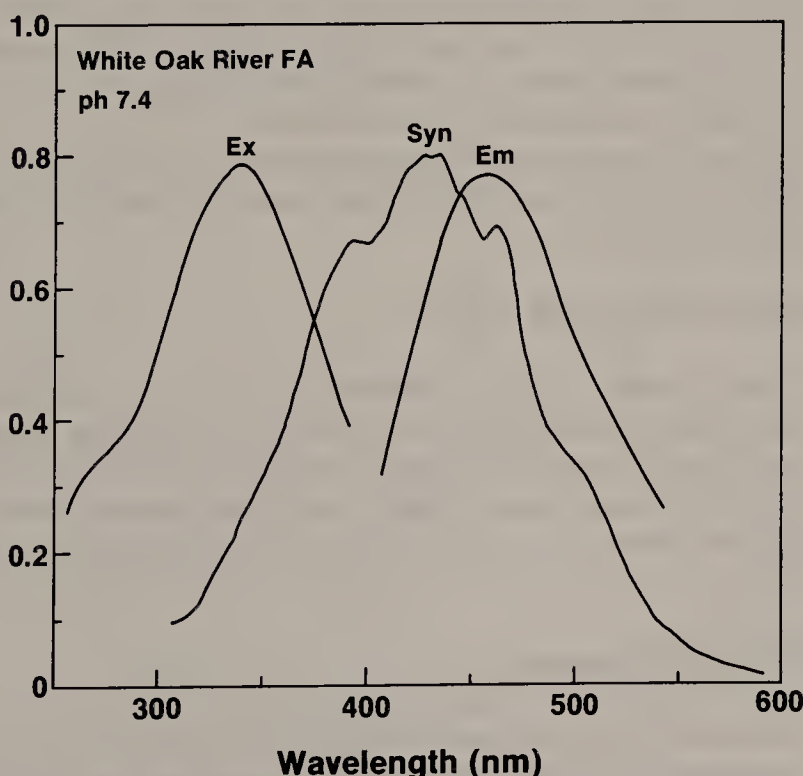


Figure 22.1. Excitation, emission, and synchronous (15-nm offset) spectra of 5 mg DOC/L White Oak River fulvic acid at pH 7.4 in 1 μ M Hepes buffer and 0.010 M NaCl.

and Shuman found peaks in river water DOM spectra that ranged from 310 nm to 470 nm using a 25-nm offset.¹⁸ Although most samples had only two major peaks, several minor peaks and shoulders were readily visible. Similarly, Miano et al. found two or three major peaks in synchronous spectra of several aquatic and soil FA samples; peaks ranged from 350 nm to 520 nm.³³ In contrast, emission spectra of all these samples showed only one peak (and often a small shoulder), while the excitation spectra showed one major peak and one minor peak or shoulder.

The better-resolved structure of the synchronous excitation spectra suggests that they can be more informative than simple excitation or emission spectra. Each of the applications discussed above might benefit from the acquisition of synchronous spectra rather than peak intensities. Two applications which have been examined are (1) as a tracer for the type and source of DOM and (2) as an indicator for different metal-binding sites on DOM.

VARIATION IN TYPE AND SOURCE OF DOM

Measurements of peak fluorescence intensity provide a one-dimensional index of the quantity of DOM. The method relies on the uniform fluorescence properties of the samples at the EEM peak. Measurements of fluorescence spectra provide a two-dimensional (vector) index of the type of DOM. Providing the different types of DOM which might be present have distinct spectral signatures, this two-dimensional measurement can estimate the types of DOM in solution.¹⁸ This method relies on variations in the fluorescence properties of the samples along the wavelength region sampled.

Since synchronous spectra are “more resolved and informative” than excitation or emission spectra,⁴⁸ they are a good candidate vector for typing or classifying DOM samples.

Distinguishing between HA and FA

Fluorescence excitation spectra of soil FA and HA have been proposed as a diagnostic for HA and FA.⁴⁸ Synchronous spectra are also able to distinguish these two operationally defined extracts. Synchronous spectra of HA show a single peak near 480 nm (18-nm offset), while synchronous spectra of FA extracted from the same source show multiple peaks and much greater sample-to-sample variation.^{33,48}

Distinguishing DOM Sources

In many studies of organic carbon cycling, mixing and transport, it is useful to know the origins of a sample of dissolved organic molecules. ¹³C and ¹⁵N isotopic analyses are useful, albeit expensive and time-consuming, tools for differentiating algal, macrophytic, and terrestrial DOM. Synchronous spectra

offer the possibility of a fast, inexpensive analysis to distinguish DOM from different sources.

One source of DOM in natural systems is the mixture of organic molecules extracted from fallen and standing plant material by falling and percolating precipitation. Leaf litter extract (LLE) obtained from leaves and bark in the laboratory is a popular surrogate for the environmental mixture.

Synchronous spectra of LLEs are better resolved than the emission spectra of the same samples.^{18,49} A comparison of synchronous spectra (25-nm offset) from LLEs of four species of plants showed substantial differences (Figure 22.2). All samples showed several peaks after 1 week of incubation; after 22 weeks, the spectra were considerably simplified, although still distinct.¹⁸ Synchronous spectra are therefore a potential indicator of DOM origin.

Distinguishing between Rivers from Different Watersheds

Since DOM samples extracted from different plants have differing spectra, it is reasonable to ask if waters from different ecosystems retain some differences in their spectra. A study of nine rivers in the piedmont and coastal plain of North Carolina indicates that synchronous spectra may be useful fingerprints for different rivers.¹⁸

Piedmont river spectra had a principal peak near 340 nm; coastal plain river

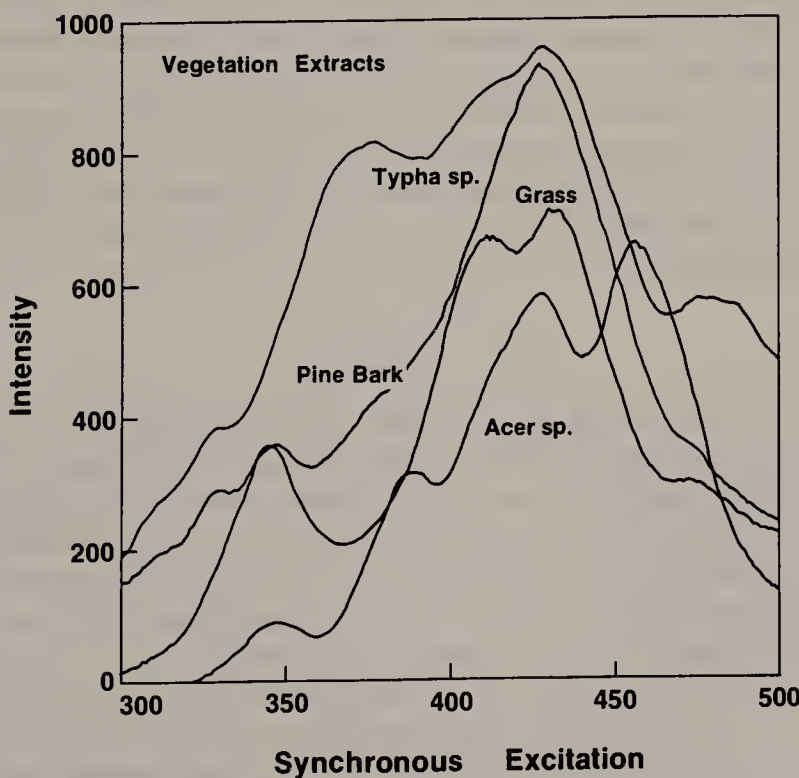


Figure 22.2. Synchronous spectra of four LLEs from maple (*Acer*), cattail (*Typha*), pine, and mixed grasses at pH = 8.2. Data from Cabaniss and Shuman.¹⁸

spectra had a peak or shoulder near 340 nm also, but were generally dominated by a major peak near 430 nm (Figure 22.3). Although spectra of these two groups of rivers could be typed or classified by the major peak, spectra within each group were readily distinguished. A mixing experiment combined different amounts of samples from four of the rivers with varying amounts of distilled water; synchronous spectra were collected for each mixture. Linear regression on each mixture spectrum was able to determine the approximate contribution by each source river.¹⁸

RESPONSE TO SOLUTION CHEMISTRY

The sensitivity of fluorescence measurements to solution conditions is a mixed blessing. Changes in peak location, intensity, and lifetime as a function of pH, metal binding, solvent type, presence of radical species, etc., permit the analyst to examine the molecular state and the immediate microenvironment of the fluorophore.⁴ On the other hand, these same changes complicate quantitation; since quantum yields may change by an order of magnitude in response to solution conditions, sample matrices must be carefully matched for quantitative work using a standard curve. Solution effects on synchronous spectra of DOM are important on both counts. For quantitative trace studies, spectral changes due to changes in solution properties are interferences which must be minimized for accurate work. For investigations of DOM interactions with metals or radical species or studies of DOM structure, spectral changes are the measured indicators of association, solvation, or fluorophore location. pH, Fe(III), Cu(II), and Mg(II) were shown to affect synchronous spectra of river water samples.¹⁸ These interferences were minimized in a mixing study by using an EDTA buffer at pH 8.2 to control the H⁺ and metal ion activities. These effects may be examined more closely to study DOM ionic binding and fluorophore structure.

pH Effects

The effect of changing pH on peak fluorescence intensity is relatively straightforward for most DOM and FA samples. Peak intensity increases sharply as the pH increases from 2 to 5, then decreases more gradually as the pH increases to 11.^{22,52} Figure 22.4a shows the effect of pH on emission spectra of FA from the White Oak River. Although the intensity changes by 10–15%, the spectral shape is hardly changed; spectra recorded at pH 2.9 and pH 10.1 are nearly identical. Structural interpretation based on fluorescence spectra alone is not generally profitable. However, a few parallels may be useful. Salicylic acid fluorescence is strongly quenched by proton binding at low pH; presumably the monoanion is rigidified by hydrogen bonding between the carboxylate oxygens and the phenolic proton. Fluorescence of many phenols is quenched by deprotonation at high pH. Since both salicylate and phenolic

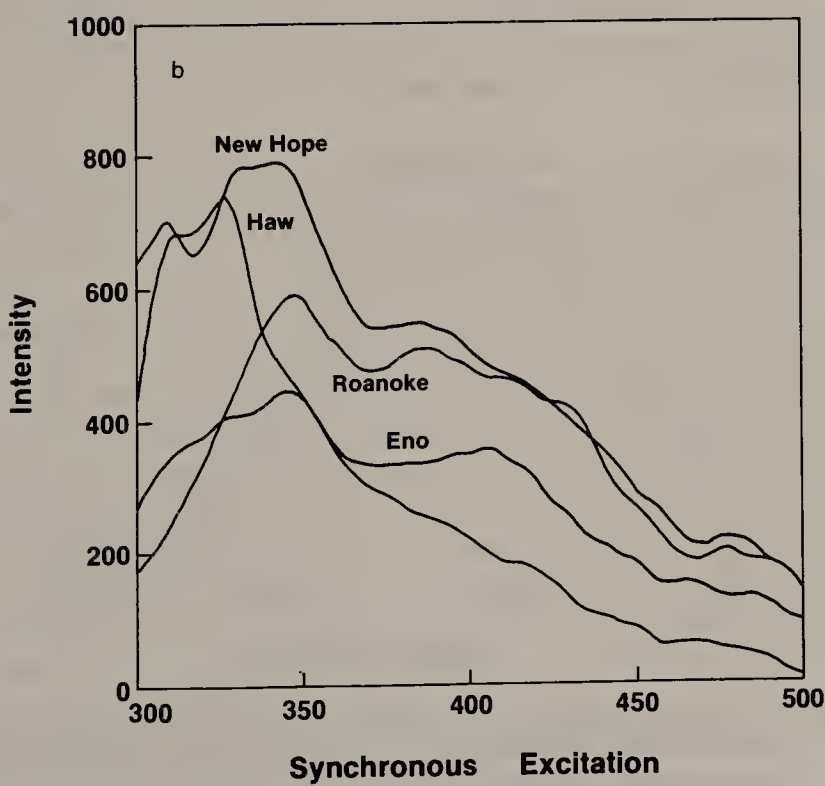
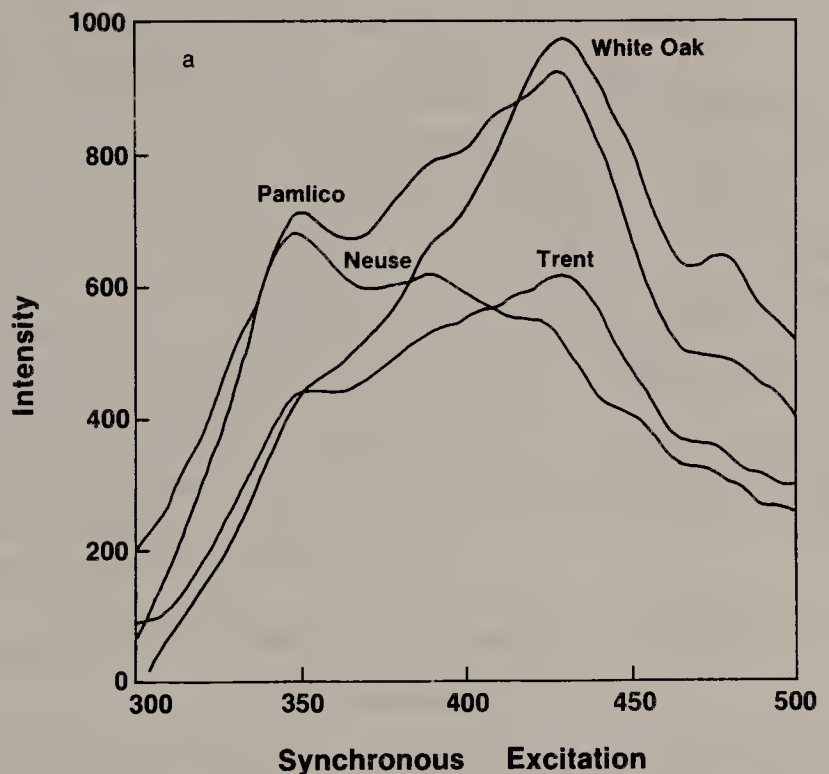


Figure 22.3. Synchronous spectra (offset = 25 nm; pH = 8.2) of (a) four coastal plain rivers¹⁸ and (b) four piedmont rivers. Data from Cabaniss and Shuman.¹⁸

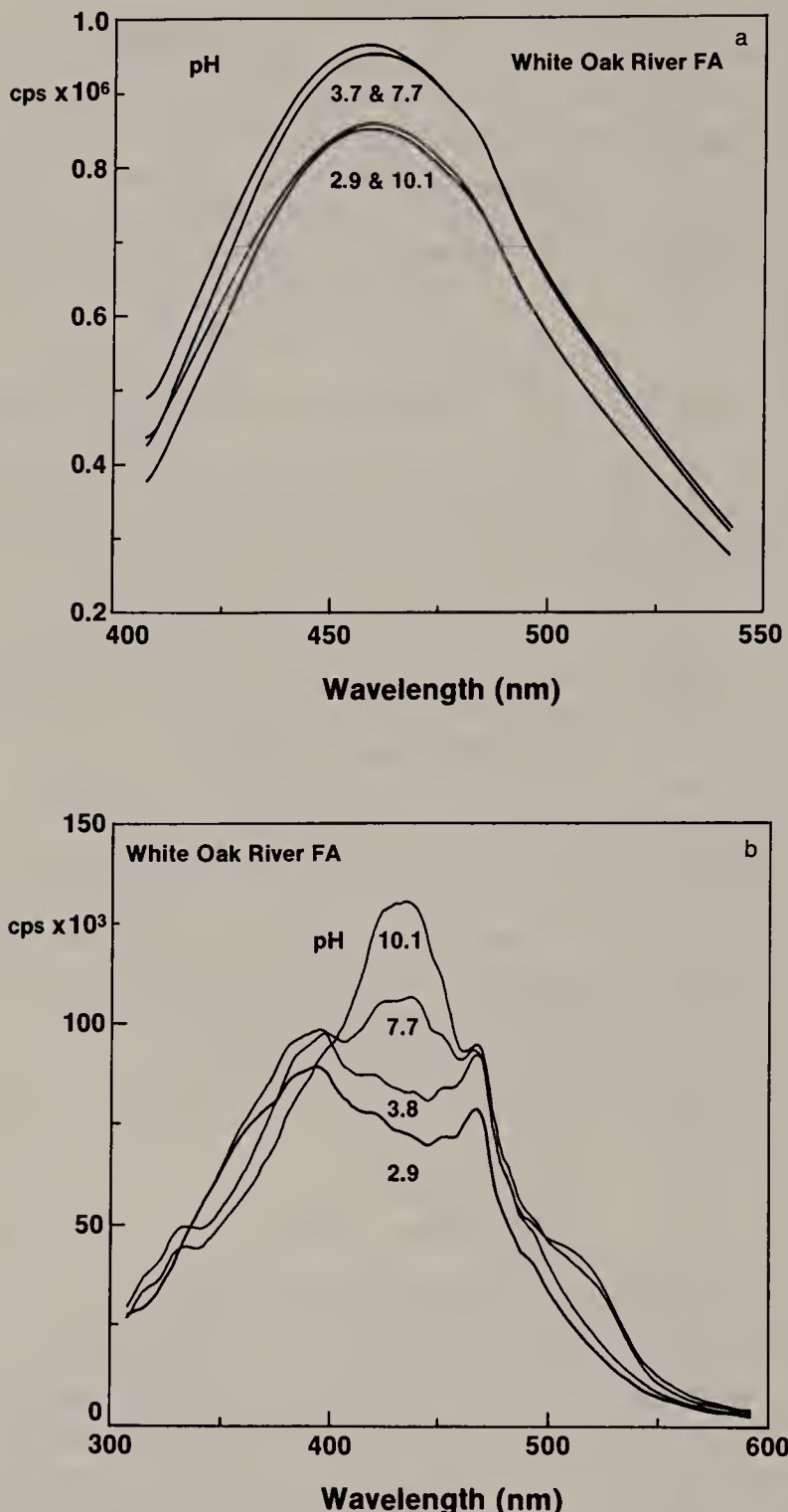


Figure 22.4. Fluorescence spectra of 5 mg DOC/L White Oak River FA at pH 2.9, 3.8, 7.7, and 10.1: (a) emission spectra (excited at 350 nm) and (b) synchronous excitation spectra (20-nm offset).

groups are believed to be present in DOM, the observed behavior is reasonable.

Changes in WORFA synchronous spectra in this pH range are much more pronounced (Figure 22.4b). Intensity increases at all wavelengths as the pH increases from 2.9 to 3.8. However, as the pH increases from 3.8 to 10.1, the peak at 395 nm is slightly quenched, that at 465 nm is unchanged, and an intense new peak is found at pH 435 nm. A shoulder at 350 nm is enhanced at low pH, while one at 520 nm is enhanced at high pH. The shapes of the spectra at pH 2.9 and pH 10.1 are markedly different. The increased complexity of the synchronous spectra changes (relative to peak intensity changes) may be useful in determining acid components of WORFA.

The effect of pH on synchronous spectra has also been examined for river water,¹⁸ HA,³³ and other samples of FA.^{18,33,50,53} It is generally complex, with both quenching and enhancement observed as pH increases,^{18,33} although one soil FA shows a simple quenching effect.⁵³

Metal Ions

Metal ions can quench DOM fluorescence either through static (equilibrium binding) or collisional (dynamic interaction) quenching.⁴ Since collisional quenching is a bimolecular process, quenching at low (< 1 μ M) concentrations is often assumed to be static quenching. Quenching of DOM fluorescence by Al(III) and divalent metal ions occurs at low metal concentrations,^{19,25} and lifetime studies of Cu-FA binding confirm that static quenching predominates in that system.

Many studies of metal-DOM fluorescence have focused on DOM fluorescence quenching by the binding of divalent transition metal ions, especially paramagnetic Cu(II).^{20-23,25-27} Even relatively small (μ M) additions of Cu(II) can measurably quench the peak intensity. Quantitative methods based on fluorescence quenching rely on an average response at the peak of the EEM; the method assumes quenching is proportional to bound metal.^{22,23,27}

Synchronous spectra can be used to examine metal binding by these metal ions. Figure 22.5a shows the Cu(II) quenching spectra of White Oak River FA, obtained by subtracting the synchronous spectrum of FA + Cu from a spectrum of FA alone at the same pH.⁵⁰ The difference spectra, like the synchronous spectra, show distinct peaks. These peaks appear to represent multiple fluorophores, since the change in relative quenching for a given addition is different for each peak. This suggests that (1) several different metal-binding sites are present in the DOM, and (2) different fluorophores are preferentially associated with sites of different binding strength.⁵⁰

Quenching spectra for Mn(II), Co(II) and Pb(II) are similar to those for Cu(II) for both Suwannee and White Oak River FA. In each case, synchronous quenching peaks appear at 395 nm, 435 nm, and 465 nm, with the peak at 435 nm dominant at high (> 10 μ M) metal concentrations. Ni(II) quenching spec-

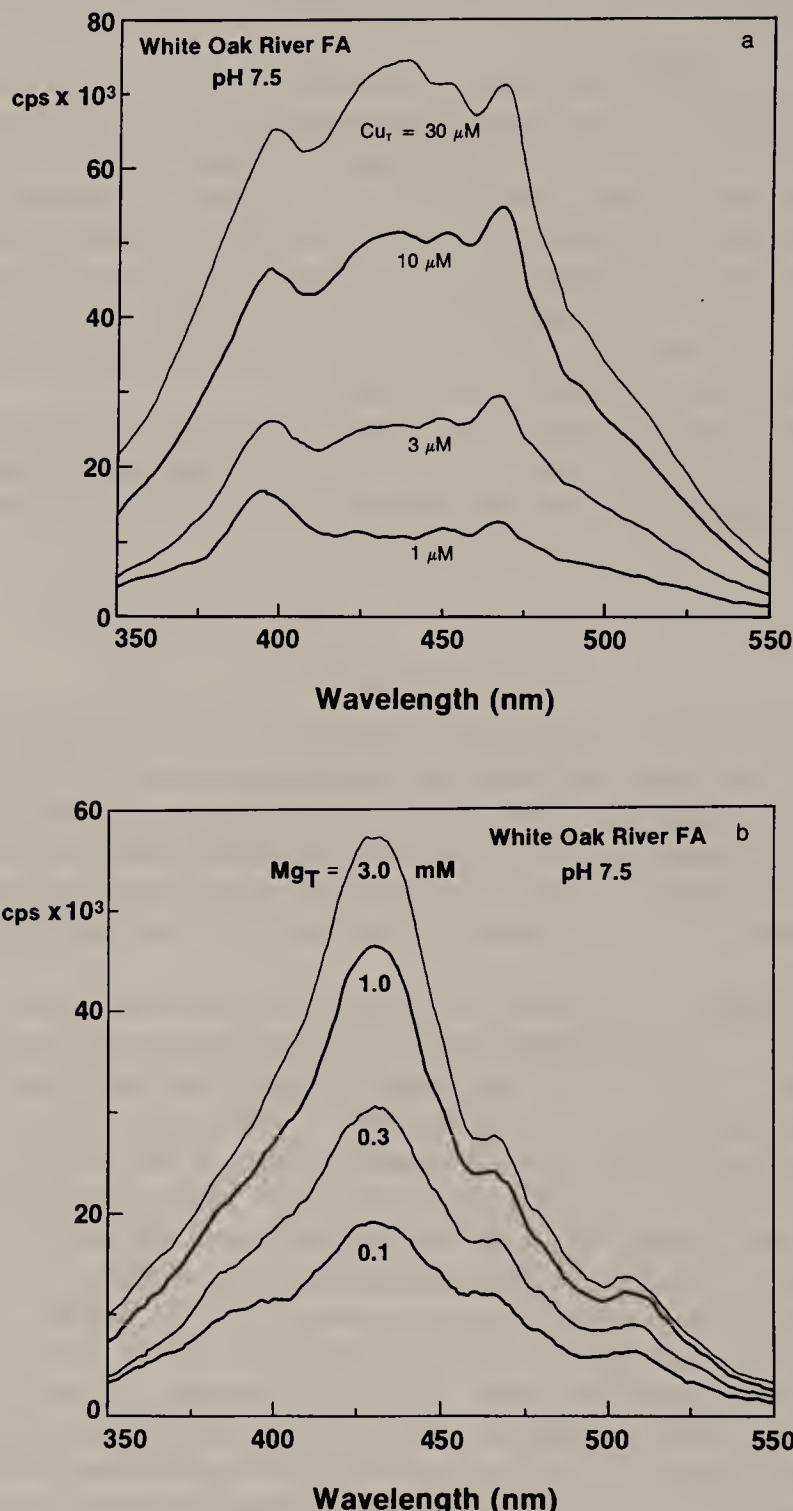


Figure 22.5. Synchronous difference spectra (offset = 20 nm) of 5 mg DOC White Oak River FA at pH 7.5: (a) quenching by Cu(II)—difference is (DOM alone)—(DOM + Cu); (b) enhancement by Mg(II)—difference is (DOM + Mg)—(DOM alone). Data from Cabaniss.⁵⁰

tra show the same set of peaks, but the peak at 465 nm dominates all the Ni(II)-WORFA spectra (II).⁵⁰

Enhancement of DOM fluorescence has been observed in the presence of Mg(II).^{17,18} Synchronous enhancement spectra obtained by subtracting the DOM spectrum from a DOM + Mg spectrum show that the enhancement occurs principally at 435 nm (Figure 22.5b). Comparing Figures 22.5a and 22.5b suggests that Cu(II) and Mg(II) are affecting different sets of FA fluorophores.

Al(III) has the interesting property of acting as a fluorescence enhancer in some systems²⁴ and a quencher in others.¹⁹ Synchronous spectra of FA and FA-Al(III) solutions indicates that the effect is quite complex, dependent on both the pH and the wavelengths used.⁵⁰

Iodide

Iodide ion, I⁻, is often used as a collisional quenching agent. The negative charge is preferentially attracted to fluorophores near positive charges and avoids fluorophores near negative charges.⁴ Consequently, it is expected to preferentially quench a different set of fluorophores than the cationic metal ions discussed above. Milne and Zika found that I⁻ efficiently quenched DOM and HA fluorescence (excitation 337 nm, emission 460 nm).⁵⁴ Anionic iodide quenching was stronger than neutral quenching by acrylamide, but weaker than cationic quenching by methyl viologen, which also showed static quenching. Although these authors obtained results consistent with the presence of a single predominant fluorophore, it is reasonable to ask whether all fluorophores in the synchronous spectra are affected by I⁻ in the same way.

Iodide quenches the spectra of White Oak River and Suwannee River FA differently. Difference spectra show that quenching of WORFA by I⁻ is very similar to quenching by divalent transition metals; quenching is nearly equally intense at the synchronous peaks 395, 435, and 465 nm. However, quenching of SRFA by I⁻ is quite different from quenching by divalent transition metals; the peak at 395 nm is preferentially quenched, while the peak at 465 nm is poorly quenched. The SRFA results suggest that I⁻ might be used as a semiselective probe for DOM fluorophores in cationic environments.

APPLICATIONS

Synchronous spectra offer a rapid and sensitive method for resolving and fingerprinting DOM fluorophores. The relative simplicity of the measurement is partly offset by the difficulty of spectral interpretation, however. Fluorescence peaks are not readily related to structure like IR and NMR spectra; neither are they highly quantitative without good matrix matching.

Synchronous spectra of DOM from different sources and watersheds are potentially useful as tracers for these sources. If specific peaks, or fingerprints,

could be correlated with structural (specific groups, individual fluorophores, particular species of plants) or functional (metal-binding, trihalomethane formation, hydrophobic pollutant solubilization) properties, synchronous spectra could prove a much more unique and useful predictor than peak fluorescence intensity.

DOM synchronous spectra are quite sensitive to metal binding by a variety of metals, including Cu(II), Co(II), Pb(II), Mn(II), Ni(II), Mg(II), Al(III), and Fe (III). By examining changes in these spectra as a function of bound metal, it is possible to determine whether two metals are competing directly for the same binding sites. These changes should be useful in constructing models of metal-DOM binding.

ACKNOWLEDGMENTS

Mark Shuman provided use of a spectrofluorometer for preliminary work and helpful discussions. Lake Drummond FA is used courtesy of Russell Christman. The author would like to thank Nicola Senesi, Garrison Sposito, and Robert Heath for useful comments.

REFERENCES

1. Kalle, K. "Fluoreszenz un Gelbstoff im Bottnischen und Finnischen Meerbusen," *Dtsch. Hydrogr. Z.* 2:117 (1949).
2. Duursma, E. K., and J. W. Rommets. "Interpretation Mathematique de la Fluorescence des eaux douces, saumâtres et marines," *Neth. J. Sea Res.* 1:391 (1961).
3. Black, A. P., and R. F. Christman. "Characteristics of Colored Surface Waters," *J. Am. Water Works Assoc.* 6:753 (1963).
4. Lakowicz, J. R. *Principles of Fluorescence Spectroscopy* (New York: Plenum Press, 1983).
5. Berger, P., R. W. P. M. Laane, A. G. Ilahude, M. Ewald, and P. Courtot. "Application of the Fluorescence Quenching Titration Method to the Complexation of Copper (II) in the Gironde Estuary (France)," *Oceanol. Acta* 7:309 (1984).
6. Donard, O. X. F., C. Belin, and M. Ewald. "Corrected Fluorescence Excitation Spectra of Fulvic Acids. Comparison with the UV/Visible Absorption Spectra," *Sci. Total Environ.* 62:157 (1987).
7. Goldberg, M. C., and E. R. Weiner. "Fluorescence Measurements of the Volume, Shape, and Fluorophore Composition of Fulvic Acid from the Suwannee River," in *Humic Substances in the Suwannee River, Georgia: Interactions, Properties and Proposed Structures*, R. C. Averett, J. A. Leenheer, D. M. McKnight, and K. A. Thorn, Eds. (Denver, CO: U.S. Geological Survey, 1989), pp. 179-204.
8. Lapen, A. J., and W. R. Seitz. "Fluorescence Polarization Studies of the Conformation of Soil Fulvic Acid," *Anal. Chim. Acta* 134:31 (1982).
9. Lochmuller, C. H., and S. S. Saavedra. "Conformational Changes in a Soil Fulvic Acid Measured by Time-Dependent Fluorescence Depolarization," *Anal. Chem.* 58:1978 (1986).

10. Milne, P. J., D. S. Odum, and R. G. Zika. "Time-Resolved Fluorescence Measurements on Dissolved Marine Organic Matter," in *Photochemistry of Environmental Aquatic Systems*, ACS Symposium Series 237, R. G. Zika and W. G. Cooper, Eds. (Washington, DC: American Chemical Society), pp. 174-190.
11. Power, J. F., R. LeSage, D. K. Sharma, and C. H. Langford. "Fluorescence Lifetimes of the Well-Characterized Humic Substance Armadale Fulvic Acid," *Environ. Technol.* 7:425 (1986).
12. Averett, R. C., J. A. Leenheer, D. M. McKnight, and K. A. Thorn. *Humic Substances in the Suwannee River, Georgia: Interactions, Properties and Proposed Structures* (Denver, CO: U.S. Geological Survey, 1989).
13. Zimmerman, J. T. F., and J. W. Rommets. "Natural Fluorescence as a Tracer in the Dutch Wadden Sea and the Adjacent North Sea," *Neth. J. Sea Res.* 8:117 (1974).
14. Willey, J. D., and L. P. Atkinson. "Natural Fluorescence as a Tracer for Distinguishing Between Piedmont and Coastal Plain River Water in the Nearshore Waters of Georgia and North Carolina," *Estuar. Coastal Shelf Sci.* 14:49 (1982).
15. Dorsch, J. E., and T. F. Biddleman. "Natural Organics as Fluorescent Tracers of River-Sea Mixing," *Estuar. Coastal Shelf Sci.* 15:701 (1982).
16. Laane, R. W. P. M., and L. Koole. "The Relation Between Fluorescence and Dissolved Organic Carbon in the Ems Dollart Estuary and the Western Wadden Sea," *Neth. J. Sea Res.* 15:217 (1982).
17. Willey, J. D. "The Effect of Seawater Magnesium on Natural Fluorescence During Estuarine Mixing, and Implications for Tracer Applications," *Mar. Chem.* 15:19 (1984).
18. Cabaniss, S. E., and M. S. Shuman. "Synchronous Fluorescence Spectra as a Tracer for Dissolved Organic Matter," *Mar. Chem.* 21:37 (1987).
19. Blaser, P., and G. Sposito. "Spectrofluorimetric Investigation of Trace Metal Complexation by an Aqueous Chestnut Leaf Litter Extract," *Soil Sci. Soc. Am. J.* 51:612 (1987).
20. Fish, W., and F. M. M. Morel. "Propagation of Error in Fulvic Acid Titration Data: A Comparison of Three Analytical Methods," *Can. J. Chem.* 63:1185 (1985).
21. Underdown, A. W., C. H. Langford, and D. S. Gamble. "The Fluorescence and Visible Absorbance of Cu(II) and Mn(II) Complexes of Fulvic Acid: The Effect of Metal Ion Loading," *Can. J. Soil Sci.* 61:469 (1981).
22. Saar, R. A., and J. H. Weber. "Comparison of Spectrofluorometry and Ion-Selective Electrode Potentiometry for Determination of Complexes Between Fulvic Acid and Heavy-Metal Ions," *Anal. Chem.* 52:2095 (1980).
23. Ryan, D. K., and J. H. Weber. "Fluorescence Quenching Titration for Determination of Complexing Capacities and Stability Constants of Fulvic Acid," *Anal. Chem.* 54:986 (1982).
24. Plankey, B. J., and H. H. Patterson. "Kinetics of Aluminum-Fulvic Acid Complexation in Acidic Waters," *Environ. Sci. Technol.* 21:595 (1987).
25. Ryan, D. K., C. P. Thompson, and J. H. Weber. "Comparison of Mn²⁺, Co²⁺, and Cu²⁺ Binding to Fulvic Acid as Measured by Fluorescence Quenching," *Can. J. Chem.* 61:1505 (1983).
26. Ryan, D. K., and J. H. Weber. "Copper (II) Complexing Capacities of Natural Waters by Fluorescence Quenching," *Environ. Sci. Technol.* 16:866 (1982).

27. Cabaniss, S. E., and M. S. Shuman. "Fluorescence Quenching Measurements of Copper-Fulvic Acid Binding," *Anal. Chem.* 60:2418 (1988).
28. *Standard Methods for the Examination of Water and Wastewater* (Washington, DC: American Public Health Association, 1985), pp. 507-515.
29. Laane, R. W. P. M. "Composition and Distribution of Dissolved Fluorescent Substances in the Ems-Dollart Estuary," *Neth. J. Sea Res.* 15:88 (1981).
30. Smart, P. L., B. L. Finlayson, W. D. Rylands, and C. M. Ball. "The Relation of Fluorescence to Dissolved Organic Carbon in Surface Waters," *Water Res.* 10:805-811 (1975).
31. Hayase, K., H. Tsubota, I. Sunada, S. Goda, and H. Yamazaki. "Vertical Distribution of Fluorescent Organic Matter in the North Pacific," *Mar. Chem.* 25:373 (1988).
32. Saar, R. A., and J. H. Weber. "Fulvic Acid: Modifier of Metal Ion Chemistry," *Environ. Sci. Technol.* 16:510A (1982).
33. Miano, T. M., G. Sposito, and J. P. Martin. "Fluorescence Spectroscopy of Humic Substances," *Soil Sci. Soc. Am. J.* 52:1016 (1988).
34. Ghosh, K., and M. Schnitzer. "Fluorescence Excitation Spectra of Humic Substances," *Can. J. Soil Sci.* 60:373 (1980).
35. Thurman, E. M., and R. Malcolm. "Preparative Isolation of Aquatic Humic Substances," *Environ. Sci. Technol.* 15:463 (1981).
36. Cabaniss, S. E., and M. S. Shuman. "Copper Binding by Dissolved Organic Matter I. Suwannee River Fulvic Acid Equilibria," *Geochim. Cosmochim. Acta* 52:185 (1988).
37. Cabaniss, S. E. "pH and Ionic Strength Effects on Nickel-Fulvic Acid Dissociation Kinetics," *Environ. Sci. Technol.* 24:583 (1990).
38. Miller, J. N. "Recent Developments in Fluorescence and Chemiluminescence Analysis," *Analyst* 109:191 (1984).
39. Christian, G. D., J. B. Callis, and E. R. Davidson. "Array Detectors and Excitation-Emission Matrices in Multicomponent Analyses," in *Modern Fluorescence Spectroscopy* Vol. 4, E. L. Wehry, Ed. (New York: Plenum Press, 1981), pp. 111-165.
40. Lloyd, J. B. F. "Prediction of Peak Wavelengths and Intensities in Synchronously Excited Fluorescence Emission Spectra," *Nature* (London) 231:64 (1971).
41. Vo-Dinh, T. "Synchronous Luminescence Spectroscopy: Methodology and Applicability," *Appl. Spec.* 36:576 (1982).
42. Inman, E. L., and J. D. Winefordner. "Constant Energy Synchronous Fluorescence for Analysis of Polynuclear Aromatic Hydrocarbon Mixtures," *Anal. Chem.* 54:2018 (1982).
43. Vo-Dinh, T. "Multicomponent Analysis by Synchronous Luminescence Spectrometry," *Anal. Chem.* 50:396 (1978).
44. Cabaniss, S. E. "Theory of Variable-Angle Synchronous Fluorescence Spectra," in press, *Anal. Chem.*
45. Latz, H. W., A. H. Ullman, and J. D. Winefordner. "Limitations of Synchronous Luminescence Spectrometry in Multicomponent Analysis," *Anal. Chem.* 50:2148 (1978).
46. John, P., and I. Soutar. "Identification of Crude Oils by Synchronous Excitation Spectrofluorimetry," *Anal. Chem.* 48:520 (1976).
47. Taylor, T. A., and H. H. Patterson. "Excitation Resolved Synchronous Fluores-

- cence Analysis of Aromatic Compounds and Fuel Oil," *Anal. Chem.* 59:2180 (1987).
48. Senesi, N., T. M. Miano, M. R. Provenzano, and G. Brunetti. "Spectroscopic and Compositional Comparative Characterization of I.H.S.S. Reference and Standard Fulvic and Humic Acids of Various Origin," *Sci. Total Environ.* 81:143 (1989).
49. Frimmel, F. H., and H. Bauer. "Influence of Photochemical Reactions on the Optical Properties of Aquatic Humic Substances Gained from Fall Leaves," *Sci. Total Environ.* 62:139 (1987).
50. Cabaniss, S. "Synchronous Fluorescence Spectra of Metal-Fulvic Acid Complexes," in press for *Environ. Sci. Technol.*
51. Ghosh, K., and M. Schnitzer. "Fluorescence Excitation Spectra and Viscosity Behavior of a Fulvic Acid and Its Copper and Iron Complexes," *Soil Sci. Soc. Am. J.* 45:25 (1981).
52. Laane, R.W.P.M. "Influence of pH on the Fluorescence of Dissolved Organic Matter," *Mar. Chem.* 11:395 (1982).
53. Senesi, N. Paper presented at the 199th ACS National Meeting, 1990.
54. Milne, P. J., and R. G. Zika. "Luminescence Quenching of Dissolved Organic Matter in Seawater," *Mar. Chem.* 27:147 (1989).

List of Authors

V. Dean Adams, Center for the Management, Utilization, and Protection of Water Resources, Box 5033, Tennessee Technological University, Cookeville, Tennessee 38505

Anders W. Andren, Water Chemistry Program, University of Wisconsin-Madison, 660 N. Park Street, Madison, Wisconsin 53706

David E. Armstrong, Water Chemistry Program, University of Wisconsin-Madison, 660 North Park Street, Madison, Wisconsin 53706

Joel E. Baker, Chesapeake Biological Laboratory, Center for Environmental and Estuarine Studies, University of Maryland, Solomons, Maryland 20688

Roger C. Bales, Department of Hydrology and Water Resources, University of Arizona, Tucson, Arizona 85721

William P. Ball, Department of Civil and Environmental Engineering, Duke University, Durham, North Carolina 27706

Diane J.W. Blum, 112 Clwyd Road, Bala Cynwyd, PA 19004

Bruce J. Brownawell, Marine Sciences Research Center, SUNY at Stony Brook, Stony Brook, New York 11794-5000

Stephen E. Cabaniss, Department of Chemistry, Kent State University, Kent, Ohio 44242-0001

Hua Chen, Department of Chemistry, Oregon State University, Corvallis, Oregon 97331-4003

Yu-Ping Chin, Ralph M. Parsons Laboratory, Department of Civil Engineering, Bldg. 48-213, Massachusetts Institute of Technology, Cambridge, Massachusetts 02139

Colbert E. Cushing, Environmental Sciences Department, Pacific Northwest Laboratory, Richland, Washington 99352

Ellen R. M. Druffel, Woods Hole Oceanographic Institution, Woods Hole, Massachusetts 02543

Brian J. Eadie, NOAA/Great Lakes Environmental Research Laboratory, 2205 Commonwealth Boulevard, Ann Arbor, Michigan 48105

David A. Edwards, Department of Civil Engineering, Carnegie Mellon University, Pittsburgh, Pennsylvania 15213

Robert P. Eganhouse, Southern California Coastal Water Research Project, 646 W. Pacific Coast Highway, Long Beach, California 90806

Steven J. Eisenreich, Department of Civil and Mineral Engineering and the Gray Freshwater Biological Institute, University of Minnesota, Minneapolis, Minnesota 55455

John T. Ellis, Graduate School of Oceanography, University of Rhode Island, Narragansett, Rhode Island 02882

Warren R. Faust, NOAA/Great Lakes Environmental Research Laboratory, 2205 Commonwealth Boulevard, Ann Arbor, Michigan 48105

C. Ellen Gonter, 1504 Timber Lake Lane, Sandusky, OH 44870

Richard W. Gossett, Southern California Coastal Water Research Project, 646 W. Pacific Coast Highway, Long Beach, California 90806

Philip M. Gschwend, Ralph M. Parsons Laboratory, Department of Civil Engineering, Massachusetts Institute of Technology, Cambridge, Massachusetts 02139

Lorraine C. Guyette, 13748 Sager, Grass Lake, MI 49240

Brian J. Harland, ICI Group Environmental Laboratory, Brixham, Devon, United Kingdom

Malcolm J. Hetheridge, ICI Group Environmental Laboratory, Brixham, Devon, United Kingdom

Douglas R. Hunter, Bennett and Williams, Inc., 2700 East Dublin-Granville Rd., Columbus, Ohio 43231

Michelle R. Kriegman-King, Department of Civil Engineering, Stanford University, Stanford, California 94305-4020

Peter F. Landrum, NOAA/Great Lakes Environmental Research Laboratory, 2205 Commonwealth Boulevard, Ann Arbor, Michigan 48105

James S. Latimer, Graduate School of Oceanography, University of Rhode Island, Narragansett, Rhode Island 02882-1197

Lawrence A. LeBlanc, Graduate School of Oceanography, University of Rhode Island, Narragansett, Rhode Island 02882

Cindy Lee, Marine Sciences Research Center, SUNY at Stony Brook, Stony Brook, New York 11794

Zhongbao Liu, Department of Civil Engineering, Carnegie Mellon University, Pittsburgh, Pennsylvania 15213-3890

Richard G. Luthy, Department of Civil Engineering, Carnegie Mellon University, Pittsburgh, Pennsylvania 15213

Robert A. Matzner, Department of Hydrology and Water Resources, University of Arizona, Tucson, Arizona 85721

Ann P. McNichol, Woods Hole Oceanographic Institution, Woods Hole, Massachusetts 02543

G. Wayne Minshall, Department of Biological Sciences, Idaho State University, Pocatello, Idaho 83209

Simon J. Molloy, ICI Group Environmental Laboratory, Brixham, Devon, United Kingdom

Michael W. Murray, Water Chemistry Program, University of Wisconsin-Madison, 660 N. Park Street, Madison, Wisconsin 53706

N. Nirmalakhandan, Department of Civil Engineering, New Mexico State University, Las Cruces, New Mexico 88003

J. Denis Newbold, Stroud Water Research Center, Academy of Natural Sciences of Philadelphia, Box 512, R.D. #1, Avondale, Pennsylvania 19311-9516

Judith A. Perlinger, Swiss Federal Institute for Water Resources and Water Pollution Control, CH-6047, Kastanienbaum, Switzerland

James G. Quinn, Graduate School of Oceanography, University of Rhode Island, Narragansett, Rhode Island 02882

Martin Reinhard, Department of Civil Engineering, Stanford University, Stanford, California 94305-4020

John A. Robbins, NOAA/Great Lakes Environmental Research Laboratory, 2205 Commonwealth Boulevard, Ann Arbor, Michigan 48105

Paul V. Roberts, Department of Civil Engineering, Stanford University, Stanford, California 94305

Martin M. Shafer, Water Chemistry Program, University of Wisconsin-Madison, 660 North Park Street, Madison, Wisconsin 53706

Robert S. Skoglund, Environmental and Occupational Health, School of Public Health, Box 197 UMHC, University of Minnesota, Minneapolis, Minnesota 55455

R.E. Speece, Department of Civil Engineering, Vanderbilt University, Nashville, Tennessee 37235

Thomas G. Stevens, National Sanitation Foundation, Ann Arbor, Michigan 48106

Deborah L. Swackhamer, Environmental and Occupational Health, School of Public Health, Box 197 UMHC, University of Minnesota, Minneapolis, Minnesota 55455

Patricia L. Van Hoof, University of Georgia/U.S. Environmental Protection Agency, Environmental Research Laboratory, College Station Road, Athens, Georgia 30613

Martha J. M. Wells, Center for the Management, Utilization, and Protection of Water Resources, Box 5033, Tennessee Technological University, Cookeville, Tennessee 38505

John C. Westall, Department of Chemistry, Oregon State University, Corvallis, Oregon 97331-4003

Wanjia Zhang, Department of Chemistry, Oregon State University, Corvallis, Oregon 97331-4003

Index

- Abietic acid, 191
Acenaphthene, 194
Acetylinic compounds, 326. *See also* specific types
Acridine, 365–380
advection-disperser model of, 375–380
batch studies of, 368
column studies of, 367–372
desorption of, 372
equilibrium model for, 376
HPLC of, 367, 368
solubility of, 366–367, 368, 373–374
sorption of, 372, 380
Acridine-octanol solubility, 368
Active sediment layer, 222
Activity coefficients, 51, 55, 60, 73
aqueous, 67
Henry's convention, 59–61
infinite dilution, 55
Raoult's convention, 59–61
Advection-dispersion model, 375–380
AE. *See* Alcohol ethoxylates
Aggregation, 297
Agricultural runoff, 320
AHD. *See* Alkyl homologue distributions
Alcohol ethoxylates (AE), 128, 129, 130, 131, 132, 133, 134, 135, 138, 142. *See also* specific types
Alcohols, 311, 314, 318, 320. *See also* specific types
halogenated, 326
long-chain, 311, 317, 320
polyvinyl (PVA), 481–489
predictability of, 338
toxicity of, 332
Aldehydes, 311, 314, 317, 318, 320, 326, 330. *See also* specific types
n-Aldehydes, 234
Algae, 100, 102
Aliphatics, 443–449. *See also* specific types
chlorinated, 332
halo-, 352
halogenated, 349
QSAR model and, 326
Alkanes, 293, 295, 311, 318, 320, 330.
See also specific types
chlorinated, 294
long-chain, 311, 314, 317
n-Alkanes, 234
Alkenes, 294, 330. *See also* specific types
4-Alkybenzenesulfonates, 128
Alkylated homologues, 200, 201
Alkylated phenanthrene, 191
Alkylation, 209
Alkylbenzenes. *See also* specific types
linear, 202
sorption of, 49–73
aqueous phase activity and, 59–63
to mineral surfaces, 50–56
particle concentration and, 56–59
sorbed phase activity and, 59–63
sorption coefficients and, 56–59
verification of method in study of, 66–68
source of, 64
Alkylbenzenesulfonates, 137–138, 140–141. *See also* specific types
Alkyl homologue distributions (AHD), 197, 202, 209
Alkyl phosphates, 429, 467
Allochthonous components, 27–29. *See also* specific types
Alumina, 298
Alumina gel column chromatography, 92
Aluminosilicates, 34
Aluminum, 34, 35, 36, 513, 515, 516
Aluminum oxide, 64
Amberlite resins, 294
Amines, 326, 330. *See also* specific types

- Amino acids, 264, 409. *See also* specific types
- Amphibole, 350
- Amphiphilic compounds, 132. *See also* specific types
- Amphipods, 172, 180, 241
- Anilines, 365
- Anionic surfactants, 127, 128, 136. *See also* specific types
- Anthracene, 195, 197, 201, 210
- Anthropogenic hydrocarbons, 234. *See also* specific types
- Anthropogenic organic compounds (AOCs), 409–418. *See also* specific types
- chemical categories of, 442
 - chromatography of, 414
 - confirmation of, 416–417
 - determination of, 471, 472–476, 477–479
 - extraction of, 414, 477–479
 - fractionation of, 414–415, 477–479
 - purification of, 414–415, 477–479
 - references on, 430–432, 471, 472–476, 477–479
 - sampling of, 412–414, 415
- Apparent effects threshold (AET), 241–243
- Aroclor, 223
- Aromatics, 193. *See also* specific types
- determination of, 443–449
 - halogenated, 285
 - polynuclear, 284, 330, 331
 - QSAR model and, 326
 - references on, 443–449
 - surface diffusivities of, 294
 - total, 194
- Artifacts, 278
- Aryl phosphates, 429, 467
- Atomic absorption spectroscopy, 20
- Autochthonous components, 23
- Autochthonous particles, 23, 229
- Autochthonous precipitates, 23
- BAF. *See* Bioaccumulation factor
- BAP. *See* Benzo(a)pyrene
- Basin geometry, 222
- Batch partitioning, 277
- Batch studies, 278–292
- of acridine, 368
- with Borden solids, 289–292
- with diffusive interpretation, 287–289
- with first-order interpretation, 284–287
- intrisorbent diffusion and, 280–283
- of PAHs, 388
- Benthic deposits, 107
- Benthic infaunal population, 241
- Benthic nepheloid layer (BNL), 172, 222, 223
- Benthic worms, 223
- Bentonite, 350, 409
- Benzaldehyde, 151, 294
- Benzene-corundum sorption, 68–73
- Benzenes, 53, 58, 64, 161, 297. *See also* specific types
- activity coefficients for, 73
 - chlorinated, 53, 285, 287–288
 - toxicity of, 332
- Benzene vapor-polystyrene system, 161
- Benzo(k)fluoranthene, 197, 206
- Benzofluoranthenes, 197. *See also* specific types
- Benzo(ghi)perylene, 181, 197, 211
- Benzo(a)pyrene, 96, 122, 123, 173, 175, 180
- accumulation of, 182
 - atmospheric concentration of, 185–186
 - biodegradation of, 210
 - concentration of, 178, 180, 185
 - decrease in concentration of, 178
 - distribution coefficients for, 183
 - in effluent, 197
 - equilibrium distribution coefficient of, 181
 - flux of, 185
 - overlying water concentration of, 180
 - sedimentary profiles of, 182, 186
 - source function and, 182–186
- Benzo(e)pyrene, 197
- Benzopyrenes, 197, 206. *See also* specific types
- Benzotriazoles, 224
- Binding coefficients of HOCs, 56

- Bioaccumulation factor (BAF), 93, 95, 96, 97, 98, 99, 101, 244
pore-water contribution to, 180
- Bioavailability, 79, 127, 171, 180
- Biodegradation, 49, 127, 192, 209, 210, 481
- Biogenic markers, 311
- Biogenic silicon, 19, 21, 24–27, 29
- Bioirrigation, 108, 118, 120, 122, 257, 260. *See also* Irrigation
- Biological properties, 323. *See also* specific types
- Bioluminescence, 241
- Biomass dilution, 100
- Bioremediation, 273
- Biotite, 350, 351, 352, 354, 356, 357, 358, 359
- Bioturbation, 171, 223
- Biphenyl, 201
- Bisnorhopane, 204, 205
- BNL. *See* Benthic nepheloid layer
- Borates, 481
- Borden field experiments, 274–276
- Borden solids, 289–292, 297, 298
- Bottom-feeding fish, 107
- Bottom sediment fluxes, 35–36
- Bottom sediment focusing factor, 35
- Boundary layer, 222, 280
- Breakthrough curves, 375–380
- Bromide, 274, 276
- Bromine, 326
- BSi. *See* Biogenic silicon
- Bubble-bursting phenomenon, 4
- Burial, 171
- Butane, 338
- Butylbenzene, 64
- Cadmium, 32, 38
- Calcite, 22–24, 27, 31–32, 36, 43
- Calcium, 22, 34, 128, 130, 131, 351
concentration of, 255
dissolution of, 262
dissolved, 252
filtrable, 20
quinolinium competition with, 365
sorption and, 138, 140, 141, 142, 143
- Capillary gas chromatography, 312–313
- Carbohydrates, 264, 409. *See also* specific types
- Carbon, 34
cycling of. *See* Carbon cycling
diffusion of, 268
dissolved inorganic, 221, 250
dissolved organic. *See* Dissolved organic carbon (DOC)
inorganic, 20, 221, 250, 298
organic. *See* Organic carbon
particulate inorganic, 20
particulate organic, 206, 265
in pore water, 264–268
remineralization of, 264
sources of, 265–268
total organic. *See* Total organic carbon (TOC)
- Carbonate, 20, 265, 268, 297
- Carbon cycling, 249–269
calcium dissolution and, 262
chemical analysis of, 252–253
isotope model and. *See* Isotope model
site description of study of, 251
- Carbon dioxide, 263, 264, 267
- Carbon-14 labelling, 493–500
- Carbon-normalized partition coefficients, 80, 93
- Carbon-normalized sorption, 284
- Carbon tetrachloride (CTET), 274, 349, 350, 352, 361
disappearance of, 356
reactivity of, 360, 362
reductant reactions with, 357
transformation of, 353, 356
- Carboxylic acid esters, 335
- Carcinogenicity of PAHs, 191
- Catalytic combustion method, 20
- Cation exchange capacity (CEC), 129, 135, 136
- Cation exchange reactions, 140
- Cationic surfactants, 127, 128, 143. *See also* specific types
- CEC. *See* Cation exchange capacity
- Cell size, 97
- Cellular metabolism, 100
- Cementation, 297

- Centrifugation, 18, 56, 57, 63, 130, 131, 149, 173, 352. *See also* specific types
continuous-flow, 17, 82
high-volume, 81
pumping-in-line sieving
continuous-flow, 17
- Cesium, 175, 180, 181, 183, 185
- CF. *See* Chloroform
- CHC. *See* Chlorinated hydrocarbons
- Chemical fractionation, 224–226
- Chemical interactions, 127, 132, 143.
See also specific types
- Chemical ionization mass spectrometry, 314
- Chemical phases, 33–35
- Chemosynthesis, 264
- Chlordane, 91
- Chloride, 274
- Chlorinated aliphatics, 332
- Chlorinated alkanes, 294. *See also* specific types
- Chlorinated alkenes, 294. *See also* specific types
- Chlorinated benzenes, 53, 285, 287–288. *See also* specific types
- Chlorinated biphenyls, 150. *See also* specific types
- Chlorinated compounds. *See also* specific types
determination of, 462–463
references on, 462–463
- Chlorinated compounds
references on, 427
- Chlorinated dibenzofurans, 453
- Chlorinated dioxins, 453
- Chlorinated ethanes, 338. *See also* specific types
- Chlorinated hydrocarbons (CHC), 186, 332. *See also* specific types
- Chlorinated pesticides, 91. *See also* specific types
- Chlorination, 338, 341, 417
- Chlorines, 98, 326
- Chlorine substitutions, 330–331, 338
- Chlorobenzenes, 341
- Chlorobiphenyl, 227, 235
- Chloroform, 349, 350, 352
- Cholesterol, 314
- Chromatography, 93, 317, 335. *See also* specific types
alumina gel column, 92
of AOCs, 414
capillary gas, 312–313
column, 92, 226, 414
gas. *See* Gas chromatography
gel permeation, 414
high-performance liquid. *See* High-pressure liquid chromatography (HPLC)
high-pressure liquid (HPLC), 95, 129, 367, 368, 414–415
high-pressure size-exclusion. *See* High-pressure size-exclusion chromatography (HPSEC)
high-resolution gas, 3, 195, 207, 226
linear column, 414
nonlinear column, 414
silica gel column, 92, 226
size-exclusion. *See* Size-exclusion chromatography (SEC)
thin-layer (TLC), 129, 194, 414
- Chromium, 32, 37
- Chrysene, 181, 194
- Chrysene/triphenylene, 197
- CI. *See* Chemical ionization
- Ciliates, 337
- Circulation, 222
- CIS. *See* Critical ionic strength
- Clay minerals, 136
- Clays, 27, 34, 56, 138, 283, 350
- CMC. *See* Critical micelle concentrations
- Cobalt, 516
- Concentration gradients, 280
- Colloidal-size particles, 63
- Colloid-associated HOCs, 69
- Colloids, 149, 222, 409. *See also* specific types
diffusivity of, 108
interstitial-fluid, 108
PAH binding to, 111
PCB complexation by, 80, 87
pore-water organic. *See* Pore-water organic colloids
separation of, 57
solution-phase, 284
sorption coefficients and, 69

- Colorimetry, 19, 20
 Column chromatography, 92, 226, 414
 Column scavenging, 36
 Column sorption experiments, 53
 Column studies, 277–278, 367–372. *See also* specific types
 Combined sewer overflows, 240
 Combustion, 20, 172, 192, 504
 Combustion PAHs, 175–180, 181, 182, 186, 191, 192, 213
 Completely stirred tank reactors (CSTR), 285, 287
 Component concentrations, 23–29
 Component fluxes, 23–31
 Component model of trace element cycling, 21–23
 Component settling rates, 23
 Component-specific metal fluxes, 32
 Conductometric titration, 151
 Connectivity indexes. *See* Molecular connectivity
 Constrictivity, 283
 Continuous-flow centrifugation, 17, 82
 Copper, 32, 37, 43, 360, 510, 513, 515
 Coprostanol, 224, 314
 Core geochronology, 175
 Corundum, 64, 68–73
 Coupled desorption, 210
 Crank's analytical solution, 158
 Critical ionic strength (CIS), 115, 116
 Critical micelle concentrations (CMC), 134, 384, 385, 386, 387, 389, 390, 391
 aqueous-phase, 393, 394, 395, 396, 397
 surfactant sorption saturation and, 398
 Cross-linking, 298
 Crustaceans, 241
 CSOs. *See* Combined sewer overflows
 CSTR. *See* Completely stirred tank reactors
 CTET. *See* Carbon tetrachloride
 Current velocity, 222
 Cycloalkanes, 295
 Cyclohexanol, 326
 DDT, 91, 100, 193, 202, 384
 Decachlorobiphenyl, 231
 Decane, 338
 Decomposition products, 250
 Degradable fractions, 257
 Dehalogenation, 349
 Dehydroxylation, 359
 Depolarization, 504
 Deposition, 32, 33, 229, 236
 Desorption, 49, 59, 209, 285
 acridine, 372
 coupled, 210
 dispersion vs., 378
 diuron, 286
 EDB, 286
 first-order rate coefficients for, 287
 HOC, 100, 150
 kinetics of, 100, 209, 210, 234
 long-term, 285
 mass transfer limitations and, 275
 nonequilibrium, 276
 particle-induced, 58
 pseudo-first-order, 375
 rate constants for, 286
 rates of, 209, 284
 resistance to, 284, 286
 slow, 378
 studies of, 286
 Desorption partition coefficients, 372
 Desorption resistant fraction, 284
 Diafiltration, 151
 Diatoms, 21, 24, 26, 31–32, 37, 97
 Dibenz(a,h)anthracene, 206, 210
 Dibenzofurans, 425, 453
 1,2-Dibromoethane. *See* Ethyl dibromite (EDB)
m-Dichlorobenzene, 52
 1,4-Dichlorobenzene, 288
 3,5-Dichlorobiphenyl, 92
 Dichloromethane, 93
 Dicyclic PAHs, 201
 Dieldrin, 91
 Diethylether, 276
 Difference index, 336
 Diffusion, 58, 121, 123. *See also* Diffusivity; specific types
 anomalous, 298
 carbon, 268
 carbon dioxide, 267
 in defined media, 292–299

- equations for, 158
- ethane, 294
- Fickian, 150, 280, 298, 299
- hexachloroethane (HCA), 360
- hydrocarbon, 293
- through immobile matrix, 283
- internal, 289
- intragrangular, 276
- intramineral, 58
- intraorganic, 66, 299
- intra-organic-matter, 66
- intraparticle equation for, 158
- intrisorbent, 278, 280–283, 287, 299
- iodide, 293
- lithium, 276
- 4-MCB, 153–154
- mechanism of, 273
- in microporous sorbent particles, 294–297
- models of
 - internal, 289
 - radial, 150, 153, 158–161, 209, 282
 - spherical, 287
- molecular, 107, 211
- natural organic matter role in, 299
- of nonelectrolytes, 298
- non-Fickian, 162, 298
- in polymers, 161–162, 297–299
- pore, 280, 281, 295–296, 298
- radial model of, 150, 282
- rate constants for, 287
- restrictive pore, 295–296
- in rock, 293–294
- solute, 161–162, 273
- sorption rate limitations and, 292–299
- spherical models of, 287
- studies of, 292–299
- surface, 280, 294–295, 298, 299
- in zeolites, 296–297
- Diffusion-advection-reaction model, 257
- Diffusion coefficients, 259, 281, 283, 285, 288, 295, 296
 - for ethane, 294
 - intraorganic, 282
 - intrinsic, 283, 293
 - meaningful, 297
- molecular, 257
- molecular size and, 299
- in polymers, 299
- pore, 298
- seawater molecular, 257
- sediment, 257, 259
- steady-state, 283
- transient, 293
- in zeolites, 297
- Diffusivity, 209. *See also* Diffusion
 - of colloids, 108
 - effective pore, 281
 - free liquid, 122
 - liquid-phase, 295
 - 4-MCB, 153
 - polymer liquid, 117
 - sediment, 122
 - zeolite, 297
- Dihaloelimination, 349
- Dioxins, 341, 425, 453. *See also* specific types
 - 9,10-Diphenylanthracene, 197, 206
- Disaggregation, 287
- Dissolution kinetics, 298
- Dissolved inorganic carbon, 221, 250
- Dissolved nutrients, 221. *See also* specific types
 - Dissolved organic carbon (DOC), 174, 180, 181, 409
 - DOM in measurement of, 504
 - in fractionation, 264–265
 - production of, 265
 - reactivity of, 265
 - Dissolved organic matter (DOM), 503–516. *See also* specific types
 - applications of, 515–516
 - experiments with, 505–506
 - fluorescence of, 503–505, 506, 508, 510, 513, 515
 - metal-binding sites on, 508
 - metal interactions with, 504, 508, 510, 513–515, 516
 - pH and, 510–513
 - in rivers, 509–510
 - solution chemistry and, 510–515
 - sources of, 508–510
 - structure of, 510
 - synchronous excitation spectra of, 506–508

- tracers and, 504, 508
 variation in type of, 508–510
 in watersheds, 509–510
- Distribution coefficients, 81, 82, 84, 87, 181, 183
- DiToro's model, 59, 72
- Diuron, 284, 286
- DOC. *See* Dissolved organic carbon
- Dodecylpyridinium (DP), 128, 129, 130, 131, 133, 134, 135–136, 140, 142–146
- Dolomite, 27, 36
- DOM. *See* Dissolved organic matter
- DP. *See* Dodecylpyridinium
- Dynamic headspace analysis. *See* Gas purging
- EA. *See* Electron acceptors
- ECD. *See* Electron capture detection
- Echirurans, 211
- EDB. *See* Ethyl dibromide
- EEM. *See* Excitation-emission matrix
- Effective pore diffusivity, 281
- Effective tortuosity factor, 283, 295
- Effluent, 192, 194
 PAHs in, 195–200
 suspended solids in, 240
 transport of particles in, 210
- EGTA. *See*
 Ethyleneglycol-bis(2-aminoethyl-ether)-N,N,N',N'-tetra-acetic acid
- EI. *See* Electron impact
- Electrochemical oxidation, 261
- Electron acceptors, 249
- Electron capture detection, 226
- Electron donors, 350
- Electron impact ionization, 314
- Electron transfer reactions, 349
- Electrostatic effects, 132
- Electrostatic energy, 133, 138, 143
- Electrostatic interactions, 127, 132, 143
- Empirical models, 55
- Energy, 133, 134–135, 138, 143. *See also* specific types
- Enthalpy, 55
- Environmental fate. *See* Fate
- EP. *See* Equilibrium partitioning
- EPICS. *See* Equilibrium partitioning in closed systems
- Equilibrium, 131, 180, 378
 approaches to, 284
 attainment of, 58
 complex, 409
 deviations from, 273
 fractional approach to, 158
 HOC-phytoplankton, 99
 lack of. *See* Nonequilibrium
 local, 276
 model of, 376
 nonattainment of, 72
 reversible, 281
 sorption. *See* Sorption equilibrium
 time to reach, 155
 true, 278
 variability in rates for, 278
- Equilibrium binding constants, 122
- Equilibrium distribution coefficients, 181
- Equilibrium partition coefficients, 108, 209
- Equilibrium partitioning, 88, 163, 243–244
- Equilibrium partitioning in closed systems (EPICS), 63
- Ethane, 293, 294, 338
- Ethers, 326. *See also* specific types
- Ethylbenzene, 64
- Ethyl dibromite (EDB), 52, 276, 286
- Ethyleneglycol-bis(2-aminoethyl-ether)-N,N,N',N'-tetra-acetic acid (EGTA), 253
- Evaporation, 210
- Excitation-emission matrix (EEM), 506, 507, 508, 513
- Excitation spectra, 506–508
- Excretion rate, 94
- External mass transfer, 280
- External transfer coefficients, 287
- Extinction coefficient, 111–112
- Extraction, 286, 352
 of AOCs, 414, 477–479
 of natural organic compounds, 313
 of PCBs, 92, 98, 224–227
- FA. *See* Fulvic acid
- Fall storms, 27

- Fate, 273, 323, 409
 of ethyl dibromite (EDB), 276
 of HOCs, 91
 models of, 323
 of PAHs, 191, 192, 206–210
 short-term biogeochemical, 206–210
 of surfactants, 127
- Fatty acids, 194
- Fecal pellet transport, 38–39
- Feldspar, 34
- Ferrous iron, 349, 350, 351, 352, 353, 356, 357
 oxidation of, 359
 reactivity of, 362
- Fickian diffusion, 150, 280, 298, 299
- FID. *See* Flame ionization detection
- Filtration, 20, 63, 81, 149
- Fine particulate organic matter, 493–500
- Fingerprinting, 515
- First-order batch rate studies, 284–287
- First-order desorption rate coefficients, 287
- First-order index, 336, 337
- First-order kinetics, 356
- First-order numerical transport models, 276
- First-order rate coefficients, 286, 378
- First-order rate constants, 291, 292
- First-order sorption models, 280
- Fish, 107, 186, 335
- Flame ionization detection (FID), 174, 313
- Flory-Huggins model, 80
- Flow fluctuations, 493
- Fluoranthene, 173, 197, 199, 202, 209
- Fluorescence, 495
 decay curves for, 503–505
 of DOM, 503–505, 506, 508, 510, 513, 515
 of fulvic acid, 503
 of humic acid, 503
 intensity of, 504, 508
 intrinsic, 503
 sensitivity to, 510
 steady-state, 506–507
- Fluorescence quenching, 111, 118, 505, 513, 515
- Fluorine, 326
- Fluorophores, 503, 507, 510, 515, 516
- Flux, 267
 benzo(a)pyrene, 185
 biogenic silicon, 26
 bottom sediment, 35–36
 component, 23–31, 33–35
 component-specific metal, 32
 estimated total, 123
 input, 15
 lead, 37
 metal, 32, 38–39, 40–44
 output, 15
 PAH, 118–123, 181–182
 preindustrial sediment, 38
 sediment trap, 23, 37–38
 total, 123
 trace element, 15, 32
 vertical, 15
 water-column-based, 40
- Focusing, 35, 181, 185, 222, 223
- Food-chain transmission, 323
- Fossil fuels, 172, 186, 191, 192, 197
- Fourier transform infrared (FTIR), 314
- Fractionation, 267, 312–313
 of AOCs, 414–415, 477–479
 of carbon isotopes, 263–264
 chemical, 224–226
 dissolved organic carbon in, 264–265
 isotopic, 250, 262–264
 size, 18–19
- Fraction organic carbon, 129
- Free liquid diffusivity, 122
- Freundlich equation, 135
- Freundlich isotherms, 135, 137–138, 155, 384
- FTIR. *See* Fourier transform infrared
- Fugacity, 4, 95
 gradient of, 95
 liquid-phase, 61
 in liquid phase, 59
 of mirex, 3
 of PCBs, 3, 10, 11
- Fulvic acid, 112, 409, 503, 504, 505, 507, 508, 513. *See also* Dissolved organic matter (DOM)

- Gas chromatography, 174, 195, 201, 226, 313, 316
capillary, 312–313
high-resolution, 3, 195, 207, 226
- Gas chromatography-Fourier transform infrared (GC-FTIR), 314
- Gas chromatography-mass spectrometry, 313–314
- Gas purging
in alkylbenzene sorption studies, 63, 64, 66
in PCB studies, 3–11
- GC. *See* Gas chromatography
- Gel permeation chromatography, 414
- Geochronology, 175
- Geometry of basin, 222
- GFAA. *See* Graphite furnace atomic absorption
- Globular protein molecular weight cutoff, 118
- Glycolates, 100
- Gold, 361
- Grain size, 238, 293
- Graphite furnace atomic absorption (GFAA), 19, 20
- Graph theory, 336
- Growth rate, 94
- Guppies, 333, 337
- HA. *See* Humic acid
- Half-lives, 323
- Halides, 349. *See also* specific types
- Haloaliphatics, 352. *See also* specific types
- Halogenated alcohols, 326. *See also* specific types
- Halogenated aliphatics, 349
- Halogenated aromatics, 285. *See also* specific types
- Halogenated compounds, 349. *See also* specific types
- Halogenated phenols, 337. *See also* specific types
- Halogens, 326, 329, 338–341. *See also* specific types
- Hazardous waste disposal sites, 276
- HCA. *See* Hexachloroethane
- Headspace analysis. *See* Gas purging
- Henry's constant, 323, 325, 338
- Henry's law constants (HLCs), 3, 4, 5, 6, 8, 9, 59–61, 66
- Hentriaccontane, 314
- Heptachlor, 91
- Heterocyclic compounds, 337. *See also* specific types
- Heterotrophs, 332, 333, 336, 338
- Hexachloreocyclohexane, 287
- Hexachlorobenzene, 91, 285
- Hexachlorobiphenyl, 284
- 2,3,4,4',5,6-Hexachlorobiphenyl, 92
- 2,4,5,2',4',5'-Hexachlorobiphenyl, 181
- Hexachloroethane (HCA), 349, 350, 352
diffusion of, 360
disappearance of, 356
reductant reactions with, 357
reduction of, 354, 359
transformation of, 353, 357, 358
- Hexacosanol, 316, 317
- Hexa-fluoro-2-propanol, 329
- Hexane, 93, 194, 195, 295, 297, 338
- Hexane/benzene, 195
- Hexane/methylene chloride, 226
- High-performance liquid chromatography. *See* High-pressure liquid chromatography (HPLC)
- High-pressure liquid chromatography (HPLC), 95, 129, 367, 368, 414–415
- High-pressure size-exclusion chromatography (HPSEC), 108, 110, 111, 112, 113, 114, 115
colloid molecular weight and, 116–118
- High-resolution gas chromatography, 3, 195, 207, 226
- High-volume filtration, 81
- HLCs. *See* Henry's law constants
- Hopane, 204, 205
- HPLC. *See* High-pressure liquid chromatography
- HPSEC. *See* High-pressure size-exclusion chromatography
- Humic acid, 409, 503, 507, 508. *See also* Dissolved organic matter (DOM)

- Humin, 163
- Hydrocarbons. *See also* specific types
aliphatic. *See* Aliphatics
anthropogenic, 234
aromatic. *See* Aromatics
chlorinated (CHC), 186, 332
diffusion of, 293
mobility of, 298
petroleum. *See* Petroleum
hydrocarbons
polycyclic aromatic. *See* Polycyclic aromatic hydrocarbons (PAHs)
saturated, 193, 194
solubility of, 385
sources of, 197
straight-chained, 297
total, 193, 194, 204, 205, 207
waxes and, 320
- Hydrodynamics, 4, 283
- Hydrogen, 108, 128, 138, 141, 143
- Hydrogen acceptors, 334
- Hydrogen bonding, 298, 326, 334, 365–366
- Hydrogen disulfide, 350
- Hydrogen donors, 334
- Hydrogenolysis, 349
- Hydrogen peroxide, 357, 359
- Hydrogen sulfide, 211
- Hydrolyzation, 336
- Hydronica, 350
- Hydrophobicity, 52, 54, 127, 132, 143, 211
relative, 61
solute, 55
of surfactants, 143
- Hydrophobic organic chemicals (HOCs), 49, 107. *See also*
Polychlorinated biphenyls (PCBs);
Polycyclic aromatic hydrocarbons (PAHs); specific types
accumulation of, 91, 92
affinity for, 493
aquatic geochemistry of, 81
aqueous phase activity of, 59–63
binding of, 118
binding coefficients of, 56
bioavailability of, 79, 180
colloids and, 69, 108
desorption of, 100, 150
- dissolved, 66
as dissolved constituents, 223
distribution of, 88, 180, 385
elimination of, 100
equilibrium between phytoplankton and, 99
fate of, 91, 102
geochemistry of, 81
lipid accumulation of, 91
measurement of, 149
modeling of, 149
organic colloid binding of, 108
particle associations with, 80, 88
particle-reactive, 123
partition coefficients of, 80
partitioning of, 52, 55, 56, 79, 154, 221
kinetics of, 93, 99–101
models of, 399–400
phytoplankton in. See under Phytoplankton
between pseudophases, 385–388
between soil and monomeric surfactants, 397–399
phytoplankton and, 102 102
reactivity of, 79
release of, 88
scagenging of, 171
in sediment amtrix, 180
sorbed phase activity of, 59–63
sorption coefficient for, 397–398
sorption of, 50–56, 221, 365
aqueous phase activity and, 59–63
kinetics of, 55
particle concentration and, 58
sorbed phase activity and, 59–63
speciation of, 79
surface interactions with, 55
surfactant solubilization of. *See*
Surfactant HOC solubilization
suspended solids and, 79
transport of, 91
uptake of, 88, 95, 96, 99, 100
- Hydrophobic partitioning, 151
- Hydrophobic sorption, 239
- Hydroxides, 295
- Hydroxyl groups, 329. *See also* specific types

ICP. *See* Inductively coupled plasma
 Illite, 409
 Immobilization, 280
 Incomplete combustion, 172, 192
 Inductively coupled plasma emission
 (ICP) spectrometry, 19
 Infinite dilution activity coefficients,
 55
 Inorganic carbon, 20, 221, 250, 298
 Input fluxes, 15
 Internal diffusion, 289
 Interstitial-fluid colloidal matter, 108
 Intragranular diffusion, 276
 Intraminerall diffusion, 58
 Intraorganic diffusion, 66, 299
 Intraorganic diffusion coefficients,
 282
 Intraparticle diffusion equation, 158
 Intraparticle porosity, 288, 289
 Intraparticle tortuosity factor, 288
 Intrasorbent diffusion, 278, 280–283,
 287, 299
 Intrinsic diffusion coefficients, 293
 Intrinsic molecular volume, 334
 Iodide, 276, 293, 515
 Iodine, 326
 Ion exchange, 365
 Ion-pair reactions, 140
 Iron, 34
 DOM and, 510, 516
 ferrous, 349, 350, 351, 352, 353,
 356, 357, 359, 362
 oxidation of, 350, 360, 361
 structural, 360
 Iron sulfides, 268, 353, 356, 357
 Irrigation, 108, 121, 260, 268. *See also*
 Bioirrigation
 Iso-octane, 150, 295
 Isotherms, 132–135, 155–157. *See also*
 specific types
 Freundlich, 135, 137–138, 155, 384
 Langmuir, 163
 linear, 134, 274
 nonlinear, 132–134, 136, 138, 143,
 282
 Isotope model
 description of, 257–260
 results of, 260–268
 Isotopes. *See also* specific types

exchange of, 264
 fractionation of, 250, 262–264
 imbalance in, 265
 profiles of, 260
 sodium, 276
 Kaolin, 409
 Kerelaar's polarizability concept, 329
 Kerogen, 163
 Ketones, 326, 330. *See also* specific
 types
 Kinetics, 130–131, 162, 211, 280,
 352–353
 algal HOC uptake, 100
 desorption, 100, 209, 210, 234
 dissolution, 298
 first-order, 356
 HOC partitioning, 93, 99–101
 HOC sorption, 55
 HOC uptake, 100
 partitioning, 149
 sorption, 55, 57, 58, 100, 149, 163,
 209, 284
 Krypton, 352
 Laboratory column studies, 277–278.
 See also specific types
 Langmuir model, 61, 62, 162, 163,
 299
 LAS, 130, 131, 132, 134, 135, 137,
 138, 141, 143
 LAS homologues, 129, 140, 143
 Lead, 32, 43, 107, 175, 180, 181
 DOM and, 513, 516
 flux of, 37
 organometallic, 429, 430
 Leaf litter, 320
 Leaf litter extract (LLE), 509
 Least-squares Gaussian fit, 183
 Ligand exchange reactions, 141, 143
 Limenite, 350
 Lindane, 97, 287
 Linear alkylbenzenesulfonate, 137–138
 Linear column chromatography, 414
 Linear partitioning, 281, 282, 287
 Linear regressions, 66, 68
 Linear solvation energy relationships
 (LSER), 334–336

- Lipids, 91, 93, 94, 95, 96, 99. *See also* specific types
- Liquid diffusion coefficient, 122
- Liquid-phase diffusivity, 295
- Liquid-phase fugacity, 61
- Liquid scintillation counting, 131, 389
- Lithium diffusion, 276
- LLE. *See* Leaf litter extract
- Log P. *See* Octanol-water partitioning
- Long-chain alcohols, 311, 317, 320. *See also* specific types
- Long-chain aldehydes, 314, 317
- Long-chain alkanes, 311, 314, 317. *See also* specific types
- LSC. *See* Liquid scintillation counter
- LSER. *See* Linear solvation energy relationships
- Macroporosity, 163
- Magnesium, 34, 351, 510, 516
- Magnetite, 350
- Manganese, 513, 516
- Marcasite, 350, 351, 356, 360, 361
- Mass spectrometry, 195, 313–314
- Mass transfer, 280
- Mass transfer coefficient, 379
- Mass transfer limitations, 274, 275, 277
- 4-MCB. *See* 4-Monochlorobiphenyl
- Mean equilibrium distribution coefficients, 181
- Mean particle settling velocities, 171
- MER. *See* Mobile environmental reservoir
- Mercury, 429
- Metabolism, 100, 210
- Metals. *See also* Trace elements; specific types
- accumulation of, 32
 - binding of, 516
 - DOM interactions with, 504, 508, 510, 513–515, 516
 - fluxes of, 38–39, 40–44
 - in particulate matter components, 36
 - partitioning of, 41–44
 - redistribution of, 43
 - removal of, 33
 - residence times for, 33, 41–44
- water-column fluxes of, 40
- Methane, 293, 294
- Methanogens, 332, 338
- Methanol, 226
- Methylacridinium, 136
- Methylene chloride, 226
- Micellar surfactants, 384–385, 399–400
- Micelle-water partitioning, 383
- Microbial degradation, 210
- Microgravimetry, 194
- Microtox, 241, 332, 335, 338, 341
- Mineralogy, 129
- Minnows, 332
- Mirex, 3
- Mixing rates, 107
- Mobile environmental reservoir (MER), 224
- Models. *See also* specific types
- advection-dispersion, 375–380
 - BET sorption, 52
 - component of trace element cycling, 21–23
 - diffusion
 - internal, 289
 - radial, 150, 153, 158–161, 209, 282
 - spherical, 287 - diffusion-advection-reaction, 257
 - DiToro's, 59, 72
 - empirical, 55
 - environmental, 149
 - equilibrium, 376
 - fate, 323
 - first-order numerical transport, 276
 - first-order sorption, 280
 - Flory-Huggins, 80
 - HOC, 149
 - HOC partitioning, 399–400
 - internal diffusion, 289
 - isotope. *See* Isotope model
 - Langmuir, 61, 62, 162, 163, 299
 - natural organic matter, 162–163
 - partitioning, 53, 399–400
 - Pelletier-Whipple-Wedlick (PWW), 185
 - predictive, 144
 - predictive ability of, 330–331
 - QSAR. *See* Quantitative

- structure-activity relationships (QSAR) model
- radial diffusion, 150, 153, 158–161, 209, 282
- rapid steady-state mixing (RSSM), 175
- Sabljić's, 338
- shale, 22
- solubilization, 80
- sorption, 52, 61, 149, 280
 - BET, 52
 - first-order, 280
 - surfactant, 144
- sorption kinetics, 209
- spherical diffusion, 287
- surfactant sorption, 144
- tortuosity, 282
- transport, 276, 291, 493
- Molar solubilization ratio (MSR), 385, 386, 387, 388, 392
- Molecular connectivity, 323, 325, 329, 330, 336–338
- Molecular diffusion, 107, 211
- Molecular diffusion coefficients, 257
- Molecular size, 110, 299
- Molecular weight, 116–118, 392–393
- Molecular weight cutoff (MWCO), 118
- Mole fraction concentrations, 51
- Mollusks, 223, 241
- 4-Monochlorobiphenyl (4-MCB), 58, 72, 150
 - diffusion of, 153–154
 - partitioning of, 154
 - partition measurements and, 151, 152
 - radial diffusion model and, 158, 160, 161
 - sorption equilibrium of, 152, 153, 154
 - sorption isotherms and, 156, 157
- Monodisperse polystyrene microspheres (MPM), 150, 151
 - partition measurements and, 151–152
 - polymers and, 163
 - radial diffusion model and, 158, 159, 160, 161
 - solute diffusion and, 162
- sorption equilibrium and, 151, 153, 154
- sorption isotherms and, 155, 156, 157
- Monomeric surfactants, 384–385, 397–399. *See also* specific types
- Monomers, 384, 386
- Monosaccharides, 409. *See also* specific types
- Montmorillonite, 138
- MPM. *See* Monodisperse polystyrene microspheres
- MS. *See* Mass spectrometry
- MSR. *See* Molar solubilization ratio
- MWCO. *See* Molecular weight cutoff
- Nannoplankton, 102
- Naphthalene, 53, 194, 195, 197, 200, 201, 393
 - removal of, 210
 - systematic changes in, 210
- Naturally occurring organic materials.
 - See* Natural organic compounds
- Natural organic compounds, 311–320, 409. *See also* specific types
 - diffusion and, 299
 - extraction of, 313
 - models of, 162–163
 - particle size analysis of, 314
 - polymers as models of, 162–163
 - sampling of, 312–314
- Nepheloid-layer terrigenous component concentrations, 28
- Neutral cation exchange, 140
- Neutral surfactants, 127, 128, 134. *See also* specific types
- Nickel, 429, 516
- Nitrobenzene, 287
- Nitro compounds, 330. *See also* specific types
- Nitrogen-heterocyclic compounds, 365.
 - See also* specific types
- 2-Nitrophenols, 61
- Nitrosomonas, 332, 338, 341
- NMR. *See* Nuclear magnetic resonance
- Nonacosane, 316, 317
- Nondegradable fraction, 257
- Nonelectrolytes, 298

- Nonequilibrium, 58, 59, 99, 276, 292
desorption, 276
sorption, 274, 275, 276
source of, 291
- Non-Fickian diffusion, 162, 298
- Nonglassy amorphous polymers, 163
- Nonionic surfactants, 127, 136, 142, 393–397. *See also* specific types
- Nonlinear column chromatography, 414
- Nonvalence index, 336–337
- Nuclear magnetic resonance (NMR), 162
- Nutrients. *See also* specific types
availability of, 249
balance of, 249
dissolved, 221
productivity enhanced by, 175
- OCN. *See* Octachloronaphthalene
- 2,2',3,4,4',5,6,6'-Octachlorobiphenyl, 92
- Octachloronaphthalene (OCN), 226
- Octane, 338
- Octanol-water partition coefficients, 91, 94, 221, 243, 323, 333–334, 392
- Octanol-water partitioning, 333–334
- Octanol-water system, 163
- 1-Octene, 295
- Oil seepage, 202, 206
- Oil spills, 210
- Oligochaetes, 180
- Optical microscopy, 19
- Organic carbon, 110, 205, 207, 221, 236, 238
concentration of, 175
dissolved. *See* Dissolved organic carbon (DOC)
fraction, 129
with inorganic carbon, 298
measurements of, 21
oxidation of, 249, 255, 263–264, 267. *See also* Carbon cycling
particulate (POC), 206, 265
partition coefficients and, 243, 409
remineralization of, 251
total. *See* Total organic carbon (TOC)
- Organic colloids. *See* Pore-water organic colloids
- Organic matter, 21–22. *See also* specific types
anthropogenic. *See* Anthropogenic organic compounds (AOCs)
dissolved. *See* Dissolved organic matter (DOM)
naturally occurring. *See* Natural organic compounds
particulate (POM), 493–500
partitioning into, 395
- Organic polymers, 297–299. *See also* specific types
- Organochlorine pesticides, 454–455. *See also* specific types
- Organometallics, 410, 429–430, 468–470. *See also* specific types
- Organophosphorus pesticides, 455–456. *See also* specific types
- Output fluxes, 15
- Oxidants, 250, 359. *See also* specific types
- Oxidation, 264
DOC and, 504
electrochemical, 361
of iron, 350, 359, 360, 361
of organic carbon, 249, 255, 263–264, 267. *See also* Carbon cycling
photochemical, 209
of pyrite, 361–362
of sheet silicates, 357–360
of sulfides, 268
- Oxyethylene, 128, 134
- Oxygen availability, 210
- Oysters, 241
- PAHs. *See* Polycyclic aromatic hydrocarbons
- Palladium, 361
- Palygorskite, 350
- Paraquat, 136
- Particle affinity, 41
- Particle-associated transport, 221–223
- Particle collision, 150
- Particle concentration, 150
HOCs and, 80, 88
low surface coverages and, 69–73

- partitioning and, 149
 PCBs and, 80
 sorption and, 149
 sorption coefficients and, 56–59
 Particle-induced desorption, 58
 Particle-particle interactions, 284
 Particle-reactive HOCs, 123
 Particle-reactive radionuclides, 107
 Particle settling velocities, 171
 Particle size analysis, 314
 Particle size distribution, 66, 91, 129
 Particulate inorganic carbon, 20
 Particulate matter. *See also* specific types
 exchange of, 4
 metal in components of, 36
 standing crop of, 17–18
 vertical flux of, 15
 Particulate organic carbon (POC), 206, 265
 Particulate organic matter (POM), 493–500
 Partition coefficients, 4, 81, 149, 281, 284, 296
 carbon-normalized, 80, 93
 classical, 59
 for column transport studies, 277
 desorption, 372
 equilibrium, 108, 209
 HOC, 80
 linear soil-water, 399
 micelle/aqueous-pseudophase, 392
 normalized, 123
 octanol-water, 91, 94, 221, 243, 323, 392
 organic carbon and, 243, 409
 rate constants with, 292
 reversible, 59
 soil-water, 399
 sorption, 372
 thermodynamic, 80
 water-particle, 93
 Partitioning, 162, 163, 171, 278, 280, 323
 batch, 277
 bioaccumulation and, 244
 direct, 222
 downgradient of, 274
 equilibrium, 88, 243–244
 of HOCs, 52, 55, 56, 79, 154, 221
 kinetics of, 93, 99–101
 models of, 399–400
 phytoplankton in. *See under Phytoplankton*
 between pseudophases, 385–388
 between soil and monomeric surfactants, 397–399
 hydrophobic, 151
 of hydrophobic organics, 239
 kinetics of, 149
 linear, 281, 282, 287
 of lipids, 95
 of 4-MCB, 154
 measurements of, 151–152
 mechanisms of, 55
 of metals, 41–44
 between micelles, 392
 micelle-water, 383
 models of, 53
 octanol-water, 333–334
 into organic matter, 395
 particle concentration and, 149
 of PCBs, 3, 81–84, 88, 149, 221, 223, 226, 235
 PCB-suspended solid associations and, 79–88
 semiempirical equations for, 82
 thermodynamic, 162
 PCDDs. *See* Polychlorinated dibenzo-*p*-dioxins
 PCDFs. *See* Polychlorinated dibenzofurans
 PCE. *See* Tetrachloroethene
 Pearson correlation matrix, 211
 Pelletier-Whipple-Wedlic (PWW) model, 185
 Pentachlorobenzene, 285, 288
 Pentacyclic PAHs, 191
 Pentacyclic triterpane, 204
 Pentane, 338
 Peptides, 409. *See also* specific types
 Perylene, 191, 194, 197, 206
 Pesticides, 410, 454–461. *See also* specific types
 chlorinated, 91
 organochlorine, 454–455
 organophosphorus, 455–456
 references on, 425–427

- sorption of, 80
triazine, 456–461
- Petroleum hydrocarbons (PHCs), 239, 410. *See also* specific types
determination of, 443–449
interlaboratory studies of, 417
PCB ratio to, 239
references on, 421–424, 443–449
- pH
acridine and, 365–380
DOM and, 510–513
surfactant sorption and, 131
- Phase separation, 63, 66
- PHCs. *See* Petroleum hydrocarbons
- Phenanthrene, 108, 111, 118, 173, 194, 199, 201, 393
alkylated, 191
removal of, 210
solubility of, 390
sources of, 234
systematic changes in, 210
- Phenanthrene/anthracene, 195, 197
- Phenanthrene/phenanthrene, 197
- Phenols, 330, 365. *See also* specific types
determination of, 464
halogenated, 337
references on, 427–428, 464
toxicity of, 332
- Phenyl polymer-modified silicon, 58
- Phosphates, 429, 467
- Photochemical oxidation, 209
- Photodegradation, 210
- Photolysis, 49
- Phthalates, 224, 428, 466. *See also* specific types
- Physical properties, 323. *See also* specific types
- Physicochemical interactions, 299. *See also* specific types
- Phytoplankton, 39, 43, 221
biomass of, 100
desorption of HOCs from, 100
equilibrium between HOCs and, 99
fate of HOCs by, 102
in HOC partitioning, 91–103
 factors controlling, 93–99
 fate and, 102
 kinetics of, 99–101
- lipid properties of, 93
in organic carbon, 264
PCBs in, 97
- Picloram, 285
- Plankton, 21, 229, 264. *See also* specific types
- Plant waxes, 311, 312, 314–315, 320
- Plateau sorption, 136
- PNA. *See* Polynuclear aromatics
- POC. *See* Particulate organic carbon
- POE. *See* Polyoxyethylene
- Point source elimination, 107
- Polarity, 336
- Polarizability, 325, 329, 330, 334, 336
- Polychaetes, 241
- Poly chlorinated dibenzo-p-dioxins, 330
- Polychlorinated biphenyls (PCBs), 79, 91, 107, 410. *See also* Hydrophobic organic chemicals (HOCs)
air-water transfer of, 3–11
apparent effects threshold (AET) and, 241–243
batch-extraction of, 92
bioaccumulation factor (BAF) for, 95
chemical nature of, 235
complexation of, 80
concentration of, 81, 87, 227–230, 236, 238
degradation of, 229
deposition of, 229, 236
determination of, 450–452
diminished levels of, 236, 238
dissolved, 93
dissolved-phase, 81, 87
distribution of, 81, 85, 87, 88, 221–244
concentration levels and, 227–230
extraction in study of, 224–227
general, 230–236
geographic, 223–224
localized, 236–240
overall, 227–230, 235
sampling in study of, 224
sediment quality and, 241–244
spatial, 224
transport and, 221–223

- distribution coefficients for, 81, 82, 84, 87
 ending of production of, 223, 224
 extraction of, 92, 98, 224-227
 field study of, 10-11
 in fish, 186
 fugacity of, 3, 10, 11
 gas purging in study of, 3-11
 general distribution of, 230-236
 grain size and dynamics of, 238
 hot spots for, 228
 interlaboratory studies of, 417
 kinetics of partitioning of, 149
 kinetics of sorption of, 149
 MPM and, 162
 octanol-water partition coefficient
 for, 243
 overall concentration of, 227-230
 overall distribution of, 227-230, 235
 particles and, 80
 partition coefficients for, 243
 partitioning of, 3, 81-84, 88, 149,
 221, 223, 226, 235
 PHC ratio to, 239
 phytoplankton and, 97, 101
 QSAR model and, 331
 references on, 424-425, 450-452
 sampling of, 224
 in sediment, 231
 solubility of, 330
 sorption of, 149, 284
 sources of, 231, 235
 spatial distribution of, 224
 suspended solids and, 79-88
 TOC ratio to, 240
 total, 227
 uptake of, 87, 98
- Polychlorinated dibenzo-*p*-dioxins
 (PCDDs), 91, 330
- Polychlorinated dibenzofurans
 (PCDFs), 91
- Polycyclic aromatic hydrocarbons
 (PAHs), 3, 79, 107, 171-186,
 191-215, 224, 410. *See also*
 Hydrophobic organic chemicals
 (HOCs); specific types
 abundance of, 192
 accumulation of, 180, 182, 211-213
 annual mass emissions of, 199-200
- batch studies of, 388
 binding of, 111
 biodegradation of, 192
 biosynthesis of, 191
 carcinogenicity of, 191
 colloid binding to, 111, 118
 colloid nonlocal exchange
 parameters and, 123
 combustion, 175-180, 181, 182, 186,
 191, 192, 213
 compositional features of, 195-199,
 200-206, 211
 concentrations of, 204, 207
 degradation of, 210, 211
 determination of, 443-449
 distribution of, 173, 191, 192, 205,
 206
 in effluent, 195-200
 environmental behavior of, 191
 fate of, 191, 192, 206-210
 fluxes of, 118-123, 181-182
 formation of, 172, 191
 global distribution of, 191
 historical rates of accumulation of,
 211-213
 input of, 207
 intense input of, 207
 inventories of, 181-182
 lost, 208, 210
 mass emission rates for, 199-200
 methods in study of, 173-175
 oil-derived, 206
 pattern in composition of, 199
 peak concentrations of, 180
 pentacyclic, 191
 pore waters and, 180-181
 postdepositional alteration in,
 210-211
 pyrogenic, 191, 211
 QSAR model and, 326, 329
 references on, 443-449
 regional accumulation of, 182
 sampling of, 194
 in sediments, 200-213
 accumulation rates for, 211-213
 composition of, 200-206
 fate of, 206-210
 postdepositional alteration in,
 210-211

- sources of, 200–206
- short-term biogeochemical fate of, 206–210
- solubility of, 384, 385, 388, 390, 391
- sources of, 178, 191, 197, 200–206, 210, 234
- structure of, 173
- surface concentrations of, 178
- tetracyclic, 191
- transport of, 178, 192
- tricyclic, 201, Di201
- uptake of, 180
- vertical concentration of, 204
- vertical distribution of, 192
- Polyelectrolytic effects, 113, 114
- Polyethylene glycol, 128
- Polymeric oxides, 295
- Polymer liquid diffusivity, 117
- Polymers. *See also* specific types
 - diffusion in, 161–162, 297–299
 - diffusion coefficients in, 299
 - as natural organic matter models, 162–163
 - nonglassy amorphous, 163
 - organic, 297–299
 - solute diffusion in, 161–162
- Polynuclear aromatics, 284, 330, 331.
 - See also* specific types
- Polyoxyethylene (POE), 384
- Polysaccharides, 112, 297. *See also* specific types
- Polysulfides, 350, 361. *See also* specific types
- Polyvinyl alcohols (PVA), 481–489
- POM. *See* Particulate organic matter
- Pore diffusion, 280, 281, 295–296, 298
- Pore diffusion coefficients, 298
- Pore size, 294
- Pore-water, 180–181, 250
 - bioaccumulation and, 180
 - calcium concentration in, 262
 - exchange between bottom water and, 260
 - exchange between overlying water and, 249
 - sources of carbon in, 265–268
- Pore-water organic colloids, 107–123
 - cooling of, 112–115
 - detection of, 111–112
 - HOC binding and, 108
 - molecular size analysis of, 110
 - molecular weight of, 116–118
 - PAH binding by, 118
 - PAH fluxes and, 118–123
 - PAH nonlocal exchange parameters and, 123
 - sampling of, 108–110
 - transport and, 211
 - uncooling of, 112–115
 - vertical distributions of, 118
- Porosity, 283, 288, 289
- Potassium, 34, 351
- Preindustrial sediment fluxes, 38
- Pressure filtration, 20
- Primary productivity, 221
- Productivity, 175, 221
- Propane, 293, 338
- Propylbenzene, 64
- Pseudo-first-order desorption, 375
- Pseudo-first order reaction constants, 352
- Pseudo-first-order sorption, 375
- Pseudophases, 383–388, 392
- Pseudo-steady state, 29
- Pulverization, 287
- Pumping-in-line sieving
 - continuous-flow centrifugation, 17
- Pump and treat remediation, 275
- Pure components, 36
- PWW. *See* Pelletier-Whipple-Wedlick
- Pyrene, 108, 111, 118, 122, 173, 393
 - desorption of, 285
 - fluoranthene ratio to, 197, 199, 202, 209
 - scatterplot of, 211
 - solubility of, 390
 - uptake of, 285
- Pyrite, 350, 351, 356, 360, 361–362
- Pyroxene, 350
- QSAR. *See* Quantitative structure-activity relationships
- Quantitative structure-activity relationships (QSAR) model, 323, 332

- methods in, 333–338
 predictive ability of, 330–331
 rationale of, 324
 solutes and, 324–329
Quartz, 27, 34
Quinoline, 365, 366, 367, 374
Quinolinium, 365
- Radial diffusion model**, 150, 153, 158–161, 209, 282
- Radioactive waste disposal**, 293
- Radiochemical impurity**, 278
- Radionuclides**, 107, 181. *See also* specific types
- Radon**, 108, 111, 120, 122, 268
- Raman spectroscopy**, 361
- Raoult's convention**, 51, 59–61
- Rapid steady-state mixing (RSSM) model**, 175
- Rate coefficients**, 286, 287, 378
- Rate constants**
 batch, 291
 desorption, 286
 diffusion, 287
 first-order, 291, 292
 primary mineral, 353
 secondary mineral, 353
- Reactivity**, 79
- Redeposition**, 172
- Redfield stoichiometry**, 250
- Redox conditions**, 210
- Redox reactions**, 357
- Reducants**, 352, 357. *See also* specific types
- Reductive dehalogenation**, 349
- Reductive elimination**, 349
- Regression coefficients**, 80
- Relaxation constants**, 298
- Relaxation times**, 162, 298, 554
- Remediation**, 275
- Remineralization**, 249, 251, 264
- Residence times**, 15, 16, 33, 40–44
 for calcite, 43
 component-specific, 33
 for metals, 41–44
- Restrictive pore diffusion**, 295–296
- Resuspension**, 27, 171, 172, 229, 236, 499
- Retene**, 191
- Reversible equilibrium**, 281
- Rhodamine**, 495, 498
- Rock**, 293–294
- Rock capacity factor**, 293
- Rotational relaxation time (RRT)**, 554
- RRT**. *See* Rotational relaxation time
- RSSM**. *See* Rapid steady-state mixing
- SA**. *See* Surface area
- Sabljic's model**, 338
- Salting out**, 62, 231
- Sampling**
 of AOCs, 412–414, 415
 of colloids, 108–110
 of natural organic compounds, 312–314
 of PAHs, 194
 of PCBs, 224
 of POM, 494
 of pore-water organic colloids, 108–110
 references on, 437–441
- Saturated hydrocarbons**, 193, 194
- Scale particle theory**, 325
- Scanning electron microscopy (SEM)**, 361
- Scavenging**, 36, 37, 171
- Seasonal resuspension**, 172
- SEC**. *See* Size-exclusion chromatography
- Secondary productivity**, 221
- Second-order index**, 337
- Sedimentation rate**, 35, 38
- Sediment focusing**, 181, 222, 223
- Sediment geochronology**, 175
- Sediment quality criteria (SQC)**, 241–244, 244
- Sediment traps**, 16–17, 23, 35–36, 37–38
- Sediment–water equilibrium partitioning**, 243–244
- Seismic profiling**, 222, 223
- SEM**. *See* Scanning electron microscopy
- Semiempirical partitioning equations**, 82
- Sesquioxide**, 138
- Settling**, 28, 171
- Sewage**, 481–489

- Sewer overflows, 240
Shale, 22, 34
Sheet silicates, 357–360
Shellfish, 107
Silica, 409
Silica-alumina catalysts, 295
Silica gel column chromatography, 92, 226
Silicates, 350, 353, 357, 357–360
Silicon, 34, 53
 biogenic, 19, 21, 24–27, 29
 filtrable, 20
 nonbiogenic, 34, 35, 36
 phenyl polymer-modified, 58
 surface-modified particles of, 58
Size-exclusion chromatography (SEC)
 charge repulsion effects in, 115–115
 high-pressure. *See* High-pressure size-exclusion chromatography (HPSEC)
Size fractionation, 18–19
Sodium, 34, 128, 131, 138, 140, 141, 142, 143, 351
Sodium isotopes, 276
Sodium tetraphenylborate, 359
Soils. *See also* specific types
 EDB persistence in, 286
 nonionic surfactant sorption onto, 393–397
 sorption of, 338
 sorption of pesticides in, 80
 surfactant HOC solubilization in, 393–397, 399–400
Solid-phase sulfides, 267, 268
Solubility, 80, 329–330, 338
 of acridine, 366–367, 368, 373–374
 of DDT, 384
 of HOCs. *See* Surfactant HOC solubilization
 of hydrocarbons, 385
 of PAHs, 384, 385, 388, 390, 391
 of phenanthrene, 390
 of pyrene, 390
 of quinoline, 366, 374
 surfactant-enhanced. *See* Surfactant HOC solubilization
Solubilization. *See* Solubility
Solutes. *See also* specific types
 diffusion of, 161–162, 273
 QSAR model for different, 324–329
 solute interactions with other, 132, 138–140
 transport of, 273
Solution-phase colloids, 284
Solvatochromatic parameters, 323, 334
Sorbate-sorbate interactions, 132, 138–140
Sorbent-surfactant combinations, 135
Sorption, 49, 79, 107, 171, 222
 acridine, 372, 380
 alkylbenzene. *See under* Alkylbenzenes
 benzene-corundum, 68–73
 capacity for, 277, 284
 carbon-normalized, 284
 chlorinated benzene, 287–288
 coefficients of. *See* Sorption coefficients
 column experiments on, 53
 1,4-dichlorobenzene, 288
 dispersion vs., 378
 diuron, 286
 hexachlorobiphenyl, 284
 HOC. *See under* Hydrophobic organic chemicals (HOCs)
 hydrophobic, 239
 instantaneous sites for, 291
 kinetics of, 57, 58, 72, 100, 149, 163, 209, 284
 mass transfer limitations and, 275
 models of, 52, 61, 149, 280
 nonequilibrium, 274, 276
 nonionic surfactant, 393–397
 particle concentration effect on, 149
 PCB, 149, 284
 PCE, 289
 pentachlorobenzene, 288
 pesticide, 80
 plateau, 136
 pseudo-first-order, 375
 rate limitations in, 273–300
 batch studies and, 278–292
 diffusion studies and, 292–299
 transport studies and, 274–278
 rates of, 209, 284
 slow, 72, 286, 378
 soil, 338

- solution properties and, 138–142
 surface, 96, 97
 surfactant. *See* Surfactant sorption
 TeCB, 289
 tetrachloroethene (PCE), 289
 theories of, 149
- Sorption capacity downgradient, 274
- Sorption coefficients, 51, 54, 55, 56, 62
 changes in, 72, 73
 colloids and, 69
 decrease in, 69
 HOC, 397–398
 measured vs. literature values for, 68–69, 70–71
 particle concentration and, 56–59, 73
- Sorption constants, 54
- Sorption energy, 134–135
- Sorption equilibrium, 57, 150, 151, 153, 155, 277, 285, 379
 anions and, 374–375
 Langmuir equation for, 61
 nonattainment of, 59, 72
 time to reach, 155
 verification of, 67
- Sorption isotherms, 132–135, 136, 137–138, 155–157
- Sorption nonequilibrium, 275
- Sorption partition coefficients, 372
- Speciation, 79
- Specific surface area, 54
- Spectrofluorometry, 111, 367
- Spectrometry. *See also* specific types
 atomic absorption, 20
 chemical ionization mass, 314
 inductively coupled plasma emission (ICP), 19
 mass, 195, 313–314
 Raman, 361
 ultraviolet, 111–112
 ultraviolet/visible, 110
 x-ray photoelectron, 261
- Spherical diffusion model, 287
- SQC. *See* Sediment quality criteria
- SRMs. *See* Standard reference materials
 Standard reference materials (SRMs), 416–417
- Standing crops, 17–18, 24, 38
- Steady-state concentration, 260, 276
- Steady-state conditions, 29, 283
- Steady-state diffusion coefficients, 283
- Steady-state fluorescence, 506–507
- Sterols, 314. *See also* specific types
- Stoichiometry, 250, 357
- Storms, 27
- Straight-chained hydrocarbons, 297.
See also specific types
- Stratification, 171
- Substituted benzenes, 332
- Substituted benzotriazoles, 224
- Substituted phenols, 332
- Sulfates, 350. *See also* specific types
- Sulfides, 349, 352, 353, 357. *See also* specific types
 iron, 353, 356, 357
 oxidation of, 268
 solid-phase, 267, 268
 surface, 350
- Sulfur, 350, 415
- Surface area, 54, 94, 97, 129, 153, 154
- Surface diffusion, 280, 294–295, 298, 299
- Surface interactions with HOCs, 55
- Surface runoff, 199
- Surface-sorbate interactions, 132
- Surface sorption, 96, 97
- Surface sulfides, 350
- Surface tension, 396
- Surface type, 94
- Surfactant HOC solubilization, 383–402
 in aqueous systems, 385–393
 experimental methods for, 388–390
 micellar surfactants and, 384–385, 399–400
 molecular weight correlations and, 392–393
 monomeric surfactants and, 384–385, 397–399
 nonionic surfactants and, 393–397
 pseudophases and, 385–388
 results of study of, 390–393
 in soil, 393–397, 399–400
- Surfactants. *See also* specific types
 anionic, 127, 128, 136

- cationic, 127, 128, 143
determination of, 465
fate of, 127
HOC solubility enhanced by. *See* Surfactant HOC solubilization
hydrophobicity of, 143
micellar, 384–385, 399–400
monomeric, 384–385, 397–399
neutral, 127, 128, 134
nonionic, 127, 136, 142, 393–397
polyoxyethylene (POE), 384
radioactivity of, 130
references on, 428, 465
sorbent combinations with, 135
sorption of. *See* Surfactant sorption
sorption isotherms of, 132–135
structural properties of, 143
- Surfactant sorption**, 127–145. *See also* specific surfactants
batch experiments on, 129–131
distribution ratios and, 129–131
isotherms in, 132–135
methods in study of, 128–131
models of, 144
pH and, 131
predictive models of, 144
solution properties and, 138–142
- Synchronous excitation spectra**, 506–508
- TAH.** *See* Total aromatic hydrocarbon
- Tannic acid**, 409
- TCE.** *See* Trichloroethene
- TCLP.** *See* Toxic contaminant leachate potential
- TeCB.** *See* 1,2,4,5-Tetrachlorobenzene
- Terrigenous components**, 28, 30, 31, 35–36, 38
- Tetrachlorinated biphenyls**, 98
- 2,3,7,8-Tetrachlorinated dioxin**, 98
- Tetrachlorobenzene**, 288
- 1,2,4,5-Tetrachlorobenzene (TeCB)**, 289
- 2,3,5,6-Tetrachlorobiphenyl**, 92
- Tetrachloroethene (PCE)**, 274, 289, 290, 291, 349, 350, 352, 354
- Tetrachloroethylene**, 54
- Tetracyclic PAHs**, 191
- Tetrahydrofuran**, 276
- Thallium**, 107
- THC.** *See* Total hydrocarbon fraction
- Thermal stratification**, 171
- Thermocline erosion**, 27
- Thermodynamic partition coefficients**, 80
- Thermodynamic partitioning**, 162
- Thermodynamics**, 55, 61, 95, 149, 162
- Thin-layer chromatography (TLC)**, 129, 194, 414
- Thiosulfate**, 350
- Tin**, 430
- TLC.** *See* Thin-layer chromatography
- TOC.** *See* Total organic carbon
- Toluene**, 64
- Tortuosity**, 163, 289, 293, 296
effective, 283, 295
intraparticle, 288
models of, 282
porosity and, 283
of sediment, 122, 259
- Total aromatic hydrocarbon (TAH)**, 194
- Total hydrocarbon fraction (THC)**, 194, 205, 208
- Total hydrocarbons**, 193, 194, 204, 205, 207
- Total organic carbon (TOC)**, 108, 110, 111–112, 224, 234, 236, 238, 239
PCB ratio to, 240
sediment quality criteria and, 244
- Total PCBs**, 227
- Toxaphene**, 91
- Toxic contaminant leachate potential (TCLP) test**, 349
- Toxicity**, 127, 332–333, 338
- Trace element cycling**, 15–44
bottom sediment fluxes and, 35–36
chemical analysis of, 19–20
chemical phases and, 33–35
component concentrations and fluxes in, 23–29
component fluxes and, 23–31, 33–35
component model of, 21–23
field studies of, 16–18
laboratory studies of, 18–20
metal fluxes and, 36–39, 40–44

- metal residence times and, 41–44
 residence times and, 15, 16, 33, 40–44
 sediment traps and, 16–17, 35–36, 37–38
 size fractionation and, 18–19
- Trace elements. *See also* Metals; specific types
 annual fluxes of, 32
 in calcite, 31–32
 cycling of. *See* Trace element cycling
 in diatoms, 31–32
 filtrable, 20, 33
 flux of, 15
 residence times for, 15, 16
 total, 20
- Transfer. *See* Transport
- Transport, 107, 211, 409
 into cell membranes, 98
 cesium, 183
 dynamics of, 192
 effluent particle, 210
 ethyl dibromite (EDB), 276
 fecal pellet, 38–39
 first-order numerical models of, 276
 HOC, 91
 hydrodynamics of, 4
 models of, 291, 493
 PAH, 178
 particle-associated, 221–223
 PCB from air to water, 3–11
 POM, 493
 radon, 122
 rates of, 273
 solute, 273
 sorption rate limitations and, 274–278
 studies of, 274–278
 tetrachloroethane (PCE), 291
 two-layer model of, 4
- Triazine pesticides, 456–461
- 1,2,4-Trichlorobenzene, 52
- Trichloroethene (TCE), 276
- Trichloroethylene, 54
- Tricyclic PAHs, 201
- Triphenylene, 181, 197
- Triterpane, 204
- Turbulence, 222
- Two-layer model of gas transfer, 4
- UCM. *See* Unresolved complex mixture
- UF. *See* Ultrafiltration
- Ultrafiltration, 108, 110
- Ultraviolet spectrophotometry, 111–112
- Ultraviolet-visible absorbance, 506
- Ultraviolet-visible spectrophotometry, 110
- Unresolved complex mixture (UCM), 195
- Valence index, 336, 337
- Vermiculite, 138, 350, 351, 354, 356, 357, 358, 359, 360
- Vertical flux, 15
- Volatilization, 49
- Waste disposal, 276, 293
- Wastewater effluent, *See* Effluent
- Wastewater treatment facility, 240, 241
- Water-column-based metal fluxes, 40
- Water quality criteria, 241
- Waxes, 311, 312, 314–315, 320
- Wilke-Chang equation, 122
- Wind-induced circulation, 222
- Worms, 107, 223
- XAD-2, 93
- XAD-4, 294
- XAD-7, 294
- XPS. *See* X-ray photoelectron spectroscopy
- X-ray diffraction, 136
- X-ray photoelectron spectroscopy (XPS), 261
- Zeolites, 294, 296–297. *See also* specific types
- Zero-order index, 336
- Zinc, 32, 37, 43
- Zooplankton, 22, 38, 39, 102, 221

Organic Substances and Sediments in Water

**An important new 3-volume set
by world leaders**

The fate and transport of natural and anthropogenic sediment-borne organic contaminants is a critical environmental issue and complex processes are involved that until now have been poorly defined. *Organic Substances and Sediments in Water* is a three-volume book that provides the best information available regarding the many interdisciplinary factors affecting organic substances associated with particulates in water. Topics discussed include absorption and transport of contaminants associated with particles; interfacial processes affecting fate and transport of organic substances associated with particles; the release of contaminants in receiving water bodies; water treatment; the role of biological factors in the fate and transport of organic contaminants in aqueous systems; development of biotransformation in natural and anthropogenic systems; the use of organic contaminant and sediment chemicals; biological and physical data to refine models to be used by resource managers; and chemical and biological processes that affect the fate and transport of organic constituents and determine degradation of contaminants and uptake in plants. This will be an important reference for environmental chemists, environmental engineers, environmental biologists, water treatment and natural system modelers, and soils scientists.



0873715284

01/19/2018 8:52-2

2-